CAMERA DE COMERȚ, INDUSTRIE, NAVIGAȚIE ȘI AGRICULTURĂ CONSTANȚA

TE-RE-RD

2014

3rd International Conference on Thermal Equipment, Renewable Energy and Rural Development

TE-RE-RD 2014

Mamaia
12-14 Iunie 2014

3nd International Conference of Thermal Equipment, Renewable Energy and Rural Development

TE-RE-RD 2014

ORGANIZERS:

University "POLITEHNICA" of Bucharest
Faculty of Mechanical Engineering and Mechatronics -
Faculty of Biotechnical Systems Engineering -

Hydraulics & Pneumatics Research Institute
(INOE 2000 - IHP), Bucharest

Chamber of Commerce, Industry, Shipping and Agriculture
Constanta – ROMANIA

PROCEEDINGS

Editors:

Prof.dr.ing. Lucian MIHĂESCU
Assoc. Prof.dr.ing.Gabriel-Paul NEGREANU

Mamaia – Romania
12-14 June 2014

ISSN 2359-7941
ISSN-L 2359-7941

Editura POLITEHNICA PRESS

COVER: Valentin Miroiu

ORGANIZING COMMITTEE

Chairman

Prof. Lucian MIHAESCU	**ROMANIA**

Co-Chairmen

Dr. Sorin-Stefan BIRIS	**ROMANIA**
Dr. Gabriel NEGREANU	**ROMANIA**
Dr. Iulian DUTU	**ROMANIA**

Members

Dr. Valentin APOSTOL	**ROMANIA**
Prof. Mircea BĂDESCU	**ROMANIA**
Dipl.Eng. Viorel BERBECE	**ROMANIA**
Dr. Crăiţa CARP-CIOCÂRDIA	**ROMANIA**
Dr. Mihaela DUŢU	**ROMANIA**
Prof. Ionel PÎŞĂ	**ROMANIA**
Dr. Elena POP	**ROMANIA**

Secretary

Dipl. ing. Adriana BAROTHI	**ROMANIA**
Dipl.ing. Cristina CIOBANU	**ROMANIA**
Dipl. Valentin MIROIU	**ROMANIA**

CONFERENCE SPONSORS

SARTOROM

Garantează. Inovează. Excelează

Sos. Bucuresti - Magurele nr. 232
051434 Bucuresti 5, Romania
Tel: +40 21 255 31 32
Fax: +40 21 255 30 66

TURBO EXPERT

Mobil 0722229638
e-mail: turboexpertromania@rdslink.ro

analytikjena

Str. Av. Vasile Fuica, Nr. 26, Sector 1
RO11795620 Bucuresti, Romania
Tel: (++40-21) 6654069
Fax: (++40-21) 2247212

Agromec Stefanesti

CONFERENCE PROFRAMME

Thursday, June 12	Friday, June 13	Saturday, June 14
	Breakfast	Breakfast
14.00-15.00 Registration of participants	08.30-09.30 Registration of participants	09.00-13.00 Visit to Ancient City of Histria
15.00-15.30 Opening ceremony	09.30-11.00 Oral presentations "Sections 1 and 2"	13.00- Participants departure
15.30-18.00 Plenary session	11.00-11.30 Coffee break	
18.00-20.00 Welcome cocktail	11.30-13.00 Oral presentations Section 1 and 2"	
	13.00-14.30 Lunch	
	14.30-16.00 Oral presentations "Sections 1 and 2	
	16.00-16.30 Coffee break	
	16.30-17.30 Workshop Efficiecy increase of the solid biomas combustion under hydrogen flow	
	19.30-22.00 Conference dinner	

CONTENTS

SECTION 1: THERMAL EQUIPMENT AND RENEWABLE ENERGY

Nr. crt	Paper	Authors	Page
1	Opportunities, challenges and future prospects of using biogas as road transport fuel in Pakistan	F. U. M. Allah	1
2	Primary resources of energy	M. Bică, M. S. Sofronie, C. D. Cernăianu, D. Muscalagiu	5
3	Experimental research on the combustion of the gases in low-power burners	M. Bică, M. S. Sofronie, C. D. Cernăianu, D. Muscalagiu	11
4	Heat measure unit for cetralized heat supply of direct subscriber stations	V. Bobilov, P. Zlatev, Z. Kolev, P. Mushakov	17
5	Increasing the energy efficiency of thermal power plant	V. Bobilov, V. Kamburova, Z. Kolev, P. Zlatev, P. Mushakov	21
6	Some aspects of cycle variability at an LPG fuelled diesel engine	Al. Cernat, C. Pana, N. Negurescu	27
7	Hot air distribution through main bustle pipe on the tuyeres of a blast furnace	E. Dimofte, Fl. Popescu, I. V. Ion	33
8	Results of operations for the storage and handling of willow energy crops	A. Domokos, L. Mihăescu, I. Pîşă, E. Pop	39
9	Analogy in processes of destruction of fragile capillary - porous coverings and metallic steam-generating surfaces in power installations	Al. Genbach, K. Olzhabayeva, I. Iliev	43
10	Study of the conditions of fragile fracture of capillary-porous coatings in thermal power plants	Al. A. Genbach, V. O. Baibekova, I. Iliev	49
11	Case of study regarding the energy requirements for a medium rural household	Al. Gruia	55
12	Simplified methodology for monitoring and assessment of the effect of energy saving measures in public buildings	V. Kamburova , I. Iliev , A. Terziev	59
13	Schemes for project financing of combined heat and power production trough biomass gasification	V. Kamburova , I. Iliev , A. Terziev	65
14	Parametric investigation study of counter-flow evaporator for waste heat recovery	M. H. K. Aboaltabooq, H. Pop, V. Badescu, V. Apostol, M. Prisecaru, C. Petcu, C. Ciobanu	71
15	Air quality in Romania. dispersion of pollutant in a urban area using CFD simulation	O. Mărunţelu, Gh. Lăzăroiu	77
16	Results on the 18 t/h boiler operation in S.C. Vrancart S.A.	L. Mihăescu, I. Pîşă, I. Oprea, G. Negreanu, A. Adam, C. Mândrean, I. Bărbieru, R. Rusu, R.Sava	83
17	Research and experimental analyses concerning the increase efficiency of solid biomass combustion in hydrogen jet	L. Mihăescu, Gh. Lăzăroiu, I. Pîşă, E. Pop, G. Negreanu,	87
18	Theoretical analysis of impact of the solid biomass combustion in hydrogen jet in developing new innovative technologies	L. Mihăescu, T. Prisecaru, Gh. Lăzăroiu, I. Pîşă, E. Pop, G. Negreanu, M.E. Georgescu, V. Berbece, M. Prisecaru	91

19	The experimental analysis on the influence of air filter, oil filter and oil on the performance of the internal combustion engine	M. D. Muscalagiu, Al.M. Dima, C. G. Muscalagiu	95
20	Design conception of a pilot burner that simulates the retrofitted burners from CHP Işalniţa	G. Negreanu, L. Mihăescu, I. Pîşă, I. Oprea, V. Berbece, A. Adam, C. Mândrean, I. Bărbieru, V. Gherghina, Al. Moga	101
21	Thermal power plant for energy willow use: design, performances	G. Negreanu, V. Berbece, L. Mihăescu, I. Oprea, I. Pîşă, D. Andreescu	105
22	The analysis of the dynamics of vegetable oils burning in power plants	B. Niculescu	109
23	Efficient use of natural gas for a medium size district heating system	I.Oprea, G. Negreanu, V. Berbece, I. Pîşă, L. Mihăescu	113
24	Pollutant emissions of a heat treating furnace	D. Pană, I. V. Ion	119
25	Hydraulic fracturing in the United States of America	D. Parascin	125
26	The effects of dimensions of combustion chamber on the heat transfer process in CFB boilers	W. Pospolita, K. Jesionek, A.Wierciak, I. Iliev	131
27	Performance analysis of a hybrid water and air solar collector with rectangular fins	Q. A. Abed, V. Badescu, I. Soriga	137
28	Cogeneration system modeling for isolated buildings	B. Radu, Al. Racovitză	141
29	Very high gas temperature turboengine	C. Sandu, I. Vladucă, B. Sacuiu, D. Amariutei, R. Cârlănescu, R. Bimbasa	145
30	Practical psychomanagerial application in order to build a behavioral holistic model of eco-awareness based on order psychology-quantum psychology® (POPQ®)	C. Sofronie, R. Zubcov	151
31	Study on combustion efficiency, technology, main factors and corrosive chemicals for the furnace	A.G. Ştefan, T. Prisecaru	157
32	Study of the PV modules inclination angle on the energy production	A. Terziev, V. Kamburova, I. Iliev, K. Mavrov, D. Deltchev	163
33	Development and testing of a solution for NOx emission reduction based on the SNCR process for high capacity steam generators	Z. Teuber, I. Bolma	169
34	Analysis on the combustion dynamics of the straw briquettes for boilers with mobile grate	M. Toader	175
35	Comfort in passive house – an adaptive approach	I. Udrea,, I. Nastase,, R. Crutescu, C. Croitoru, V. Badescu	179

SECTION 2 : BYOTECHNICAL SYSTEMS, RENEWABLE ENERGY AND RURAL DEVELOPMENT

Nr. crt	Paper	Authors	Page
1	Determination permeability of transparent covers for solar collectors	D. G. Atanasov, M. S. Minchev, A. I. Tashev	183
2	Research on valuable recovery of oil from grape seeds	S.Șt. Biriș, C.I. Covaliu, G. Paraschiv, V. Vlăduț, A. Atanasov	187
3	Elimination of parasitic weed seeds from the mass of seeds of agricultural crops through wet magnetic separation	V. G. Ciobanu, A. Paun	193
4	Influence of cinematic regime and quantity of material on efficiency of sifting process	G.Al. Constantin, Gh. Voicu, M.E. Ştefan	199
5	Heavy metals removal from wastewater using magnetic nanomaterials based adsorption strategies	C.I. Covaliu, G. Paraschiv, S.Șt. Biriș, E. Matei, I. Filip, M. Ionescu	205
6	Structural analysis of the reciprocating rod in the driving mechanism of the mas-220 machine	A.D. David, E. Maican, Gh. Voicu, M.F. Duţu	209
7	The common agricultural policy in the European Union and Romania: past, present and future	O. David, S. Maiduc (Osiceanu)	215
8	The influence of heavy metals on biogas production during the anaerobic digestion process	M. Dincă, G. Moiceanu, G. Paraschiv, Gh. Voicu, N. Ungureanu, L. Toma, M. Ionescu	219
9	Mathematical modeling of vertical oscillation of a tractor for a model with four degrees of freedom when traveling on an agricultural land and an unpaved road	M.F. Duţu, G. Simion, I. Duţa, A.D. David, S. Osiceanu (Maiduc)	225
10	Antimicrobial action of some essential oils from indigenous flora against fungal contaminants in food	M. Ferdes, A. Pruteanu	231
11	Convection dryers with increased energy independence	I. C. Gîrleanu, Gh. Sovăială, G. Matache	237
12	Parameters influencing the screw pressing process of oilseed materials	M. Ionescu, Gh. Voicu, S.-Şt. Biriş C. Covaliu, M. Dincă, N. Ungureanu	243
13	Micro greenhouse climate management based on the Arduino	G. Ipate, Gh. Voicu, E. M. Stefan, N. Ungureanu, C. Nutescu	249
14	The use of electric field for pollutant removal from contaminated soils	I.A. Istrate, T. M. Oprea	255
15	Current state of fuel cells and hydrogen for European road transport sector	E. Maican	261
16	The potential of biomass from agricultural activities available for energy purposes	Gr. Marian, Al. Muntean, A. Gudîma, A. Pavlenco	267
17	Biogas, the future of modern society	G. Moiceanu, M. Dincă, G. Paraschiv, Gh. Voicu, M. Chiţoiu	273
18	Experimental research regarding chamomile inflorescences mechanized harvesting process	A. Muscalu, A. Pruteanu, L. David	279
19	Research on optimization of parameters of plows with variable working width	C. Nuţescu	285
20	The shredding of soft-textured food materials by means of unheated metal wire cutting	C. Olaru, V. Nedeff, M. Panainte - Lehăduș, I. Olaru, E. Ciobanu	291

21	Efficiently extraction of bioactive compounds from medicinal plants using organic and sustainable techniques	A. Pruteanu, A. Muscalu, M. Ferdes	297
22	Results from implementation of energy saving measures in the educational buildings of university of food technologies. Block 4	V. Rasheva, N. Kalojanov, S. Tasheva, M. Minchev, G. Valtchev	303
23	Characterization of rainfall with rainfall indices in the city of Bucharest in (2009-2012)	C. O. Rusănescu	307
24	Lagoon systems for extensive wastewater treatment plants from the rural agglomerations	V.V. Safta, M. Dincă, G.A. Constantin, A. Boureci	311
25	HACCP approach to pastry products	G.C. Simion, M. F. Duţu	317
26	Study on the specific energy consumption for drying blueberries in convective solar dryer	D. Stoev, A. Tashev, N. Penov	321
27	Special construction autonomous station for the dynamic monitoring of surface water quality indicators	C. Vîlcu, Gh. Voicu, G. Paraschiv, A. Petcu, A. Nedea	325
28	Experimental research on the determination of the lower calorific power of the Miscanthus briquettes compared with that of the sawdust briquettes	I. Voicea., Gh. Voicu, V. Vladut, G. Găgeanu, P Cârdei	331
29	The study of Miscanthus rhizomes distribution at the semiautomatic planters	Gh. Voicu, G. Paraschiv, P. Cârdei, M. Dincă, I..C. Poenaru	337

SECTION 3 :HYDRAULICS, PNEUMATICS, ELECTRONICS, MISCELLANEOUS

Nr. crt	Paper	Authors	Page
1	Biodegradability of hydraulic fluids	S. Anghel, A. I. Popescu, C. I. Garleanu	343
2	Study of optical fiber sensors regarding corrosion detection for building efficiency improvement	A. Badea, Fl. Dragan, L. Fara, P. Sterian	347
3	An innovative technique of car noise analysis based on multiresolution algorithms	L. M. Caligiuri, F. Lamonaca, A. Nastro, M. Vasile	353
4	Combined systems using renewable sources – a solution for increased energetic autonomy	C. Dumitrescu, H. Sundt, P. Drumea, L. Dumitrescu C. Cristescu	359
5	Analysis of charge transport in Dye-sensitized solar cells (DSSC) using a Monte Carlo simulation	C. Dumitru, Vl. Muscurel, L. Fara, P. Sterian	365
6	Hydrothermal treatment for the production of calcium phosphate biomaterials	D. Grimaldi, D. L. Carnì, F. Lamonaca, A. Nastro, M. Vasile	371
7	Medium and high pressure actuators pneumatic system	G. Matache, Gh. Sovaiala, R. Radoi, I. Pavel	377
8	Electro hydraulic system for speed control of a hydraulic motor using a PI controller	R. I. Rădoi, I. C. Duţu	383
9	Impact of noise and vibrations on the ship microclimate	K. Uzuneanu, I. V. Ion	387

OPPORTUNITIES, CHALLENGES AND FUTURE PROSPECTS OF USING BIOGAS AS ROAD TRANSPORT FUEL IN PAKISTAN

Fazal Um Min Allah[1]
University of Craiova

ABSTRACT

Fossil fuels are depleting and causing more global warming. To decrease dependency on fossil fuels we will analyze potential, possible outcomes and challenges of using biogas as road transport fuel in Pakistan. It has potential of producing biogas from animal, food and household waste by using anaerobic digestion process. We will analyze implications of distribution and economics scenarios of producing biogas and to compare it with existing natural gas usage. This paper aims to make recommendations and to draw a conclusion on the basis of studying existing practices regarding waste to wheel approach.

1. INTRODUCTION

For its energy needs, primarily, Pakistan is dependent on fossil fuels. It has to import fossil fuels to fulfill its energy demands. Main cause of environment pollution is usage of fossil fuels in Pakistan. To make itself less dependent on conventional energy resources, Pakistan should use renewable energy resources. Transport sector in Pakistan is heavily dependent on compressed natural gas (CNG). Due to the shortage of CNG transport sector has to face supply cuts for several days in a month. It will face even worse situation in the future. Prices for CNG fuel are also increasing as demand is growing. This demand can be fulfilled by alternative energy resource like biogas because country has the huge potential to produce it [5]. Biogas is being used as vehicle fuel in Sweden and its consumption is increased over the years. Number of filling stations for biogas is increased from 6 to 122. Biogas can also be used as fuel in modified diesel engines. This experiment is done in Ireland and it has reduced dependency on fossil fuels and caused 12% decrease in green house gas emissions. Main source for biogas production in UK is animal waste. To make it usable for engines, it should be upgraded to increase the percentage of methane. Studies show that by using biogas as transport fuel, GHG emissions can be reduced up to 200%. It's an environmental friendly fuel compared to other fossil fuels. As a fuel, biogas offers fewer prices than fossil fuels. Sweden, France and Switzerland are already using biogas fuel for road transport. UK has limited potential to replace natural gas with biogas as transport fuel but in Pakistan it can play a huge role as transport industry is heavily dependent on CNG [1-5]. This paper aims to evaluate opportunities, future prospects and challenges of using biogas as road transport fuel in Pakistan keeping in view the experience gained from its usage in developed countries.

2. METHODOLOGY

2.1. CNG status in Pakistan

In Pakistan CNG as vehicle fuel was introduced in 1982 and in 2010 it became world's largest CNG user in transport sector. Competitive price and government policies played an important role in growth of its consumption in transport sector. 89% of the registered vehicles

[1] Craiova, Str. Libertății, Căminul 3, Ap. 306, 0721737661, fazaluminallah@hotmail.com

are using CNG as transport fuel [6]. The demand has increased rapidly in past 10 years. The demand is increasing at average rate of 2% annually. Although Pakistan has good potential to produce natural gas but to meet the growing demand it has to import from its neighboring countries. Pakistan uses 8% of its natural gas production in transport sector. Comparison is shown in figure 1 between consumption of natural gas by different sectors.

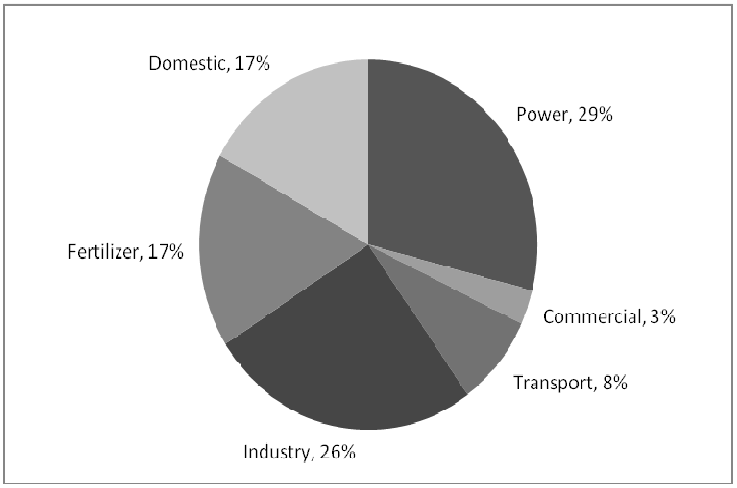

Figure 1: Natural gas consumption by sector in Pakistan 2011

Pakistan is facing following problems with the usage of CNG in transport sector.

1. Supply and demand gap is widening and government has to close CNG stations for three days in a week.
2. Government offers subsidy to the household natural gas users. Due to higher demand in transport sector officials have to cut the supplies for household customers.

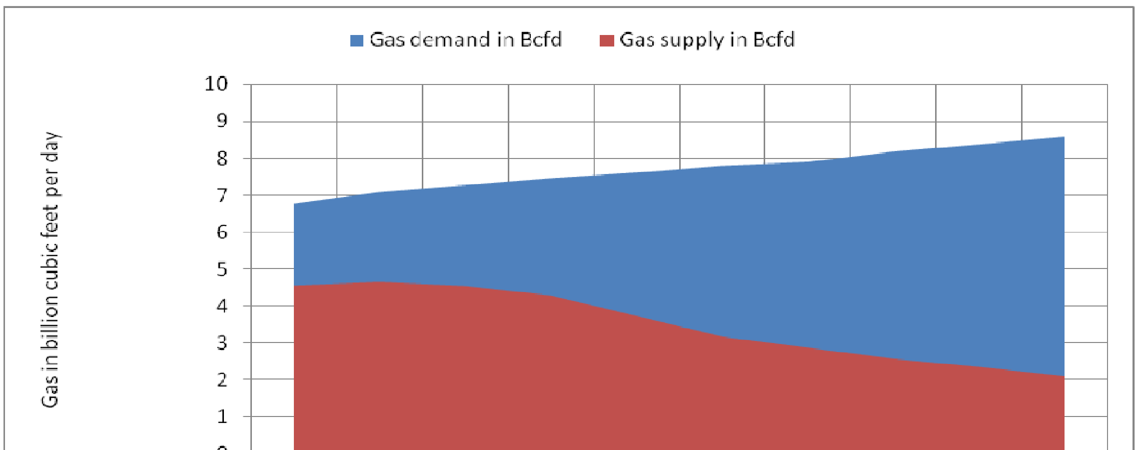

Year	2011	2012	2013	2014	2015	2016	2017	2018	2019	2020
Gas demand in Bcfd	6.77	7.09	7.27	7.46	7.61	7.8	7.9	8.18	8.38	8.58
Gas supply in Bcfd	4.55	4.64	4.54	4.28	3.73	3.17	2.87	2.57	2.35	2.11

Figure 2. Comparison between projected demand and supply of natural gas in Pakistan

3. The standards for CNG vehicle safety are not being followed and consequently CNG vehicles are facing more accidents every year.

2.2 Biogas Potential in Pakistan

Pakistan needs to focus on alternative resources to meet the energy demands of transport sector. Pakistan is an agricultural country and it has abundant biomass resources in the form of waste from food, animals and corps. There are 159 million animals whose manure can be used to produce biogas.

Table 1: Livestock sector strength

Species	2011-2012 (in Millions)	2012-2013 (in Millions)
Cattle	36.9	38.3
Buffalo	32.7	33.7
Sheep	28.4	28.8
Goat	63.1	64.9
Camels	1	1
Horses	0.4	0.4
Asses	4.8	4.9
Mules	0.2	0.2

Source: Pakistan economic survey 2012-2013

Livestock strength is growing annually by 4%. From the waste of these animals, 16.3 million m^3 of biogas can be obtained daily. Biogas can also be obtained from waste of paper and sugar industries, slaughter houses and household. Domestic biogas plants are already in use in different rural areas for cooking purposes. Fertilizer and sugar industries are already producing biogas from their waste to produce electricity. Biogas from these resources can be upgraded to be used as vehicle fuel.

2.3. Waste to wheel approach

Sewage sludge, agriculture waste, animal manure, food and household waste are used to produce biogas. Inorganic material will be separated from organic material. The shredding of the material will be done. Main process in production of biogas is anaerobic digestion. Waste material is degraded in the presence of bacteria in airtight vessel. Biogas is obtained from digesters and then upgraded to use it as vehicle fuel. Carbon dioxide, hydrogen sulphide, ammonia and water contents have to be removed to get 95-98% methane by volume.
Upgraded biogas can be stored in the form of CNG or liquefied form. Methane number and Wobbe index are important parameters to determine quality of gas. Cars can use bi-fuel system or can be designed to operate on single fuel system with CNG. In Pakistan, most of the vehicles are using CNG as fuel and it has already a distribution network for CNG.

2.4 Economics of Biogas

Following elements affect the biogas economics.

1. Manufacturing and production cost of biogas
2. Storage and distribution cost related to biogas
3. Governmental Taxes

Usage of biogas as road transport fuel proved to be more expensive in France and Sweden. Infrastructure, maintenance costs are similar to that of CNG. Vehicles using CNG as fuel are more expensive than other vehicles.

2.5. Comparison between natural gas and biogas

Natural gas and biogas both consist of methane. Composition of biogas depends upon the nature of resource and process from which it is obtained. Major difference is that biogas has less CO_2 emissions than natural gas.

Table 2 Properties of biogas and natural gas [7]

Property	Biogas	Natural Gas
Density (kg/Nm^3)	1.2	0.83
Wobbe Index, upper	27	55
Methane number	>135	72
Hydrogen sulphide (Parts per million)	<500	3
Calorific value ($MJ/\ Nm^3$)	35	0.9
Carbon dioxide (% volume)	30-40	-
Nitrogen (% volume)	0.2	0.3
Oxygen (% volume)	0	0
Ammonia (Parts per million)	100	0

Biogas is a renewable fuel which helps to reduce carbon emissions. It also helps us to be independent of fossil fuels especially oil which results in better energy security. Both waste management and energy production can be obtained by biogas usage. Less exhaust emissions help to improve air quality.

3. CONCLUSIONS

The aim of the paper was to determine the opportunities and future prospects of the usage of biogas in transport sector of Pakistan. Currently, Pakistan is facing CNG shortage and to overcome this it has to look for alternative solutions. Pakistan has huge potential to produce biogas from waste and it can be used as vehicle fuel. It already has storage and distribution system. Production of biogas is not as cost efficient as CNG but it is more environmental friendly. In order to achieve biogas production targets, policy makers and government institutions have to play their role.

References

[1] Mirza U., Ahmad N., Harijan K., Majeed T., *Identifying and addressing barriers to renewable energy development in Pakistan.* s.l. : Renewable and Sustainable Energy Reviews 927–931, 2009, Vol. 13 .

[2] Munawar A., *Energy and renewable energy scenario of Pakistan.* s.l. : Renewable and Sustainable Energy Reviews 354–363, 2010, Vol. 14 .

[3] Olsson L., Fallde M., *Waste(d) potential: a socio-technical analysis of biogas production and use in Sweden.* s.l. : Journal of Cleaner Production 1-9, 2014,

[4] Makareviciene V., Sendzikiene E., Pukalskas S., Rimkus A., Vegneris R., *Performance and emission characteristics of biogas used in diesel engine operation.* s.l. : Energy Conversion and Management 224-233, 2013, Vol. 75.

[5] Murphy J.D., McCarthy K., *The optimal production of biogas for use as a transport fuel in Ireland.* s.l. : Renewable Energy 2111-2127, 2005, Vol. 30.

[6] Khan M., Tabassum Y., *Development of natural gas as a vehicular fuel in Pakistan: Issues and prospects.* s.l. : Journal of Natural Gas Science and Engineering 99-109, 2014, Vol. 17.

[7] Eriksson O., Environmental Technology Assessment of Natural Gas Compared to Biogas, Natural Gas, Primoz Potocnik (Ed.), (2010). ISBN: 978-953-307-112-1

PRIMARY RESOURCES OF ENERGY

Marin BICĂ[a] , Marius Sorin SOFRONIE[b]
Corina DanaCERNĂIANU[c], Daniel MUSCALAGIU[d]
[1]University of Craiova, Faculty of Mechanics, Calea Bucuresti,107, Romania
[a] marinbica52@gmail.com, [b]sofronie@yahoo.com, [c]cernaiananu_corina@yahoo.com
[d]daniel_muscalagiu@yahoo.com

ABSTRACT

The paper presented is a bibliographical study of primary energy resources and global trends in this area. The increase of the oil prices caused a special attention to the burning installation of solid fuels and the production of energy from renewable sources. The use of solid fuels in power plants is treated with interest by all countries.

1. STATISTICAL ANALYSIS

.

Statistics shows a decrease of the petroleum resources which require specialists to rethink the production of electricity using solid fuels and unconventional energy. At present, over 80 per cent of primary energy consumed worldwide is obtained from fossil fuels. In the last decade, the increase in world energy consumption was based, at the rate of 85% by fossil fuels. The estimates of future energy consumption on current policies and developments indicate a continuation of this dependence to this type of fuel. These trends are not compatible with the necessity to attenuate the effects of climate change and can lead to an increase in the average temperature of the globe with 3 or 4 degrees Celsius, according to the International Energy Agency (IEA) and, respectively, a report commissioned by the World Bank.

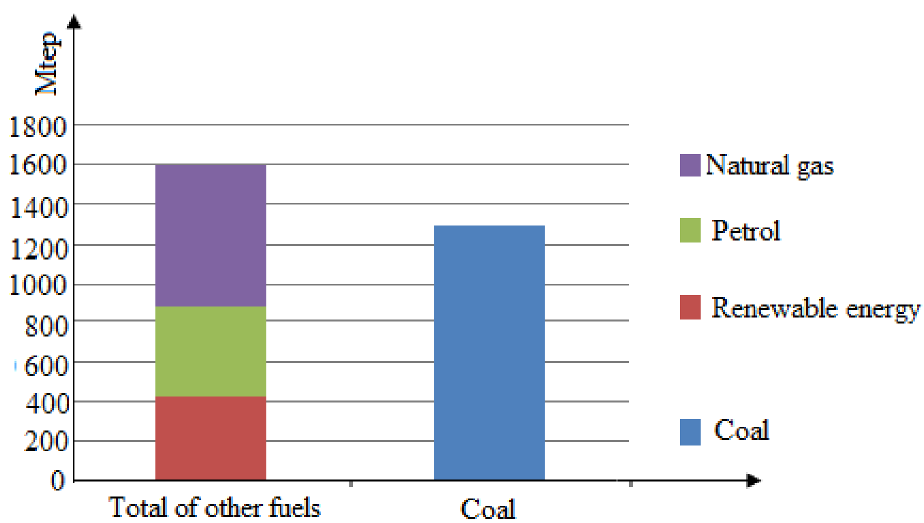

Figure 1: The increase of global demand in fuels 2001-2011

If the prices are compared the coal has a net advantage over the natural gases. In these conditions the coal is reconsidered as a raw material for the production of electricity. As a result, coal power plants are being retooled to be brought up to current standards on emissions of polluting gases and particles into the atmosphere. The carbon dependence increases, CO_2 emissions are increasing being necessary technical solutions that contribute to reducing the global warming effect. Emissions policies during the crisis have resulted in increasing the number of remaining unused, 955 million in 2012, with the upward trend to about 2 billion. It causes a drop in the price of coal which becomes attractive in economic terms with the negative consequences of the pollution. Each country in the EU will ensure the production of coal for power plants at the rate of about 73%. Coal is used mainly in Europe for the production of electricity. Overall, the consumption of lignite and hard coal in the EU increased to 712.8 Mt in 2010 at 753.2Mt in 2011, representing around 16% of the total consumption of energy. Although the share of coal in electricity production to the EU dropped slowly until 2010 (when he reached about 25%), in the fallowing year began to increase again, as described above.

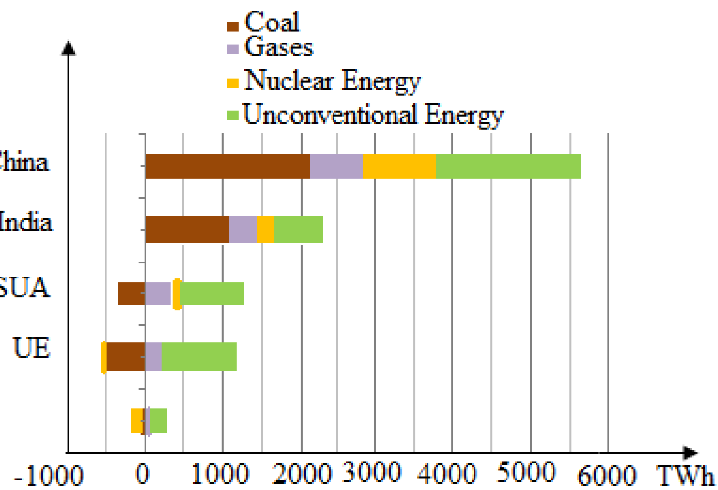

Figure 2: The changes in the production of electric energy in some parts of the world 2010-2035

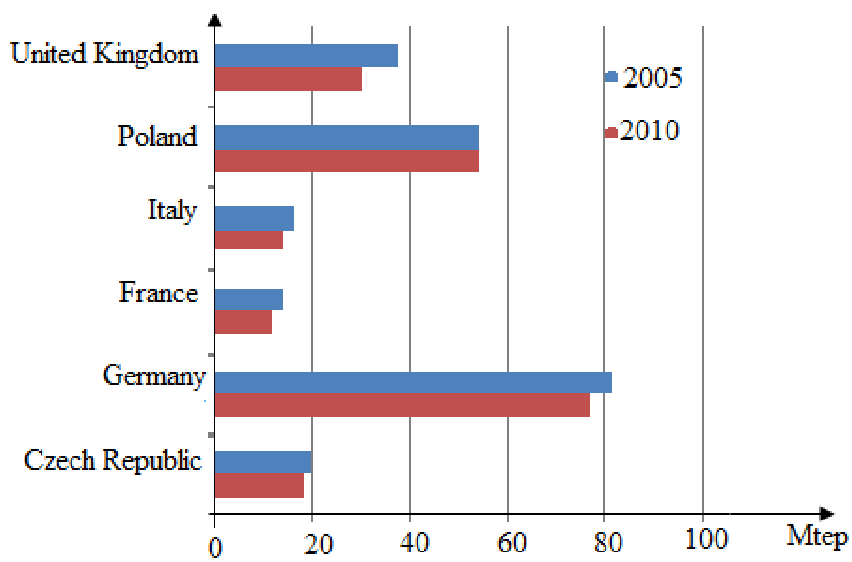

Figure 3: The main consumers of coal in UE in 2010

In Europe there are significant regional differences. While the share of coal in energy production in some member states (for example, Sweden, France, Spain and Italy) are well below 20%, other member states such as Poland (88%), Greece (56%), Czech Republic (56%), Denmark (49%), Bulgaria (49%), Germany (42%) and the United Kingdom (28%), is based largely on coal. The yield increase in combustion plants necessitated the design of new processes, particularly in the case of coal. The fluidized bed combustion has proved his efficiency and with small amounts of particulate matter. For high-capacity energy installations the burning of solid fuels is realized in pulverized state.

2. PRIMARY ENERGY RESOURCES

The deficit of primary energy in the global energy balance has imposed the burning of solid waste resulting from industrial or technological processes in agriculture. The main types of waste that can be used for energy purposes or for heating can be categorized as follows:

- *Combustible wood waste*. These waste results from the exploitation of forestry, different kind of sawmill and furniture. They are used in particular for heating of houses in the countryside while being a source of fires:

- *Combustible vegetal waste*. Are obtained from the processing of plants grown from what is called big culture: straw, corn cob, remnants of sunflower, waste from the processing of sugar cane. These wastes have a high moisture content (40 ...60) %. If the temperature in the heating stove is high at the burn of straws occurs large desposits on the surfaces of heat exchangers. Burning the vegetal waste must be avoided on crop fields for several reasons:

- the air pollution due to the resulted smoke
- the impoverishment of the soil in-organic matter;
- earthworms and other soil creatures are destroyed
- the water is evaporated from the upper layer of the soil and through cracks resulted the depth water is lost.
- the arable land is harder to cultivate and the fuel consumption increases.

- *Waste from the industry*. These materials come from hemp, flax, cotton and leather. It has been observed from these wastes special problems regarding burning due to diffusion of oxygen on difficult surfaces.

- *Combustible waste from chemical processes*. These are obtained from the processing of crude oil in order to obtain superior fuel.

- petroleum coke characterized by low volatile matter and moisture. The absence of volatile materials generates problems to ignition.

- celolignina is a powdery waste obtained from the extraction of furfulol from vegetal products (seed husks, corn). These waste have a good behavior in burning but the ash has tendency of slug and the burning gases contain compounds that adheres to the heat exchange surfaces.

- *Household waste*. These waste results in significant quantities, especially in the city. The preparation for burning often involves briquetting and selecting on categories of materials (paper, plastics, e.g.). They have a high content of ash with characteristics very different due to varied composition of these types of wastes.

Negative impacts on the environment should not be attributed only to fuel-burning process. As well as these other polluting industries are radioactive materials, other non-metallic substances, minerals and rocks. The exploitation of non-renewable or renewable resources or lead to unpredictable developments with consequences difficult to removed.

The highest consumption of primary energy resource is recorded from coal. In 2011, the highest coal consumption was registered in China-1,839 billion tons of oil equivalent (tons), USA-501.9 million toe and India-295.6 million tons. In the European Union consumption was 285,9 million tons and represented 7.7% of world consumption.

Table 1: Production of coal in the world

Operation expressed in thousands of tones						
Nr.	Country	1970	1980	1990	2000	2004
1.	Germany	406.034	387.930	356.524	167.724	181.926
2.	USA	5.963	42.300	82.608	77.620	75.750
3.	Greece	8.703	23.207	49.909	63.948	71.237
4.	Russia	128.100	141.500	138.500	86.200	70.300
5.	Australia	25.648	32.895	47.725	67.363	66.343
6.	Poland	36.118	36.866	67.584	59.505	61.198
7.	China	16.960	26.288	44.520	42.774	50.000
8.	Czech Republic	84.894	90.145	80.205	51.063	48.290
9.	Turkey	4.400	16.967	46.892	61.315	43.754
10.	Serbia	18.341	27.921	45.376	34.037	35.620
11.	India	3.908	4.548	14.110	22.947	30.341
12.	Romania	15.575	28.128	34.897	26.882	28.648
13.	Bulgaria	31.806	29.946	31.532	26.183	26.455
14.	Thailand	441	1.427	12.421	17.714	20.060
15.	Hungary	26.102	22.636	15.842	13.532	12.730
16.	Canada	3.919	5.971	9.407	11.190	11.600
17.	Bosnia	7.340	11.174	18.160	7.441	9.000
18.	Macedonia	4.940	7.519	6.640	7.516	8.500
19.	Spain	3.121	15.390	20.870	8.524	8.147
20.	North Korea	5.700	10.000	12.500	6.500	6.500
21.	Austria	4.045	2.865	2.448	1.255	235
...	World	869.626	1.080.335	1.153.970	877.417	915.789

Table 2: The classification of coal in Romania

Class	Group
Peat	-
Brown coal	Brown coal earthy
	Brown coal woody Lignite
	Mat Brown coal
	Brown coal with gloss
Brown coal	-
Coal (H)	Coal with long flame
	Coal gas
	Fat coal
	Coal coke
	Coal lean
	Anthracite coal
Anthracite	-

3. OBJECTIVES

The general objectives of the researches in energy resources consist in:

- research on the physical properties of the fuels and energy characteristics;
- research on the processes of combustion and flame propagation;

In addition to the objectives mentioned the aim is to develop and implement an experimental base to meet the requirements imposed by the regulations in the field of combustion of solid fuels. Given the new european approach, which imposes stringent rules on emissions of pollutants is necessary the modification of the conception regarding the design, verification and monitoring in exploitation of energy and combustion installations of low power. At the same time, the paper proposes the realization of analyses of the cases when fire are generated, the propagation mode, the thermodynamic study, considering the blaze as a complex process of combustion, with indeterminate growth, and other phenomena including physical, chemical, biological (heat transfer, the exchange of gases with the environment, the formation of flames, structural transformations). The energy sector, which uses solid fuel, has to be a dynamic sector, actively to support the economic development of the country, for the purpose of reducing gaps regarding the European Union.

In this way, the general objective of the energy sector is to meet the energy needs both in present and for medium term and long at a low price appropriate to a modern market economy and a standard of civilized life, in terms of quality, food safety, while respecting the principles of sustainable development.

The main direction of action of energy policy of Romania converging with those of the European Union’s energy policy is:

- the increase of safety in energy supply.
- the increase of energy efficiency.

- the achievement of the objectives of protecting the environment and reducing CO_2 emissions;

Considering these main directions of action, the objectives of the development of the energy sector in Romania, are:

- the improvement of energy efficiency throughout the production chain:-resources-transport-distribution-consumption;
- reducing the negative impact of the energy sector on the environment.

4. SPECIFIC MEASURES IN THE FIELD OF ENERGY

The energy production will follow a process of restructuring and renewal of energy capacities through the rehabilitation of existing viable units, closing non-viable units and the construction of new production capacities. The investment effort will be supported mainly by privatization.

In order to ensure balanced energy productions, priority will be given to investments in units of energy production that uses:

- renewable sources of energy;
- charcoal by clean technologies;
- nuclear energy technologies through secure and with low environmental impact.
- the use of wood for heating in households;
- use plant debris.

5. CONCLUSION

Research conducted in the field of production, transport and consumption of energy are focused on new energy sources, renewable sources, reducing the quantities of triatomic gases emitted into the atmosphere. The development of energy consumption determined the return to the production of coal-based energy.

References

[1] Comisia europeana pentru energie, Bruxelles 2013.
[2] Eurostat, Comisia Europeană.
[3] AIE, World Energy Outlook 2012.
[4] Barbu, I. ş.a. A doua tinereţe a cărbunilor, Editura Albatros, Bucureşti, 1986.
[5] Bejan M., Rusu T. (2007), O sursa de energie regenerabila – biogazul din deşeurile organice, Buletin AGIR nr. 1, ianuarie-martie, pp. 13-19.

EXPERIMENTAL RESEARCH ON THE COMBUSTION OF THE GASES IN LOW-POWER BURNERS

Marin BICĂ[a], Marius Sorin SOFRONIE[b],
Corina Dana CERNĂIANU[c], Daniel MUSCALAGIU[d]
[1]University of Craiova, Faculty of Mechanics, Calea Bucuresti,107, Romania
[a] marinbica52@gmail.com, [b]sofronie@yahoo.com, [c]cernaianu_corina@yahoo.com
[d]daniel_muscalagiu@yahoo.com

ABSTRACT

Gaseous fuels have a physical-chemical characteristic, which recommends them for use in medical applications, research labs, but also in the industrial field. The present paper aims to highlight the advantages of using gaseous fuels, especially in small power plants, but also issues which arise with regard to the burning with stable flame. We propose to analyze burners used in low-power applications with the possibility to ease the ignition and stabilizing combustion. Gases used in combustion plants have chemical compositions specific to each area, which involves different burning speeds and propagation of the flame. Adjusting these installations must be made in such a way to not cause the interruption of the flame.

1. PHYSICAL-CHEMICAL CHARACTERISTICS OF GASEOUS FUELS

The composition of these fuels is different from area to area. In all situations they contain combustible gases, nitrogen and oxygen in small or very small proportion and other gases. In Romania methane (CH_4), is found in higher proportion in the composition of combustible gas. The composition of a fuel gas is expressed in percentages and is reported to the anhydrous state:

$$CO^{anh} + CO_2^{anh} + H_2^{anh} + H_2S^{anh} + CH_4^{anh} + \Sigma C_mH_n^{anh} + O_2^{anh} + N_2^{anh} + ... = 100\% \qquad (1)$$

In combustion plants the gaseous fuel is used to the flow through the pipeline. The calculation of the burn is made at wet condition, written in the form:

$$CO^i + CO_2^i + H_2^i + H_2S^i + CH_4^i + \Sigma C_mH_n^i + O_2^i + N_2^i + w_t^i + ... = 100\% \qquad (2)$$

In table 1 is presented the composition of the oil gas in Romania.

Table 1: The composition of the oil gas

Name of the gas	Composition in (%) of volume						
	Methane CH_4	Ethan C_2H_6	Propane C_3H_8	Butane C_4H_{10}	Pentane C_5H_{12}	Hexane C_6H14	Dioxide of carbon CO_2
Rich gas of Boldeşti – Prahova	78	9,24	6,23	3,46	1,10	1,77	0,20
Poor gas of Moreni – Gura Ocniţei	95,93	1,19	1,35	0,73	0,46	0,34	-
Poor gas of Măneşti – Vlădeni	99,80	-	-	-	-	-	0,20
Poor gas of Ariceşti	95	2	-	-	-	-	3

In general, saturated gases contain methane in the highest proportion, but other combustible and inert gases. There are situations when they contain water vapor with concentration below saturation temperature appropriate for use. In Romania, the Transylvania basins are the most important for their composition to the petrochemical industry. Table 2 shows the composition of these deposits.

Table 2: The composition of the deposits in Transylvania

Basin	CH_4	C_2H_6	C_3H_8	C_4H_{10}	C_5+	Other compounds
Transylvan basin 1	99,92	0,06	0,02	-	-	-
Transylvan basin 2	99,72	0,08	0,02	-	-	0,18
Transylvan basin 2	99,57	0,06	0,06	-	-	0,20
Subcarpatic zone	95,26	0,79	0,79	0,53	1,69	-

From the table is observed that natural gases from Transylvania have a special purity.
For industrial use, of interest are some properties showed in table 3.

Table 3: The gas properties from Transylvania

Zone	Density ρ (kg/m^{3}N)	Relative Density δ	CH_4			C_2H_6			Caloric power			
									sup.		inf.	
			% volume	% Weight	g/m^{3}N	% volume	% Weight	g/m^{3}N	Mj/m^{3}N	Kcal/m^{3}N	Mj/m^{3}N	Kcal/m^{3}N
Copșa Mică	0,718	0,556	99,60	99,25	713	0,40	0,75	5	39,69	9480	35,69	8525
Noul Săslac	0,719	0,556	99,55	99,16	713	0,45	0,84	6	39,69	9480	35,71	8530
Bazna	0,721	0,558	99,16	98,44	710	0,84	1,56	11	39,82	9510	35,82	8555
Șincai	0,719	0,556	99,50	99,03	712	0,50	0,97	7	39,71	5485	35,73	8535
Saraș	0,721	0,557	99,25	98,60	711	0,75	1,40	10	39,79	9505	35,80	8550
Boguța de Mureș	0,719	0,556	99,45	99,03	712	0,55	0,97	7	39,73	9490	35,73	8535

From the experimental research on the burner described in Figure 1, the measurements being carried out with a thermo anemometer type Kimo shows that the burning speed for a normal flame becomes constant at a given temperature of the combustion gases. It was found that the temperature of the combustion gases increases in a transitional regime by order of seconds (from laboratory determinations about 30 seconds)

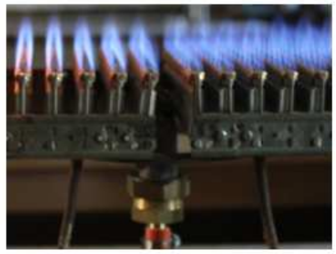

Figure 1: The burner used tor experimental determination

Table 4: The limits of ignition

Fuel	Symbol	The minimum concentration of ignition [%] volume of gas in oxygen		Stoichiometric blend		Blend in which the speed of the flame is maximum		The minimum concentration of ignition [%] volume of gas in oxygen	
		min	max	[%] vol. gas	u_n [cm/s]	[%] vol. gas	u_n max, [cm/s]	min	max
Hydrogen	H_2	4	74.2	29.5	160	42	267	4.65	93.9
Carbon oxide	CO	12.5	74.2	29.5	30	43	42	15.5	93.9
Methane	CH_4	5	15	9.5	28	10.5	37	5.4	59.2
Ethan	C_2H_6	3.22	12.45	5.64	-	6.3	40	4.1	50.5
Propane	C_3H_8	2.37	9.5	4.02	-	4.3	38	2.3	55
Butane	C_4H_{10}	1.86	8.41	3.12	-	3.3	37	1.8	49
Pentane	C_5H_{12}	1.4	7.8	2.55	-	2.92	38.5	-	-
Hexane	C_6H_{14}	1.25	6.9	2.16	-	2.52	38.5	-	-
Heptane	C_7H_{16}	1.00	6.0	1.87	-	-	-	-	-
Octane	C_8H_{18}	0.95	-	1.65	-	-	-	-	-
Ethylene	C_2H_4	3.75	29.6	6.5	50	7	63	2.9	79.9
Acetylene	C_2H_2	2.5	80	7.7	100	10	135	3.5	89.4
Benzene	C_6H_6	1.41	6.75	2.71	-	3.34	40.7	2.6	30
Methyl alcohol	CH_3OH	6.72	36.5	12.44	-	-	-	-	-
Ethyl Alcohol	C_2H_5OH	3.28	18.95	6.52	-	-	-	-	-
Carbon sulphur	CS	1.25	50	6.52	-	8.2	48.5	-	-
Water gas		6.0	70	-	-	-	-	-	-
Coke gas		5.6	28-30.8	-	-	-	-	-	-
Natural gas		5.1	12.1-25	-	-	-	-	-	-
Furnace gas		35	65-73.9	-	-	-	-	-	-

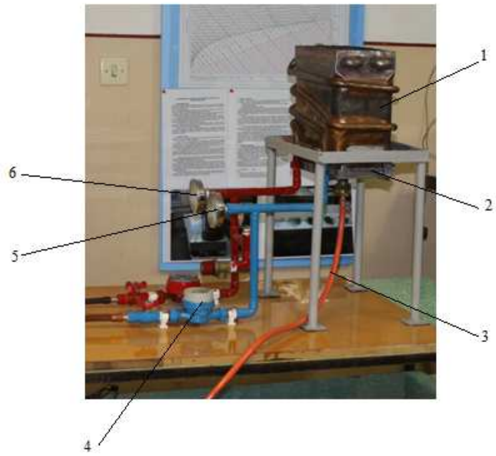

1-heat exchanger; 2- gas burner; 3- special hose for gases; 4-water debit meter; 5-thermometer for the measurement of cold water; 6- thermometer for the measurement of hot water.
Figure.2. Stand with heat exchanger for burner testing

2. DETERMINATION OF THE BURNER PERFORMANCE

The tests performed in the laboratory were intended to determine the ability of a burner to burn gas fuel with stable flame. The tests were performed in the laboratory for Thermal Engineering of the Faculty of Mechanics at a temperature of 25 °C, atmospheric pressure of p_a=1013 mbar and relative humidity of φ= 50%. Were used 9 regimes at different loads. Modification of gas flow to the burner was made concurrently with the modification of the water flow in the heat exchanger used for water heating.

Table 5: The parameters of burning regimes (gas from the local network of distribution)

Nr.	V_{gas} [m^3] measured	V_{gas} [m^3] measured	V_{water} [m^3] measured	V_{water} [m^3] heated	t_{ai} [°C]	t_{ae} [°C]	τ minutes
1	11,683	0,043	131,190	0,006	26,1	72,2	3
	11,726		131,196				
2	11,777	0,045	131,203	0,007	25,2	64,3	3
	11,822		131,210				
3	11,841	0,045	131,220	0,008	25,5	55,4	3
	11,886		131,228				
4	12,008	0,046	131,244	0,009	25,3	51,4	3
	12,054		131,253				
5	12,098	0,045	131,263	0,01	25,6	48,5	3
	12,143		131,273				
6	12,218	0,046	131,291	0,0 12	25,2	44,3	3
	12,264		131,303				
7	12,319	0,046	131,318	0,014	25.4	41,4	3
	12,365		131,332				
8	12,422	0,046	131,350	0,017	25,1	38,2	3
	12,468		131,367				
9	12,500	0,045	131,379	0,019	24,6	35,5	3

The flame was stable during experimental determinations. The stand used is presented in figure 2. For the combustion process in the mixture must be a minimum concentration of oxygen and the temperature to be higher than the temperature of oxidation for the reaction to start. During the test these conditions are met because the burn is atmospheric and the temperature of the front flame measured is greater than that required to start combustion. For the flame to not interrupt the gas flow the speed of gas is adjusted in such a way that the gas flow velocity is equal to the speed of propagation of the flame front. The concentration limits of ignition for different gases are presented in table 4. The values refer to the atmospheric pressure and a temperature of 20 ° C. For the burner tested measurements were carried out for gases from the local network of distribution and gases obtained from a gas cylinder fueled at a station with GPL alimentation. For this type of burner, with multiple slits, used in low-power heating plants of family type shows a bigger yield to the burn of liquefied gas and this performance is due to the liquid gas qualities, the lack of impurities, and a higher calorific value.

Table 6: The parameters of burning regimes. Liquefied gas (Cylinder stove)

Nr.	V_{gas} [m^3] measured	V_{gas} [m^3] consumed	V_{water} [m^3] measured	V_{water} [m^3] heated	t_{ai} [^oC]	t_{ae} [^oC]	τ minutes
1	12.632	0,050	132,342	0,0082	21	68,2	3
	12.682		132,350				
2	12,720	0,052	133,411	0,007	22	72,3	3
	12,772		133,418				
3	12,775	0,053	133,622	0,006	23	75,1	3
	12,828		133,628				
4	12,311	0,047	133,802	0,006	21	67,4	3
	12,358		133,808				
5	12,911	0,043	133,902	0,0092	22	47,5	3
	12,954		133,9112				
6	12,962	0,046	133,950	0,0 11	22	51,2	3
	13,008		133,961				
7	13,121	0,048	133,982	0,012	21	49,3	3
	13,169		133.994				
8	13,172	0,051	134,012	0,013	22	43,6	3
	13,223		134.025				
9	13,228	0,049	134,500	0,007	23	58,7	3
	13,277		134,507				

The heat lost in the surrounding atmosphere has a significant share in the total efficiency of the installation. To limit these losses the inside of the heat exchanger was shielded.

Table 7: The parameters of burning regimes (gas from the local network of distribution)

Nr.	V_{gas} [m^3] measured	V_{gas} [m^3] consumed	V_{water} [m^3] measured	V_{water} [m^3] heated	t_{ai} [^oC]	t_{ae} [^oC]	τ minutes
1	13,412	0,062	134,600	0,008	22,5	72,2	3
	13,474		134,608				
2	13,480	0,065	134,700	0,0084	23,2	75,1	3
	13,545		134,784				

3	13,560	0,053	134,800	0,0086	24,1	71,4	3
	13,613		134,086				
4	13,650	0,059	134,900	0,0079	22,6	71,4	3
	13,709		134,9079				
5	13,750	0,062	134,910	0,009	23,2	69,2	3
	13,812		134,919				
6	13,815	0,054	134,920	0,011	22,4	62,5	3
	13,869		134,931				
7	13,870	0,063	134,940	0,012	21,3	57,3	3
	13,933		134,952				
8	13,950	0,055	134,960	0,013	23,2	52,4	3
	14,005		134,973				
9	14,010	0,058	134,980	0,007	23,4	73,2	3

Obtaining very good performance of this type of burner has been reduced by difficulties in adjusting the gas flows for a stable burn. The apparition of the lateral flame is explained by an uneven distribution of gas in the burner.

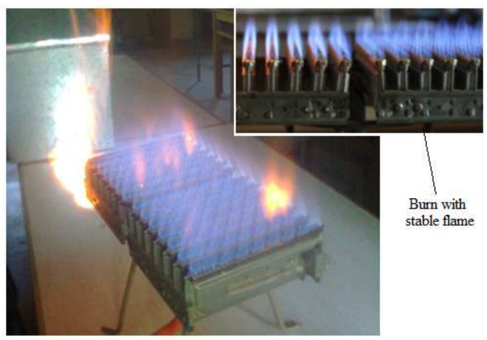

Figure 3 The apparition of the carburate flame and the interruption of the flame

At the increase of the flow the interruption trend appears to the flame. At the power installations for heating the gas flow is adjusting in combustion regimes. In the laboratory we forced the limits of normal combustion to obtain these undesirable regimes. From the observation of several power installations of low power results that each type has a predefined normal regimes, the adjustment being made automatically.

3. CONCLUSIONS

The combustion of gaseous fuels requires heightened security measures to prevent the extinguishment or interruption of the flame. The burner studied in laboratory has a good stability of the flame when is fueled with liquefied gas and the gas from distribution network.

References

[1] Alexandru, D., Nagi, M., *Utilizarea gazelor petroliere lichefiate in sisteme autonome* ISBN (10) 973-661-933-8, (13)978- 973-661-933-5, Mirton, Timisoara 2006
[2] Iordache, I., Mihăescu, L., *Cercetări privind lungimea flăcărilor difuzive de ardere a combustibililor gazoşi în jeturi libere turbulente cu secţiune dreptunghiulară,* A V-a Conferinţă Naţională de Echipament Termomecanic Clasic şi Nuclear şi Energetică Urbană şi Rurală,., Bucureşti, 2006, pp. 95-98.
[3] Stambuleanu, A., *Flacăra Industrială,* Editura Tehnică, Bucureşti, 1971.
[4] Bică,M., Nagi, M., Cernăianu, C.D., Bara, N., Transfer de căldură, Editura Universitaria, Craiova, 2011.

HEAT MEASURE UNIT FOR CETRALIZED HEAT SUPPLY OF DIRECT SUBSCRIBER STATIONS

Valentin Bobilov[1], Pencho Zlatev[1], Zhivko Kolev[1], Plamen Mushakov[1]
University of Ruse

ABSTRACT

This article provides an analysis of heat consumption of University of Ruse at different regimes of operation including work and holyday time and the increase of energy consumption as result of adding new energy efficient buildings. It was found that the temperature schedule of distribution network differs from standardized and established a possible reason for this discrepancy. Identification of possibilities to improve the accuracy of measuring of the heat energy consumption was done and proposed new scheme of central heat measuring unit. The new scheme of central heat measuring unit will make it possible to control the mixing ratio and to maintain adequate parameters of the heat transfer medium for the direct connection scheme

1. INTRODUCTION

Aim of this report is study the possibility of using direct heating substations in centralized district network at University of Ruse.

Changing the type of substations implies the compilation of statistics of the parameters of the heat carrier in the external heat transmission network under various operating conditions and ambient temperatures including both periods of full load of buildings and periods in which buildings are used only partially.

The report presents statistics on the thermal power in Ruse University for the past four heating seasons. Also has been analyzed heat consumption at University when connected to a distribution network of new buildings. An analysis of data from instrumentation and measures have been outlined for improving the accuracy when measuring the consumed thermal energy.

The heating of the university includes 20 separate buildings with a total heating area of 45607m^2. Campus has a heat transmission network in impassable collectors as individual buildings are connected differently. There are buildings in which heating is a direct and indirect type of such heating substations with fast water heaters and several new buildings with plate heat exchangers.

2. METHODOLOGY

2.1. Statistics of heat meter readings

Compile statistics of the meter readings cover a period of four years from the beginning of the heating season in 2010. By the end of the heating season in 2014, the total number of the data amounts to 377 as the period during which the measurements were performed is different. Weekdays measurements were performed every day at 09:00 am and at weekends Saturday and Sunday measurements were not performed, and then the amount of the energy consumed covers a period of three days from Friday to Monday at 9:00 am

Measurements of heat consumption are carried out in the beginning of the campus heat networks by using heat meter Kamstrup [1], which is a device for commercial accounting of the thermal energy and is owned by the University.

Besides readings of the consumed thermal energy measurements were carried out of the pressure and temperature of the heat carrier in the transmission network as well as meteorological data were collected on campus using a Davis Weather Station Model Vantage 2 Pro Plus

The main weather information is speed and wind direction, minimum, maximum and average daily temperature and quantity of solar energy on a horizontal surface.

The results with the ambient temperatures and the temperature of the heat carrier in transmission network are shown in Figure 1. for each heating season.

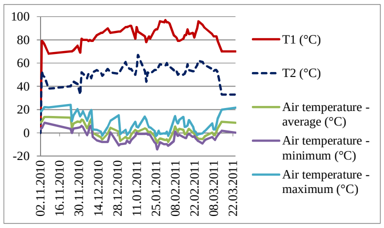

Heating season 2010/2011

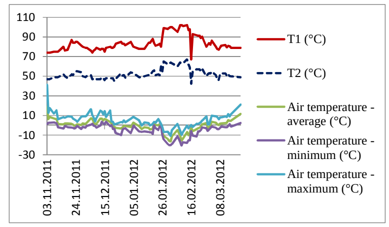

Heating season 2011/2012

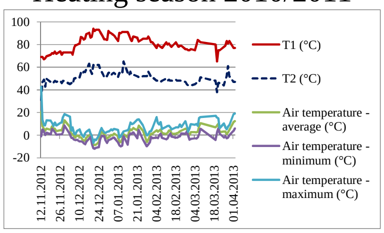

Heating season 2012/2013

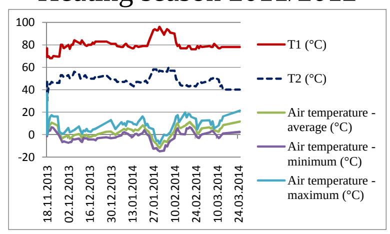

Heating season 2013/2014

Figure 1: Statistics of temperatures

In Figure 1 with T1 is represented heat carrier temperature in the supply pipe of the network and with T2 is represented the temperature of the return heat carrier pipe. Statistics of heat consumption over the last four years are shown in Figure 2.

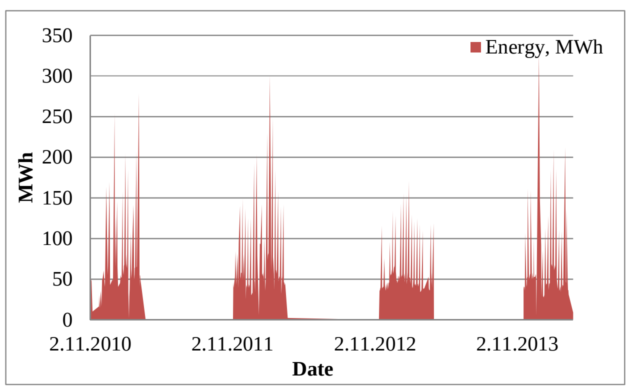

Figure 2: Statistics of energy consumption for heating

Summary data for the heat consumption during the last four heating seasons are presented in Table 1.

Table 1 Summary data for heating seasons

Heating season	Duration, Days	Energy for the period, MWh	Heating degree-days at 12.0°C
2010/2011	150	5017.3	1322.05
2011/2012	152	6508.5	1700.82
202/2013	151	5131.38	1242.52
2013/2014	145	5426.4	1130.45

2.2. Analysis of experimental data

From the data for the change in temperature of the heat carrier and the environment during the heating season is apparent that the temperature of the heat carrier in the supply heat pipeline varying from 70 ° C to 100 ° C depending on the climate outside temperature. The change in temperature of the heat carrier in the return pipeline varying from 40 °C to 70 °C.

Standardized scheduling of the heat carrier temperature in the district network for Ruse is 120 °/70 °C [2]. The change of the temperature of the hot heat transfer medium should be in the range from 120 ° C to 70 ° C depending on the climatic conditions and the change of the temperature of the cold heat transfer medium should be in the range from 70 ° C to 40 ° C.

Therefore, the temperature schedule of transmission network in the city does not meet the standard. Possible reason for this is outdated heat transmission network and in order to reduce accidents in the expansion joints is reduced medium temperature. Covering the heating load is done by increasing the volume flow of the heat transfer medium.

Heat consumed by the group of buildings is calculated by month and then is determined the average thermal power of the complex.

The average thermal power of the buildings as a function of the average temperature of the environment is shown in Figure 3

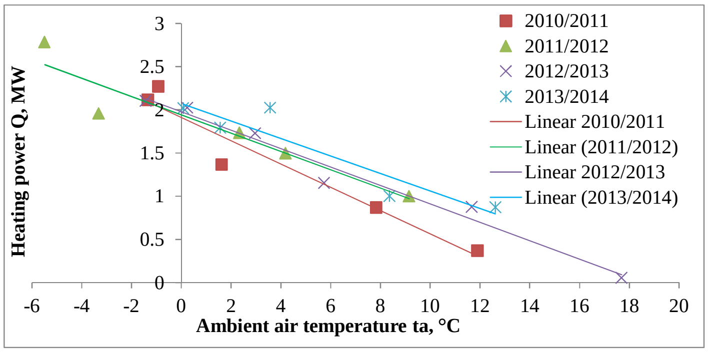

Figure 3 Average heating power

It has been done a regression analysis of the average thermal power of the buildings over the years. The regression equations are shown in Table 2.

The data shows that during the heating season 2011/2012 and in 2012/2013 slope of the straight line decreases due to the commissioning of the new building with high energy efficiency. During the heating season 2013/2014 was put into operation another such building as seen from the slope of the strait line.

Logically connection of new buildings to the district network leads to increased energy consumption. Dissipated the less heating degree-days during the heating season 2013/2014 compared to the previous season.

Table 2 Linear regression of heating power

Heating period	Equation	R-squared value
2010/2014	Q=-0.111*ta+1.9336	R^2=0.9254
2010/2011	Q=-0.1346*ta+1.9113	R^2=0.9365
2011/2012	Q=-0.1058*ta+1.9415	R^2=0.8947
2012/2013	Q=-0.1066*ta+1.9797	R^2=0.9752
2013/2014	Q=-0.101*ta+2.0726	R^2=0.8652

2.3. Identify possibilities to improve accuracy of measuring of the heat energy consumption

In some of the buildings attempts have been made using hybrid heating substations / combination of the direct and indirect substation/ and the results are optimistic.

The remaining heating substations are based on outdated indirect water heaters "pipe in pipe" or plate heat exchangers, Bulgarian production that are morally and physically outdated. Also in the most of substation is missing equipment and measurement systems.

Possible measures to improve the accuracy of the measured amount of heating energy are:

- Construction of a monitoring system which covers all buildings irrespective of the manner their connection to the district heating network;
- Installation of second flow meter in the heat measure unit at entrance of University district heating network and connecting of present heat meter and new flow meter with monitoring system;
- Reconstruction of old substations including replacement of the heating equipment and allows for connection of the building to the district heating network in direct scheme.

2.4. Scheme of centralized heat meter unit

The report proposes to reconstruct the heat meter unit at the entrance of the University district heating network to allow remote reading and eventually regulate the quantity of consumed heat when implementing direct substations for individual buildings.

The principle scheme of the proposed heat meter unit is shown in Figure 4.

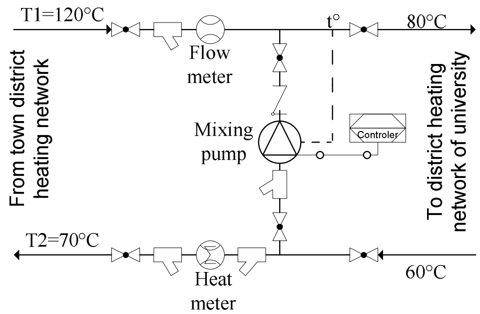

Figure 4 proposed scheme of heat meter unit

3. CONCLUSIONS

The proposed scheme of the heat meter unit for centralized supply of the direct heating substations provides an opportunity to its connection to the monitoring system and using the additional flow meter to display of emergency accident scenarios such as break in the system [3, 4].

Construction of the bypass connection with mixing pump will make it possible to control the mixing ratio and to maintain appropriate the parameters of the heat carrier for direct connection scheme of substations

The use of a direct scheme will achieve following advantages:

- Saving funds for reconstruction of old heating substations;
- Maintain the heat transfer medium temperature close to the designed for most of the buildings;
- achieving savings of electricity from substations circulating pumps;
- Operation of the heating system in the building even when power supply interruption.

References

[1] http://kamstrup.com/

[2] Nikolov, N. Regimes of heat consumption and regulation of the district heating systems. Technics, Sofia, Bulgaria, 1979 (in Bulgarian).

[3] Skriver, G. Smart heat metering with consumer related services - automatic functions in smart energy meters secure both consumer comfort and operation efficiency. International magazine on district geating and cooling “HOT/COOL”, DBDH, №4, 2012.

[4] Werner, B. 27 childcare institutions in the municipality of Odense protected from damage from leaks and seepage from the water and heating installations. International magazine on district geating and cooling “HOT/COOL”, DBDH, №1, 2013.

INCREASING THE ENERGY EFFICIENCY OF THERMAL POWER PLANT

Valentin Bobilov[1], Veselka Kamburova[2], Zhivko Kolev[1], Pencho Zlatev[1], Plamen Mushakov[1]
[1]Department of Thermotechnics, Hydraulics and Ecology,
University of Ruse, Ruse 7017, Bulgaria
[2]University of Ruse - Branch Razgrad, Razgrad 7200, Bulgaria

ABSTRACT

The purpose of the work is to analyze the activities taken to increase the energy efficiency of the Thermal Power Plant which is a part of the overall Sugar Plants facility located in the industrial zone of the city of Gorna Oriahovitsa, Bulgaria.

1. INTRODUCTION

The Thermal Power Plant (TPP) is a part of the overall Sugar Plants facility located in the industrial zone of the city of Gorna Oriahovitsa [2, 4, 5]. TPP has been constructed for the combined production of electric and thermal energy.

The thermal energy sent to the steam turbine installation has been divided in two components:

- thermal energy to consumers;
- thermal energy for electric energy production.

To increase the energy efficiency of TPP the following reconstructions have been carried out:

- one of the steam turbines has been replaced in the scheme;
- heat exchanger station in TPP has been built;
- heat supply system for overheated water steam has been replaced with such for hot water.

2. METHODOLOGY

2.1. DESCRIPTION AND ENERGY BALANCE OF TPP

The total area of the plant is 11,500 m^2. The TPP includes four steam boilers - two Russian made BKZ-75-39 boilers produced by the Barnaul boiler works, one PK–35-39 boiler and one KM-12 both of Bulgarian origin produced by the G. Kirkov boiler works in Sofia. The two BKZ-75-39 boilers and the PK–35-39 boiler are coal fired and the KM-12 boiler is heavy fuel oil fired.

The combined cycle has been realized with backpressure turbines. The technological structure of the TPP at Sugar Plants is centralized: all steam generators send steam to a single collector, which in its turn distributes it and sends it to the steam turbines.

Three independent branches of the heat supply system structurally form the steam transfer network of the company have served the main technologic capacities – the Sugar Refinery, the Ethanol Factory and the Confectionery Plant. The basic branch has been Branch №2, which has served the units TPP – Repair-Mechanical Works – Sugar Refinery –

[1] Department of Thermotechnics, Hydraulics and Ecology, University of Ruse, "Studentska" St., 7017 Ruse, Bulgaria, +359 82 888 304, zkolev@uni-ruse.bg

Administration (Company Management) – Greenhouse. This branch is subject to the present research. Branch №2 has been fed with heat carrier from collector 0.6 MPa of the TPP.

During 2004 (the last year before the made reconstructions) TPP has produced 236,571 tons of steam, which has been distributed as follows:

- steam from the TPP 160,218 tons;
- auxiliary needs of the TPP 76,353 tons;
- steam passed through turbines 207,678 tons;
- steam from steam reducing and cooling unit 28,893 tons.

The total heat production of TPP Sugar Plants for 2004 year has been177,507 MWh, which has been distributed for:

- electricity production 19,041 MWh;
- heating purposes of TPP and losses 32,790 MWh;
- consumers of heat energy 125,675 MWh.

The thermal energy balance of the TPP has been made in accordance with the structural equation 1 [1, 3].

$$Q_{TPP} = P_{EL} + P_{MT} + P_G + Q_{BPT} + Q_{RD} + Q_{pl} + \Delta Q_{SG}, \qquad (1)$$

where: Q_{TPP} is total thermal consumption of the power plant, MWh;

P_{EL} - produced electric energy from the generators, MWh;

P_{MT} - mechanical losses of the turbine, MWh;

P_G - generator losses, MWh;

Q_{BPT} - heat from the backpressure turbine;

Q_{RD} - heat from the steam pressure reducing device;

Q_{pl} - losses in pipelines;

ΔQ_{SG} - losses in the steam generator.

In the concrete case the components of equation (1) for 2004 had the following values:

Q_{TPP} = 177,507 MWh;

P_{EL} = 9,265 MWh;

$P_{MT} + P_G$ = 32,790 MWh;

$Q_{BPT} + Q_{RD}$ = 125,676 MWh;

ΔQ_{SG} = 52,675 MWh.

2.2. DESCRIPTION OF THE SYSTEM – AN OBJECT OF RESEARCH

In figure 1 a principal scheme of the system from TPP which has been an object of research is shown. As is shown in the principal scheme, the steam turbine 1 has worked with backpressure 8 ÷ 13 bar. In this case, the thermal energy required for heating, ventilation and domestic hot water (DHW) to the consumers included in the heat supply system Branch № 2 has been provided from overheated water steam.

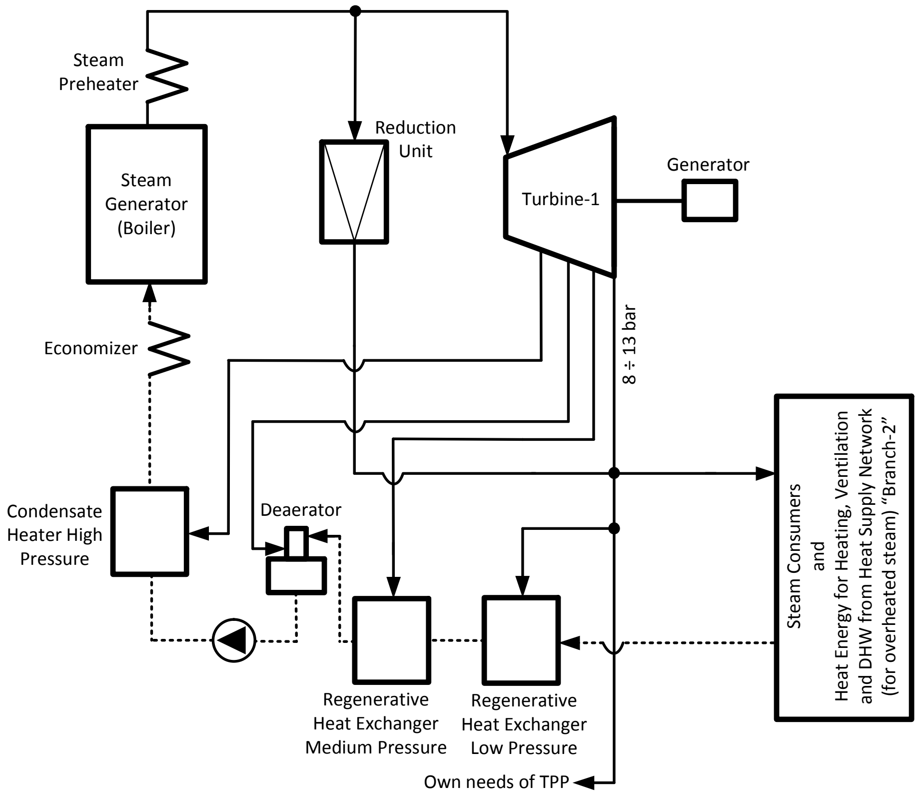

Figure 1: Principal scheme of the system from TPP - an object of reconstructions

The heat balance for 2004 of the overheated steam consumers, connected to Branch №2 is presented in тable 1.

Table 1: Energy balance of the heating capacities of the consumers connected to Branch №2

№	***The name of the consumer***	***Heating capacity of the branch №2 (calculation regime)***			
		Heating	***Ventilation***	***DHW***	***Total***
	-	**t/h**	**t/h**	**t/h**	**t/h**
1	Thermal Power Plant	798	112	726	1,636
2	Repair Mechanical Factory-RMF	1,815	173	294	2,282
3	Sugar Plant	3,436	98	980	4,514
5	Block№6 (Institute for sugar production)	845	0	251	1,096
4	Administrative building (Company management)	747	0	225	972
6	Block №15	394	0	133	527
7	Block №16	233	0	74	307
8	Block №9	184	0	55	239
9	Block №10	184	0	55	239
10	Greenhouse	429	0	0	429
	Total for branch №2:	**9,065**	**383**	**2,793**	**12,241**

The specific characteristics of the heat supply system of Branch №2 have been as follows:

A. The steam line has been designed for heating capacities considerably exceeding the present needs. This fact has led to occurring of two serious issues related to decrease of the heat carrier flow rate and change in the degree of the simultaneous exploitation of the consumers. The effect from this is negative and regarded the following:

A.1. reduction of the steam velocity, which leaded to increase of the steam line heat losses;

A.2. the transportation in saturated state required a compulsory blow-down of the pipe network, which leaded to additional energy losses of heat and condensate;

A.3. in order to reduce the length of the heat network sections, working at regime of saturated water steam, the TPP has forced to enhance the temperature of the output overheated water steam from a collector of 0.6 MPa, which has reflected negatively on the electricity production and on the total heat losses from the heat feeding system.

B. Condensate from the consumers, included in the studied Branch №2 has not returned. This peculiarity has formed the substantial part of the energy inefficiency of the existing heat supply system.

C. The general state of the heat insulation of the steam line, especially in the section between the Sugar Refinery and the Administration has been unsatisfactory. The state of the underground sections, between Administrative building and the connected to it end consumers – units No. 6, 15, 16, 9, 10 and Greenhouse, has been similar.

D. The pipelines and the supporting elements of the pipelines have required additional investments for preventive maintenance and repair.

E. The steam line has been type III category in accordance with the Ordinance №15 and has been subject to technical supervision.

As is seen from the listed disadvantages of heat supply system Branch №2, there has been an objective need to change the scheme in accordance to increase the energy efficiency of TPP.

2.3. RECONSTRUTIONS IN THE SCHEME IN ACCORDANCE TO INCREASE THE ENERGY EFFICIENCY OF TPP

To increase the energy efficiency of TPP in accordance with the listed disadvantages of heat supply system Branch №2 the following reconstructions in the scheme have been proposed and implemented:

► The steam turbine 1 has been replaced in the scheme with a steam turbine 2 which has two adjustable steam extractions (one for overheated steam at a pressure of 8 ÷ 13 bar and one for saturated steam at a pressure of 1.2 ÷ 2.5 bar). Thus, on the one hand achieves an increase in the quantity of electricity output from the turbine with the same amount of steam supplied from the steam generators (turbine 2 has a bigger work surface). On the other hand concerning the reduction of thermal energy consumption for heating, ventilation and DHW it enables this heat to be provided from steam to a lower pressure (1.2 ÷ 2.5 bar).

► In order to reduce the heat losses from the transportation of the heat energy required for heating, ventilation and DHW, a Heat Exchanger Station in the TPP has been built.

► The heat supply system Branch №2 has been reconstructed from heat supply system for overheated steam (p = 5 bar, t = 240 °C) in heat supply system of hot water (t = 95/70 °C), supplied by the built Heat Exchanger Station.

In figure 2 a principal scheme of the reconstructed system is shown.

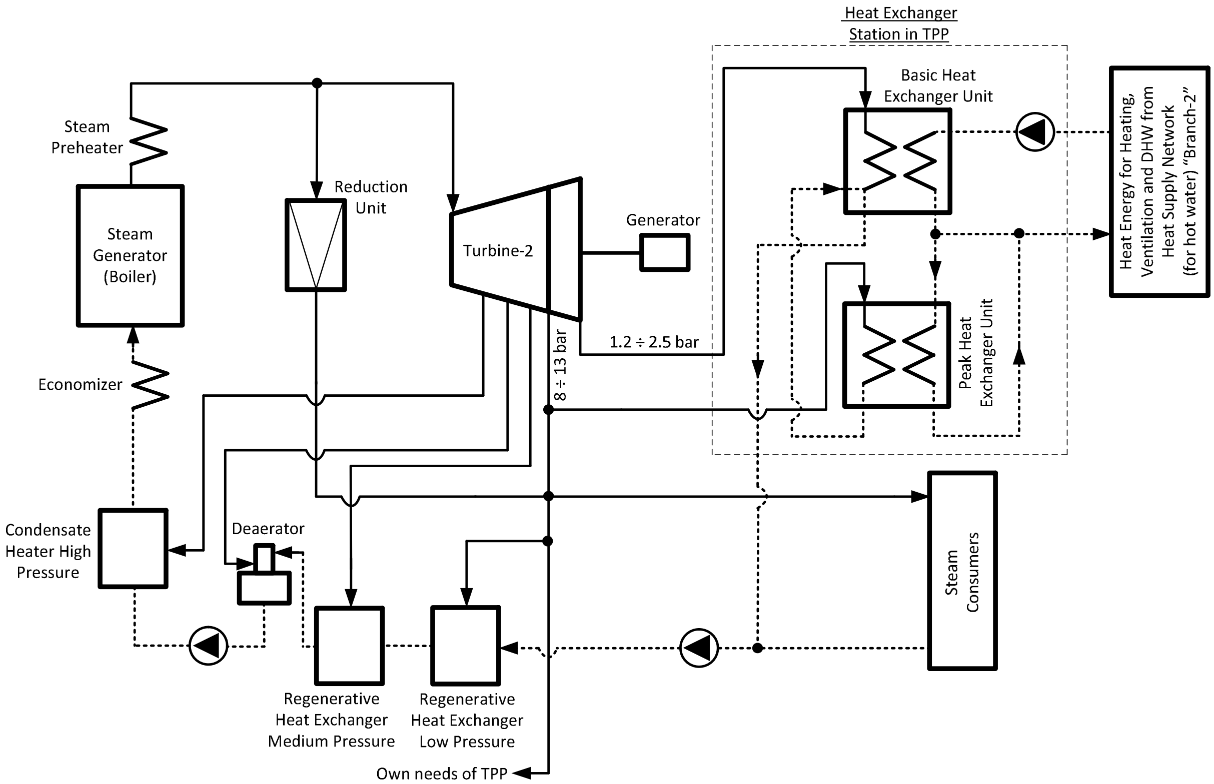

Figure 2: Principal scheme of the reconstructed system

2.4. RESULTS FROM THE MADE RECONSTRUTIONS

Table 2 shows a comparative analysis of the annual energy losses for one calendar year of the steam heat transfer network and the hot water transfer network of Branch №2 as a result of the made reconstructions in the scheme. The parameters have been estimated on the base of the individual network subbranches' characteristics and the working regime of the heat energy consumers.

Table 2: Energy losses before and after replacement of the heat supply network

Losses	Summer regime	Winter regime	Total	Dimension
Heat transfer losses	1,174	1,492	2,666	MWh/yr
Warming losses			101	MWh/yr
Blow down losses	476	605	1,081	MWh/yr
Losses from nonreturn condensate	537	2,305	2,842	MWh/yr
Total annual losses before reconstruction			**6,690**	**MWh/yr**
Heat transfer losses	285	362	646	MWh/yr
Electricity consumption for pumps	163	207	371	MWh/yr
Total annual losses after reconstruction			**1,017**	**MWh/yr**

The results in table 2 shows that the reconstruction of the heat supply system Branch-2 leads to significant reduce of the energy losses and this is a reason for increasing of the TPP energy efficiency.

3. CONCLUSION

The new technical solution – replacement of the heat network from overheated steam to hot water 95/70°C has leaded to the following results:

- the expenses from not returned condensate have been eliminated;
- the losses from heating up and blow through of the pipes have been eliminated;
- the heat losses from the steam transfer have been reduced significantly;
- new opportunities have appeared for more efficient regulation of the heat power of the consumers, this has leaded to additional energy savings;
- the generated by the TPP electricity has increased due to the replacement of the steam turbine;
- increased operational reliability of the heat supply system;
- the category of the heat supply network has changed from III to IV according to Ordinance №15, which allows the supervision to be performed by company or authorised person.

References

[1] Simões-Moreira, J. *Fundamentals of Thermodynamics Applied to Thermal Power Plants*. http://www.springer.com/978-1-4471-2308-8.
[2] www.chambersz.org
[3] www.iipnetwork.org
[4] www.zaharnizavodi.com
[5] www05.abb.com

SOME ASPECTS OF CYCLE VARIABILITY AT AN LPG FUELLED DIESEL ENGINE

Alexandru Cernat[1], Constantin Pana, Niculae Negurescu
University Politehnica of Bucharest

ABSTRACT

Liquid Petroleum Gas fuel can be a viable fuel due to its ability of diesel emissions and fuel consumption reduction. Its special physic-chemical properties, which make is suitable for spark ignition engines, lead to specific aspects of the in-cylinder combustion and engine mechanical running for diesel engines. The main aspects of LPG combustion variability in the diesel engine are analysed from the point of view of maximum pressure rate, maximum pressure timing, maximum heat release rate, following the criteria of reduction of combustion variability in terms of indicated main effective pressure and maximum pressure. Comparative to the classic diesel engine fuelled only with diesel fuel, the cycle variability increases for dual fuelling. The cycle variability is influenced in a direct way by the increase of LPG cycle dose which will lead to the increasing of the cycle variability coefficients values, maximum pressure, maximum pressure rate, heat release rate and cycle angle points of burn mass fractions. The calculated values of these parameters are bigger comparative to the normal values of diesel engines, but don't exceed the maximum admitted values that provide engine reliability. From the analysis of COV values of the engine parameters, the maximum admitted values of LPG cycle dosage are also established.

1. INTRODUCTION

Nowadays, Liquid Petroleum Gas is a worldwide alternative fuel used on a large scale for internal combustion engines. The mixture forming, the heat release, the energetically and pollution performance of the engine are influenced by different vaporization and burning properties of the LPG comparative to diesel fuel. Higher combustion rate of air-LPG mixtures leads to the increase of maximum pressure and maximum pressure rate rise, with consequences on cycle variability. Thus, the maximum LPG cycle quantity admitted inside the cylinder can be limited for efficiency, mechanical reliability, noise, smooth running reasons. The higher auto ignition temperature of the LPG, in the field of 481...544°C versus 225°C for diesel fuel, can allow the use of excessive values for the compression ratio and may required the use of additives for CN improvement or of the diesel fuel pilot injection for air-LPG mixture ignition. The use of LPG at diesel engine, operating on diesel cycle, will required the use of diesel fuel pilot for LPG ignition. LPG raised vapour pressure assures forming of air-LPG mixtures of higher homogeneity. Higher octane number (ON propane = 111, ON n-butane = 102 and ON i-butane = 94), a burning laminar velocity comparable with the one of gasoline (0.46 m/s) [1], [2] makes the LPG a suitable fuel for SI engines. Starting the combustion into a relative lean high homogeneity air-LPG mixture influences the combustion process and cycle variability. Also, wide inflamabillity limits of the liquid petroleum gas 2,1…10,4 % versus 0,6 … 5,5 % for diesel fuel, smaller combustion temperature and the its lower carbon content will influence the combustion cycle variability and may lead to an improvement of the combustion process and of the pollutant emissions, [1], [2], [3], [5], [6]. The cycle variability for air-LPG mixtures is analyzed comparative to diesel fuel fuelling for a 1,5 litre direct injection supercharged engine, type K9K from Dacia Logan.

University Politehnica of Bucharest, Splaiul Independentei no. 313, 0723470021, cernatalex@yahoo.com

The engine is fuelled with diesel fuel and liquid petroleum gas by diesel gas method, the LPG cycle dose is injected inside the inlet manifold and electronic controlled by a secondary ECU connected with the main engine ECU.

2. ASPECTS OF CYCLE VARIABILITY STUDY

Difficulties for LPG use at the CI engine (a lower cetane number, high autoignition temperature) implied special solutions for mixture forming and combustion control. The air-LPG mixture in a higher state of homogeneity, due to propane higher vapour pressure will lead to a high velocity combustion process, after the flame nucleus is forming inside the cylinder next to the diesel fuel jet boundary, [1], [2], [3].

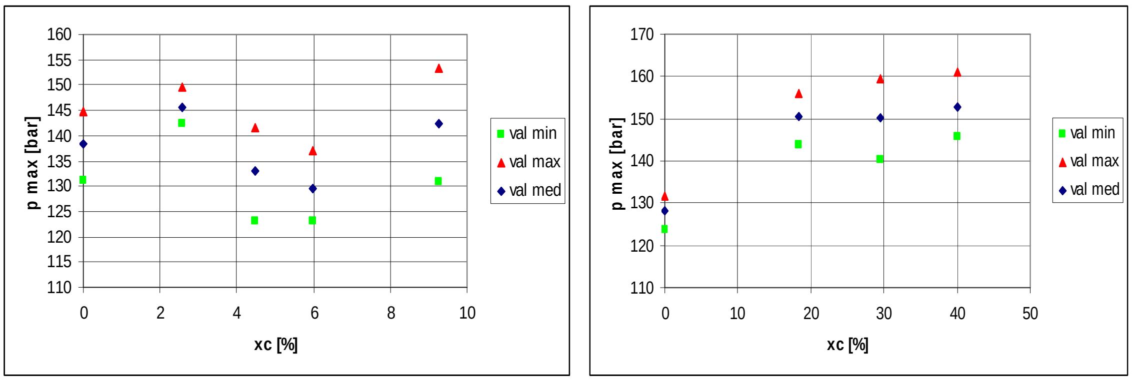

Figure 1. Maximum pressure at 2000 rev/min (left), 4000 rev/min speed (right) and 100% load regime, for different substitution ratios

For different energetically substitute ratio of diesel fuel by LPG, xc, were analyzed individual pressure and heat release diagrams, in terms of maximum pressure, maximum pressure rate rise and heat release rate. For full load and 2000 rev/min regime, the increase of LPG cycle dose leads to the increase of cycle maximum pressure and maximum pressure cycle dispersion, thus the dispersion of successive running cycles increases, figure 1. Also, the angle value for maximum pressure, α_{pmax}, is registered closer to the TDC, with is generally related to a rapid, brutal combustion. This aspect is related with the increase of maximum pressure values and of maximum pressure cycle variability when the LPG dose increases.

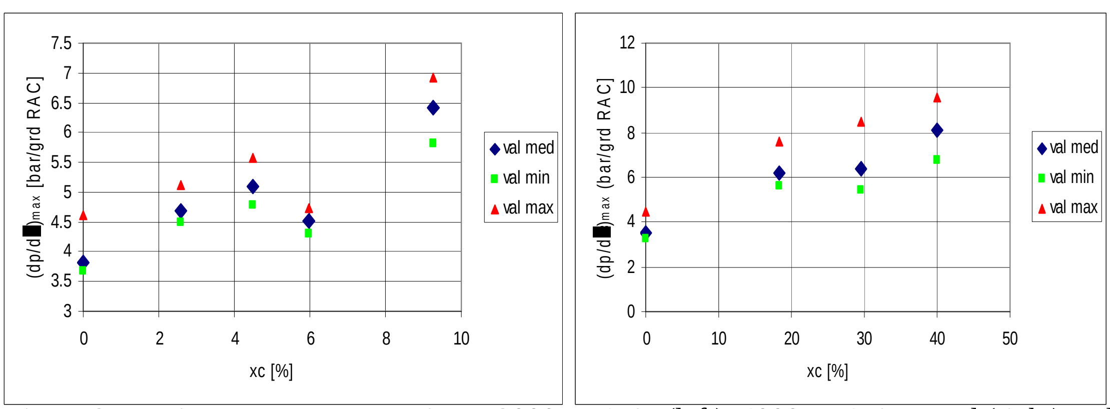

Figure 2. Maximum pressure rate rise at 2000 rev/min (left), 4000 rev/min speed (right) and 100% load regime, for different substitute ratios

The forming of higher homogeneity air-LPG mixture leads to higher combustion velocity, during the performing mixtures combustion phase, by kinetics of chemical reactions at low temperatures. This fact implies the increase of in-cylinder maximum pressure with 10% at maximum diesel fuel-LPG substitute ratio, and also the increase of maximum pressure rate rise value, figure 1, 2. For this operating regime the values registered for averaged cycles, shown as “val med”, are completed with the minimum and maximum values registered in the individual cycles, shown as “val min” and “val max”, respectively. The increase of maximum pressure rate rise is maximum for xc=9,25 and is with 68% bigger comparative to the reference value. This increasing in maximum pressure rate rise will be limited thru the value of substitute ratio at xc=10, at maximum torque regime, leading to values that don’t exceeded 7 bar/CA deg. For the other xc substitute ratios, the increasing percents in maximum pressure rate rise are much lower, 23% for xc=2,59 and 33,8% for xc=4,48, respectively. The lower increasing comparative to the reference regime is for xc=5,98 with 18%, with an absolute value of 4,5 bar/CA deg, [3].

At 4000 rev/min speed regime, the LPG cycle quantity is much bigger and the in-cylinder pressure reach values with 23% higher comparative to the diesel fuel fuelling, for xc=40. Values of 160 bar registered in some cycles, lead to necessity of substitute ratio limitation in order to maintain engine reliability. From xc=20, the cycle dispersion of maximum pressure angle increases comparative to maximum pressure values, figure 1. Also the maximum pressure rate rise registered increased values comparative to the only diesel fuel fuelling, figure 2. The most important increase of 130 % is for xc=40 substitute value, for which the maximum pressure rate rise is in the area of 8…10 bar/CA deg. For the other substitute ratios the increasing percents for maximum pressure rate rise remains significant: 74% for xc=18,3 and 82% for xc=29,5 versus diesel fuel. For a energetically substitute ratio of xc= 30…35, the maximum pressure rate rise values are in the area of xc=9,25 from maximum torque speed, 2000 rev/min. For xc=40, the maximum pressure rate rise climbs to higher values around 10 bar/CA deg. This fact becomes a new limitation criterion for the substitute ratio value. The limitation of xc is also required by variability coefficients in terms of maximum pressure rate rise $(COV)_{(dp/d\alpha)max}$, 5,129 % at xc=0, 2.761 % at xc=2,58, 3,624 % at xc=5,98%, 4,124 at xc =9,25 for 2000 rev/min and 8,496% at xc=0, 6,641% at xc=18,3, 9,207 % at xc=29,5, 7,835 % at xc=40% for 4000 rev/min.

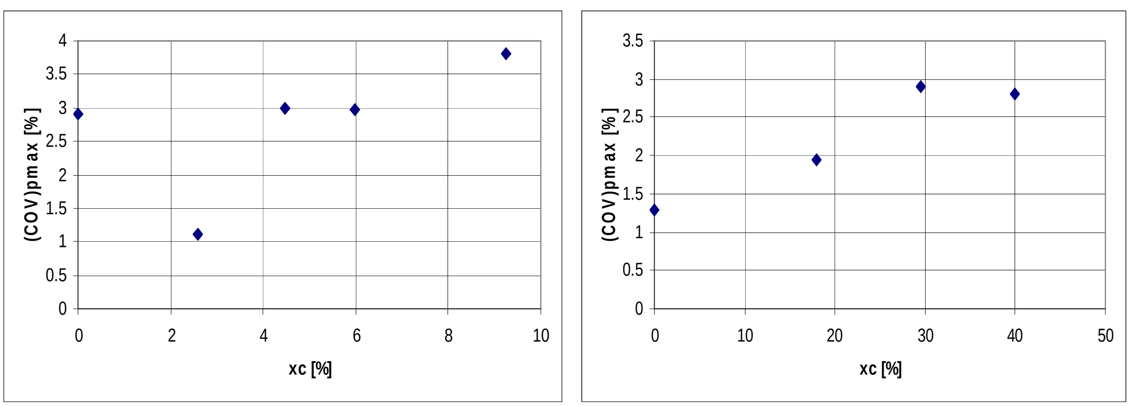

Figure 3. Variation of coefficient $(COV)_{pmax}$ with substitute ratio at 2000 rev/min (left), 4000 rev/min speed (right) and 100 % load

Following the aspects that lead to the establishing of a maximum substitution ratio, can be also taken into consideration the values of cycle variability coefficients for in-cylinder maximum pressure and IMEP, $(COV)_{pmax}$ and $(COV)_{pi}$, respectively. The cycle variability can be very well appreciated by the values of these two coefficients, and they are related with the engine adaptability for traction. The normal automotive manoeuvrability is assured if $(COV)_{pmax}$, respectively $(COV)_{pi}$, don't exceeded 10 %. [8]. The coefficient $(COV)_{pmax}$ don't exceed values of 4 % at 2000 rev/min speed and full load, figure 3, being registered a slightly increase of the coefficient value with the LPG dose. At 4000 rev/min speed regime, the higher dose of LPG leads to a much significant continuously increase of $(COV)_{pmax}$. Even the maximum value doesn't exceed 3%, with no reason for xc limitation, the further increase tendency of $(COV)_{pmax}$ with xc, especially for xc>30%, can be take into consideration, figure 3. For MTB speed regime, IMEP cycle variability $(COV)_{pi}$ is 3 times higher for maximum LPG cycle dose comparative to diesel fuelling, figure 4. From this point of view the substitute ratio limitation at xc = 9.25 % obvious. If is admitted as limit value $[(COV)_{pi}]_{max}$ = 10 %, a limit value in substitute ratio of xc = 8 % results, [3].

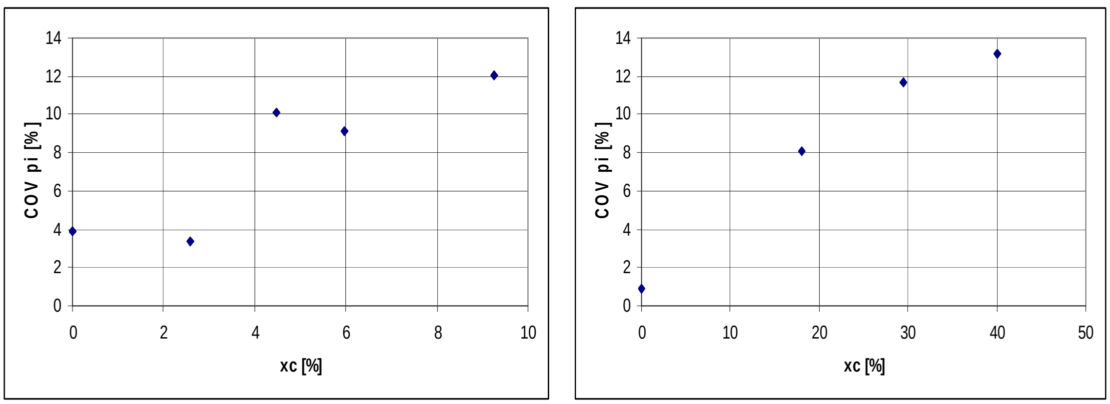

Figure 4. Variation of coefficient $(COV)_{pi}$ with substitute ratio at 2000 rev/min (left), 4000 rev/min speed (right) and 100 % load

For xc=40% the value of coefficient $(COV)_{pi}$ is 14 times bigger comparative to reference value, figure 4. Thus, become necessary the limitation of the LPG dose at 40 % in order to maintain the normal engine running for dual fuelling.

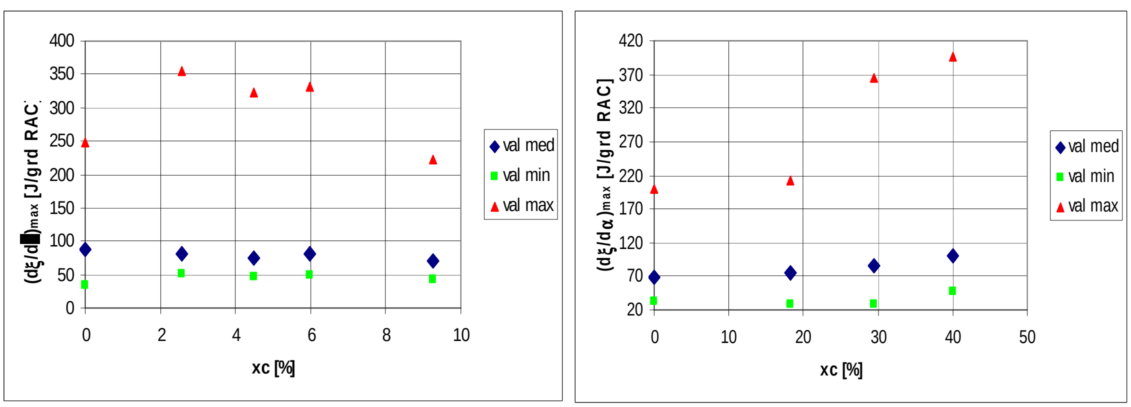

Figure 5. Maximum heat release at 2000 rev/min (left), 4000 rev/min speed (right) and 100 % load

If the admitted limit is $[(COV)_{pi}]_{max}$ = 10 %, then the substitute ratio will be limited to xc = 25 %. Thus, the maximum pressure and maximum pressure rate rise are limited at p_{max} =

150 bar and $(dp/d\alpha)_{max}$ = 6 bar/CA deg, respectively. At 4000 rev/min, the significant increase in LPG cycle dose leads to the increasing of in-cylinder maximum pressure rate due to the increase of cycle heat release, seeing that is no variation for the medium values of maximum cycle heat release $(d\xi/d\alpha)_{max}$, in the investigated rage of xc, figure 5. The maximum values of the heat release rate, from the individual cycles, continuously increase. The maximum heat release obtained values are according with the variation of the maximum pressure and with the variation of the maximum pressure rate rise at the same operating regime. The maximum heat release rate diagrams present beside values from the averaged cycles, "val med", also the minimum and maximum values from the individual cycles, "val min" and "val max", respectively. The most important increase of 160% is registered for the maximum LPG dose, for the other quantities the increasing percent being 39% at xc=18.3 and 28 % at xc=29.5. Thus, the higher values lead to the limitation of the LPG dose at 40%. The calculated values for maximum heat release rate cycle variability coefficients, $(COV)_{(d\xi/d\alpha)max}$, are 34,1% at xc=0%, 86,22% at xc=2,58, 56,54% at xc=5,98, 52,01% at xc=9,25 for 2000 rev/min and 35,35% at xc=0, 22,85% at xc=18,3, 62,73% at xc=29,5 and 32,66% at xc=40 for 4000 rev/min. The position of the burned mass fractions of 5, 10, 50 and 90% versus TDC is directly influenced by these phenomena's. For 2000 rev/min, the conventional 5% and 10% of heat release appears much earlier comparative to diesel fuel, for all substitute ratios, in a direct proportional dependence with the increase of LPG dose. The 90% burned mass fraction is archived later on cycle comparative to diesel fuel, because of a lower heat release quantity during the main phase, 50%. The increase tendency of combustion process variability, reflected in the variability of the angles α_5, α_{10} and α_{50}, with the increasing of the LPG cycle dose is also remarked. Thus, only for diesel fuelling the values of the cyclic variability coefficients increases from $(COV)\alpha_5$=28.3 %, $(COV)\alpha_{10}$=33 %, $(COV)\alpha_{50}$=30 %, $(COV)\ \alpha_{90}$=29.9 %, to values of $(COV)\alpha_5$=49.4 %, $(COV)\alpha_{10}$ =80 %, $(COV)\alpha_{50}$ =31.3 %, $(COV)\ \alpha_{90}$ =34.7 % for the maximum LPG dose, xc= 9.25, [3]. For 4000 rev/min appear the same phenomena of an earlier release of 5% and 10% of burned mass fraction for dual fuelling. The increasing of LPG dose leads to the acceleration of the heat release during combustion, the acceleration of the combustion process and of the sooner achieving on cycle of the 50% and 90% burned mass fractions, comparative to diesel fuelling. Also the amplification of the combustion cycle variability, explained by α_5, α_{10}, α_{50} angles variability is present when the LPG cycle dose increases. For diesel fuel fuelling the values of coefficient $(COV)\alpha_5$=45.5 %, $(COV)\alpha_{10}$ =29.5 %, $(COV)\alpha_{50}$ =4.5 %, $(COV)\ \alpha_{90}$ =6.1 %, are much lower comparative to the values registered for diesel fuel -LPG fuelling: $(COV)\alpha_5$=89.5 %, $(COV)\alpha_{10}$ =64.1 %, $(COV)\alpha_{50}$ =84.6 %, $(COV)\ \alpha_{90}$ =46.8 %, values calculated for maximum LPG dose, xc= 40, [3]. Also this phenomenon is related with a combustion process closer to TDC and leads to the increasing of the maximum pressure rate rise during the combustion process.

3. CONCLUSIONS

The experimental study shows the main characteristics of the engine running for diesel fuel and diesel fuel-LPG fuelling. Thus, the main conclusions can be formulated:

1. The diesel fuel and LPG engine fuelling leads, comparative to classic diesel fuel fuelling to an increase tendency for maximum pressure rate rise $(dp/d\alpha)_{max}$ and cycle variability $(COV)_{pi}$ increasing.

2. The diesel fuel substitute ratio by LPG, xc, is limited by the maximum values or by the maximum variation interval of same running characteristic parameters of the engine, as is follows: if the maximum admissible level of the cycle variability is $(COV)_{pi}$ = 10 %, for IMEP, then the substitute ratio will be limited to xc = 8 % for 2000 rev/min and to xc = 25 % at 4000 rev/min, respectively; if the maximum pressure rate rise is limited to the value $(dp/d\alpha)_{max}$ = 8 bar/CA deg, then the LPG substitute ratio will be limited to xc = 10 % at 2000 rev/min and to xc = 40 % at 4000 rev/min, values that will lead to a maximum acceptable in-cylinder pressure level of 160 bar;
3. The partial substitution of diesel fuel by liquid petroleum gas leads to the increasing of the heat release rate during the rapid combustion phase, showed by the raised level of the maximum heat release rate $(d\xi/d\alpha)_{max}$ and earlier achievement per engine cycle of 5% and 10% of burn mass fractions from the heat release (decreasing of α_5 and α_{10} angles values). This influence is correlated with the increasing tendency for maximum pressure rate rise values and for in-cylinder maximum pressure values;
4. The partial substitution of the diesel fuel by LPG leads to the increase of cycle variability for the beginning of the combustion process, shown by the variability of the angles α_5 and α_{10} with a direct influence on cycle variability for indicated main effective pressure IMEP, $(COV)_{pi}$ and maximum pressure, $(COV)_{pmax.}$

References

[1] Popa M. G., Negurescu N., Pana C., "*Motoare Diesel. Procese.*" volum I si II, Editura MatrixRom, Bucuresti, 2003.

[2] Pana C., Negurescu N., Popa M. G., Cernat A., *Experimental Aspects of the Use of LPG at Diesel Engine*, Buletinul stiintific UPB, Seria D nr. 1, Bucuresti, 2010.

[3] Cernat A., "*Contributii la studiul functionarii unui motor diesel la alimentarea cu motorina si gaz petrolier lichefiat*", Universitatea Politehnica Bucuresti, teza de doctorat, Bucuresti, 2010.

[4] Negurescu N., Pană C., Popa M.G., G.Boboc, Cernat A, *"Performance of a Diesel Engine Fueled by LPG,"* 5th International Colloquium FUELS 2005", Technische Akademie Esslingen, Germania, ISBN 3-924813-59-0, pp.143-148, 6 pag. January 12-13, 2005

[5]Pana C., Negurescu N, Popa M.G., Cernat A, Bujgoi Fl, *Sistem dual de alimentare cu combustibili alternativi pentru ecologizarea motoarelor diesel de automobil – DGPL*, contract de cercetare nr. X2C10, proiect CEEX/2006, 2006-2008

[6] Pană C., Negurescu N., Popa M., G., Boboc G., Cernat A, „*Reduction of NOx, Smoke and BSFC in a Diesel Engine Fueled with LPG*", MECCA, Journal of Midle European Construction and Design of Cars, Vol III, No. 4, December 2005, Praha, Czech Republic, ISSN 1214-0821, pp37- 43, 7 pag., ..2005 indexata in baza de date internationala MECCA: http://www.bozek.cvut.cz/mecca/2005/4_05-pana-en.pdf, cod CNCSIS 500) Tomul L (IV), Fasc. 6D, , pp 89-97, 9

[7] Negurescu N., Pana C., Popa M.G., Cernat A., Boboc G., Soare D., *„GPL – combustibil alternativ pentru motorul diesel"*, ZILELE ACADEMICE TIMISENE, Editia a IX-a, Simpozionul OMUL SI MEDIUL, Editia a IV-a, Politehnica din Timisoara, ISBN973-625-225-6, Editura Politehnica, 2005

[8] Heywood J. B.," *Internal Combustion Engines Fundamentals*." McGraw-Hill Book Company, New York, 1988

[9] Goto S., Lee. D., Wakao Y. Honma H., Moiri M., Akasaka Y., Hashimoto k., Motohashi M., Konno M., *Development of an LPG DI Diesel Engine Using Cetane Numbet Enhancing Additives*, SAE Paper 1999-01-3602, in Alternative Fuels 1999, SP-1482

[10] Goto S., Shakal J., Daigo H., *LPG engine research and development in Japan*, Int'l Congress on Transportation Electronics, 1996

[11] Goto S., Lee. D., Shakal J., Harayama H., Honjyo F., Ueno H., *Performance and emissions of an LPG lean-burn engine for heavy duty vehicles*, SAE Paper 1999-01-1513, 1999

[12] Goto S., Lee. D., Harayama H., Honjyo F., Ueno H., Honma H., Wakan Y., Mori M., *Development of LPG SI and CI Engines for Heavy Duty Vehicles*, F2000A171, Seoul 2000 FISITA World Automotive Congress, 15-20 iunie 2000, Seul, Coreea

HOT AIR DISTRIBUTION THROUGH MAIN BUSTLE PIPE ON THE TUYERES OF A BLAST FURNACE

Eugen Dimofte[1], Florin Popescu, Ion V. Ion
"Dunărea de Jos" University of Galati

ABSTRACT

The paper consists in the numerical modelling of the hot air distribution in the tuyeres based on the air flow intake into the main bustle pipe of a blast furnace. As a result of the analysis, the minimum hot blast air flow can be determined that must enter the main bustle pipe in order to ensure a uniform distribution of the air in each tuyere.

Key words: Numerical modelling, discretization web, main bustle pipe, tuyeres, blast furnace.

1. INTRODUCTION

The accomplish of physical and chemical processes that occur in a blast furnace requires a high temperature, temperature that is obtained by hot air coming from cowpers and reaching the furnace by blowing hot air installation. Air from blowers is introduced in cowpers and heated to a temperature of about 1200°C. From cowpers, the hot air is introduced into the annular duct to the furnace at a pressure of 3.5 bar. From ring pipe, the warm air enters through elbows in the tuyeres of furnace. For proper development of physicochemical processes, the distribution of warm air inside the furnace must be uniform. This uniform distribution is achieved through the installation of hot air blowing into the furnace, which is composed of annular pipe, elbows and tuyeres. The number of elbows and tuyeres varies depending on the size of the blast furnace. The analyzed air feeding plant has 32 elbows and tuyeres.

2. PURPOSE OF THE WORK AND APPROACH

This paper consists of the numerical modeling of the pressure distribution of hot air inside the tuyeres depending on the inlet pressure of the hot air in the annular pipe of a furnace. To solve this problem it was used the Ansys CFD (Fluent).

The purpose of this paper is to determine the optimal input pressure in annular pipe so that to obtain an uniform outlet pressure for all the 32 wind holes. In this respect, three simulations were performed varying the inlet pressure in annular pipe.

3. DATA PREPROCESSING

Whatever the numerical methods used in solving a certain flow problems, the simulation is done in the same sequential stages, namely:

1. Setting the simulation goals, step in which the problem is analyzed and the parameters of interest are set up, i.e. the unknown quantities to be calculated, which are significant for the studied problem;

[1] Galati, 47 Domneasca St., E-mail: eugen.dimofte@yahoo.com

2. Defining of domain analysis, stage in which it is determined the geometrical shape of the domain that provides both spatial framing of the studied problem and the possibility of correct setting of boundary conditions. At this stage, the domain is drawn also.
3. Meshing of analysis area, step in which the analysis is divided into finite elements, also known as cells.
4. Definition of mathematical models, stage in which the set of equations that models the phenomena characteristic of the studied problem is chose. The set of equations includes the constitutive equations describing the physical properties of substances.
5. Introducing of boundary conditions. A number of parameters required for numerical calculation are defined, parameters usually known at the limits of the analysis domain.
6. Numerically solving of problem. The unknown quantities are calculated.
7. Graphical post-processing of results. Derived parameters from those obtained in the numerically solving stage are calculated and are drawn a number of graphical representations of the results.

The first five stages of simulation represent preprocessing and are essential in defining a problem that is solved numerically. Usually, a good part of the time required by a numerically solving of a problem is assigned to this stage.

3.1 Drawing of model

The model drawing can be achieved by using any CAD/CAE package. In fact this is just the calculation domain for the established problem. In this respect, the refractories inside the ring pipe, elbows and hot air feeding pipe will not be plotted, but actually just the calculating domain for the given flow problem.

The graphical representation was made using the CATIA software by respecting the size of components of hot air blowing plant into the blast furnace as they result from the technical documentation of the blast furnace. The Figure 1 shows the facility of hot air blowing into the furnace.

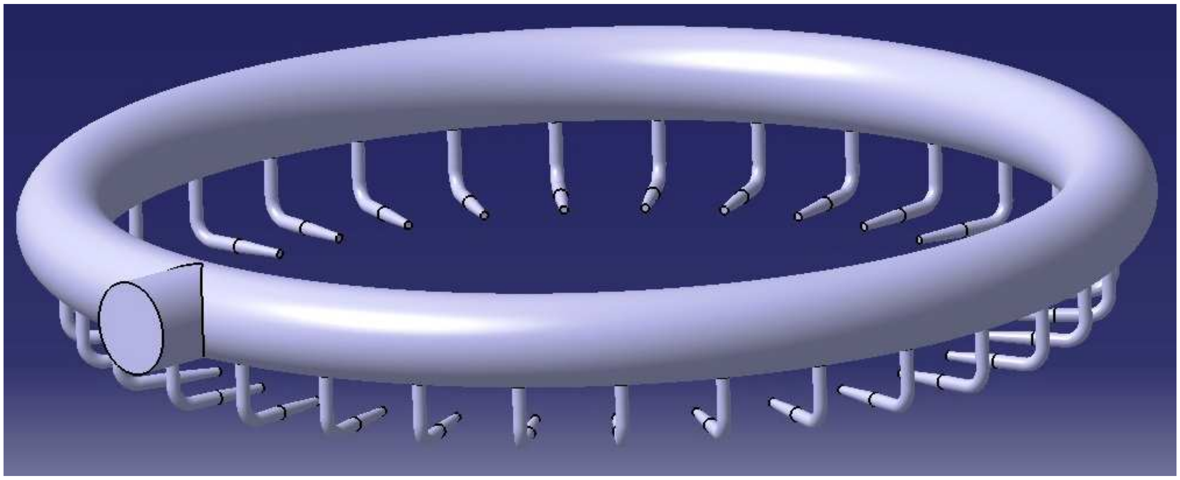

Fig. 1. Plant of hot air blowing into the furnace.

3.2 Meshing of analysis domain

After the drawing of analysis domain this must be discretized. Ansys CFD (FLUENT) has a solver for unstructured networks, so there is no limit for the meshing of domain, the most appropriate meshing could be chose to geometry and problem. Are supported both structured network, multi and unstructured networks.

In the studied problem, due to the geometry complexity of the domain analysis, the mesh network is unstructured. The figure below provides mesh network domain analysis.

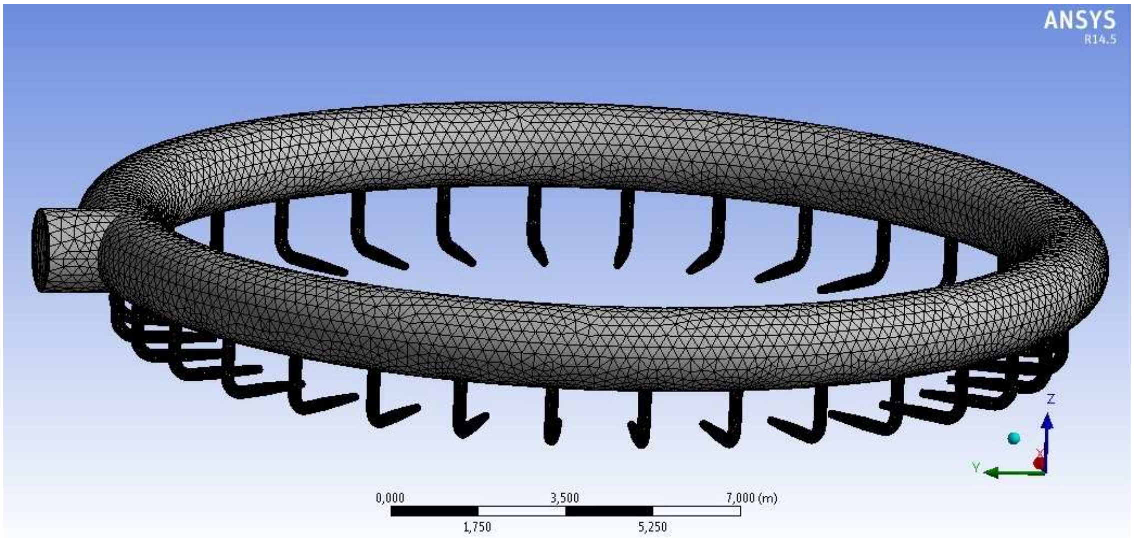

Fig. 2. mesh network of analysis domain.

3.3 Alegerea modelelor matematice si definirea conditiilor la limita

As a mathematical model was chosen the viscosity model because the fluid flow velocities are high. The Boundary Conditions are imposed in some points for the calculation variables. The values of these parameters are introduced before the start of the calculation itself and have a significant impact on the results, so they must be defined correctly as possible. For the analyzed case, the pressure at annular duct inlet is 3.5 bars and the temperature is 1200°C (1473 K). At exit, the pressure is 0 and the temperature is the same as for entering. Although circulated air temperature is quite high due to excellent thermal insulation that is lined both annular pipe and elbows and tuyeres, the temperature variation inside the warm air blowing plant is neglected.

3.4 Numerically solving of problem

To solve the proposed problem, the convergence criteria were met after a total of 200 iterations.

4. DETERMINATION OF INLET MINIMUM PRESSURE

Determination of the entrance minimum pressure for which the pressure for all tuyeres is approximately the same, was accomplished by successive attempts, using three input pressure values 1.5, 2.5 and 3.5 bars and following the distribution of pressure on those 32 tuyeres. The Figures 3, 4, and 5 show the distribution of pressure on each tuyere as function of the inlet pressure in annular pipe.

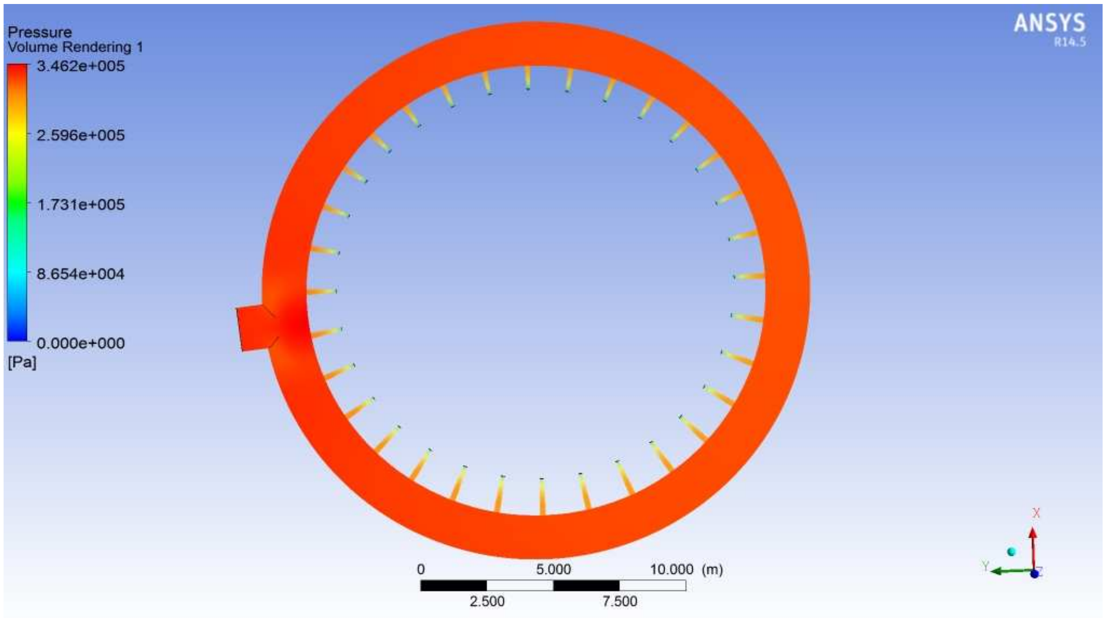

Fig. 3. Distribution of pression on tuyeres for an inlet pressure of 3.5 bars.

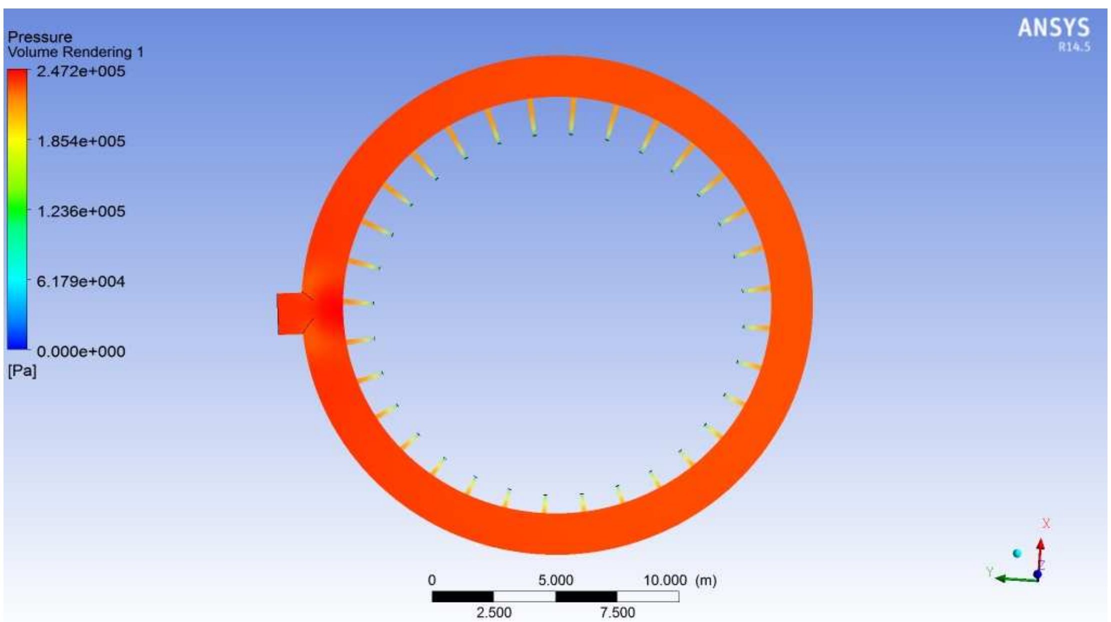

Fig. 4. Distribution of pression on tuyeres for an inlet pressure of 2.5 bars.

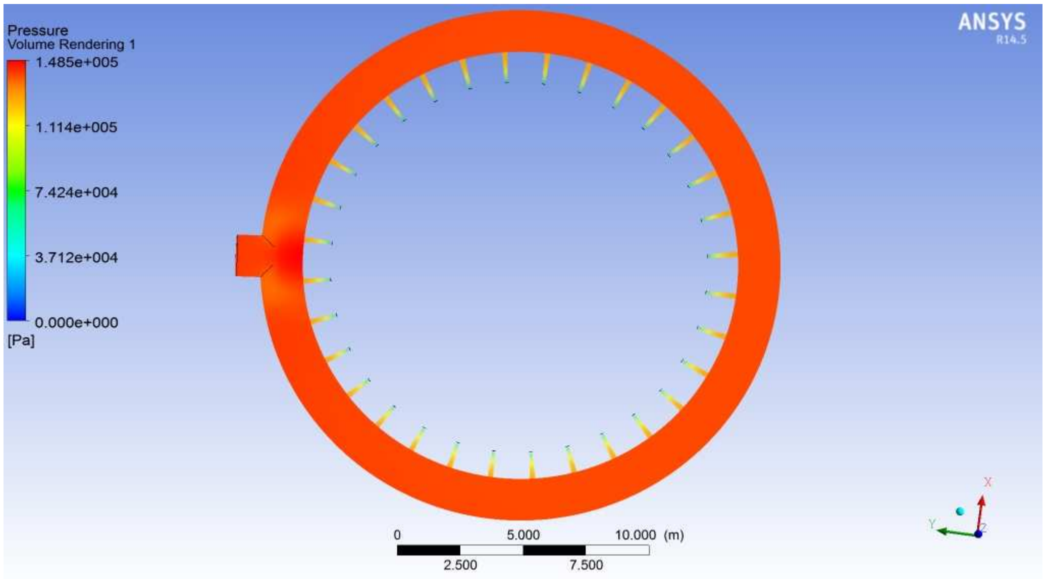

Fig. 5. Distribution of pression on tuyeres for an inlet pressure of 1.5 bars.

5. RESULTS ANALYSIS

As seen from the distribution of pressure on the tuyeres for the three values of inlet pressure for which the analysis of the proposed problem was made, the inlet minimum pressure for each tuyere is approximately equal to 3.5 bars. In the Figure 6 is shown a longitudinal section of ring pipe at the value of inlet pressure of 3.5 bars.

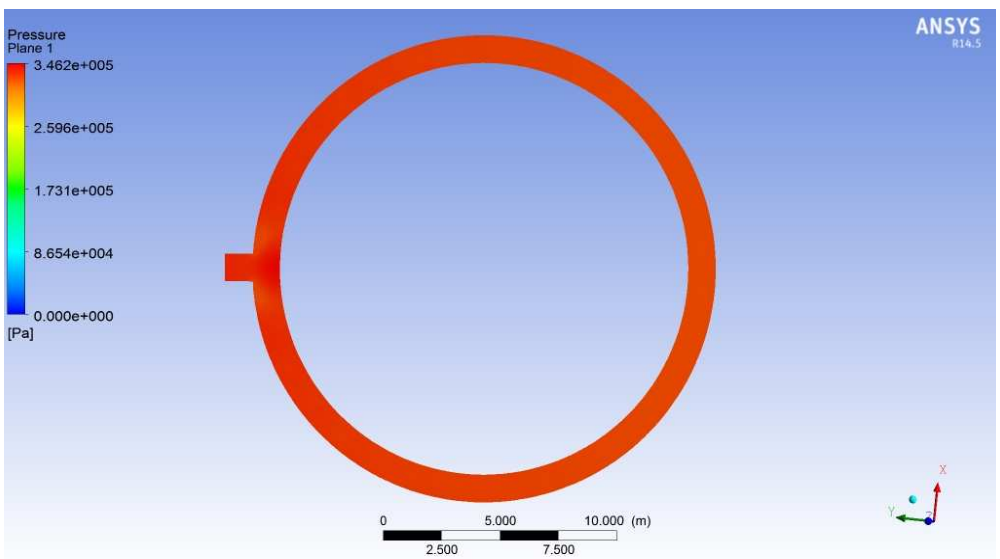

Fig. 6. Pressure distribution in longitudinal section of ring pipe at the inlet pressure of 3.5 bars.

In Figure 6 can be noted an approximately equal distribution of pressure in the analysed section and therefore an even distribution of pressure on all tuyeres.

6. CONCLUSIONS

According to the obtained results the minimum value of the pressure of warm air at blowing facility inlet for which a uniform distribution of pressure was obtained on the 32 tuyeres is 3.5 bars. For an inlet pressure less than this value the pressure distribution becomes non-uniform with negative implications on physical and chemical processes taking place in the blast furnace.

Due to the large gap between the annular pipe section in relation to the amount of the exit sections of tuyères, the annular pipe stores a considerable amount of air playing the role of an air tank.

Playing the role of air reservoir, the annular pipe ensures an uniform distribution of pressure on tuyeres when the inlet pressure is adequate.

References

1. Popescu F., *Modelare si validare experimentala in curgerea fluidelor*, Editura Fundatiei Universitare "Dunarea de Jos" Galati, 2004.
2. *** CATIA V5-6R2013 software
3. *** ANSYS Fluent software

RESULTS OF OPERATIONS FOR THE STORAGE AND HANDLING OF WILLOW ENERGY CROPS

Arpad Domokos[1], Lucian Mihăescu[2], Ionel Pîşă[2], Elena Pop[2]

ABSTRACT

Energy willow cultivation began, at European level, in the 1970s. Today, renewable energy production, captures the interest of more and more.

Is the aim of achieving some hybrids (today there is about 300, of which 12 have excellent results), with a long period of recovery, up to 25-30 years.

Romania has integrated this trend by cultures made according to possibilities of the investors.

There is no centralized actions, the area has a wide range of estimates, from 600 ha to 2000 ha. It is estimated, however, that there is propitious surface culture of about 500 000 ha, represented by land with high humidity. At the moment there is no legislation that actually support crops, but is to be expected of such a legal framework.

The current stage, however, needs to respond to opportunities to exploit the willow harvested. For these answers depend further development of future crops.

It is noted that the theoretical research, experimental and applied even on combustion technologies are in advanced stage, with certain achievements. For this purpose it is noted, thermal power boilers (designed and built) for willow chips between 20-1000 kW.

There are still problems to solve, related to the dynamics of harvest, transport and storage. Regarding storage is mentioned that energy willow represents an agricultural plant, already registered in the Official Catalogue of Plant Varieties of Culture in Romania, which has a number of features of positive energy. These features give it a prominent place on the level of energy plants cultivated in Europe. Compared to the rest of the plant, salicin content represents an undeniable advantage.

Salicin as a material preservative ensures willow (as chips) the opportunity to be stored for long periods (even years), only on a concrete platform and without a roof. The experiments carried out have confirmed this.

Harvesting energy willow is made with different machines, in most cases combine the cut, chop and throw the resulting product in a trailer.

The town Poieni, Miercurea Ciuc, but also in Sweden, Hungary, Slovakia, samples were made samples storage with willow chips for different periods of two months, one year, two years and three years, making in parallel determinations for moisture and calorific power.

In Poienile - Covasna were initially grown in 22 hectares, the first mechanical harvesting is carried in February 2012 with a Jonh Deere machine. Harvesting speed was about an hour to hectare.

Chips willow transportation can be done with walking floor semitrailer for longer distances and with trailers (30-40 cubic meter) or special container for smaller distance. The trailer and container loading is made by front loader. After harvesting in February 2012, has revealed the importance of binomial harvesting, transport and storage.

If the storage platform is channeled (or drain water), so that chopped willow does not sit in water and chopped willow dumps is 2-3 m tall, were found the following:

[1] Association Green Energy, Sfantu Gheorghe, Covasna County, Romania, email: office@greenenergycluster.ro

[2] University Politehnica of Bucharest, Faculty of Mechanical Engineering and Mechatronics, tel. +40214029158.

- moisture at harvest is 53-55%; after two months was reduced to 20-21% and after approx. 3 months was stabilized at 15-16%;
- the waste dump surface to a depth of 10-15 cm has been observed water intrusion resulting from rain or melting snow layer that has changed color, becoming darker. After some time (a few days) without precipitation, this layer dries in the hot season. Winter wet layer freezes, forming a hard shell, but below this layer material kept at 15-16% humidity;
- analysis of calorific power revealed that the calorific value increased with of the decreasing of the humidity, and this was the same (close) at different points of the heap, including the top layer;
- the willow dump condition after different periods is not damaged, with few exceptions, when for various reasons, rainwater could not drain and chopped willow stayed long time in water. In these cases found no visible damage, but after drying, was found minor deviations of calorific values.

Figure 1 and 2 present aspects of open and closed storage activity at the base of Poienile.

Figure 1. Open storage of the energy willow. Poienile Village

Figure 2. Aspects of closed storage activity at the base of Poienile.

The transport and storage container is shown in Figure 3. Such a construction ensures operation of a 350 kW boiler in St. George at a sausage factory.

Figure 3. The transport and storage system

All issues related to the development of energy chopped willow is solved considering two major targets:
- for heating by hot water producing in specialized boilers;
- for the production of electricity, with or without cogeneration (production and heat).

If the first possibility of recovery, are somewhat lower consumption and local storage can be accepted at a distance from the harvesting area in the second case it is obvious that the power plant location to be in the vicinity of the plantation.

For heating, especially for those in urban areas, was developed the transport and storage in high volume containers. Containers replaced deposit being changed after consumption.

Case studies and feasibility studies have indicated that power plants less than 250 kW are the most economical. This implies a plantation size about of 100 ha. The power plant is higher, the energy production is more efficient, but increases exponentially issues of storage and handling of energy willow.

This work was supported by a grant of the Romanian Authority for Scientific Research, CNCS-UEFISCDI, project number PN-II-ID-PCE-2011-3-0698.

ANALOGY IN PROCESSES OF DESTRUCTION OF FRAGILE CAPILLARY - POROUS COVERINGS AND METALLIC STEAM-GENERATING SURFACES IN POWER INSTALLATIONS

Alexander Genbach[1], Karlygash Olzhabayeva[2], Iliya Iliev[3]

ABSTRACT

In the given article the analogy in the processes of a limit condition of weak capillary-porous coverings and a metal heating surface is drawn. It was considered that real factors of development of concentrators of tension are revealed on the basis of the physical model of development of a steam phase in capillary and porous coverings. The role of thermal tension of compression and stretching, depending on brought thermal streams, is shown, at the time of their coming, the sizes of coming-off particles of a destroyed material and depth of penetration of thermal waves in studied materials.

1. INTRODUCTION

The inner thermohydraulical characteristics of boiling liquids inside, as well as on the surfaces of capillary-pore structures [1] are examined in order to create reliable cooling systems for the heat-loaded units in heat and power installations.

Capillary and porous structures can be made of mesh, fibrous, ceramic, felt materials. It is possible to use fragile capillary and porous coverings for their modeling. In this connection, we'll draw an analogy in destruction processes of the fragile coverings with metal protecting construction that differ in small porosity and heat conductivity.

2. METHODOLOGY

The dynamics of tension in steam bubbles existing in capillary and porous structures is presented in figure 1. Rapid shooting allows to observe and generalize internal characteristics of boiling liquids [2-4].

Both the tension of compression waves and the expansions of steam bubbles that extend into a steam-generating surface, or in steam volume, can be destructive ("deadly") – i.e. death of a steam bubble, or creative ("viable") – i.e. the birth explosion of a steam germ, which will have a number of stages in its development (a critical stage and a silence stage) when relaxation, rest, stability of phases, structure, order, balance and symmetry are observed.

The model of the generation process, development and the separation of a steam bubble in an active stage of the steam-generating wall,covered by porous structure, is presented in figure 2.

The model of tension representation of the dynamics and "life" of a steam phase allows to model and draw analogies in processes «bank of a crack disclosures», and to reveal the main components of thermal tension in the destruction mechanism of capillary-porous coverings.

[1] Professor Dr.Sc., AUES, Kasachstan, katerina-1@rambler.ru; cell phone: +78727 2630601

[2] Ph.D. Student, AUES, Kasachstan, karla210784@mail.ru; cell phone: +78771 415 35 71

[3] Professor, PhD, Ruse University, Ruse, Bulgaria, e-mail: iiliev@enconservices.com; cell phone: +359 887306898

Tension dynamics in life of (light) phase in steam capillary porous structure

↓	↓	↓	↓	↓	↓	↓	↓
The spontaneous (explosive) birth of a bubble of the critical size (tension birth) in the center of activation	Speed of a bubble's development Form and bubble outlines	Time of existence (life) of a bubble	Intensity of pulsations of a bubble	Density of the centers of bubbles regeneration	Frequency of bubbles generation	Detachable diameter at the moment of death ("death") of a bubble (tension removal)	Time of the silence center (balance, stability)
Rebirth of a new steam germ in the activation center (in a tension concentrator)							

Figure 1. Dynamics of tension in a steam (easy) phase existing, alternating in its development the tranquility, balance and stability to a catastrophic disorder in cells of capillary and porous structure

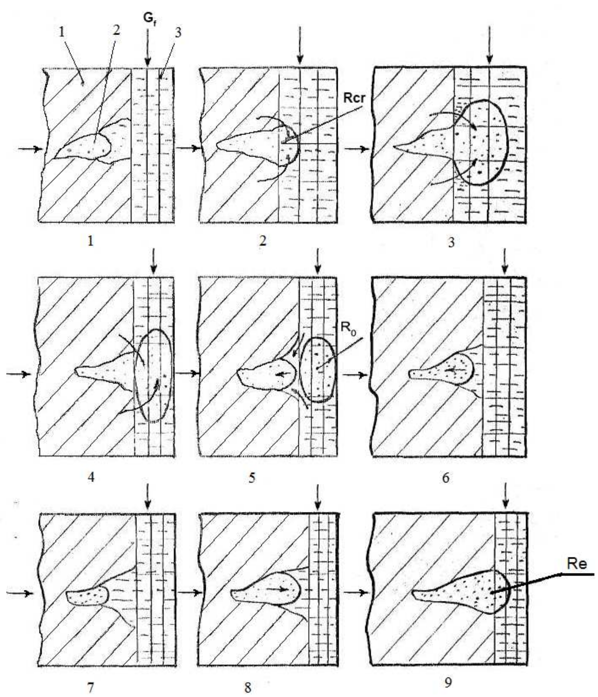

The fig. 2 Illustration of process of appearance, development and the separation of a steam bubble in an active time of the steam-generating wall, covered with porous structure: 1 – wall; 2 – hollow; 3 – porous structure.

Regarding the thermal destruction of weak capillary-porous coverings and a metal wall in power installations, it is required to find out the influence of the specific thermal stream size, which is brought to a surface, and the time of its impact on the creation of breaking points, granulometric structure of coming-off particles, and for metals – the depth of penetration of temperature indignation. In some works, the crucial part in the destruction is assigned to the thermal tension of stretching, as the value of strength of weak porous coverings on compression is more than 10 (20÷30) times above the limit of the strength of stretching, and in metals - several times higher. It is considered that the stretching tension causes only cracking of a covering and doesn't define peeling it, i.e. they aren't decisive for thermal destruction, and the main breaking points are shift.

According to the estimates of tension compression size, with the increase of circumstance's temperature in very short periods, the dynamic effects become quite considerable, and tension compression reaches high values as well, often exceeding the strength of a material on compression by several times. Therefore, it is necessary to consider this tension in the mechanism of thermal destruction of a porous material. It is required to find out what type of tension reaches its limit values for brought thermal streams earlier.

We will consider a plate, free in all its aspects, and of 2h thickness. To Z surface = + h, since the moment of $\tau = 0$, here, it a constant specific thermal stream of q is brought. The bottom surface of Z = - h and lateral edges of a plate – heat-insulated [2].

The heat conductivity equation with boundary conditions will register as follows:

$$a_w \frac{\partial^2 T}{\partial z^2} = \frac{\partial T}{\partial \tau}, \tag{1}$$

$$\lambda_w \frac{\partial T}{\partial z} = q, \quad z = +h, \tag{2}$$

$$\lambda_w \frac{\partial T}{\partial z} = 0, \quad z = -h. \tag{3}$$

Temperature distribution on thickness depends on the heat-physical properties of a material, the size of a thermal stream and the time of its appearance:

$$\lambda_w \frac{\partial T}{\partial z} = 0, \quad z = -h. \tag{4}$$

where $\mu = \lambda_w / h$; n – whole positive numbers.

Having been informed about the temperature distribution in a plate, it is possible to calculate the thermal tension of stretching and the compression, appearing at some moments τ at various depth from a surface δ_i ($h=z_i$) at this value of a thermal stream of q.

The plate from a variable on thickness temperature is in plain tension. Tension is defined with accordance to the following equation:

$$\sigma_{xx} = \sigma_{yy} = -\frac{\alpha' E}{1-\nu} T(\frac{z}{h};\tau) + \frac{1}{(1-\nu)2h}\int_{-h}^{+h} \alpha' E T\left(\frac{z}{h};\tau\right) dz, \tag{5}$$

Where the first member – making compression tension, and the second – stretchings; α' – coefficient of linear expansion; E – Jung's module.

Work (α' E) doesn't depend on the temperature, therefore the expression for tension of stretching becomes simpler.

Setting the limit values of tension of compression, stretching for each covering and metal, a functional dependence on time and penetration depth of the thermal stream demanded for destruction arises. Besides, when equating plate surface temperatures to temperature of melting of both the covering and the metal, the values of the specific thermal streams, necessary for the melting of of the top layer in various period of their action, are determined Thus, in each specific case present are functional dependences of a thermal stream from the time of its influence on the covering and metal surface:

- melting of a plate surface
-

$$q_1 = T_{пл} / \left\{ \begin{aligned} &\frac{\mu}{2(c\rho\lambda)_{CT}}\tau + \frac{2}{3\mu} - \frac{4}{\pi^2 \mu} \times \\ &\times \sum_{n=1}^{\infty} \frac{(-1)^n}{n^2} \exp\left[-(n\pi\mu)^2 \tau / 4(c\rho\lambda)_{CT}\right] \cos n\pi \end{aligned} \right\}; \tag{6}$$

- Creation of limit tension of compression

$$q_2 = \frac{(1-\nu)\sigma_{\lim.compr}}{\alpha' E} / \left\{ \begin{array}{l} \dfrac{\mu}{2(c\rho\lambda)_w}\tau + \dfrac{3z^2/h^2 + 6z/h - 1}{12\mu} - \dfrac{4}{\pi^2\nu}\times \\ \times\sum_{n=1}^{\infty}\dfrac{(-1)^n}{n^2}\exp\left[-(n\pi\mu)^2\tau/4(c\rho\lambda)_w\right]\cos\left[\dfrac{n\pi}{2}\left(\dfrac{z}{h}+1\right)\right] \end{array} \right\} \quad (7)$$

- Creation of limit tension of stretching

$$q_3 = \frac{(1-\nu)\sigma_{\lim.str.}}{\alpha' E} / \frac{\mu}{2(c\rho\lambda)_{CT}}\tau. \quad (8)$$

For the plates executed of quartz, granite, *teshenit* and metallic coverings, functional dependences of q_1, q_2, q_3 are calculated on a computer. Thermo-mechanical characteristics of rock and metals are submitted in [2].

Results of calculations are shown on schedules (fig. 3 - 6). In case of a porous quartz plate, thermal streams are counted for very a wide interval of time ($10^{-8}\div10^{3}$ s) by the village Nizhny, where the limit of this interval (10^{-8} s) is the relaxation time. From figure 3, it is visible that for time intervals ($10^{-8}\div10^{-3}$s) from a ratio of the sizes q_1 and q_2, representing curves of hyperbolic type in coordinates (q; τ), lose physical meaning as in this task the heat conductivity equation is assumed as a basis. For the accounting of micro processes, it is necessary to add, that the member like K $\partial^2T/\partial\tau^2$. As far as a thermo destruction is regardes as a macro process, we accept that it proceeds for the time ($5\cdot10^{-3}\div10^{3}$) sec.

On the condition of covering destruction only by compression, a number of curves were received, each of which matches a certain thickness of a coming-off particle. The maximum thickness of the particles which are coming off under the influence of forces of compression for quartz and granite makes $(0{,}25\div0{,}3)\cdot10^{-2}$ m , which is confirmed by the experiment, received as a result of high-speed film removable SKS – IM (fig. 7).

Sites of compression curves defining a separation of particles with thickness $\delta > 0{,}3*10^{-2}$ m for big thermal streams and small τ are shielded by a curve of II melting, and in case of small thermal streams and considerable intervals of time – a curve of I stretching. The curve of surface melting of a quartz covering is much higher, than that of a granite one, which goes to show the weak destruction of quartz.

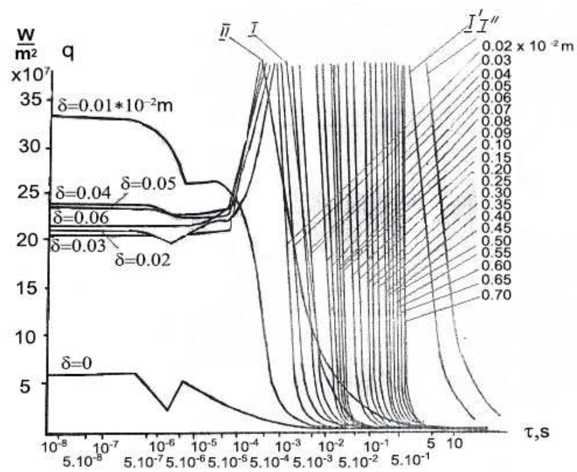

Dependence of Thermal Streams causing tension of compression of a quartz covering, depending on action time for various thickness of coming-off particles: The fig. 3

I – stretching tension, sufficient for destruction;

I', I'' – copper and stainless steel, h=0,1*10^{-3} m, II – melting surfaces. Curves of II' and II'' for copper and steel almost coincide with a curve of I in area τ=(0,01÷0,1) sec the following figure:

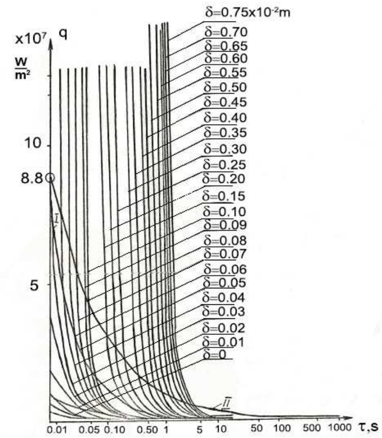

The fig.4 Dependence of Q=f (τ), presented in fig. 3 in the range τ=(0,01÷1000)s. Curves of II' and II'' for copper and steel almost coincide with a curve of I in area τ=(0,01÷0,1)s

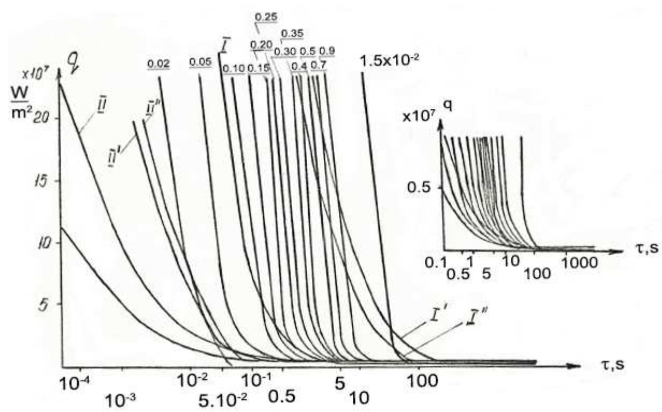

The fig. 5: Dependence of Thermal Streams causing tension of compression of a covering from granite, depending on action time for various thickness of coming-off particles: I – stretching tension, sufficient for destruction;

(I', I'' – copper and stainless steel, h=0,1×10^{-3} m) the m, II – surfaces (II', II'' – copper and stainless steel, h=0,1×10^{-3} m).

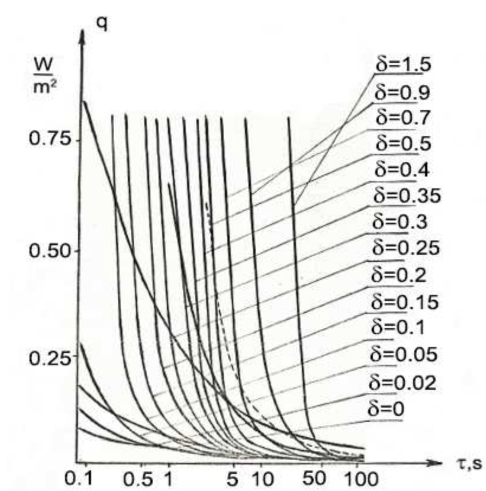

The fig. 6: Dependence of q=f(T), presented in fig. 5 in q=(0,25…0,75)·10^7 W/m^2.

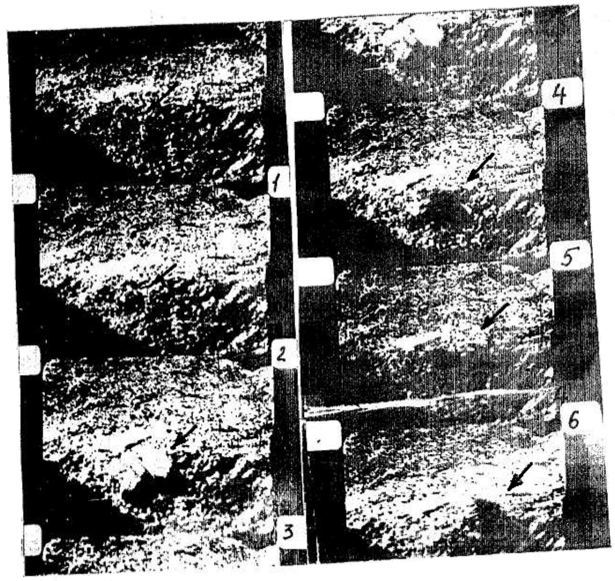

The fig. 7: Fragment of High-speed Filming of Destruction Process of a Teshenitny Coverings at the specific thermal stream equal $1,2\times10^6$ to W/m^2. Time of formation of a particle (particles) the size $2,5\times10^{-3}$ m makes 2,2 pages. The line of destruction of "equal opportunities" is accurately visible.

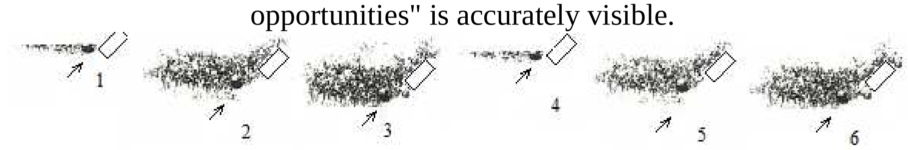

To figure 7. Flight of a broken particle (particles)

CONCLUSIONS

1. The drawn analogy in processes of weak destruction of non heat-conductors capillary and porous coverings and metals, allows us to establish the nature of materials and their behavior, depending on specific thermal streams, time of their influx, the sizes of coming-off particles of a destroyed material and the depth of penetration of thermal waves in studied materials. In the mechanism of a limit condition of a surface, the role of thermal tension of compression and stretching comes to light.
2. Dynamics of tension in the life cycle of the steam phase and the model of development of steam bubbles show the real sources of concentration of destructive thermal tension up to emergence of fatigue cracks of the critical (destructive) sizes.

References

[1]. Polyaev V. M., Genbach A.A. the growth rate of steam bubbles in porous structures//News of higher education institutions. Mechanical engineering. -1990. No. 10. – P. 56-61.

[2]. Polyaev V. M., Genbach A.N., Genbach A.A. a limit condition of a surface at thermal influence//TVT. -1991. – T.29, No. 5. – With. P. 923-934.

[3]. Polyaev V.M. Genbach A.A. Control of Heat Transfer in a Porous Cooling System//Second world conference on experimental heat transfer, fluid mechanics and thermodynamics. -1991. – Dubrovnik, Yugoslavia, 23-28 June. – P.639-644.

[4]. Polyaev V. M., Genbach A.A. management of internal characteristics of boiling in porous system//Cryogenic equipment and conditioning: Sb.Trudov of MGTU. 1991. – P. 224-237.

STUDY OF THE CONDITIONS OF FRAGILE FRACTURE OF CAPILLARY-POROUS COATINGS IN THERMAL POWER PLANTS

Alexander Alexievich Genbach[1], Vera Orazievna Baibekova[2], Iliya Iliev[3]

ABSTRACT

The conditions of the destruction of fragile capillary - porous coatings were investigated. The traditional approach shows two basic conditions of destruction: tensile stresses and shift. However, only destructive pressure of compression occurs to cover with granite $t = (0,1 \div 1)$, and only when $t \succ 1$c, in some region $\Delta \approx 0,6 \cdot 10^{-2}$ m, they pass into the tensile stresses in a very short period. To cover granite intervals of heat flows within which there is such destruction will be: $q_{max} = 1 \cdot 10^7$ Vt/m²; $q_{min} = 2,1 \cdot 10^5$ Vt/m².

1. INTRODUCTION

Capillary-porous coating can be used to create high-intensity and high-cooling systems. Coatings are applied to the boiling surface. Due to the mass and capillary forces, a cooler is supplied to the coating. A physical model of the processes of heat and mass transfer may look as shown underneath in Fig. 1[1-9].

The normal process of cooling can be violated in case of a heat transfer crisis occurrence (termination of a supply cooler, ultra-high heat fluxes) [9]. The coating can then start to degrade.
Of interest to the simulation of the destruction process is the investigation of the behavior offragile capillary-porous coatings, which will allow relatively low heat fluxes and temperature to identify the mechanism of the destruction process.

A variety of rocks that are whether easily or intricately destroyed by the heat flow through the surface installation can be used as simulating fragile coatings, or in the case of direct exposure by flame burners, including high-temperature supersonic.
Currently, there are is a significant number of works devoted to the exploration of the mechanism of rock failure by thermal method burner of missile type, criteria for thermo destruction.

2. METHODOLOGY

The works devoted to the theory of thermal destruction, which gives an opportunity to explore the impact of certain physical properties of rocks, physical and chemical processes as well as properties of the high-temperature supersonic gas flow process.

During the thermal destruction of rocks some regions of the surface coating are exposed by a burner, resulting in part of the surface rocks being heated to the temperature Ts, whilst in other parts of the rocks the temperature remains T0. Under the irradiated surface of the rocks the temperature gradient ascends, as a result of which the rocks unevenly expand.

[1] Professor Dr.Sc., AUES, Kasachstan, katerina-1@rambler.ru

[2] Ph.D. Student, AUES, Kasachstan, vera0382@mail.ru

[3] Professor, PhD, Ruse University, Ruse, Bulgaria, e-mail: iiliev@enconservices.com; cell phone: +359 887306898

Surrounding unheated layers are able to countervail this expansion. As a consequence thermal stress occurs both in the heated part of the rocks, and in like manner in the surrounding unheated array. That stress can reach annihilative values.

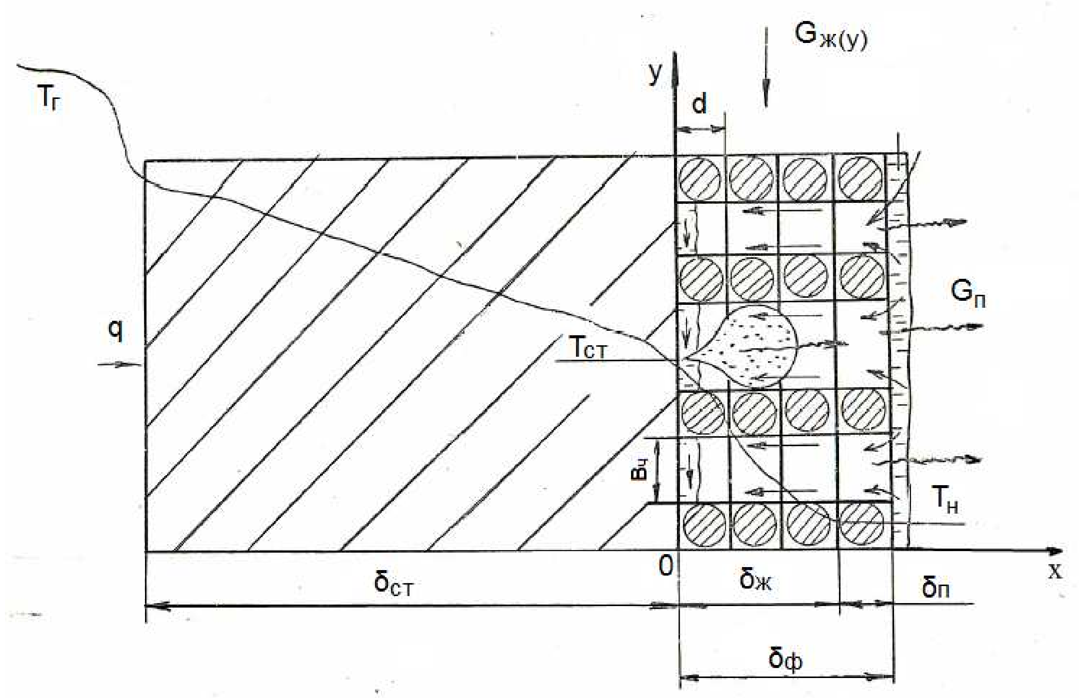

Figure 1. Physical model of the processes of heat and mass transfer in porous structure, covering the cooling surface: straight lines - fluid flow; wavy line - pair movement: q is the heat flux; Tg, TST,Tn-temperature of gases, walls, saturation; Gж ,Gп - consumption of liquid and vapour; δст, δф , δж , δп-width of the adjacent surface of porous coatings, liquid and vapour; VG, d - cell width of porous coating and the diameter of pores.

The rate of the temperature increase on the irradiated high-temperature jet surface is proportional to the difference of the final temperature Ts and current T,moreover according to one of the models,one can assume that the temperature of the heated surface changes with regard to the following law:

$$T = T_0 e^{-kt} + T_S (1 - e^{-kt}),$$

where K- coefficient; t-time.
If the rocks were to expand freely without resistance, then there would not be any strain inside, as the reason for its appearance is the resistance of the surrounding materials extension.

$$l_{св} = \alpha L (T - T_0),$$

where lсв - increment coverage L; alpha - coefficient of linear thermal expansion. Stress caused by the heating (or cooling) of rocks, are considered as temperature (thermal). The utmost stress may be observed if the ends of the rod (the model of the rock) are ??? fixed

$$\sigma_{\max} = -E \frac{l_{св}}{L} = -\alpha E (T - T_0),$$

where E - module of elasticity.
In fact, the rod is lengthened with l, which is less than $l_{св}$

$$l = l_{св} - l_{сж},$$

$l_{сж}$- the result of a compressed rod,surrounding rocks

$$l_{сж} = -\frac{1}{E}\sigma_T L,$$

$\sigma_T -$ thermal stress compression. Then

$$l = l_{св} - l_{сж} = \alpha L.$$

$$\sigma_T = -E\left[\alpha(T - T_0) - \frac{l}{L}\right]$$

Since the stress caused by the heated surface is always compressive and compression strength is higher than tensile strength and shear, it could be expected that the destruction will be called by the final stresses that really formed in the rock.
We should mark out two layers or rod (one makes to another bottom). Tensile σ_P stress will arise in the lower terminal when heated i.e.

$$l_1 = \alpha_1(T_1 - T_0)L - \frac{1}{E_1}\sigma_1 L;$$

$$l_2 = \alpha_2(T_2 - T_0)L - \frac{1}{E_2}(\sigma_2 - \sigma_p).$$

But $l_1 = l_2$ and $\sigma_p \equiv \sigma_{растяг}$;

$$\frac{\sigma_p}{E} = \Delta\left\{\alpha(T - T_0) - (\frac{\sigma_T}{E})\right\}.$$

More precisely

$$\frac{\sigma_p}{E} = l_x[\alpha + (T - T_0)\frac{\partial\alpha}{\partial T} - \frac{\partial}{\partial T}(\frac{\sigma_T}{E})]\frac{\partial T}{\partial x},$$

Where E – module of elasticity;

α – coefficient of linear thermal expansion;

l_x - factor, with dimension of length and modulo equal to one.

The aforementioned ratio shows that tensile stress σ_P increase with the growth of the temperature gradient, provided that the coefficient of linear expansion also increases with the temperature. $\left(\frac{\partial\alpha}{\partial T} \succ 0\right)$.

The condition of the destruction of tensile stresses is as follows:

$$\frac{P_1}{E} \le l_x[\alpha + (T - T_0)\frac{\partial\alpha}{\partial T} - \frac{\partial}{\partial T}(\frac{\sigma_T}{E})]\frac{\partial T}{\partial x}$$

P_1 – the limit of the tensile strength.

Tension strains can cause gaps in coverage in the form of cracks, located in planes, which areperpendicular to the surface; these cracks are not decisive in the sense of the thermal destruction. Moreover, it hampers the process of thermal destruction, namely the separation of plates on the planes parallel to the surface rocks. Such plates may be separated as a consequence of deformation and shift. The shear τ is calculated by the law:

$$\tau = G\gamma = G\frac{l_1 - l_2}{\Delta x} = G\frac{\Delta l}{\Delta x}$$

Δx – thickness of deformed layer;

G - shear modulus.

Then $\tau = G\frac{\partial l}{\partial x}$ substituting *l, we get the following*

$$\tau = GL\frac{\partial}{\partial x}\left[\alpha(T - T_0) - \frac{\sigma_T}{E}\right]$$

So, for shearing stress

$$\frac{\tau}{G} = L\left[\alpha + (T - T_0)\frac{\partial \alpha}{\partial T} - \frac{\partial}{\partial T}\left(\frac{\sigma_T}{E}\right)\right]\frac{\partial T}{\partial x}$$

i.e. shear stress has the property to accumulate ($\tau \sim L$).

The condition of the destruction by shift

$$\frac{P_2}{G} \leq L\left[\alpha + (T - T_0)\frac{\partial \alpha}{\partial T} - \frac{\partial}{\partial T}\left(\frac{\sigma_T}{E}\right)\right]\frac{\partial T}{\partial x}$$

P_2- tensile-shear.

Destruction leads to the appearance of cracks, parallel to the irradiated surface of the rocks. If we consider that the ultimate strength of rocks stretching P1 and shift P2 are the values of the same order, and P2 contains the length L, which is missing in the first condition (P1) and can take large values, it can be argued that the second condition (P2) can be performed more often than the first.

Progress in the research of thermo elasticity, photo-elasticity, holography and high-speed photography [1,3,5] allows to explain the mechanism of formation of thermal stresses, deformations [1], displacements and the emerging paramount efforts in capillary-porous coatings.

However, the magnitude of the applied specific heat fluxes qi, their duration t and depth of penetration z of temperature waves in thickness h of coverage will pose an influence onthe reasons for the destruction of the capillary-porous coating. This ultimate goal can be solved using the equation of unsteady heat conduction with boundary conditions of the second kind [2,3]. Figure 2 shows a plot of stresses over the thickness h of capillary-porous coatings, made of granite. Limiting heat flow, causing stress fracture melting, compression and tensile, respectively form q_1, q_2 and q_3, and voltages $\sigma_1, \sigma_2, \sigma_3$.

It turned out that the heat flux compression $q_2 \prec q_3$, than stretching, and a $q_1 \succ q_2$ and $q_1 \succ q_3$. Fig.2 shows the interrelation between the stresses of compression and tension inside coatings for various time intervals, beginning with the submission of heat flow. At small $t = (0{,}1 \div 1)$ c only pressure of compression occurs.

Starting with c $t \succ 1$c in a certain field $\Delta(z_i - h)$, equal to $6 \cdot 10^{-2}$ m, tension compression pass into the tensile stresses for a very short period of time, and for various intervals of time they are located at different depths of the surface of the capillary-porous coating. Most of the shear layers of coating will be observed in the transitional region of compressive stress in tension strains. Following some time, shear stresses reach their limit values later than the destructive stress of compression and, obviously, sometime before the maximum tensile stresses.

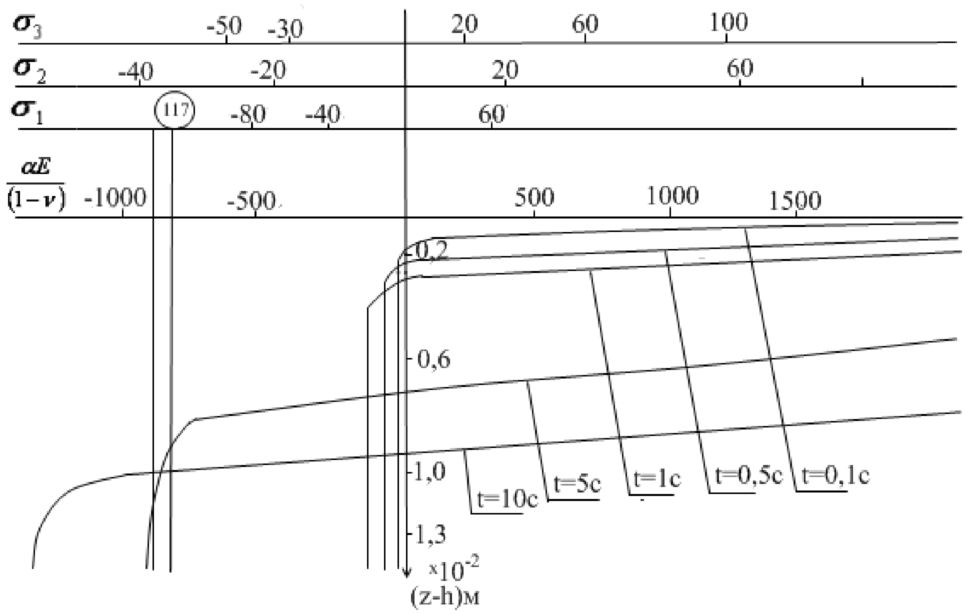

Figure 2. The stress distribution over the thickness of the coating in the form of a granite plate with different heat fluxes and time of their action: $q_1 = 0{,}142 \cdot 10^7$ Vt/m²; $q_2 = 0{,}042 \cdot 10^7$ Vt/m²; $q_3 = 0{,}075 \cdot 10^7$ Vt/m²; - limit of tensile strength: σ, x10^5, N/m^2; E, x10^5, N/m^2.

CONCLUSIONS

1. So the destruction of rocks under the action of compression forces occur much earlier in time than the forces of stretching. The destruction will probably take place under the action of compression forces and shift. To cover granite intervals of heat flows, within which such a destruction appears, will be: $q_{max}= 1 \cdot 10^7$ Vt/m²; $q_{min}= 2{,}1 \cdot 10^5$ Vt/m². Each thickness δ_i of the given particles under the action of compression forces meet their limits of heat flow, both within the given interval. For a cooled metal surface (see figure 1) in case of a violation of the operation of the cooling system $q_{min} = 1 \cdot 10^4$ Vt/m², and in the case of capillary-porous cooling system, employed by the combined action of capillary and mass forces ($\Delta P_{g+ кап}$), the value of $q_{мак} \approx (1 \div 2) \cdot 10^6$ Vt/m².
2. The role of compression stress grows with the increase of size q in the heated layer of the coating and consequently reduces the heating time t, despite of the fact that high compression resistance destruction from compressive stresses occurs instantly and in very small volumes in more auspicious conditions.

References

[1]. Polyaev V., Genbach A.N., Genbach A.A. An experimental study of thermal stress in porous material by methods of holography and photoclasticity // Experimental thermal and fluid science, avenue of the Americas.-New York, volume 5. Number 6, November.-1992.-P.697-702.
[2]. Genbach A.A., Burmistrov A.V. Investigation of the thermal condition of the cylinders of steam turbines// Industry of Kazakhstan, №2 (65).-2011. -P-93.
[3]. Poliaev V.M., Genbach A.N., Genbach A.A. Ultimate state of the surface of the thermal effects// Thermal physics of high temperature.-1991.-T, №5.-P-934.
[4]. Polyaev V.M., Genbach A.A. Control of Heat Transfer in a Porous Cooling System// Second world conference on experimental heat transfer, fluid mechanics and thermodynamics.-1991.-Dubrovnik, Yugoslavia, 23-28 June.-P.639-644.

[5]. Poliaev V.M., Genbach A.A. Management of internal boiling characteristics in porous system, Cryogenic equipment and air conditioning: Collected proceeding MSTU.-1991.-P-237.
[6]. Poliaev V.M., Genbach A.A. Management of heat transfer in porous structures// proceedings of the Russian Academy of Sciences. Power engineering and transport.-T, №6.-P 110.
[7]. Poliaev V.M., Genbach A.A. Heat transfer in porous system operating under combined action of capillary and gravitational forces, "Heat and power engineering.-1993, .№7-PP.-58.
[8]. Poliaev V.M., Genbach A.A. The Intensity of heat porous system in the gravitational field// School's news. Power Engineering 1993, №.1,2-P-95.
[9]. Poliaev V.M., Genbach A.A. Limiting thermal load in porous structures// School's news. Aerotechnique.-1991 №.1.-PP. 33-37.

CASE OF STUDY REGARDING THE ENERGY REQUIREMENTS FOR A MEDIUM RURAL HOUSEHOLD

Alexandru Gruia[1]
University of Craiova

ABSTRACT

The paper presents a case of study for meeting the energy demands for a medium rural household regarding the most accessible renewable energy resource.

1. INTRODUCTION

For many people living in remote areas, connecting to the main power grid is not an option or the costs of connecting tot the grid are very expensive. Therefore, they must produce their own power. Many people are resorting to petrol or diesel generators, but these are noisy, maintenance intensive and environmentally damaging. In more recent years, other cleaner forms of power generation have become available. The most known is solar power but there are other forms of generating power like wind power, water power, biogas that are becoming more common. Unlike fossil fuel powered petrol or diesel generators, these technologies are known as renewable energy. In this document is a comparison on the new types of renewable energy electrical generating technologies that can be used in a rural area household and can provide an independence of the grid. On the market there are a couple of new and green technologies that can solve the electrical energy requirements of a medium rural home. Electrical energy generation is more problematic than thermal energy generation in a rural household because the thermal energy requirements in a medium rural area household are achieved by using biomass that can be found in the area such as: wood, straw, corn cobs. That can be burned in a stove, fireplace, heater to produce thermal energy for cooking and heating.

2. METHODOLOGY

The electrical energy requirements of a medium rural household are about 283kw/month this means 9,43kw/day. But this consumption can be lowered by 30% using more energy efficient light bulbs and appliances. The drawbacks in this new technologies is the price than can be higher than the normal cost of the power consumed of the grid over a period of 20 years which is the guaranteed lifespan of a renewable energy system. The advantages are that this form of producing is green and has smaller carbon foot print than conventional energy use and you will not be defendant on the electrical company for power.

Solar energy is the most used electrical energy generating technology. Solar power generates electrical and thermal energy; the electrical power is generated via photovoltaic panels. This technology works by converting solar radiation in to direct current electricity using semiconductors. This is done by using the photovoltaic effect of the semiconductors materials. The solar panels are made using a series of solar cells that contain photovoltaic material. The majority of cells are made of water based crystalline silicone or thin film cells based on cadmium telluride or silicon. The panels that are usually sold now are of two

[1]Craiova, 0767140877, gruia.alexandru87@yahoo.com

typesmonocrystalline and policrystaline the first is more expensive and has an efficiency of 15-18% the others are less expensive and have o efficiency of 13-15% and the power varies from 30w to 300w per module.

The solar panels can be mounted on a fix mounting system or a mobile 1axis system that it is linked to a sun tracker, this will increase the efficiency of the panels by 20%. Using an off-grid system will require a regulator and a battery pack to store the energy produced by the system. The system will require an inverter to convert the DC current that the panels generate to AC current that is used on household appliances; the power of the inverter is calculated by the power of the solar system. To achieve total Of-grid independence you would need a solar system to produce 3396kw/year. But considering than in the winter the system has a lower efficiently, the system should be a 5000kw/year system which has a medium price of 12000€.The price in Romania is 11€/100kw this means 31,13€/month= 373,56€/year power consumed by the household in 1 year if we make a calculus it will mean that the system will be paid in 32,1 year. This is inefficient because the system is rated for 20 years. In extreme weather conditions like a week of clouded sky the batteries may be depleted an you may need a backup generator to power the system which will raise the cost of the entire system and you would need also to buy fuel for the generator which will raise the of producing the power. Also the system is prone to problems in hail storms or heavy snow falls.

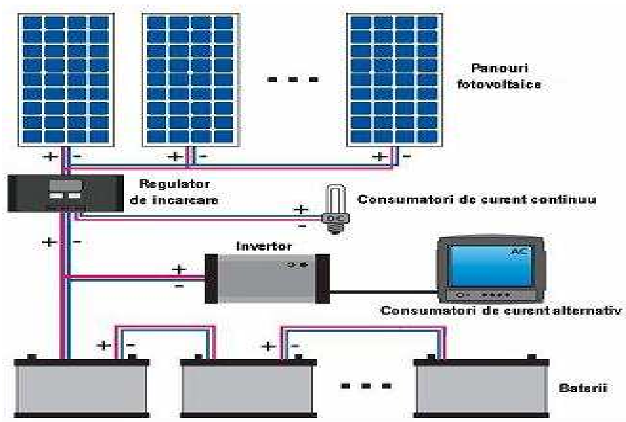

Figure 1: Solar energy system

Wind powered is the conversion of wind energy in to electrical energy using wind turbines. Wind turbines convert kinetic energy to electrical energy that it is used to charge the batteries. Modern turbines are manufactured in variable sizes and being vertical or horizontal axis design. A wind powered turbine can extract 59% from the total kinetic energy of the air flowing through the turbine, this is the maximal achievable extraction of wind power according to Betz' law , that the conservation of mass requires as much mass of air exits the turbine as it enters it. But the efficiencies of a modern wind turbine is at 75% of the Betz limit for the wind power extractable at rated operational speed because there are loses in the blade rotor friction and drag, generator and convertor loses, gearbox loses. The small wind turbines are for household uses because there are of a small size are more cost effective than the large commercial wind turbines used in wind farms .The small scale turbines have a range from 2m to 7.5m in diameter and produce rated electricity from 300 to 10000 watts at rated optimal wind speed. The vast majority of small wind turbines are horizontal axis turbines. The generator of a small wind turbine produces AC current that is converted in to DC current to charge the batteries. The small wind turbines use dynamic braking to regulate their speed at high wind speeds. For a small wind turbine the size of the tower varies from 7m to 15m and it must be placed at a distance from 150m from any object higher than the turbine. The components of a small wind turbine design for household of grid use are: The upper part of the turbine composed of the blades and housing which has the rotor, gearbox, generator, convertor, the pole upon the housing sits the charger and the inverter that convert the current from the generator to the battery pack and household electrical grid. To produce electrical energy for a medium household you would need 5000kw/year system. The medium costs of the system are 11000€ including the montage. The price in Romania is 11€/100kw this means 31,13€/month= 373,56€/year this means that the system will be paid in 29,9 year. This is inefficient because the system is rated for 20 years. In extreme weather conditions like a week without wind the batteries may be depleted an you may need a backup generator to power the system which will raise the cost of the entire system and you would need also to buy fuel for the generator which will raise the of producing the power. Also the system is prone to problems in heavy wind and to be used as a standalone system you would need to live in an area with constant wind activity.

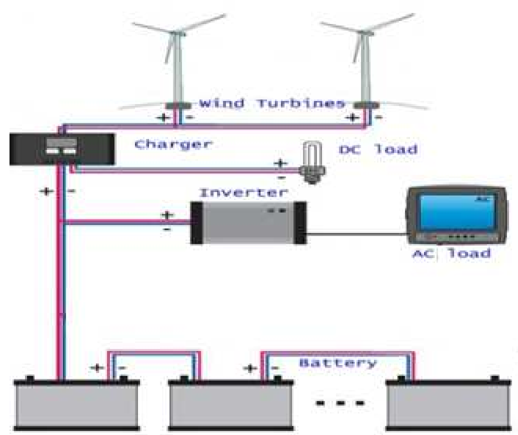

Figure 2: Wind turbines system for producing electricity

Water based electricity producing systems, if the local area has a stream or a river flowing near your house you can harness the power of the flowing water to create a micro hydroelectric plant. In our country approximately in any village there is a stream of water that passes it. This type of system can be created to provide auxiliary power and can be linked to photovoltaic system of a wind turbine system. The water flow can be harvested in a couple of ways the first would be that you make a small channel of water that runs along the river. The channel would have to have a drop from whom the water would be channeled in to a funnel that will turn a turbine linked to a generator and then the water that passed the turbine should flow back in to the river. The generator would be linked to a charger and then to the batteries. This system can be linked to a 150w up to 600 w generators depending on the water speed and flow. This system has reduced costs but depends on the position and the flow of the river. The other option is to build a micro dam and a micro basin like a miniature hydro plant and have the water funneled to a small turbine that will be linked to a generator. The cost of this system would be higher because you would have to build the dam out of concrete and you have to dig the small basin, but it can have a larger generator an you can produce more power, if you have enough river flow you can power the entire household. The system would provide the most power in spring and fall; it can be affected by drought in the summer and freezing in the winter. This system can be used as an auxiliary system in hybrid system with classic generators and wind turbine systems, it can’t be used so well with solar systems because in the winter booth system will have a small efficiency and you would need a fuel generator.

The cost of these systems can’t be approximated because they depend on the landscape, position and power requirements of the household.

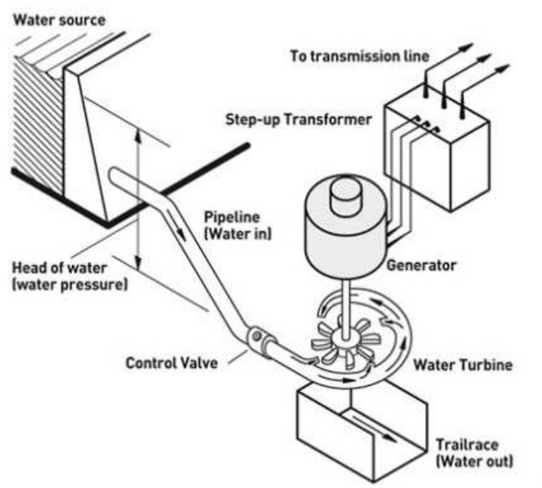

Figure 3: Water based system for electrcity generation

3. CONCLUSIONS

To make a system that would be cost efficient we would need to build a hybrid system that will combine more than one system. A combined solar and wind energy will reduce the cost of the system because it will share some of the components like the battery back and inverter. If we used a hybrid system we would need a 4500kw/year system because it can work independent. A 3000kw/year system has a medium cost of 5000€ and a wind turbine of 1500kw/year has a medium cost of 2000€ and you can ad for extreme situations a 3,5kw generator which is 500€ the cost of the whole system would be 7500€. This means 7500€/375,33€ year = 19,98 years the system will be played by the power consumption made. This system is cost efficient. The prices of On grid power is also staidly rising and the system may pay itself sooner than 20 years. This calculation is made without adding the cost of a linkage to the power grid which is about 1000 € if the house is near the power grid and it will be much higher if the household is further from the grid. The balance in powers of the components on the system may vary according to the geographical location of the household. In an area with more wind activity the power of the wind turbine may be grater that of the photovoltaic system or the power of the system may be smaller if you use other auxiliary systems like a micro hydro plant or the backup generator may run on biogas from a small biogas plant. If the you would use more energy efficient appliances and rationing the energy consumption of big energy consumers the yearly consumption cam be smaller an the size of system can also be smaller.

References

[1] Houston C., Gyamfi S., Whale J., *Evaluation of energy efficiency and renewable energy generation opportunities for small scale dairy farms: A case study in Prince Edward Island, Canada*, Renewable Energy**,** volume 67, July 2014, Pages 20–29

[2] Ding W., Wang L., Chen B., Xu L., Haoxu L., *Impacts of renewable energy on gender in rural communities of north-west China*, Renewable Energy**,** volume 69, September 2014, Pages 180–189

[3] Cotana F., Belardi P.,Petrozzi A., *TIAR: Renewable Energy Production, Storage and Distribution; A New Multidisciplinary Approach for the Design of Rural Facility,* Energy Procedia**,** volume 45, 2014, Pages 323–332

SIMPLIFIED METHODOLOGY FOR MONITORING AND ASSESSMENT OF THE EFFECT OF ENERGY SAVING MEASURES IN PUBLIC BUILDINGS

Veselka Kamburova , Ruse University; Iliya Iliev , Ruse University; Angel Terziev, Technical University of Sofia

ABSTRACT

The object of the study is development of simplified methodology for monitoring and assessment of the effect of implemented energy efficiency measures in public buildings.

Several EU programs provide funds for the implementation of energy efficiency measures in public buildings. When applied beneficiaries provide energy audits with estimated energy savings based on which base they are selected.

After the implementation of energy efficiency measures in order to justify the savings a monitoring is needed. The report proposes a simple methodology for energy monitoring in buildings with various types of heating - central heating, electricity, light fuel oil, gas and biomass boilers.

The methodology is consistent with the beneficiary's education background in the field of energy. However the presented methodology gives complete information to verify the foreseen in the audits savings through the introduction of energy efficiency measures.

1. INTRODUCTION

The goal of sustainability in the building sector requires a tremendous effort to reduce energy demand, boost energy efficiency and increase the share of renewable energy sources. According to the analysis made, buildings are one of the largest energy consumers. Summarized data for the European Union show that 40% from the entire energy consumption comes from the 160 million existing buildings in Europe and 3/4 from the consumed energy is used for heating and cooling.

The households and business in Bulgaria consume considerably more energy for heating and cooling compared to other countries in Europe. According to the Agency for Sustainable Energy Development (ASED) the consumption of energy in the housing sector is more than1/3 from the entire energy consumption in the country.

Several EU programs in Bulgaria provide funds for the implementation of energy efficiency measures in public buildings. The main purpose of these measures is to reduce energy demand in the buildings.

2. MEASUREMENT AND VERIFICATION OF ENERGY SAVINGS

Energy savings cannot be measured directly. In general, the energy-saving can be calculated as the difference between the consumption according to the energy efficiency measures (EEM) and the consumption prior to the energy efficiency measures implantation.

$$AES = BLEU - PREU \ , \tag{1}$$

where AES - annual energy saving, BLEU - baseline energy use or demand, PREU - Post-retrofit energy use or demand.

The baseline energy use presents the energy consumption by the building for a certain period in the pre-retrofit period. Selection of the period and duration of the baseline period is an important decision to be made during the savings determination process. The baseline period must end before the period of implementation of the energy efficiency measures so the data for the baseline period must not include any measurements taken during the installation period.

The post-retrofit energy period includes the data for the energy consumption that are collected after the implementation of energy efficiency measures. The defined post-retrofit period is usually called “performance period”, which can vary from about two weeks to 12 months, depending on the type of energy efficiency measures and technology [2].

Power consumption, however, depends on different variables like weather, usage or occupancy of the building, which makes a direct comparison difficult since it might not be obvious if the observed difference is caused because of implementation of energy efficiency measures or other effects. At best case the two periods which is to be compared should have the same conditions (e.g. for the same time of the year with the same weather conditions). Where this cannot be achieved, suitable adjustments have to be made.

$$AES = BLEU - PREU - A, \tag{2}$$

where A is the adjustment.

The calculation of baseline can start with short-term or continuous measurements of key operating parameter(s) (sub-metering energy efficiency measures affected system), consumption measurements of the entire building and calibrated simulations.

The methodology to be used for determination of the baseline and to make the necessary adjustments should be easy to implement, deliver accuracy, useful and transparent results and – quite important – has to be adaptable for this type of project.

Measurement and verification (M&V) methods are used to measure and verify, in a defined, rigorous and transparent way, the energy savings resulting from the implementation of energy conservation measures, that have been planned and designed to improve the energy performance of a specific facility or group of facilities. This is done without regard to the energy performance of any facility other than the one at which a change in energy infrastructure is implemented. M&V provides certainty that reported results are real and verifiable.

The four approaches to determining savings use similar concepts in savings computation. They differ in their ways of measuring the actual energy use and demand quantities to be used in savings determination. This clause summarizes the three approaches for determination of energy and demand savings [1, 3].

A. Partially Measured Retrofit Isolation. Savings are determined by partial field measurement of the energy use of the systems to which an energy conservation measure was applied separate from the energy use of the rest of the facility. Measurements may be either short-term or continuous. Partial measurement means that some but not all parameters may be stipulated, if the total impact of possible stipulation errors is not significant to the resultant savings. Detailed review of energy conservation measures design and installation will ensure that stipulated values fairly represent the probable actual value. Stipulations should be shown in the M&V Plan along with analysis of the significance of the error they may introduce. The energy savings are defined through the simple engineering calculations for short term or continuous post-retrofit measurements and stipulations.

B. Retrofit Isolation. Savings are determined by field measurement of the energy use of the systems to which the energy conservation measure was applied separate from the energy use of the rest of the facility. Short-term or continuous measurements are taken throughout the post-retrofit period. The energy savings are obtained by engineering calculations using short term or continuous measurements.

C. Entire Facility. Savings are determined by measuring energy consumed by entire facility level. Short-term or continuous measurements are taken throughout the post-retrofit period. The energy savings are obtained by analysis of whole facility utility meter or sub-meter data using techniques from simple comparison to regression analysis. Energy consumption is defined through the gas and electric utility meters for a twelve month baseline period and throughout the post-retrofit period.

D. Calibrated Simulation. Savings are determined through simulation of the energy consumption of separate measure or the entire facility. The accepted simulation procedures must demonstrate adequately the actual energy consumption in the facility. This option usually requires considerable skill in calibrated simulation. The energy savings are obtained by energy use simulation, calibrated with hourly or monthly utility billing data and/or end-use metering. Multifaceted energy management program affecting many systems operating in a building where no baseline data are available. Post-retrofit period energy consumption is measured by the gas and electric utility meters. Baseline energy consumption is determined by simulation using a model calibrated by the post-retrofit period utility data.

Options A and B focus on the performance of specific ECMs. They involve measuring the energy consumption of systems affected by each ECM separately from the rest of the facility. Option C focuses on the energy savings for the entire facility. Option D is based on simulations of the energy performance of equipment or entire facilities to enable determination of savings when baseline or post-retrofit data are unreliable or unavailable.

3. METHODOLOGY FOR ASSESMENT THE SAVING OF ENERGY EFFICIENCY MEASURES FOR PUBLIC BUILDINGS

As it was noted above several EU programs in Bulgaria provide funds for the implementation of energy efficiency measures in public buildings. The main purpose of these measures is to reduce energy demand in the buildings. The common measures are as follow:

- Replacement of windows;
- Thermal insulation - rehabilitation of walls;
- Thermal insulation - rehabilitation of roofs/attics;
- Thermal insulation - rehabilitation of floor;
- Replacement/modernization of the heating system;
- Energy efficient optimization of the electrical system.

The four first energy efficiency measures are related with the building envelope which is composed of walls, floors, roof, doors, and windows. The effect from the implementation of each of those measures and on fifth measure defines the energy needed for heating and cooling.

The baseline for each building is preliminary defined in the prepared energy audits. The energy audits are prepared according on the European Standard ISO 13790:2004 through the specialized software EAB approved by SEDA for Bulgaria. Baseline was calibrated in relation with day degrees for the specific climatic database.

The main purpose of the monitoring is to determine energy savings regardless of the implemented energy efficiency measures.

The authors have extensive experience in the monitoring of the public buildings.

The first step of the monitoring procedure is development of M&V. The plan includes the following activities:

- Configuration and testing of the measuring equipment;
- Performance of series of tests on-site before installation;

- Installing of the equipment at the preliminary selected measuring points;
- Performing measurements and data collection;
- Checking the availability and reliability of the data collected during monitoring period;
- Testing the performance of the equipment after measurements are completed;
- Downloading and processing the data; and
- Saving the data on the computer.

The following measurements should be performed for 14 days during technical monitoring period:

- Flow rate heat pipe measurements;
- Heat pipe temperature measurements (in-flow and out-flow);
- U-value measurements;
- Boiler efficiency determination;
- Indoor temperature measurements;
- Outdoor temperature measurements; and
- Light intensity measurements.

As a result of performed measurements were obtained the data of: daily consumptions of thermal energy for heating the building, the average daily temperatures in the building, and average daily maximum and minimum outdoor temperatures in the technical monitoring period. The average daily temperature was calculated as a daily average of temperatures in reference rooms.

The indicator of the specific energy consumption per m^2 and degree hour (K_{TM}, kWh/m^2/DH) was calculated on the base of measurement data. This indicator is generally characterized by thermal-technical features of the observed buildings. Based on this, it is possible to further carry out analyses in terms of:

- comparison with other buildings that have similar purposes;
- comparison with the buildings with different structural and environmental characteristics;
- estimate (forecasts) of the consumption of thermal energy for heating reaching different levels of comfort in the building, different observation periods at different climate conditions.

The annual thermal energy consumption (Qg,a), calculates with the following relation:

$$Q_{g,a} = K_{TM}.A_g.DH_{g,a}\,, \tag{3}$$

where A_g - total heated area, $DH_{g,a}$ - average annual degree hours for the heating season, K_{TM} - heat transfer coefficient denoting the amount of heat transferred through the walls, windows, doors, and floors of the building.

Under the current methodology the consumption of the thermal energy of the building defines on the base of 14 days monitoring period and further multiplication for the entire heating period.

The Authors' experience shows that the proposed methodology gives good results and the deviations in determination of the consumed energy are negligible.

A disadvantage of the proposed methodology may be pointed the need of usage of specialized measuring devices and highly educated staff. Hence the relatively high price of the monitoring process.

Concerning current case this methodology is inapplicable because of the great number of buildings and the budget for the monitoring process is limited. It means that the mechanism of obtaining data during measuring period should be simple in order to be accomplished by non-professional in the energy area people.

In this case is very important the type of measuring devices the boiler room is equipped with and the boiler by itself. It is also should be proposed the different methodologies in accordance with specifics in heating the building.

In central heating systems in the boiler room is usually installed heating meter. The data about consumed thermal energy can be obtained directly without additional measuring devices. Collecting data can be performed daily or weekly. It is recommended to record meter readings daily at a certain hour.

When local heating system is available it is easier to measure the consumed amount of fuel (natural gas, LHO or wood pellets) than the consumed amount of energy needed for heating the building. The amount of the consumed fuel can be accounted on a daily bases with gas meter or level of the LFO in the tank. Concerning this the thermal energy supplied to the building needs to be calculated on the base of boiler efficiency and the fuel caloricity. The caloricity of the fuel during the heating season changes insignificantly. The boiler efficiency defines at the beginning of the heating season when adjusting the burner.

The results of the monitoring needed to be filled in the preliminary prepared table (Table 1). Thus can be account the real consumption of heat energy and the amount of fuel for heating the building neglecting the specific terms – thermal comfort and outdoor temperature.

It is highly recommended in the representative rooms in the building to be installed a several temperature sensors. The number of installed temperature sensors in the rooms should be at least equal to number of riser pipes coming from the distributing header. The temperature data need to be stored in the data loggers where the temperature readings are recorded at specified intervals and then averaged. That is the way to determine the daily average temperature.

The data about the outdoor temperature can be obtained either by direct measurements or the closest meteorological station. The temperature sensors measuring the outdoor temperature must not be installed on the facades adjacent to technical rooms, kitchens, heating devices and others where presence of huge amount of heat.

Based on the collected data about the internal and external temperature is possible to be calculated the day degrees then the measurements for the consumed energy are adjusted and the referent consumption of energy can be determined.

$$Q_{g,a} = \frac{Q_M . DD_{g,a}}{DD_M}, \qquad (4)$$

The resulting energy consumption for post retrofit period is compared to the base line identifying energy savings.

The obtained results of the energy monitoring should be deeply analyzed and compare with expected values calculated with the specialized software. In case of significant deviations needs to find the reason.

The most common reasons for deviation from predefined parameters according international experience are:

- Wrong set up of the thermostatic regulator;
- Wrong set up of the system for automatic control;
- Significant part of the windows that are left open;
- Damages in the regulating valves;
- Leakages in the distributing network;
- Damages in ventilating systems;

- Incorrect filling of the heating system causing air pockets into the system and the inability to maintain the indoor air quality and etc.;

In the weekly (manually or automatically) collection of data it is more easily to find the damages in the systems or in the set ups without leading serious financial consequences. This increase the quality of the performed analysis about annual energy consumption and the associated costs.

Table 1: Measurement Data

Data				
Outside temperature, ºC				
Average inside temperature, ºC **1. ....** **2. ....** **3..** **4..**				
Heat energy consumption, kWh				
Fuel consumption, (m^3, litters, kg)				

3. CONCLUSIONS

The simplified methodology for assessment of savings as a result of implementation of energy efficiency measures in public buildings is presented. The presented methodology is based on the collection of data for the consumed heat energy or amount of fuel and further correction with the information about the actual day degrees calculated after proper measurement of internal and outdoor temperature. The methodology is developed for the Beneficiaries who mostly are not professionals in the field. This methodology is simplified but still gives information about achieved energy savings.

References

[1] Guidelines for Verifying Existing Building Commissioning Project Savings, resources.cacx.org/library/holdings/

[2] International Performance Measurement & Verification Protocol Concepts and Options for Determining Energy and Water Savings, Volume I, International Performance Measurement & Verification Protocol Committee, 2002, DOE/GO-102002-1554

[3] Measurement of Energy and Demand Savings, ASHRAE Guideline 14-2002, ISSN 1041-2336

SCHEMES FOR PROJECT FINANCING OF COMBINED HEAT AND POWER PRODUCTION TROUGH BIOMASS GASIFICATION

Veselka Kamburova[1], Iliya Iliev[2], Angel Terziev[3]

Summary

The current report aims is to analyze the system for combined heat and power production through biomass gasification system. Special attention is paid on the process of synthetic gas production in the gasifier, its cleaning and further burning in the co-generation unit. A financial analysis is made regarding the investments and profits generated by the combined heat and power production.

A scheme for project financing, characterized by low interest rates, for funding of renewable energy sources by export credit agencies is analyzed. Comparison between the standard funding grant schemes and the project financing schemes was made.

The presented conclusions can be used for making important investment decisions on various renewable energy sources projects.

1. INTRODUCTION

Combined heat and power production process also known as cogeneration, is the simultaneous production of thermal and electric energy from a single fuel source (oil, gas, biomass, biogas, coal, etc.). Currently the CHP systems are affordable not only for commercial buildings but also for homeowners. The CHP engines producing electricity that can be internal combustion or Stirling engines. The micro-CHP installations applicable for residential buildings usually run on propane, natural gas, or even solar energy or biomass. The CHP systems offering combined heat and power have efficiency of approximately 90%.

Here is reviewed the CHP system by using biomass as a fuel source. The process of the syngas production is through biomass gasification. Currently such power plants produce up to 100 kW electric energy and 150 kW thermal energy. The calorific value of the syngas produced by the process of biomass gasification reaches up to 11 000 kJ/m^3 or more than double the values of autothermal gasification process. The total efficiency of the power plant is 81%, as cold gas efficiency is in the amount of 70%, electrical efficiency is 33% and thermal efficiency is 48%.

2. GENERAL INFORMATION ABOUT CHP POWER PLANT

The annual consumption of wood waste is 1,152 tons per year. The wood waste material is from wood industry. The wood material will be delivered to the plant's storage. A wheel loader will be used for filling the container (with volume of 12 t) with wood waste. The material will then be delivered by transport belt to each gasifier systems' hermetic storages (each 12 t load is capable of supplying raw material to the gasifier for 6 to 8 hours). The two gasifiers are filled

[1] Ruse, Bulgaria, e-mail: vkambourova@enconservices.com; cell phone: +359 885955347 Ruse University

[2] Ruse University, Ruse, Bulgaria, e-mail: iiliev@enconservices.com; cell phone: +359 887306898 Ruse University

[3] Technical University, Sofia, Bulgaria, e-mail: aterziev@enconservices.com; cell phone: +359 885955183

with dry wood material through feeding screws from the biomass storage. The heat needed for pyrolysis is delivered to the gasifier system using air ducts. Before reaching the gasifiers, the air passes through heat exchangers. The temperature of the air reaches up to 600ºC accelerating the gasification reaction and decreasing formation of dioxin.

The entire power plant consists of two different size gasifiers. The gasifier system with the capacity of 100 kW consumes 110 kg/hour wood waste and 190 kg/h air generating approximately 298 kg/h biogas. The gasifier for 30 kW installation consumes 34 kg/hour wood waste and 59 kg/h air generating approximately 91 kg/h biogas. The annual wood waste consumption of both gasifiers is 1,152 t/y. Combined, the gasifiers generate approximately 400 kg/h biogas. The components of the biogas generated in the gasifiers are shown on Table 1.

Table 1: Components of the generated biogas

The gas components					
CO	***H_2***	***CH_4***	***CO_2***	***N_2***	***H_2O***
20-21%	22-23%	1-3%	4-6%	48%	1-3%

3. THE PROCESS OF GASIFICATION AND CALCULATION OF ENERGY PRODUCTION

The purpose of the implementation of CHP system is the production of electric energy to be sold to the local electricity company at a preferential feed in tariff, and the production of thermal energy for selling to a wood waste delivery company and greenhouses.

The raw material is wood waste from the wood industry (branches, tree-tops, trunks, rind peelings and etc.) and wood pellets. The wood waste is delivered from the biomass storage to the gasifier. In bottom of the gasifier, the biomass is burned and in the top part, the biomass is heated for syngas production. Then the syngas is cooled with water before entering the cyclone filter. The cooled syngas passes through a cyclone filter where the hard particles like coke are separated from the gas. The exhaust gases from the burning process are filtered before being cooled. The hard particles, are separated from the syngas, are then returned for burning. The waste products of the chemical cleaning are separated in a settling tank and the particulate residue is returned to the burning chamber, while the remaining ester is delivered to the rinse. The exhaust gases of the gas engine's burning chamber, after cooling, pass through a cyclone filter where the ashes are separated from the exhaust gases. After filtration the cleaned exhaust gases are mixed with the exhaust gases of the gas engine and the combined exhaust gases are released through the chimney.

Cleaning of the syngas, after the gasifier, is according to the following cleaning system:

- *Cyclones* – used for separation of larger dust particles (98%) from the gas flow leaving the reactor zone.
- *Heat exchanger* – The gases are cooled by passive cooling tower. The temperature is reduced from 180ºC to 70 ºC;
- *10-micron filter* - The filter for the 30 kW system has 70 m^3/h capacity and for the 100 kW system has 200 m^3/h capacity. The filters also separate water and moisture from gases at a rate of 15 ml/h;
- *1-micron filter* - The filter is made by INFASTAUB and has a 70 m^3/h capacity (for the 30 kW installation) and 200 m^3/h capacity (for the 100 kW installation).

The biogas is burned in a gas generation module producing 130 kW electrical energy from the modules. The biogas produced by pyrolysis process is completely burned in the gas generators. The motors' manufacturer is GM and generator type is FLD274DL14 Stamford.
The technical parameters of the 100 kW gas engine and the electrical generator are as follows:

Electrical output (kVA):	109
Voltage (V):	*400*
Engine Type:	*GM*
Number of cylinder:	*12*
Engine speed (rpm):	*1500*
Fuel consumption:	*1kW/kWel*
Generator type:	*FLD274DL14 Stamford*

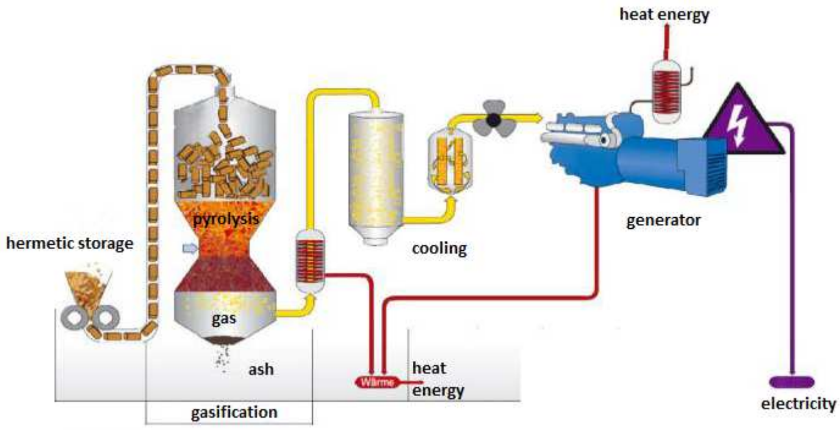

Figure 1: General Components of the Biomass Gasification Plant [1]

The installation will be used for combined thermal and electricity production.

This analysis assumes that 300 kg/hour of biogas is fired in the 100 kW generator and produces approximately, 307 kWh/hour. The electrical efficiency of the system is 39% thus the net electricity production is 100 kWh. The thermal efficiency of the system is 48 % so net thermal energy is 150 kWh. The thermal balance for the 100 kW biomass installation is presented in Figure 2.

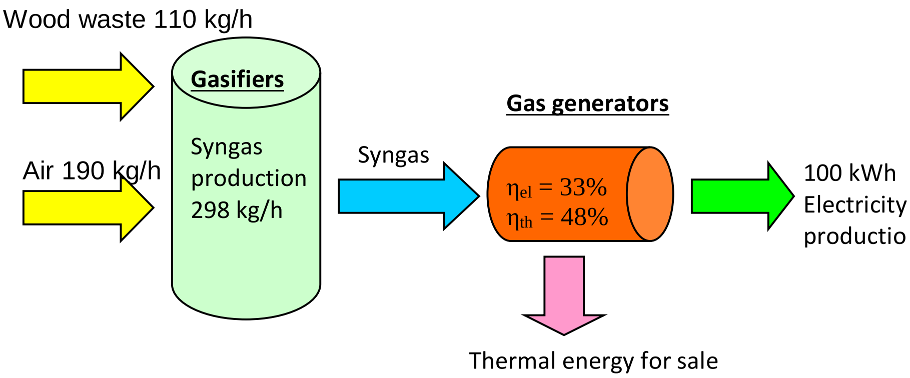

Figure 2: Thermal balances of the biomass installation [4]

4. FINANCIAL ANALYSIS

The profitability of a certain project depends not only by the technical parameters but also by the financing scheme. The funding method and the associated costs can sometimes make a good project unattractive to investors and prevent further implementation. On the other hand with suitable financing scheme a project with seemingly unprofitable and accompanied by high risks parameters can be implemented.

To be comparable here it is assumed that the lending period is 8 years (based on the simple payback period – the investment costs are in the amount of 622 500EUR and net savings are in the amount of 88 417 EUR) and the amount of credit is 100% of the investments.

Based on the abovementioned here an analysis of three possible financing schemes concerning the project have been studied and presented.

The first scheme is standard financial scheme with no extra terms for beneficiaries with annual interest rate in the amount of 8.0 %. The second scheme utilizes grant financing with a corresponding incentive of 15 % of the loan and the same financial terms (annual interest rate 8.0%) as first scheme. The third scheme is project financing under the credit line of Exim Bank in as much as the equipment is American.

Ex-Im Bank's "Renewable Express" is designed to provide streamlined post-completion project financing to small renewable-power producers that meet Ex-Im Bank's credit standards. This initiative meets the increased demand for financing of small renewable-power transactions.

- Ex-Im Bank's provides **medium and long-term direct loans and loan guarantees** to international buyers of the US equipment and related services;
- Ex-Im Bank's guarantees coverage for 100% of commercial and political risks;
- Ex-Im Bank's loans and guarantees cover 85% of the US equipment cost and up to 30% of local project costs (design, construction and installation works) and ancillary services such as financial, legal or local bank fees;
- No limits on transaction size. There is no minimum or maximum limit to the size of the export sale that may be financed with Ex-Im Bank's loan guarantee;
- Products must be shipped from the U.S. to a foreign buyer;
- Ex-Im Bank's loans and medium-term guarantees include repayment terms of up to 7 years for financed amounts of $10 million or less;
- Ex-Im Bank's medium-term guarantees and loans for projects that are over $10 million. Repayment terms are typically up to 10 years, but can be up to 12 years for large power plants and up to 18 years renewable energy and water sector exports;

- Direct Loan Costs
  - Letter of Interest processing fee - $100 (one-time payment);
  - An exposure fee based on risk (one-time payment)

Creditworthiness Group of Project Sponsors	Medium-Term 7-Years	Long-Term 10-years
State Owned Entities and Exceptionally Good Credit Quality Private Entities	4.74%	6.72%
Very Good Credit Quality Entities	5.53%	7.87%

Good to Moderately Good Credit Quality Entities	6.59%	9.41%

- Interest rate

Loan Terms	**Interest Rate**
Up to 5 years (including) ≤ 5 years	1.69%
Between 5 and 8.5 years (including)	2.58%
Between 8.5 and 12 years (including)	3.29%

Project financing differs with its substantially lower interest rate (with up to 4-5 percent points, in comparison with standard financing). Aside from that, the preferential prices of the regulatory organ are reduced with regard to the level of the incentive grant, and furthermore, the reduced price of the purchased electricity from renewable energy sources is effective during the whole period of 15-20 years. Consequently, that is why most companies circumvent grant financing. Below is provided the short financial analysis, concerning the project investments, cash flow generated by the power plant during the period of operation and operational and maintenance costs.

The allocation of sold heat production, electricity production, electricity own needs, wood consumption and O&M cost savings in Figure 3.

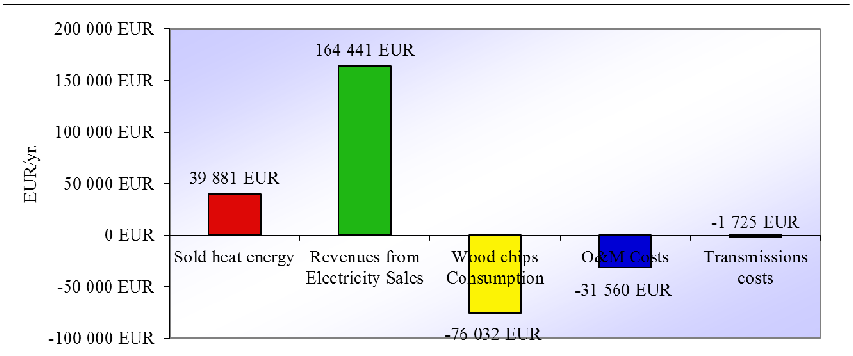

Figure 3: Allocation of sold heat production, electricity production, electricity own needs, wood consumption and O&M cost savings

The revenues from the purchase electricity produced by the power plant according the prices announced in the Resolution No Ц-018/28.06.2012 [3] of SEWRC.

The approximate base project costs are presented in Table 2.

Table 2: Base project costs

(EUR)		Design	Equipment	Total Project Cost
ECO	Implementation of renewable project producing heat and electricity from waste wood	49,200	573,300	622,500

The investments for the implementation of such systems are in the amount of 1 915 EUR/kW installed capacity.

The financial analysis was made for the abovementioned three financial scheme. The initial data for the analysis are as follow: 100% loan in the amount of EUR 622 500 and the loan is granted for a period of 8 years.

Liquidating plan was prepared for the three financial schemes. In the first funding scheme for a loan of EUR 622 500 for a period of 8 years interest payable amounted to EUR 201 275 or 32.3% of the loan amount;

In the second financial scheme the interest rate remain the same (8%) but in addition as a result of implementation of energy efficiency or renewable energy project 15% incentive grant of the loan is applied. Concerning this for the same loan amount the interest payable amounted to EUR 171 084 or 27.5% of the loan amount.

The last proposed financial scheme employs financing under the credit line of Exim Bank. Based on the terms of the Bank the proposed in the section 4 tables the interest payable amounted to EUR 64 911 (at 2.58% interest rate). The utilization of loan at lowest interest can be compared with obtaining grant in the amount of 67.8% of the loan amount. Even the requested loan to be for a period between 8.5 and 12years (interest rate in the amount of 3.29%) the interest payable amounted to EUR 103 254 or can be compared with obtaining grant in the amount of 58.9% (for a period of 10 years). The summarized results are presented in the table below.

Period, years	Loan amount, EUR	Interest payable at 8% interest rate, EUR	Interest payable at 8% interest rate and 15% incentive, EUR	Interest payable at 2.58% interest rate, EUR	Interest payable at 3.29% interest rate, EUR
8	622 500	201 275	171 084	64 911	
10	622 500	251 075	213 414		103 255

5. CONCLUSIONS

1. The caloricity of the produced syngas is higher than the gas obtained by the standard gasification process;
2. Higher efficiency (81%) of the CHP plant (33% electrical and 48% thermal efficiency) resulted in significant amount of thermal and electricity production, respectively considerable incomes;
3. The presented power plant is compact and has low operational and maintenance costs;
4. The proposed scheme of financing shows definitely better parameters of the project because of lower interest rate and higher purchase price of electricity due to absence of grant.

References

[1] Richard Drummond - Legal adviser, office of the general counsel, Export Credits Guarantee Department, UK, Role of Export Credit Agencies in Project Financing, ABA Section of International low, November 2008.
[2] Implementation of Renewable Project Producing Heat and Electricity from Wood Waste, Nova Energia Lozen Ltd, March 2013
[3] Resolution NoЦ-018/28.06.2012 of State Energy and Water Regulatory Commission, June 2012

PARAMETRIC INVESTIGATION STUDY OF COUNTER-FLOW EVAPORATOR FOR WASTE HEAT RECOVERY

Mahdi Hatf Kadhum Aboaltabooq[1], Horatiu Pop, Viorel Badescu,
Valentin Apostol, Malina Prisecaru, Cristian Petcu, Cristina Ciobanu
University Politehnica of Bucharest, Faculty of Mechanical Engineering and Mechatronics

ABSTRACT

Organic Rankine cycle system (ORC) may be used to recover waste heat from an internal combustion engine (ICE). The evaporator design in such a system is a very important task. For a successful ORC system, the amount of heat that can be received in the evaporator should be determined.

In this paper, the performance of a counter-flow evaporator used to recover exhaust waste heat from a diesel engine is presented. First, depending on the measured data, the exhaust heat of the diesel engine is evaluated. Then, a mathematical model of the evaporator is developed based on the detailed geometry and the specific ORC working conditions. The evaporator is subdivided into three zones, i.e preheater, boiler and superheater. The results show that the percentage heat flux for preheater zone is approximately 47.4% from total heat while for boiler zone it is 38.01% and for superheater zone is 14.59%. Furthermore, the heat transfer rate of each zone is proportional to that of the overall heat transfer rate when the engine operating condition changes. Consequently the percentage area for preheater zone is approximately 71% from the total area while for the boiler zone it is 26%; for superheater zone it is 3 % (in case of evaporation temperature 120ºC and superheating degree 10ºC). Results were compared with literatures and shows a very good agreement.

1. INTRODUCTION

One of the methods to improve the thermal efficiency of an internal combustion engine is the usage of, Organic Rankine cycles (ORCs) to recover the waste heat. Many studies analyzing the ORC performances have been conducted recently [1–7]. The available heat which is called as waste heat is transferred to the organic working fluid by an evaporator in an ORC, where the organic working fluid changes from a liquid state to a vapor state under a high pressure. Then, the organic working fluid, which has a high enthalpy, is expanded in an expander, and output power is generated. Therefore, the evaporator is an important part of the ORC for an engine waste-heat recovery system. In this study, the parametric investigation of a counter-flow evaporator designed to recover the exhaust waste heat from a diesel engine is evaluated theoretically. The working fluid R245fa is selected as the working fluid. A mathematical model of the evaporator is developed according to the detailed dimensions of the designed evaporator and the specified ORC working conditions.

2. SYSTEM DESCRIPTION

The schematic of an ORC for exhaust heat recovery of a diesel engine is shown in Figure 1. The pressure of fresh air is increased by the compressor. Then, the air enters the engine cylinders, which combusts with the injected fuel. After expanding in the cylinders, the high-temperature gas is exhausted to the turbine to be expanded further. In the turbine outlet, the temperature of the exhaust gas is still high between 170 ºC and 480 ºC depending on the load variations [8]. This high-temperature waste heat can be use as a heat source for ORC, for

[1]Splaiul Independenței 313, Bucharest 060042, Romania and Foundation of Technical Education, Technical College Najaf, Iraq, Tel. 0040734322783, e-mail: hatfmahdi@yahoo.com.

evaporating the working fluid in the evaporator. The evaporator, which will be used in this study is of counter - flow type.

3.NUMERICAL APPROACH

The approach used in this work draws inspiration from the work of Vargas et al. [9] where such an evaporator is assumed to be divided into three zones i.e. a preheater (Pr) , a boiler (B) and a superheater (Sp) as shown in Figure 2.

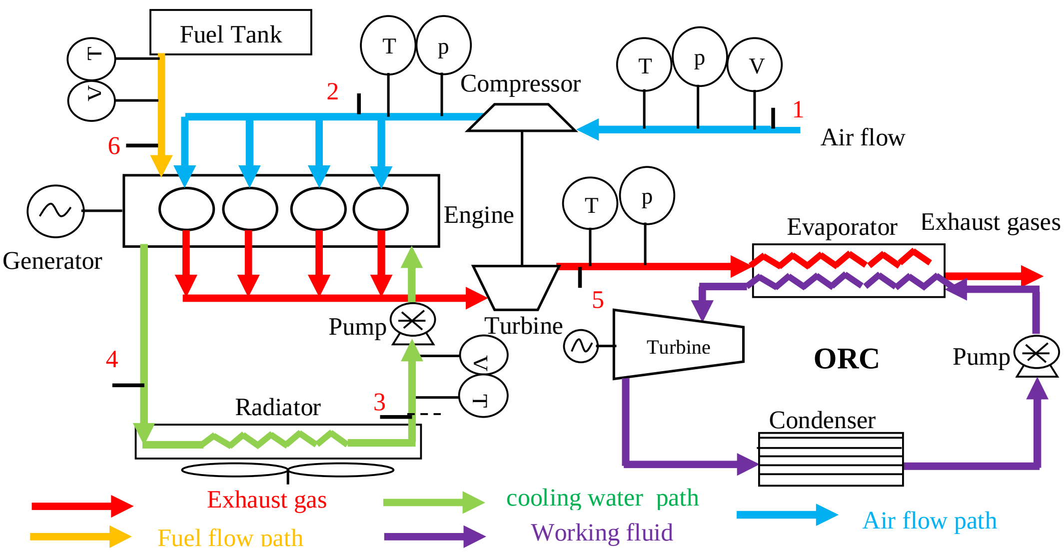

Figure 1: Schematic diagram for ICE and

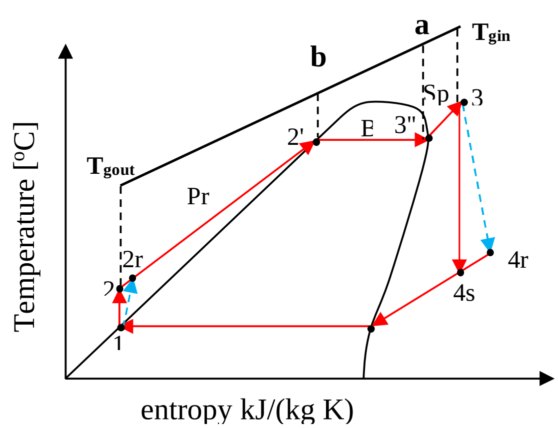

Figure 2: T-s diagram for ORC.

4. MATHEMATICAL MODEL

The mathematical model was developed based on a set of thermodynamic equations written for each zone of the evaporator and corresponding inlet and outlet parameters.

Firstly, the thermodynamic properties of the exhaust gas and the working fluids are calculated for each zone, based on the corresponding temperature and pressure levels.

Secondly, according to the energy balance, the heat transfer rate for each zone is obtained. Then, depending on the relative correlations, the heat transfer coefficients are estimated. Finally, the heat transfer area of each zone is determined.

The waste heat from exhaust gas can be determined as:

$$\dot{Q}_g = \dot{m}_g\, c_{p,g}(T_{g,in} - T_{g,out}) = \dot{m}_{ref}\,(h_{out} - h_{in}) = \dot{m}_{ref}\,(h_3 - h_{2r}) \quad [kW] \tag{1}$$

where $\dot{m}_g$ is the exhaust gases mass flow rate in [kg/s]; $\dot{m}_{ref}$ is the refrigerant mass flow rate in [kg/s]; h_3, h_{2r} are the enthalpies of refrigerant on the inlet to evaporator and outlet from evaporator, respectively in [kJ/kg K].$c_{p,g}$ is the specific heat at constant pressure of exhaust gases in [kJ/(kg K)] and $T_{g,in}$, $T_{g,out}$ are the temperatures of exhaust gases at inlet to the evaporator and outlet from evaporator, respectively in [K]. Table 1 shows the measurement data which are used in this study. The enthalpies of refrigerant on the inlet to evaporator (point 2r) and outlet from evaporator (point 3) depend on the properties of working fluid and can be calculated by using the EES program [10]. With some changes at equation (1), the refrigerant mass flow rate can be calculated as:

$$\dot{m}_{ref} = \frac{\dot{Q}_g}{(h_3 - h_{2r})} \tag{2}$$

The exhaust gases mass flow rate and the temperature of exhaust gases at inlet to the evaporator are calculate from experimental work as shown in Figure 1 [8] but the temperature of exhaust gases at evaporator outlet is assumed to be 140°C [11].

Table 1: Main parameters used in the study.

Property	Value	Unit
Exhaust gases temperature at inlet evaporator [$T_{g,in}$]	480	ºC
Exhaust gases temperature at outlet evaporator [$T_{g,out}$]	140	ºC
Exhaust gases mass flow rate [m_g]	192.6	kg/s
Expander efficiency [η_{ex}]	0.9	—
pump efficiency [η_p]	0.9	—
Ambient temperature [T_{amb}]	22	ºC
Inside diameter of evaporator inner tube [d_i]	0.08	m
Outside diameter of evaporator inner tube [d_o]	0.09	m
Outside diameter of evaporator outer tube [d]	0.1	m

The specific heat at constant pressure of exhaust gases is depending on the medium temperature for each zone and the percentage volume of components for exhaust gases and is determined from Ref.[12,13,14]. Now the heat transfer rates of all zones are obtained from the following equations:

$$\dot{Q}_{pr} = \dot{m}_{ref}\,(h_2' - h_{2r});\dot{Q}_b = \dot{m}_{ref}\,(h_3'' - h_2');\dot{Q}_{sp} = \dot{m}_{ref}\,(h_3 - h_3'')\ [kW] \tag{3}$$

There are two sides in evaporator tube; the refrigerant side and exhaust gases side, so many equations are used to determine the heat transfer coefficients [15,16,17]. Then the overall heat transfer coefficient is determined as:

$$U_{overall} == \frac{H_{ref} * H_g}{H_{ref} + H_g} \tag{4}$$

The log mean temperature difference (LMTD) method is often used to predict the performance of a heat exchanger [18]. The LMTD is defined as:

$$\Delta T_{m,j} = \frac{\Delta T_{max} - \Delta T_{min}}{\ln\left(\frac{\Delta T_{max}}{\Delta T_{min}}\right)} \tag{5}$$

Then, the heat transfer area for each zone is calculate as:

$$A_j = \frac{Q_j}{U_j \, \Delta T_{m,j}} \tag{6}$$

where j represents preheater or boiler or superheater zones.

5. RESULTS

Based on the mathematical model, a program has been developed in EES [10,13]. The program input data is from Table 1. The results are presented in Figures (3-6). From Figure 3 it can be observed that the amount of heat for preheater and boiler zones decreases with superheating degree and for superheater zone is increasing. In conditions of constant heat input in the evaporator, the superheating increase leads to a increase of the heat received in the superheater zone and a corresponding decrease of the heat input in the preheater and boiler zones. Also, the percentage heat flux for preheater zone is approximately 47.4% from total heat while for boiler zone it is 38.01% and for superheater zone is 14.59% (with 30 ^{o}C superheating degree).

Figure 4 shows effect of inlet turbine temperature (ITT) on the heat flux for each zone of evaporator. It can be seen another style which is the heat flux for preheater and superheater zones is increasing with (ITT) but the heat flux for boiler zone is decreasing.

Figure 5 shows effect of superheating degree on the area for all zones. It can be observed from this figure that increase in superheating degree leads to increase in the area of superheater and preheater zones while the area of boiler is decreasing. The high value is for preheater zone while the lower value is for superheater zone. In another side the effect of (ITT) on the heat exchange area of each zone is shown in Figure 6 and from this figure it can be seen a slight increase in area of superheater zone with (ITT) but in preheater zone there is marked increases. In another way in the boiler zone the area is decreasing.

From Figure 7 it can be observed that the overall heat transfer coefficient for all zones is decreasing with superheating degree and the high value is associated with the boiler zone while the lower value is for preheater zone.

Finally the effect of ITT on overall heat transfer coefficient of each zone can be seen in Figure 8 and clearly shows a slight increasing in preheater zone and high increasing in superheater zone while decreasing in boiler zone.

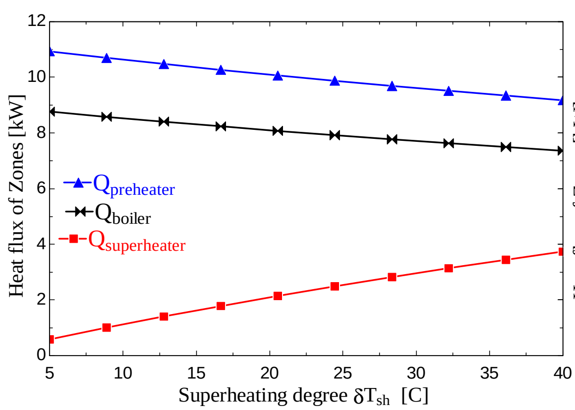

Figure 3. Effect of (SD) on the heat flux at T_c=27^{o}C T_{ev}=120 ^{o}C.

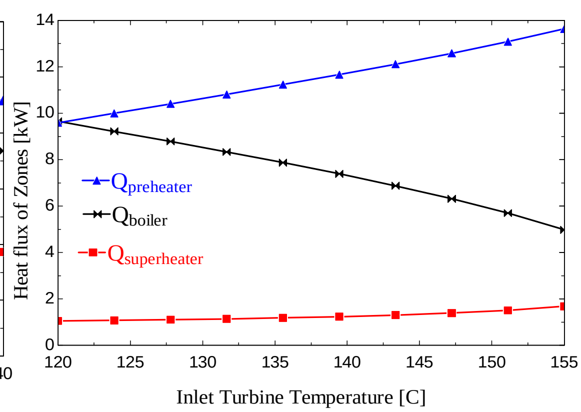

Figure 4. Effect of (ITT) on the heat flux of zone at T_c=27^{o}C, SD=10^{o}C.

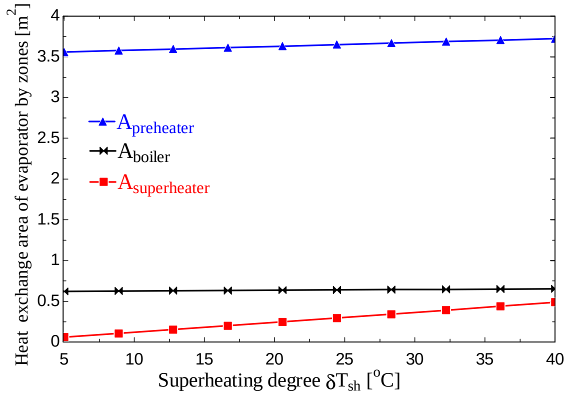

Figure 5. Effect of (SD) on the area of zone at T_c=27ºC T_{ev}=120 ºC.

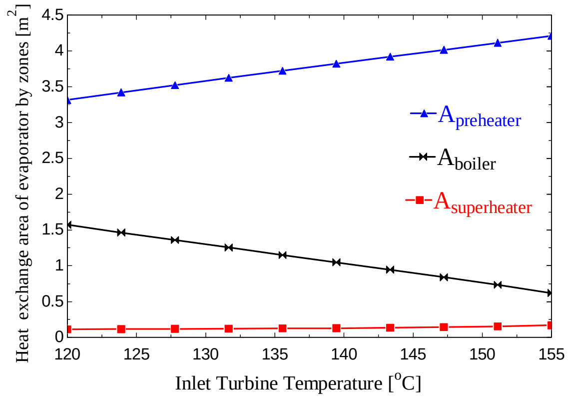

Figure 6. Effect of (ITT) on the area of zones at T_c=27ºC, SD=10ºC.

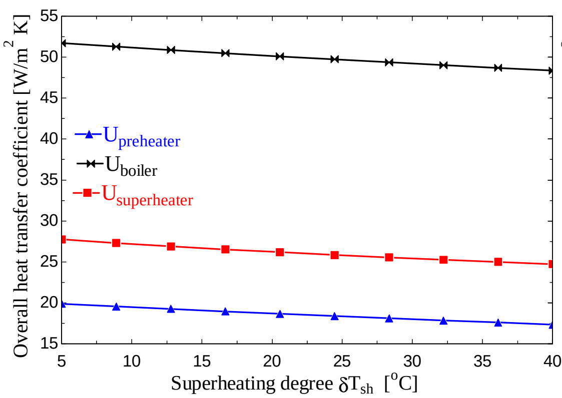

Figure 7. Effect of (SD) on the heat transfer coefficient at T_c=27ºC T_{ev}=120 ºC.

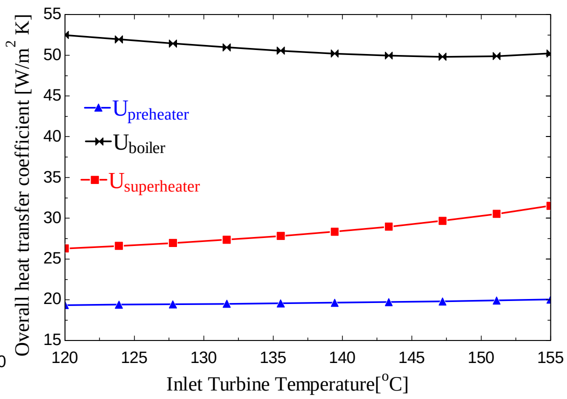

Figure 8. Effect of (ITT) on the heat flux of zone at T_c=27ºC, SD=10ºC.

6. Comparison

To check the validity of the results, it was necessary to compare the results with literature. The present model and calculation procedure were successfully validated by comparison with results found in Ref. [12]. The input data used in comparison are as follow:
The exhaust gases temperature at evaporator outlet is 197 ºC ; exhaust gases Temperature at the evaporator inlet is 528 ºC; evaporation temperature T_{ev}= 131.5 ºC; Degree of superheat is 35 K; Mass flow rate of exhaust gases is 0.188 kg/s. The comparison with Ref.[12] shows very good agreement.

6. CONCLUSIONS

In this study, the heat transfer characteristics of an ORC system combined with diesel engine were analyzed by using measured data such as flue gas mass flow rate and exhaust gas temperature at evaporator outlet. A mathematical model was created and developed with regard to the preheated zone, the boiler zone, and the superheated zone of a counter flow evaporator. The performance of the evaporator was evaluated under variations of superheating degree and inlet turbine temperature. Based on our analysis, the following points can be concluded:
1. The heat transfer rate of the preheated zone is the largest and is more than half of the overall heat transfer rate. The heat transfer rate of the boiler zone is higher than that of the

superheated zone. Furthermore, the heat transfer rate of each zone is proportional to that of the overall heat transfer rate when the engine operates in variable condition. In conditions of constant heat input ($\dot{Q}_g$) in the evaporator, the superheating increase leads to a increase of the heat received in the superheater zone ($\dot{Q}_{sp}$) and a corresponding decrease of the heat input in the preheater ($\dot{Q}_{pr}$) and boiler zones ($\dot{Q}_b$). Also, the percentage heat flux for preheater zone is approximately 47.4% from total heat while for boiler zone it is 38.01% and for superheater zone is 14.59% (with 30 ^oC superheating degree).
2. The area of superheater and preheater zones are increased with superheating degree while the area of boiler is decreased with superheating degree and high value was for preheater zone while the lower value was for superheater zone .The percentage area for preheater zone is approximately 71% from total area while for boiler zone it is 26% and for superheater zone it is 3 % (for evaporation temperature 120 ^oC and superheating degree 10 ^oC).

Acknowledgments

One of the authors (M.H.K.Aboaltabooq) acknowledges support from the Iraqi government through grant and the Romanian government through Research grant ," Hybrid micro-cogeneration group of high efficiency equipped with an electronically assisted ORC", 1st Phase Report, 2nd National Plan, Grant Code: PN-II-PT-PCCA-2011-3.2-0059, Grant No.: 75/2012.

References

[1] Kang SH. Design and experimental study of ORC (organic Rankine cycle) and radial turbine using R245fa working fluid. Energy 41 (2012) 514–524.
[2] He C, Liu C, Gao H, Xie H, Li Y, Wu S, et al. The optimal evaporation temperature and working fluids for subcritical organic Rankine cycle. Energy 38 (2012) 136–143.
[3] Sun J, Li W. Operation optimization of an organic Rankine cycle (ORC) heat recovery power plant. Applied Thermal Engineering 31 (2011) 2032–2041.
[4] Wang EH, Zhang HG, Fan BY, Ouyang MG, Zhao Y, Mu QH. Study of working fluid selection of organic Rankine cycle (ORC) for engine waste heat recovery. Energy 36 (2011) 3406–3418.
[5] Rentizelas A, Karellas S, Kakaras E, Tatsiopoulos I. Comparative technoeconomic analysis of ORC and gasification for bioenergy applications. Energy Convers Manage 50 (2009) 674–681.
[6] Gewald D, Karellas S, Schuster A, Spliethoff H. Integrated system approach for increase of engine combined cycle efficiency. Energy Convers Manage 60 (2012) 36–44.
[7] Vélez F, Chejne F, Antolin G, Quijano A. Theoretical analysis of a transcritical power cycle for power generation from waste energy at low temperature heat source. Energy Convers Manage 60 (2012) 188–195.
[8]Research Grant," Hybrid micro-cogeneration group of high efficiency equipped with an electronically assisted ORC", 1st Phase Report, 2nd National Plan, Grant Code: PN-II-PT-PCCA-2011-3.2-0059, Grant No.: 75/2012.
[9] J.V.C. Vargas, J.C. Ordonez, A. Bejan. Power extraction from a hot stream in the presence of phase change, International Journal of Heat and Mass Transfer 43 (2000) 191-201.
[10] Engineering Equation solver program from website: http://www.fchart.com/ees/
[11] Panoiu Nicolae, Cazane de abur, Ed. Didactica si pedagogica, Bucuresti (1982).
[12] H.G. Zhang, E.H. Wang, B.Y. Fan. Heat transfer analysis of a finned-tube evaporator for engine exhaust heat recovery, Energy Conversion and Management 65 (2013) 438–447.
[13] M.H.Kadhum, "Mathematical Modeling Of Organic Rankine Cycle For Waste Heat Recovery From Internal Combustion Engine", scientific 2nd report, University Politehnica of Bucharest, Faculty of mechanical engineering and mechatronics, April (2014).
[14] Guopeng Yu, Gequn Shu, Hua Tian, Haiqiao Wei, Lina Liu. Simulation and thermodynamic analysis of a bottoming Organic Rankine Cycle (ORC) of diesel engine (DE). Energy 51 (2013) 281-290.
[15] J.P.Holman, Heat Transfer, Tenth edition, Published by McGraw-Hill, New York (2010).
[16] H., Kakac S. Heat exchangers; Selection, rating and thermal design. Florida : CRC Press, (2002) .
[17] Sun L, Mishima K. An evaluation of prediction methods for saturated flow boiling heat transfer in mini-channels. Sol Energy 52 (2009) 5323–5329.
[18] Bergman TL, Lavine AS, Incropera FP, Dewitt DP. Fundamentals of heat and mass transfer. 7th ed. USA: John Wiley & Sons; (2011).

AIR QALITY IN ROMANIA. DISPERSION OF POLLUTANT IN A URBAN AREEA USING CFD SIMULATION

Oliver MĂRUNŢĂLU[1], Gheorghe LĂZĂROIU[2]
University Politehnica of Bucharest, Romania

ABSTRACT

The ambient air quality in Romania is made permanently trough 138 automated stations that are part of National Network for Air Quality (R.N.M.C.A) distributed throughout the country. The following pollutants are taken into consideration when evaluating the air quality: SO_2, NO_2, NOx, PM_{10}, $PM_{2.5}$, B, C_6H_6, CO, O_3, As, Cd, Ni, Hg, and HAP. In studies of air quality in rural and urban areas need to know the answers to some basic questions you should ask them. Some of these questions are: What is the contribution of source A to the concentration of pollutants at site B?; What is the most effective strategy for reducing the concentration of pollutants to meet air quality standard?; What will be the air quality tomorrow or in the days following?.
In this paper is studied the pollutants dispersion from multiple sources, punctual and mobile, continuous or instantaneous, in an urban area using CFD simulation. Finally presented solutions for reducing emissions in the atmosphere and associated conclusions.

1. INTRODUCTION

Romania has the obligation to limit annual emissions of acidification, eutrophication and ozone precursors' greenhouse pollutants under the values of 918 thousand tons/year of sulphur dioxide (SO2), 437 thousand tons/year for nitrogen oxides (NOx), 523 thousand tons/year for non-methane volatile organic compounds (NMVOC) and 210 thousand tons/year for ammonia (NH3), values that are national emission ceilings. National emission ceilings for sulphur dioxide, nitrogen oxides, volatile and ammonia organic compounds, set for 2011 are those provided in the Protocol to the 1979 Convention on long-range transboundary air pollution, to reduce acidification, eutrophication and troposphere ozone levels, adopted in Gothenburg, on 1st of December 1999, ratified by Law no. 271/2003 and represents the maximum amount of pollutant that can be emitted into the atmosphere at national level in a calendar year. Romania submits annual estimates of emissions of air pollutants covered by Directive no. 2001/81/EC on national emission ceilings for certain atmospheric pollutants (NEC Directive) and the Protocols to the Convention on Long-range Transboundary Air Pollution, done at Geneva on 13th of November 1979 (UNECE/CLRTAP).

In this sense, the final national inventory of emissions of sulphur dioxide, nitrogen oxides, volatile organic compounds, ammonia, powders, heavy metals and persisting organic pollutants is drawn up for a period of two years after the present year and the preliminary national inventory of emissions of sulphur dioxide, nitrogen oxides, volatile organic compounds and ammonia is drawn up for the year before the present year. Emissions were also recalculated for the period 2005-2011, using emission factors from the new guide EMEP/EEA 2009, concerning the elaboration of the emission inventories.

[1]Splaiul Independenței nr. 313, olivermaruntelu@yahoo.com, 0743196458

1.1. Evolution of SO_2, NOx, NMVOC and NH_3 emissions for the period 2005-2011

SO_2 emissions corresponding to 2011 are characterized by a decrease of about 48.8% compared to 2005; significant decreases occurring in areas like "Burning in the metallurgic industry" (73.07%), and "Production of heat and power "(45.11%).

In 2011, the largest contribution to the national total was from the large combustion plants, which are sources of the "Production of heat and power" sector, whose emissions were about 282.882 kt (85.44%). Emissions from burning in the steel industry had a share of 7.13% and those in other industries had a share of 3.94% of the national total.

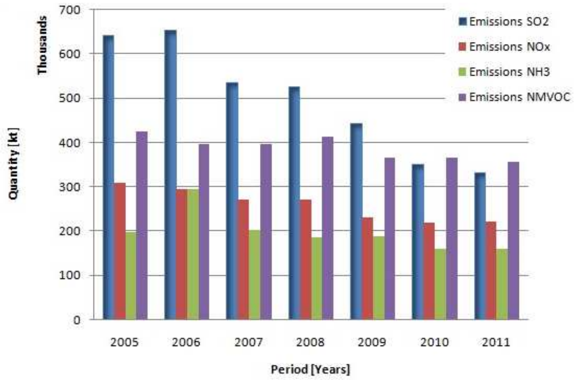

Figure 1.1 Evolution of SO_2, NOx, NMVOC and NH_3 emissions for the period 2005-2011

Year	Emissions SO_2 [kt]	Emissions NOx [kt]	Emissions NMVOC [kt]	Emissions NH_3 [kt]
2005	642584	309056	198049	424813
2006	653491	294556	294556	396344
2007	534933	271684	202325	396408
2008	525771	269567	185931	412274
2009	443579	230052	186398	365674
2010	350344	217916	159814	365397
2011	331083	221606	159204	355870

Table 1.1 Evolution of SO_2, NOx, NMVOC and NH_3 emissions for the period 2005-2011

The total NOx emissions in 2011 amounted to 221.606 kt, compared to 309.056 kt. in 2005. NOx emissions derive especially from the "Road Transport" sector (36.18%) and the "Production of heat and power" (25.77%). NOx emissions calculated for 2011, which saw declines compared to 2005, were the ones from sectors like "Production of heat and power" (40.15%), "Burning in metallurgic industry" (69.6%) and "Burning in the commercial/institutional sector" (26.57%). Increases in NOx emissions compared to 2005 were recorded in "Burning in the residential sector" (2.17%).

NH3 emissions have decreased by 19.61% compared to 2005. During the analyzed period, the highest value was recorded in 2006 (294.556 kt). In 2011, total NH3 emissions were 159.204 kt. Change in emissions from livestock activities is explained by fluctuations in the number of livestock. The most important share in the national total is represented by the manure management from dairy cows breading (22.42%), sows (24.75%) and laying hens (13.71%) and the waste water treatment (9.69%).

NMVOC emissions decreased in 2011 compared to 2005 by 16.23%. An increase is noted, mainly due to the "Fugitive emissions coming from natural gas extraction" (33.97%), "Burning in the residential sector" (14.88%).

In the year of 2012 the ambient air quality assessment in Romania was made permanently through 138 automated stations that are part of the National Network for Air Quality

Monitoring (RNMCA) distributed throughout the country. The stations are equipped with automatic analyzers that continuously measure the ambient concentrations of the following pollutants: sulfur dioxide (SO_2), nitrogen oxides (NO_2, NOx), carbon monoxide (CO), benzene (C_6H_6), ozone (O_3), particulate matter (PM_{10} and $PM_{2,5}$). Also included are laboratory equipment used to measure the concentrations of heavy metals, lead (Pb), cadmium (Cd), arsenic (As), nickel (Ni) of suspension particles and debris.

2. DISPERSION OF POLLUTANTS IN THE ATMOSPHERE

In studies of air quality in rural and urban areas need to know the answers to some basic questions you should ask them. Some of these questions are: What is the contribution of source A to the concentration of pollutants at site B?; What is the most effective strategy for reducing the concentration of pollutants to meet air quality standard?; What will be the air quality tomorrow or in the days following?

Equations underlying the dispersion of pollutants in the atmosphere are three dimensional and non-linear equations, according to three components u, v, w of the velocity in the three directions x, y, x, and time-dependent, are the following:

- Pollutant transport equation (function Φ)

$$\frac{\partial \rho \Phi}{\partial t}+\frac{\partial(\rho U\Phi)}{\partial x}+\frac{\partial(\rho V\Phi)}{\partial y}+\frac{\partial(\rho W\Phi)}{\partial z}+\frac{\partial}{\partial x}\frac{\mu_t}{Pr_m}\frac{\partial \Phi}{\partial x}+\frac{\partial}{\partial y}\frac{\pi_t}{Pr_m}\frac{\partial \Phi}{\partial y}+\frac{\partial}{\partial z}\frac{\mu_t}{Pr_m}\frac{\partial \Phi}{\partial z}+S\Phi \tag{2.1}$$

-Density continuity equation (ρ)

$$\frac{\partial}{\partial t}+\frac{\partial(\rho U)}{\partial x}+\frac{\partial(\rho V)}{\partial y}+\frac{\partial(\rho W)}{\partial z}=0 \tag{2.2}$$

-Navier-Stokes equation (by function k) in the x direction

$$\frac{\partial \rho U}{\partial t}+\frac{\partial(\rho UU)}{\partial x}+\frac{\partial(\rho UV)}{\partial y}+\frac{\partial(\rho UW)}{\partial z} = \frac{\partial p}{\partial x}+\frac{\partial}{\partial x}\mu_\varepsilon\frac{\partial U}{\partial x}+\frac{\partial}{\partial y}\mu_\varepsilon\frac{\partial U}{\partial y}+\frac{\partial}{\partial z}\mu_\varepsilon\frac{\partial U}{\partial z}+\frac{\partial}{\partial x}\mu_\varepsilon\frac{\partial U}{\partial x}+\frac{\partial}{\partial y}\mu_\varepsilon\frac{\partial V}{\partial x}+\frac{\partial}{\partial z}\mu_\varepsilon\frac{\partial W}{\partial x}-\frac{\partial}{\partial x}\frac{2}{3}\rho k \tag{2.3}$$

- Navier-Stokes equation (by function k) in the y direction

$$\frac{\partial \rho V}{\partial t}+\frac{\partial(\rho UV)}{\partial x}+\frac{\partial(\rho VV)}{\partial y}+\frac{\partial(\rho WV)}{\partial z} = \frac{\partial p}{\partial y}+\frac{\partial}{\partial x}\mu_\varepsilon\frac{\partial U}{\partial x}+\frac{\partial}{\partial y}\mu_\varepsilon\frac{\partial U}{\partial y}+\frac{\partial}{\partial y}\mu_\varepsilon\frac{\partial U}{\partial z}+\frac{\partial}{\partial x}\mu_\varepsilon\frac{\partial U}{\partial y}+\frac{\partial}{\partial y}\mu_\varepsilon\frac{\partial V}{\partial y}+\frac{\partial}{\partial z}\mu_\varepsilon\frac{\partial W}{\partial y}-\frac{\partial}{\partial y}\frac{2}{3}\rho \tag{2.4}$$

- Navier-Stokes equation (by function k) in the z direction

$$\frac{\partial \rho W}{\partial t}+\frac{\partial(\rho UW)}{\partial x}+\frac{\partial(\rho VW)}{\partial y}+\frac{\partial(\rho WW)}{\partial z} - \frac{\partial p}{\partial z}+\frac{\partial}{\partial x}\mu_\varepsilon\frac{\partial U}{\partial x}+\frac{\partial}{\partial y}\mu_\varepsilon\frac{\partial U}{\partial y}+\frac{\partial}{\partial x}\mu_\varepsilon\frac{\partial U}{\partial z}+\frac{\partial}{\partial y}\mu_\varepsilon\frac{\partial U}{\partial z}+\frac{\partial}{\partial z}\mu_\varepsilon\frac{\partial V}{\partial x}+\frac{\partial}{\partial z}\mu_\varepsilon\frac{\partial W}{\partial x}-\frac{\partial}{\partial x}\frac{2}{3}\rho \tag{2.5}$$

3. MODELING AND SIMULATION OF POLLUTANT EMISSIONS IN A URBAN AREEA

CFD (Computational Fluid Dynamics) use numerical methods and algorithms to solve and analyze problems that involve fluid flows. Computers are used to perform the calculations required to simulate the interaction of liquids and gases with surfaces defined by boundary conditions. With high-speed supercomputers, better solutions can be achieved. Modeling is based on solving a set of differential equations of conservation equations supplemented by numerous additional models often semi empirical. These equations are discretised by different methods, the method of finite differences, finite elements, finite volumes or border elements. Model domain is divided into small parts, resulting mesh networks with many nodes. The equations are written for each node is assembled in a overall equation which is then solved.

Urban area which is studying the dispersion of pollutants is Bucharest which is located in southeastern Romania with global coordinates 44º26' N, 26º03' E.

Air quality in Bucharest is monitored using six fixed monitoring stations located in areas: Lacul Morii, Cercul Militar Naional, Mihai Bravu, Drumul Taberei, Titan si Berceni. These monitoring stations are of three types: urban stations(Lacul Morii), traffic stations(Mihai Bravu and Cercul Militar National) and industrial stations(Drumul Taberei, Titan si Berceni). Data collected from these stations are sent to ANPM (National Agency for Environmental Protection).

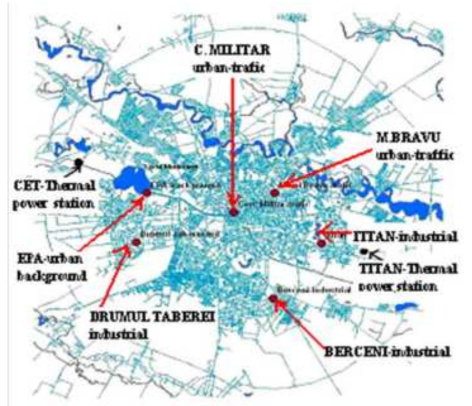

Figure 3.1 Air quality monitoring station of Bucfarest

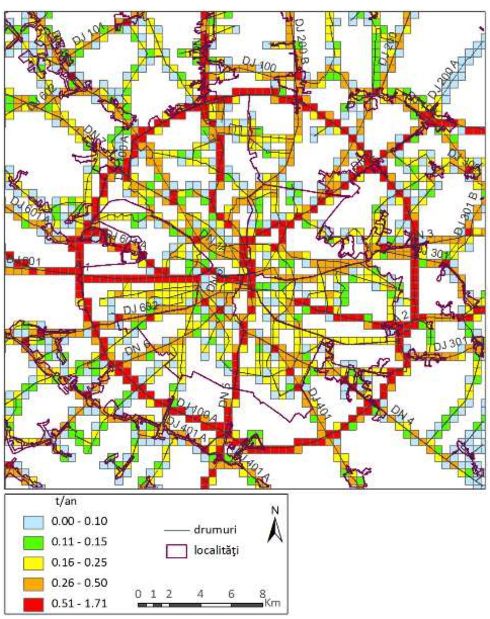

Figure 3.2 NOx distribution from linear sources

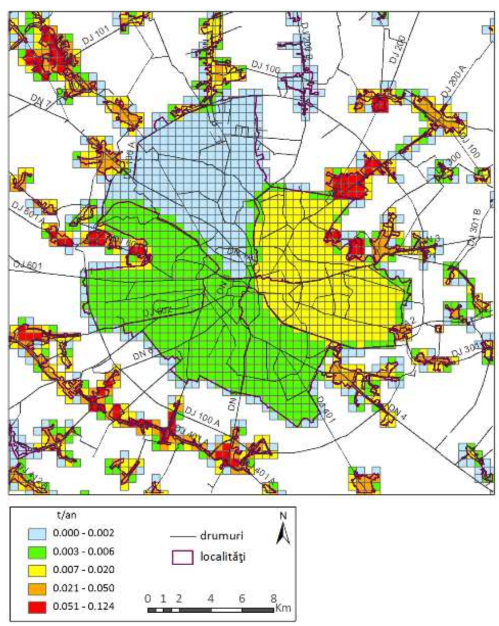

Figure 3.3 NOx distribution from surface sources

Wind direction and speed greatly influences the dispersion of pollutants in the air. These wind characteristics are obtained from ANM.

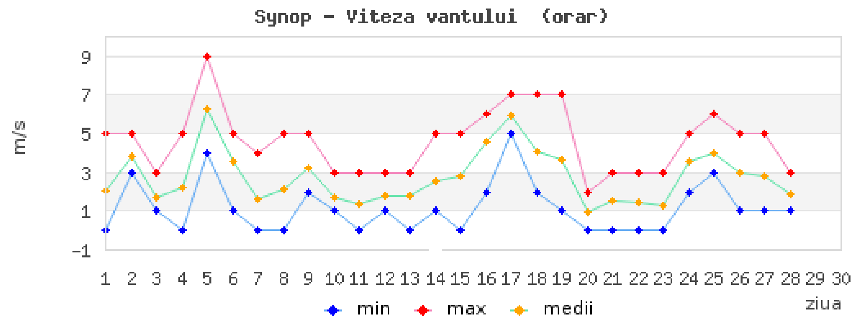

Figure 3.4 Wind speed for 20.04.2012

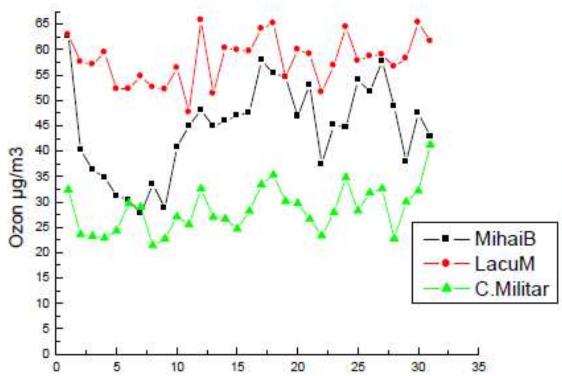

Figure 3.5 Ozone concentration 2010

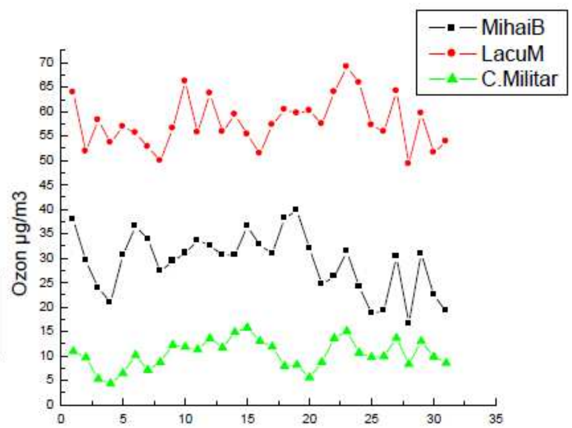

Figure 3.6 Ozone concentration 2011

4. SOLUTIONS TO REDUCE THE POLLUTANT EMISSIONS INTO THE ATMOSPHERE

The most important solutions to reduce emissions in the production of electricity and heat are processes for desulphurization (wet, semi-dry and catalytic), promotion of electricity produced from renewable energy sources (wind, solar, biomass, geothermal, hydraulic, tidal) and nuclear energy which is one of the bets accepted by everyone as a solution to reduce pollutant emissions and protect the environment.

In automotive the reduction solution refers to advanced combustion processes that are injection direct and controlled auto injection, variable distribution, multiple injections, reducing displacement, continuously variable transmission, manual-automatic transmission.
It is estimated that by implementing advanced systems to the engine, transmission and vehicle structure, in 2050 year, might reduced, relatively low cost, fuel consumption by up to 40%.

Scenarios provided by the ONU for global energy sector can be summarized as follows:
- The baseline scenario (starting) for 2050, which represents further evolution without major surgery, involves unacceptable increase CO2 emissions by 37% compared with 2003, the rapid increase in prices of conventional fuel and fuel doubling conventional in this period;
- ACT scenario (the Accelerated Technology) requires accelerated introduction of new energy technologies, and automotive diversifying conventional propulsion and use of biofuels, which can be reduced to half of the consumption of hydrocarbons and only a slight increase in emissions CO2;

- TECH Plus scenario, the most optimistic, assume for the road transport sector, the use of bio-fuels and hydrogen fuel cells and will reduce 16% of CO_2 emissions and maintaining the consumption of hydrocarbons at current levels, despite the rapid growth of the vehicle fleet.

5. CONCLUSIONS

Air quality in recent decades was changed therefore should not be neglected, we have to bring solutions to improving it because the air is very important factor for the existence of life. Need to support energy production by renewable energy.

LIST OF ABBREVIATIONS AND ACRONYMS

ANM	AGENTIA NATIONALA DE METEOROLOGIE
ANPM	AGENTIA NATIONALA PENTRU PROTECTIA MEDIULUI
CFD	COMPUTATIONAL FLUID DYNAMICS
NMVOC	COMPUSI ORGANICI VOLATILI NONMETANICI
R.N.M.C.A	RETEAUA NATIONALA DE MONITORIZARE A CALITATII AERULUI

References

[1] Agentia Nationala pentru Protectia Mediului www.anpm.ro .

[2] Administratia Nationala de Meteorologie www.anm.ro .

[3] Parlamentul României. “Legea nr. 104/15.06.2011 privind calitatea aerului înconjurator.” In: Monitorul Oficial al Romaniei, Partea I 452 (June 2011).

[6] Caracterizarea meteorologică a anului 2012 în România - Administraţia Naţională de Meteorologie .

[7] Strategia Națională a României privind Schimbările Climatice 2013-2020 - Ministerul Mediului și Schimbărilor Climatice.

[8] Inventarul Național al Emisiilor de Gaze cu Efect de Seră 2013 (INEGES-2013) - Ministerul Mediului și Schimbărilor Climatice.

RESULTS ON THE 18 T/H BOILER OPERATION IN S.C. VRANCART S.A.

Lucian Mihăescu[1], Ionel Pîşă[1], Ion Oprea[1], Gabriel Negreanu[1],
Adrian Adam[2], Cristian Mândrean[2], Ion Bărbieru[2], Romeo Rusu[3], Romeo Sava[3]

1. INTRODUCTION

VRANCART S.A. Adjud is one of the most important producers of corrugated cardboard, paperboard and tissue paper in Romania, with over 35 years of activity in this field. The heating system from VRANCART S.A. is equiped with a stream boiler of 18 t/h nominal flow rate and 5 bar nominal pressure, with solid fuel resulted from manufacturing processes and with natural gas as support fuel.

The initial project was requested by S.C. VRANCART S.A. Adjud from the necessity to eliminate the soil and underground water pollution due to storage of sludge and waste byproducts from production process on dump, in order to recover biomass energy from sludge and waste.

The boiler is designed for the following operating modes:

-mixed supply, constantly with dried sludge/dried waste and natural gas (support combustion + addition to boiler load);

-sludge + gas supply, or waste + gas supply, avoiding sludge + waste + gas supply whitch does not allow a stable combustion to maintain the boiler performance;

-only gas supply was also taken into account.

The pressure body of the boiler consists of a horizontal mono-block and with fume tubes construction with three gas pass and a submerged entry chamber. It mainly consists of a welded layer between two tubular plaques; in this assembly there are mounted flame tubes and smoke pipes.

The first gas path having heat exchange consists of the flame tubes – the focus, of Ø 1200 mm external diameter. The convection part of the boiler consists of second gas path composed of smoke pipes, welded between front tubular plaque and intermediate tubular plaque of the boiler.

The combustion chamber for solid fuel is placed under the (cilindrical) pressure body, inside walled antefocus, made of refractory brick. The turning back chamber is a welded construction, uncooled and sealed, placed in the lower part of the cylindrical pressure body; it allows the exit for gas from second path and the passage to the air preheater. The main combustion installation includes the grate with push forward and consists of three monoblock burners mounted above the grate. The three burners are monoblock type, having the thermal power P = 4000 kW.

The grate is made of steel profiles, on which the cross elements made of refractory iron are based. In the lower part of the slanted grate there is a horizontal grate.

Behind the boiler there is mounted the air preheater, and after there is the exhauster for hot gas which extracts the gas resulted in combustion, through pipes to several cyclone, preheater and then exit to the chimney of the power plant.

[1] University Politehnica of Bucharest, Faculty of Mechanical Engineering and Mechatronics
[2] ICEMENERG Bucharest
[3] SC VRANCART SA

The primary air fun is installed on the air preheater; it suckes the combustion air and blowes that under the slanted grate. The preheated air flows through pipes to below grate. Preheated air flow is adjusted with three flaps and another flap between the air preheater and secondary air fan.

The secondary combustion installation consists of two monoblock burners on natural gas with continuous adjustment of air – fuel, having each of them the thermal power P = 10000 kW and being installed in the back side of the slanted grate, at the 2,8 m level.

By design, the boiler had the main role in thermal waste treatment, burning sludge with moisture content of 40% with natural gas support.

2. TESTS AND CALCULATIONS

The measurements determinate the combustion performance, the temperatures in the focus and on the masonry walls, also the boiler efficiency, if an operating regime agreed.

The operating conditions included a solid fuel flow of 1450 kg/h, consisting of:

-850 kg/h of sludge with moisture content of 40%;

-400 kg/h waste;

-200 kg/h of polyethylene waste.

The calorific value of the solid fuel was calculated based on the following composition:

-sludge, with a calorific value of 5780 kJ/kg and the mass ratio of 55%;

-waste, with a calorific value of 15100 kJ/kg and the mass ratio of 25%;

-polyethylene waste, with the mass ratio of 20%. The polyethylene with the composition $(C_2H_4)_nH_2$ has a calorific value of 37700 kJ/kg.

With this composition, the calorific value of the solid fuel has resulted as 14450 kJ/kg.

The natural gas flow was determined at a load of 60 %, 5% and 59 % for the burners installed in the combustion chamber. The natural gas flow was in this case of 496 Nm^3/h, compared to the total obtainable flow of 1200 Nm^3/h (41,33 % load). Each secondary burner was charged at 5% load, making a total flow of 200 Nm^3/h, compared to the total obtainable flow of 2000 Nm^3/h (10% load).

The measurements on the operatin mode during the tests shown:

-the input temperature in the secondary burners of 950-1050^{0}C

-the outlet temperature from the boiler for combustion gases: t_{ev} = 148 – 150 ^{0}C;

-the air excess at the end of furnace: λ_f = 0,97;

-massive emissions of carbon monoxide at the end of focus: CO=18000-20000 ppm;

-increasing of the air excesse up to the air preheater: λ_{PA} = 2,39 and up to the exit from boiler: λ_{ev} = 2,58, values manifested by burning carbon monoxide to the value of 12-13 ppm;

-the temperature measured by pyrometer of 1150°C in the first third of the layer on the grate, of 1350-1370°C for the final combustion on the grate and of 1100-1200°C for the brick at the turning back chamber.

The unburnt content in the discharged material from the focus, as ICEMENERG's samplings and determinations, was 8,32%. The method used is STAS 10274/15-1975. The value is usual for such combustion technology. The air deficiency measured at the end of the focus required a verification of the calculation for the air required by the combustion. This stoichiometric air deficiency has the value of 1040 Nm^3/h and it will be compensated by an additional injection. We recommend an injection of air into the last third of the grate with 1300 Nm^3/h, at an air excess of 1,25. Currently, the operating conditions considered by the owner of the boiler include:

-operating with a solid fuel made of sludge, waste and polyethylene waste, having a calorific value of 14450 kJ/kg;

-a medium flow for solid fuel of 1450 kg/h;

-a charge for natural gas burners placed in furnace of 40-45%;

-a charge for secondary natural gas burners of 10-15%;

-temperatures resulted at input in the secondary burners of 950-1000^{0}C, with maintenance of the minimum value;

-the flow of the air under the grate of 80-90% compared with project value;

-increasing the life time of the refractory brick by using 60A type, which has the compressive deformation temperature of 1450^{0}C.

The calculated value of the efficiency for the operating mode was 80,7%. We see that the value for the efficiency is the same as the project value, so the operating mode proposed by VRANCART S.A. is an acceptable regime because it provides an efficiency very close to the project.

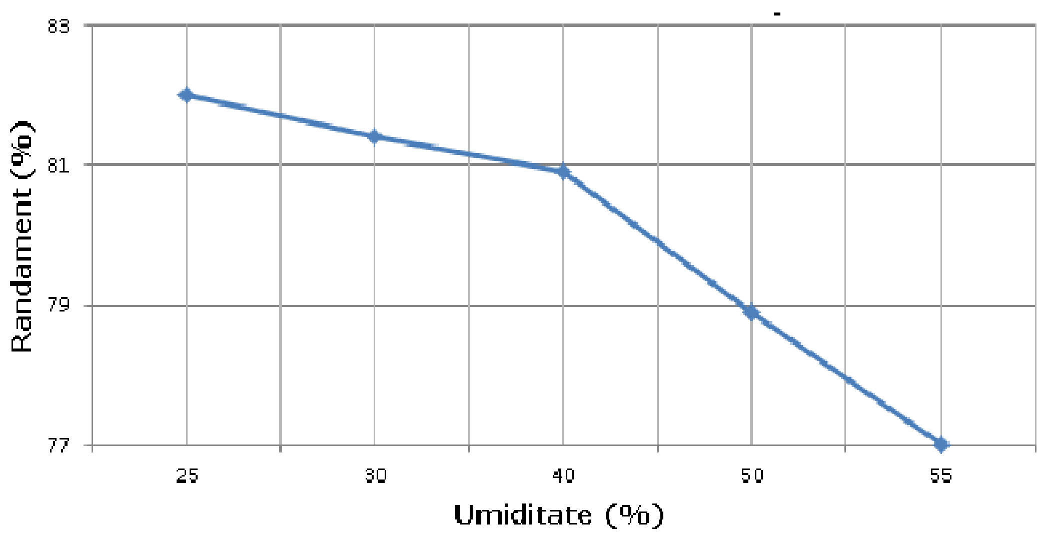

Figure 1 Variation of the project efficiency with the fuel moisture

After proposed retrofitting, it is mentioned that the estimated operating period between two repairs will increases at about 4 months, which is an acceptable economic stage for the currrentcondition of the boiler.

According to the contract, S.C. VRANCART S.A. Adjud sent to ICEMENERG two mobile plates from combustion grate, an unused plate (marked PN) and an old plate which was deformed and fractured during operating (marked PV), in order to analyze the state of metallic material and eventually to detect the causes of deformation and cracking durin operation.For both plates there were made visual checks (macroscopic) and dimensional measurements and samples were taken for chemical analysis, metallographic analysis and Brinell hardness tests.

The results of complete chemical analysis on both plates are shown in the table no. 1 and in the test reports of the UPB-CCEEM-ECOMET: no. 100 EOS/14.03.2014 (PV) and no. 101 EOS /14.03.2014 (PN), Table no. 1 complete chemical analysis on both plates

Marking plate	C %	Si %	Mn %	P %	S %	Cr %	Mo %	Ni %	Al %	Cu %	Brand resulting
PV	3.141	5.1	0.515	0.063	0.071	0.512	0.015	0.067	0.015	0.327	FrSi5
PN	3.073	5.318	0.589	0.084	0.087	0.710	0.008	0.088	0.011	0.183	FrSi5
FrSi5	2.5-3.2	4.5-6.0	Max. 0.80	Max. 0.30	Max. 0.12	0.5-1.2	-	-	-	-	

The results show that both plates are made of refractory iron FiSi5 according to STAS 6706-79.

Both plates have medium values of Brinell hardness (HB) of 258 HB (PN) and 250 HB (PV), both values below 300 HB, according to STAS 6706-79 for FrSi5. The two plates analyzed (PV and PN) are made of refractory iron with lamellar graphite FrSi5 – STAS 6706-79, which maximum temperature is usually 700 °C. The unused plate – PN, shows smooth surfaces (processed) and it has the project value. The old plate (used) – PV, shows that:

-A crack in width at the top, the crack is located at 65 mm from the front edge (F);

-On the top there is a layer consists of deposition of oxide (tundish) and combustion products, thicker than the portion of face (F) placed in the focus

-the deformation is 2,2% on length and 10,0% on width compared to the new plate (PN), the maximum deflection being at the front end (F), on the portion located in focus. Also there is a deformationof the front end (F) on the thickness (heigh) of the plate of 10,5% compared to the new board (PN).

So we can conclude that the old plate – PV worked at very high temperatures, above the maximum operating temperature (700 0 C) prescribed for refractory iron with lamellar graphite FrSi5, which leds to very large dilatation (possibly prevented dilatation due to the friction) and also to deformation and cracking of the slab. In order to prevent future damage of the plates there are recomanded:

-use refractory iron in the manufacturing of the plates, with high alloy in Cr or Al, according STAS 6706 – 79, type:

a) FrCr30 – maximum temperature of 1000 0 C;

b) FrAl22 – maximum temperature of 1100 0 C;

c) FrAl30 – maximum temperature of 1100 0 C.

Refractory brick is considered necessary to be change by switching from 50 A to 60A quality, with an increase in the deformation temperature at compressive with 130 0 C.

3. **CONCLUSIONS**

Theoretical and experimental measurements and analysis made by ICEMENERG and University Politehnica of Bucharest showed the viability of the new operating mode, and the boiler capability to operate economically using a different fuel from the design one.

RESEARCH AND EXPERIMENTAL ANALYSES CONCERNING THE INCREASE EFFICIENCY OF SOLID BIOMASS COMBUSTION IN HYDROGEN JET

Lucian Mihăescu[1], Gheorghe Lăzăroiu, Ionel Pîşă, Elena Pop, Gabriel Negreanu,
Universitatea Politehnica Bucuresti

ABSTRACT

The paper analyzes the experimental combustion efficiency of solid biomass in the form of willow chips in hydrogen jet (gas enriched in hydrogen - HRG). The experiments has been performed on a 2 MW boiler from the Polytechnic University of Bucharest. We used a 600 kW burner with HRG injection in the supply pipe for willow chips. The main contribution of the hydrogen consisted in a massive reduction of CO, mainly because of a higher combustion rate.

1. INTRODUCTION

An inovative and efficient technology for burning solid biomass as willow is the combustion in air jet. This technology allows the combustion of solid biomass in form of chips, as was harvested. We distinguish the following aspects related of efficiency:

- no need for mechanical processing for willow after harvest;
- increased thermal power that recommand the process for energy production;
- a swift and efficient combustion.

Typically, the CO emission is quite high for solid biomass combustion, regardless of technology. Combustion in a stream of hydrogen, with a thermal participation up to 8% allows to control CO emissions, at the end of furnace reaching the generally accepted values of max 100 ppm.

Achieving high power plants using solid biomass involves compliance with the environmental protection regulations. CO is the main pollutant that must be removed; consequently, the combustion of solid biomass with hydrogen is an effective way to solve this problem.

2. WILLOW COMBUSTION EFFICIENCY IN JET OF AIR AND HYDROGEN

Combustion of solid biomass in airflow is similar with pulverized coal combustion. Consequently, the combustion chamber (the furnace) will be equipped with a suitable burner. In our previous research, two burners of 600 and 620 KW have been built.

Hydrogen was introduced with the willow chips in the burner, resulting a perfect blend between solid phase, air and hydrogen. The analysis of safety concluded that the continuous supply system of hydrogen and solid fuel besides the high speed air jet into the furnace does not allow for the return of the hydrogen flame. The return of the flame may be possible due to the poor burn rate between hydrogen and biomass.

Figure 1 shows a scheme of the solid biomass burner and the hydrogen (HRG) injection.

[1]University Politehnica of Bucarest, 313 Splaiul Independentei st. 060042 Bucharest, Romania; tel: +404029158;
E-mail: lmihaescu@caz.mecen.pub.ro

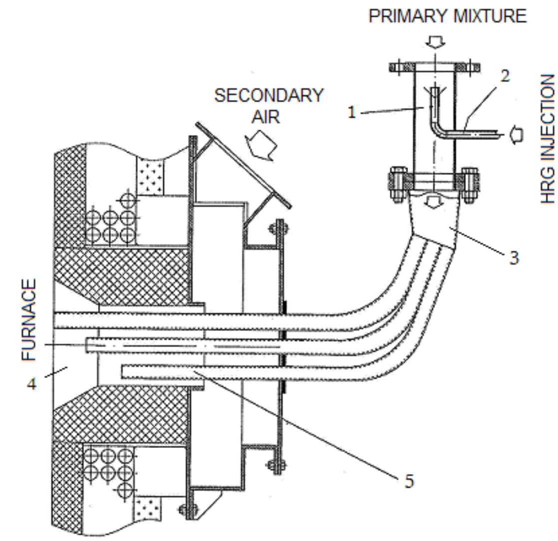

Figure 1: HRG Injection system
1-Injection channel; 2-HRG injector; 3-distribution channel;
4-embrasure; 5-fuel channel.

Elemental analysis of the solid fuel is:

C^i = 40 – 44,8%; H^i = 4,3 – 4,8%; O^i = 33 – 36,3%; N^i = 0,7 -1%; A^i = 2,3 – 5,6%; W^i_t = 9,8 – 13,7%.

Heating value varied in range 14 115 – 19860 KJ/kg.

3. WORKING METHODOLOGY

Swirling type burner with secondary and tertiary air flows was designed and executed by UPB ICEMENERG SA, with the following features:

a) thermal power: maximum 600 KW;
b) low weight (up to 50 kg);
c) self-supporting construction (all subassemblies are welded to the central channel with primary agent, an element that supports the whole building);
d) radial size allows its implementation in furnace embrasure.

Hydraulic resistance of pneumatic circuit connected to the burner was thus calculated to create compatibility with the boiler auxiliaries. Thus, for the primary agent (air and solid biomass particles), for the secondary and tertiary air circuit, hydraulic resistance is less than 100 mmH2O and it is performed by the ventilation system;

The thermal regimes of fluid circuits are in the following range:

- The temperature of the primary agent: 60 - 90^{0}C; The value is imposed by the solid biomass humidity at the entrance of the supply system and the primary air temperature;
- Depending on the heat load of the system, the temperature of the primary air will have values of about 150 - 200 ^{0}C. In order to avoid possible ignition of solid biomass (of the volatiles released in the contact with the hot primary air), a higher concentration of oxygen coming from flue gas recirculation, will be used;
- Secondary air temperature is 150 - 220^{0}C;
- Tertiary air temperature is 150 - 220^{0}C.
- Primary air accounted for 30-40% of the total combustion air.

Excess air at the end of the furnace is imposed λ_f = 1.25, common value for high efficiency biomass boiler.

The parameters that characterize the installations functioning are presented below:

1. The thermal support combustible quota:
   - Mass participation ratio:

$$q_B = B_g \,/\, B \tag{1}$$

where B_g is the flow rate of hydrogen, and B - biomass flow rate.

   - Thermal participation rate:

$$q_B = \frac{B_g \cdot Q_g}{B \cdot Q_i^i + B_g Q_g} \tag{2}$$

where Q_g is the calorific value of the fuel gas and Q^i_i calorific value of biomass.

2. Capacity of pneumatic transportation of biomass, defined as volume concentration in transportation air:

$$c = \frac{B}{\dot{V}_a} \tag{3}$$

where $\dot{V}_a$ is the air flow of pneumatic transport, m^3/s

In mass proportions, the transport concentration of solid biomass will be:

$$c = \frac{B}{\dot{V}_a \cdot \rho_a} \tag{4}$$

where p_a is the density of air for solid biomass transportation (corrected for real temperature regime) in kg/m^3

3. Thermal loading of burner embrasure:

$$q_a = \frac{B \cdot Q_i^i + B_g Q_g}{S_a} \tag{5}$$

where S_a is the burner embrasure surface, m^2.

4. Thermal loading of furnace volume

$$q_v = \frac{B \cdot Q_i^i + B_g Q_g}{V_f}$$

where V_f is the active volume of the furnace, m^3.

The effectiveness of combustion in a stream of hydrogen has been characterized as a result of experiments by the following performance criteria:

- the thermal support combustible quota:

  q_B = max 0,03 kg HRG/kg solid biomass

  q^*_B *=2,9%*

The calorific value of HRG was: Q_g = 10760 KJ/m^3_N (18240 KJ/kg), biomass flow rate being B = 82 kg/h with Q^i_i = 17000 kJ/kg.

- thermal loading of furnace volume: q = 0,04 - 0,0041 MW;

As the thermal load may be raised to values of 0.1 - 0.12 MW, results the possibility of charging of the furnace with a volume of 10 m^3, with two burners having increased flow rate up to 120 kg/h

- the pneumatic transportation capacity;

The solid biomass mass concentration in the transportation air was: c = 0,24 kg/m^3 and c^* = 0,19 kg/kg

- during the tests, the air excess value was:
  O_2 = 1,2 – 6,6%
  λ = 1,06 – 1,45
- the carbon monoxide emission was:
  CO = 20 – 40 ppm

This value is incontestable lower comparing to the layer burning technology. The NO_x emission was NO_x = 375 – 387 mg/m^3.

4. CONCLUSIONS

The burner operating parameters recommends a transportation air flow rate of 25-35 m/s, for secondary air, about 30 - 35 m/s and for tertiary air, about 30 - 35 m/s

The designed burner successfully achieved the rated thermal power 620 KW, for a solid biomass flow capacity of 80 – 85 kg/h and 4 m^3_N/h gas HRG. It is recommended a proportion for transportation air of about 35 – 40%.

The flame had high brilliancy aspect and filled the entire furnace volume. Under the influence of HRG, the burning was stable and the emissions were low. The CO emission, which is high when using layer burning biomass, was extremely low, under 40 ppm, when using suspension burning solid biomass. This aspect offers an advantage to suspension burning of solid biomass as also the possibility of higher power archievements.

Experiments have shown that hydrogen is more effective in reducing CO emissions than natural gas or LPG. Considering the economical aspects related to the use of hydrogen, can be specified that because of its very low proportions, will not act as a financial inhibitor.

Acknowledgement

This work was supported by a grant of the Romanian National Authority for Scientific Research, CNDI-UEFISCDI, PN-II-ID-PCE-2011-3-0698.

References

[1] Mihăescu, L., Pîşă, I., Negreanu, G., Berbece, V., „*Arderea pulverizată a tocăturii de biomasă – premisă pentru producerea de energie electrică*”, rev. Energetica

[2] Mihăescu, L. E. Pop, M. E. Georgescu, G. Lăzăroiu, I. Pişă, G.P. Negreanu, C. Ciobanu „*Testing of a 620 KW burner for sawdust in suspension and gas enrichen in hydrogen (HRG)*, 2th International Conference of Thermal Equipment, Renewable Energy and Rural Development, TE-RE-RD 2013, Baile Olanesti, 20-22 June 2013.

[3] Prisecaru, T., Petcu, C., Prisecaru, M., Pop, E., Ciobanu, C., Pîşă, I. „*Co-combustia cărbunelui cu gaz îmbogăţit în hidrogen (HRG)* pp 145-149, a IX Conferinţă Naţională de Echipament Termomecanic Clasic şi Nuclear şi Energetică Urbană şi Rurală, Bucureşti, 25 iunie 2010, ISSN 1843-3359

[4] Mihăescu, L., Prisecaru, T., Georgescu, M., Lăzăroiu, Gh., Oprea, I., Pîşă, I., Pop, E., Berbece, V.,”*Construction and testing of a 600 KW burner for sawdust in suspension”*, COFRET12, 11-13 June Sozopol, Bulgarie

THEORETICAL ANALYSIS OF IMPACT OF THE SOLID BIOMASS COMBUSTION IN HYDROGEN JET IN DEVELOPING NEW INNOVATIVE TECHNOLOGIES

Lucian Mihăescu[1], Tudor Prisecaru, Gheorghe Lăzăroiu, Ionel Pîşă, Elena Pop, Gabriel Negreanu, Manuela-Elena Georgescu, Viorel Berbece, Malina Prisecaru
University Politehnica of Bucharest

ABSTRACT

The experience and positive results obtained in combustion of solid biomass with hydrogen allowed the development of innovative technologies for renewable solid fuels. Two concepts for efficient combustion of solid biomass with hydrogen have been developed: combustion in a tunnel burner attached to a low thermal power boiler respectively combustion in complex power plants comprising gas-producing, internal combustion engine, steam boiler and steam turbine.

1. INTRODUCTION

Experimental researches on solid biomass combustion efficiency with hydrogen intake have been conducted in the laboratory of fuels and combustion installations from the University Politehnica of Bucharest. The research has been focused on two technologies for wood chips combustion (sort 0-30 mm), in compacted form or in stream of air. The first technology is an application of fluidized bed combustion, fluidizing taking place only in a room located in the furnace, and the second has similarities with the combustion in pulverized condition.

The research focused particularly on the combustion efficiency for the sort 0-30 mm wood biomass or willow chips, in order to reduce costs on its additional machining after harvest (sort 0-30 mm resulting either once with harvesting or later after harvest).

The use of hydrogen was evaluated from the point of view of reducing flame length and reducing carbon monoxide emissions by experimental research [1].

By use of hydrogen to support the combustion of solid biomass has been achieved excellent performance, particularly in reducing the emission of carbon monoxide by 30 - 100 times. CO emissions were below 40 ppm for all cases tested. Burning rate of wood biomass minced to 0-30 mm was 17 m/s, a very high value.

2. INNOVATIVE TECHNOLOGIES FOR EFFICIENT COMBUSTION OF SOLID BIOMASS

From the results of experimental research concerning solid biomass combustion in hydrogen jet, two innovative technologies have been proposed.

a) The combustion of solid biomass with hydrogen in a tunnel or in a combustion chamber located before the furnace of the boiler.

[1]University Politehnica of Bucarest, 313 Splaiul Independentei st. 060042 Bucharest, Romania; tel: +404029158;
E-mail: lmihaescu@caz.mecen.pub.ro

This combustion technology, presented in the diagram from figure 1, has applications for low thermal power boilers, whose furnace, having small size, does not allow complete combustion. The technology refers to wood biomass combustion, including willow chips.

Such combustion is performed in two stages, the ignition and combustion of fine fraction in the tunnel and the completion of combustion in the burner combustion chamber. Hydrogen will be admitted into the burner tunnel, where by its high speed combustion will catalyze the thermo-gas-dynamic processes.

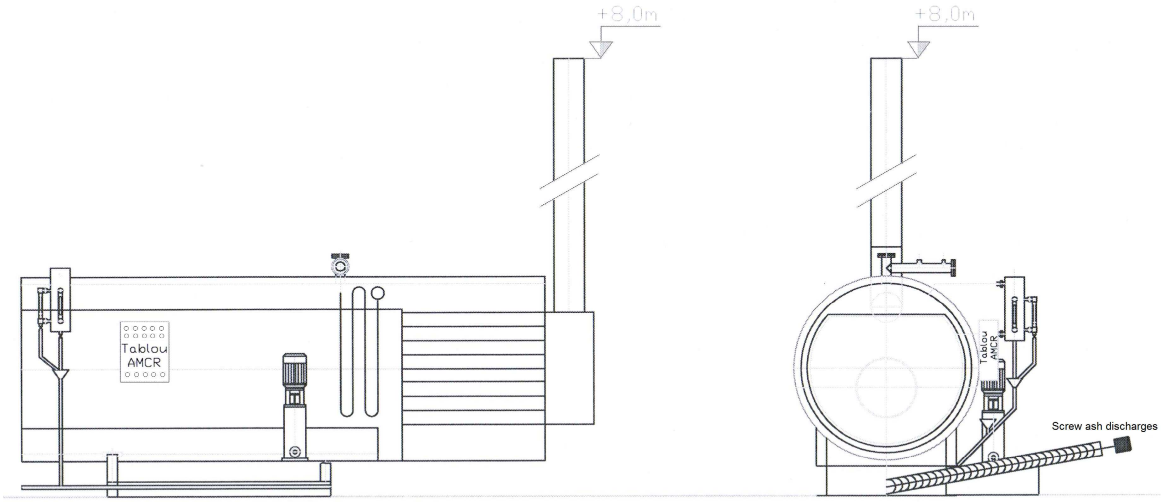

Figure.1. Boiler with tunnel burner

For overall efficiency, the combustion will be achieved in a proportion of not less than 70% in the tunnel burner. It will be maintain the thermal proportion of hydrogen determined from the previous program of experimentation of 2.8 to 4.8%.

These data are for an averaged analysis of wood, close to those imposed by willow combustion, according to data from Table 1 [2].

Table 1

Proximate analysis [% by weight, as received]		**Ultimate analysis [% by weight, on dry basis]**	
moisture	17	C	47,3
volatiles	67,1	H	5,66
fixed carbon	13,6	N	1,4
ash	2,3	O	42,8
Heating value [KJ/kg as received]		S	0,05
LHV a.r. (as received)	15400	Cl	0,018
Elementary analysis [mg/kg on dry basis]			
Al	70	Mg	600
As	1,3	Mn	11
B	12	Na	190
Ca	7700	Ni	25
Co	0,6	P	860
Cr	8,2	Si	220
Cu	7,6	Ti	2,8
Fe	81	V	0,2
K	2700	Zn	130

With this technology it is estimated that boilers with very low superheated steam flow in range of 1.3 to 4.8 t/h will be designed, enabling the development of micro electricity production plant of 100-600 kW. Such a micro power plant, possibly in a cogeneration cycle will achieve our economic target "energy crop - local use in energy production." This concept will shape the size of the renewable fuel culture and will guide the financial efficiency only on energy production.

b) Solid biomass combustion in boilers with gas producer thermal support

Positive results from biomass combustion with hydrogen support can be extended to biomass combustion with gas producer support. Energy is thus obtained in a complex power plant comprising:

- Gas-producing or pyrolyzer for solid biomass;
- Installation for producing mechanical work with gas producer or pyrolysis gas comprising an internal combustion engine or gas turbine;
- Steam boiler firing biomass with producer gas or pyrolysis gas support, coupled to a turbine.

This power plant guides gaseous fuel obtained from solid biomass to two users, one direct energy producer and one, user for thermal support to a steam boiler. Figure 2 shows schematically the proposed power plant.

The power plant allows greater heat generation in CHP scheme, with applications especially when using gas turbines.

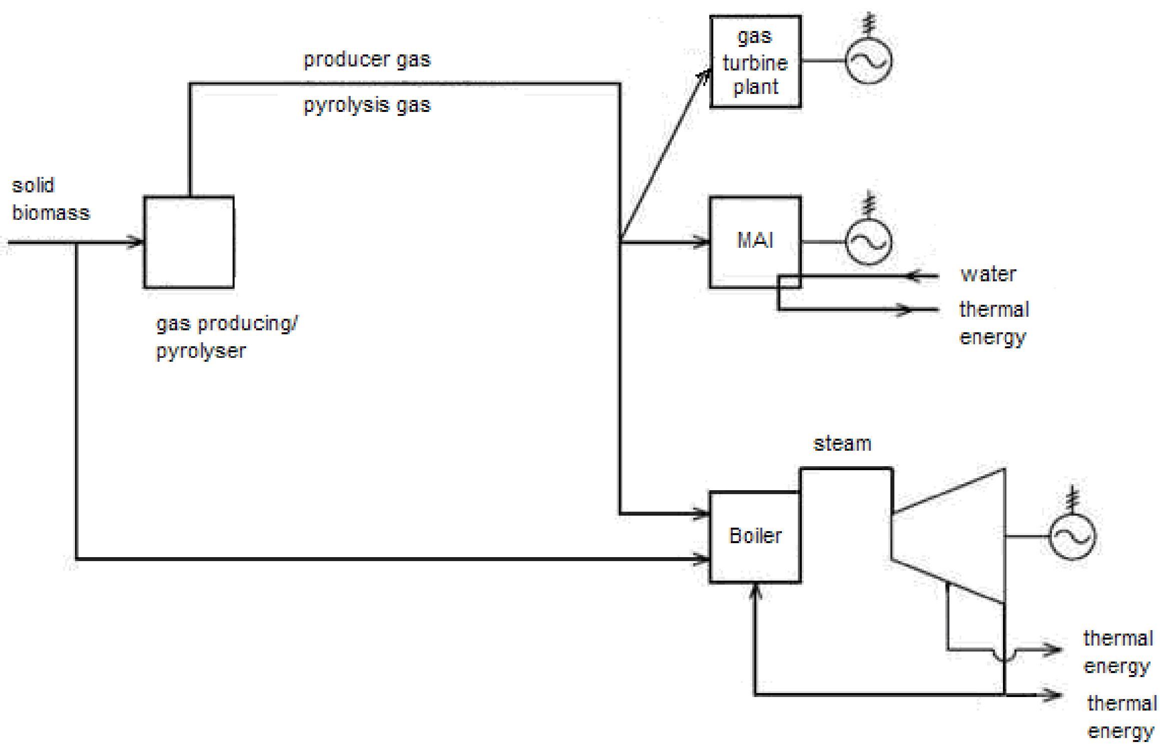

Figure 2. Innovative energetic concept for solid biomass energy recovery

3. CONCLUSIONS

The combustion of solid biomass has not only positive results for majority technologies of combustion on grate. The hydrogen support, a gas with high combustion rate, theoretically and experimentally has proved to be very beneficial. Starting from this result, there are proposed two combustion technologies that consider a minimum processing of solid biomass for burning.

First innovative combustion technology proposed aims to achieve its highest proportion before the boiler furnace in order to be implemented to low power installations.

The second innovative technology proposes achievement of power plants for solid biomass combustion, with gasification or pyrolysis in parallel with burning installations both for gaseous fuel and solid biomass.

Acknowledgement

This work was supported by a grant of the Romanian National Authority for Scientific Research, CNDI-UEFISCDI, PN-II-ID-PCE-2011-3-0698.

References

[1] Mihăescu, L. E. Pop, M. E. Georgescu, G. Lăzăroiu, I. Pişă, G.P. Negreanu, C. Ciobanu „*Testing of a 620 KW burner for sawdust in suspension and gas enrichen in hydrogen (HRG)*, 2th International Conference of Thermal Equipment, Renewable Energy and Rural Development, TE-RE-RD 2013, Baile Olanesti, 20-22 June 2013.

[2] J. Boyd,"*Energy from Willow*" SAC, West Mains Road, Edinburgh Eh 9 3JG, UK, The Scottish Agricultural College, December 2000

THE EXPERIMENTAL ANALYSIS ON THE INFLUENCE OF AIR FILTER, OIL FILTER AND OIL ON THE PERFORMANCE OF THE INTERNAL COMBUSTION ENGINE

Marius Daniel Muscalagiu[1], Alexandru Mihai Dima, Cosmin Gabriel Muscalagiu
University of Craiova, Faculty of Mechanics

ABSTRACT

In case of a long period of parking of a car engine and non usage of it, its integral parts wich have capstan-turned surfaces may bee atacked by corrosion and the properties of oil and gas may decrease. That is the reason why it is recommended that the engine shoulb be booted from time to time after shorts periods of idling. When an internal combustion engine parked for a long period of time the first parts that are affected in their perfomance are the air filter, oil filter, fuel filter, oil and coolant fluid.
In this article we present a methodology that would allow an experimental analysis of air filter, fuel filter performance and fuel performance also.

1. INTRODUCTION

Previous studies in the field of internal combustion engines were focused mainly on reducing the wear and the fuel consumption during the function period of those engines. There are few researches about the effect of a log period of parking on the internal combustion engine. In this experiment we intend to study the possibility of reducing the engine wear and the fuel consumption as the idling of an engine can cause serious damage to the power system, to the cooling system and to the road-crank mechanism.

The engine is a technical system able to transform any form of energy into mechanical power. If the initial energy is obtained by burning a fuel-air mixture the engine is called heat engine (combustion engine) [1], [2].

The performances of internal combustion engines are characterized by the existence of several areas on charge and in relative movement some towards others. Under these circumstances it is necessary to reduce the frictional effects on the surfaces and to spread among them a fluid that would adhere to surfaces and to be a sliminess one; this way the pressure that occurs would maintain the surfaces to a certain distance [1], [2], [6].

Fuel filters have a particular significance in the function of an engine because they block the pollutants form the fuel in order to ensure the best performance of an engine. Hole injector clogging due to the deposits of pollutants in the fuel is a major problem to an engine because it decreases its power and increases fuel consumption [3], [4], [5], [7].

Air filter is an important component of an engine as every engine has one since the earliest models and all have the same goal to clean up the air before it reaches the intake and the engine.

Besides the methodology herein this article our purpose is to analyse the following experiment set out on a Volkswagen Golf VI 1,4MPI 80 CP engine, fuel consumption, gasses emission coming from the internal combustion and the functional parameters of the engine : speed, position of throttle valve coolant fluid temperature, intake air temperature and inlet pressure. These experiments presented in the article are the first step to further analysis of air filters, fuel filters and fuel properties in case of a long period of parking

[1]Craiova, 0720064495, daniel_muscalagiu@yahoo.com

2. METHODOLOGY

Experimental measurements have been performed on a Volkswagen Golf VI 1,4MPI 80 CP engine assembled on a stand. In the first figure (Figure 1) is presented this type of stand. The test was being held at ambient temperature of 23°C and the fuel used the test for the internal combustion engine was unleaded petrol with octane value 95.

On this type of stand the test was being held on an idling engine. The air filter, clean fuel, new fuel filter were all tested in order to see their influence on the function of internal combustion engine (effects on the fuel consumption, exhaust gases resulting from fuel consumption).

Functional parameters (speed, position of throttle valve, coolant fluid temperature, intake air temperature and inlet pressure) were determined using the auto diagnosis program VCDS

Fuel consumption was determined by measuring the amount of fuel combusted after each part of the experiment.

The pollution rate was also determined. This with the aid of gas analyzer CAPELEC CAP 3200 GO which can measure the coefficient of air excess lambda and density of the following gases: CO, CO2, HC, O2, AFR(BNZ).

Experimental stand characteristics:

- Manufacturer: VW Volkswagen
- Model: Golf VI 5K1
- Key Number: 0603 / AMD
- Power: 59 kW / 80 hp
- Engine code: CGGA
- Cylinder capacity: 1,390
- Built: 2009 – until 2012
- Engine type: petrol engine, MPI
- Cylinders: 4 inline
- Fuel System: multi point injection
- Bord voltage: 12 volt.

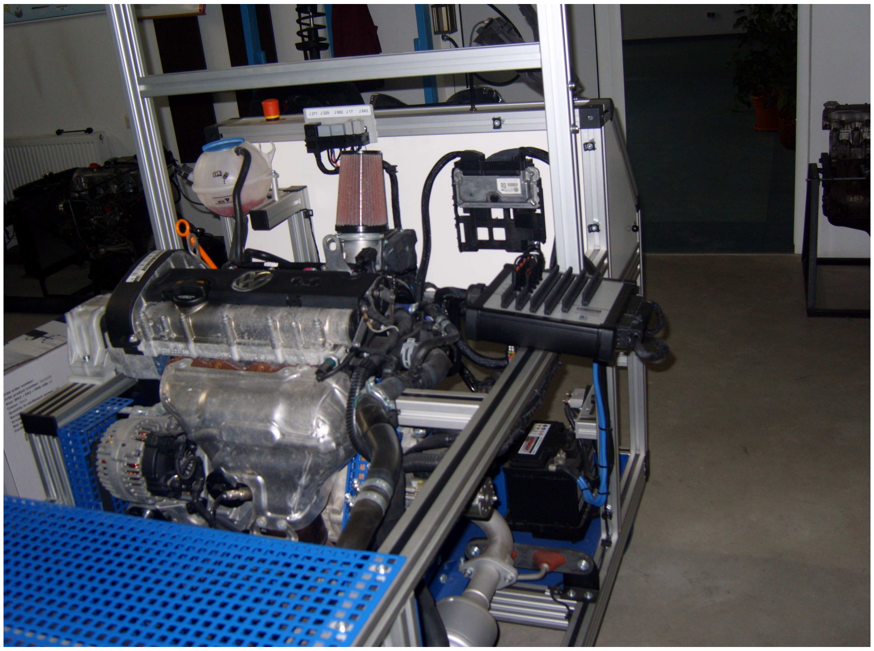

Figure 1: Experimental stand–view of the engine Volkswagen Golf VI 1,4MPI 80CP

2.1 EXPERIMENTAL ANALYSIS

In Tabel 1 are presented all the characteristics resulted at the end of the experiment as shown on the diagnosis programme VCDS.

Tabel 1 Measured parameters with the help of the diagnosis VCDS

Nr. crt.	N	Throttle position	T_{water}	T_{air}	P_{inlet}	$T_{environement}$	Time	Consumption	Consumption /hour
[-]	[rot/min]	[%]	[C]	[C]	[mbar]	[C]	[min]	[ml]	[l/hour]
1	783	12.5	60.5	26	300.1	23	15	100	0.4
2	1016	12.7	84.5	34.5	264.5	23	5	59	0.7
3	1513	13.5	87	37.5	246.9	23	5	75	0.9
4	2091	14.1	87.5	39	222.2	23	5	116	1.4
5	2509	14.5	87	40.5	231.4	23	5	127	1.5
6	3024	15.7	87	41.5	208.7	23	5	150	1.8
7	3505	16.1	87.5	41	190.4	23	5	185	2.2
8	3970	16.9	90	42	200	23	5	210	2.5

On the whole have been held eight tests with a different engine speed, whose final purpose was to measure the following funtional parameters:

- throttle position;
- coolant fluid temperature;
- inlet air temperature;
- inlet air presure;
- fuel consumption;

For the first test the engine was hold on idle position at 783 rpm during 15 minutes and after the engine has reached its normal operating temperature of 87° C the etest were carried out at 1000 rpm for 5 minutes. The test were repeated increasing the rotative speed by 500 rpm.

The values obtained at the final of all tests have been settled on diagrams with parameters measured according to the engine revolution.

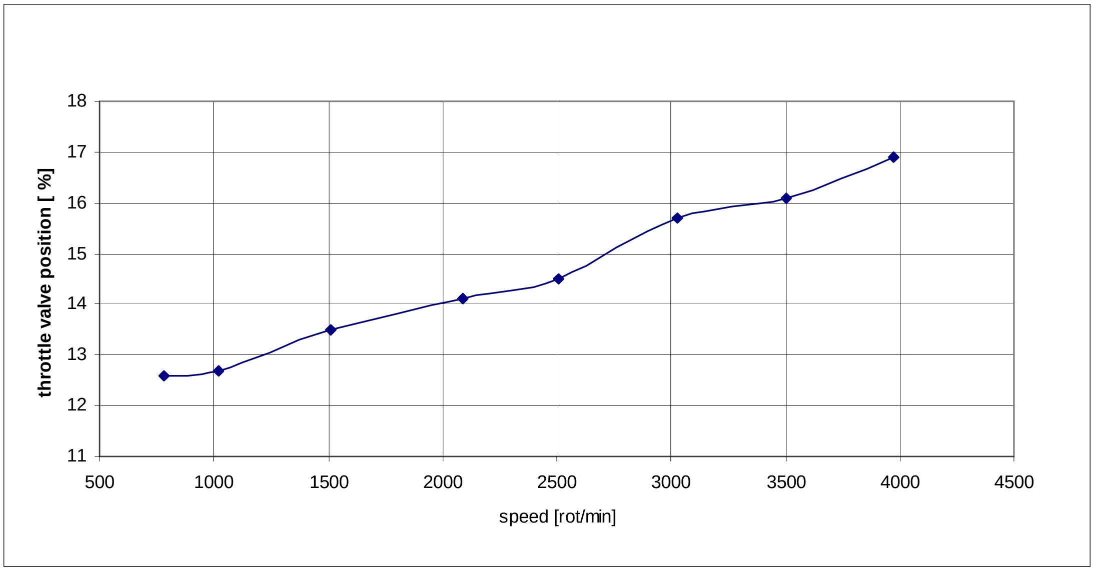

Figure 2: The throttle position fluctuation depending on the engine speed

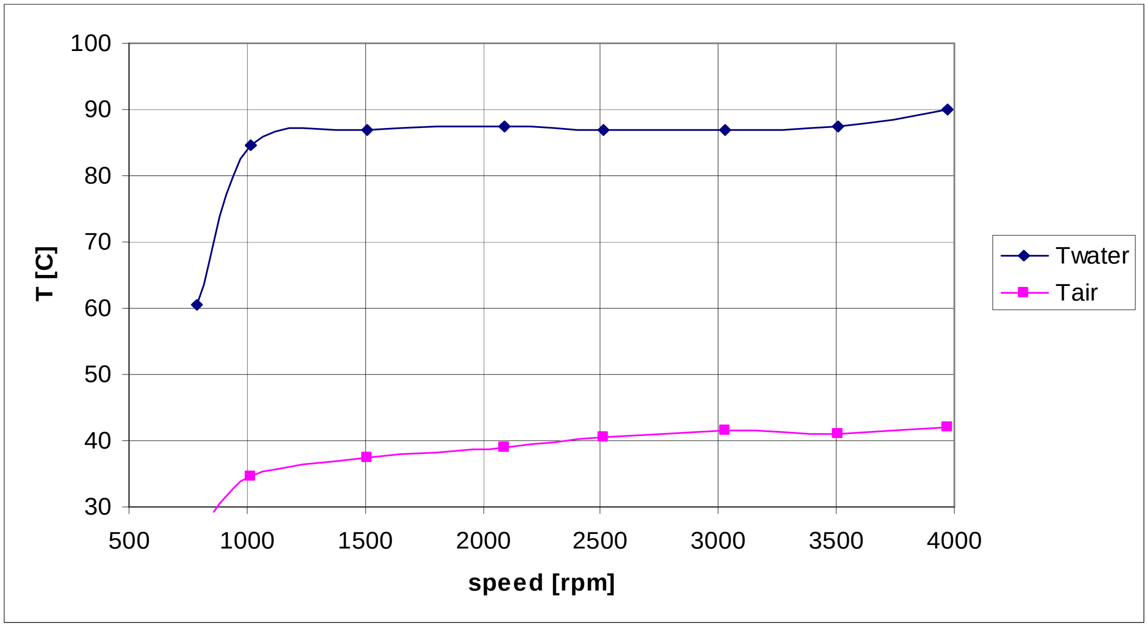

Figure 3: Fluctuation of air temperature and the coolant fluid depending on the engine speed

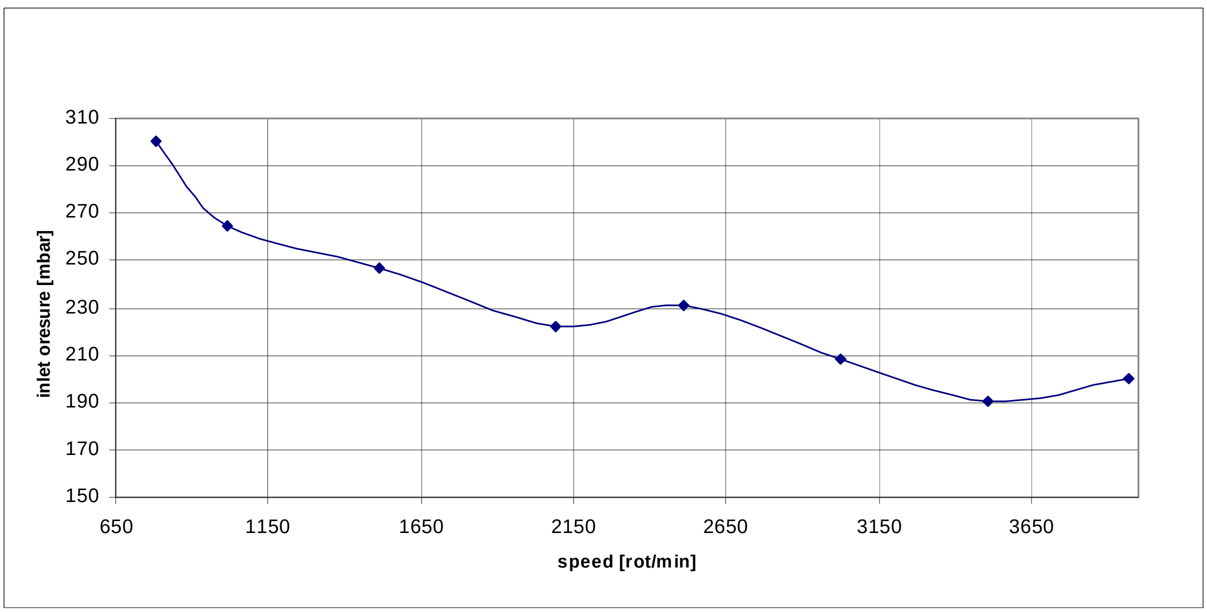

Figure 4: Fluctuation of inlet pressure depending on the engine speed

Table 2 presents the results obtained on the final experiment carried out with the aid of the diagnosis programme CAPELEC CAP 3200.

Eight tests were conducted as a result of the engine revolution in order to analyse the stages of the following gases: CO; CO_2; HC; O_2; COcorr and lambda values.

The first test was being held on an idle engine at 880 rpm during 15 minutes with the oil temperature of 90° C and after then engine has reached his normal operating temperature all tests were carried out at 1000 rpm for 5 minutes. After these operations the test was repeated increasing the engine revolution by 500 rpm.

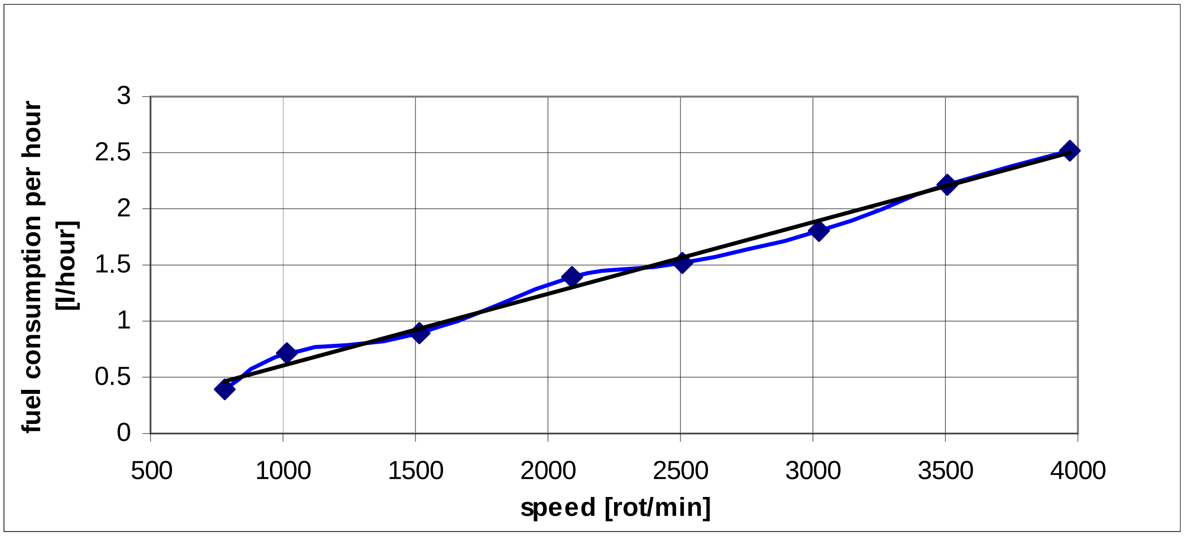

Figure 5: Fuel consumption per hour depending on the engine speed

Table No. 2 Measured parameters with the aid of the diagnosis programme CAPELEC CAP 3200.

Nr. crt.	CO	CO_2	HC	O_2	LAMBDA	CO corr	AFR(BNZ)	Speed	TEMP.
[-]	[%]	[%]	ppm	[%]		[%]		RPM	[C]
1	0,0	10,9	1	0,34	1,02	0,0	15,10	880	90
2	0,0	10,9	0	0,04	1	0	14,8	1030	92
3	0,0	10,9	0	0,04	1	0	14,8	1510	93
4	0,0	10,9	0	0	1	0	14,8	2000	94
5	0,0	10,9	0	0	1	0	14,8	2500	94
6	0,0	10,9	0	0	1	0	14,8	3000	96
7	0,0	10,9	0	0	1	0	14,8	3500	96
8	0,0	10,9	0	0	1	0	14,8	4000	97

3. CONCLUSIONS

In case of a long period of idling a car engine some components with their surfaces capstan- turned are subject to corrosion and the properties of oil and gas additives may decrease. It is believed to be neccesary to boot the engine at short periods of time.

During the staying of a heat engine the most afeected components are the oil filter, the air filter, the coolant fuid, the oil and the fuel.

Fuel filters have a particular significance in the performance of an engine because they block the pollutants from the fuel in order to ensure optimum function of the engine.

Hole injectors clogging due to the deposits of pollutants from the fuel is a major problem for the engine and it getting bigger as the burden regimes gets worse.

Air filter is an important component of an engine and each car has one no matter the model and all air filters have the same purpose to clean up the air before it reaches the intake gallery and the engine.

Using the tests results presented herein it can easily be observed that once we increase the engine speed the temperature raise also in the intake gallery due to the raise of engine temperature but decreases the inlet presure and increases the fuel consumption.

It can also be observed that simultaneously with the increment of engine speed, the oxygen resulting from exhaust gases disappears and CO_2 remains constant no matter the speed ot the temperature of the engine.

References

[1] Aramă C., Grunwald B. – *Motoare cu ardere internă ed.* 1966 – *Procese şi caracteristici*.

[2] Băţagă N., Tănase F., Zătreanu Gh., Dăscălescu D., Caramavru N. – *Motoare termice* ed. bucuresti 1979.

[3] Rădulescu G.A – *Combustibili, lubrifianţi şi materiale specifice pentru automobile, ed. Bucureşti, pag 35-40;51-58;58-65;170-173;*

[4] Mateescu M., Blejoiu S. - *Combustibili, lubrifianţi şi materiale speciale pentru autovehicule rutiere*, Craiova 1998 pag 14-32;32-36;66-83;99-101;

[5] Gailis M., Pirs V. *Research in influence of engine air filter replacement periodicity*. In proceedings of 10th International Scientific Conference ENGINEERING FOR RURAL DEVELOPMENT, May 26 – 27, 2011, Letonia.

[6] Filtru combustibil. Adresa:http://newpartsauto.wordpress.com/2012/08/23/filtru-combustibil.

[7] Filtre carburant bosch. Adresa:http://www.bosch-auto.ro/noutati/de-80-de-ani-filtrele-de-carburant-bosch-asigura-functionarea-optima-motoarelor/

DESIGN CONCEPTION OF A PILOT BURNER THAT SIMULATES THE RETROFITTED BURNERS FROM CHP IŞALNIŢA

Gabriel Negreanu[*1], Lucian Mihăescu[*], Ionel Pîşă[*], Ion Oprea[*], Viorel Berbece[*],
Adrian Adam[**], Cristian Mândrean[**], Ion Bărbieru[**], Viorel Gherghina[***], Alexandru Moga[*]

University Politehnica of Bucharest[*]
ICEMENERG Bucharest[**]
CE Oltenia CHP Isalnita[***]

ABSTRACT

The paper presents the results of the third phase of a research grant [1] with the purpose of decrease of NOx emissions, using a staggered combustion new lignite burner. Until now, the research team has tested the burner on the wind tunnel and by numerical modeling. After design and manufacturing, the burner will be tested in a 2 MW_{th} pilot boiler in order to simulate the behavior of the combustion system to be retrofitted at CHP Işalniţa. Due to the modular construction, it is possible to multiply the operational results of a single experimental burner to the whole structure of the industrial burner. In the next pages we will present the design approach of this burner.

1. INTRODUCTION

The research developed in our project [1] aims to create a new lignite burner with lower NO_x emissions meant for the replacement of the burners belonging to the current combustion system of the steam generators installed at CHP Işalniţa. The new burners will use the staggered combustion technology, by means of the aerodynamics remodeling, especially for the secondary air flow, which will have a long-drawn admission related to the exit section of the burner.

Because the industrial burner has a modular construction, with 16 modules, the tests performed for one module, in a lower thermal power furnace (a pilot furnace of 2 MW_{th} from University Politehnica of Bucharest), will produce results that can be replicated in the large power steam generator.

In order to achieve the project main task, the following research stages have been completed in 2013:

- Testing of the burner aerodynamics on the wind tunnel, with atmospheric air;
- Numerical modeling of the burner.

The tasks of 2014 stage are:

- Design of the pilot burner;
- Manufacturing and installing the pilot burner on the experimental furnace;
- Testing the combustion efficiency.

2. GENERAL CONDITIONS FOR THE DESIGN OF EXPERIMENTAL BURNER

[1]Tel: +40214029158, email: gabriel.negreanu@gmail.com

The sizing of the experimental burner should satisfy the aerodynamics of primary air jet (coal dust with the assembly of fluids discharged by the mill: primary air, water vapors from the coal drying process, recirculated flue gasses) and the secondary air jet.

The mass-flow of primary air is related to the coal quality. The initial coal elemental analysis is presented in Table 1:

Table 1 The elemental analysis of the lignite

	UM	Value	Method of determination
Total moisture W^i_t	%	41,86	SR 5264:95
Ash A^i	%	22,23	ISO 1171:1997/+CI:1998
HCV, initial condition	kJ/kg	8947	ISO 1928:2009
LCV, initial condition	kJ/kg	7553	ISO 1928:2009
Carbon, C^i	%	22,8	PO-SME-16
Hidrogen, H^i	%	2,08	PO-SME-16
Nitrogen, N^i	%	0,51	PO-SME-16
Sulphur, S^i_c	%	0,74	PO-SME-16
Oxigen, O^i	%	9,78	PO-SME-16
Volatile	%	29,06	STAS 5268-90

The burner will be installed on the embrasure of the experimental furnace. The lignite dust will be obtained by grinding of crushed shreds in a mill fan with direct injection, like those installed at the steam generator from CHP Isalnita. In order to remove the lignite wetness, the crushed coal is transported through the pre-drying tower with hot flue-gasses in the mill suction section.

The dimensions of the air slots should respect the following conditions:

- Reaching the velocities from the pre-sizing stage;
- Fitting of the burner in the embrasure.

The burner will be reinforced by a circular base-plate with minimal diameter of 500 mm and a minimal thickness of 4 mm, in order to support its weight and discharge the forces to the connection system to the embrasure and other pipes.

For the fuel quality presented in Figure 1, after solving the stoichiometric equations of the combustion, the following values have been computed:

- The volume of theoretical humid air: $V^0_{aum} = 2{,}32\ \mathrm{m^3_N/kg}$; (1)
- The volume of $(CO_2 + SO_2 = RO_2): V_{RO_2} = 0{,}43\ \mathrm{m^3_N/kg}$; (2)
- The volume of nitrogen: $V^0_{N_2} = 1{,}8\ \mathrm{m^3_N/kg}$; (3)
- The volume of water vapor from flue-gasses: $V_{H_2O} = 0{,}79\ \mathrm{m^3_N/kg}$; (4)
- The volume of flue-gasses (stoichiometric): $V^0_g = 3{,}02\ \mathrm{m^3_N/kg}$; (5)
- The flow-mass of the lignite was $B = 200\ \mathrm{kg/h}$ (6)

In order to obtain a lower NO_x concentration during the first phase of the combustion, the burner will be designed for substoichiometric conditions, with an air mass-flow rate of 90 % from the nominal one. The necessary stoichiometry will be achieved by supplementary air injection and external air leakages, allowing an excess air coefficient at the end of the furnace λ_f = 1,15 -1,2.

Admitting that the exit temperature from the mill is about 105^0C, the mass-flow rate of the primary working fluid (coal dust, recirculated flue-gasses, vapor, air) is $\dot{V}_{ap} = 0{,}104\ \mathrm{m^3/s}$. The necessary surface of the slots for primary working fluid is computed for a velocity $v_{ap} = 15\ \mathrm{m/s}$, imposed by the coal quality (ratio ash/moisture):

$$A_p = \frac{\dot{V}_{ap}}{v} = \frac{0{,}104}{15} = 0{,}0069 \quad \text{m}^2 \tag{7}$$

For a slot width of 0,083 m, required by the framing of rectangular slots in a circular embrasure, it results a high of 0,08 m. It may be allowed deviations of ± 12% from these dimensions, resulting an unessential change of the primary working fluid velocity.

For the secondary air slots II, the section dimension are 0,280 x 0,140 m, imposed by the structure of air supply network. While the velocity of the secondary air was optimized by experiment [2] on wind tunnel, $(v_{asII} = 40 \ \text{m/s})$, the mass-flow rate of the secondary air II, represents 70 % of the total secondary air mass-flow, meaning 0,06 m^3/s. with these figure it is possible to calculate the surface of the slots for the secondary air II: A_{asII} = 0,0015 m^2.

The rest of the secondary air will be injected trough the space between the embrasure and the channels for primary working fluid and secondary air II.

The burner design should satisfy the following hydraulic conditions:

- Losses of pressure on the circuit of primary working fluid circuit, 10–20 mm H_2O;
- Losses of pressure on the circuit of secondary air I, 20–40 mm H_2O;
- Losses of pressure on the circuit of secondary air II, 20–40 mm H_2O;

In Figure 1 are shown the details of the preheated air supply and mixed air-coal supply.

Figure 1 details of the preheated air supply and mixed air-coal supply

The pressure losses on the circuit of primary working fluid circuit will be covered by mill ventilation. The 0,2 t/h fan mill provides an overpressure of minimum 90 mm H_2O. The pressure losses from the particle separator of the mill to the burner is maximum 20 mm H_2O. A rectangular supply network with smoothly curved shape, with a length of maximum 1,5 m, transporting a fluid with a velocity of 15 m/s causes a pressure loss of 10–15 mm H_2O, then the burner design respects this criterion.

While the central preheated air network has a static overpressure of 150 mm H_2O, , the pressure losses from the secondary air I and II can be easily covered. Eventually, a control and measurement system (valve and diaphragm) of the mas-flow rat can also be installed.

In figure 2 are shown the general conception of burner connection to the supplying circuits of the furnace.

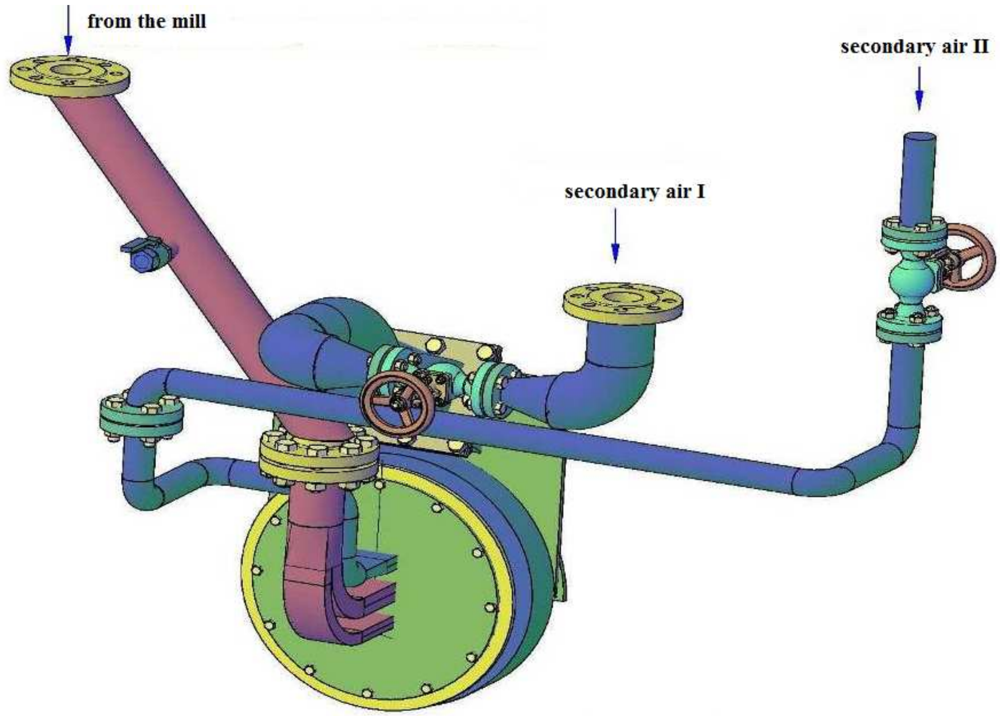

Figure 2. General conception of burner connection to the supplying circuits with primary air+coal dust, and secondary air I and II

4. ACKNOWLEDGMENT

This work was supported by a grant of Romanian National Authority for Scientific Research CNDI-UEFISCDI, project number PN-II-PT-PCCA-2011-3.2-1292, contract number 33/2012, HOLGRUP.

References

[1] * * *, Management and psychology applied to a holistic integrated coal energy system in order to reduce pollution and increase quality of life – HOLGRUP. Project ID: PN-II-PT-PCCA-2011-3.2-1292; University Politehnica of Bucharest – Center of Thermal Researches, 2012-2016.

[2] G. P. Negreanu, D. Stanciu, L. Mihăescu, I. Pîşă, I. Oprea, „Testing the operation of a new lignite low NOx burner module by experiment and modeling", International Conference on Applied Energy, ICAE 2013, Jul 1-4, 2013, Pretoria, South Africa

[3] Ungureanu, C., Zubcu , V., Pănoiu, N., Ionel, I., „Combustibili, Instalaţii de ardere, Cazane", Ed. „Politehnica", 2006, ISBN 973-9389-21-0.

[4] Mihăescu, L., Prisecaru, T., Popa, E., Grămescu, S., „Cazane de abur şi apă fierbinte", Ed. Perfect în colaborare cu Ed. Printech, 2007, ISBN 978-973-7984-32-6.

[5] Prisecaru, M., Mihăescu, L., Prisecaru, T., Popa, E., „Construcţia şi exploatarea cazanelor de abur şi apă fierbinte", Ed. Politehnica Press, 2009, ISBN 978-606-515-011-9.

[6] Popper, L., Mihăescu, L., Iliescu, M., „Eficienţa economică a sistemelor de energie", Ed. Perfect, Bucureşti, 2011, ISBN 978-973-798 4-86-9

THERMAL POWER PLANT FOR ENERGY WILLOW USE: DESIGN, PERFORMANCES

Gabriel Negreanu[1*], Viorel Berbece[*], Lucian Mihăescu[*],
Ion Oprea[*], Ionel Pîşă[*], Dan Andreescu[**]

[*]*University Politehnica of Bucharest*
[**]*Turboexpert Romania*

ABSTRACT

In last few years, in Romania, the energy willow crops exceeded 1200 hectares, with an average yield of 50 t/ha at 50 % of moisture. The entrepreneurs are selling the chopped biomass with 50 €/t to the firms and individuals, mainly for heating purposes, to be burned in stoves and hot water boilers.
The purpose of the paper is to analyze the opportunity to increase the overall efficiency of the biomass conversion, using a thermal power plant based on Rankine-Hirn thermodynamic cycle. The innovation of our research is related to the concept of integrated use of the biomass in energy purposes, from the crops formation and initiation up to the electricity and heat markets. The analysis of the different constructive solutions of the low-size steam turbines allows the estimation of the technical performances and economic indicators, in order to obtain a successful project.
Several constructive and functional schemes for steam power plants in the range of 200-2000 kW_e are studied in comparison. The main goals are to maximize the internal efficiency of the turbine at lowest rated load and to obtain positive economic indicators (payback period, net present value, internal rate of return)

1. INTRODUCTION

Today, in Romania, energy willow crops are booming, the cultivated area is over 1000 ha. In 2013, Covasna County held its first energy harvesting willow, with a production of 50 t/ha at harvest moisture of 50%. The local use in small heating installations is restricted by complicate transport and storage. The design of power plants with an output of 200-2000 kW, allows an efficient recovery, especially in locations near the crops. The high calorific energy willow chips (about 16,000 kJ/kg) will expect that power.

Only a steam boiler with efficient and environmental friendly combustion to be coupled with a turbine in current production is the main need for harnessing energy willow crops. The selected combustion technology (willow chips entrained by the primary air) imposes a tunnel-burner attached to the combustion chamber. Superheated steam conditions are required by the turbine input parameters, while the steam exhaust pressure is higher than usual.

2. TECHINCAL SOLUTIONS

Two constructive and functional schemes for steam power plants are studied in comparison. The main goals of the research are to prove the technical feasibility, to maximize

[1] 313 Splaiul Independentei, Bucuresti, Romania, Tel. +40214029158, email: gabriel.negreanu@gmail.com.

the internal efficiency of the turbines and to obtain positive economic indicators (payback period, net present value, internal rate of return)

The first chosen solution is shown in figure 1 and inspired from [1].

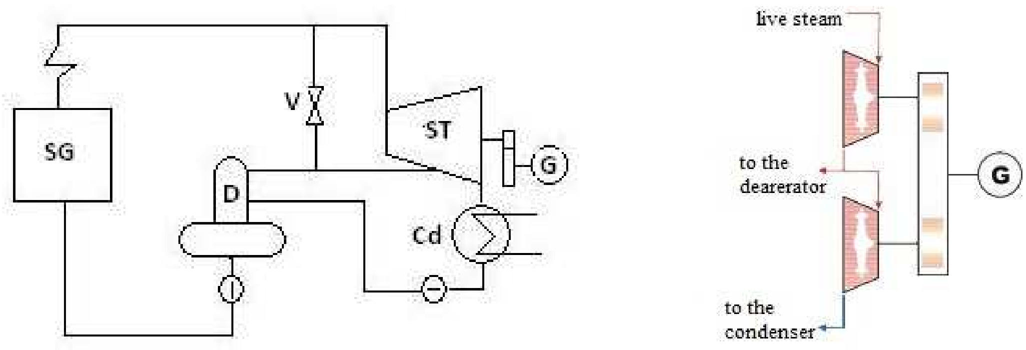

Figure 1 The 200 kW_e power plant scheme and the steam turbine

The micro power plant is composed of:

- A superheated live steam generator (p_0=27 bar, t_0= 275 °C, t_{al}=120 °C) fuelled by dry chopped energy willow (B[kg/s]), generating 0,55 kg/s live steam;
- A steam turbine (P_e= 200 kW_e, p_c=0.15 bar, n=12000 rpm) composed of two velocity compounded Curtis stages in sequence;
- An electric generator with 4 poles coupled to the both turbines trough a gearbox;
- A deaerator supplied with live steam trough a lamination valve;
- The condensate pump and the feed-water pump.

Admitting that the isentropic enthalpy drop is divided equally between the two Curtis stages, the overall design performances of the plant are presented in Table 1

Table 1 Design and performance data of the 200 kWe TPP

$P_{BG\ ST1}$ [kW_e]	88	$\eta_{i\ ST1}$	0.482
$P_{BG\ ST2}$ [kW_e]	112	$\eta_{i\ ST2}$	0.558
$P_{TH\ SG}$ [kW_{th}]	1688	η_{SG}	0.88
B[kg/s]	0.1055	η_{EA}	0.1135

The second chosen solution is shown in figure 2, taken and processed from [2]

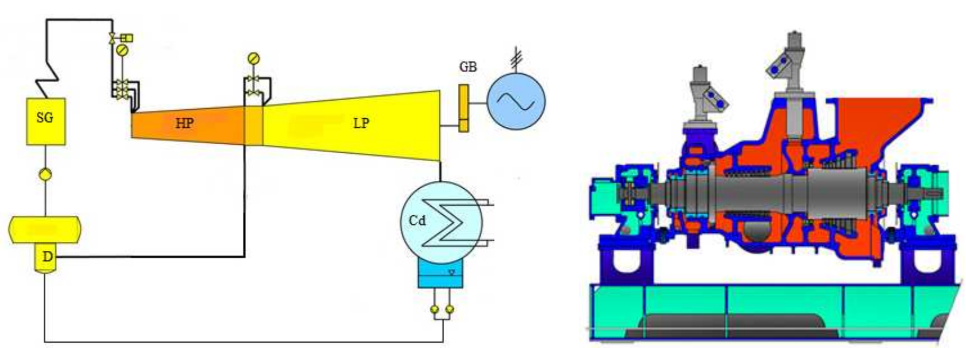

Figure 2 The 2000 kW_e power plant scheme and the steam turbine

The mini power plant is composed of:

- A superheated steam boiler (p_0=35 bar, t_0= 350 °C, t_{al}=135 °C) fuelled by dry chopped energy willow B[kg/s]), generating 2,92 kg/s live steam;
- A steam turbine (P_e= 2000 kW$_e$, p_c=0.1 bar, n=10500 rpm) composed of two sections, each one with a Rateau control stage and many pressure compounded stages;
- An electric generator with 4 poles coupled to the turbine trough a gearbox;
- A deaerator;
- The condensate pumps and the feed-water pump.

The original steam turbine had a controlled extraction at the pressure of 3 bar, but we have computed the turbine like two serial condensing turbines (high pressure –HP and low pressure –LP). The overall design performances of the plant are presented in Table 1

Table 1 Design and performance data of the 2000 kWe TPP

$P_{BG\ HP}$ [kW$_e$]	993	$\eta_{i\ HP}$	0.785
$P_{BG\ LP}$ [kW$_e$]	1007	$\eta_{i\ LP}$	0.793
$P_{TH\ SG}$ [kW$_{th}$]	8213	η_{SG}	0.90
B[kg/s]	0.5133	η_{EA}	0.2435

3. ECONOMIC ANALISYS

The economic analysis is carried on a period equal to the lifetime expectance of the equipments (usually 20 years). The cash-flow source is represented by the money value of the available electricity generated during this period. There are two income components: the market price (p_{el}= 40 €/MWh) and the support scheme for the energy produced from renewable sources (3 green certificates of p_{GC}=27-52 €/MWh).

The expenses are represented by the annual return of the investment, the interest (if the investment cost is covered even partially by a loan), the fuel cost, O&M cost, insurance, etc.

Considering an annual discount rate a, it is possible to compute the economic indicators, such as: simple payback time (T_s), net present value (NPV), internal rate of return (IRR). The conditions for a good micro gas turbine system are: NPV > 0, IRR > a, T_s < lifetime and related to the investor satisfaction.

$$NPV = \sum_{t=0}^{n} \frac{V_t - C_t}{(1+a)^t} \; ; \qquad \text{IRR} = a^* \text{ for } NPV = \sum_{t=0}^{n} \frac{V_t - C_t}{(1+a^*)^t} = 0 \; ; \qquad \sum_{t=0}^{n_{\min}=T_s} (V_t - C_t) \geq 0$$

where: - V_t – revenues of year t; C_t – expenses of year t; - n – power plant lifetime.

The study case is based on the installation of a TPP producing P_{BG} and delivering to the network (1-ε)·P_{BG}, ε being the internal electricity consumption (assumed 10%). The annual operation period was estimated at 7000 hours, in integration with the forest activity (energy willow crop)

The common input figures for the economic analysis are:

- O&M costs $C_{O\&M}$ = 30,000 €/MW$_{ei}$+4 €/MWh$_e$[3];
- Energy willow price p_{ew} = 20 €/t; (the willow culture and the power plant are integrated in the same business, so the price is lower than 50 €/t)
- Electricity market price p_E = 40 €/MWh$_e$;
- Green certificate price p_{GC} = 40 €/MWh$_e$;
- Discount rate a = 10%;
- Planned payback period T_p = 7 years;
- The investor has the money for the project and don’t borrow it from the bank.

In table 2 are represented the components of the capital costs:

Table 3 Components of the capital costs of the biomass TPP

No.	Component	200 kW_e	2000 kW_e	M.U.
1	Turbine+annexes+gearbox+electric generator	300,000	3000000	€
2	Steam generator+deaerator	60,000	400000	€
3	Pumps	30,000	240000	€
4	Fuel supply and storage plant	20,000	100000	€
5	Chimney	20,000	106154	€
6	Total equipments	430,000	3,846,154	€
7	Services & labor	87,000	769,231	€
8	Contingency	43,000	384,615	€
9	Capital cost	560,000	5,000,000	€
10	Specific capital cost	2,800	2,500	€/kW_{ei}

The results of economic analyze are shown in table 3.

Table 3 Results of the economic analyze of the biomass TPP

No.	Economic criteria	200 kW_e	2000 kW_e	M.U.
1	T_s	8.3	5.3	years
2	NPV	970,892	24,671,709	€
3	IRR	14.09	21.50	%

4. CONCLUSIONS

Analyzing these numbers, we can draw the conclusion that both projects are feasible. However, a slight slippage of a single input data (such as the value of the green certificates, or even the interruption of the support mechanism) can easily bring looses to the project and put the investor in a difficult situation. It is also possible to increase the revenues of the plant if the electricity market price will rise in the future. The 2000 kW_e TPP has an overall efficiency twice then the 200 kW_e TPP, but its capital cost is quite double. For the 200 kWe TPP the necessary crop area for energy willow is about 160 hectares/2 year harvest, while for the 2000 kW_e TPP is about 776 hectares.

After the comparative analysis of the studied technical schemes, the following conclusions were drawn:

- The smaller TPP is suitable to work in remote areas, while the larger one is better to be connected to the grid.
- While the nominal power increases, the economic indicators are increasing too.
- The support mechanisms for renewable energy sources (green certificates) are vital for the project success.

References

[1] http://www.etgroup.nl/?steam-turbine-mk-7,25

[2] http://www.ttk.hr/en/?page_id=351

[3] Technology Data For Energy Plants, energynet.dk, ISBNwww: 978-87-7844-931-3

[4] A. Leca, V. Muşatescu,...G.P. Negreanu,...et all, „Managementul energiei”, Editura AGIR, ediția a II-a 2008, 745 pagini, ISBN 978-973-720-190-4.

[5] L. Mihăescu, I. Oprea, G. Negreanu, I. Pîşă, M. Ceclan, Mălina Prisecaru, Elena Pop, Manuela Georgescu, V. Berbece, „Sisteme şi echipamente termice pentru producerea energiei – Construcție, funcţionare, management”, Ed. Printech, ISBN 978-606-521-872-7, Bucureşti 2012, 386 pag.

THE ANALYSIS OF THE DYNAMICS OF VEGETABLE OILS BURNING IN POWER PLANTS

PhD student Eng Bogdan Niculescu
Faculty of Power Engineering, University Politehnica of Bucharest

1. THE ENERGETIC HARNESSING OF VEGETABLE OILS

The energetic harnessing of vegetable oils represents an economical and ecological solution if it is resorted only to conventional combustion installations. The development of a special technology of burning would lead to additional investments, which would be hard to amortize.

The vegetable oils used for energy purposes differ from the bio fuels used in internal combustion engines and that through special treatments follow a different financial course.

The harnessing of vegetable oils that are pure or mixed with liquid fossil fuels in electrical installations includes boilers of hot water and steam, destined for residential and industrial heating and the heating of technological steam or steam for turbines coupled with electrical generators.

Analyses that were conducted in the past few years on the energetic characteristics of crude vegetable oils indicate they are approaching those of fossil fuels.

The research on the process of burning vegetable oils, starting from their energetic characteristics, is imposed concurrently by two methods, analytical and experimental. It is estimated that only after a concordance of the experimental results with the theoretical results occurs, a certain burning technology can be validated.

The most common mixing situation is with the liquid fossil fuels.

The light liquid fuels, like the crude vegetable oils, are characterized by the temperature of vaporization situated under the one of ignition, with the burning being influenced adequately.

2. COMPUTATION MODELS APPLICABLE TO THE BURNING OF VEGETABLE OIL DROPS

Mathematically, the modelling of the burning processes for vegetable oils will be derived from the one for light fossil fuels.

There exist several mathematical models that approach the burning of light liquid fuels.

The first step in choosing the mathematical model will depend on the comparative analysis of the energetic characteristics for the crude vegetable oils and the light liquid fuels.

The following structural models are defined:

-the Hitrin model, considers that the liquid drops receive warmth from the environment through convection and the time of burning is imposed by the time of vaporization:

$$\tau = \frac{\rho_e \frac{L}{\lambda} R_O^2}{2\left(T_m - T_f\right)} \left[s\right] \qquad (1)$$

where: T_f is the boiling temperature, K; T_m – the temperature of the environment, K; R_0 –the ray of the fuel particle, m; q_l – the liquid density, kg/m^3, L – the latent heat of vaporization, K kg; λ – thermal conductivity, W/ (mK).

- the Varsavski model considers the heat to be received from the particle through conductivity; as a result it has more precision for the fine drops.

$$d_\tau = -\frac{\left(1-\frac{R}{R_a}\right) R \rho_e dR}{\frac{\lambda_0 T_0}{a}\Phi} \qquad (2)$$

where: R and R_a are the rays of the fuel particle, respectively of the front flame, m; λ_0 –the conductivity coefficient at 0^0C; a = λ/(ρ c_p); Φ correction function with the report T_g/T_m.

- the Godsave model considers decisive the influence of the radiation over the burning time

$$\tau = \frac{\left(1-\frac{R}{R_a}\right) R^2 \rho_e c_p}{3\lambda \ln\left(1+\frac{c_p \Delta T}{\Delta I}\right)} [s] \qquad (3)$$

where: c_p is the specific heat of the fuel, kK/(kgK); ΔI - the amount of heat for evaporation and lifting the temperature of the fuel up to the value of balance for the surface

-the Spalding model considers the burning in a stationary film at the edge of the drop under the influence of the flux of the fuel-air diffusion

$$\tau = \frac{\rho_e R_0^2}{2D\rho \ln(1+B)} [s] \qquad (4)$$

where: D is the coefficient of the diffusion of fuel-air, m^2/s, B- the heat transport parameter, q – the density of the burning gases, kg/m^3

$$B = \frac{H_i^i}{\Delta I}\frac{m_{O_2}}{\beta} + c_p \frac{T_g - T_s}{\Delta I} \qquad (5)$$

in which H^i_i - is the calorific power of the fuel, KJ/kg; m_{O_2} - the gravimetrical concentration of the oxygen in a gaseous medium, β - the oxygen needed for the burning of the unit of fuel, T_g – the temperature of the burning gases, K; T_s – the temperature of the particle's surface, which can be approximated with the temperature of vaporization, K..

As a result of the analysis of the energetic characteristics of the crude vegetable oils, shown in table number 1(conducted by ICEMENERG in year 2012), characteristics that are very close to the light liquid fuel from the diesel fuel class can be distinguished.

The flammability point is of 320-330^{0}C for the sunflower oil, of 250 – 260^{0}C for the canola oil and of 82 – 87^{0}C for the diesel fuel mix.

The higher value of the vaporization and ignition temperature for the vegetable oils implies the choice for the numerical simulation of the Spalding model, dominated by the burning in a single film on the edge of the particle and determined by the time of the oxygen diffusion.

Table 1

The energetic characteristics of crude vegetable oils

The fuel	**The energetic characteristic**					
	the boiling temperature ^0C	**density kg/m^3**	**Specific heat ĶJ/(kgĶ)**	**Latent heat ĶJ/kg**	**Conductivity W/(ms)**	**Calorific power H^i_i ĶJ/kg**
Sunflower oil	210-230	915-930	1,80-1,86	500-530	0,18-0,184	39000-39400
Canola oil	220-245	915-930	1,75-1,80	500-520	0,18	39900-40100
Diesel fuel	230	858	1,74-1,76	430-445	0,169-0,171	40600
Sunflower oil 40% and diesel fuel mix	220	880	1,8-1,83	480-488	0,177	39800-39900

In figure number 2, it is presented the variation of the viscosity with the preheating temperature.

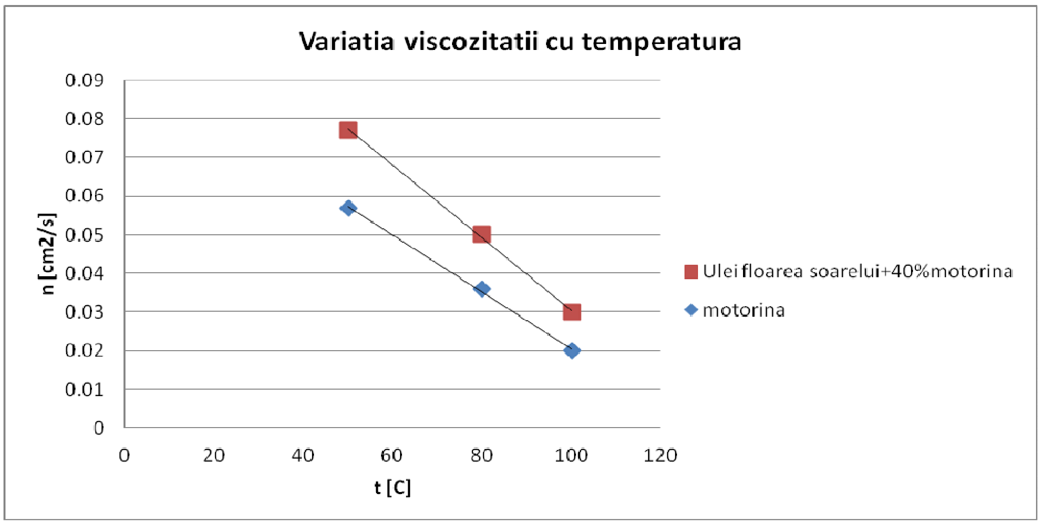

Figure 2. The variation of the viscosity with the temperature

The length of the flame of the liquid fuel particle, after paper [2], can be determined with the relation:

$$L = \frac{ut}{[1+A]^2}\,[m] \qquad (6)$$

where: u is the speed of the flow in the output section in the burner, m/s; t – the time, s.

The A coefficient has the structure:

$$A = 1 + \frac{2.4}{\tau_e}\left(\frac{\rho_a}{\rho_e}\cdot\frac{\upsilon_a}{\upsilon_e}\right)^{1/2}\cdot\left(\frac{d_j}{d_0}\right)^{1,5} \qquad (7)$$

where: τ is the superficial tension of the liquid, N/m, ρ_a, ρ_e – the air density, respectively of the liquid fuel, kg/m^3; υ_a, υ_e – the air viscosity, respectively of the liquid fuel, m^2/s; d_j, d_0 – the diameter of the fuel squirt, respectively the output section, m.

3.THE ANALYTICAL RESULTS CONCERNING THE BURNING OF VEGETABLE OILS

In figure 3, the length of the flame for burning the sunflower oil in a crude state and additivated with 40% diesel fuel is presented.

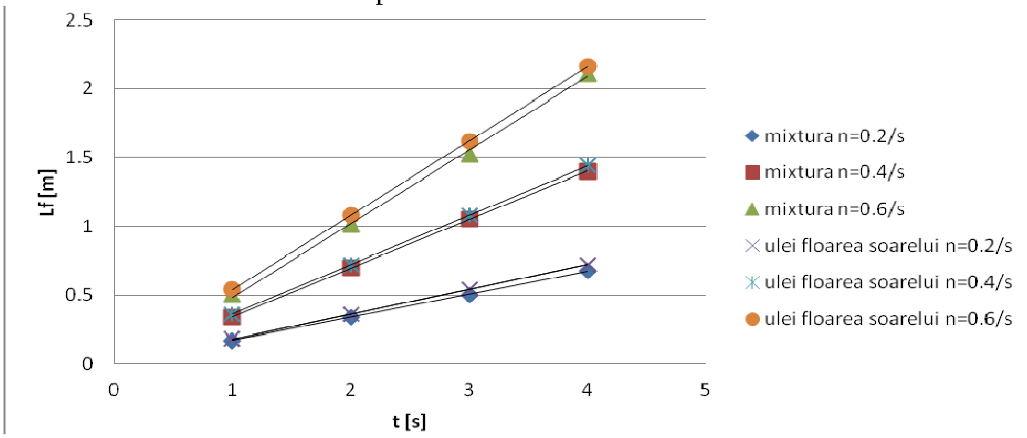

Fig.3. The length of the flame depending on the speed of the fuel at the injector exit

The speed of exit from the injection orifice was considered in the 0,2 m/s domain, a domain applicable for a burner of low flow, which can be applied in the harnessing of vegetable oils. The data are for a report d_j/d_0 and a preheat temperature of the fuel of 90^0C.

In order to determine the time of burning in correlation with the length of the flame, applications for the Spalding model have been chosen, relation (4). Quantity ΔI was chosen as equal with the latent heat of vaporization L. The physical quantities have the following values:

- for the sunflower oil: H^i_i = 39400 KJ/kg; L = 500 KJ/kg; m_{O2} = 0,23 kg/kg; β = 3,48; c_p = 1,86 KJ/(kgK)

- for the sunflower oil and 40% diesel fuel mix: H^i_i = 39900 KJ/kg; L = 480 KJ/kg; m_{O2} = 0,23 kg/kg; β = 3,48; c_p = 1,83 KJ/(kgK); $T_g - T_s$ = 1100, λ = 0,18 W/(ms)

After calculations, the results were the following:

-crude sunflower oil

$$B = \frac{39400}{500}\cdot\frac{0.23}{3.48} + 1.86\frac{1100}{500} = 9.3$$

- for R_0 = 40 µm

$$\tau = \frac{915\cdot 1.86\cdot (0.04)^2}{2\cdot 0.18\cdot \ln(1+9.3)} = 3.24\,s$$

- for R_0 = 50 µm

$$\tau_a = \frac{915\cdot 1.86\cdot (0.05)^2}{2\cdot 0.18\ln(1+9.3)} = 4.25\,s$$

A compatibility between the time of burning and the length of the flame, presented in figure number 3, can be distinguished, for installations of reduced thermal powers, with the lengths of the firebox of under 1,2 m and an increased adaptability for installations of large and medium thermal power.

References

1. Lemneanu, N., ş.a. „Instalaţii de ardere cu combustibili lichizi” ed. Tehnică, 1982
2. Stambuleanu, A. „Flacăra industrială”, ed. Tehnică, 1971
3. Mihăescu, L. ş.a. „Valorificarea energetică a uleiurilor vegetale brute”, ed. Printech, Bucureşti 2011, ISBN 978-606-521, 690-7

EFFICIENT USE OF NATURAL GAS FOR A MEDIUM SIZE DISTRICT HEATING SYSTEM

Ion Oprea[1], Gabriel Negreanu, Viorel Berbece, Ionel Pîşă, Lucian Mihăescu
Politehnica University of Bucharest

ABSTRACT

Cogenerative combined cycles are now the best commercial technology for energy production. They achieve the higher overall efficiency then other operational power plants, low greenhouse gases and good capital cost. The modern gas-turbines, with high inlet temperature, give the possibility to increase the thermal efficiency and the economic results both in electric and cogeneration operation. Based on literature and own research this paper emphasizes the opportunity to obtain better economic results for natural gas use as fuel for the district heating of a medium size district system. The case study involves not only the thermal efficiency but also the capital costs, fuel price, operational and maintenance costs, and the taxes imposed.

1. INTRODUCTION

The new power plants must meet three major requirements: minimum investment, maximum efficiency and reduced emissions. From this point of view the cogeneration combined cycles are the optimal solution being most modern technology in commercial power generation. Combined cycle fuel used must be a superior fuel, gaseous or liquid that burns in the combustion chamber of the gas turbine. Most power plants operate today in the most efficient combined cycle using natural gas as fuel.

Cogeneration of electricity and heat in gas-steam combined cycle ensure thermodynamic and economic benefits for certain. The thermal potential of a combined cycle is higher, given that for the same value extracted for heating steam temperature, enthalpy drop in the combined cycle compared to the classic. Heat input gas-steam combined cycle is at a higher temperature, corresponding to gas Brayton cycle.

2. OPERATIONAL SOLUTIONS

Combined cogenerative cycle systems operate now in three basic constructive solutions [2]:

- Heat recovery steam generator;
- Backpressure steam turbine (fig. 1);
- Extraction condensing steam turbine (fig. 2).

All these three variants bring additional power and better performance flexibility using supplementary firing, with the ability to independently adjust the production of electricity and heat. Gas turbine power controls electric power generation and supplementary firing allows controlling the flow of steam and heat. Another solution that improves the peak loading is complementary firing system, which involved a supplementary industrial sized gas turbine.

In combined cycle with heat recovery boiler, the missing of the regenerative circuit in the Rankine makes dominant the external cogeneration index (power to heat ratio in cogeneration). Another feature is the high minimum value of this index. The cogeneration index of combined cycles is significantly affected by three parameters:

[1]Splaiul Independenţei 313, sector 6, Bucharest, PC RO-060042, oprea@caz.mecen.pub.ro

- The size of the final condensing region of the steam turbine;
- Steam pressure value to the consumer or industrial areas;
- Supplementary amount of fuel burned.

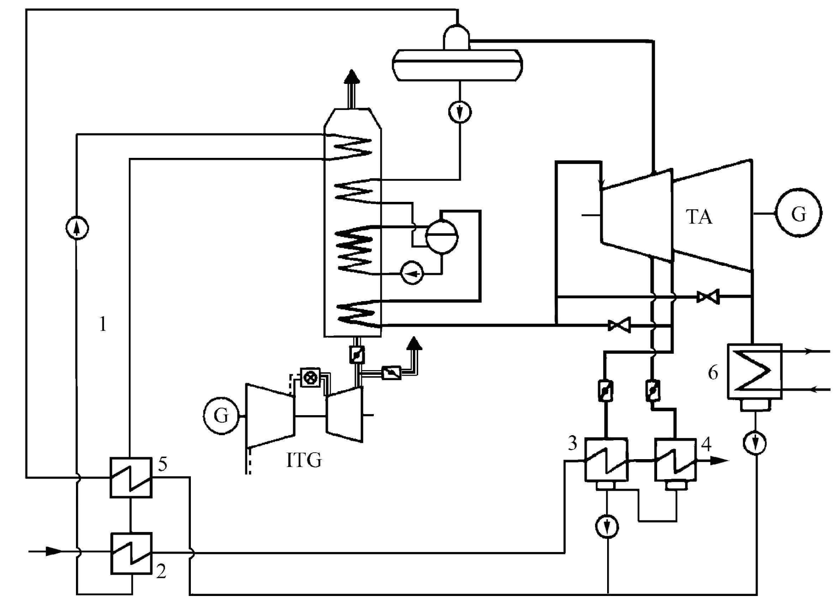

Figure 2: Combined cogenerative cycle with single-pressure heat recovery boiler and extraction condensing steam turbine
1 – additional heating circuit; 2 – preheating stage I ; 3 and 4 – preheating stage II and III; 5 – low pressure preheater; 6 – condenser.

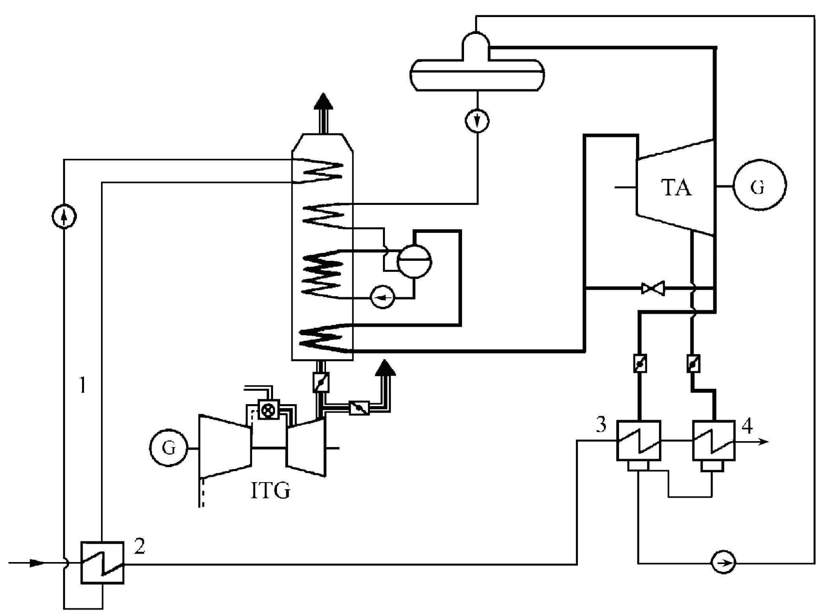

Figure 1: Combined cogenerative cycle with single-pressure heat recovery boiler and backpressure steam turbine
1 – additional heating circuit; 2 – preheating stage I ; 3 and 4 – preheating stage II and III.

The modern gas turbines with high inlet temperature make no advantage the supplementary heating. More over the supplementary firing diminishes the cogeneration index value that means a decrease of the thermodynamic efficiency. For better efficiency, combined cogenerative cycles are recommended to be used only in relatively high cogeneration indexes.

Extracting condensing steam turbines as compared to the backpressure turbines are characterized by smaller internal efficiency, higher dimensions and costs. But they have some indubitable advantages. These steam turbines can operate independently of heat demand and have high operational flexibility, covering broad areas of demand for electricity and heat. The ability to produce additional electricity in the condensing region makes possible an increasing of the cogeneration index. As it increases, decreases the overall efficiency of the combined cycle, which at very high cogeneration index approaching the combined cycle without cogeneration. This makes the backpressure turbine to be preferred for combined cogeneration.

In modern power combined cycle, with triple pressure, the live steam condition of the heat recovery steam generators is close to those used in classical cycles. Under these conditions the pressure steam extracted to provide heat consumption has a major influence on the combined cycle characteristics. In contrast to boilers with lower parameters and single-pressure, without supplementary firing, the level of the live steam pressure plays an important role. Thus, the high pressure steam is extracted, so it is necessary to adopt a higher pressure of the live steam, in order to ensure a sufficiently high enthalpy drop in the turbine between the two pressure levels. By increasing the live steam pressure decreases the degree of heat recovery and the introduction of an additional heating loop become necessary.

To be effective the steam extract temperature for district heating should be as small and live steam pressure greater than for no cogeneration cycle. The optimum steam extracted temperature is determined so as to obtain maximum electrical power and lowest cost to transport heat.

3. CASE STUDY

The new combined cycle power plants set new world records with both their electrical efficiency of more than 60 percent and un unmatched supply of thermal energy for municipal district heating. The fuel utilization rate of natural gas fuel increases in cogeneration above 85 percent.

The objective of the case study is to emphasize the high efficiency of a triple pressure cogenerative combined cycle and the possibility to obtain better economical results for natural gas using. The thermodynamic analyze includes a model for the heat exchange in the steam recovery boiler, that get the possibility to find the steam condition for the all three steam circuits.

On consider a cogenerative triple-pressure combined cycle that has a thermal output of 180 MWt, corresponding to a medium municipal district heating. Heat is supply by an extracting condensing turbine as is shown in figure 3.

The gas turbine has maximum temperature of 1427 ^{0}C, pressure ratio 18,1, exhaust mass flow 650 kg/s and exhaust temperature 640 ^{0}C. For the Rankine cycle steam condition is: live steam p_o = 110 bar, t_o = 565 ^{0}C, one stage of reheat t_{01} = 565 ^{0}C, the intermediate steam pressure p_{01} = 26 bar, the low steam pressure p_{02} = 3.7 bar, condensing pressure p_c = 0.07 bar. The recovery het boiler arrangement is shown in figure 3 and the minimum temperature difference was considered δt = ^{0}C. An intermediate temperature for high pressure vaporization circuit was considered. The equation system for heat exchange is given below:

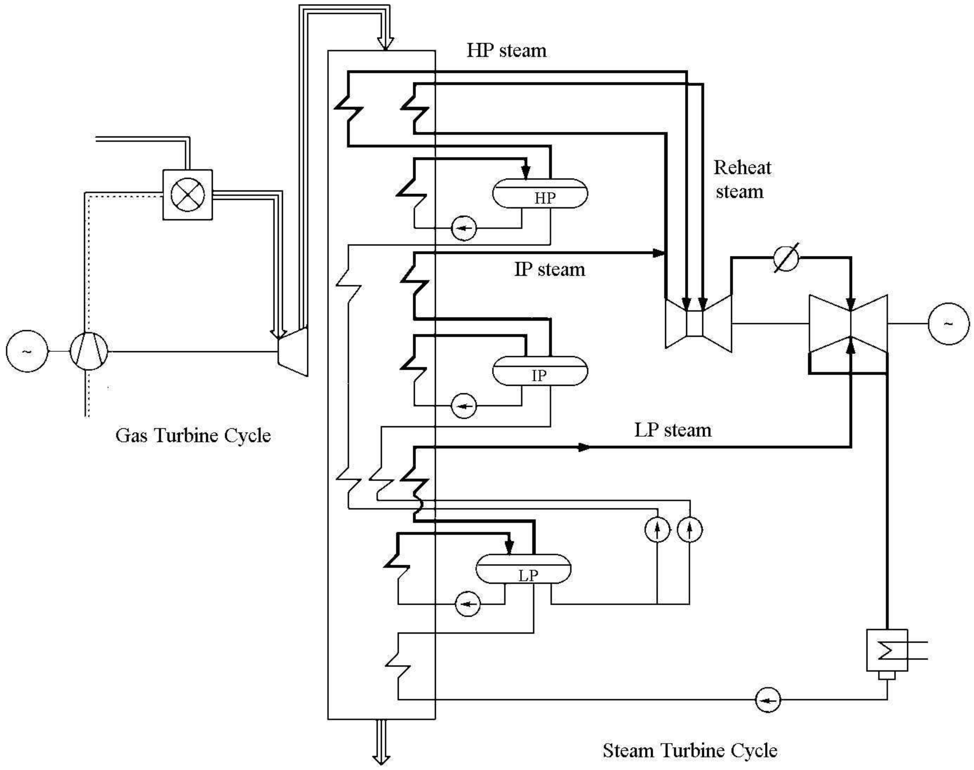

Figure 3: Cogenerative combined cycle with triple-pressure heat recovery boiler and condensing steam turbine

$$\left(t_{gev}\cdot C_{pg}\left(t_{gev}\right) - t_{gx1}\cdot C_{pg}\left(t_{gx1}\right)\right)\cdot\eta_{rec} = \left(m_0 + m_1\right)\cdot\left(h_{01} - h_{evCIP}\right) \tag{1}$$

$$\left(t_{gx1}\cdot C_{pg}\left(t_{gx1}\right) - t_{gx2}\cdot C_{pg}\left(t_{gx2}\right)\right)\cdot\eta_{rec} = m_0\cdot\left(h_0 - h''_0\right) \tag{2}$$

$$\left[t_{gx2}\cdot C_{pg}\left(t_{gx2}\right) - \left(t_{s0} + \delta t\right)\cdot C_{pg}\left(t_{s0} + \delta t\right)\right]\cdot\eta_{rec} = m_0\cdot r_0 \tag{3}$$

$$\left[\left(t_{s0} + \delta t\right)\cdot C_{pg}\left(t_{s0} + \delta t\right) - t_{gx3}\cdot C_{pg}\left(t_{gx3}\right)\right]\cdot\eta_{rec} = m_1\cdot\left(h_{evCIP} - h''_1\right) \tag{4}$$

$$\left[t_{gx3}\cdot C_{pg}\left(t_{gx3}\right) - \left(t_{s1} + \delta t\right)\cdot C_{pg}\left(t_{s1} + \delta t\right)\right]\cdot\eta_{rec} = m_1\cdot r_1 + m_0\cdot\left(h'_0 - h_{a1}\right) \tag{5}$$

$$\begin{aligned}\left(t_{s1} + \delta t\right)\cdot C_{pg}\left(t_{s1} + \delta t\right) - t_{gx4}\cdot C_{pg}\left(t_{gx4}\right)\cdot\eta_{rec} = {} & m_0\cdot\left(h_{a1} - h'_2\right) \ldots \\ & + m_1\cdot\left(h'_1 - h'_2\right) + m_2\cdot\left(h_{02} - h''_2\right)\end{aligned} \tag{6}$$

$$\left[t_{gx4}\cdot C_{pg}\left(t_{gx4}\right) - \left(t_{s2} + \delta t\right)\cdot C_{pg}\left(t_{s2} + \delta t\right)\right]\cdot\eta_{rec} = m_2\cdot r_2 \tag{7}$$

$$\left[\left(t_{s2} + \delta t\right)\cdot C_{pg}\left(t_{s2} + \delta t\right) - t_e\cdot C_{pg}\left(t_e\right)\right]\cdot\eta_{rec} = \left(m_0 + m_1 + m_2\right)\cdot\left(h'_2 - h_{aa}\right) \tag{8}$$

where:

– t_{gev} , t_{gx} , t_e , - exhaust gas turbine temperature, intermediate gas temperatures in heat recovery steam generator and stack flue gas temperature;
– h_{aa} - feed water temperature;
– m_0, m_1, m_2 - relative mass steam flow;
– η_{rec} - heat recovery steam generator efficiency.

The relative mass steam flows corresponding to each pressure are: m_0 = 0.1264, m_1 = 0.02 and m_2 = 0.017. The flue gas temperature to the heat recovery steam generator exhaust was obtained t_e = 87 ^{0}C.

The simple gas cycle efficiency is 39%, combined cycle gross efficiency is 0.61 and the overall fuel utilization ratio in cogeneration is in excess of 70%. In district heating operational mode the extracted steam ensures the thermal output of 180 MWt with a loss in power of about 50 MW.

4. ECONOMICAL ANALYSIS

The economical analysis will be conducted on a period equal to the lifetime expectance of the equipments (usually 20 years). The two positive cash-flow sources are represented by the money value of the available electricity and heat generated in a year, including two bonuses (for high efficiency cogeneration and CO_2 saving).

The expenses are represented by the annual return of the investment, the interest (if the investment cost is covered even partially by a loan), the fuel cost, O&M cost, insurance, etc.

Considering an annual discount rate (*a*), it is possible to compute the economic indicators of the case, such as: payback time (T_s), net present value (NPV), internal rate of return (IRR). The conditions for a good electric and heat cogeneration system are: NPV > 0, IRR > a, T_s < lifetime and related to the investor satisfaction.

$$NPV = \sum_{t=0}^{n} \frac{V_t - C_t}{(1+a)^t} \tag{9}$$

$$\text{IRR} = a^* \quad \text{for} \quad NPV = \sum_{t=0}^{n} \frac{V_t - C_t}{(1+a^*)^t} = 0 \tag{10}$$

$$\sum_{t=0}^{n_{\min}=T_s} (V_t - C_t) \geq 0 \tag{11}$$

where:

- V_t – revenues of year t; C_t – expenses of year t; - n – power system lifetime.

The analysis was performed for the above case study. The annual operation period was estimated at 8160 hours (4400 winter time).

The input figures for the economic analysis are:

- Specific capital cost I_{sp} = 583 €/kW$_i$;
- O&M costs $C_{O\&M}$ = 3.4 €/MWh$_e$+4.5 €/kW$_i$;
- Natural gas tariff p_{gas} = 0.29 €/m^3_N;
- Electricity tariff p_E = 35 €/MWh$_e$;
- Heat tariff p_Q = 36 €/MWh$_t$;
- Discount rate a = 10%;
- Planned payback period T_p = 7 years.

After running the operational case, we have obtained the following results:

- NPV = 69,920,000 €;
- IRR = 12.65 %;
- T_s = 8.9 years.

Looking to these values, it is obviously that the project is successful for a high efficiency use of the natural gas, but it is sensitive to the value of support-mechanisms.

5. CONCLUSIONS

The paper is an application that shows the benefit of the natural gas utilization in a cogenerative combined cycle for a medium district heating.

The choice of a triple pressure cycle ensures the better performances both in electrical and heating operational modes. The presented case studied for natural gas fuel have demonstrated an efficiency of 61% in condensing mode and the fuel utilization rate over 70% in heating mode. The extraction condensing steam turbine is capable of satisfying heat demand of 180 MWt for the municipal district heating system. The analyzed solution has a high operational flexibility, good part-load efficiency, minimum impact on environmental and huge reduction of CO_2 emissions.

The economical study of the cogenerative combined cycle have proved that the project is successful for a high efficiency use of the natural gas, but it is sensitive to the value of support-mechanisms.

References

[1] Horlock J.H., *Advanced Gas Turbine Cycles*, Elsevier Press 2003.

[2] Kehlhoferr.H., Plancherel A., Stirnimann F., Rukes. B., Combined Cycle Gas & Steam Turbine Power Plants, PennWell Corporation 2009.

[3] Oprea, I., *Heat recovery in micro gas turbines for cogeneration.* 1st International Conference on Modern Power Systems MPS, November 8-11, 2006, Cluj-Napoca, Romania.

[4] Oprea I., *Steam and Gas Turbines*, Ed. Printech, Bucharest 2004.

[5] Leca., A., Muşatescu., V., ..., Negreanu G.P., et all., Managementul energiei, Editura AGIR, 2006.

[6] Bejan A., *Termodinamica tehnica avansata*, Ed. Tehnica, Bucuresti 1996.

[7] Mihaescu L., Oprea I., Negreanu G.,…, Sisteme si echipamente termice pentru producerea de energie, Ed. Printech 2012.

[8] Chacartegui R.**,** Sánchez D, Muñoz de Escalona J.M., Muñoz A., Sánchez T. “Redesigning gas and steam combined cycles for low BTU syngas fuels utilization”.

POLLUTANT EMISSIONS OF A HEAT TREATING FURNACE

Daniela Pană[1], Ion V. Ion
"Dunărea de Jos" University of Galaţi, Romania

Abstract

The NO_x and CO emissions are regulated pollutant emissions. In order to have an insight into the degree of the amount of pollutant emission, especially at the modification of combustion conditions in the furnace is necessary to know the generation mechanisms and the influence of different parameters on their formation. In this paper, the mathematical models to quantify the generation rate of CO and NO_x in a heat treating furnace, on the basis of the chemical equilibrium and chemical kinetic mechanisms have been developed.

1. INTRODUCTION

European environmental regulations continue to reduce the CO and NO_x emissions from the combustion plants, production and processing of metals and other industrial activities [1]. Furthermore, the holders of stationary combustion plants that generate emissions of pollutants in the atmosphere are obliged to pay taxes to the Environment Fund in the amount and for substances listed in Annex. 1 of the Government Emergency Ordinance no. 196/2005, approved with amendments by Law no. 105/2006, as amended and supplemented.

The role of a heat treating furnace is to heat the material to a uniform temperature in order to change their shape or properties by using fuel as less as possible. The metal processing including iron production is one of the largest energy consumers in the manufacturing sector. To improve the energy efficiency many techniques have been developed. The most used techniques are: combustion with minimum excess air, correct heat distribution, furnace waste heat recovery, improved design of burners, combustion control, and instrumentation [2]. Combustion with minimum excess air is the first option in increasing energy efficiency as it is more economically convenient.

The normal operation of most burners of a furnace for heat treating is with as low as possible excess air to avoid metal oxidation. Therefore much attention should be paid to the CO emissions and combustion efficiency. The low excess air in flame combined with techniques to reduce NO_x emissions (steam or water injection into the flame, air and/or fuel staging, flue gas recirculation, ultra-lean premixing, and eliminating preheating of the fuel and/or combustion air) leads to increased emission of CO. During the start-up of furnace the burners produce cooler flame because the furnace walls, which are cold, absorb much radiant energy from the flame than they do when they are hot and because the furnace is full of ambient air which is entrained by the flame leading to the cooling of the flame. The steep decrease of flame temperature has as result the increase in CO emission.

CO emission is very important especially at small heat treating furnaces where the CO can come out from furnace into the atmosphere around the furnace. It is known that the

[1] Galati, 47 Domneasca St., E-mail: danyela_mail@yahoo.com

concentration of CO in the air of 100 mg/m^3 is fatal to the person who draws air loaded with CO [3].

In order to have an insight into the degree of the amount of pollutant emission, especially at the modification of combustion conditions in the furnace is necessary to know the generation mechanisms and the influence of different parameters on their formation.

In this paper, the mathematical models to quantify the generation rate of CO and NO_x in a heat treating furnace, on the basis of the chemical equilibrium and chemical kinetic mechanisms have been developed.

2. CO AND NO_X GENERATION MECHANISMS

Pollutant genesis in combustion processes is closely related to individual chemical reactions that sustain combustion. Formation of carbon monoxide and nitrogen oxides depends very much on the ratio in which the two reactants involved in the reaction - the fuel and air of combustion and the temperature at which combustion takes place [5]. With the increase in air/fuel ratio, under adiabatic conditions, the concentration of CO in the flue gas decreases and the NO_x increases to reach a maximum, and then decreases. Increasing the combustion temperature leads to an increased concentration of NO_x and to a lower CO concentration.

At chemical equilibrium there is enough time for all combustion reactions to proceed to perfection, so that chemical kinetics is less important. The chemical equilibrium describes composition of the reaction products tat can be achieved if the system is kept sufficiently time at constant temperature and pressure. Experience has shown that most combustion processes take place in finite time and thus chemical kinetics is important [4]. In order to understand the factors influencing the chemical pollutant emissions is necessary to study the rate at which the chemical system closes to the final equilibrium state [6].

The mechanisms that describe the combustion include a large number of reactions, even for simple hydrocarbons. Description of combustion kinetics of usual fuels is complicated by lack of knowledge of the composition of fuels. Once initiated combustion, combustion reactions take place quickly. The pollutant formation processes involve physical processes or slow reaction that impede the equilibrium reaching during combustion or as the combustion products are cooled and lead to partial oxidation of the fuel [6].

Detailed description of the dynamics of the multitude of simultaneous reactions requires finding the solution of a large number of ordinary differential equations [6]. Integrating these equations is difficult because they contain very different time scales, from short times of free radical reactions to long times of initiation reaction. One way to overcome these difficulties consists in modeling the combustion reactions in the processes represented by a small number of synthetic reactions, each of which describes the results of a number of stages of the basic reactions. These mechanisms called "global mechanisms" are stoichiometric equations that can be developed for approximate kinetic expressions. The overall reaction rate expressions may be derived from detailed kinetic mechanisms by taking into consideration appropriate simplifications, such as steady state or partial equilibrium. Another alternative is to use the correlation between concentration profiles, experimentally determined, of the species, the flame velocity measurements or other experimental data for parameters estimating of the overall rate [6].

The global mechanisms greatly reduce the complexity of the kinetic calculations because a small number of steps are used to describe the behavior of a large number of reactions [6]. In addition, the simplified reactions involve generally the major stable species, reducing the number of chemical species that should be followed. Minor species greatly influences the formation of pollutants and that is why the simplified overall mechanisms may not contain sufficient detail to describe chemical pollutant formation steps [107].

The hydrocarbons are consumed quickly during combustion generating CO, H_2 and H_2O. The oxidation of CO to CO_2 occurs at very low rate [107]. This difference in reaction rates may be taken into account using the two-step model, which separates the rapid oxidation of the hydrocarbon to CO and H_2O from the slow oxidation of CO to CO_2 [107]:

$$\begin{aligned} & C_mH_n+\left(\frac{m}{2}+\frac{n}{4}\right)O_2 \xrightarrow{k_A} mCO+\frac{n}{2}H_2O \\ & CO+\frac{1}{2}O_2 \xrightarrow{k_B} CO_2 \end{aligned} \tag{1}$$

The rate of reaction A is expressed by the same empirical equation used for the one-step reaction model [107]:

$$v_A = k_A[C_mH_n]^a[O_2]^b \, [\text{mol/m}^3\cdot\text{s}] \tag{2}$$

The rate of CO oxidation is given by the empirical equation [107]:

$$v_A = k_B[H_2O]^c[O_2]^d[CO] \, [\text{mol/m}^3\cdot\text{s}] \tag{3}$$

where the concentration of [H_2O] is included in equation because the largest share of CO is consumed by the reaction with OH, which is supposed to be in equilibrium with H_2O [6].

According to Dryer şi Glassman [107], the oxidation rate of CO in the two-steps model, can be described by the following equation:

$$v_{CO} = -1.3\cdot 10^{10}[CO][H_2O]^{0,5}[O_2]^{0,25}e^{-\frac{20130}{T}} \quad [\text{mol/m}^3\cdot\text{s}] \tag{4}$$

The two-steps model, although does not describes accurately the processes that occur at the beginning of combustion, represents an improvement of the one-step model, because it is considered that the CO oxidation reaction occurs at much lower rate than the rate at which fuel is consumed [6].

During the experiments accomplished on a small metal treatment furnace it was observed that at the cold start up, CO emission is high due to rapid cooling of the flame which loses heat to the cold walls and cold metal parts in furnace (Fig. 1). Heat exchange between the flame and the furnace walls occurs at higher rate than is normally done when the furnace is hot. This is in agreement with the results of numerical simulation using two-steps combustion mechanism of hydrocarbons combustion and CO formation (eq. 4). After separation of the variables, the equation (4) has been integrated considering the flue gas mixture composed of the reactants CO, H_2O, O_2, and the inert gas N_2 and CO_2.

Figure 2 presents the variation of the CO concentration with flame temperature for different residence times of reactants in furnace, and in Fig. 3 the variation of CO concentration with flame temperature for three values of the oxygen excess in flame. There is an increased conversion of CO to CO_2 for high values of flame temperature. The residence time of the reactants in flame greatly influences the CO concentration. A high residence time leads to a low concentration of CO. The oxygen excess in flame influences to a small extent the CO concentration. The concentration of CO decreases with increasing of oxygen concentration in flame because the excess oxygen compensates for imperfections in mixing of the reactants and because of the gas mixture dilution.

The combustion of organic fuels leads to the formation of nitrogen oxides. About 95 % of nitrogen oxides from the flue gases are in the form of nitrogen monoxide and 5% in the form of nitrogen dioxide. Nitrogen oxides are formed from two sources via three mechanisms:

- molecular nitrogen contained in the combustion air, which at high temperature conditions in flame reacts with oxygen from the air, forming the so- called thermal nitrogen monoxide. Thermal NO generation in the flame core occurs during the combustion of majority of fuel;
- nitrogen contained in fuel, in the form of compounds which decompose during the combustion process forming the so- called fuel nitrogen monoxide;
- molecular nitrogen contained in the combustion air which is combines with hydrocarbon free radicals that exist only in the oxidation zone forming so-called prompt nitrogen monoxide.

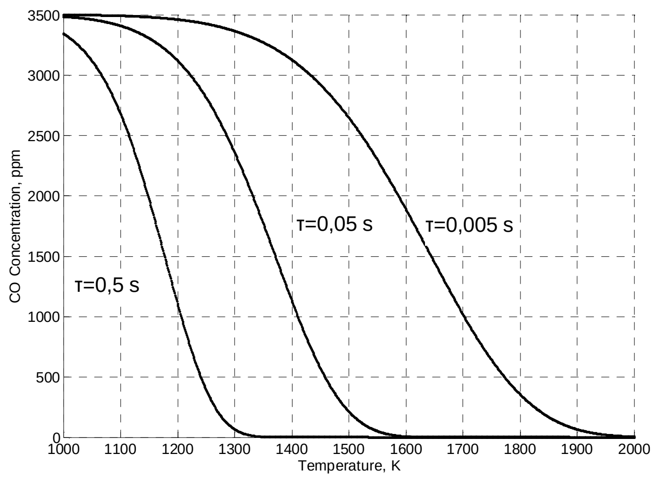

Fig. 2. Variation of CO concentration with flame temperature, for 3 values of residence time.

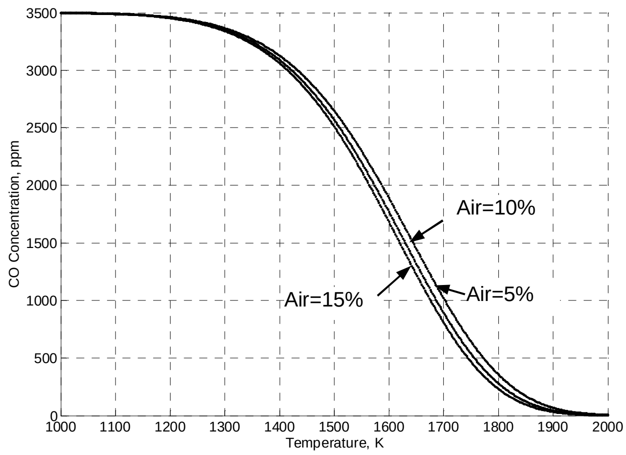

Fig. 3. Variation of CO concentration with flame temperature, for 3 values of excess air in flame.

About 85% of nitrogen oxides in the flue gas are thermal NO and the rest are fuel NO or prompt NO [5]. Nitrogen dioxide is formed at low temperatures by exothermic reactions of

NO [105]. The NO_2 formation is favored by rapid cooling of the flue gas in the presence of the large amount of O_2 [4].

The rates of NO generation and destruction, respectively, are [6]:

$$v_{NO}^{+} = 1.35 \cdot 10^{16} \rho [N_2][O_2] \frac{1}{T} e^{-\frac{69160}{T}} \tag{5}$$

$$v_{NO}^{-} = 22.5 \rho [N_2]^2 [O_2]^{-0.5} \frac{1}{T} e^{-\frac{47355}{T}} \tag{6}$$

The rate of prompt NO generation is given by the following equation [6]:

$$v_{NO} = 1.9 \cdot 10^3 ([N_2][O_2]_i [CH_4]_i)^{0.45} \frac{1}{T} e^{-\frac{16000}{T}} \tag{7}$$

where „*i*' denotes the initial concentration.

Reactions at chemical equilibrium involving NO, NO_2, N_2 and O_2 and their equilibrium constants are [4]:

$$\tfrac{1}{2} O_2 + \tfrac{1}{2} N_2 \Leftrightarrow NO$$

$$K_{p,NO} = 4{,}71 e^{-\frac{10900}{T}} = \frac{[NO]}{[N_2]^{\frac{1}{2}} [O_2]^{\frac{1}{2}}} \tag{8}$$

$$NO + \tfrac{1}{2} O_2 \Leftrightarrow NO_2$$

$$K_{p,NO_2} = 2{,}5 \cdot 10^{-4} e^{-\frac{6923}{T}} = \frac{[NO_2]}{[NO][O_2]^{\frac{1}{2}}} \tag{9}$$

This model allows to estimate the concentration of NO and NO_2 in flue gas as function of temperature and excess air. Excess air influences in two ways the concentration of NO and NO_2: more air in flue gas means more nitrogen that can be converted into NO and NO_2, but more air in flue gas leads to lower flame temperature and hence to reduced emission of NO (NO_2). To see the influence of excess air on the emission of nitrogen oxides have been calculated and presented graphically concentrations of NO and NO_2 at equilibrium (Fig. 4).

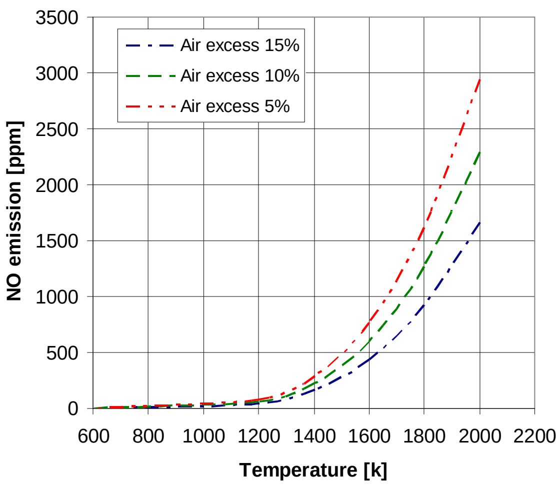

Fig. 4. NO and NO_2 concentration as function of temperature and excess air.

The NO_x concentration increases greatly with temperature increase over 1200 K. A lower excess air means a higher NO_x concentration. Less air in flame means higher temperature and therefore higher NO_x concentration.

3. CONCLUSIONS

European environmental regulations continue to reduce the CO and NO_x emissions from the combustion plants. In order to find out how the CO and NO_x emissions are influenced by the flame temperature, excess air and residence time simple models based on chemical kinetics and chemical equilibrium have been developed to estimate the CO and NO_x emissions. Using these models, the CO and NO_x concentrations have been calculated and plotted. There is an increased conversion of CO to CO_2 for high values of flame temperature. The residence time of the reactants in flame greatly influences the CO concentration. A high residence time leads to a low concentration of CO. The oxygen excess in flame influences to a small extent the CO concentration. The concentration of CO decreases with increasing of oxygen concentration in flame because the excess oxygen compensates for imperfections in mixing of the reactants and because of the gas mixture dilution. The NO_x concentration increases greatly with temperature increase over 1200 K. A lower excess air means a higher NO_x concentration. Less air in flame means higher temperature and therefore higher NO_x concentration.

Bibliografie

1. *** Directive 2010/75/EU of the European Parliament and of the Council of 24 November 2010 on industrial emissions (integrated pollution prevention and control)
2. Baukal C.E., *Industrial Combustion Pollution and Control*, Marcel Dekker, New York, NY (2004).
3. *** Ministerul Mediului şi Pădurilor. Agenţia Naţională pentru Protecţia Mediului. Poluanţii aerului (http://www.calitateaer.ro/parametri.php).
4. Baukal C.E., Jianhui Hong, Richard T. Waibel, Wes Bussman, *Controlling Emissions During Cold Furnace Startup*, CEP (Chemical Engineering Progress), February 2007.
5. Heinsohn, R.J., Kabel, R.L., *Sources and control of air pollution*, Pearson Education-Prentice Hall, 1999.
6. Flagan C.R., Seinfeld H.J., *Fundamentals of Air Pollution Engineering*, Prentice Hal, 2012.
7. *** *Perry's Chemical Engineers' Handbook*, 7th Ed., McGraw-Hill, Editor Don W. Green, 1997.
8. El-Mahallawy F., El-Din Habik S., *Fundamentals and Technology of Combustion*, Elsevier Science, 2002.

HYDRAULIC FRACTURING IN THE UNITED STATES OF AMERICA

Dan Parascin[1],

Process Improvement Manager, OneSubsea - a Cameron and Schlumberger company

ABSTRACT

Large amounts of hydrocarbons (specifically gas) could not be recovered economically from low permeability, gas-saturated sandstone. Generally, a formation permeability of less than 0.1 millidarcy is unsuitable for conventional drilling and recovery methods. Geologists and oil producers became increasingly aware of the huge untapped hydrocarbon reserves contained in low permeability formations.

A new method, the hydraulic fracturing, was first experimented in 1947. Since 1949 it was used extensively to reinvigorate declining production of conventional wells. In the past ten years the hydraulic fracturing (fracking) became the preferred method to design new wells into formerly inaccessible hydrocarbon reserves. **More than two and a half million** hydraulic fracturing jobs were performed in the world, with about **one million in the US alone**.

1. WHAT IS HYDRAULIC FRACTURING ?

Hydraulic fracturing is a technique used to maximize reservoir production of shale gas by creating small fractures (typically less than 1mm) into the formation to increase permeability. A directional well is drilled in the pay-off zone and water mixed with sand and various chemicals is injected into the well at very high pressure. The applied pressure opens small fractures. After the hydraulic pressure is removed, the fractures are kept open by the grains of sand or aluminum oxide that were mixed with the hydraulic fluid.

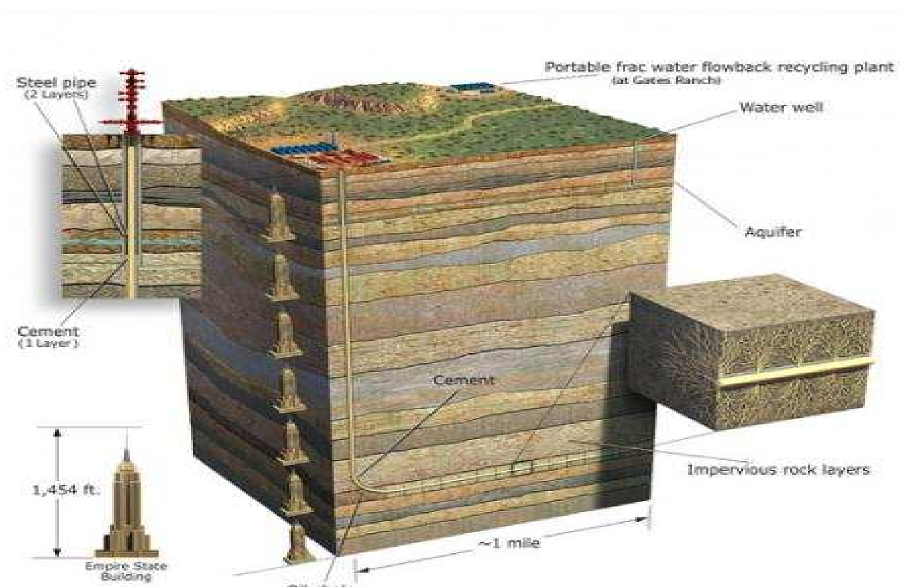

Figure 1 Hydraulic fracturing

[1] 5106 Danebridge Dr,Houston, TX 77084, USA, 1 281 770 7711, e-mail:d.parascin@hotmail.com

2. BENEFITS OF FRACKING

Less than a decada ago, government studies and industry analysts predicted that the United States will run out of gas. Extensive use of hydraulic fracture made these studies obsolete. The US shale gas production increased over eight times in less than 10 years.

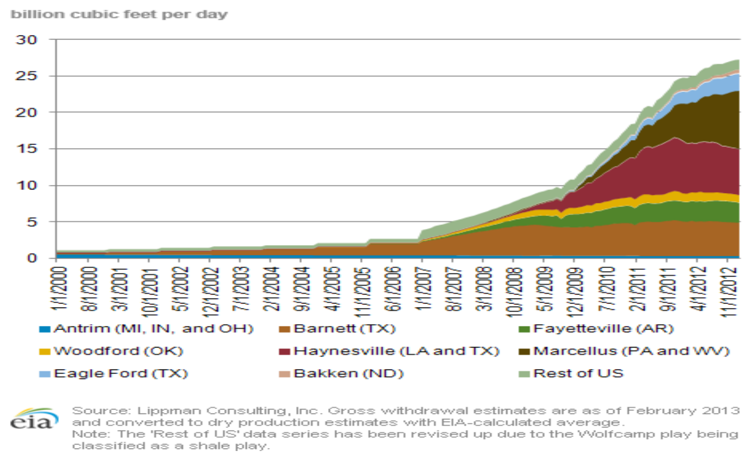

Figure 2 Monthly dry shale gas production

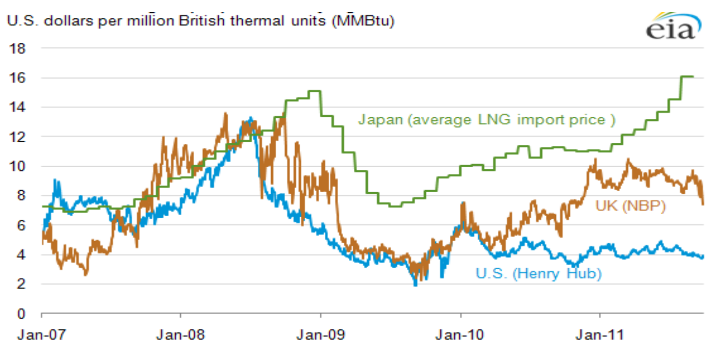

Figure 3 Trends in natural gas spot price

At the same time with increased shale gas production, the natural gas prices, in US, dropped from a peak of $13 per million Btu in 2008 to a low of $2 per million Btu in 2009. Current prices, set by the demand and supply mechanism, are around $4 per million Btu. In 2012, in Japan, the cost of Btu (LNG) was roughly four times higher than in the US.

It is predicted that by the year 2016, the United States will become a natural gas net exporter.

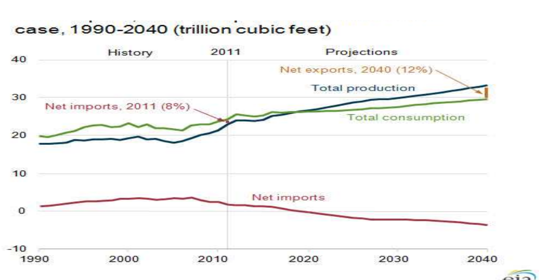

Figure 4. Total U.S. natural gas production, consumtion and imports

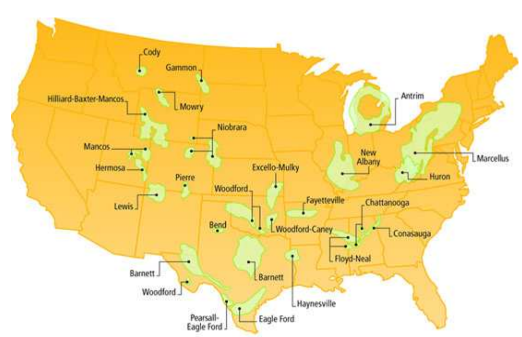

Figure 5 Main shale gas fields in the US:

In addition to the pure domestic economic benefit, the high production of natural gas in the US and the export availability has a significant geo-politic and economic impact. United States could become an important player in the global energy market, especially in the natural gas and LNG sectors, currently dominated by few suppliers and in certain cases by producers with monopoly power.

Natural gas is the cleanest fossil fuel. It produces about 29% less carbon dioxide per Joule delivered than oil. When compared with coal, the difference is even more significant: natural gas produces 44% less CO_2 per Joule delivered than coal. According to the IPCC Fourth Assessment Report, in 2004, natural gas produced about 5.3 billion tons a year of CO_2 emissions, while coal and oil produced 10.6 and 10.2 billion tons respectively. According to an updated version of the Special Report on Emissions Scenario by 2030, natural gas would be the source of 11 billion tons a year, with coal and oil now 8.4 and 17.2 billion respectively because demand is increasing 1.9 percent a year. Total global emissions for 2004 were estimated at over 27,200 million tons. Other pollutants, such as sulfur dioxide, carbon monoxide and nitrous oxides are produced in much lower amounts by the combustion of natural gas, when compared to any other hydrocarbon fuels. Vehicles powered by liquefied natural gas, propane or compressed natural gas run cleaner than cars with either gasoline or diesel in the tank. According to the Department of Energy, if the transportation sector switched to natural gas, it would cut the nation's carbon-monoxide emissions by at least 90 percent, carbon-dioxide emissions by 25 and nitrogen-oxide emissions by up to 60.

Coal-fired electric power generation emits around 2,000 pounds of carbon dioxide for every megawatt hour generated, which is almost double the carbon dioxide released by a natural gas-fired electric plant per megawatt hour generated. Because of this higher carbon efficiency of natural gas generation, as the fuel mix in the United States has changed to reduce coal and increase natural gas generation, carbon dioxide emissions have unexpectedly fallen. Those measured in the first quarter of 2012 were the lowest of any recorded for the first quarter of any year since 1992 (Rachel Nuwer: A 20-Year Low in U.S. Carbon Emissions)

2. CHALLENGES AND CONTROVERSIES

a) Water Recycling: Hydraulic fracturing uses a lot of water. It can take as much as 27,000 cubic meter of water to process just one well, although these are extreme cases. Most wells will take between 10,000 and 15,000 cubic meter of water. At least one third of this water will be trapped deep in the shale. Fracking operations can contribute to the depletion of water supplies in drought-stricken areas. Comprehensive studies of the region's water supply should be conducted before the fracking operations begin. To put things in perspective, hydro-geologist David Yoxtheimer of Penn State's Marcellus Center for Outreach and Research notes: "Of the 9.5 billion gallons of water used daily in Pennsylvania, natural gas development consumes 1.9 million gallons a day (mgd); livestock use 62 mgd; mining, 96 mgd; and industry, 770 mgd."

Depending on the type of reservoir, 20 to 80% of the water injected flows back in the early stages of production.

All the flow back water is treated to remove pollutants, (such as solid particles, hydrocarbon molecules, salts) that are picked up as the water flows through the reservoir rock. In addition, fracking additives must also be removed before the water is return to the ground. Modern treatment processes allow up to 90% of the water to be recycled.

A different method that is investigated by the oil companies is to use deep saline aquifers, whose water is unsuitable for human consumption, as a new source of water supply.

b) Protecting Aquifers: Drilling deep holes in the ground will reach aquifers. This is not something new to the industry and it is not restricted to hydraulic fracturing operations. It was true at the time of the Spindletop and it is true today. The industry developed very effective methods to protect the sources of underground fresh water by isolating the well bore with successive barriers. A typical well design is shown below.

Historically, there were incidents were a poor cement job, inadequate casing program or other causes led to underground water contamination. These occurrences are not specific to hydraulic fracturing. They are risks associated to any drilling in the ground beyond a certain depth. The problem can be corrected by using stronger cement and processing casings to create a better, impermeable seal.

The iconic image captured in 2010 in the "GasLand" documentary that shows a man's kitchen faucet with flames coming from the pipes has been explained.

The entire scene appears a damning indictment of the gas drilling nearby. However, Colorado officials determined the gas wells were not to blame. The homeowner's own water well had been drilled into a naturally occurring pocket of methane.

Figure 6 Drilling cross-section

c) Radioactivity: Uranium isotopes such as radium-226 and radium 228 are part of the shale formation. It is a natural phenomenon used by geologists and drillers to measure and chart the underground. The higher the radiation levels, the greater the likelihood of gas deposits in that section. But that does not necessarily mean the radioactivity poses a public health hazard. Tests conducted in Pennsylvania compared the radiation level of fracking fluids that return to the surface to the radiation level of naturally occurring water that contains radioactive elements and found no evidence of elevated radiation levels. Conrad Dan Volz, former scientific director of the Center for Healthy Environments and Communities at the University of Pittsburgh, is a vocal critic of the speed with which the Marcellus is being developed—but even he says that radioactivity is probably one of the least pressing issues. "If I were to bet on this, I'd bet that it's not going to be a problem," he says.

d) Transparency: Oil and gas producers invoked proprietary privileges to keep secret the type and quantities of the chemical compounds used in their wells. This is changing, as Texas was the first state to pass a law, in 2010, requiring full public disclosure. Following the new regulations, we learned that the ingredients include such benign products like instant coffee and walnut shells, but also some known and suspected carcinogens, including benzene and methanol. Some 5000 gallons of additives are used every 1 million gallons of water and sand. That is only 0.5%, however the large amount is more significant than the concentration. The real question is what to do with this fluid once it returns to the surface. Depending on the formation porosity, this wastewater can be re-injected into the impermeable rock some 1.5 miles deep. This method is not possible at some other locations (such as Marcellus Shale) where the underlying rocks are not porous enough. New methods of wastewater treatment are developed and several facilities are approved to process these fluids. Most companies use the unprocessed water to drill their next well.

e) Pollution: It is clearly established that natural gas has a lower carbon footprint than any other fossil fuel.
However, bringing the gas to the surface is an energy intensive task. Drilling and production sites rely on large diesel engines and generators running around the clock. Heavy truck and equipment traffic is common.
The industry response is not less drilling for gas but more equipment running on natural gas.
Another pollution concern is the methane, extensively used in the drilling process, with potential to escape from poorly designed and maintained equipment. Methane is a significant greenhouse gas.
Robert Howarth at Cornell University has calculated that methane losses could be as high as 8 percent. Industry officials concede that they could be losing anywhere between 1 and 3 percent. Some of those leaks can be prevented by aggressively sealing condensers, pipelines and wellheads.

f) Earthquakes: Using hydraulic fracturing to open fractures triggers minute tremors within the source rock. These movements are termed "micro-seismic events." Although significant enough to induce fracturing within the rock, they can be detected only by the most sensitive instruments because of their extremely low magnitude: typically -3 to -2 on the Richter scale, or even at most +0.5. Humans can only detect earthquakes with a magnitude of at least +3 (which is a million times higher than the -3 induced by fracking). And every day, seismographs record several thousand quakes with a magnitude of less than +2.
It is true that slightly stronger tremors indirectly linked to hydraulic fracturing have been reported, for example in the United Kingdom. Studies have shown that these phenomena are due to the unusual combination of two factors: the pressure exerted on the rock by water injection and the presence of a naturally fractured, seismically unstable zone. Prior geological surveys and continuous monitoring of rock behavior during fracturing operations should prevent this type of incident, by enabling operations to be halted immediately.

"It should be noted, however, that after hundreds of thousands of fracturing operations, only three examples of felt seismicity have been documented. The likelihood of inducing felt seismicity by hydraulic fracturing is thus extremely small but cannot be ruled out." (Richard Davis – Induced Seismicity and Hydraulic Fracturing for Recovery of Hydrocarbons – Durham University)

The Royal Society and the Royal Academy of Engineering, Shale gas extraction in the UK, June 2012 noted that *earthquakes of magnitude 3.0, which are more intense than the larger of the two quakes caused by Cuadrilla (2.3 magnitude) are: "Felt by few people at rest or in the upper floors of buildings; similar to the passing of a truck."*

3. CONCLUSIONS

Not even the most vocal opponents of "fracking" will deny the benefits of the additional quantities of natural gas recovered using hydraulic fracturing: smaller carbon footprint than any other fossil fuels, reduced energy dependence, low energy cost, job creation and industrial development.

However there is a heated debate with regard to the process itself. Arguments and positions on one side or the other should be strictly based on scientific research, concrete data and facts.

Honest debates are beneficial and help both public acceptance and operators restrain and control.

Safe drilling and exploitation activity are possible without affecting the environment or the public health. Communities should be educated about the process, so they can clear balance benefits vs. risks.

Modern technologies and regulations aroused from the public debate. The oil and gas companies are under increased scrutiny and government regulating bodies should be the enforcer of rules and regulations compliance.

Excesses or half-truths are toxic on both sides.

References

[1] Chesapeake Industry
[2] United States Department of Energy
[3] United States Environmental Protection Agency
[4] United States Energy Information Administration
[5] Total International
[6] Royal Society UK
[7] Royal Academy of Engineering UK
[8] Richard Davis- Induced Seismicity and Hydraulic Fracturing for Recovery of Hydrocarbons
[9] Rachel Nuwer – A 20-Year Low in U.S. Carbon Emissions

THE EFFECTS OF DIMENSIONS OF COMBUSTION CHAMBER ON THE HEAT TRANSFER PROCESS IN CFB BOILERS

Wojciech Pospolita[1], Krzysztof Jesionek[2], Adam Wierciak[3], Iliya Iliev[4]

,

ABSTRACT

Boilers with circulating fluidized bed are technolgy with many adventages, such as low emission of harmful substances, fuel elasticity and proper operation in large load range. To achieve all of these advantages it is very importannt to design the combustion chamber in proper way.

The paper contains short introduction into combustion process in CFB boilers. The most important parameters were chosen and described by appropriate equations. Paper contains also calculations of circulating bed density by using factors and values which are described before. There are figures which show correlations between those parameters

1. INTRODUCTION

Nearly 50 years of development in CFB boilers technology has given knowledge about internal processes. According to this knowledge, engineers and scientists can accomplish projects of boilers that fully take advantage of CFB combustion, like lower emission and equal temperature profile in combustion chamber. First one is an important factor due to EU environmental needs, second eliminates a number of operational problems.

By analysis of data, it is possible to avoid several problems at the boiler design stage. Project of combustion chamber has to provide e.g. correct temperature of superheaters pipes or optimal flow of ash. This increases reliability of CFB unit by lowering the number of emergency stoppages. Thus, the cost of boiler operation could be lower too.

CFB combustion technology in one of the ways to combine coal firing with several environmental restrictions. It still needs research to be sure, that all the correct solutions from well-known 100÷200 MW units, will be successfully transferred into designed ones.

2. BASICS OF COMBUSTION IN CFB

Combustion in Circulating Fluidized Bed boilers is a complicated process which depends on many factors. The most important are those, which determine the parameters of the circulating material flow. Mass flow is made up of [1]:

$$\dot{m}_s(h) = \dot{m}_c(h) + \dot{m}_{inert}(h) + \dot{m}_{fumes}(h), \qquad (1)$$

where: – m_c is mass flow of fuel [kg/s],

– m_{inert} is mass flow of inert material [kg/s],

– m_{fumes} is mass flow of fumes [kg/s],

[1] Wroclaw University of Technology, Poland,e-mail:wojciech.pospolita@gmail.com; cell phone: +48 537651824

[2] Wroclaw University of Technology, Poland, e-mail:Krzysztof.Jesionek@pwr.edu.pl; cell phone:+48713441207

[3] Wroclaw University of Technology, Poland, adam.wierciak@o2.pl; cell phone +48 514784171

[4] Ruse University, Bulgaria, e-mail: iiliev@enconservices.com; cell phone: +359 887306898

– h is chamber height [m].

The mass flow of the circulating material depends on distance from the bottom of the chamber. It is connected with a phenomenon of burning coal and drooping larger grains back to the bottom. Consequently, the density of the material decreases. The density of bed material is described as [2]:

$$\rho_s = \frac{KR \cdot \Psi}{V_{fumes}}, \tag{2}$$

where: – KR is circulation rate,

– $\psi=2\div5$ is factor which defines the internal circulation of particles in furnace [2],

– V_{fumes} is a gas volume per unit of fuel [m^3/kg].

KR gets values from 40 to 60, lower for lignite coal fire units. It is a relation between fuel (coal) mass flow and inert material [4]:

$$KR = \frac{\dot{m}_{inert}}{\dot{m}_c}. \tag{3}$$

According to KR values, fuel is only around 3 % of the whole material.

Value of bed density is parameter, which directly affects heat transfer processes because of two reasons. Firstly, in contrast to traditional steam boiler, most of the heat is transferred by convection. It is a consequence of lower temperature in chamber, around 850 °C. There are some experimental relations between bed density and convection coefficient of heat transfer. According to [3], this correlation for high power units is described as:

$$\alpha_c(h) = 30 \cdot \rho_s(h)^{0,5}, \tag{4}$$

where – α_c is convection coefficient of heat transfer [$W/(m^2 \cdot K)$].

Due to equation (4), bed density should be chosen so as to ensure optimal heat mass to working fluid into evaporator pipes.

The second important parameter which is influenced by density is flow per unit mass G. It is described as [1]:

$$G(h) = \frac{\dot{m}_s(h)}{A} - \rho_{fumes} \cdot w_{fumes}, \tag{5}$$

Where: – ρ_{fumes} is fumes density [kg/m^3],

– A is chamber cross section [m^2].

– w_{fumes} is fumes velocity [m/s],

$$A = \dot{m}_c \cdot V_{fumes} \cdot \frac{273 \cdot t}{273 \cdot w_{fumes}}, \tag{6}$$

where – t is temperature in combustion chamber [°C].

Changes of ρ_{fumes} is skippable, also w_{fumes} is selected as average for whole chamber.

Appropriate analysis of G factor forces provide secondary air on correct height of chamber. It has to ensure accurate coal burn while low emission of NO_x.

In equation (6) temperature t appears. Most of CFB boilers operate at 850 °C average temperature in the combustion chamber. Thus, the obtained possibility to insert calcium sorbent directly into bed greatly reduces emission of sulfur. This temperature is also lower than the temperature of ash softening. It makes heating surfaces less susceptible contamination by ash.

3. CALULATIONS

During calculations, some parameters were chosen to show how their influence on the combustion process. As a base, served values from table 1.

Table 1: Base parameters.

Fuel	Lignite
m_c [kg/s]	100
V_{fumes} [m^3/kg]	3,7
KR	50
T [°C]	850
ψ	3,5

According to equation (6) and chosen velocities of fumes, the cross section of the chamber was computed. Velocities should be within the range of 4 to 10 m/s [2]. If the velocity in the chamber is out of range, there is a risk that fluidization will stop.

Table 2: Combustion chamber cross sections.

Fumes velocity [m/s]	4	5	6	7	8	9	10
Chamber cross section [m^2]	285,4	228,3	190,3	163,1	142,7	126,8	114,2
T [m]	23,9	21,4	19,5	18,1	16,9	15,9	15,1
B [m]	11,9	10,7	9,8	9,0	8,4	8,0	7,6

Values T and B are the lengths of the chamber walls. Between them, there is a correlation [2]:

$$\frac{T}{B} = 2 \tag{7}$$

For boilers with a higher power, it is very important to ensure adequate penetration inside the chamber by circulating material mass.

In work [1] quoted exemplary range of G values. For chosen value of m_c, G should stay in the range of 5÷15 kg/(s·m^2). In Figure 1, there is a function which approximates G as a function of h. Chamber height is 42 m.

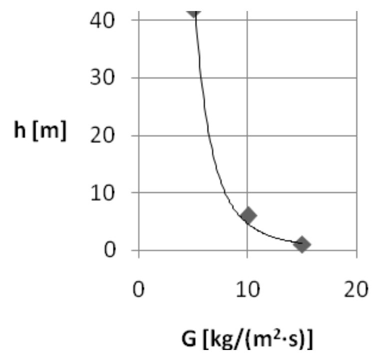

Figure 1: Flow per unit mass G versus chamber height.

Approximate function, including results for all velocities, appears as:

$$G(h) = G_{start} \cdot 2{,}19 \cdot h^{-0{,}246}, \tag{8}$$

where – G_{start} is G from equation (5) for data from table 1 and 2 [kg/(m^2·s)].

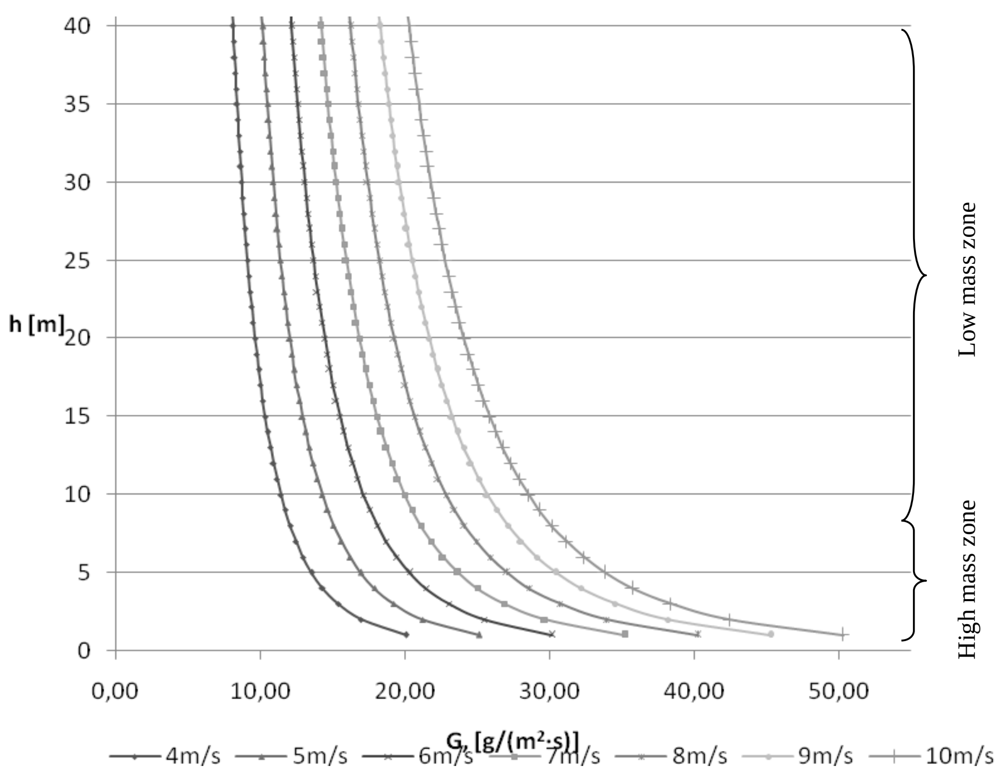

Figure 2: G versus chamber height for chosen velocities.

Figure 2 includes results of computing for all velocities that were chosen. It seems to be, that higher velocity (smaller cross section) incereases range of flow per unit mass. As a consequence, during design of chamber, for higher velocities, higher flow of secondary air should be assured. Ussualy flow of secondary air is around 40 % of whole air fed to the boiler [5]. For highiest velocities it is a good solution to divided air into three flows. For all velocities, there is a devison between two zones of high and low mass flow of per unit mass. The division border seems to be on around 5÷7m. This is a value, where evaporator walls shoud apper instead of brick bottom nozzle.

Next important parameter, which takes part during computing was bed density. Acorrding to [3], bed density changes in range from 70 to 7 kg/m^3. For those values, function appears as:

$$\rho(h) = \rho_{start} \cdot \sqrt[-0,129]{\frac{h}{0,0033}}, \tag{9}$$

where – ρ_{start} is ρ from equation (2) for data from table 1, [kg/m^3].

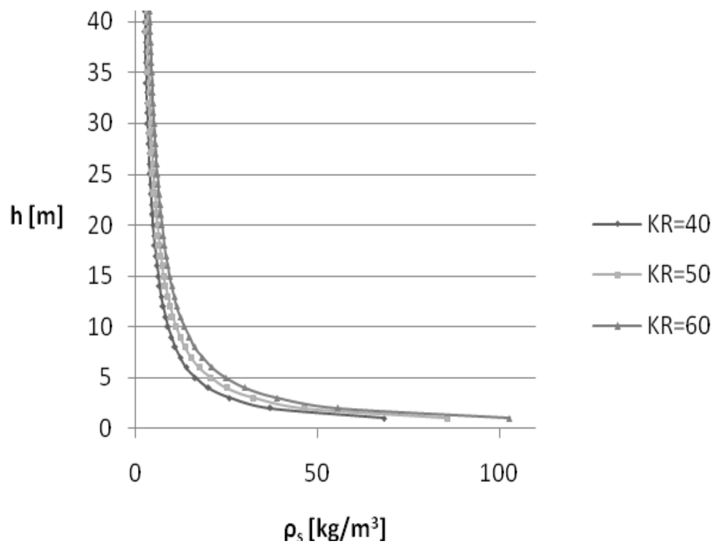

Figure 3: Bed density ρ_s versus chamber height for chosen KR values.

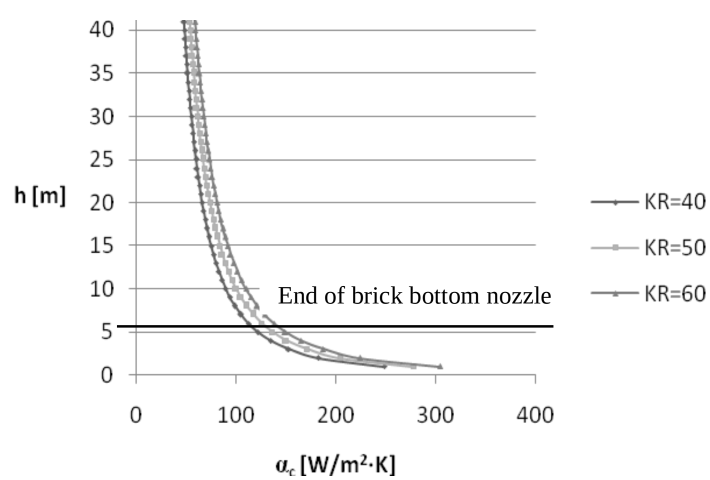

Figure 4: Convection coefficient of heat transfer a_c versus chamber height for chosen KR values.

Figures 3 and 4 show results of computing for variable values of KR. In figure 3, there are little differences between density level for each KR value, but it seems that it is better to use higher KR values for boilers with higher productivity of steam. In both figures, similar to figure 2, there is very clear border between low and high density area. To protect evaporator pipes from overheating, it is good solution to design brick bottom nozzle min. 5 m tall. In range of 1÷5 m is this part of the chamber where convection coefficient of heat transfer is the highest. To take full advantage of this fact, very often designers place there special heating surfaces, which are immersed directly into the bed. Those surfaces are also adapted to adopt extremely high heat flux, often take role of last stage of superheater.

Figure 4 clearly shows that α_c level still decreases. Conclusion is that in lower part of the chamber, convection takes more important part then in top of the chamber, where radiation starts to dominate.

Keeping α_c on a medium level is also an important issue. This is one of the reasons way boilers with a higher productivity have taller combustion chambers.

4. CONCLUSIONS

To provide an adequate combustion conditions is one of the most important tasks of the designers. Only in this way they can fully utilize all the advantages of fluidized bed boilers. It is important to use the available data to choose KR and dimensions of the chamber, to ensure proper distribution of bed density and its temperature.

An important issue is the appropriate design of brick bottom nozzle, on one hand to prevent overheating of lower part of the evaporator, and on the other to be able to use the heat flux gathered there to ensure appropriate parameters of the steam flowing to turbine.

References

[1] Bis, Z., *Kotły Fluidalne. Teoria i praktyka,* Wydawnictwo Politechniki Częstochowskiej, Częstochowa, 2010.

[2] Kruczek, S., *Kotły parowe. Konstrukcja i obiczanie,* Oficyna Wydawnicza Politechniki Wrocławskiej, Wrocław, 2001.

[3] Dutta A., *Heat transfer in circulating bed boilers*, Dalhousie University, Halifax, Nova Scotia, 2002.

[4] Badur J., Topolski J., *"Optymalna krotność recyrkulacji w palenisku z atmosferycznym złożem fluidalnym"*, Instytut Maszyn Przepływowych PAN, Gdańsk 2002.

[5] Pawlik M., Strzelczyk F., *Elektrownie,* Wydawnictwo WNT, Warszawa, 2012.

PERFORMANCE ANALYSIS OF A HYBRID WATER AND AIR SOLAR COLLECTOR WITH RECTANGULAR FINS

QAHTAN ADNAN ABED[1,4], VIOREL BADESCU[2], IULIANA SORIGA[3]

[1]Phd student,Universitatea POLITEHNICA din Bucureşti, Facultatea Inginerie Mecanică şi Mecatronică

[2]Prof.dr.ing., Universitatea POLITEHNICA din Bucureşti, Facultatea Inginerie Mecanică şi Mecatronică

[3]Dr.ing., Universitatea POLITEHNICA din Bucureşti, Facultatea Inginerie Mecanică şi Mecatronică

[4]Foundation of Technical Education, Najaf Technical College, Iraq.

Abstract: In this presented paper a hybrid solar collector with two fluids (water and air) is investigated. The studied configuration consists of rectangular fins in the lower air channel that are arranged perpendicular to the direction of air flow to enhance the heat transfer rate and efficiency. The effect of solar irradiation, ambient temperature, air and water inlet temperatures on the useful energy and thermal efficiency were studied. The indicated results show that the maximum efficiency obtained by using 10 rectangular fins at a constant mass flow rate of 0.1 kg/s was 65.8 %.

Keywords: hybrid solar collector, rectangular fins, solar water heater; solar air heater.

1. INTRODUCTION

Among the solar thermal technology, collectors have been widely used for water or air heating. There are many studies reporting solar water heating or solar air heating efficiency improvement methods. The solar water heater has been used in domestic purposes, and various types of solar water heater system were studied, such as flat plate collectors [1], concentrating collectors [2],evacuated tube collectors [3] and integrated collector storage system [4].Also, researches have been made on the efficiency and water outlet temperature of solar collectors when integrated in thermosyphon systems [5]. The solar air heaters are used for applications at low and moderate temperatures. Several solutions have been proposed in order to improve the heat transfer efficiency of air collectors, like the development of various types of baffles [6], or modifying the dual- function solar collector by adjusting the interior air gap and changing the shape of the absorber [7].

In the present work we perform the analysis of a hybrid solar collector (HSC) for water and air heating with rectangular fins in the air channel.

[1] Corresponding author, email qahtan77@yahoo.com

2. MATHEMATICAL MODEL OF HSC

2.1 Description of the collector

Detailed description of HSC design and construction details are presented in figure 1. The absorber plate covers the full aperture area of the collector, absorbs incident solar irradiance and conducts the heat to water through 10 copper tubes welded at the top, and to the air that flows through the bottom side. To enhance the heat transfer to the air, galvanized fin located below, inside the 6 cm high air channel, and the amount of heat lost back to the surroundings is reduced to minimum. The collector tilt from the horizontal is 35^o.

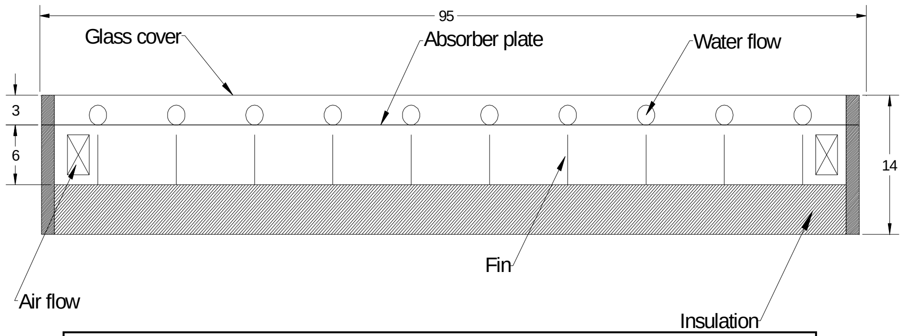

Fig. 1. Configuration of the HSC. (All dimensions in cm)

2.2. Theoretic modeling of the HSC

The essential components of the HSC for water and air heating are the glass cover, the back plate and the absorber. The performance of the HSC has been tested theoretically in the real operating conditions of Timisoara, Romania. (45° 44' 57" N / 21° 13' 38" E).

The performance of a hybrid flat-plate solar collector for water and air can be described by the useful heat gain from the collector, given as [8]:

$$q_{u,f} = F_{R,f}\, A_p\, S - U_{L,f}\, A_p\, (T_{f,in} - T_{amb}) \qquad (1)$$

where: A_p is the collector gross area (m^2), S is incident solar flux absorbed by the absorber plate (W/m^2), $U_{L,f}$ is the overall loss coefficient for fluid (water or air) (W/m^2 K), $T_{f,in}$ is inlet fluid temperature (K), T_{amb} ambient temperature (K) and $F_{R,f}$ is collector heat removal factor for fluid (water or air) [9]:

$$F_{R,f} = \frac{\varepsilon_f\, \dot{m}_f\, C_{p,f}}{U_{L,f}\, A_p + \varepsilon_f\, \dot{m}_f\, C_{p,f}} \qquad (2)$$

where: ε_f is heat exchange effectiveness of fluid (water or air) and $C_{p,f}$ is specific heat (J/kg.K).

The heat transfer coefficient between water and the tubes is calculated from the Nusselt number:

$$h_f = \frac{k_f}{d} Nu_f \qquad (3)$$

The heat transfer coefficient in the air channel with rectangular fins is calculated with the following formula [10]:

$$h_f = \frac{k_f}{d} Nu_a = 0.023\, \mathrm{Re}_a^{\ 0.8}\, \mathrm{Pr}^{0.4} \qquad (4)$$

The thermal efficiency, which is defined as the ratio of the useful energy to the total incident solar radiation is expressed by the Hottel-Whillier-Bliss equation [8].

$$\eta = \frac{q_{u,f}}{A_p \; I_T} \tag{5}$$

3. RESULTS AND DISCUSSIONS

The daily solar irradiation and ambient air temperature during one day in Timisoara, Romania (45° 44' 57" N / 21° 13' 38" E) are presented in Fig. 2. The maximum solar irradiation and the maximum ambient temperature were 884 W/m^2 and 31 ^{o}C, respectively. The daily average ambient air speed was 0.54 m/s, ranging from 0.29 to 1.5 m/s.

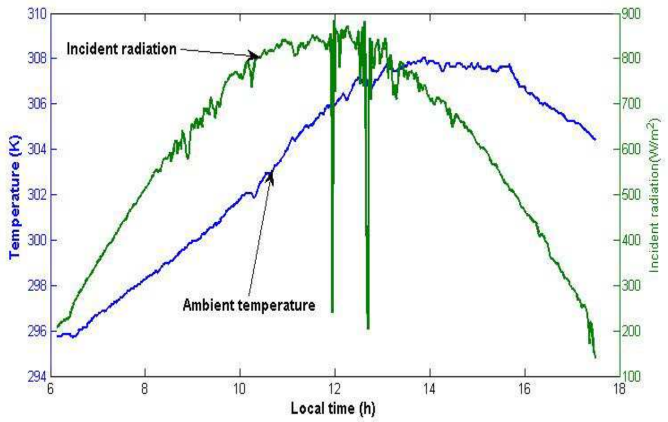

Fig.2. Variation of ambient air temperature and solar radiation intensity on 01/July/ 2010.

The mathematical algorithm presented above was implemented and solved in MATLAB. The variation of water outlet, air outlet and plate mean temperatures, respectively, are shown in Fig. 3. The maximum water and the air outlet temperature were 48 ^{o}C and 34 ^{o}C, respectively, results obtained for the water inlet temperature fixed at 40 ^{o}C.

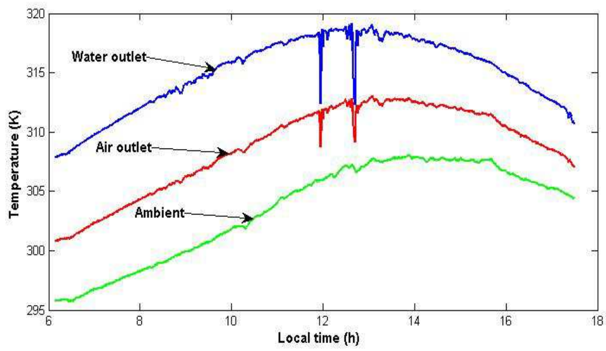

Fig.3. Variation of water outlet, air outlet and plate mean temperature

Figure. 4a shows the useful heat gain for water and air during the day as they were obtained from the computations. The average value of the useful heat gain for water is 534 W varying from 24 to 924 W, and the average value of the useful heat gain for air is 124 W, varying from 37.8 to 173.4 W.

The instantaneous efficiency of the HSC follows the same trend as the useful heat flux. It increases until noon time and then decreases as shown in Fig. 4b. The maximum efficiency value equals 65.8 % and occurs at 02:33.

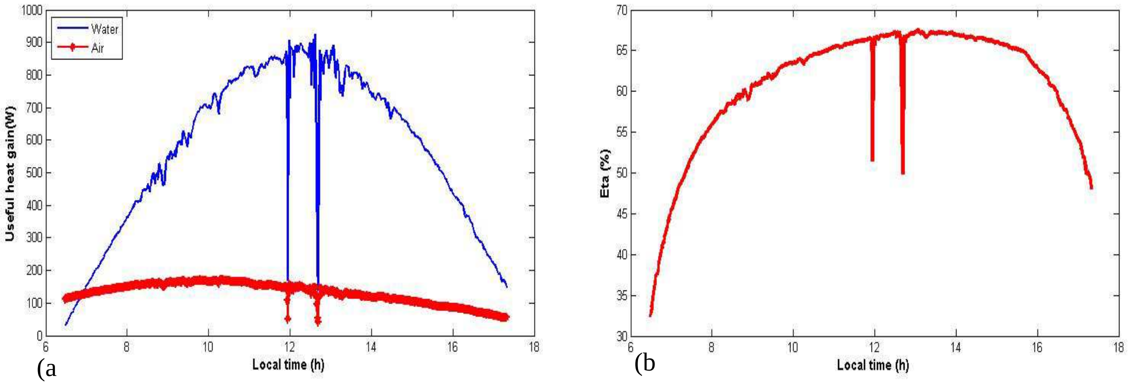

Fig. 4. Variation of useful heat gain and instantaneous efficiency with

4. CONCLUSION

The performance of a hybrid solar collector with rectangular fins has been simulated with a variable value of solar radiation and air inlet temperature, maintaining the water inlet temperature constant. The efficiency of the HSC with rectangular fins varied between 10 to 65.8 %, with air outlet temperature from about 307 to 319 K.

REFERENCES

[1] E. Zambolin, D. Del Col. Experimental analysis of thermal performance of flat plate and evacuated tube solar collectors in stationary standard and daily conditions. Solar Energy, vol. 84, 2010, p. 1382–1396.

[2] H. Zhai, Y.J. Dai, J.Y. Wu, R.Z. Wang, L.Y. Zhang. Experimental investigation and analysis on a concentrating solar collector using linear Fresnel lens. Energy Conversion and Management, 2010, p. 48-55.

[3] Gang Pei, Guiqiang Li, Xi Zhou, Jie Ji, Yuehong Su. Comparative experimental analysis of the thermal performance of evacuated tube solar water heater systems with and without a mini-compound parabolic concentrating (cpc) reflector(c < 1). Energies. Vol. 5, 2012, p. 911-924; doi:10.3390/en5040911.

[4] M. Souliotis , P. Quinlan, M. Smyth, Y. Tripanagnostopoulos, A. Zacharopoulos, M. Ramirez, P. Yianoulis. Heat retaining integrated collector storage solar water heater with asymmetric CPC reflector. Solar Energy. Vol. 85, 2011, p. 2474–2487.

[5] Jaisankar, S., Radhakrishnan, T.K., Sheeba, K.N. Studies on heat transfer and friction factor characteristics of thermosyphon solar water heating system with helical twisted tapes. J. Energy, vol. 34, 2009, P. 1054–1064.

[6] Ben Slama R., Bouabdallah M., Mora J. C. Air solar collector with baffles: Aerodynamics, heat transfer and efficiency. RERIC International energy journal, vol. 18, No.1, 1996.

[7] Jinwei Ma, Wei Sun, Jie Ji, Yang Zhang, Aifeng Zhang, Wen Fan. Experimental and theoretical study of the efficiency of a dual-function solar collector. Applied Thermal Engineering, vol. 31, 2011, p. 1751-1756.

[8] Duffie, J.A., Beckman, W.A. Solar Engineering of Thermal Processes, (Toronto, John Wiley 1991).

[9] Assari, M.R., Basirat Tabrizi, jafari, i., Experimental and theoretical investigation of dual purpose solar collector, Solar Energy, vol. 85, 2011, p. 601–608.

COGENERATION SYSTEM MODELING FOR ISOLATED BUILDINGS

Bogdan Radu[1], Alexandru Racovitză

University "POLITEHNICA" Bucharest, Faculty of Mechanical Engineering
Dept. of Thermodynamics, Engines, Thermal and Refrigerant Machines

ABSTRACT

Cogeneration systems highlight a certain way to increase the efficiency of internal combustion engines use for energetic purposes and therefore consist in a valuable source to supply isolated objectives, such as hospitals, hotels or small residential places with electric energy and hot water when no connection to standard utilities networks is available. The main goal of the analyzed model is to evaluate the fuel consumption for a building that requires electric energy and hot water as well. Thus, based on the operation of an internal combustion engine and heat exchangers a calculation model has been proposed, in which certain operating parameters depending on specific delivery situations have been defined. The below presented model allows the calculation of the fuel consumption for every operating regime.

1. INTRODUCTION

Cogeneration refers to the production of electric energy in parallel with waste heat recovery (WHR) to be further used for central heating or hot water preparation. Some results show the fact that engine efficiency in terms of fuel combustion could increase from 30% to 80% in certain cases when using co-generation systems [1][2]. In this work, authors propose a schematic formed by an engine and three heat exchangers to take the recovered heat from the engine exhaust gases, cooling water and oil [1].

Other exergetic and thermo-economical analysis of a cogeneration system equipped with a diesel engine are also presented [3][4]. This refers to a general exergetic modeling of a system deserving an electric plant of 25 MW. Besides the specific thermodynamic calculations, a balance of the entire system costs is either presented.

The present work is trying to highlight a real possibility to assemble and to use a heat recovery system for a given situation. The design of the compounding elements is inspired from other technical data [5].

2. THE SCHEMATIC OF THE INSTALLATION

The model consists in a diesel gas engine connected to an electric generator and to a water circuit designed to deliver hot water to the user. This circuit first passes through a water-water heat exchanger which extracts the heat from the engine cooling water and then passes through a gas-water heat exchanger supposed to take the heat from the engine exhaust gases. Finally, the water circuit contains a gas boiler needed to set the hot water parameters requested by the user.

In the following figure (fig.1), circles mark the points in which agents' temperatures are measured (U for the user water flow, W for the engine cooling water and G for the engine exhaust gases). Each heat exchanger features a faucets system in order to modify the flow rates of the agents depending on the heat flow rates adjustments, related to the engine as to the

[1]313 Splaiul Independentei, sect.6, 060042, Bucharest, tel.: 0040-21-4029451, e-mail: bobitaradu@yahoo.com

user. These adjustments are necessary for each kind of operating regime. For the water cooling system a radiator equipped with a ventilator is needed to cover the situation for which the heat offered by the cooling water overpass the necessary heat to be further transferred.

The other elements have been designed to take the maximum amount of disposable thermal energy from the engine when operating at minimum load. In case of engine operating at part-loads the transferred heat has to be evaluated consequently to the agents streaming conditions and to the corresponding engine operating temperatures.

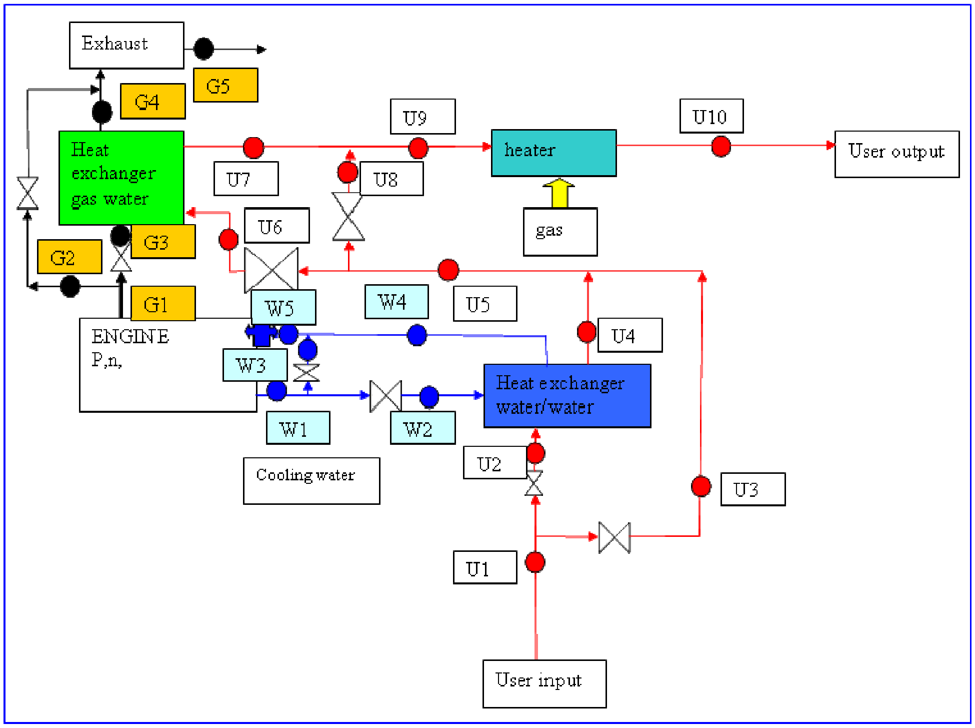

Figure 1: The schematic of the installation

3. MODELING OBTAINED RESULTS

It is considered that the engine can run at any speed, corresponding to the optimal regime consumption because the system is equipped with an electronic device that modifies the frequency at high efficiency. It is also presumed that the engine minimum output power is 20 kW, expressing the minimum necessary continuous power. The maximum water flow rate is 0.85 kg/h (approx. 3.06 m^3/h), to be delivered at 90°C. The system behavior has been analyzed for several operating conditions, characterized by the necessary electric produced power and the hot water flow rate.

For a first scenario, considered to reach an upper functional limit, electric power is at its minimum, 20 kW while the water flow gets its maximal value. In these conditions, the water temperatures are varying upon the next graphic, versus the engine speed (see fig.2).

It is pointed out that the temperature in the boiler inlet increases from 30°C to 40°C with the increase of the engine speed. The gas consumption remains quasi-constant and the global efficiency varies in-between 55% and 62%.

For a second scenario, the produced electric power keeps its same minimum value, but the hot water flow decreases to 0.2 kg/h. The corresponding temperature measurements vs. the engine speed are plotted in fig.3. It also clearly appears that for some values of the engine speed it becomes not anymore necessary the use of the water boiler, so any other gas consumption for the boiler is no more needed. The natural gas consumption for the engine and the boiler varies with the engine speed (at basic load) as shown in fig.4.

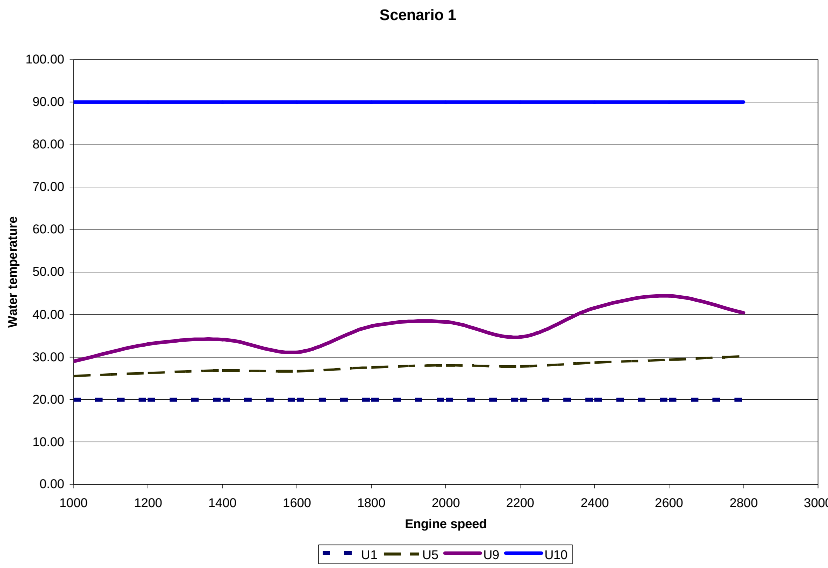

Figure 2: Water temperatures vs. engine speed for Scenario 1

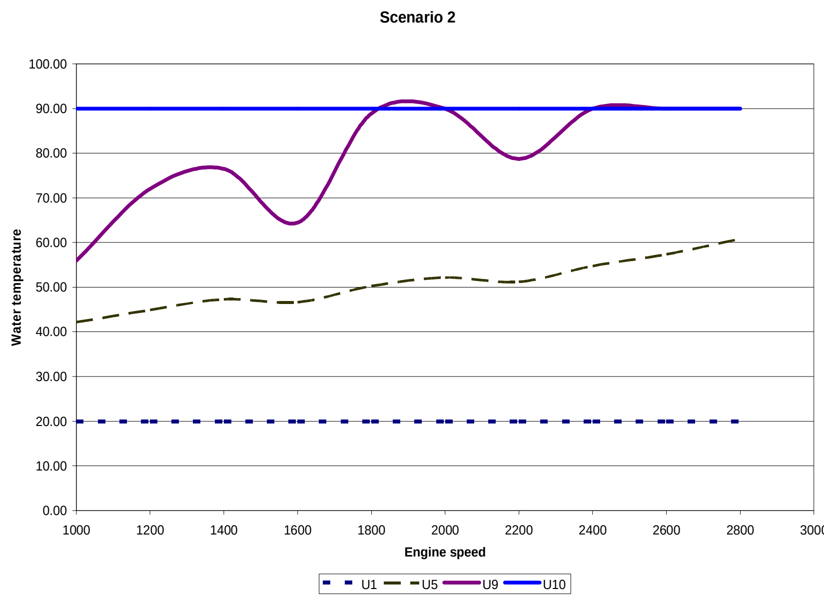

Figure 3: Water temperatures vs. engine speed for Scenario 2

The operating domain of the system covers the range between maximum electric power with zero hot water flow and minimum electric power with maximum hot water flow; there are also extreme cases in which the electric power is maximal and the hot water flow rate varies in-between its limits. In order to get optimal engine efficiencies it is necessary to choose certain water and gas flow rates passing through the heat exchangers. These flow rate values could be consequently calculated.

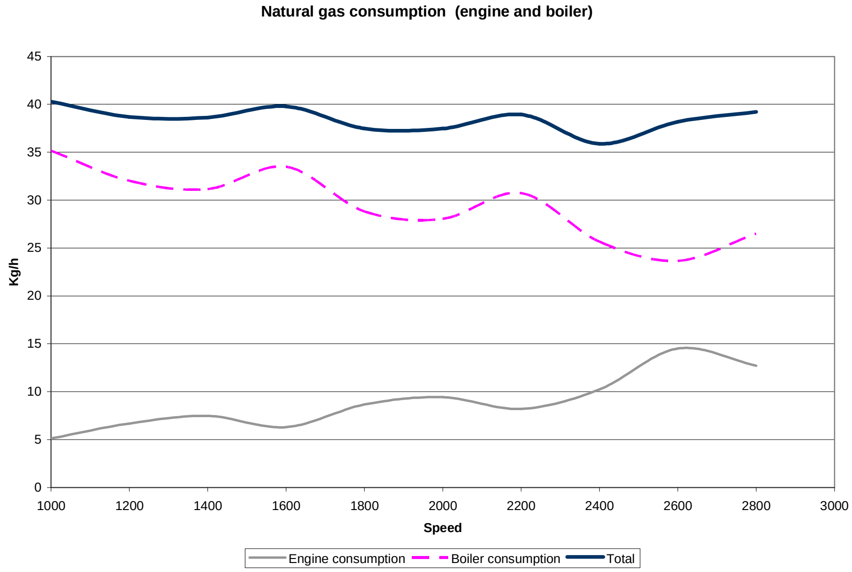

Figure 4: Natural gas consumption vs. engine speed

4. CONCLUSIONS

This paper is proposing the modeling of a waste heat recovery system, transferring the heat of a diesel engine exhaust gases and cooling water to a building water heating system in parallel with the electric energy generation.

The diesel gas engine could furnish energy to the electric generator at any revolution speed, fact which allows the optimization of the engine fuel consumption at any operating regime.

This model could be successfully applied to any other similar energetic system configuration.

References

[1] Aussant, C. D., Fung, A.S., Ugursal, V.I., Taherian, H., *Residential application of internal combustion engine based cogeneration in cold climate*, Canada, Energy and Builduings 41 (2009), 1288-1298.
[2] Lozano Serrano, M.A., Saravia, J.R., *Optimal Cogeneration Technology Selection for Residential and Commercial Buildings*, Distributed Generation & Alternative Energy Journal 25:4,8-19.
[3] Abusoglu, A., Kanoglu, M., *Exergetic and thermoeconomic analyses of diesel engine powered cogeneration: Part 1* – Formulations Applied Thermal Engineering, 29 (2009) 234-241.
[4] Abusoglu, A., Kanoglu, M., *Exergetic and thermoeconomic analyses of diesel engine powered cogeneration: Part 2* – Application Applied Thermal Engineering, 29 (2009) 242-249.
[5] Ştefănescu, D et al., *The heat exchange in Technics. Applications for engineers*. Technical Press, 1982 (in Romanian).

VERY HIGH GAS TEMPERATURE TURBOENGINE

Constantin Sandu[1*], Iulian Vladucă[1], Bogdan Sacuiu[1], Dumitru Amariutei[1],
Razvan Cârlănescu[1], Razvan Bimbasa[1]
[1]*COMOTI, Bucharest, Romania*
[*]Corresponding author: E-mail : Iulian.Vladuca@comoti.ro

ABSTRACT

This paper presents a new type of turboengine having very high gas temperature in front of turbine. It is known that the maximum gas temperature in front of turbine is the best method to increase the efficiency of turboengines and of any thermal engine. However, this temperature can not be too high because the limited strength of turbine blades. The turbine blades of present turboengines are cooled with air taken from engine compressor. However, this method does not permit increasing of burnt gases temperature over 1450 ºC. This is happened because the thermal transfer between the blade metal and cooling air has a low intensity due to low density of cooling air. This drawback can be eliminated if the turbine blades are cooled with liquid instead of air. The present paper presents the possibility to cool the turbine blades with liquid fuel for gas turbines ('Kerosene'). The liquid fuel is circulated through cooling holes in turboengine blades before to be injected in combustor. Thus, the heat extracted from turbine is completely recuperated because, after cooling the turbine blades, the liquid fuel is injected and burnt in combustor.

Keywords-turbine blade cooling with liquid, turboengine, high gases temperature in front of turbine.

NOMENCLATURE

c_p -specific heat (kJ/kg/K)
d* -characteristic dimension (m)
H_c -heat of combustion for Kerosene (kj/kg)
F_c -fuel consumption (kg/s)
l_{hev} -latent heat of evaporation (kj/kg)
l_{bc} -blade chord
M_a -mass flow of air through turboengine (kg/s)
Nu -Nusselt number (dimensionless)
Pr -Prandtl number (dimensionless)
P_t -power absorbed by Kerosene in turbine rotor
q_{cgb} -The specific heat flux due to convection from burnt gases to blade (W/m^2)
Re -Reynolds number(dimensionless)
S_{teab}-total area of external surfaces of all turbine blades (m^2)
T -temperature (K)
T_{meg} -mean temperature of burnt gases (K)
T_{mesb}-mean temperature of turbine blade surface (K)
T_H -absolute temperature of the high-temperature reservoir for Carnot cycle (K)
T_L -absolute temperature of the low-temperature reservoir for Carnot cycle (K)
t -time (s)
w -speed of burnt gases relatively to turbine blade (m/s)

Greek

α_{cgb}-coefficient of heat transfer due to convection from burnt gases to blade external surface (W/m^{2}K)
η_{Carnot} -the thermal efficiency of Carnot cycle (dimensionless)
η_t - the thermal efficiency of simple gas turbine cycle (Joule/Brayton cycle) (dimensionless)
λ_{meg} -mean coefficient of heat transfer by conduction for burnt gases [W/(m K)]
ν- kinematic viscosity , $\nu = \mu/\rho$ (m^2/s)
ρ-density (kg/m^3)

Numerical symbols

1*, 2*, 3* points of decelerate (total) state of working gas (air) in the diagram enthalpy-entropy of engine cycle

1. INTRODUCTION

As it is known, the theoretical limit of thermal efficiency of a heat engine is given by Carnot cycle [1]. This limit, η_{Carnot}, is given by [1, 2]:

$$\eta_{Carnot} = 1 - \frac{T_L}{T_H} \qquad (1)$$

(T_L = minimum absolute temperature of cycle; T_H =maximum absolute temperature of cycle).

In the case of gas turbine engine, i.e. an engine composed of mainly of a compressor, combustor and a turbine, the maximum thermal efficiency $\eta_t^{(max)}$, is given by:

$$\eta_t^{(\max)} = 1 - \sqrt{\frac{T_1^*}{T_3^*}} \qquad (2)$$

where T_1^* and T_3^* are the total temperature at compressor and turbine inlet, respectively [3].

Therefore, increasing of temperature T_3^* is the best method for improving the efficiency of these type of engines. For the case of aeroengines, increasing of T_3^* has a greater importance because it leads to decreasing of the specific weight and frontal area of the engine.

2. THE PRESENT COOLING SYSTEMS OF TURBINE BLADES

The need to increase T_3^* led to the need of turbine blade cooling. The preferred cooling systems use cold air taken from compressor [1, 3]. On average, despite sustained efforts, from 1970 to 1997, T_3* increased by 10 K per year [4]. For example, if this rate of gain will be kept, T_3* will reach 2500 K after seventy years.

There are 3 basic air-cooling systems [5, 6]:

- Convection cooling;
- Film cooling;
- Air transpiration cooling.

Convection cooling is the mostly used. Cold air taken form compressor cools the disc faces then enter through holes in turbine blades cooling them (fig.1). Due to mechanical and manufacturing constraints, blades have a limited internal cooling surface and air is not an efficient cooling fluid. When temperature at turbine inlet becomes very high, the amount of air required for cooling increases too much [6].

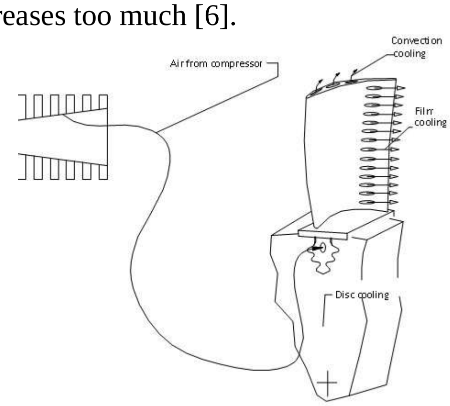

Fig.1-Convection cooling and film cooling.

Film cooling systems blast cold air on the external surface of turbine blades. A drawback of this system is the difficulty of controlling the flow of cold air around the blade surface; see again fig.1. This system produces only marginal T_3*gains. The maximum temperature at turbine inlet provided by air-cooling systems is about 1800 K [2, 5].

Currently, transpiration (effusion) cooling appears to be an efficient cooling method. This transpiration system attempts to isolate turbine blades from burnt gases using a thin layer of cold air [1,6]; in this case, blades need to be coated with a porous material in order to allow the air efflux, see fig. 2.

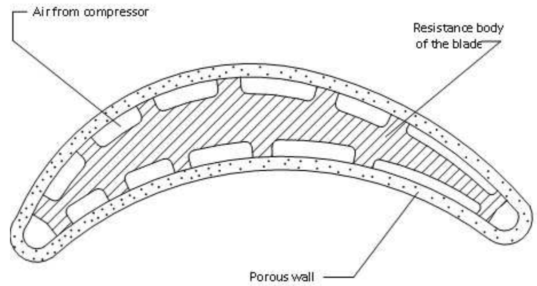

Fig. 2 – Transpiration (effusion) cooling for turbine blades.

However, the experiments shown that the porous material is subject to excessive wear, fatigue and corking. Strength of porous coating is low while the maximum mechanical and thermal stress is reached on the blade surface.

The air film disturbs the flow pattern of burnt gases leading to power losses [6]. Due to mechanical vibrations and combustion processes, the flow of burnt gases is turbulent [7], therefore, the thin layer of cold air is difficult to maintain.

The main problem is that the burnt gases contain impurities in plastic state due to high gases temperature and occlude the external pores of the blade. As a result, cooling is greatly reduced.

3. A NEW TURBINE BLADE AND DISC DESIGN SOLUTION

This paper proposes a new design of cooling system for turbine blades and discs using liquid fuel (Kerosene) as coolant. This is possible now because it was accumulated much experience in the field of high speed seals used for transfer of Kerosene fuel from static part of engine to rotor (this kind of seal is used in the case of some helicopter turboshaft engines) (fig.3 [8]). At those engines, the liquid fuel (Kerosene) enters the engine rotor through engine shaft by means of an axial carbon seal placed at the front of engine shaft. After that, the fuel circulates through engine shaft to the injection disc which injects fuel in engine combustor. Such kind of engines already accumulated millions of flight hours without events.

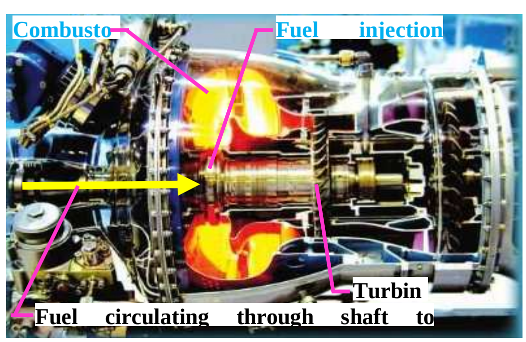

Fig. 3 – Engine having fuel circulation through shaft

The main idea exposed in this paper is that before injection in combustor, the fuel is circulated through the turbine disc and blades cooling them in this way (fig.4). The cooling holes in disc and blades look like in fig.4 when turbine disc and blades are made as a single piece. If turbine blades and disc are separated pieces, the disc can have configuration given in fig.5.

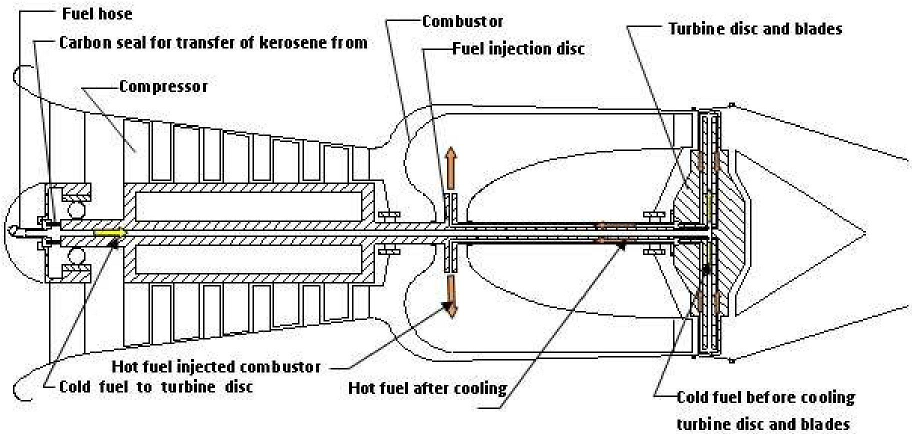

Fig. 4 – Engine having fuel circulation through shaft, cooling of turbine disc and blades with fuel and injection of fuel in combustor by means of a injecting disc

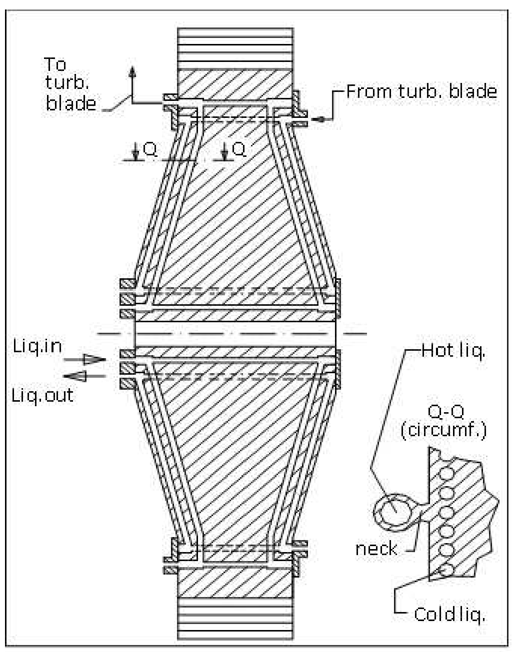

Fig. 5 – Disc cooling

Kerosene has important properties making it appropriate for cooling. Kerosene density is 780÷810 kg/m^3, i.e. a little under density of water and much higher than air density. The specific heat of Kerosene is c_p=2.01 kJ/kg/K. The specific heat of vaporization is l_{hev}=251 kJ/kg. In addition, Kerosene has other physical important properties like:

- Not reacting with engine materials (such as ducts, blades and discs materials).
- Low viscosity
- High latent heat of vaporization (when vaporization is used)
- Lubricating capacity

Turbo-engines have specific fuel consumption from 8.696 g/KN/s (CF6-General Electric) to 33.8g/kNs (Olympus 593-a SNECMA-Rolls-Royce engine). Obviously, the fuel consumption is great in the case of turboengines being for the most of engines of many kilograms per second. For example, in the case of engine Olympus 593, the engine thrust is 169.2 kN. Fuel consumption is then:

F_c=169.2x33.8=5.718 kg/s (3)

Kerosene is taken from the aircraft tanks. Its temperature varies from about 15ºC at ground level (in normal ambient conditions) to -55ºC at 11.000 m. So, when the aircraft is in flight the quantity of heat which can be extracted from turbine blades is higher because Kerosene temperature is lower than at ground level.

Kerosene is obtained from the fractional distillation of petroleum between 150 °C and 275 °C. Assume an average distillation temperature (150+275)/2 = 212.5 ºC. Then, in the case that Olympus engine is in flight, the quantity of heat which could be extracted from turbine blades by Kerosene through heating from -55 ºC to 212.5 ºC is:

$$P_{t1} = F_c \cdot c_{p\cdot} \cdot \Delta T \;= 5718 \cdot 2.01 \cdot (212.5 - (-55) = 3074 kW \qquad (4)$$

Assume that the Kerosene is vaporized inside turbine blades and then goes to injection disc to be burned in combustor. The additional heat extracted by Kerosene from turbine blades due to vaporization is:

$$P_{t2} = F_c \cdot l_{hev} = 5718 \cdot 251 = 1435 kJ/s = 1435 kW \qquad (5)$$

The total thermal power extracted from turbine blades is:

$$P_t = P_{t1} + P_{t2} = 3074 + 1435 = 4509 kW \quad (6)$$

This value is very high showing how important is recovering of thermal heat extracted from turbine blades during cooling process.

Let's consider now the same turboengine presented in paper [9]. The specific heat flux due to convection from burnt gases to blade, q_{cgb}, is given by:

$$q_{cgb} = \alpha_{cgb} \Delta T_m = \alpha_{cgb} (T_{meg} - T_{mesb}) \qquad (7)$$

where α_{cg} -is the heat transfer coefficient through convection from burnt gases to turbine blade external surface, T_{meg}-is the mean temperature of burnt gases, T_{mesb} is the mean temperature of turbine blade surface. In paper [9] was found that coefficient of heat transfer through convection from burnt gases to blade external surface is α_{cgb}=8169 (W/m^2/K), being given by formula:

$$\alpha_{\square} = \frac{\square \lambda \square}{\square} = \frac{\square \lambda \square}{\square} \qquad (8)$$

where l_{bc}-blade chord was taken 25 mm, λ_{meg} -mean coefficient of heat transfer by conduction for burnt gases was taken ≈0.1012 W/mK, and Nu (Nusselt number) = 2018 (dimensionless) being calculated with formula:

$$\square = \square \cdot \square \cdot \square \qquad (9)$$

In formula (9), Re (Reynolds number) = 1.038·10^6 (dimensionless) (calculated with formula $\mathrm{Re} = w \cdot \frac{d^*}{\nu}$, where w and ν are the burnt gases speed relatively to turbine blade and kinematic viscosity, respectively and d*= l_{bc})

Pr (Prandtl number) = 0.71 (dimensionless) (calculated with formula $\mathrm{Pr} = \rho \cdot \frac{c_p}{\lambda}$, where ρ, c_p and λ are the density, specific heat at constant pressure and heat conductivity of burnt gases respectively).

Assume the average temperature of turbine blade external surface is T_{mesb}=1173 K (900 ºC). In paper [9], the calculated area of external surfaces of all blades was found S_{teab}=0.089608 m^2 .

The total amount of heat transmitted through convection from burn gases to blades surfaces is given by:

$$Q_{cgb} = q_{cgb} \cdot S_{teab} = 8169 \cdot (1879 - 1173) \cdot 0.089608 = 516.8kW \qquad (10)$$

where T_{meg}=1879K, T_{mesb}=1173 K. On the other hand, the fuel consumption for the turboengine given in [9] is:

$$F_c = M_a \cdot (T_3^* - T_2^*) \cdot c_p / H_c = 15.7 \cdot (2050 - 748) \cdot 1/43500 = 0.47kg/s \qquad (11)$$

where M_a=15.7 kg/s (mass airflow), T_3* was taken 2050K (maximum temperature of gases), T_2*=748 K (air temperature after compressor), c_p=1kJ/kg (specific heat of air), H_c=45500kJ/kg (heat of combustion for Kerosene).

The maximum heat which can be extracted by Kerosene is:

$$P_t = P_{t1} + P_{t2} = F_c \cdot c_p \cdot (212.5 - (-55)) + F_c \cdot l_v = 0.47 \cdot (2.01 \cdot 267.5 + 251) = 370.7kW \qquad (12)$$

It can be seen that Pt/Q_{cgb}=71.7%, i.e. 71.7% from the heat extracted during turbine cooling can be totally recuperated busting turboengine efficiency to high values. Only 100-71.7=28.3% of heat should removed using classic cooling methods with air.

4. CONCLUSIONS

To raise the thermal efficiency of gas turbine engines, the temperature at turbine inlet must increase. This temperature is limited by the heat transfer capacity of cooling systems that are used for turbine cooling. Reaching of very high gas temperatures in front of turbine is no longer possible if only cooling with air is used. Cooling with liquid should be used in combination with cooling with air or instead cooling with air.

This paper proposes cooling of turbine blades and discs using the engine fuel (Kerosene). For the given example, the fuel can extract 71.7% of heat from turbine blades when T_3*=2050K. This heat is completely recuperated. Only the rest of 28.3% of heat should be removed using classic cooling methods with air. This paper completes the paper [9] which deals with cooling of turbine blades using liquid circulated in closed loop.

References

1. Bathie, W. W.: Fundamentals of Gas Turbines, 2nd edition, John Wiley & Sons Inc., N.Y., 1996, pp. 30, 318-325.
2. Vincent, E. T.: The Theory and Design of Gas Turbines and Jet Engines, 1st edition, McGraw-Hill, NY, 1950, pp. 92-94,140.
3. Oates, G. C.: Aerothermodynamics of Gas Turbine and Rocket Propulsion, 3rd edition, AIAA Reston VA, 1997, pp. 136-137, 220.
4. Giampaolo, T.: The Gas Turbine Handbook: Principles and Practices, The Fairmont Press Inc., Lilburn, GA, 1997.
5. Cohen, H. et al.: Gas Turbine Theory, 4th edition, T. J. Press, 1996, pp. 25, 237, 320-324.
6. Boyce, M. P.: Gas Turbine Engineering Handbook, Gulf Publishing Co., Houston, 1982, pp. 264-278, 319.
7. Anderson, D. J: Modern Compressible Flow with Historical Perspective, McGraw-Hill, N.Y., 1982, pp. 4, 75.
8. http://www.google.ro/books?hl=ro&lr=&id=Ly66eNVjtfEC&oi=fnd&pg=PP1&dq=convection+heat+transfer+in+gas+turbines&ots=qxLmQyvXMO&sig=YVwldwYPFgOEZ8zhUeaU9HjA8LI&redir_esc=y#v=onepage&q=convection%20heat%20transfer%20in%20gas%20turbines&f=false
9. Sandu, C., Brasoveanu, D., Relative Cooling with Liquid for Gas Turbines-A solution for Exceeding 2000K at Turbine Inlet, Proceedings of DETC/CIE 2001 ASME Technical Conference, September , 2001, Pitsburg, PA, USA, DETC2001/CIE-21763 (part 1 and 2).

PRACTICAL PSYCHOMANAGERIAL APPLICATION IN ORDER TO BUILD A BEHAVIORAL HOLISTIC MODEL OF ECO-AWARENESS BASED ON ORDER PSYCHOLOGY-QUANTUM PSYCHOLOGY® (POPQ®)

Corneliu Sofronie, Ruxana Zubcov
Centrul de Formare si Perfectionare Perfect

ABSTRACT

In the social field experts noted in time a more individualized social reality. The need to protect Human, the essential factor of the preservation and evolution of species, requires an adaptation of methodologies and methods of knowledge for an intervention in favor of keeping life at higher levels of evolution of matter, at leading information existing in science.
This article is a synthesis of research works aimed at training and developing a model of a high environmental consciousness based on a complex instrument which makes the individual a responsible person.

1. INTRODUCTION

The study subject to our research, seen from the perspective of management and applied psychology within Sucursala Electrocentrale Craiova, Isalnita Facility, in order to reduce the polluting emissions and increase the quality of life, has a holistic and eco-ergonomic nature, the relation between man and equipment being characterized by the synergetic role of the environment in validating such relation.
During the first stage one has conducted the initial ergonomic study of work places in the context of the triad: man-equipment–environment aimed at preparing a model for shaping and developing an ecological awareness compatible with the environmental protection requirements set forth by EU.
The results obtained, having as a benchmark the objectives of the current stage of the study, can be summarized into two points regarding the holistic eco-ergonomics of the work place, as follows:

- **Conditions for performance of the activity** (materialized in the ergonomic study of the work place, based on the tool for holistic determination of the occupational environment ergonomic potential).
- **Professional quality of the activity** (determined based on the responses received following application of the method for evaluation of the vocational training).
- **Synergy between the first two points** having as an effect **the type of eco-awareness of the employees from Isalnita Facility, completed by a holistic model of eco-awareness** with which we have compared the results obtained during the field research conducted with the beneficiary.

2. METHODOLOGY

The methodology and psychosocial-management tools are built on principles of feed-before cybernetics, serving to prevent the occurrence of events, incidents and accidents and also meet the requirements of OHSAS 18001 for health and safety at work, and of ISO 14000 - creating conditions for environmental protection. By satisfying the conditions of ISO 14000, the overall methodologies become a powerful tool for training among the population of the energy group, of a higher environmental consciousness in agreement with the European Union on the need to approach the human factor.

3. RESULTS OBTAINED AND CONCLUSIONS

Table no. 1. General holistic model of awareness built on the basis of sustainable development principles included in the Rio Statement

ECO-AWARENESS MODEL					
Perspective on the relation with nature	**Perspective on life in general**	**Type of necessity satisfied / unsatisfied by the relation with nature**	**POP Q scale**	**Type of emotion caused by nature understood in broad terms**	**Attitudes towards natures and environment**
Integration in nature Solophilia	Spiritual	Ideality, stable balance	Cp	Ecstasy/ happiness	Attachment
Love for nature Solastalgia	Moral	Harmony with the world, with the others, morality	Cg	Joy	Empathy
Wisdom in the relations with nature (Rationality)	Rational-utilitarian	Need for usefulness	Cl	Pleasure	Sympathy
DETACHMENT					
Ambiguous towards nature (schizoid)	Emotional-negative, dynamic balance	Inner disharmony, uncertainty	I	Unconcern	Antipathy
Vengeful on nature (sadistic-paranoid)	Antagonist-conflicting	The feeling of losing identity	R	Defiance	Hatred
Negativist (catatonic)	Depressive	Losing the sense of existence	H	Apathy	Indifference

One has addressed the following five **criteria:**

1. Perspective on the relation with nature
2. Perspective on life in general
3. Type of necessity satisfied/unsatisfied by the relation with nature
4. Type of emotion caused by nature understood in broad terms
5. Attitudes towards nature and environment

Table no. 2. Conclusions

Criterion	**Subjects with higher education**		**Subjects with high school**	
	Ratio	**Comments**	**Ratio**	**Comments**
1	**93%**	They consider themselves as integrated in nature	**94%**	They consider themselves as integrated in nature
2	**95%**	One reports rationally, general optimist answers	**92%**	One reports rationally, general optimistic answers
3	**94%**	Satisfied-the necessities related to freedom and ideality generating the feeling of power and uniqueness	**75%**	Satisfied-the necessities of morality, causing the feeling of perfection, harmony
4	**60%**	They feel no emotion for	**67%**	Positive emotions for

		nature (age-over 40 years)		nature
5	The reaction varies depending on the professional age. If subjects with the professional age of 7-16 years have a totally positive attitude towards the environment, subjects belonging to the category 0-7 are reluctant, assessing the environment in which they carry out their activity at the level of limit certainty, which means the existence of a distress in the relation between the subjects and work environment. For the categories of age 16-24, respectively 24-33-categories which suppose a wide experience in the context of the current work environment, the trend is over the ceiling between limit certainty and uncertainty, which emphasizes forms of slight to major distress, evolving to conflict between the subject and his/her work environment		An uncertain reference to the environment is obvious. The attitude towards the environment ranges between appreciation and disappointment, even if the latter is not directly expressed, but indirectly, by the refusal to assess the attitude towards the work place by a certainty grade (8, 9 or 10).	

BEHAVIORAL HOLISTIC MODEL OF ECO-AWARENESS BASED ON ORDER PSYCHOLOGY - QUANTUM PSYCHOLOGY® (POPQ®)

The POPQ human behavior model has been created based on experiment. This experiment has involved over ten years more than 5,000 subjects. We have developed a human behavior model that we will use also in the context of this study for creating the eco-awareness behavioral model. Eight fundamental models have resulted:
MMR – male-male rational; MFR – male-female rational;FMR – female-male rational;FFR – female-female rational;MMI – male-male irrational;MFI – male-female irrational;FMI – female-male irrational;FFI – female-female irrational
Each having 4 levels of manifestation: higher, medium, lower and regressive:

Table no. 3. Higher eco-awareness

MMR Competitive	Authentic behavior, focused on finding efficient solutions in the relations with nature; sympathy for nature
MFR Expert	Knowledge-focused, visionary behavior and active and innovative participant in the relations with the environment, with nature
FMR Altruist	Empathic, generous and thoughtful behavior towards the natural environment
FFR Perfectionist	Highly accountable behavior, based on attachment towards nature; it refers to nature as to a Supreme Moral Law
MMI Hero	Heroic behavior, with a sacrifice spirit in relation to nature and environment; facts and actions giving the subject the feeling that he/she is strong, a savior of humanity
MFI Innovator	Lover of nature, sensitive and receptive to what happens in the environment; creative, original
FMI	Enthusiastic, with the capacity of anticipating future actions related to

Energetic	nature, realistic and productive
FFI Pacifist	Composed, calm and harmonious in the relations with nature, passive but capable to follow role models and successful examples in the relations with nature and with environment

Table no. 4. Medium Eco-awareness

MMR Competitive	Pragmatic, adaptable, wanting to excel, conditioning the involvement in actions with environment or nature on a gain brought to his/her own image
MFR Expert	Cerebral type: perceptive, innovator, secretive and isolated, with the propensity to become apathetic and disinterested the moment he/she has no longer the motivation necessary to get involved in the relations with the environment
FMR Altruist	Generous, demonstrative, aimed at pleasing the others, easily switching between the need to consider himself/herself as indispensable for the ones from his/her environment, and to consider himself/herself completely intrusive
FFR Perfectionist	Serious minded, principled, applied, but with the feeling of doing what he/she is doing out of obligation, which often impacts on his/her health condition
MMI Hero	Pragmatic and enterprising, but with the propensity of being overproud and not accepting proposals and solutions provided by others
MFI Innovator	Tendency to behave as if the center of the universe and to be too permissive with the others, when noticing aggressive actions of the others on the environment
FMI Energetic	Bohemian, relatively unfocused and distracted behavior, a little excessive in manifestations yet efficient
FFI Pacifist	Generally modest and pleasant, still resigned; it is hard to convince him/her to participate in actions related to environment or nature in general

Table no. 5. Lower Eco-awareness

MMR Competitive	Unscrupulous, aggressive and conventional behavior; insincerity in the attitude towards environment and nature
MFR Expert	Disconnected from everything around him/her and concerned about his/her problems only, separated from the environment he/she is living in
FMR Altruist	Despotic and coercive towards the environment, based on having adverse feelings, disappointments
FFR Perfectionist	Inflexible, contradictory and confusing behavior towards the environment and nature
MMI Hero	Feeling the need to be megalomaniac, aggressive and destructive to the environment and nature
MFI Innovator	Distant, with tendencies of denying life, with a detesting behavior towards the ones in his/her interaction environment
FMI Energetic	Imprudence in the relation with environment and nature; incapability of facing difficult situations
FFI Pacifist	Careless, disoriented, prone to commit errors or blamable deeds most of the time by accident and unintentionally

Table no. 6. Regressive/pathological eco-awareness

MMR Competitive	Sadistic behavior, lack of feelings and inner emptiness in relation to nature, neurotic reaction towards nature
MFR Expert	Schizoid behavior, with full loss of interest in the world, environment and nature
FMR Altruist	Forms of hysterical behavior, aggressive manifestations and inappropriate extremist tendencies against environment and nature
FFR Perfectionist	Living high intensity moments of disillusion and depression towards the environment and nature; obsessive thinking and compulsive behavior; feeling of debilitating guilt towards environment and nature
MMI Hero	Paranoiac, vengeful behavior towards environment and nature which are deemed guilty for his/her frustrations and failures; lack of eco-awareness and of empathy towards environment and nature
MFI Innovator	Syndrome of narcissist, avoiding personality; strong feeling of self-estrangement and estrangement from others; explosion of fury, hostility and hatred
FMI Energetic	Maniac-depressive, careless behavior towards environment and nature
FFI Pacifist	Depressive disorder, extreme denial of environment and nature, obstinacy and rejection of helping efforts

CONCLUSIONS regarding the behavioral holistic model of eco-awareness built based on the methodology of Order Psychology - Quantum Psychology® (POPQ®)

The level of behavioral eco-awareness has been investigated by means of POPQ® methodology. The aim has been to determine by higher, medium, regressive and pathologic levels, the forms of behavior that make up the behavioral eco-awareness model with S.E.Isalnita.

Table no. 7. Conclusions regarding the behavioral holistic model of eco-awareness built based on the methodology of Order Psychology - Quantum Psychology® (POPQ®)

Behavior level	Subjects with university education level		Subjects with pre-university education level	
	Personality type	Ratio of subjects	Personality type	Ratio of subjects
Higher	***Hero*** -sacrifice spirit in the relation with nature and environment -it occurs in difficult situations -it defines subjects with a high awareness of the world	17%	***Perfectionist*** - Highly accountable behavior, based on attachment towards nature; - specific behavior in critical, difficult, catastrophic situations.	24%
Medium	***Energetic*** - Bohemian, relatively unfocused and distracted behavior, a little excessive in manifestations yet efficient. –it occurred in	62%	***Competitive*** - Pragmatic, adaptable, wanting to excel, conditioning the involvement in actions with environment or nature on a gain brought to	49%

	ordinary, normal situations -proper to subject in whom the self-awareness and the awareness of the worlds are equiprobable.		his/her own. –it occurs in ordinary, normal situations.	
Lower	***Expert*** -The subject is disconnected from everything around him/her and concerned about his/her problems only, -the self-awareness is dominant.	18%	***Energetic*** - Imprudence in the relation with environment and nature - individual behaviors, based on personal disappointments and frustrations.	22%
Regressive	***Pacifist*** - Depressive disorder, extreme denial of environment and nature, obstinacy and rejection of helping efforts (he/she is highly present in cases of social and economic crisis).	3%	***Expert*** - Schizoid behavior, with full loss of interest in the world, environment and nature. Such outbreaks occur especially during crisis and social and economic uncertainty periods.	5%

The methodological model developed in the context of the research work is a genuine model placing in a consistent relation: MAN - TECHNIQUE - ENVIRONMENT**,** providing, in the end, a comprehensive guide including the main assumptions for increasing the quality of life.

4. ACKNOWLEDGMENT

This work was supported by a grant of Romanian National Authority for Scientific Research CNDI-UEFISCDI, project number PN-II-PT-PCCA-2011-3.2-1292, contract number 33/2012, HOLGRUP.

References

[1] Bateson, G.: *Mind and Nature*, E.P. Dutton, 1979
[2] Bélanger, David, Dion, Kenneth şi Adair, G. John: *Advances in Psychological Science. Récents dévelopements en psychologie scientifique* (vol I şi II), Psychology Press-Montreal, 1998
[3] Bohm, David: *Plenitudinea lumii şi ordinea ei, (Plenitude of the world and its order),* Ed. Humanitas, Bucuresti, 1995
[4] Boutot, Alain: *Inventarea formelor, (Invention of shapes)*, Ed. Nemira, Bucuresti, 1997
[5] Capra, Fritjof: *Conexiuni ascunse, (Hidden Connectings)*, Ed. Tehnică, Bucuresti, 2004
[6] Capra, Frjtiof: *Înţelepciune aparte, (Uncommon Wisdom),* Ed. Tehnică, Bucuresti, 2004
[7] Dawkins, Richard: *Gena egoistă, (Selfish gene)*, Ed. Tehnică, Bucuresti, 2006
[8] Deutsch, David: *Textura realităţii, (The Fabric of Reality)*, Ed. Tehnică, Bucuresti, 2006
[9] Drăgănescu, Mihai: *Informaţia materiei, (Information of matter),* Ed. Academiei Române, Bucuresti, 1990
[10] Drăgănescu, Mihai: *Eseuri (Essays)*, Ed. Academiei Române, Bucuresti, 1993
[11] Fuller, Ray (coordonator): *A Century of Psychology. Progress, paradigms and prospects for the new millenium*, by Routledge London and New York, 1997

STUDY ON COMBUSTION EFFICIENCY, TECHNOLOGY, MAIN FACTORS AND CORROSIVE CHEMICALS FOR THE FURNACE

Gabriel Adrian Ștefan, Tudor Prisecaru
Universitatea Politehnica din Bucuresti

Abstract

One of the most important research and development in engineering and technology is the continuous technological improvement and innovation with direct applications in people's lives. This innovation cannot be found without a continuous and detailed research for all the technologies and methods of combining them to increase efficiency and constant lowering the exhaust emissions. The main expected results from human society is a continuous decrease of the cost for producing heat and electricity while reducing the amount of pollutants and ash that may affect the environment.

Keywords: solid fuel, co-combustion, biomass pilot plant, technical optimization, efficiency, emission, dust and ash.

1. INTRODUCTION

Technology for the production of heat and electricity does not seem to have changed much compared to 20-30 years ago, but researchers were able to continuously improve the thermal efficiency of the plant and equipment, using innovative materials and control systems. The most important aspect of this technology is the possibility of lifting the thermal efficiency reduced periods of time to cover the top of the heat consumption in some periods specific zones of human activity. [1]. Increasing efficiency by a few percent without affecting thermal systems and equipment, and to reduce emissions at the same time was a difficult goal to achieve.

Biomass continue to make a vital contribution and represents the most important renewable successfully replaces coal in thermal plants without major changes involves the technologies or equipment. The main advantages it has over coal biomass availability and purchase price are much lower. [2]

2. THE MAIN PURPOSE OF MY STUDY

In the last decade the attention of researchers has focused on the modification of equipment and systems to increase the thermal efficiency of the plant at a high level for longer periods of time with less fuel consumption and therefore harm reduction for the envirenment. Another aspect to consider is keeping in good condition and clean installation of heating appliances harmful residue resulting from combustion and heat recovery process. This is possible due to control programs and simulations for the burning and the way of combining air with fuel particles without soiling outbreak walls.

Another way to protect the environment is through the retention and storage of ash or slag results after combustion and the use of effective filters for smoke and smog particles.[1]

3. THE OPTIMAL CONDITIONS FOR OPTIMISING THE THERMAL PROCESS IN FURNACE

The past decade has increased the demand and needs to diversify energy sources predominantly in the direction of partial or total replacement of classic fuels , especially coal renewable fuels such as biomass and especially plant biomass .Particularly important in thermal equipment's operation and regulation is the cleaning and maintenance of facilities. Chemical compounds that form and can adhere to the walls of the combustion furnace major influence and gas temperature. The main chemical compounds that are found in clay or ash discharged from the plant In the case of boilers and heat exchange heating water main factors that can affect the installation and the installation of heating appliances are high temperature and dew temperature and dew acid. The maximum temperature obtained in a combustion process theory, assuming that there is direct heat exchange with the outside is called the theoretical temperature of combustion gases and corresponding theoretical enthalpy of combustion gases according to the relation [3]:

$$t_{ga}^{0} = \frac{I_{ga}^{0}}{V_{ga}^{0} \cdot C_{ga}\Big|_{0}^{t_{ga}^{0}}} \quad [^{0}C] \tag{1}$$

This temperature cannot be achieved in real installations; it is a limit to be achieved in real plants. Dew temperature and dew temperature acid is an important feature in exploiting installations. The dew point temperature - saturation temperature corresponding to the partial pressure of water vapor in the flue gas. This is given by:

$$p_{H_2O} = p\frac{V_{H_2O}}{V_{gu}} \quad [MPa] \tag{2}$$

Where: p - the pressure of the combustion plant, in MPa; VH2O VGA - Volume of water vapor in the flue gases and the respective actual volume of flue gas in m^3_N/kg fuel. At the indicator λ = 1.6 wood to give a dew temperature tr = 323-325 K (500C). dew point between 25 and 70 ^{0}C (according to **Fig.1**)
Acid dew point temperature can be calculated using the equation:

$$t_{ra} = t_r + \frac{\beta_a \sqrt{S_c^{rap}}}{1{,}05^{4{,}19(1-\eta_{zg})A^{rap}}} \quad [^{0}C] \tag{3}$$

Where: t_r - water dew point in ^{0}C; B_a - coefficient which takes into account the coefficient of excess air in the combustion chamber, the values β = 195 at λ_f = 1.2 and β = 208 at λ_f = 1.6; S_c $_{rap}$ - sulfur fuel reported in[% kg / kJ]; A_{rap} - ash reported in [% kg / kJ].

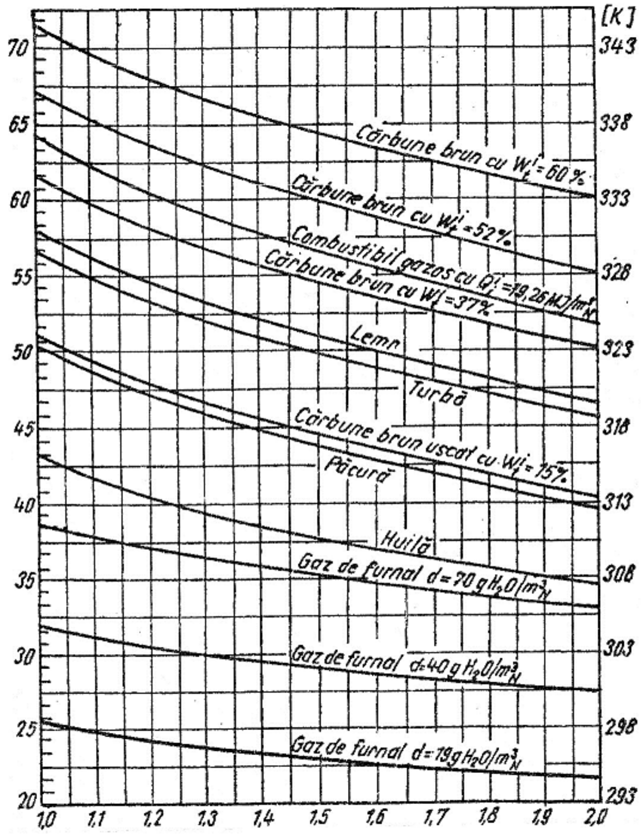

Fig1.Variation of dew point temperature depending on the type of fuel used and the coefficient λ.

To achieve complete combustion and high efficiency of 92 % is introduced considerable flow of warm air through the grate steps directly into the combustion chamber[3].Calorific value of biomass (corn cobs) was calculated and is Q^i_{ib} = 18500 KJ/kg and low calorific lignite value Q^i_{il}= 16383KJ/kg ;The amount of fuel introduced into the combustion chamber was calculated from 300kg / h to an outbreak of dimensions 3m long , 2m wide and 1.3m average height, resulting V_f = 7.8 m3.

$$q_v = \frac{B \cdot Q_i^i}{V_f} \quad \left[\frac{kW}{m^3}\right] \tag{4}$$

Heat supply volume of the combustion chamber has a high value and was calculated approximately $q_{vbiomasa}$ = 200 kW/m^3, $q_{vlignit}$ = 175 kW/m^3 and $q_{v\ co\text{-}comb}$ = 184 kW/m^3. The ash from combustion can be used in some cases as agricultural fertilizer.

4. THE STUDY FOR CO-COMBUSTION LIGNITE AND BIOMASS

Co -firing biomass with coal is an optimal technical solution to improve combustion will lead to a more complex energy recovery technology but with lower emissions. Experimental research on biomass and co -combustion of pulverized coal were instrumental demo efficient validation efficient solutions for implementing this optimal technologies. The experiments were performed using pilot plants and technic characteristics as an industrial facility originally designed to burn only pulverized coal, thermal plant with a maximum power of 2MWt. The first attempts were made in 2012 and 2013 on a high power pilot outbreak. The outbreak has all the facilities for fuel and equipment for the collection of experimental data. The installation with grill facilities in post combustion stage located at the bottom of the furnace above the funnel and allowed to co - firing biomass combustion waste grain high and very high . The experiment aimed to explore the possibility of recovery in terms of the energy for dry corn cobs after more than a year stoking, in case of co-combustion of lignite coal particle with biomass. The lignite came from Rovinari area, fuel that is mixed in a mass ratio of 30 %, 40 % corn cobs. The coal mass flow was kept constant at over 200 kg/h , and the flow of gas when used for lifting or maintaining constant temperature in furnace helped by a constant rate of 30 m^3_N/ h methan gas. The biomass was brought form Ialomita county area, and has been stored for a long time more than a year to reduce the moisture content from 40-50 % to 9-10 % . Laboratory analysis indicated the cobs stored volatile matter content of 45.9 % and a moisture content of 9-10 % , values close to those of lignite.

Experiments have revealed a biomass gasification delayed particles from those of lignite which led to ignition delay for corn cobs-lignite mixture in the furnace. There were no noted deficiencies in the process of grinding , drying and transport dust in case of the mixture .The operating characteristics were assigned to the industrial operation for such a mixture , even for thermal support given the absence of methane . Conclusion experimentation recommend the possibility of using biomass dry and stored for a significant period by direct determination in coal grinding plants before fuel preparation. The experiment included co-firing pellet from corn chips together with lignite. The burning was done on the grill that has stepped role after burning through the food counter pulverized coal flame .Small parts of corn stalks were between 9 and 15mm diameter and height of 3- 40 mm.

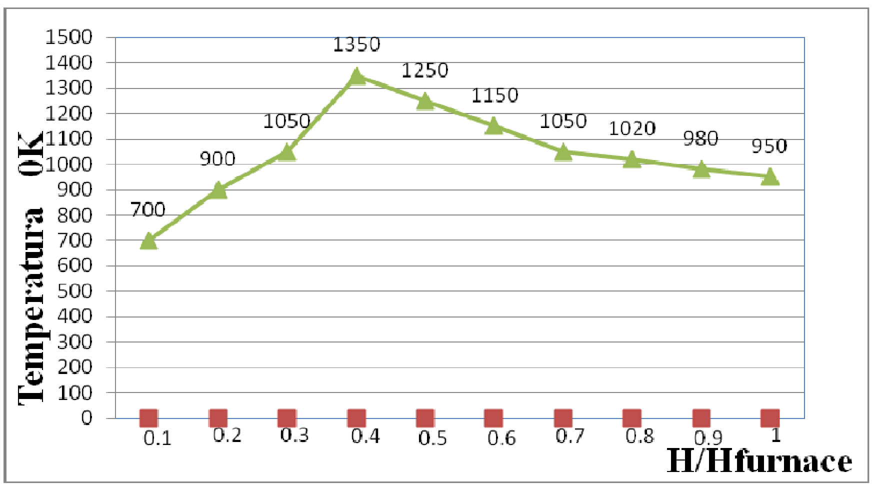

Fig.2 The height variation of temperature furnace for burning lignite with biomass degraded after 1 year which includes corn cobs of corn stalks or wood chips.

Visualization method to follow the evolution process of ignition and combustion process, determining the speed of ignition, burning rate and temperature field for all samples analyzed. Flow of coal for co-firing research focus properly 170-225kW/m3 pilot industrial burning of such inferior coal, lignite pulverzat. Excess air at the end of the outbreak was 1.4 to 1.65. Combustion efficiency varied in the 92-95% and CO emissions were 20-30 ppm NOx emission in the range 185-225 ppm.[5][6]

Table.1

Pollutant emissions when burning pulverized lignite and its co-firing 30% to40% biomass,O_2 maxim 7%.

Fuel mass flow	Pneuma -tic injection and hot air 5 bar	Renewable in fuel	Gas Temperature in Furnace	Gas sample taken from near the mouth Injector Analyzer Horiba PG250 point P9					Gas sample taken at the exit of the combustion chamber to P2 Analyzer Horiba PG250				
				SO_2	CO_2	O_2	CO	NO	SO_2	CO_2	O_2	CO	NO
Kg/h	/	[%]	[^{0}C]	ppm	[%]	[%]	ppm	ppm	ppm	[%]	[%]	ppm	ppm
300	No	40	1072	1270	14.85	3.87	14.4	217	1294	14.85	4.31	15.3	225
300	Yes	40	1080	1004	13.59	5.32	7.6	258	1005	13.59	5.78	9.8	242
285	No	30	1043	1021	14.49	4.28	12.2	178	1036	14.49	4.23	13.3	185
285	Yes	30	1056	1001	13.23	5.74	7.0	202	1009	13.23	5.69	9.0	206

Table.2

Comparative chemical analysis of ash (slag) as a percentage of the outbreak[5][6]

Fuel	Al_2O_3	CaO	MgO	Na_2O	K_2O	P_2O_5	Cr	SO_3	Cl	Zn
U.M.	[%]	[%]	[%]	[%]	[%]	[%]	[%]	[%]	[%]	[%]
Biomass 60kW pilot plant	1,8	8,5	3,9	0,30	7,7	2,28	0,41	1,72	1,4	3,0
60kW pilot plant biomass(wood pellets) and lignite	1,6	6,5	2,8	0,40	8,9	2,05	0,71	2,12	1,1	2,0
Lignite for 2MW pilot plant	2,75	9,8	3,1	0,1	3,2	2,3	1,8	0,9	0,2	5,3
Co-combustion for 2MW pilot pilot plant lignite&biomass 30%	2,29	8,47	2,75	2,31	11,3	3,52	0,97	2,84	0,89	8,97

5. CONCLUSIONS

To maximize combustion efficiency and complete as it requires a considerable amount of excess air at least 175-250 kW/m^3. The cyclone filter efficiency is 72%.
From the experimental data presented here, important information about the efficiency of the combustion and emission levels and ash. A more complete combustion of solide fuel has reduced the amount of environmental damage occurs due to burning of biomass ash in combination with lignite.
The results can be exploited in the construction and operation of woody biomass for energy recovery.
Even a small modification in design or intelligent fuel supply is a step forward for engineering technique .This can later transform in one percent in the pilot plant global thermal improvement that can be very important in terms of fuel efficiency and energy supply.

References

[1]Tudor Prisecaru,Emil Enache,Lucian Mihaescu,Ionel Pisa,Gabriel Negreanu,Malina Prisecaru, Berbece Viorel,Popa Elena - Wood biomass energy exploitation and wood processing technologies

[2] Nicolae Pãnoiu,Constantin Cazacu, Lucian Mihãescu,Cristian Totolo, Alexandru Epure - Instalații de ardere a combustibililor solizi , Editura Tehnicã, Bucundrești – 1985;

[3] Corneliu Ungureanu,Nicolae Pănoiu,Victor Zubcu,Ioana Ionel – Combustibili Instalatii de ardere cu cazane, Editura Politehnica,Timisoara 2006
[4]Emil Enache, Lucian Mihaescu, Ionel Pisa,Tudor Prisecaru,Gabriel Negreanu,Malina Prisecaru, Berbece Viorel,Pop Elena – Achievements in the construction of boilers for agricultural biomass combustion
[5]Ionel Pisa,Gheorghe Lazaroiu,Corina Radulescu,Lucian Mihaescu – Experimental studies on the corrosion occurrence during biomass combustion process,
[6] Lucian MIHĂESCU, Ion OPREA, Gabriel Paul NEGREANU, Tudor PRISECARU, Laurenţiu Popper, Ionel PIŞA, Elena POP,Gabriel POPPER,Adrian ADAM, Adelina PANAIT -Valorificarea energeticã a uleiurilor vegetale brute –, Editura PRINTECH, Bucuresti 2011;

STUDY OF THE PV MODULES INCLINATION ANGLE ON THE ENERGY PRODUCTION

Angel Terziev[1], Veselka Kamburova[2], Iliya Iliev[3], Kiril Mavrov[4], Deyan Deltchev[5]

ABSTRACT

The energy produced by the PV panels depends generally on several parameters – local weather data (solar intensity, amount of impurities in the air (Linke Turbidity Factor), temperature, wind speed and etc.), type and orientation of the PV panel.

The impact of local data and type of the PV panels on the production of electricity was discussed and presented in the previous works [1], [2].

The aim of the current study is to show the impact of the inclination angle of the PV panels on the electricity production. Generally, depending on the type of mounting, the PV systems are divided into free-standing and building integrated. Concerning the tracking options the systems are classified into: fixed, tracking in vertical and inclined axes and 2 axis tracking. Here is presented a study on the electricity production for different systems and angle orientations. Mainly focuses on the fixed systems, fixed systems with a single change of the angle during different seasons, and 2 axis tracking systems. Simplified financial analysis based on the energy generated by the PV modules, investments for the implementation of the reviewed systems in respect with the angle change is presented.

1. INTRODUCTION

The photovoltaic modules use energy from the sun to produce electricity. At present the highest possible sunlight conversion rate is about 20% [3] which is typically lower than the efficiencies of the separate cells in isolation. The optimal absorption of the solar irradiation flux is guarantee for maximal energy production and higher profit.

In current paper is discussed the impact of the inclination angle of the PV panels on the energy production. In addition it is also presented the impact on the local atmospheric data (geographical location) on the energy production. The analysis includes 6 different sites evenly distributed on the territory of Bulgaria. For a couple of the sites the PV farms are in operation for more than one year providing additional information for the analysis. The simplified financial analysis was made based on the system investment costs and revenues generated.

2. LONG-TERM DATA ANALYSIS

Site specifics and long term data interpretation

The current study is focused on the energy production of the photovoltaic modules installed at different locations on the territory of Bulgaria (Figure 1) [4]. The selected six locations are close to the following populated areas: Ihtiman, Varna, Vidin, Dobritch, Dolna

[1] Technical University, Sofia, Bulgaria, e-mail: aterziev@enconservices.com ; cell phone: +359 885955183
[2] Ruse University, Ruse, Bulgaria, e-mail: vkambourova@enconservices.com ; cell phone: +359 885955347
[3] Ruse University, Ruse, Bulgaria, e-mail: iiliev@enconservices.com ; cell phone: +359 887306898
[4] Technical University, Sofia, Bulgaria, e-mail: kmavrov@enconservices.com ; cell phone: +359 885956209
[5] Technical University Dortmund, Germany, e-mail: deyan.deltchev@gmail.com; cell phone: +359 887 918028

Lipnitza and Elhovo. Concerning the geographical location the spots are characterized with specific solar irradiation, air temperature, humidity, amount of impurities in the air (Linke turbidity factor) and etc.

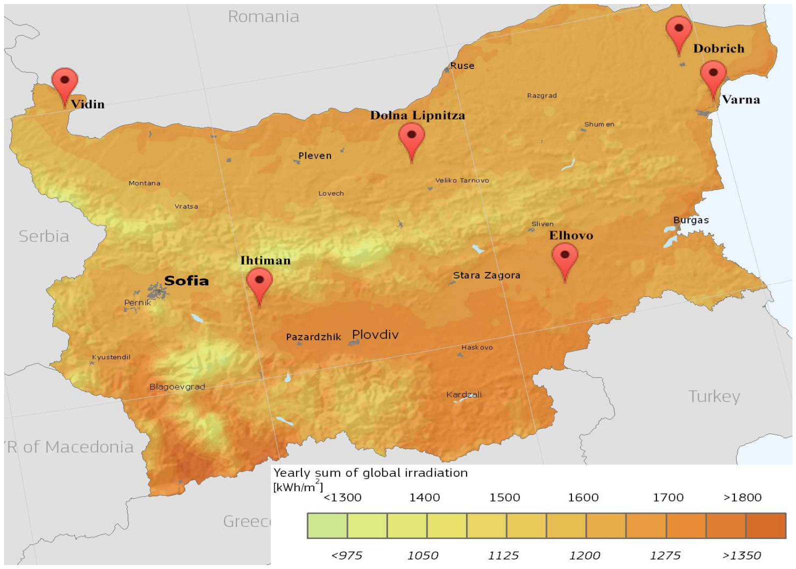

Figure 1: Location of the selected sites on the territory of Bulgaria

Figure 2 presents the yearly energy yield for the concerned six places at optimal inclination angle fixed for the entire year. The presented energy yield concerns the crystalline silicon PV panels. It is obvious that annually the specific solar energy yield varies between 60 and 145kWh/kWp. On monthly bases the highest difference in electricity production among the selected six place is observed during the winter period, and it is in the amount between 17 and 20%. During the rest of the year the discussed difference is between 6 and 8% among the places. Here it should be pointed that in about 80% of the annual energy production is between March and October. The places were selected because the PV farms are already installed. PV farm located close to the Dolna Lipnitsa village is in operation since December 2012. Hence the specific analysis made further in the paper refer to this location.

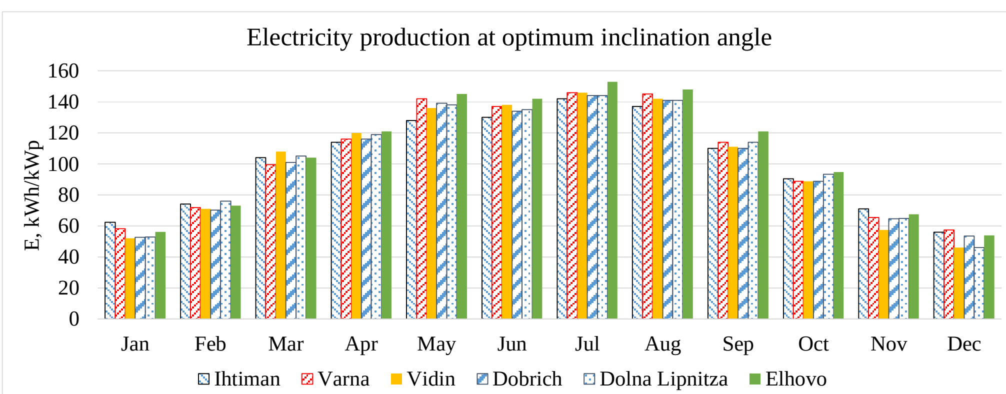

Figure 2: Specific energy yield for the selected locations

As discussed in [1] and [2] the energy yield of the specific location is mainly affected by the parameters of the atmospheric air – temperature, relative humidity and amount of impurities in the air (Linke turbidity factor). The yearly distribution of the air parameters are presented in the figures below.

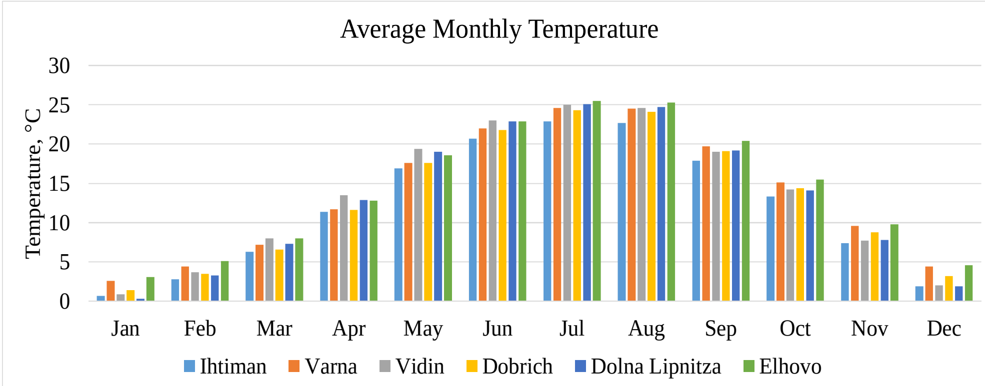

Figure 3: Annual temperature distribution for the selected locations

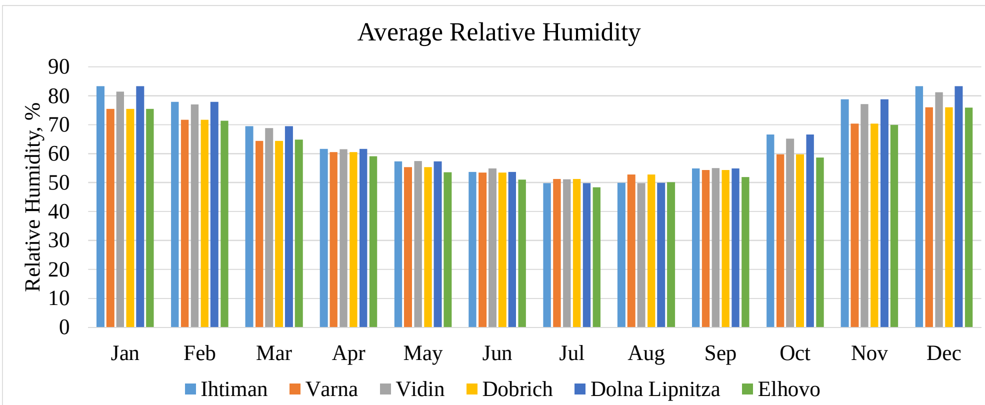

Figure 4: Annual relative distribution for the selected locations

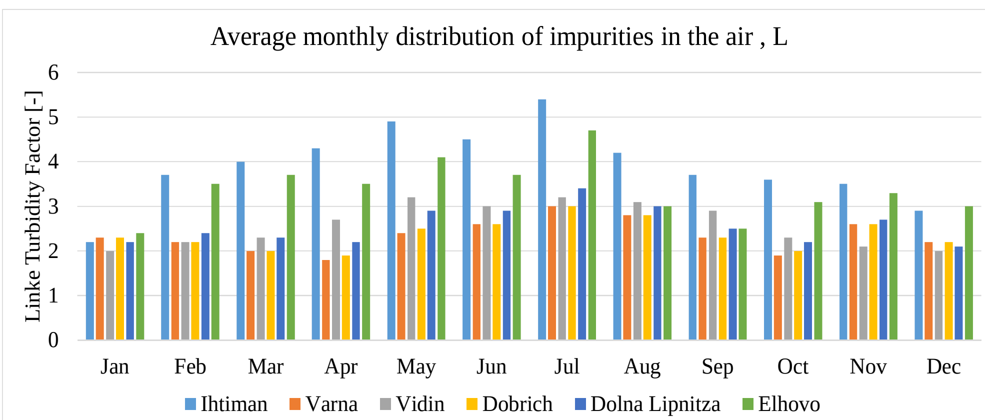

Figure 5: Annual Linke turbidity factor distribution for the selected places

As discussed in [1] and [2] the energy yield of the specific location is mainly affected by atmospheric air parameters.

Figure 3 shows that the average temperature distribution for the sites changes annually insignificantly. Greater difference in temperatures are visible during only the winter season. However, these differences are not significant and they will not have significant impact on energy production. Humidity distribution for the places is presented on figure 4. In relation with temperature the higher values of this parameter are observed during the winter period. Higher values of the relative humidity are observed for the sites close to Ihtiman, Vidin and Dolna Lipnitza.

On figure 5 is presented the degree of pollution of the air. Sites located close to Ihtiman and Elhovo are characterized with higher values of Linke turbidity factor all year long. The higher values affect the energy production from the PV panels [1], [2].

Analysis of the impact of the inclination angle on energy production

The proper selection of the panels' inclination angle is crucial for the energy production. On figure 6 is presented the specific energy production for the selected sites gained by the change of the angle of the panels.

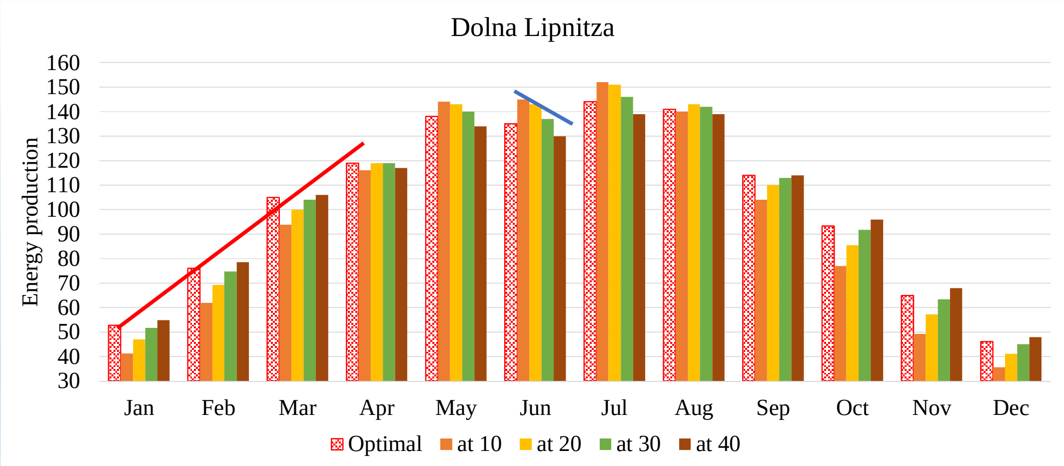

Figure 6: Average monthly energy production for the selected locations at different inclination angles

Figure 6 shows the energy output from the PV panel for a site located close to the Dolna Lipnitza village at different inclination angles. It is obvious that for the first 4 months of the year the energy output is maximum at optimal inclination angle recommended for the site. During next three months (May – July) the maximum energy output can be reached at small inclination angles (up to 20^o). For the August the output at different inclination angles remains the same. This is determined by the geographical location of the site (respectively horizon angle). For the rest of the year the maximum utilization of solar radiation can be expected at large inclination angles (optimal or larger).

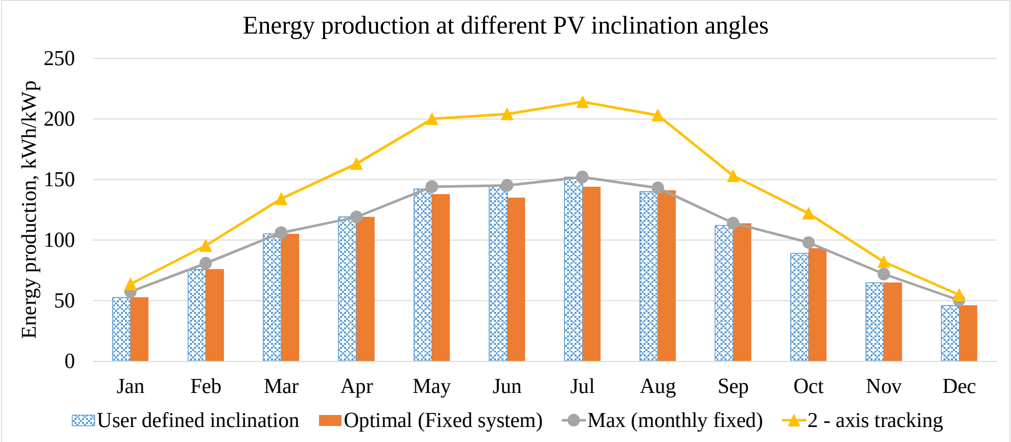

Figure 7: Estimated energy production at various systems (fixed and tracking)

Based on this on figure 7 is presented the energy yield for the location Dolna Lipnitza for different types of systems. The study shows that when a system is fixed over the year at optimal inclination angle the energy production is in the amount of 1228 kWh/kWp. Currently the inclination angle of modules of the PV farm changes four times per year (at 10, 25 and 35 degrees). The study shows that the energy production is in about 1243kWh/kWp or in about 2% higher than optimal angle. The third option is to adjust the optimal angle monthly. In this case the energy production is in the amount of 1281kWh/kWp (or 4.3% higher than the yearly fixed optimal inclination angle). When the system is equipped with 2 axis tracking system then the energy production is estimated to 1689kWh/kWp (or 37.5% higher than the fixed system at optimal inclination).

Regression analysis

The data for the selected sites were analyzed and the regression statistic were presented. The initial parameters for the regression model are the impurities in the surrounding air (Linke turbidity factor, X_1), air temperature (X_2), relative humidity of the air (X_3) and inclination angle (X_4). The resulting function Y is energy production presenting in accordance with the site specifics. Through the non-linear regression the following expression was obtained:

$$Y = a.X_1 + b.X_2 + c.X_3 + d.X_4, \quad (1)$$

where a, b, c and d are regression results (relevant for 99% Confidence interval) presented in the table below.

Table 1: Components of the generated biogas

Variable	Value	99% (+/-)	Lower Limit	Upper Limit
a	17.36393298	33.70409126	-16.34015827	51.06802424
b	-3.10877712	4.842039289	-7.950816409	1.733262169
c	-4.414273335	2.993990372	-7.408263707	-1.420282963
d	11.76658603	7.025533324	4.741052704	18.79211935

The regression shows maximum Error (%) in the amount of -10% for the data related with highest air relative humidity. The proportion of variance explained is 95.85%. The adjusted coefficient of multiple determination (Ra^2) is 0.945.

3. FINANCIAL ANALYSIS

Here is presented a simplified financial analysis for the abovementioned systems as a function of inclination angle. To assess the economic impact of different types of systems it is necessary to estimate the amount of the increased electricity production as a function of the increased investment and operational costs. The selected photovoltaic system in Dolna Lipnitza is with installed capacity of 1,184.4 kW and total investment costs of EUR 2,467,872. Annually the PV inclination angle of the system changes 4 times per year resulting in annual energy production in the amount of 1,457,252 kWh/per year. Accepting the current fixed purchase price of the electricity of 0.24828 EUR/kWh [5] and annual O&M costs of EUR 36,425 the resulting yearly income is about 325,386 EUR/yr. Taking into account that change of the inclination angle for the presented PV system is manually accomplished the investment and operational costs for the fixed systems and with manual inclination angle selection can be considered to be the same.

The two-axis tracking system requires significantly higher investment, as well as operational costs. Concerning [6] the average investment costs for the implementation of a two-axis tracking system is 40.54% more expensive than the fixed one. Also the operational costs are 41.09% higher. In table 2 is given summary of the economic indexes of the different types of systems, considering the different investments and operational costs.

Table 2: Financial analysis for different type of inclination angle management

	Fixed system at optimal inclination	User defined inclines	Maximal inclination	Two-axis tracking
Energy yield, kWh	1,441,306	1,457,253	1,502,044	1,980,330
Investment	2,467,872	2,467,872	2,467,872	3,468,236
Yearly incomes	357,852	361,812	372,933	491,683
O&M costs	36,425	36,425	36,425	51,391
Net yearly income	321,427	325,387	336,508	440,292
Simple payback	7.68	7.58	7.33	7.88
NPV (in 20 years)	€2,121,829	€2,178,364	€2,337,163	€2,818,747

After 20 years of operation under specific local conditions, despite of the higher initial investment and the highest simple payback period, a system with two-axis tracking has the higher NPV factor (at discount rate 3.45%), thus the two-axis tracking system is the most economically viable.

4. CONCLUSIONS

An analysis about the energy production of different types of PV systems (fixed and with changed of PV modules inclination angle) here is presented. For this purpose six different locations on the territory of Bulgaria were selected and analyzed. In order to be assessed the impact of the inclination angle the site specifics were carefully analyzed and considered in the regression model. Relation between inclination angle, site specifics and energy production were presented. Simplified financial analysis was provided about the profitability of the introduced PV systems.

References

[1] Terziev A., I. Iliev, V. Kamburova, D. Deltchev, Analysis of the degradation factor of photovoltaic modules operating under field conditions, 2nd International Conference of Thermal Equipment, Renewable Energy and Rural development, TE-RE-RD 2013y., Baile Olanesti (Valcea County), Romania, ISSN 1843-3359

[2] Iliev I., V. Kamburova, A. Terziev, P. Gramatikov, Comparable analysis of estimated and real energy production from photovoltaic system “Paunovo”, Scientific conference 2010 of Ruse University “Angel Kantchev”, Proceedings of Ruse University “Angel Kantchev”, 29-30.10.2010y Ruse, vol. 49, series 1.2, p.p. 8-13

[3] http://www.solarplaza.com/top10-monocrystalline-cell-efficiency/

[4] http://re.jrc.ec.europa.eu/pvgis/cmaps/eu_cmsaf_opt/G_opt_BG.png

[5] http://www.dker.bg/files/DOWNLOAD/res-preftseni-20-06-2011.pdf

[6] http://eujournal.org/index.php/esj/article/download/994/1024

DEVELOPMENT AND TESTING OF A SOLUTION FOR NOx EMISSION REDUCTION BASED ON THE SNCR PROCESS FOR HIGH CAPACITY STEAM GENERATORS

Zoltan Teuber, ERC GmbH, Buchholz, Germany[1], Ion Bolma, ECOTECH Proiect srl, Bucharest, Romania[2], Ion Pisc, Complexul Energetic Oltenia, Sucursala Electrocentrale Rovinari[3]

The SNCR process is not new. It has been applied since many years for boilers of low and medium capacity. The application of this process to the high-capacity steam generators involves a number of features for both the plant itself and the process parameters.

A test application of the SNCR process in a steam generator of 1035 t/h concretely revealed that this method is viable even in the high capacity level and can be, along with a process of limiting NOx formation (primary measure), a solution to solve the legal requirements concerning the NOx emission.

1. FACTORS INFLUENCING THE NOx REDUCTION PROCESS

The selective non-catalytic NOx reduction is based on the reaction of nitrogen oxides (NO and NO_2) by some compounds such as urea ($(NH_2)_2CO$) or ammonia (NH_3) according to the following overall reaction:

$$2\,(NH_2)_2CO + 4\,NO + O_2 \Rightarrow 4\,N_2 + 2\,CO_2 + 4\,H_2O, \quad 4\,(NH_2)_2CO + 2\,NO_2 + 4\,O_2 \Rightarrow 5\,N_2 + 4\,CO_2 + 8\,H_2O$$

or

$$4\,NH_3 + 4\,NO + O_2 \Rightarrow 4\,N_2 + 6\,H_2O, \quad 8\,NH_3 + 6\,NO_2 \Rightarrow 7\,N_2 + 12\,H_2O.$$

These reactions are strongly influenced by various factors present in the processes of steam generators. The ways how the most important of these factors are involved in the reduction of nitrogen oxides are briefly explained below.

The efficiency of this overall reaction and the extent of side reactions is strongly dependant on the reaction temperature. The temperature controls the duration of the reduction reaction. The highest efficiency is achieved at temperatures between 880°C and 1080°C.

Flue gas composition influences the optimal reaction temperature. Thus the higher the oxygen concentration, the lower the optimal temperature range. Carbon monoxide as well as hydrogen and vaporous water influence the NOx decomposition in a similar way.

Flue gas velocity determines the residence time in the injection area of the reduction agent. Thus the lower the flue gas velocity, the longer the residence time of the flue gas in the reaction area. This way lower temperature can be accepted.

Non reacted ammonia in the flue gas causes some side reactions. Various products are formed which may have an impact on the environment or which may damage the boiler. The most frequently resulting compounds of the side reactions are ammonium sulphate,

[1] Contact: ERC Technik GmbH, Bäckerstrasse 13 D-21244 Buchholz i.d.N., Germany,
e-mail: zteuber@ erc-technik.com, tel:+49 4181 216 115
[2] Contact: ECOTECH PROIECT SRL, Bl.Camil Ressu nr.38, Bucureşti, Romania,
e-mail:ion.bolma@ecotech-proiect.ro, tel:+40 31 40 70 390
[3] Contact: Complexul Energetic Oltenia S.A., Electrocentrale Rovinari, str Energeticeanului nr 25, Rovinari,
- e mail: ionpisc@gmail.com, tel: +40 253 371580

$(NH_4)_2SO_4$, ammonium bisulphate, NH_4HSO_4, ammonium chloride, NH_4Cl and nitrous oxide, N_2O.

2. SNCR SOLUTION DESIGNED TO BE APPLIED FOR HIGH CAPACITY STEAM GENERATORS

In high capacity steam generators, due to their large geometric dimensions, flow processes, combustion and heat exchange induce major unevenness regarding temperature, flow velocity, concentrations of CO, which are precisely the factors that influence most the non catalytic reduction process. Disregarding these non-uniformities in obtaining the desired denitrification yield would result in high reagent consumption and at the same time in high even unacceptable ammonia in the flue gas and in the fly ash. Furthermore, it is even possible to not achieve the target NOx concentration in the flue gas.

In order to obtain information about the temperature distribution in the furnace cross section, to the SNCR process itself a temperature measurement system based on modern techniques was assigned.

The use of urea instead of ammonia in steam generators of large dimensions is essential. Research has shown that the successive vaporization of water followed by thermal decomposition of urea gradually generates amine radicals (NH_2). Thus, these radicals can penetrate into the core of the flue gas stream where the NOx concentration is the highest.

In high capacity steam generators it is imperative to use several injection levels (at least two), in order to enable, depending on the load at which the steam generator is operating and on the evolution of the flue gas temperature in the furnace, for the reagent the injection into the level where the reaction temperature is optimal.

3. TESTING THE SNCR SOLUTION FOR A BOILER OF 1035 T/H IN THE POWER STATION ROVINARI

Between 9 and 19 March 2013 tests were carried out with the SNCR solution adopted for high capacity steam generators at a boiler of 1035 t/h in the Power Station Rovinari. An aqueous urea solution of 40 % enriched by additives was used as reduction agent.

The main goal of the test was to achieve a NOx emission reduction from 350 mg/Nm³ to 200 mg/Nm³ by applying the SNCR process. Furthermore possibilities of optimizing the reagent injection were analyzed in order to reduce reagent consumption without affecting the yield of reduction.

3.1 SNCR Process Testing Plant

The testing plant according to the SNCR process comprised:

- the NOx reduction agent storage
- the mixing and dosing module
- the distributors and the injection system.

The storage vessel for the reduction agent was the tank truck itself. It was placed on ground level. For this test a total quantity of 3 tank trucks having a volume of 20 m^3 was used.

The structure of the mixing and dosing module was designed and adapted to the requirements of the test. It assured the metering and dosing of the amounts of reduction agent and dilution water according to the requirements, see Figure 1, left. During the test this module was placed on level 45.00 m. The atomization air for the distribution of the NOx reduction agent in the furnace was adjusted in a separate facility by means of a pressure control valve (Figure 1 right).

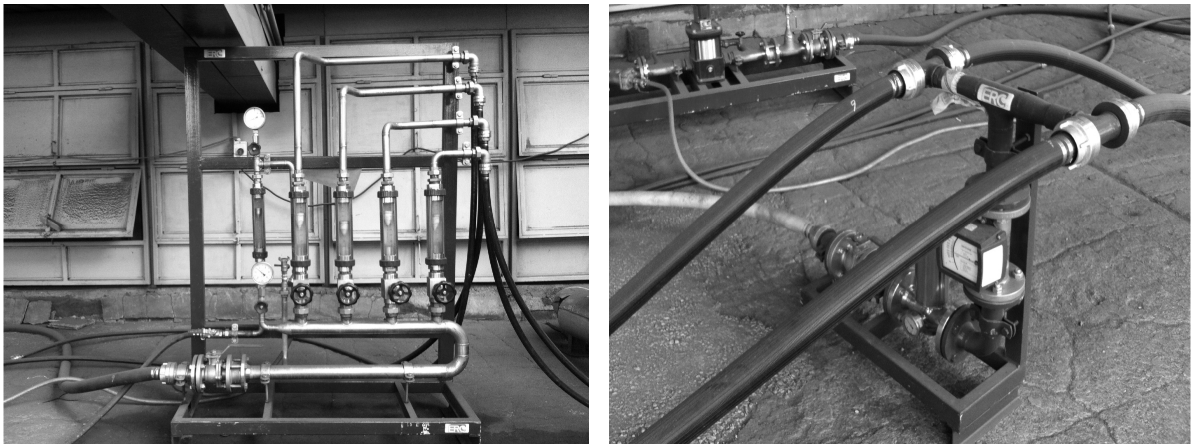

Figure 1: Mixing and dosing module for reduction agent and dilution water (left) and Control module for atomization air (right)

The diluted reduction agent was driven to 4 distributors, each feeding a part of the injection lances. Atomization air was distributed separately but in a similar way in 4 distributors located on the front and the rear and on the right and left side of the furnace. The injection system for the test was composed of 22 injection lances installed on the 4 walls of the furnace on level 45.00 m. The locations of the injection lances and their relative positions versus the furnace walls were determined by the real situation on site in accordance with the goal to cover with the injection jets as much as possible of the flue gas stream.

The NOx emissions were measured by the customer's analysers which were already installed in the flue gas duct downstream the electrostatic precipitator. The flows of reduction agent, dilution water and atomization air were adjusted manually.

The operation parameters of the steam generator were followed in the control room of the power station and the processing information were extracted from the records of the DCS.

3.2 Performed Tests and Analysis of Results

Test no.1 was performed on 14.03.2013, at high boiler load, about 300 MWel, in frequency – power operation mode, with load variations of ± 15 MWel around the setpoint.

The test itself started at 11:00 and took 6.5 hours. The baseline NOx emission at the beginning of the test was about 350 mg/Nm³, see the diagrams in Figure 2. As displayed in the graphic the NOx level dropped sharply to 200 mg/Nm³ (at 6 % of vol. O_2 in the dry flue gas) immediately after starting the injection of the reduction agent into the furnace and was maintained at this level during the whole duration of the test, with slight fluctuations of approximately 25 mg/Nm³. During the test the injection had to be interrupted for about 25 minutes in order to change the reduction agent tank truck.

NOx concentration decrease was due solely to the NOx reduction process initiated by injecting the diluted reduction agent. It can be seen that the oxygen concentration throughout the test, both on the left and the right side, has not changed, except small fluctuations of about 0.5 % around the average value, indicating that there was no change in the combustion process which could result in changes in NOx formation.

The fact that the oxygen concentration did not change reveals another aspect: the operation regime of the coal mills remained relatively optimal, even with load fluctuations dictated by the operating conditions of the boiler, i.e. there was no need to introduce

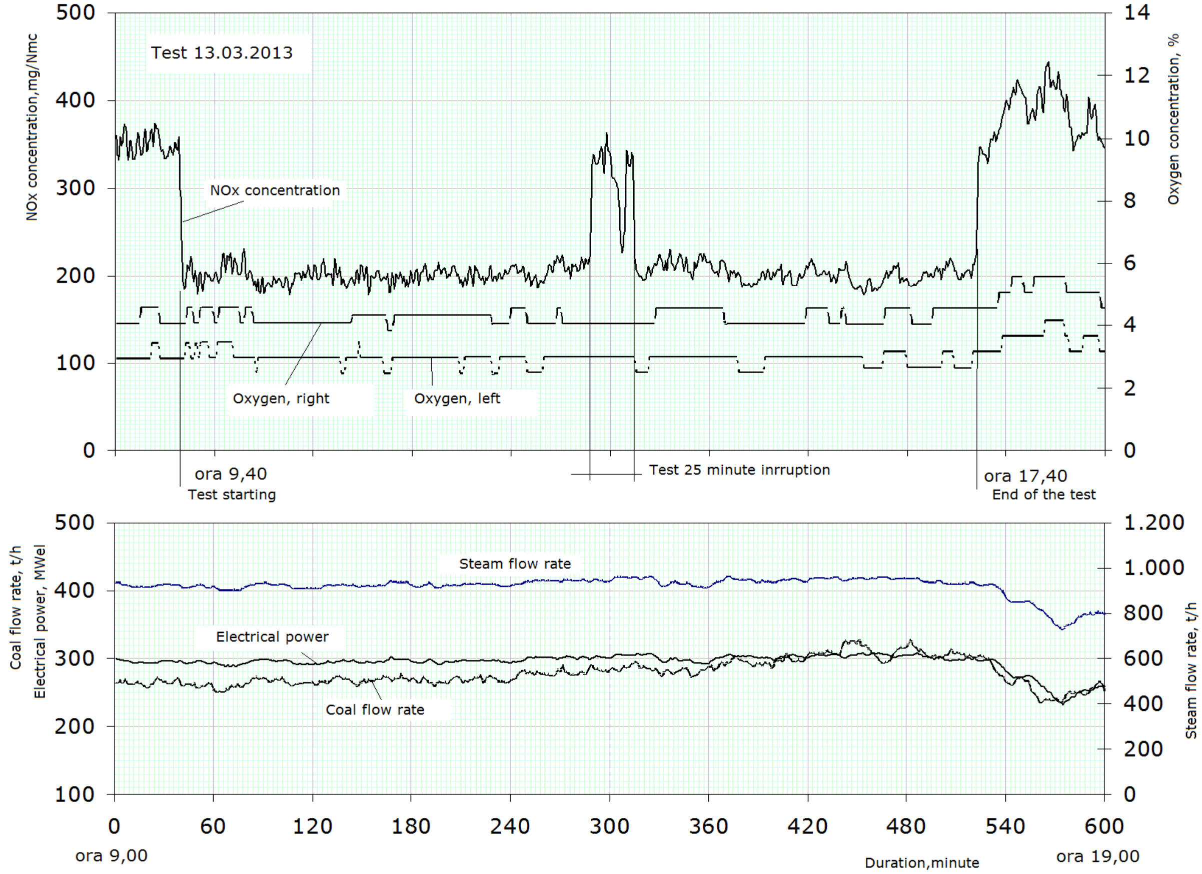

Figure 2: Test results at high boiler load

additional air for temperature regulation at the separators (proven by the almost constant oxygen concentration). Thus the reducing atmosphere was maintained and consequently the NOx formation remained relatively constant, about 350 mg/Nm³.

The flue gas temperatures, measured in the vicinity of the furnace walls with the installed equipment of the boiler (the flue gas stream temperature in the core was about 100 K higher), were around 825 – 855 °C on the left side and 750 – 790 °C on the right side, thus providing an acceptable thermal level for the purposes of the NOx reduction reaction.

Test no. 2 was on 18.03.2013, between 11:00 and 16:00. The boiler load was 260 – 280 MWel, in frequency – power operation mode.

The baseline NOx level at the beginning of the test was 340 – 360 mg/Nm³. Shortly after starting the injection of the reduction agent the NOx level sharply dropped to an average level of 190 mg/Nm³. Although the goal to reduce NOx to a level of 200 mg/Nm³ was achieved, similar to test no.1, differences can be observed in the evolution of the parameters between the two regimes.

The NOx concentration during Test no. 2 fluctuated with significantly higher amplitude than in Test no. 1 (Figure 3). By analysing the operation regime during the test it is obvious that these strong fluctuations are not caused by the way of reagent injection but by the way how NOx formation evolved during combustion process. This can be seen first of all by

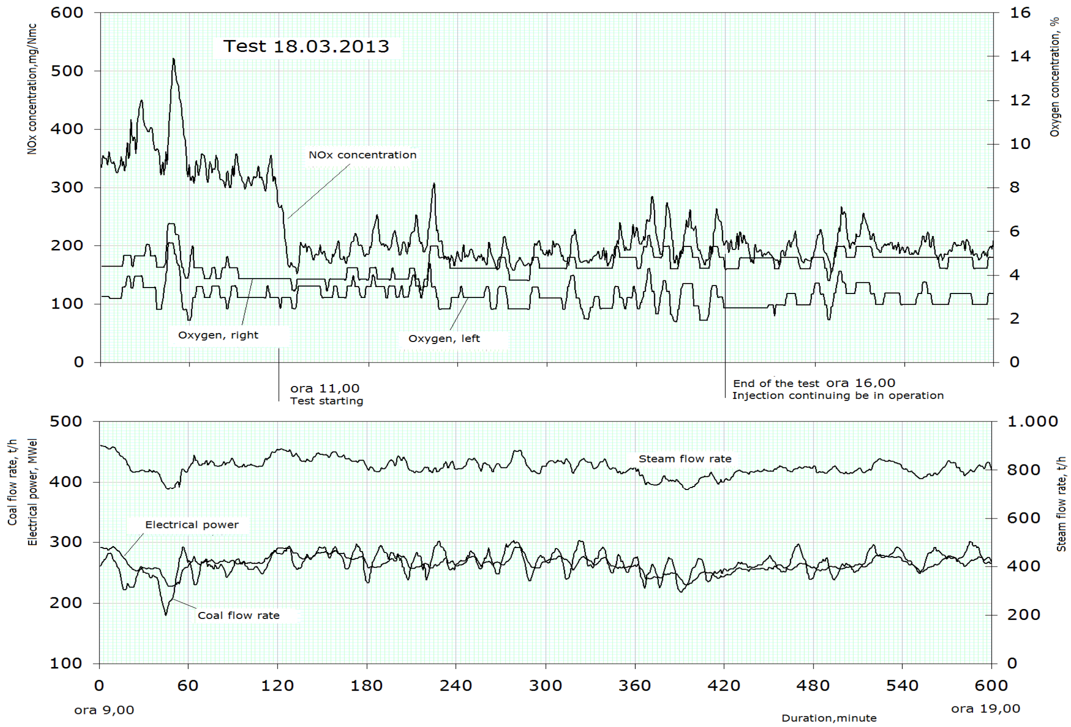

Figure 3: Test results at medium boiler load

comparing the evolution of the NOx concentrations before starting the tests: it has much larger fluctuations before Test no. 2 which is due to higher amplitudes in the oxygen concentration. On its turn, the level of oxygen concentration is a consequence of the stability of the combustion process indicated by modifications of the flue gas temperature and of the opening degree of the directing flaps of the air fans, etc.

Test no.3 was in the night from 18. to 19.03.2013, between 0:00 and 5:30. The boiler load was 160 – 175 MWel, in frequency – power operation mode. The evolution of the NOx concentration before and during the test is displayed in Figure 4, along with the evolution of other parameters, presented for the purpose of comparative analysis together with the previous two tests.

The main remark is the fact that at the beginning of the reagent injection the reduction was significantly lower than during the previous two tests. The factors leading to this result are the way of preparation and combustion of pulverized coal. Both the coal flow rate and the load of the boiler had huge fluctuations (variations in the flow rate of the coal were about 40 % around the average value), denoting a high instability of the combustion process. Only three coal mills were in operation, all on quite low capacity, requiring injection of primary air to control the temperature at the separators. Due to fluctuations of the opening degrees of these flaps, driven by the regulators of the control loops, the amount of combustion air couldn't be adequately controlled in relation to the incoming fuel flow. The consequences of this can be seen in the evolution of the oxygen concentration.

On the right side the average oxygen concentration was of 6.4 % having a pronounced oscillation with amplitude of maximum 2.5 %. On the left side the average oxygen concentration was 5.7 % still evolving pronounced oscillatory with amplitude of 4.1 %. The effect on the NOx formation is not only the high level but also the highly oscillating appearance before start of the test, as displayed in Figure 6.

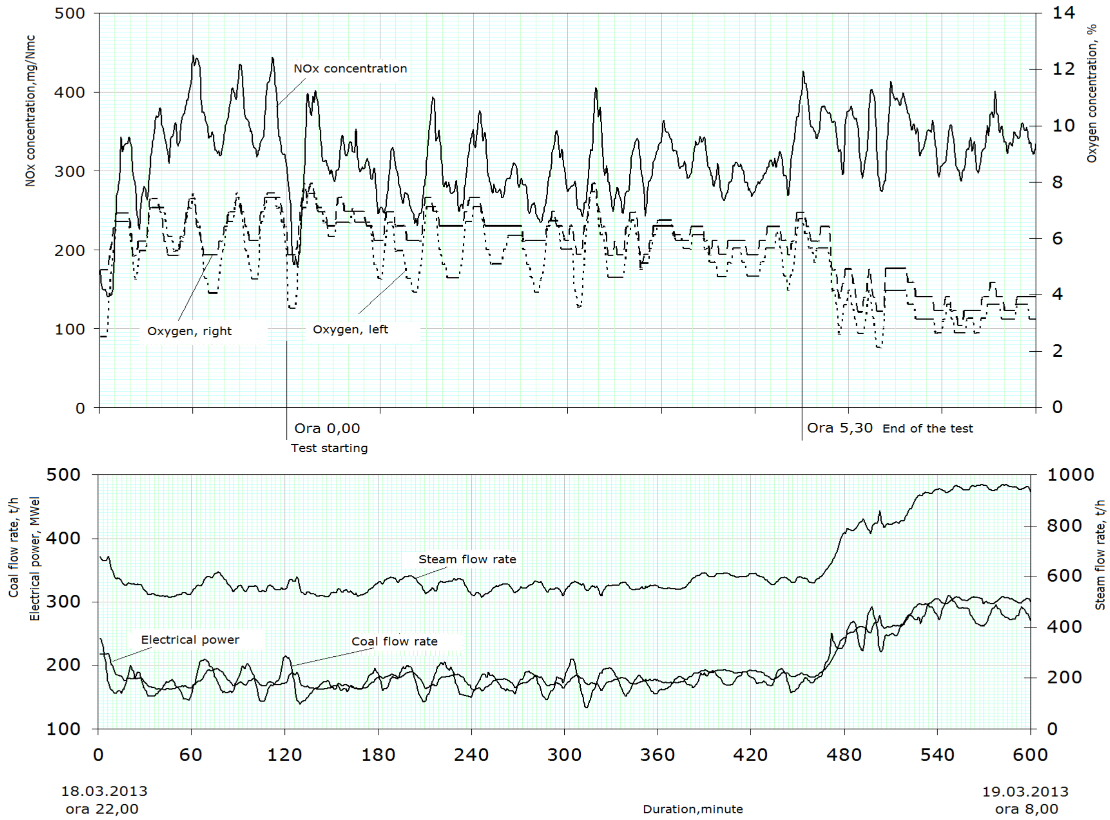

Figure 4: Test results at low boiler load

The flue gas temperature level and evolution in the injection zone contributed substantially in the NOx reduction efficiency. At this low boiler load the temperature at the end of the furnace dropped below 800 °C, which is insufficient for the NOx reduction reaction. The test revealed the imperative need to use several injection levels for high capacity steam generators. The activation of the required level is dictated by the temperature in the furnace, which on its turn is depending on the steam generator load.

4. CONCLUSIONS

The NOx emission reduction tests by applying the SNCR process showed that it can be successfully applied to large capacity steam generators operating on lignite. It is possible to achieve NOx values below 200 mg/Nm³ and reduction rates of more than 40 %.

In order to control the reduction process along the entire operating range of the steam generator and to run with low consumption of reduction agent it is necessary to know the thermal regime in the injection area. Therefore an advanced and fast temperature measuring system is required.

Taking into account the strong variation of the flue gas temperature in flow direction according to the boiler load it is imperative to install at least two levels of injection.

The tests have revealed the essential role of the combustion process in the NOx formation and, consequently, in the reduction based on the SNCR process. For this reason, the successful implementation of the SNCR process is influenced by the primary measures for limiting the NOx formation.

ANALYSIS ON THE COMBUSTION DINAMICS OF THE STRAW BRIQUETTES FOR BOILERS WITH MOBILE GRATE

Ph. D student. Eng . Mihai Toader

ABSTRACT

Achievements in straw energy recovery. According to the economic analysis in agriculture, Romania has an energetic potential for cereals straw estimated to 6 - 7 million tonnes annually. These achievements are still incipient, with indubitable success for the combustion in the form of pellets.

1. INTRODUCTION

Mathematical analysis on the fixed bed pellets combustion dynamics resulted as a consequence of the achievements of a new boiler - designed by BPU - CCT and machined by the E Milling Company having a heat output of 150 KW .
The boiler was built in a version that included a fireplace with a flame tube in order to significantly reduce the gas temperature to avoid the ash fusibility. Such a temperature was acquired at the combustion gases discharge from the flame tube 650 - 850C .
Figure 1 shows the construction of the boiler.

Figure 1 . 150 kW boiler

The combustion installation comprises a mobile grate and a post grate fuel pusher to realize a controlled and efficient combustion. Figure 2 shows the geometry of the lighters. In terms of burning and manufacturing technology, lighters with an empty backbone are preferred.

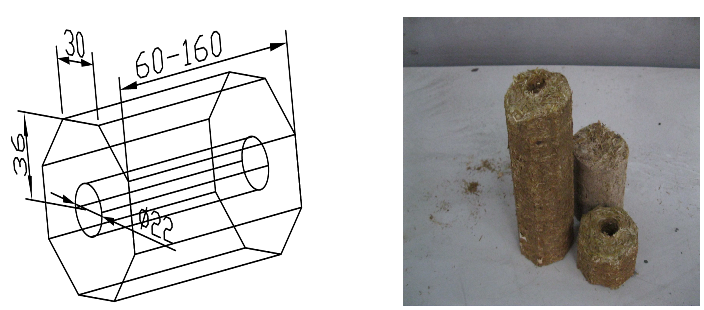

Figure 2 Briquette geometry

2. THE BURNING RATE OF THE BRIQUETTES LAYER

Due to the relatively high fuel layer, the burning phenomenon primarily involves the dependency of the burning velocity on the air admission. The oxygen consumption rate finally controls the carbon dioxide formation. An incomplete combustion results in the emission of carbon monoxide.

The model on the combustion rate has been developed according to the theory of air filtration through layer, combined with the kinetics of the carbon combustion [1] [2].

If σ denotes the fuel cylinders' section (briquettes) and N is their number, for a baseline height of the layer, its porosity can be defined by the relation:

$$m = \frac{S - N\tau}{S} \tag{1}$$

where S is the layer surface.

The section of the air passing through N_1 - number of cylinders with hollow section, σ_1, is determined by the relationship:

$$\omega = \frac{N_1 \sigma_1}{S} \tag{2}$$

For an air flow rate through the hollow cylinders denoted by u and through the cylinders porous mass denoted by *v*, the quantity of air that passes through the fuel layer is dependent on the m and ω coefficients. If the equivalent radius of the lighters of r size is denoted,

$$R = r\frac{\omega}{3}\sqrt{\frac{2}{1-m}} \quad [m] \tag{3}$$

The combustion equation will be:

$$\frac{dC}{dz} = -\alpha C, \tag{4}$$

With
$$\alpha = \frac{\alpha m + \frac{\omega}{1-m}\frac{2}{R}\alpha_k}{v + \frac{\omega}{1-m}u} \tag{5}$$

The carbon oxidation reactions have been taken into account:
$$C + O_2 = CO_2$$
$$2C + O_2 = 2CO$$
$$CO + 0{,}5O_2 = CO_2$$

As the reduction of the carbon reaction, C + CO^2 = 2CO, is not significant for combustion at low temperature, the combustion equation becomes:

$$\frac{dCO_2}{C_{O_2}} = -(\alpha + \alpha_2)z \tag{6}$$

where $C^0_{O_2}$ and C_{O_2} is the initial and current oxygen concentration , and α_1 , α_2 , and α_3 are the constants of the three combustion reactions, in the order of the presentation . As $\alpha_1 + \alpha_2 >> \alpha_3$, the calculation relationship simplifies to the form:

$$\alpha_1 + \alpha_2 = \frac{15}{ru}\left(10{,}8 \cdot e^{-\frac{41000}{RT}} + 0{,}6^{-\frac{29000}{RT}}\right) \tag{7}$$

where T is the combustion average temperature, in K.

Integrating it resulted :

$$C_{O_2} = C^0_{O_2}\, e^{-(\alpha_1+\alpha_2)z} , \tag{8}$$

where z is the height of the layer.

For combustion at 1100K, lighters of radius r = 0.05 m and air velocity u = 2 m / s, it results $\alpha_1 + \alpha_2 = 22.22$ m / s. Reducing the diameter of the lighters at 0.03 m, resulted in the increasing of the burning rate at the value $\alpha_1 + \alpha_2$ value = 37.05 m / s.

The rate of carbon dioxide formation is characterized by the following equation :

$$C_{CO_2} = C_{O_2}^{O} e^{-\alpha_4 z} \qquad (9)$$

With $\alpha_4 = \frac{15}{ru}\left(3{,}9e^{-\frac{40000}{RT}}\right)$

According to the elemental analysis of the fuel, the energetic characteristic β can be calculated by using the following relationship :

$$\beta = 2{,}37\left(H^i - 0{,}125O^i + 0{,}038N^i\right)/C^i \qquad (10)$$

The carbon monoxide formation results from the relationship of the mass balance of the oxygen consumption:

$$C_{CO} = \frac{C_{O_2}^0 - C_{O_2} - (1+\beta)C_{CO_2}}{0{,}605+\beta} \qquad (11)$$

3. EXPERIMENTAL RESULTS

The calculation for the combustion of fuel layer is based on the results of the oxygen consumption for the 150 KW boiler, results that are presented in [2] .

The analysis of the results on the oxygen consumption of fuel layer – which are presented in [2] – indicates the efficiency of using speeds below 2 m/s for the air crossing the layer. Therefore, for the air speed of 2 m/s, the height of the layer is recommended to be up to 200 mm and for the air speed of 1 m/s, 100 mm.

The optimum height of fuel layer resulting from the combustion dynamics must be correlated with the height of the grate and with its thermal loading. Therefore, the 150 KW boiler has an active volume of combustion consisting of:

- Mobile and fixed grate;
- Space of post grate combustion.

The grate has 3 rows of bars, two mobile and one fixed (the total combustion volume in the grate area is 0,009 m3). The total volume for the combustion space is 0,256 m3.

The mass loading of the fuel layer q_m is of maximum 400 kg/(m^2/h). For a density of 900 kg/m_3 and a porosity $\varepsilon = 0{,}5$, there results the height of the combustible h, based on the relation:

$$h = \varepsilon \frac{q_m}{\rho_c}\left[\frac{m}{h}\right] \qquad (12)$$

Figures 3 and 4 show the variation in the CO2 concentration based on the oxygen consumption inverse proportionality.

In order to pass to volume units, the result was reported to the maximum concentration of carbon dioxide (CO_2^{max}).

The maximum percentage of CO2 is determined by the relation $CO_2^{\max} = 21/(1+\beta)$, and the maximum CO emission with the relation $CO^{\max} = 21/(0.605+\beta)$.

For straw briquettes with elemental analysis:

$C^i = 42\%$, $H^i = 6{,}4\%$, $N^i = 0{,}64$, $O^i = 34\%$, $W^i_t = 11{,}99\%$, $A^i = 4{,}97\%$, it results:

$\beta = 0.12, CO_2^{\max} = 18.75$ and $CO^{\max} = 28.9\%$

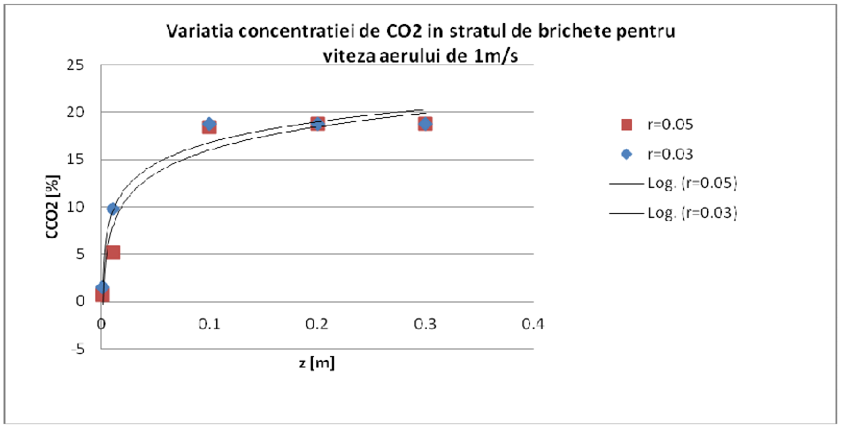

Figure 3. The variation in the CO_2 concentration in the briquettes layer for the air velocity u = 1 m/s

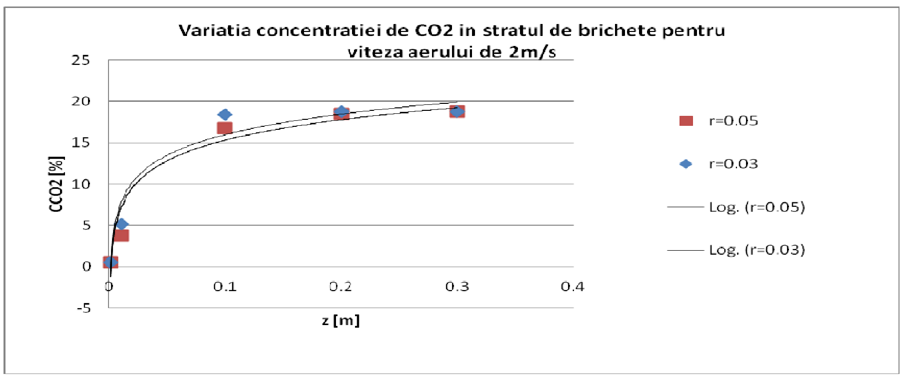

Figure 4. The variation in the CO_2 concentration in the briquettes layer for the air velocity u = 2 m/s

4. CONCLUSIONS

Inquiries complete the data on the dynamics of combustion within a layer of straw briquettes starting from the evolution of the oxygen concentration. There is an intensive burn to a height of 0.1 m and a completion of combustion above this value, regardless of the briquettes size and of the air blowing speed.

It follows a possible charge of the fuel layer above the height of 0.1 m to the height resulted from the achieving of the grate thermal burden.

Bibliography

1. Mihăescu, L., Domokos, A., Pîşă, I., Oprea, Bartha, S., “Results of the First Energetic Willow Crop in România”, Lozenec, 12 – 13 june, 2013 - Bulgaria.
2. Mihăescu, L. ş.a. “Straw in boiler manufactured in România, Chech University of Live Schience” Prague 3 – 5 september, 2013, Czech Republic.
3. Mihăescu, L., Lăzăroiu, Gh., Prisecaru, T., Pîşă, I., Pop, E., Berbece, V., Negreanu, G.” Problems Regarding the Endurance of Boilers when using straw from N – E Region of Romania”, Saint Maloo, 2nd – 4th of April, 2013, France.
4. Panoiu , N., Mihăescu , L. "Modernisation of industrial boilers combustion instalation", Technical Publishing, Bucharest, 1993 , ISBN 973 - 31-0261 -x .

COMFORT IN PASSIVE HOUSE – AN ADAPTIVE APPROACH

Ioana Udrea*[1], Ilinca Nastase[2], Ruxandra Crutescu[3], Cristiana Croitoru[2], Viorel Badescu[1]

[1]Polytechnic University of Bucharest, Faculty of Mechanical Engineering and Mechatronics, Thermodynamics Department, Spl. Independentei 313, 060042, Bucharest, Romania
[2] Technical University of Civil Engineering in Bucharest, Building Services Department, 66 Avenue Pache Protopopescu, 020396, Bucharest, Romania
[3]Spiru Haret University, Faculty of Architecture, Bucharest, Romania

Abstract

Global current requirement is to reduce energy consumption which results in a reorientation in terms of energy saving. The question is to construct and operate buildings with low energy consumption as passive buildings. It happens sometimes that these measures of energy savings lead to a reduction of a comfort reduction. A field survey was therefore carried out in summer, in a passive house office building. A campaign of measurements to determine the comfort on building has been performed in summer. A questionnaire has been filled on by a group of subjects working in the building.

This paper investigates the subject's thermal sensation trend, their thermal acceptance and their perception of overall comfort.

1. INTRODUCTION

As it's an undisputable fact that modern man spends much more time indoors than outdoors, human thermal comfort ("the state of mind which expresses satisfaction with the thermal environment") is a very important aspect of building design. However, defining it in a mathematical-physical way appears to not be an easy and already achieved goal. Understanding and modeling human thermal comfort is a field of study whose interdisciplinary character is extremely pronounced. Although some research studies have gone well beyond the Fanger (Fanger 1970) and adaptive human thermal comfort models (de Dear 1997), the two are still the only mentioned in widely used thermal comfort standards related to buildings.

There is no assurance that comfort studies results performed in climate-control chambers, offices or university classrooms reflect the thermal sensation and preference of the people working in a passive office building like surveyed building. Furthermore, the everyday environment of building with special characteristics such as, offices, hospitals, universities and school classrooms are different to an extent, which suggests that occupants probably adapt to different thermal conditions.

In the studies about hospitals (Khodakarami and Nasrollahi 2012), (Meldaho et al. 2005), (Skoog et al. 2005), (Croitoru et. al 2013) it is showed that the thermal preference of medical stuff differ from patients preferences and that the actual comfort standards are not adapted to this. In (Teli et al. 2012) are described the atypical thermal response of schools pupil. From adaptive studies in universities we mention (Buratti and Ricciardi 2008). The main conclusion in all this cases of buildings is that each of them have specific traits and that standards must to be changed in order to be suitable for each. Passive building is a special category, low energy consumption building that fulfil special requirements according to Passivhaus Institute (PHI 2014). The aim of this paper is to analyze thermal comfort in a passive building according to questionnaire surveys.

* Corresponding author: Ph.D. Student Ioana Udrea Tel.: +040 744 661303
E-mail address: udreaioana@yahoo.com

2. METHOD

2.1. AMVIC DESCRIPTION

Amvic (figure 1) is a passive office-building, located in Bragadiru (latitude 44.4°N), a small town 10 km south of Bucharest, Romania. It is a ground floor and four levels office building inaugurated in February 2009 (Hera el al. 2008).

For the exterior walls was used AMVIC constructive system. They are provided with low-emissivity triple-pane glazing windows with reduced overall heat transfer coefficient U and high solar transmission factor.

The main functions of the Amvic office building are listed now. On the ground floor there is a wide open space where the sales department and the secretary's office are located. In a separated area there is a service room. The first, second and third floor are wide open office areas. On the top floor there are five apartments. Amvic PH is well documented (Badescu et al. 2010, 2011) and has been monitored for a relatively long time (2009-2013). For the internal heat sources and sinks details are given in (Badescu et al. 2010, 2011).

From the thermal comfort approach Amvic building meats two traits: low energy consumption building according to Passivhaus and office building. In July 2013, when was undertaken present thermal comfort survey the building belong to Arco company, and some interior changes were made.

Figure 1. AMVIC office building. South façade (courtesy of Dr. Ruxandra Crutescu).

2.2. PEOPLE QUESTIONNAIRE SURVEYS

The field study presented here included people questionnaire surveys and simultaneous measurements of the environmental variables in relation with thermal comfort. In this survey were given to people 142 questionnaire in 16 different days.

The dates requested by questionnaire were: date and time of filling, the floor and the office number, the working place (POST), information about the person who had completed the questionnaire (name, age and sex). For the assessment of the thermal sensation (TSV) the subjects chose an option on the ASHRAE 7-points rating scale, they also chose what thermal preference had at the time of completion, they had to answer about the acceptability of the thermal environment and if to answer they felt some local thermal discomfort. The questionnaire included a checklist with clothing items for the peoples to choose from. They had to specify the activity they had been doing in the last 15 minutes before the moment of questionnaire filling.

3. RESULTS AND DISCUSSION

Figure 3.a shows the distribution of the thermal sensation votes (TSVs), and figure 3.b shows the distribution of the thermal preference votes (TPVs) for the entire sample. It can be seen that the TSVs are centred on ‘OK’ (0) with almost symmetrical distribution of the votes of (‘A bit warm’ and ‘A bit cold’) and, after that, with a little shift towards warm thermal sensations. The TPVs are centred on ‘0’ (‘No change’) and ‘1’ (‘A bit warmer’).

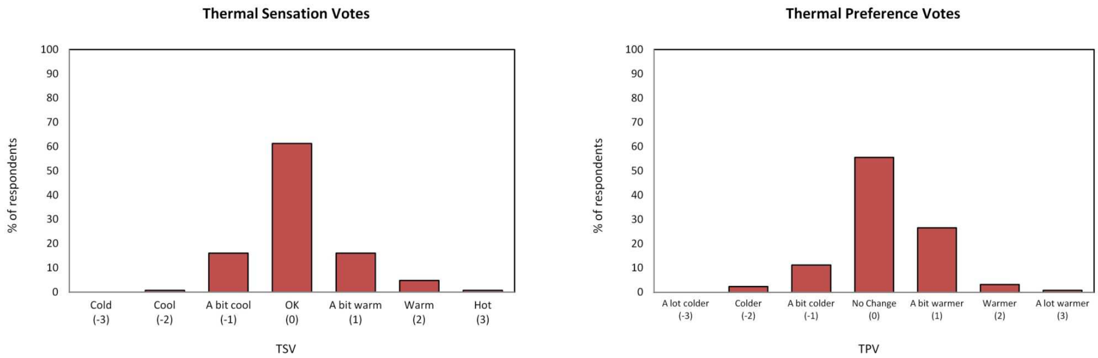

Figure 3. Relative frequency of: a. Thermal Sensation Votes (TSVs); b. Thermal Preference Votes (TPVs)

Comparative distribution of Thermal Sensation Votes (TSVs) and Thermal Preference Votes (TPVs) on buildings levels can be seen in figure 4. On TSVs distribution can be observed a bigger concentration of votes on ‘OK’ (0) than in the TPVs distribution of ‘No change’ (0) votes.

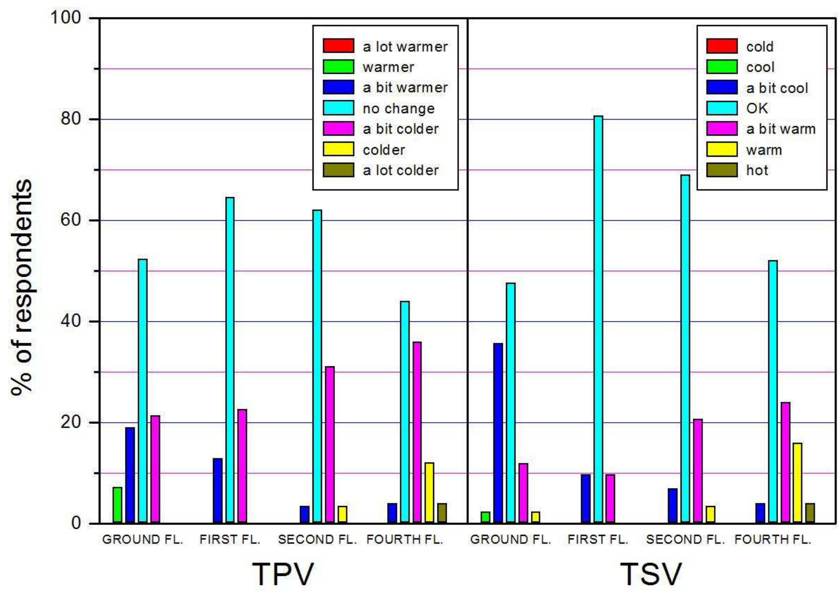

Figure 4. Comparative distribution of Thermal Sensation votes (TSVs) and Thermal Preference votes (TPVs) on buildings floors

Figure 5 shows the distribution of thermal sensation votes in relation to thermal preference for all survey period. As can be seen, the majority of people voting for a specific thermal sensation preferred the conditions which would bring them to neutrality, as would be expected.

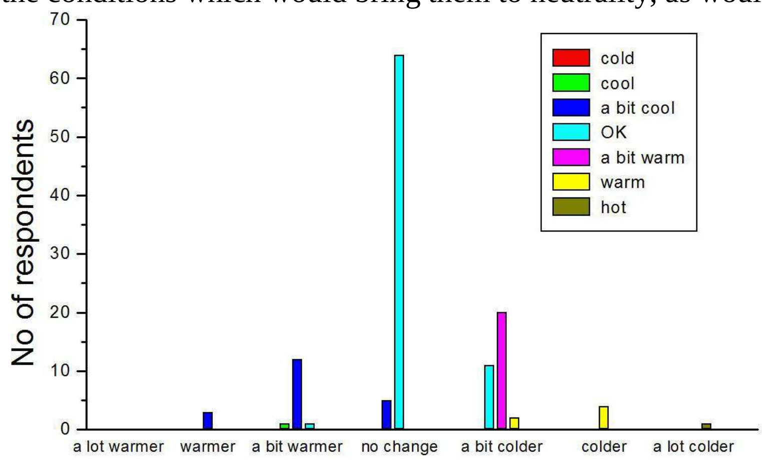

Figure 5. Thermal sensation vote (TSV) by thermal preference vote (TPV)

4. CONCLUSIONS

The distribution of the thermal sensation votes (TSVs) during the entire period of survey is centred on 'OK' (0), with a percentage of 61.29% as can be seen in figure 3. The distribution of the thermal preference votes (TPVs) during the entire period of survey is concentrated to 'No change' (0), too, with a percentage of 55.65% as can be seen in figure 4.

The repartition of thermal sensation votes and thermal preference votes on building floor has an obvious ascending tendency, from 'Cold' to 'Warm', respectively from 'To be warmer' to 'To be colder', beginning to ground floor, then first floor, second floor and third floor. This thing happens because of stratified placement of temperatures on the levels of a building, in summer from cold to warm beginning from down to up.

REFERENCES

1. Badescu V, Laaser N, Crutescu R. , (2011a), Warm Season Cooling Requirements For Passive Buildings In Southeastern Europe (Romania). Energy; 2010; 35:3284-3300.
2. Badescu V, Laaser N, Crutescu R, Crutescu M, Dobrovicescu A, Tsatsaronis G. Modeling, (2011), validation and time-dependent simulation of the first large passive building in Romania. Renewable Energy; 2011; 36:142-157
3. Buratti A. and Ricciardi P., (2008), Adaptive analysis of thermal comfort in university classrooms: Correlation between experimental data and mathematical models, Building and Environment 44 (2009) 674–687
4. Croitoru C., Vartires A., Bode F., Dogeanu A., (2013), „*Survey Evaluation of The Indoor Environment Quality In A Large Romanian Hospital*", INCAS Bulletin,Vol 4/2013 December 2013
5. de Dear, R., Brager, G. and Cooper, D. (1997). Ashrae rp-884; Developing and adaptive model of thermal comfort and preference. Technical report, The American Society of Heating, Refrigeration and Air-Conditioning Engineers, Inc., and Environmental Analytics, editor. Atlanta
6. Fanger P.O (1970), Thermal Comfort. Analysis and Applications in Environmental Engineering. Published in the United States by McGraw-Hill Book Company 1972. Originally presented as the author's thesis, Danmarks Teknishe Højskole 1970
7. Hera D, Drughean L, Ilie A, Crutescu R, (2008), "*Climatizarea unei case pasive cu functiune mixta*", a XV-a Conferinta; Confort, Eficienta, Conservarea energiei si Protectia mediului, 26 – 27 noiembrie 2008.
8. Khodakarami J., Nasrollahi N. (2012), „Thermal comfort in hospitals – A literature review". Renewable and Sustainable Energy Reviews 16 (2012) 4071– 4077
9. Meldaho M., Beyer P., Hensen J. Siqueira L. (2005), "The thermal comfort, the indoor environment control, and the energy consumption in three types of operating rooms." In: Building simulation , 9th International IBPSA Conference.
10. PHI (2014), Passivhaus Institut, The independent institute for outstanding energy efficiency in buildings, http://passiv.de/en/, [accessed: March 2013]
11. Skoog J, Fransson N, Jagemar L. (2005) „Thermal environment in Swedish hospitals summer and winter measurements." Energy and Building 2005;37:872–7.
12. Teli D., Jentsch M. F., James Patrick A. B., Bahaj AbuBakr S., (2012), "Field study on thermal comfort in a UK primary school ", Proceedings of 7th Windsor Conference: *The changing context of comfort in an unpredictable world* Cumberland Lodge, Windsor, UK, 12-15 April 2012. London: Network for Comfort and Energy Use in Buildings, http://nceub.org.uk

DETERMINATION PERMEABILITY OF TRANSPARENT COVERS FOR SOLAR COLLECTORS

Dimitar Georgiev Atanasov, Mincho Stoianov Minchev, Atanas Ivanov Tashev
UFT-Plovdiv, Bulgaria

ABSTRACT

Lately the focus is on using solar radiation in collectors for air heating. Basic indicator, for the performance of solar collectors is their efficiency, which represents the ratio between the absorbed and the fallen solar radiation. The permeability of the transparent covers has fundamental influence over efficiency.

1. INTRODUCTION

The flat solar collector is a simple and widely spread device for transformation of solar energy into useful heat.

For minimizing heat losses in the environment the absorbing surface is covered with a covering which is transparent for the solar radiation (made of glass or plastic). The most common transparent covering is glass [7]. It is an artificial, inorganic product obtained through melting and subsequent cooling without crystallization [9]. Basic requirements of the covering are thermal stability, high permeability for solar radiation, strength and resistance against ambient and radiation (ultraviolet radiation) influences.

According to the actual world standards the testing of collectors is carried out by inclining and orientating the latter in a way that the incidence of solar rays is perpendicular to the surface of the absorber. In reality in solar systems the angle under which the solar rays fall on the collector surface changes permanently as well as the direct solar radiation flux proportionally to cos θ (where θ is the angle between the solar rays direction and the normal of the collector's surface). The actually fallen radiation on the absorber surface depends on the collector's optical efficiency ($\tau\alpha$).

The permeability of the transparent cover relative to the short-wave solar radiation is dependent on the angle of incidence. Energy is wasted during reflection from the glass surface and as well as during its absorption. These losses increase with increasing the angle of incidence [7]. The influence of the angle of incidence of the radiant flux is investigated by [4]. The glass thickness must not be greater than necessary. Special glasses have better thermal insulation characteristics. They are transparent for solar radiation and opaque for infrared rays.

For each partially transparent material there exists such a thickness at which the surface becomes practically opaque for the fallen radiation.

The transmittance coefficient depends on the wavelength λ, the direction of the incident radiation (β, θ), the refractive index and the attenuation coefficient k.

The refractive index of air is n = 1, and for the most commonly used ordinary glass in heliotechnics n = 1, 5 ÷ 2; [3, 7]. The glass with reduced iron content has higher permeability.

Most transparent covers let through selectively, i.e. the transmittance coefficient depends on the wavelength of the incident radiation. The glass with a low content of Fe_2O_3 is practically transparent to the solar spectrum and becomes opaque for wavelengths greater than 3 μm.

The transparent covering of the solar collectors can be made from plastic materials in which case the transmittance coefficient changes strongly by the wavelength. In these cases it is good to know the spectral characteristics of the covering.

In contrast to glass most transparent plastics have a high transmittance coefficient in the infrared range of the spectrum at $\lambda > 3\ \mu m$ [7]. Optical characteristics of transparent plastic coverings have been also studied by the authors [1, 2, 5].

Theoretical strength of glass reaches about 32 GPa. The actual lower strength of the glass (about 45 MPa tensile strength) is due to the inevitable defects during manufacturing and depends on many factors (e.g., load duration).

Improving the constructive properties of the glass is achieved by two main types of processing - hardening and laminating. Hardening aims at creating a pressure on the surface (where tension is expected due to bending during exploitation). In general hardening means heating and subsequent rapid cooling of the glass. During cooling compressive stresses occur on both surfaces of the glass which is counterbalanced by tension on the inner side (where there are no defects and the tensile strength is very high).

In glass elements residual bearing capacity is obtained through laminating. Laminated glass consists of two or more sheets of glass (in general with different thicknesses and if present degree of hardening), stuck together using a transparent polymer (usually polyvinyl butyral – PVB). After breaking the laminated glass keeps its position due to the polymer and may continue to bear external load until its replacement [9].

The properties of one of special kinds of glass namely the borosilicate glass are: high corrosion resistance, smooth surface without pores, ecologically clean, high temperature stability and low linear expansivity. The composition of the borosilicate glass is 13% boric oxide B_2O_3, 4% alkalis Na_2O, 2% other impurities, 81% silica SiO_2.

The borosilicate glass deforms only at temperature close to that of a transition phase (about 525 ° C). At lower temperatures the borosilicate glass retains mechanical strength. A permissible operating temperature, however, is significantly lower. Generally, the maximum operating temperature of glass components is 200 ° C, in rare cases up to 300 °C, they can be safely used at temperatures up to -80 ° C. The abrupt change of temperature variations leads to an increase in thermal stress [8].

Multi-wall polycarbonate sheets Policam (PCMW) have the following properties: 80% light transmission, low weight, operation over a temperature range of -40 ° C to 120 ° C [6].

Purpose of the work

The goal of this work is experimental determination of permeability of various types of transparent coverings, which are used in solar collectors. The permeability is defined as the ratio between the intensity of radiant flux which has passed through the transparent cover and the intensity before passing trough the transparent cover. The measurement of the intensity of the radiant fluxes is performed with solar radiation sensor model PYR, Decagon Devices, USA.

2. METHODOLOGY

Permeability of the following types of transparent covers was investigated: polycarbonate, borosilicate glass, common (white) glass, low emission (K) glass with hard coating and low emission (K) chemical glass.

The measurements are made with two sources of radiation – natural (the sun) and artificial (halogen lamp). The measurements were made at various angles of radiation - 90^o, 45^o, 30^o.

The measuring is done in the following steps: the incident radiant flux $\mathbf{I_0}$ which falls on the solar radiation sensor is measured, after that the glass is placed and the flux of radiant energy which has passed through **I** is measured. The measurements are repeated 10 times for each of the experiments in order to avoid an accidental error. A scheme of the experimental set-up is presented in fig. 1.

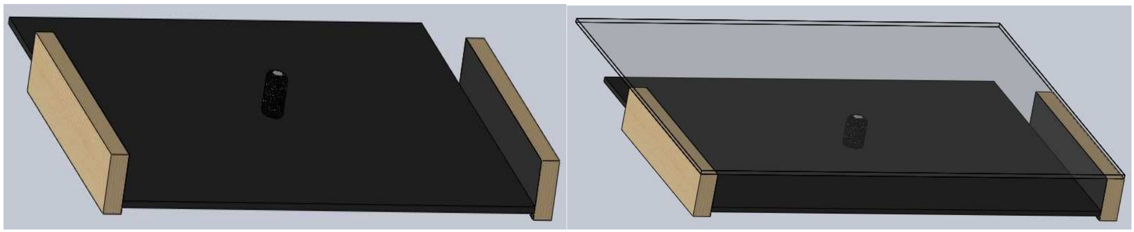

a) b)

Fig. 1 Scheme of the measuring system for a) direct radiant energy,
b) radiant energy let through

The glasses have a thickness of 4 mm except the polycarbonate which has a thickness of 8 mm. The width of the glass is 450 mm. The base is made of black aeroflex with a thickness of 5 mm, and the sides are wooden blocks with a thickness of 18 mm and a height of 45 mm coated with a matte black paint to reduce the secondary reflection.

During the experiments with an artificial source of radiation the halogen lamp is placed 280 mm away from the sensitive element of the solar radiation sensor with the radiant flux falling at an incidence of 90°. The change in incidence of the radiant flux is achieved through rotation of the lamp.

Results

Experimental results for the permeability of the described transparent covers have been obtained. Close values have been established for the permeability when comparing the results with natural and artificial light.

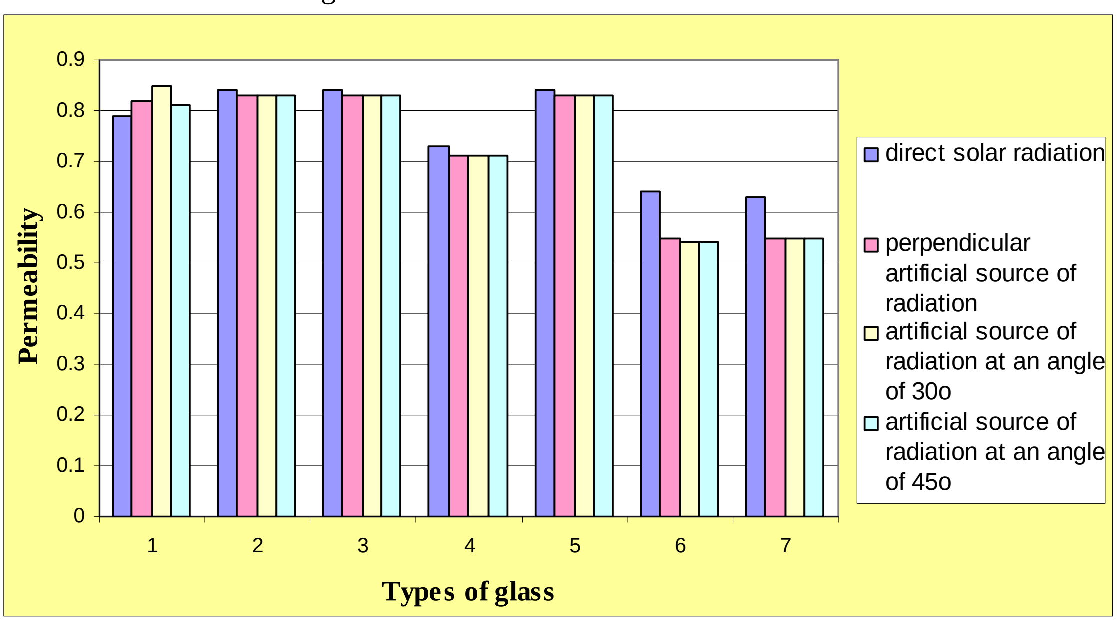

Fig. 2.Permeability of various types of glass.

1- polycarbonate transparent cover; 2 - chemical low-emission glass (coating is upside); 3 - chemical low-emission glass (coating is downside); 4 - borosilicate glass; 5 - common (white) glass; 6 - low-emission glass with hard coating (coating is upside); 7 - low-emission glass with hard coating (coating is downside).

The permeability of radiant energy is estimated by:

$$(I/I_0).100, \% \qquad (1)$$

During the experiments the test samples of the transparent covers are placed in a horizontal plane. The experiments using direct solar radiation are conducted under normal incidence of the radiant flux on the transparent cover surface. The experiments with artificial source are performed in several different angles of incidence of the radiant flux – 90^o, 45^o and 30^o.

The analysis of the experimental results (fig. 2) shows that the radiation flux source influences only the permeability of the low-emission glass with hard coating. It lets the solar radiation trough of about 10 % more (in both directions) than the artificial radiant flux. Minimal differences can be observed in the other transparent coverings, but their values are much lower.

The incidence angle of the radiant flux has a weak influence (up to 6%) only in the case with the polycarbonate transparent covering. For all other coverings such influence is not observed.

3. CONCLUSION

From the obtained results the following conclusions can be drawn:

1. The transparent coverings with the highest permeability are: common (white) glass, low-emission chemical glass and polycarbonate transparent covering.
2. From an economic point of view – the cheapest option is the common (white) glass.

Acknowledgements

The research is sponsored by fund “Science” (Contract № 11/13-H on "Experimental study and modeling of solar collectors for air heating").

References

1. Chandra, A., L. Turng, P. Gopalan, R. M., Rowell, Sh. Gong, Study of utilizing thin polymer surface coating on the nanoparticles for melt compounding of polycarbonate/alumina nanocomposites and their optical properties, Elsevier, Composites Science and Technology 68 (2008)768–776

2. Danchova, N., Obtaining and properties of the doped sol-gel materials, (in Bulg.), Abstract, SU „St. Kliment Ohridski”, Sofia, 2012

3. Geometric optics, MGU „St. Ivan Rilski”, (in Bulg.), Copyright © 2012 http://mgu-physics.com/e107_files/downloads/physics2/Geometrichna_optika.pdf

4. Kostov, K., P. Tsankov, T. Tanev, I. Ivanov, Experimental stand of air solar collector, (in Bulg.), ISSN 1314-2550 Heat engineering, year 3, book 1, Published by Technical University - Varna, 2012

5. Moretti, E., M. Zinzi, E. Belloni, Polycarbonate panels for buildings: Experimental investigation of thermal and optical performance, Elsevier, Energy and Buildings 70(2014)23-35

6. Signum Engineering Ltd., Sofia, (in Bulg.), http://www.signum-plast.com/ploskosti/polikarbonatni-ploskosti.html

7. Spassov, K., M. Balabanov, At. Stankov, Design and construction of thermal solar installations, (in Bulg.), Technics, Sofia, 1988

8. Tau engineering, Moscow, (in Russ.) http://www.pprus.ru/info/materials/Borosilicate/

9. Trifonov, S., Enclosing constructions of glass and aluminum. Overview of the field and topic for future research., (in Bulg.), XI International Science Conference VSU’2011

RESEARCH ON VALUABLE RECOVERY OF OIL FROM GRAPE SEEDS

S.Șt. Biriș[1], C.I. Covaliu[1], G. Paraschiv[1], V. Vlăduț[2], A. Atanasov[3]
[1]Politehnica University of Bucharest, Faculty of Biotechnical Systems Engineering, Romania
[2]INMA Bucharest National Research Institute, Romania
[3]University of Rousse "ANGEL KANCHEV", Bulgaria

ABSTRACT

Grape growing and wine making lead to the obtaining of subsidiary products (various wastes and by-products) which are not further used as for example: grape pomace, vine prunings, grape stalks, yeast lees, grape seeds, tartrate, carbon dioxide and wastewater. Oil from grape seed was not produced on a large scale until the 20th century because of the complicated technology involved for obtaining it and also because grape seeds contain a decreased percentage of oil compared to other oil-producing seeds such as sunflower seeds. This article presents a number of value adding technologies for the valorization of the subsidiary products and the experimental part is about the obtaining of oil from grape seeds by extraction.

1. INTRODUCTION

Since grape seed oil can be a profitable sideline of wine making process, as well as a byproduct that can be successfully marketed, the valuable recovery of oil by various techniques as for example extraction is required. Grape seed oil is light in color and flavor, and has many nutrients. Some of the health benefits of grape seed oil conferred by the presence of certain specific chemical compounds are presented in Table 1 [1,2,3].

Table 1. Grape seed oil benefits

Benefit	**Description**
strong antioxidant	- due to flavonoid such as oligomeric procyanidin (Fig. 1a), found in grape seed oil; -procyanidins from grape seed oil are chains of (+)-catechin molecules (Fig.1b) found in teas and may be absorbed in their chained forms. -about 50 times stronger than antioxidants like, vitamin C and E. -provide protection against free radicals (oxidative stress) - help in preventing cancer
Improves heart function and cardiovascular system	- by lowering the level of bad LDL cholesterol (bad Cholesterol) and increasing the level of HDL cholesterol (good cholesterol), which can reduce the risk of coronary diseases - because of the content of Omega-3, Omega-6, and Omega-9 which are the fatty acids found in this oil.
Consolidates health status for people having diabetes	- because it contains linoleic acid (76 %), which is a polyunsaturated fatty acid that can improve the health status for people having diabetes Fig.1c.

[1]Bucharest, Splaiul Independentei, 313, +40744756832, biris.sorinstefan@gmail.com

Anti-inflammatory properties	-it can be used in releasing pain and swelling caused by arthritis.

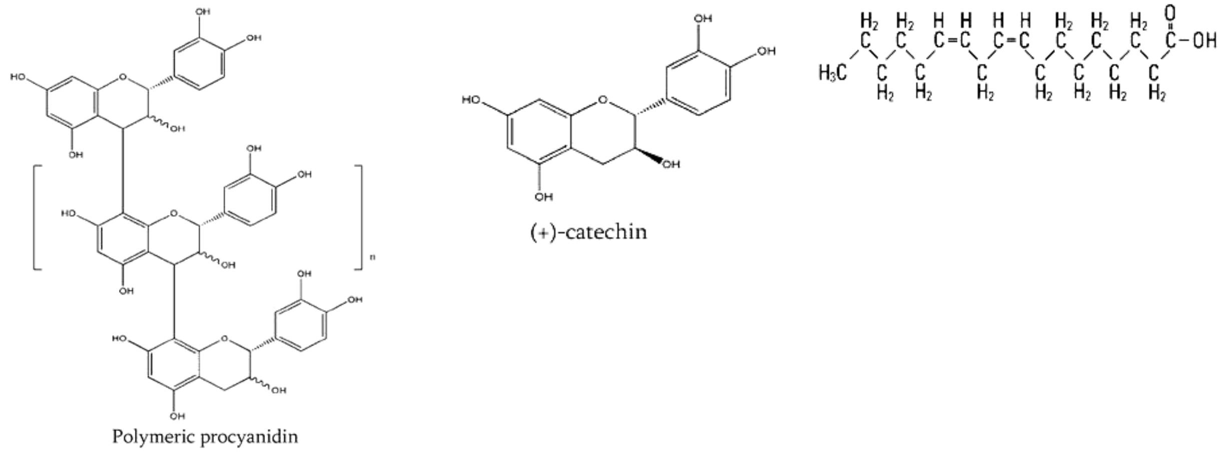

Figure 1: Structural formula of oligomeric procyanidin (a), catechin (b) and linoleic acid

In the 20th century, grape seed oil started to be to be processed and marketed starting with the United States and Europe. Because each seed yields a small amount of oil, grapeseed oil is usually chemically extracted. The chemical extraction has a decreased impact on the flavor of the oil, but it makes it very accessible. The structure of grape seed is presented in Fig. 2 and the grape composition is outline in Tabel 2.

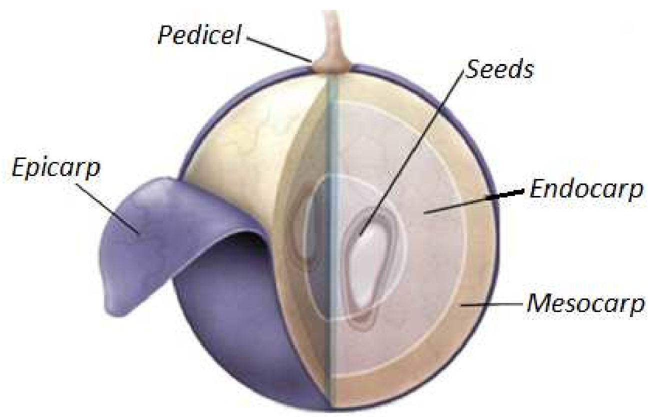

Figure 2: The structure of grape seed

Table 2. The grape structure

GRAPE	BUNCH (3-8 %)	
	BOBSLED (92-97 %)	PEEL (7-12 %)
		PULP (80-92 %)
		SEEDS (2-8 %)

Grape seed oil can be obtained by using press process or solvent extraction. It can be safely used for heating because it has a high smoke point, around 216°C. Consequently, it is safe for cooking food. The processing routes and derived products from grape seeds are presented in Fig.3. For example, grape seed oil is used as cosmetic ingredient for treatment of damaged and stressed tissues, for possessing regenerative and restructuring qualities which allow a better control of skin moisturization and protection [4].

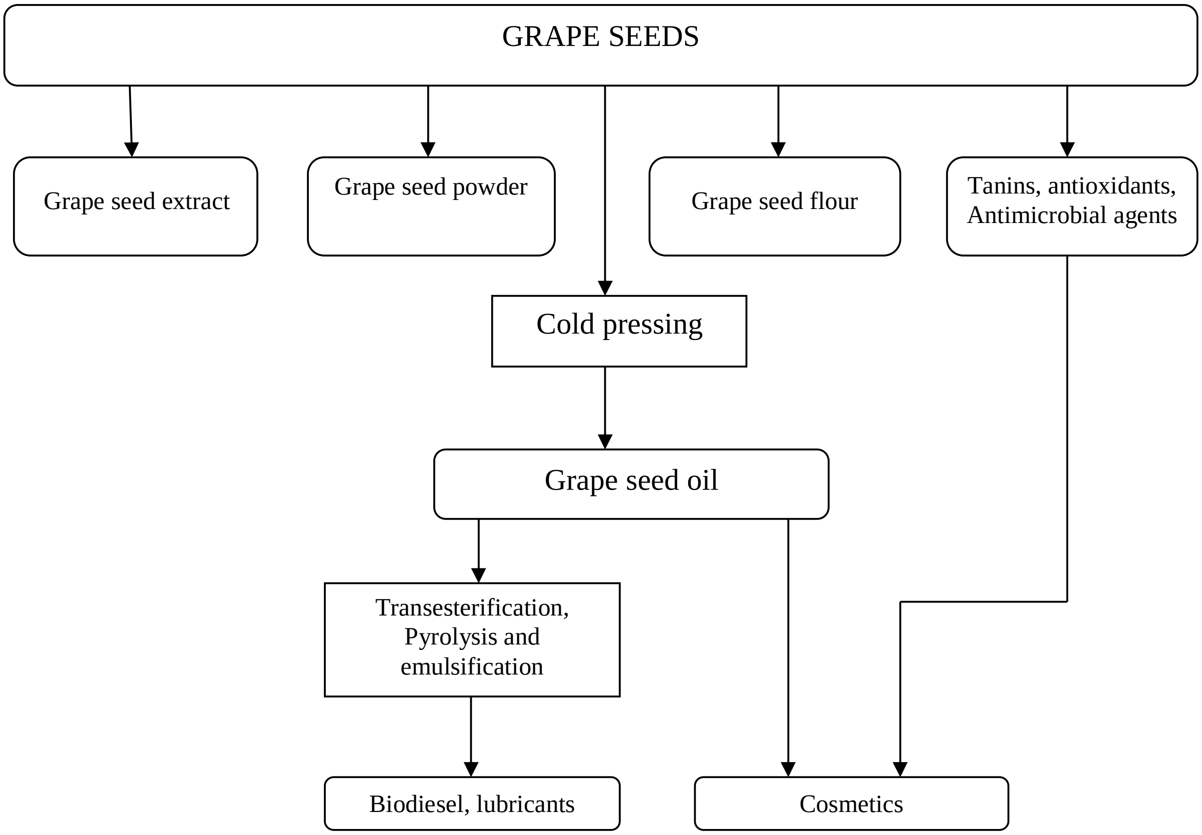

Figure 3: Processing routes and derived products from grape seeds

2. METHODOLOGY

Separation of grape seed pomace can be done in several ways [5]:

a) by mixing the pomace with water and sieving on a sieve seed.

b) mixing the pomace with water and separating the seeds by using a hydrocyclone.

c) drying the pressed pomace.

In addition to these methods exist other ways of separation such as: separating the seeds by using an electromagnetic field or a hydraulic flow line.

In Fig. 4 is presented OVS-2 seeds separator which consists of scraper elevator, smashing tiller with horizontal blades (I), site block arranged in cascade (II, III), transverse ventilator (IV), frame and a piston actuator.

Pomace from the press of the extractor, taken by the feed elevator with scrapers, is directed to the hopper separator equipped with a crusher tiller with horizontal hammers, which performs grinding of blocks of pressed pomace. From here shredded pomace is directed using the sieves and inclined planes system arranged in cascade, which performs pomace separation by size of seeds.

The cleaning process is amplified by the action of the air stream made by transversal ventilator. The evacuation of the separated fractions is performed by collecting channels.

Pomace is fed to the equipment of loosening (I) and at the bottom of the separator are discharged the pomace without seeds (1) and the grape seeds (12).

In Fig. 5 are presented the different constructive and functional alternatives of grape seeds separation equipments, which were the subject of a recent patent [6]. The invention describes a method and equipment for separating grape seeds from the pulp and skin of a grape consisting of depositing grapes on a plate having apertures there- through and driving the grapes across the plate by using a blade such that the grape seeds and juice will pass through the apertures of the plate while holding the grape skin.

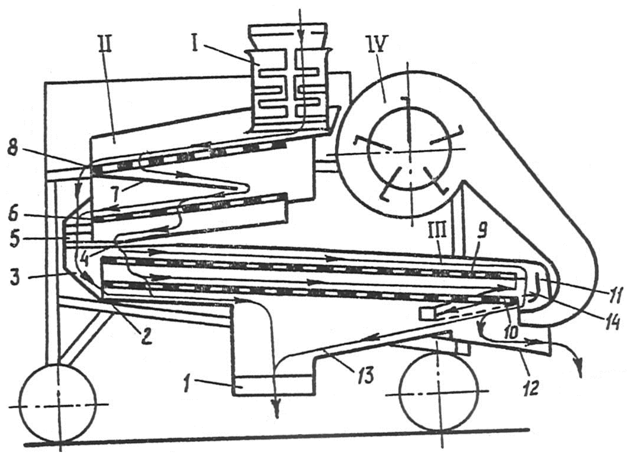

Figure 4: The seeds separator OVS-2

Then the grape juice could be separated from the seeds and recombined with the pulp and skin for the fermentation operation in order to produce a wine possesing improved flavor profiles because of the different tannin contents of the skin and seeds. Also the patent describes a method and equipment for opening grape berries without fracturing their grape seeds [6].

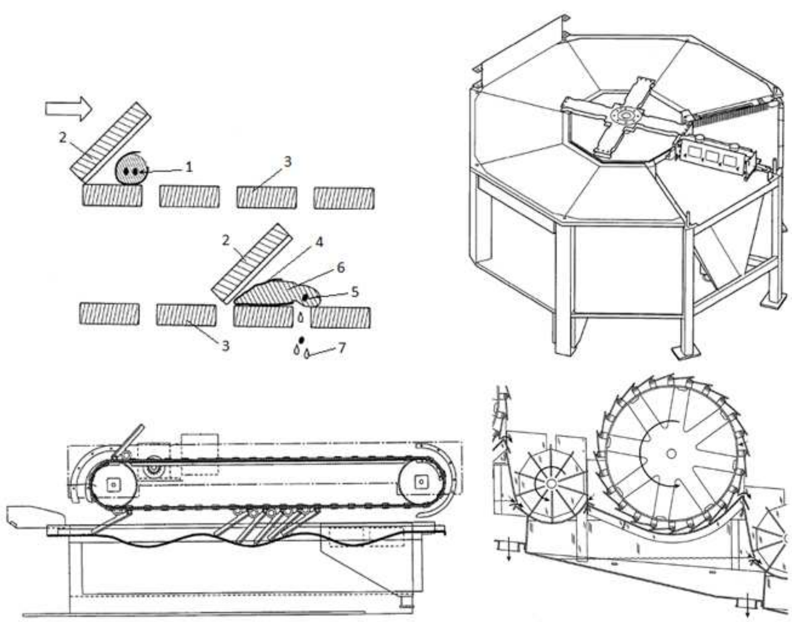

Figure 5: Various types of seed separators [6]

For separation of oil from grape seed can be used, mechanical presses with continuous functioning of small capacity as in the Fig. 6. These presses of small capacity are designed for cold pressing, without preheating and treatment of oilseeds before pressing. Moreover, these presses are designed for those who worked only ten pounds of seed per hour. The equipment is slightly unstable, compact, simple and easy to use. They are used not only for conventional oilseeds such as canola, sunflower, flax, but especially for pressing technical oilseeds such as artichoke, hemp, grape seeds, etc.

Figure 6: Mechanical presses with continuous functioning of small capacity [7]

The application of extraction technique for obtaining an increased yield of grape seed oil in comparison with that obtained by pressing operation was the aim of the experimental part. For conducting the experiments focused on the grape seeds oil extraction were used as starting materials: seeds of white grapes and chloroform solvent ($CHCl_3$) of analytic purity (min.99%) from Chimactiv S.R.L.

Experiments were carried out using the following set of parameters: contact time of 48 h, temperature 30°C, particle diameters 1.0–1.4 mm. Seeds sample were first dried at 103°C for 1 h and then were mill ground to obtain a mean particle seeds size of 1.0–1.4 mm. Based on the literature data [8] the extraction yield was 10.1%, which represents an increment of approximately 50% over oil yield obtained by pressing operation.

3. CONCLUSIONS

Our preliminary study indicates and sustain that the extraction using solvent technique may certainly be used to enhance oil extraction in comparison with pressing. More experiment will be performed to complement the experimental research.

References

[1] Dorobanţu, P., Beceanu, D., *Importanţa alimentară şi dietetică a uleiurilor vegetale*, Lucr. Ştiinţifice U.Ş.A.M.V., Seria Agricultură, vol.50, Iaşi,2007.
[2] Carlson S., Peng N., Prasain J.K., Wyss J.M., *Effects of botanical dietary supplements on cardiovascular*, cognitive, and metabolic function in males and females, Gend Med.,5 Suppl A:S76-90, 2008.
[3] Fitzpatrick D.F., Bing B., Maggi D.A., et al. *Vasodilating procyanidins derived from grape seeds*, Ann N Y Acad Sci.,957, 78-89, 2002.
[4] Neranzis, E., Tataridis, P., *Integrated Enology- Utilization of winery by-products into high added value products*, e-Journal of Science & Technology (e-JST), No. 3, 2006.
[5] Cebotărescu, I.D., Neagu, C., Bibire, L., *Utilaj tehnologic pentru vinificație*, Ed. Tehnică, București, 1997.
[6] Margolis, G., Gallo, E., *METHOD AND APPARATUS FOR REMOVAL OF GRAPE SEEDS FROM GRAPE SKIN*, United States Patent Application Publication, US 2007/0104842 A1, 2007.
[7] * * *, *Farmet-Prese de capacităţi mici*, http://www.farmet.ro/tehnologia-de-prelucrare-a-semintelor-oleaginoase/prese-de-capacitati-mici
[8] Dorobanțu, P., Berceanu, D., *Studii privind uleiul extras din semințe de struguri, aparținând unor soiuri diferite de Vitis Vinifera*, Lucr. Ştiinţifice U.Ş.A.M.V., Seria Agricultură, vol.51, Iaşi, 2008.

ELIMINATION OF PARASITIC WEED SEEDS FROM THE MASS OF SEEDS OF AGRICULTURAL CROPS THROUGH WET MAGNETIC SEPARATION

PhD. Stud Eng Valeria Gabriela Ciobanu[1],[2], PhD. Eng Anisoara Paun[1]
[1.]National Institute of Research – Development for Machines and Installations Designed to Agriculture and Food Industry – INMA, Bucharest
[2]. University Politehnica of Bucharest - Faculty of Biotechnical Systems Engineering

ABSTRACT

The quality and production of any agricultural crop (whether it is intended for human or animal consumption) is determined both by the factors that directly influence the seeds before sowing as well as of those which act from the moment of sowing and up to storage.

An important problem facing the Romanian agriculture is represented by the high degree of weed encroachment, especially the development of parasitic weeds affecting both the quality of perennial forage leguminous crop production as well the animal health.

The most dangerous and harmful parasitic weed is the dodder, reason for which combating it is a necessity for all the factors involved in the processing chain (the farmers and all the units wich responsible for the ensuring of some quality agricultural productions), which can not be completely eliminated than by the method of wet magnetic separation.

In this paper is presented the most safest method of fighting against these parasitic weeds from the mass of seeds ever since the establishment of the crops, which can not be completely eliminated that only by the method of wet magnetic separation.

1. INTRODUCTION

Ensuring the obtaining of a rich agricultural crop is conditioned by using at sowing of a seeding material with an as high germinating power, as clean, free of any seeds and especially parasitic weeds.

Before of sowing the seeds are subjected to some preparatory operations regarding the conditioning and quality control of them .

The seed conditioning includes all the operations applied to seeds provided in the standards and normative documents regarding the material used for planting.

These operations are: drying, cleaning, sorting, processing, packaging and storage.

Weeds are much better adapted to the environment and more resistant to adverse conditions than the cultivated plants. Their root system is well developed, deep, with great power of absorption of nutrients and water.[5,10]

The most dangerous parasitic weed is the dodder, plant of quarantine registered in the list of risk factors for the production of many crops, including: clover, alfalfa, flax, willow, which degrades the quality of production of these plants. .[5,10]

In our country, Romania, the area of spreading of the dodder weed is very high, being reported in all the counties of the country, from the sea level and up to the altitude of 1800 m.

Out of the 17 species of dodder that are found in our country the most dangerous are campestris dodder and trifolii dodder, that produce great damage of the crops of clover and alfalfa, epilinum dodder which do immense damage to crops of hemp, hops and vegetables and monogyna dodder which cause damage to orchard of nurseries, at forestry and agroforestry shelterbelts.

[1]1. PhD. Std. Eng. Ciobanu Valeria Gabriela from National Institute of Research – Development for Machines and Installations Designed to Agriculture and Food Industry – INMA, Bucharest, ROMANIA, 6 Ion Ionescu de la Brad, Blv, sector 1, Bucharest 71592, OP 18, Phone: 004021-269.32.55, e-mail :dns.gabriela@yahoo.com

Currently there is no established culture in which is not reported the dodder, so if no action is taken for its combating, this is multiplying very quickly and as its expansion the plants dry up and are perishing, the production of cultivated plants being reduced up to 90% or even 100%.[3,5,6]

In the doders combating an important role is played by the preventive measures of fighting with the doders. A major preventive measure is represented by use of clean seed to crop establishment.

Besides diminishing of production, dodder is also dangerous under aspect toxic, because it contains substances harmful to animals health, thus depreciating the quality of forages.

Thus the high levels of dodder from green or dry fodder for animal nutrition are poisonous in case are consumed for several weeks leading to the occurrence of liver damage associated with bleeding throughout the body, abdominal pains and weight loss of the animals and also the behavior of the affected animal can be erratic and unpredictable.

The most efficient spreading of dodder is throught seeds, which keeps the germination capacity 12-15 years in deposits and up to 6-8 years into soil, crop residues and manure.

Animals that consumes contaminated fodder with dodder seeds spread these seeds through dejections, because dodder seeds is not affected by enzymatic substances of the digestive system, thus keeping the germination.[9,10]

An important measure in connection with dodder combating is the separation of wet seeds in magnetic field, which is possible only with special machines equipped with magnetic drums, in order to perform a cleansing neat of the sowing material, that is made and when the field is completely devoid of weeds.[1,4,7]

2. METHOD OF WET MAGNETIC SEPARATION WITH MD 400 MACHINE

An interesting application of the iron powder, in agriculture, is to be used in the separation of seeds that can not be completely separated according to customary methods: sieve,air currents, etc..

The method of the wet magnetic separation based on the iron filings, applies to eliminate the parasitic weed seeds, especially the dodder (Fig. 1), from the mass of seeds of crops, which is based on the property of seeds to be coated with a very fine powder, prepared specifically and which contains iron, property directly related to the surface condition of the seeds (Fig. 2), which as have the surface ridgyer, spongy, wrinkled so it covers more well with fine powder on are wet, thus gaining the properties of the ferromagnetical bodies and being able to be easily attracted by the magnets with wich the equipment is endowed, while the basic seeds of culture, having the smooth outer surface will not be attracted by the magnetic field.[2,3,8].

Figure 1: Dodder

Figure 2: Dodder seeds [12]

From table 1, which presents data on the the roughness of some cultural plant seeds and weeds, it is found that the weeds which are found in shown crops have almost entirely roughness, while the seed culture are smooth favoring the application of magnetic separation method, namely the separation of seed mixture after their surface condition.[1,2,3]

Table 1: Roughness of some seeds

Cultural seeds	Percentage of smooth seeds	Percentage with roughness seeds	Weeds	Percentage of smooth seeds	Percentage with roughness seeds
Clover	73-93	1-5	Dense buckwheat	-	96
Alfalfa	91	1	Corn	-	98
Sparceta	93	2	Tares	0,2	92
In	93	5	Pigeon crop	-	94
			Dodder	-	100
			Raigras	-	100

Figure 3: Dodder in clover [12]

Figure 4: Dodder in alfalfa[13]

Accession of iron powder to roughness of dodder seeds is conditioned by finesse of the filings and by the presence in its composition of pure element Fe or Fe_3O_4 for magnetic permeability.

Figure 3: Iron powder

Mixing of seeds with iron powder is done completely in closed containers where the seed is mixed continuously and in which is dripping water (in small amounts) to increase the adhesion of the powder to the dodder seeds. The use of closed containers is imposed as a necessity as it the magnetic qualities of the iron filings depreciates in contact with water, due to the oxidation of the iron (Fe) contained in filings.

It is recommended to use in a short time or keeping away from moisture in sealed vessels of the iron powder.

The seed material, before being subjected to the action of magnetic field, must be pre-cleaned, where a lot of impurities are removed from the basic seeds, thus the work on electro-magnetic and magnetic machines is making easier, the iron powder consumption is reduced and the yield qualitative and quantitative increases in favor of reducing the cost price.

Figure 5 shows schematically the working principle of the machine MD 400 for cleaning and sorting seeds in magnetic field using the wet method. [6,7,8,11,14]

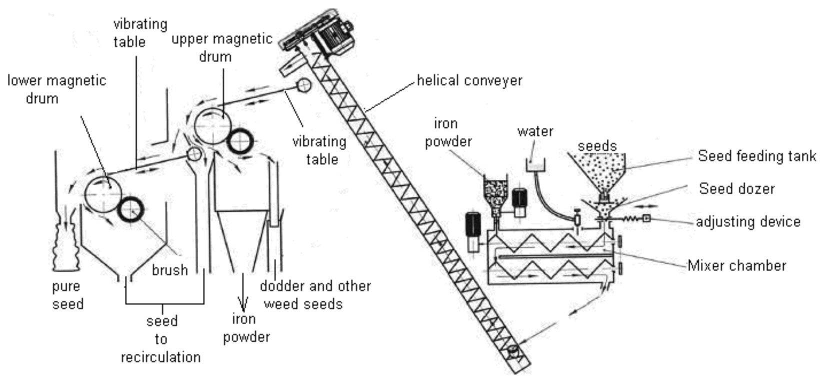

Figure 5: Schematic of MD 400 machine of the disposal of dodder seeds in magnetic field[2]

The machine for removing dodder seeds MD 400 presented in figure 6, equipped with magnetic ferrite drums, is designed to pick out the seeds of perennial fodder vegetables, flax, hemp, carrots, onion, chive, spinach, tomatoes, etc., in view of removing the dodder seeds, a parasite quarantine plant.

The machine is composed of a front frame that supports the selecting system endowed with magnetic drums and the electrical panel and a rear frame on which are fitted the mixer with the dampening unit and the powder dozer, the seed feeding tank and the helical conveyer.

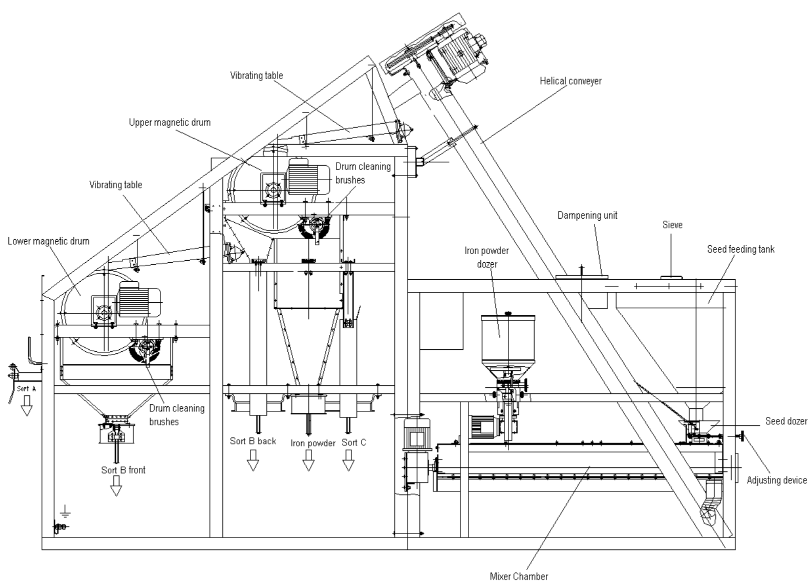

Figure 6: MD 400 Machine [6]

The technological process of the MD 400 machine

The seeds intended for cleaning are introduced through the feed tank equipped with a sieve, which avoid the ingress of the straw or other foreign bodies in the machine. The seeds flow into the mixer, where they are wetted with water and in which is dispensed also the iron powder in accordance with a "recipe" predetermined that requires certain quantities of seed, water and iron powder depending on the degree of infestation of the seeds (fig.7).

Figure 7 :Seeds feeding tank with water and iron powder dozers

The seed mass thus treated is taken over by a screw conveyor which discharges the seeds on the upper vibrating table to upper magnetic drum (fig.8), where the where the seeds of weeds and sharps covered with iron filings are removed from the drum with the help of the rotating brush (Figure 9) to the collection funnel Sort B back, the seeds wich the seeds containing predominantly of dodder and iron powder are directed through a collection hopper Sort C (Figure 10), and the recovery of iron powder is done into a special vessel.

The seeds of basic culture, at which do not have joined the particles of iron filings, are directed further to the second magnetic drum for extracting of the remnants of dodder seeds, sharps that had escaped from the first magnetic drum. [2,3,6]

Figure 8: The first and second separation of the mixture of seeds

Figure 9: Rotative brush [6]

At the passage of seeds over the lower magnetic drum it produces a new separation, where the seeds with a very high content of the good seeds are collected in sort A (fig.10), and those with a high content of good seeds, but in which there are also sharps and dodder seeds in a relatively low percentage are guided to a mouth of bag through the front funnel B.

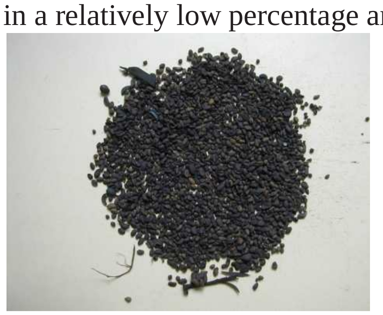

Figure 9: Sort C (weeds and dodder seeds) [3,6]

Figure 10**:** Sort A (clean alfalfa seeds) [3,6]

Front and back sort B are introduced again in the machine, the purpose of recovering of the good seeds remaining in them and the Sort C will not be recovered, entering into the technological losses.

The number of changeovers at seeds for removing dodder seeds from crop seeds can vary depending of purity, number of dodder at kg, water and iron powder tanks.
Generallyit is customary to put the opinion the seed through the machine by 2-4 times.

3. CONCLUSIONS

In this paper was presented the most effective and safe process of parasitic weeds control, especially of dodder, which can ensure a good quality of seed material.

The method of wet magnetic separation is based on the property of some seeds that can be covered up with very fine powder, prepared in a particularly mode and containing iron, operation performed with the MD400 machine for separation of seeds with magnetic drums following their surface texture.

The machine for dodder removing can be fitted and used both in stations of seeds separation as well as in agricultural farms and livestock in rural areas, decreasing the production costs and making savings regarding the transportation of raw material.

In this way is combated the spread of the parasitic plants in agriculture by the cultivators and also by the seed processing units that are responsible to ensure a high quality to the agricultural productions.

References

[1] A. V. Krasnicenko, Constructor's handbook of agricultural machinery (Vol 2), Technical Publishing House, 1964.

[2] Ciobanu, V., Căsăndroiu, T., Ciupercă, R, Păun, A., Researches on seeds mixture mechanical separation systems according to their surface, Renewable Energy and Rural Development, TE-RE-RD, Baile Olanesti, 20-22 June, (Issn 1843-3359); pag. 133-138 , 2013.

[3] Ciobanu, V., Structural and functional aspects and the process work of technical of the equipment for separating seeds after their surface condition, Seminar paper 1, Politehnica University, Bucharest, 2013.

[4] Dragomir, N., Cuscuta - A great danger for crops of perennial legume from Romania, articol publicat in Revista Ferma nr 4.(36), 2005.

[5] Emil Chesches, Measures to combat of the dodder seeds in the agricultural crops of our country, Red. Rev. Agricole, Bucharest; 2010.

[6] Fader, T., Pop, A., M.L., Stanciu, A., Experimental researches concerning realization of a technology and an installation for separating parasite dodder seeds, using a magnetic field, for obtaining a quality prime seed material for fooder plants, INMATEH Magazine IV; 2007.

[7] Fader, T, Studies and researches concerning the separation of dodder of onion and carrot seed, ICPITMUA Institut, Bucharest; 1989.

[8] Harmond, E., Robert Brandenburg, N., Klein, M., Mechanical seed cleaning and handling, Agriculture handbook ,no 354; 1968.

[9] Onisie, T., Zaharia, M., Agrotechnics, University of agricultural sciences and veterinary medicine “Ion Ionescu de la Brad”, IAȘI; 2002.

[10] Tanase Maria, Stanciu Mirela, Moise C. , Gheorghe M.., Ecological and economic impact of dodder species (Cuscuta spp. Convolvulaceae) on pratological ecosystems, JOURNAL of Horticulture, Forestry and Biotechnology, Volume 16(3), 93- 97, 2012.

[11] Kiyazev, V.F., Production and use of iron and alloy powders, Central Scientific-Research Institute of Ferrous Metallurgy, No.11, pp.28-30, 1981

[12]http://extension.missouri.edu/p/IPM1023-19

[13] Department of Crop and Soil Sciences East Lansing, MI 48824-1325, ww.msuweeds.com, 2010

[14] POPA, C., Researches concerning the influence of constructive and functional parameters of the active bodies of equipment used for for cleaning and sorting of seeds on the working the quality indices and exploitation, Academy of Agricultural and Forestry Sciences PhD THESIS; 2004.

INFLUENCE OF CINEMATIC REGIME AND QUANTITY OF MATERIAL ON EFFICIENCY OF SIFTING PROCESS

Gabriel-Alexandru CONSTANTIN[1], Gheorghe VOICU, Mădălina-Elena ŞTEFAN
University Politehnica of Bucharest, Faculty of Biotechnical Systems Engineering

ABSTRACT

In milling industry, two processes present a character of high repeatability, having a particular importance on the flour extraction. These are grinding and sifting, which can be made up to twenty times on the technological flow. After grinding, obtained grist is a mixture of particle with a wide variety of sizes and composition (bran, endosperm). In order to continue grinding the endosperm, up to the dimensions of flour, is required sorting on fractions of the grist, fractions that presents a certain particle size uniformity. This uniformity is necessary for structural and functional parameters of grinding equipment to be established in correlation to the size and composition of the particles of processed fraction. Within plansifter compartments, grist are sorted into fractions so that a certain percentage of flour to be extracted, and the rest to be divided on fractions that are returned to a grinding equipment, with well-defined structural and functional parameters.

This paper presents the results of laboratory tests on a grist obtained at the pair of grinding rollers of the first technological passage of reduction phase at a milling plant with capacity of 4.2 t/h, on the degree of extraction of sifted material from the initial mixture, according to the revolution speed of actuation mechanism and the amount of material at feeding.

INTRODUCTION

It is known that, in practice, sifting is never complete, in the sense that in the refuse of sieve will be found each time a percentage of undersize particles, which have not reached entirely to carry out the sifting conditions and were not separated. For a more complete sifting is required, either a sieve having a great length, either repeating several times of sifting on a identical separating surface, which leads to an increase in working time.

At sifting on sieves with oscillatory motion, for undersize particles can be separated, is first necessary for them to have time to pass through the apertures. Therefore, if sifting time is limited, a percentage of undersize particles (higher or smaller) may not never reach to be separated, first that small particles do not have time to traverse the general layer of material, and secondly because it will not have time to be engaged in passing through apertures. In order to be engaged in passing through the apertures, small particles must reach over apertures and then have time to fall vertical a height at least equal to half the thickness of wire, plus half the height of the particle. This percentage is correlated with kinematic regime of sieve, respectively with the amount of material that reaches the sieve in order to separate.

For plansifters at which the sifting movement is one of circular translation movement, is important, revolution of actuation mechanism (period of circular motion).

Efficiency of sifting process of plansifters can be determined by finding the amount (or number, for computer-assisted simulation) of undersize particles that are rejected by sieve together with oversize fraction, on each sieve of equipment. Different parameters of sifting equipment affect the performance of sieve, as ex.: revolution of equipment, feeding rate, inclination angle of sieves, eccentricity of actuating mechanism etc. Most of the paper from the specialty literature approaches the factors that influence the sifting efficiency, [1,2,3,4], but also kinetics of sifting, [5].

[1]Splaiul Independentei, 313, District 6, Bucharest, Romania, 0727651064, gabriel.constantin@upb.ro.

In paper [6], Alkhaldi and Eberhard (2007) presents a numerical model for studying of particles sifting process (using the discrete element method), which treats movement of each particle, individual. The authors analyze the influences that have inclination angles of sieves, type of feed, eccentricity and revolution of actuator mechanism of plansifters on sifting process.

Revolution of actuating mechanism should be chosen so that sorting on fractions to be as effective as, undersize particles have time to sift and not stay stuck in oversize fraction of the sieve, and larger particles but with sizes close to fabric apertures does not stay blocked in apertures, [6].

Kelly and Spottiswood, [7], claim that although some optimal height of the layer of material on the sieve is difficult to specify, there is a certain height that produces maximum of sifting efficiency. So, has been differentiated three types of stratification for which loading with particle are increased. Stratification I characterized by insufficiency of particles to form an even layer on the sieve surface, leading to a reduced rate of sifting, because the particles tend to move chaotically, and sifting surface is incomplete used. At Stratification II, have at least one uniform layer of particles which leads to greater efficiency of sifting. For this stratification particles have a controlled movement, and undersized particles have a higher probability of passing through the fabric aperture. Lowest efficiency of sifting occurs at Stratification III, when the particles layer is excessively high, and particle motion is almost blocked due to the large amount of oversized particles and insufficient separation of particles through the sieve apertures.

1. METHODOLOGY

At experimental determination was used a sample of grist from fraction that feed the plansifter compartment of reduction roll M1 of a milling plant. Testes were made at four different revolution speed (115, 125, 136, 150 rot/min) and three different quantities of material (100, 200 and 300 g) on a sieve shaker with circular translational motion, using a sieve with metal fabric with aperture side of 315 μm and active surface of 30.86%. For all samples the sieve was weighed (with refusal on it) every minute, on a 9-minute test period, to monitor the amount of undersized particles that is stuck in the refusal of sieve. The experimental results are shown in table 1.

It was considered that undersized particles separate completely (approximately) when at three successive determinations difference was less than 0.1 g. Curves drawn by regression analysis based on experimental points show an asymptotic variation, in the sense that the major part of the undersized particles was separated (see fig. 1).

In table, on columns P was noted the amount of undersized particles blocked in the refusal fraction. To know exactly when undersized particles were separated totally from refusal, during the experiments was drawn refusals curve aiming when it becomes asymptotic. Value from which the curve becomes asymptotic was found to be the boundary that separates refusal fraction from the sifted fraction, at this value sifting being almost complete. Watching values in table 1 can see that for some revolutions this boundary is not reached (100 g - n_4; 200 g - n_2; 300 g - n_1, n_2). In this case there are three possible reasons for which not have been reached the maximum efficiency: was required a higher time for sifting, stratification of material on sieve prevented the separation or revolution was too high.

From table 1 and fig. 1 it can be seen that in case of the samples of 100 g sifting maximum efficiency was obtained for revolution n_1 = 115 rot/min, although revolutions n_2 = 125 rot/min and n_3 = 136 rot/min had good results. For the first revolution was obtained the highest percentage of sifting after the first minute. It can be said, in case of revolution n_4 = 150 rot/min, that due to oscillation frequency too large particles tend to move uncontrollably after their trajectories on the sieve, thus preventing separation. Possible that if time were greater than 9 minutes, undersize particles may be separated, however, from the refusal fraction. For experimental data obtained at revolution n_4, amount of undersized particles stuck in refusal was calculated by deducting the value 21.9 % (corresponding to revolution n_1 and obtained at sifting time of 8 minutes) from sieve refusals value at each determination (in percentage).

Table 1. Influence of revolution and quantity of material subjected to sifting on separation efficiency

$M_{material}$ = 100 g												
	n_1 = 115 rot/min			n_2 = 125 rot/min			n_3 = 136 rot/min			n_4 = 150 rot/min		
Time, (min)	R (%)	T (%)	P (%)	R (%)	T (%)	P (%)	R (%)	T (%)	P (%)	R (%)	T (%)	P (%)
1	28.80	71.20	7.00	29.10	70.90	7.30	28.90	71.10	7.10	36.90	63.10	15.10
2	25.50	74.50	3.70	25.40	74.60	3.60	25.70	74.30	3.90	32.50	67.50	10.70
3	24.00	76.00	2.20	23.90	76.10	2.10	24.40	75.60	2.60	30.40	69.60	8.60
4	23.00	77.00	1.20	23.00	77.00	1.20	22.90	77.10	1.10	29.30	70.70	7.40
5	22.40	77.60	0.60	22.40	77.60	0.60	22.40	77.60	0.60	28.40	71.60	6.60
6	22.00	78.00	0.20	21.90	78.10	0.10	22.00	78.00	0.20	27.70	72.30	5.90
7	22.00	78.10	0.20	21.90	78.10	0.10	22.00	78.00	0.20	27.00	73.00	5.20
8	21.90	78.20	0.10	21.80	78.20	0.00	21.90	78.10	0.10	26.10	73.90	4.30
9	21.90	78.20	0.10	21.80	78.20	0.00	21.90	78.10	0.10	25.40	74.60	3.60
$M_{material}$ = 200 g												
	n_1 = 115 rot/min			n_2 = 125 rot/min			n_3 = 136 rot/min			n_4 = 150 rot/min		
Time, (min)	R (%)	T (%)	P (%)	R (%)	T (%)	P (%)	R (%)	T (%)	P (%)	R (%)	T (%)	P (%)
1	35.15	64.85	12.25	34.50	65.50	11.60	32.80	67.20	9.90	32.00	68.00	9.10
2	29.10	70.90	6.20	29.50	70.50	6.60	28.25	71.75	5.35	27.65	72.35	4.75
3	26.55	73.45	3.65	27.45	72.55	4.55	26.30	73.70	3.40	25.60	74.40	2.70
4	25.05	74.95	2.15	26.25	73.75	3.35	25.20	74.80	2.30	24.30	75.70	1.40
5	24.00	76.00	1.10	25.40	74.60	2.50	24.30	75.70	1.40	23.55	76.45	0.65
6	23.20	76.80	0.30	24.70	75.30	1.80	23.60	76.40	0.70	22.95	77.05	0.05
7	23.00	77.00	0.10	24.60	75.40	1.70	23.25	76.75	0.35	22.95	77.05	0.05
8	22.95	77.05	0.05	24.30	75.70	1.40	22.95	77.05	0.05	22.90	77.10	0.00
9	22.90	77.10	0.000	23.95	76.05	1.05	22.95	77.05	0.05	22.90	77.10	0.00
$M_{material}$ = 300 g												
	n_1 = 115 rot/min			n_2 = 125 rot/min			n_3 = 136 rot/min			n_4 = 150 rot/min		
Time, (min)	R (%)	T (%)	P (%)	R (%)	T (%)	P (%)	R (%)	T (%)	P (%)	R (%)	T (%)	P (%)
1	47.80	52.20	23.73	40.73	59.27	16.67	38.13	61.87	17.07	36.37	63.63	12.30
2	35.03	64.97	10.97	31.80	68.20	7.73	30.80	69.20	6.73	29.80	70.20	5.73
3	31.13	68.87	7.07	28.70	71.30	4.63	28.13	71.87	4.07	27.27	72.73	3.20
4	29.00	71.00	4.93	27.00	73.00	2.93	26.63	73.37	2.57	25.90	74.10	1.83
5	27.40	72.60	3.33	25.83	74.17	1.77	25.50	74.50	1.43	24.87	75.13	0.80
6	26.50	73.50	2.43	25.03	74.97	0.97	24.77	75.23	0.70	24.10	75.90	0.03
7	26.27	73.73	2.20	24.83	75.17	0.77	24.50	75.50	0.43	24.10	75.90	0.03
8	26.03	73.97	1.97	24.60	75.40	0.53	24.13	75.87	0.07	24.07	75.93	0.00
9	25.87	74.13	1.80	24.33	75.67	0.27	24.10	75.90	0.03	24.07	75.93	0.00

Experimental data, for percentages of refused material by sieves at every test minute, were correlated with the power law type using the program MS Excel 12.0, represented by the relation:

$$R(x) = \alpha \cdot e^{-\beta} \tag{1}$$

Values of coefficients α and β for experimental data correlated with power law type (ec. 1), and the values of correlation coefficient R^2 are shown in table 2. It can be seen that distribution law (1) correlates sufficiently well the experimental data, being obtained values of correlation coefficient of $R^2 \geq 0.939$.

Table 2. Coefficient values for experimental data correlated with power law type (ec. 1), α and β, and the coefficient of correlation R^2

Experimental parameters	n_1 = 115 rot/min			n_2 = 125 rot/min			n_3 = 136 rot/min			n_4 = 150 rot/min		
	α	β	R^2	α	β	R^2	α	β	R^2	α	β	R^2
$M_{material}$ = 100 g	28.021	0.127	0.950	28.175	0.132	0.948	28.248	0.130	0.953	36.676	0.162	0.995
$M_{material}$ = 200 g	33.795	0.198	0.961	33.474	0.163	0.973	32.007	0.164	0.981	30.979	0.156	0.950
$M_{material}$ = 300 g	44.123	0.272	0.939	38.360	0.229	0.950	36.378	0.207	0.961	34.607	0.188	0.940

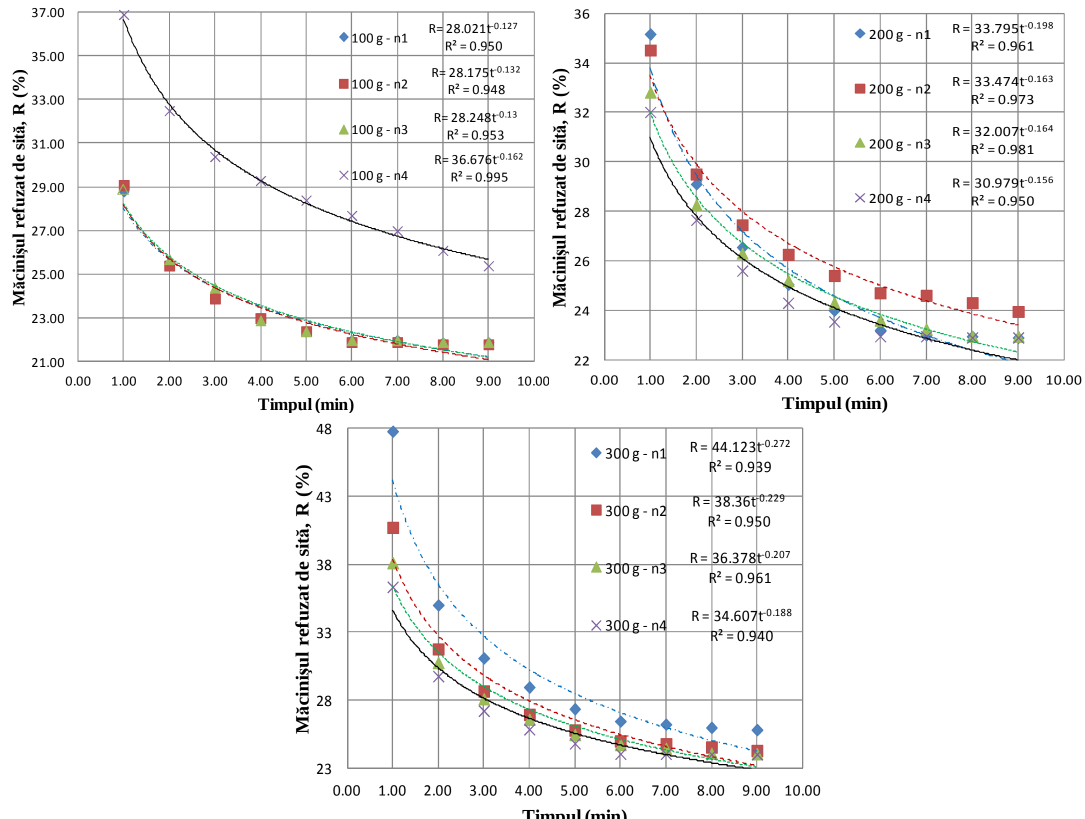

Fig. 1. Influence of the revolution speed on the efficiency of sifting process for three different quantities of material (100 g, 200g and 300 g)

In case of 200 g samples, maximum efficiency was achieved for revolution n_4 = 150 rot/min, although it can be seen (table 1 and fig. 1) the results are good for all the other three revolution. At revolution 150 rot/min small particles were separated in the shortest time, so that it can be said that in experimental conditions, undersized particles were separated from the fraction of refusal and managed to pass quickly through the sieve apertures. As in the case of 100 g samples, for amount of 200 g processed at revolution n_2 = 125 rot/min sifting is incomplete, being required more sifting time (probably still 1 – 2 minute). For this sample, the amount of undersized particles blocked in the refusal was calculated by deducting the value 22.95 % from the refusal values for each of the 9 minute test.

For 300 g samples total separation in a short time of undersized particles from the sample mass was also performed for revolution n_4 = 150 rot/min, separation being obtained in the range of 5-6 minutes from the beginning of sifting. Good results have been obtained in the case of revolution n_3 = 136 rot/min, but in the range of 8-9 minutes from the beginning of sifting. For revolutions n_1 = 115 rot/min and n_2 = 125 rot/min, sifting time was too small, and sifting was incomplete. For these two revolutions quantities of undersized particles blocked in refusal were obtained by deducting the value 24.10 % from sieve refusal values at every minute for the 9-minute test.

In fig. 2 is presented the influence of the mass of material on the effectiveness of sifting for the four revolution experienced. It can be seen that both the amount of material and revolution have a pretty big impact on complete separation of undersize particles from refusal fractions. For some samples, 9-minute test time was insufficient, and a certain amount of undersize particles remains stuck in refusal of the sieve. In the process of sifting stratification, being made by the density of the material, it seems that the revolution of actuating mechanism has an important influence.

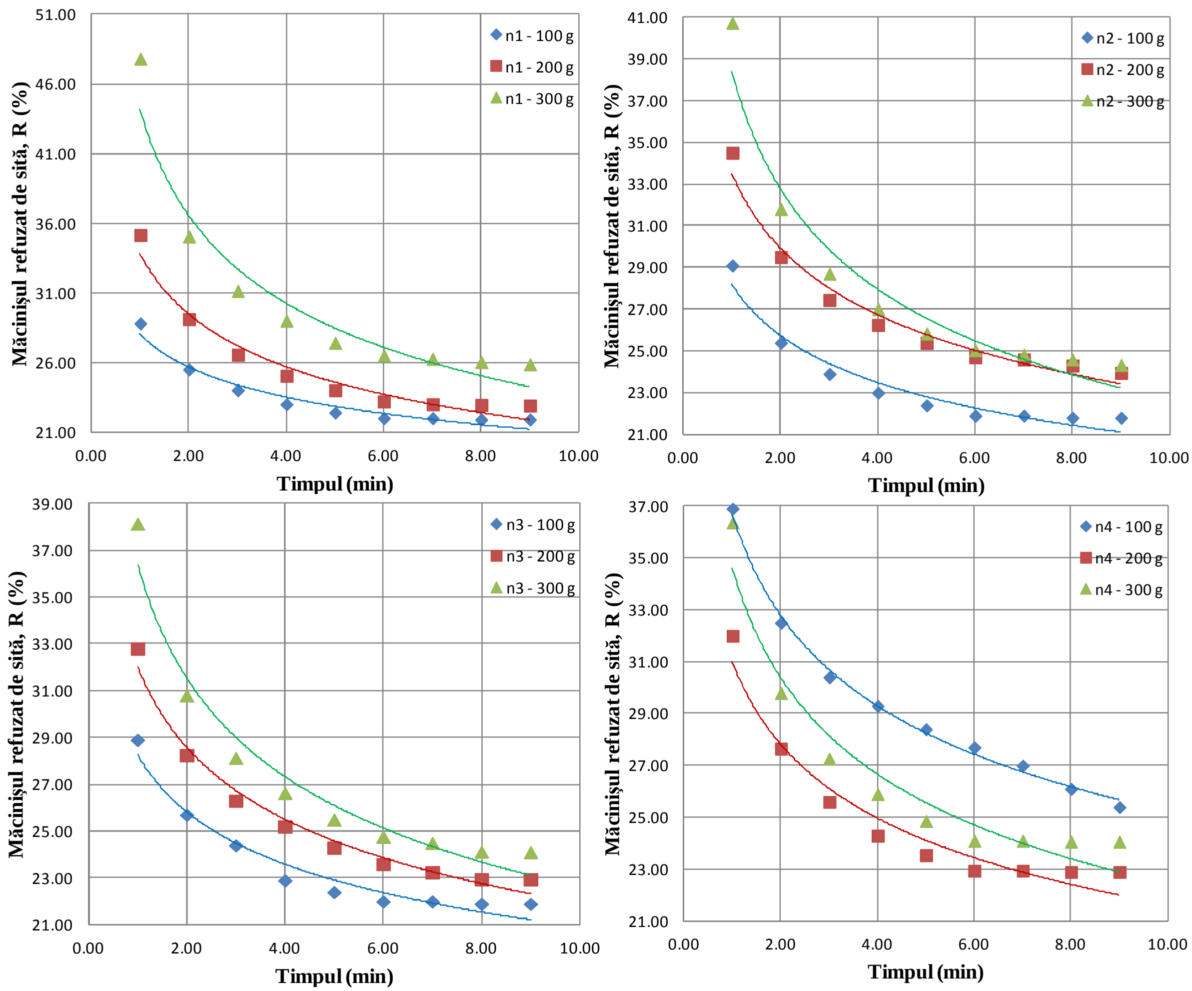

Fig. 2. Influence of the amount of material on the efficiency of the sifting process for the four revolutions (n_1 = 115 rot/min, n_2 = 125 rot/min, n_3 = 136 rot/min and n_4 = 150 rot/min)

Analyzing the data in table 1 and graphics from fig. 1 and 2 it can be said that at small amount of material on sieve (and, consequently, low height of material layer) are required small values of revolution (115 - 136 rot/min), high revolutions resulting in uncontrolled movements of undersize particles through the layer of material, while density stratification and individual particle mass worsens this process.

For average quantities of material are required average or high values of revolution (136 - 150 rot/min under the conditions of this experiment), but also low speeds showed good results. In the case of the average quantity of material, the speed range which can be used for separation is fairly broad, because it can get pretty good results and at low revolutions, but also at high revolutions.

In the case of large quantities (great heights of grist on sieve surface), in order to achieve high efficiency, high revolutions are required. Particles of refusal, tending to block the sieve apertures larger inertial forces are required to remove the refusal particles from apertures and sifting to be done in good conditions. At the same time, at high revolutions undersize particles get faster in contact with the sieve even if stratification is increasing and have a greater possibility to sift through the sieve aperture, if the time of engagement at passing through apertures is sufficient.

3. CONCLUSIONS

It was found that by increasing the revolution speed of actuating mechanism the percentage of undersize particles blocked in the refusal fraction increase at small amount of feeding material, in exchange for greater quantities of material, revolution increase is beneficial, undersize particles percentage blocked in refusal decreasing with increasing of revolution speed.

It follows that there is an optimum both for revolution value, and on the mass of feeding material at which undersize particles have enough time to go through the layer of material and then to be engaged in passing through the sieve aperture. For the analyze case this optimal corresponds to a revolution of 150 rot/min and a quantity of feeding material of 200 g (that is, the height of the layer of material of about 12 mm on the sieve).

References

[1] Jansen M., Glastonbury J., *The size separation of particles by screening*, Powder Technology 1, p.: 334-343, 1967;

[2] Standish N., Meta I., *Some kinetic aspects of continuous screening*, Powder Technology, 41, p.: 165-171, 1985;

[3] Standish, N., Bharadwaj, A., Hariri-Akbari, G., *A study of the effect of operating variables on the efficiency of a vibrating screen*, Powder Technol. **48**, 161–172, 1986;

[4] Li J., Webb C., Pandiella S., Campbell G., *Discrete particle motion on sieves – a numerical study using the DEM simulation*, Powder Technology, 133, p.:190 – 202, 2003;

[5] Kaye B., Robb N., *An algorithm for deducing an effective sieve residue from the rate of powder passage through a sieve*, Powder Technology, 24, p.: 125-128, 1979;

[6] Alkhaldy H., Eberhard P., *Particle screening phenomena in an oblique multi-level tumbling reservoir – a numerical study using discrete element simulation*, Granular Matter 9 (6), p.: 415-429, 2007;

[7] Kelly, E. G. and Spottiswood, D. J., *Introduction to Mineral Processing*, John Willey & Sons, New York, USA), pp 172 and 182, 1982.

HEAVY METALS REMOVAL FROM WASTEWATER USING MAGNETIC NANOMATERIALS BASED ADSORTION STRATEGIES

C.I. Covaliu[1]*, G. Paraschiv[1], S.Șt. Biriș[1], E. Matei[2], I. Filip[3], M. Ionescu[1]

[1]University POLITEHNICA of Bucharest, Faculty of Biotechnical Systems Engineering, Bucharest, Romania
[2]University POLITEHNICA of Bucharest, Faculty of Materials Science and Engineering, Bucharest, Romania
[3]University POLITEHNICA of Bucharest, Faculty of Mechanical Engineering and Mechatronic, Bucharest, Romania

ABSTRACT

In recent years, the removal of toxic heavy metal ions from sewage, industrial and mining wastewaters has been widely studied. Their presence in surface and underground water has been responsible for several types of health problems in animals and human beings. The present paper is focused on utilization of the magnetic nanomaterials adsorbents for the removal of heavy metal ions such as Cu^{2+}, Zn^{2+}, Cr^{2+}, Cd^{2+} and Ni^{2+} from model acidic wastewater. Quantitative elemental information regarding the wastewater treatment performance of two magnetic nanomaterials (Fe_3O_4, Fe_3O_4-PVP) was investigated by atomic absorption spectroscopy.

1. INTRODUCTION

The term “heavy metals” refers to any metallic element with atomic density higher than 4 g/cm^3 or five times or more higher than water, that has a relatively high density and is toxic even at low concentration [1]. The toxic heavy metals, existing in high concentrations (even up to 500 mg·L^{-1}), have to be efficiently removed from water. Some natural and antrophic source of drinking water pollution with heavy metals and their corresponding concentration related by U.S. Environmental Protection Agency are presented in Tabel 1.

Table 1. List of drinking water heavy metals pollutants [2]

Pollutant substance	**Concentration (mg/L) [2]**	**Sources of Pollutant in Drinking Water**
Cadmium	0.005	Erosion of natural deposits, anticorrosion coating, electroplating, alloying activity in solders, stabilizer in plastics (organic cadmium), pigments, drying of zinc concentrates and roasting, smelting, refining of ores corrosion of galvanized pipes, discharge from metal refineries, runoff from waste batteries
Zinc	7	Protecting steel against corrosion, brass and other alloys, automotive equipment, household appliances, fittings, tools, toys, building and construction, pharmaceuticals, medical equipment, cosmetics, tyres and rubber goods, fertilizers, animal feed.

*[1]313 Splaiul Independentei Street, 060042, Bucharest, Romania; +40722791791; cristina_covaliu@yahoo.com

Pollutant substance	Concentration (mg/L) [2]	Sources of Pollutant in Drinking Water
Chromium	0.1	Erosion of natural deposits, discharge from steel and pulp mills.
Copper	1.3	Erosion of natural deposits, industrial operations such as smelters, foundries, power stations, incinerators, various combustion sources, corrosion of household plumbing systems.
Lead	0.015	Erosion of natural deposits, corrosion of household plumbing systems, industries such as the petroleum, mining, smelting, lead-acid battery manufacturing, waste incinerating, mining industries.
Mercury	0.002	Erosion of natural deposits, discharge from refineries and factories, runoff from landfills and croplands, medicinal industry, cosmetics industry, waste incineration, coal combustion, base metal smelting, chlor-alkali industry.

Mining activities and other geochemical processes often are the sources of acid mine drainage formed when pyrite (FeS_2) and other sulphide minerals in the aquifer are exposed to air and water to produce metal ions, sulphate and acidity [3].

$$2FeS_2 + 7O_2 + 2H_2O \longrightarrow 2FeSO_4 + 2H_2SO_4$$
$$2FeSO_4 + 2H_2SO_4 \longrightarrow Fe_2(SO_4)_3 + SO_2 + 2H_2O$$
$$Fe_2(SO_4)_3 + 2FeAsS + 9/2O_2 + 3H_2O \longrightarrow 2H_3AsO_4 + 4FeSO_4 + S$$

If the wastewaters containing heavy metals were discharged directly into natural waters, will constitute serious risks for the aquatic ecosystem and public health, whilst the direct discharge into the sewerage system may affect negatively the efficiency of wastewater conventional treatment [3].

There have been reported the following toxic effects to the human body associated with cadmium, lead, arsenic, mercury, zinc, and copper poisoning: tremor, the gastrointestinal disorders, diarrhea, stomatitis, hemoglobinuria causing a rust–red colour to stool, ataxia, paralysis, vomiting and convulsion, depression, and pneumonia when volatile vapours and fumes are inhaled. The nature of effects may be toxic (acute or chronic), neurotoxic, carcinogenic, mutagenic or teratogenic [4].

The current physico-chemical processes for heavy metals removal as for example: precipitation, reduction, ion-exchange etc. are considered expensive and having low efficiency in treating large quantities.

One of the most efficient technologies for reducing or removal the heavy metal is through adsorption using various adsorbents; activated carbon being the most commonly used adsorbent [5].

Due to development in nanotechnologies, nanostructured materials have been developed for wastewater treatment Fig. 1.[6].

Recently, scientists have used magnetic iron oxides nanoparticles for removel of heavy metal ions and organic pollutants from wastewater [7]. This is because magnetic iron oxide nanoparticles have not only strong adsorption potential, but also the benefit of being easily separated and recover through the application of an external magnetic field [8,9].

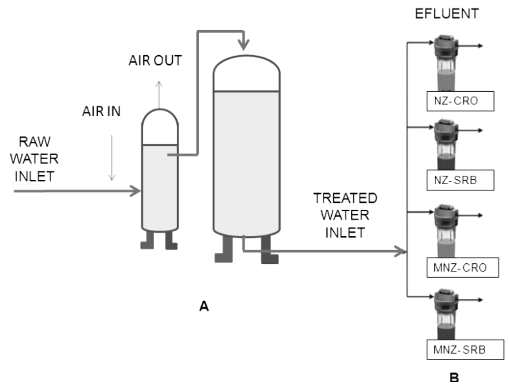

Figure 1: Scheme of drinking water production plant (A) and pilot plant “filter guards” (B) using nanostructured adsorbants (NZ-, MNZ-CRO natural and modified zeolite from Croatia; NZ-, MNZ-SRB natural and modified zeolite from Serbia).

2. METHODOLOGY

Two nanomaterials, magnetite (Fe_3O_4) and a hybrid (magnetite coated with polyvinylpyrrolidone, noted as Fe_3O_4-PVP) were used as adsorbents for Zn (II), Cd (II), Cu (II), Cr (VI) and Ni (II) from synthetic aqueous wastewater Table 2.

Table 2. Wastewater treatment efficiency (η %) of two nanomaterials studied on metal ions (Cr, Cu, Zn, Ni, Cd)

Metal ion	**C₀,**	**Fe_3O_4, η %**			**Fe_3O_4-PVP, η %**		
	mg/L	0.05 g	0.1 g	0.2 g	0.05 g	0.1 g	0.2 g
Cr (VI)	20	80	79	78	82	80	80
	50	78	77	76	78	71	72
	100	79	75	70	75	69	68
Cu (II)	20	76	76	72	75	72	70
	50	75	74	70	72	70	67
	100	75	73	68	70	66	65
Zn (II)	20	76	74	71	75	72	69
	50	75	72	70	72	70	68
	100	74	71	67	70	66	64
Ni (II)	20	74	70	69	70	68	65
	50	72	68	67	68	66	64
	100	69	65	64	67	65	64
Cd (II)	20	70	68	65	76	75	73
	50	67	65	61	74	73	72
	100	65	63	60	74	72	70

It can be seen that the maximum efficiency is up to 80% for Cr(VI) and between 74 – 76% for the other heavy metals. For uncoated Fe_3O_4, the percentage of removal efficiency decreased in the order: Cr(VI) > Cu(II) > Zn(II) > Ni(II) > Cd(II).

Adsorption can be explained by the zero point of net charge pH_{pnzc} of magnetite which is 6.5. Below this value, the adsorbent surface is more positively charged and anions are adsorbed by electrostatic attraction. Above this value of pH_{pnzc}, the adsorbent surface is more negatively charged and the metal ions are adsorbed on the magnetite.

The uptake of Cr (VI) ions will decrease with an increase of pH, because in the aqueous phase the surface of the metal oxides is covered with hydroxyl groups that vary at different pH values.

The available sites for nanoparticles are mostly present on the surface and based on this assumption a higher surface area will provide more sites for adsorption.

With respect to the Fe_3O_4-PVP hybrid (45% wt Fe in mass of polymer) the adsorption phenomena appears as follows: Cr(VI) > Cd(II) > Cu(II) ~ Zn(II) > Ni(II) (Table 2). The adsorption could be explained based on the tendency of nitrogen or oxygen from polymer composition to bind the heavy metal ions from wastewater. The results indicate that Fe_3O_4-PVP maintained the removal efficiency for metal ions at approximately the same values as for the uncoated Fe_3O_4. The values indicate that Fe_3O_4-PVP hybrid is a good adsorbent for studied heavy metal ions.

3. CONCLUSIONS

The aim of this study was to demonstrate the use of magnetic nanomaterials as adsorbent for removal of heavy metal ion. The hybrid Fe_3O_4-PVP could be used as adsorbent with the same performance as uncoated Fe_3O_4 having the advantage of its stability in real conditions when the industrial wastewaters have a low pH value.

References

[1] Hutton M, Symon C, The Quantities of Cadmium, Lead, Mercury and Arsenic Entering the U.K. Environment from Human Activities, Sci. Total Environ., 57, 129-150, 1986.

[2] http://www.epa.gov/safewater/mcl.html#/mcls

[3] Ogwuegbu M.O.C., Muhanga W., Investigation of Lead Concentration in the Blood of People in the Copperbelt Province of Zambia, J. Environ.,1, 66 – 75, 2005

[4]Matis K.A., Zouboulis A.I., Gallios G.P., Erwe T. and Blocher C., Application of flotation for the separation of metal-loaded zeolites, Chemosphere, 55, 65–72, 2004.

[5] Lo M.C.I., .Hu J., Chen G., Iron-Based Magnetic Nanoparticles for Removal of Heavy Metals from Electroplating and Metal-Finishing Wastewater, 213-264. In Zhang C.T. et al. (eds.) American Society of Civil Engineers, Virginia, 2009.

[6] McCluggage D., Heavy Metal Poisoning, NCS Magazine, Published by The Bird Hospital, CO, U.S.A., 1991 (www.cockatiels.org/articles/ Diseases/metals.html).

[8] Liang X., Xi B., Xiong S., Zhu Y., Xue F., Qian Y., Porous soft magnetic material: The maghemite microsphere with hierarchical nanoarchitecture and its application in water purification, Materials Research Bulletin. 44: 2233–2239, 2009.

[9] Booker N.A., Keir D., Priestley A.J., Ritchie C.B., Sudarmana D.L., Woods M.A., Sewage clarification with magnetite particles, Water Sci. Technol., 23, 1703–1712, 1991.

[10] Orbell J.D., Godhino L., Bigger S.W., Nguyen T.M., Ngeh L.N., Oil spill remediation using magnetic particles—an experiment in environmental technology, J.Chem. Educ., 74,1446–1448, 1997.

STRUCTURAL ANALYSIS OF THE RECIPROCATING ROD IN THE DRIVING MECHANISM OF THE MAS-220 MACHINE

PhD. Stud. Eng. Alexandru-Dorin David - National Institute of Research - Development for Machines and Installations Designed to Agriculture and Food Industry - INMA [1],
PhD. Eng. Edmond Maican – University Politehnica of Bucharest, Faculty of Biotechnical Systems Engineering [2],
PhD. Eng. Gheorghe Voicu – University Politehnica of Bucharest, Faculty of Biotechnical Systems Engineering[3],
PhD. Eng. Mihaela Florentina Duţu - University Politehnica of Bucharest, Faculty of Biotechnical Systems Engineering[4]

ABSTRACT

The deep soil loosening machine MAS – 220 is a mounted machine with active furrows powered by means of a quadrilateral mechanism from the tractor's PTO. Following the kinematic analysis of the driving mechanism one can determine the stress from the main component parts. Structural analysis determines the minimum and maximum values of the total deformation and equivalent stresses in the analyzed structure, allowing its shape and size optimization.

1. INTRODUCTION

The driving mechanism of the deep soil loosening machine consists of crank handle (1), reciprocating rod (2), reciprocating lever (3) and four rotation couplers (R). It contains the initial mechanism, driving group R and modular group 3R.

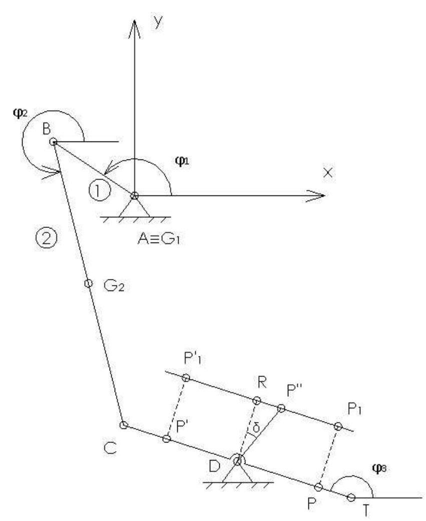

Figure 1: The diagram of the quadrilateral mechanism

The deep soil loosening machine MAS – 220 is mounted on the three-point hydraulic system on 180-220 HP tractors and has the following main features [1]:

[1]Bd. Ionescu de la Brad Ion, 6, Bucuresti-Sector 1, Bucuresti, somy_alex_07@yahoo.com
[2] Splaiul Independenţei, nr.313, corp D, sector 2, Bucureşti, e.maican@gmail.com
[3] Splaiul Independenţei, nr.313, corp D, sector 2, Bucureşti, 0214029649, ghvoicu_2005@yahoo.com
[4] Splaiul Independenţei, nr.313, corp D, sector 2, Bucureşti, 021.402.9637, dutumihaelaflorentina@gmail.com

- The number of active parts – 2
- The mobile blade oscillation frequency – 9.16 Hz
- Maximum working depth – 80 cm
- The amplitude of the oscillations – 18 mm

2. METHODOLOGY

When tested in field conditions with the T-195 tractor on compacted soil in the experimental perimeter from INMA, a 160 daNm driving torque and a traction force of 4580 daN were recorded.

The components of reaction R_{12} in joint B for a rotation of the crank, have a variation shown in Figure 2.

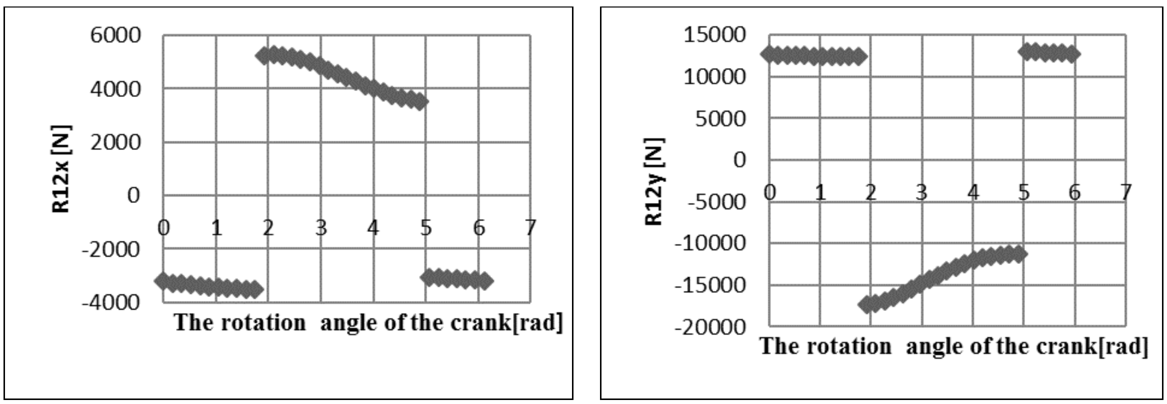

Figure 2: The variation of reaction R_{12} on the coordinate axes depending on the angle of rotation for the crank

The connecting rod of the quadrilateral mechanism driving the cutter of the deep soil loosening machine is subject to tension when the cutter angle of rotation ω_3 is less then zero, and compression when $\omega_3 > 0$ (the angle of rotation of the crank $f_1 = 1.92 \div 4.88$ rad). Figure 3 shows the variation of reaction R_{12} on the coordinate axes and in Figure 4 the variation of reaction R_{12} depending on the angle of rotation for the crank when $\omega_3 > 0$.

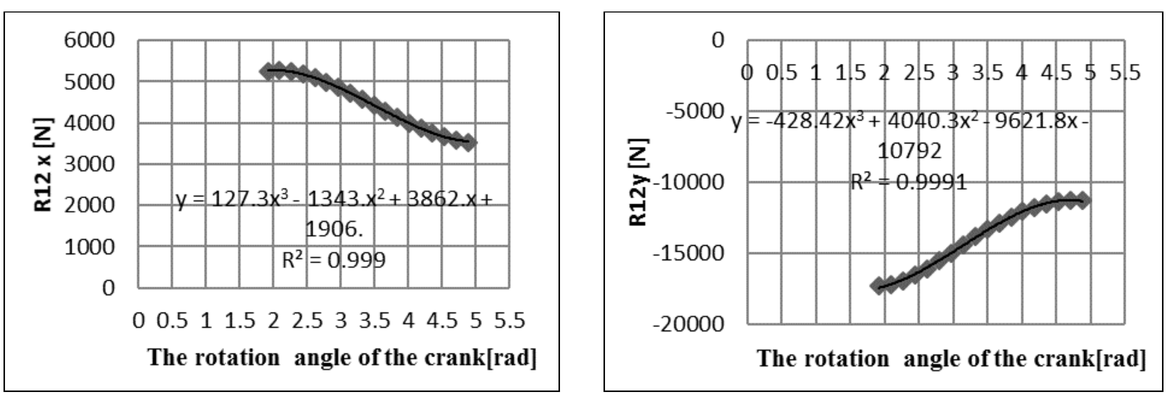

Figure 3: The variation of reaction R_{12} on the coordinate axes for compressive stresses ($\omega_3 > 0$)

Formulas for calculating these reactions are:

$$R_{12xi} = 127.3 \cdot \varphi_{1i}^{3} - 1343 \cdot \varphi_{1i}^{2} + 3862 \cdot \varphi_{1i} + 1906$$

$$R_{12yi} = -428{,}42 \cdot \varphi_{1i}^3 + 4040{,}3 \cdot \varphi_{1i}^2 - 9621{,}8 \cdot \varphi_{1i} + 10792 \quad (1)$$

$$R_{12i} = 446.2 \cdot \varphi_{1i}^3 + 4251 \cdot \varphi_{1i}^2 + 10319 \cdot \varphi_{1i} + 10885$$

where $i = 1 \div 36$ is the crank position corresponding to one complete rotation.

The compressive forces reach a maximum for the position i = 12 of the mechanism, were the angle of rotation of the rod $\varphi_{12} = -1.284$ rad has the maximum value (rotational angle of the crank $\varphi_1 = 1.92$ rad), while the connecting rod and crank are overlapping and point C is in the highest position. The maximum value of compressive forces is $R_{12} =$ 18075.21 N and are distributed on half of the surface of the bearing.

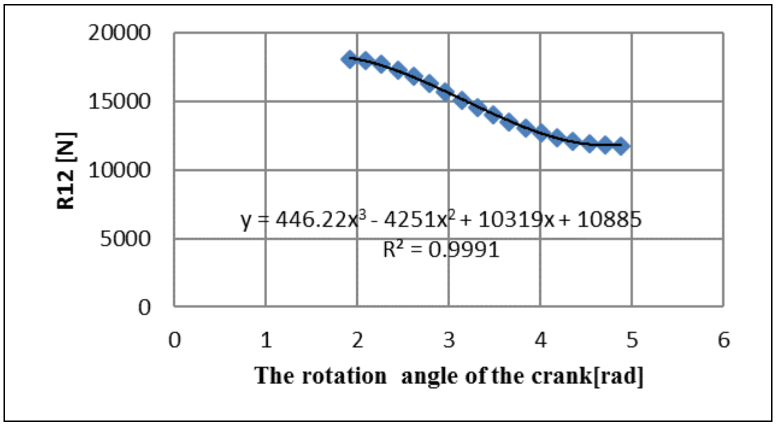

Figure 4: The variation of reaction R_{12} depending on the crank angle of rotation, for $\omega_3 > 0$.

The geometry of the connecting rod is generated in the CAD program SolidWorks and is shown in Figure 5. Structural analysis is performed using the finite element analysis program ANSYS.

Figure 5: 3D model of the rod

The structure has five solid components that are considered in contact with connection type "Bonded", that work together as a single body. Meshing is made with tetrahedral 3D type elements (Figure 6) and contains 11025 elements and 21417 nodes.

The structural analysis type is static linear elastic. The structure is loaded on the bearing with a force specified by means of its three-components. Figure 7 shows the surface on which the force is acting. The structure of both the rod as well as the other component is built of steel, with material the following constants:

- mass density: 7850 kg/m3;
- 250 MPa yield strength (both tensile and compressive);
- tensile ultimate strength: 420 MPa.

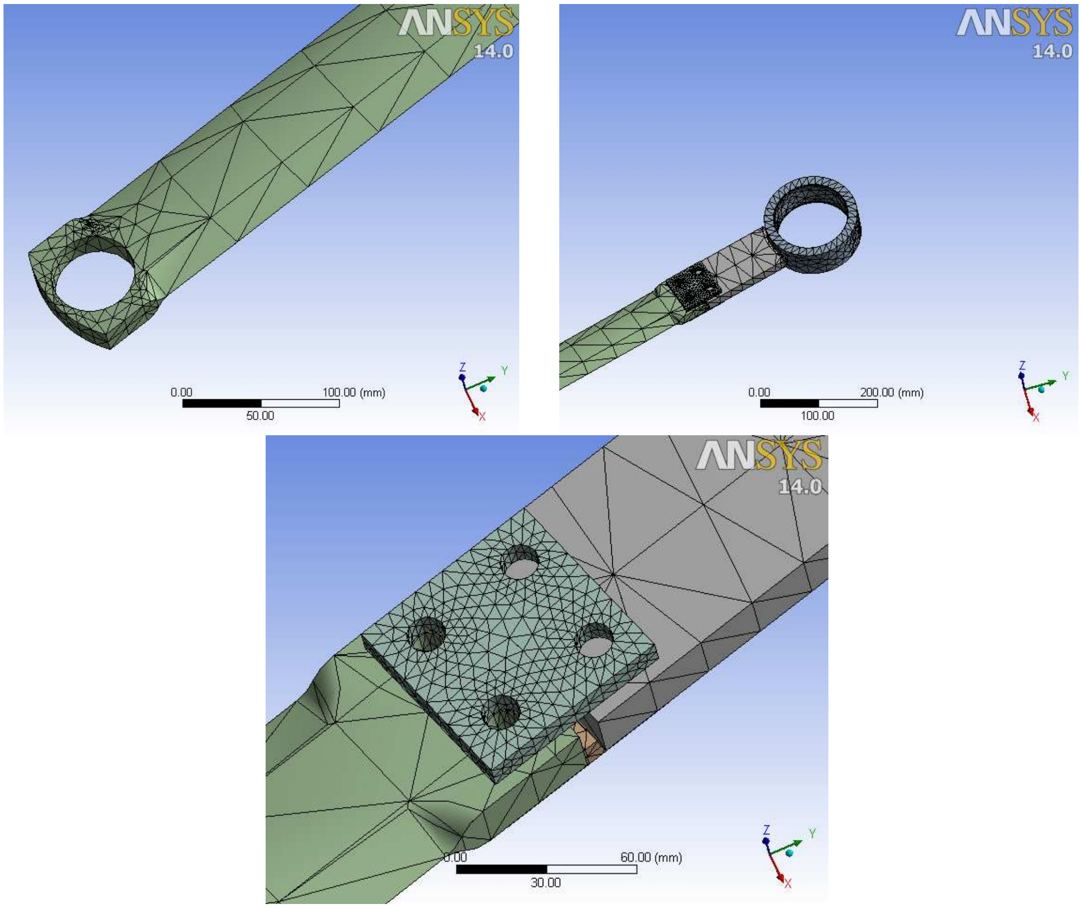

Figure 6: Meshing the rod with 3D tetrahedral elements

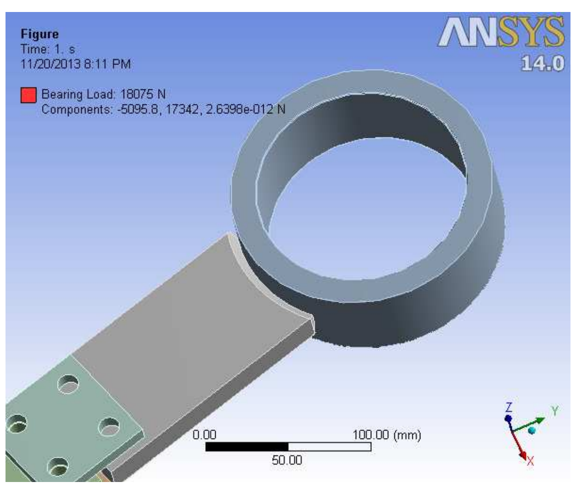

Figure 7: Loading in the plane xOy

Main results of the analysis is the minimum and maximum total deformation (Figure 8) and equivalent stress in the structure analysis. The distribution of equivalent stress is presented in Figure 9 and in Figure 10.

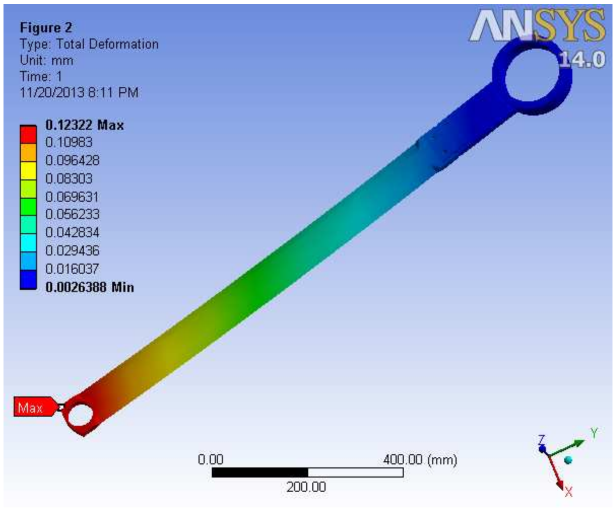

Figure 8: The total deformation distribution values

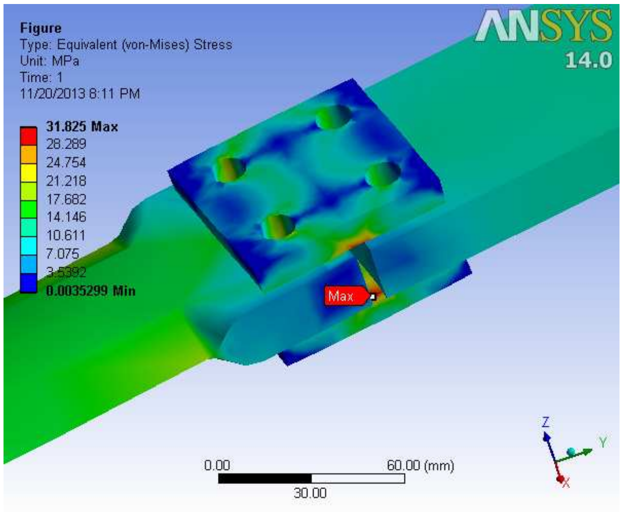

Figure 9: The equivalent stress values distribution in the area of connecting plates

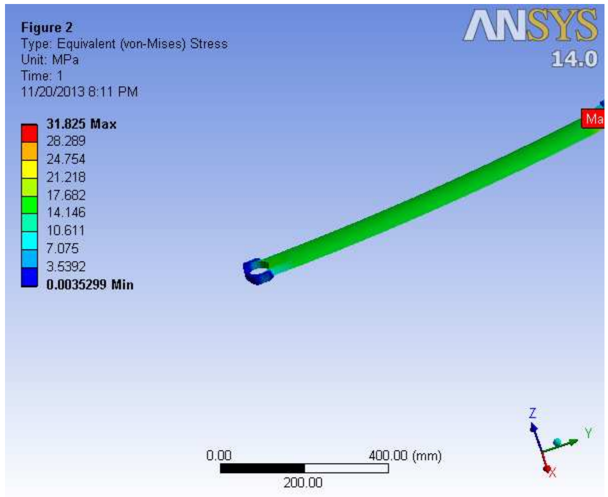

Figure 10: The equivalent stress values distribution for the entire arm

Main results of the linear static analysis are summarized in Table 1.

Table 1. The results of structural analysis of the connecting rod

	Equivalent stress, [MPa]	Total deformation [mm]
Maximum value	0.003	0.003
Minimum value	31.825	0.123

3. CONCLUSIONS

The main conclusions resulting from the structural analysis of the rod from the cutter drive mechanism are:

- The entire structure works in a linear elastic domain, considering that the maximum equivalent stress (31.825 MPa) is much lower than the material's tensile yield strength (250 MPa);
- The area the most intensely used, under the given circumstances, is at the clamping plates of the two parts of the connecting rod arm, in their midst, on the side contacting the arm. The arm undergoes a bending effect.
- The maximum relative deformation takes place in the opposite zone of the ring where the structure is loaded, the maximum value being of the order of one tenth of a millimeter;
- Safety factor calculated in relation to the yield strength (ratio between the material's yield strength and the maximum equivalent stress) is 7.85, which is much too large for agricultural machinery structures, where a normal coefficient should take values between 3 and 3.5.

References

[1] *Vergil Gangu, Cojocaru Iosif, Constantin Nicolae, Koloszvari Constantina,* Prototype test report for the deep soil loosening machinery for 180-220 HP tractors MAS - 220, produced within the method of improving water resources and soil air by conducting a soil deep refining machinery tractors destined for 180 - 220CP, Bucharest,2005

THE COMMON AGRICULTURAL POLICY IN THE EUROPEAN UNION AND ROMANIA: PAST, PRESENT AND FUTURE

Oana David[1], Sanda Maiduc (Osiceanu)[2]
University Politehnica of Bucharest

ABSTRACT

This paper aims to make a foray into the Common Agricultural Policy of the European Union since its occurrence, showing that evolution has had over the years. It illustrates the main ideas that started the realization of this policy, the advantages and disadvantages inherent in something new. Along came time passed a series of amendments aimed at improving policy and adapt it to situations arising in the new Member States of the EU, as is the case of Romania. It also presents an overview of the common agricultural policy for the coming years.

1. INTRODUCTION

A decade after the Community started its activity, agriculture represented one of its main sectors, which was the reason of including it into the *Treaty of Rome* or the *Treaty establishing the European Economic Community* (TEEC), signed by Germany, France, Italy, Belgium, Luxembourg and the Netherlands on March 25, 1957 and became effective on January 1, 1958.

The first approach of the Common Agriculture Policy (CAP) targeted objectives such as the increase of efficiency via promoting the technical advancement and providing the logical development of the agricultural production, as well as the optimum use of the production factors, the assurance of decent life standards for the people in rural areas, regulation of the markets, guarantee in the security of supplies and also in affordable prices for the agriculture products towards the consumer.

Along the years, CAP has matured itself in an attempt to be able to face the incoming challenges, as below: responding to the surging concerns related to the food safety in the European Union and worldwide; improving the sustainable management of certain natural resources, as water, air, biodiversity and the soils; dealing with both rising pressure upon the agriculture production conditions, derived from the ongoing climate changes and also the necessity that the agriculture workers reduce the greenhouse gas emissions; maintaining and increasing competitiveness in a world defined by a more visible globalization and a higher price volatility; a better use of the diversity in the agriculture structures and of the production systems in the EU.

2. PAPER CONTAIN

At the beginning, CAP focused on boosting the increase in the agriculture production in order to provide the consumers with a constant supply with food products at affordable prices and also to build a viable agriculture sector for the European Union. The CAP has helped the agriculture workers receive grants and systems that guaranteed them high prices to stimulate a higher production. There were also the financial aids that aimed to reorganize the agriculture, as well as to support the investments in farms for a better ability to manage and develop their

[1] Splaiul Independentei nr.313, sector 6, Bucharest; 0040214029268 and davidgioana@yahoo.com
[2] Splaiul Independentei nr.313, sector 6, Bucharest; 0040214029742 and sanda.osiceanu@gmail.com

technological skills so as to be able to adjust to the economic and social conditions of that time. CAP has also brought a positive contribution to the economic growth and succeeded to secure the supply of the European consumer with a wide range of food products at affordable prices. Thus, until the mid 90's, CAP represented the most important community policy and the European Union turned into the main world exporter of agriculture products. The system showed a series of flaws when the Community started piling large food quantities, thus being compelled to raise its tax percent that required the collective agreement of the member states.

In June 1992, the Board of Agriculture formally adopted the CAP Reform. Even though the level of expenses has remained the same, the measures taken have eliminated the expansionist dynamics of CAP and prepared the ground for the future reform.

Agenda 2000 brought new changes to CAP, in lowering the subventions by 15% for grains and 20% for the beef meat, without substantially affecting the subventions for the dairy products. The *Agenda 2000* reform backed up the competitiveness of the European agriculture and introduced a new and fundamental element – the policy of rural development meant to boost numerous rural initiatives by supporting the agriculture workers in the restructuring of the farms and in the diversifying and improving the sales of the products.

In 2003, a new common reform in the agriculture policy was agreed upon – those measures are still applied to this day, where the key element is the demand and the agriculture workers are no longer paid to only bring forth products.

The agriculture sector in Europe uses safe, clean, ecological production methods, which provides getting quality products that satisfy the needs of the consumer. The agriculture sector of the European Union serves the rural communities and its role is not to generate food but to secure the survival of the rural area and help with its tourism development.

Currently, the main actions of CAP consist in the growth of farms efficiency and granting incentives. In time, they have led to a significant increase in the production level and self-supply, as the earnings of the farms rose along with a step-up in their size (the farms would merge when the agriculture workers left this sector).

The issue of the surpluses has been solved by their withdrawal from the market and by subsidizing the storage of the products or by a funded exploitation of the products in third countries, so as to avoid the price lowering of the farm production.

One of the most important exigencies of CAP is the quality of the food products. The Union defends this exigency via diverse measures, such as increase in the safety and hygiene of the food products, definition of clear labeling norms, regulations concerning the health of animals and plants with a focus on the welfare of animals, the control of the pesticide residues and of the additives in the food products, as well as supply of information regarding the nutritional qualities of the food products. Starting with the 1992 Summit in Rio de Janeiro, known as the United Nations Conference on Environment and Development (UNCED), the issue of protecting the environment, people and animals has gained a new form, as the most developed countries started the marathon of adopting and implementing the ecological policies. Today, the European Union is the leader in the environment protection sector from the perspective of norms.

The ecological measures have been implemented, mainly within CAP, and the ecological agriculture represents a production method that preserves the structure and fatness of the soil, promotes a high standard of animal welfare, and avoids the use of pesticides, herbicides, of the chemical fertilizers or of the growth stimulants, as well as antibiotics or the genetically modified organisms. Another CAP segment targets the assistance for the rural communities by various means, such as training for new agriculture techniques and rural crafts; support for the accommodation of the young agriculture workers; assistance for the agriculture in the mountain areas and in other disfavored zones; boosting the tourism; preservation and protection of the rural heritage, etc.

In order to meet the CAP goals, a complex system of rules and mechanisms has been set up that regulates the production, trading and the processing of the agriculture products, systematically grouped under the name of Common Market Organizations, which has replaced in time the similar national associations in the respective fields, under the jurisdiction of CAP. To implement the common measures of regulating the markets, the Community has available the following instruments, such as the prices, the intervention in the market, the financial aids, the production quotes, the joint customs protection.

As for the prices and at the request of the European Commission and following the consultation with the European Parliament and the Board of Ministers, the Commission sets up three distinct prices, artificially, at the beginning of every trading campaign: an indicative price, a threshold price (a minimum price agreed in trading the important products) and an intervention price (a guaranteed minimum price). The other types of assistance consist in farm payments, production aids, subsidies for raising cattle or compensatory amounts. The purpose of financing is to stimulate the trading and the competition of the products. Similarly, measures of market aid are being taken when sick animals are identified.

Since January 1, 2007, Romania has been a full-right member state of the European Union. As a member, Romania is entitled to all the privileges granted to a new member state less economically developed (aids from the Union budget to various precarious activity sectors); at the same time, Romania must comply with the common regulations, from which CAP does not make any exceptions. Since the pre-accession time, Romania has been imposed to adopt a series of legal regulations and norms specific to the European Union, such as the implementation of the community *acquis* or the restructuring of various key sectors (justice, army, industry, economy, etc.).

According to the report of the Department of Agriculture, Food and Forestry in the year of 2001, the contribution of the agriculture and forestry to the Romania GDP between 1989 and 2000, was constantly significant, thus asserting an increase from 13.7% in 1989 to 18.6% in 1992. This percentage was maintained until 1996, and then it lowered to 12.9% in 1999 and 11.4% in 2000. The rural areas in Romania are spread on 87.1% throughout the country, including circa 45.1% of the production. For 2007-2013, the Department of Agriculture, Food and Forestry created the National Program of Rural Development, meant to investigate the current status of the Romanian agriculture, to provide a general perspective and, finally, to help drafting the plans by which the Romanian citizens will be able to benefit from the structural funds derived from the budget of the European Union.

The plan proves the desire of Romania to fully implement the community regulations in the field of CAP; the following step is to establish, in accordance with the art 68 in the EC Regulation 1698/2005, the National Network of Rural Development, with the purpose of classifying (at a national level) the organizations and the authorities involved in the process of rural development. Its objectives were to build an agriculture and forestry economy, based on exploitations that will favor modernization, biodiversity and environment preservation, improvement in the life quality and the economic development in the rural space, the progress in the local governance so as to devise and apply the strategies for local development.

Romania finds itself in a privileged position from the perspective of the agriculture resources; since the agriculture areas in our country amount to 39.5% of the total surface of the territory, this is often looked at as the main beneficiary of the CAP funds.

Likewise, beyond the opportunities that Romania has in terms of the European funds, the application of a more stable and predictable regulation framework as a result of CAP implementation could have positive effects upon the freeze of prices. The full capitalization of the advantages brought about by the Romania's accession into the European Union could open new doors for the Romanian farmers who can supply a market with a population exceeding 80 million people.

While the agriculture policies and the official institutions have formally fulfilled all the criteria of accession to the European Union, the agriculture sector itself is not ready yet to efficiently use the opportunities in sight and appropriately respond to the new challenges.

Even though Romania has 14.7 million hectares of agriculture land, the crops are rather modest and very vulnerable to weather extremes, while the animals raising takes usually place at small size farms. Romania is not able to cater to its internal needs of agriculture and food products, which led to a constant deficit of the balance of trade during the post-communist time that exceeded 1.8 billion euros in 2007.

While the agriculture percentage in GDP decreased to only 6.6% at the beginning of the 90's, this was much higher than the European average in 2005. Also, the percentage of the people employed in agriculture is still very high. After a peak of 41% between 1999 and 2001, when a large part of the laid off workers in the mining and processing industry joined the agriculture sector, it remained constant at 30% in 2006.

The three main objectives of the future CAP up to 2020 will be:

1. *Viable food production*, which aims to derive agriculture income and limit its variability, to improve the competitiveness of the agriculture sector.
2. *Sustainable management of natural resources and climate action* intends to guarantee the sustainable production practices and secure improved supplies of environmental public goods.
3. *Balanced territorial development* involves supporting the rural employment and maintaining the social structure of rural areas.

3. CONCLUSIONS

Generally speaking, CAP was created with the purpose to bring performance to the economies of the European Union member states.

This context can only be a win situation for Romania, so much for the fact that our country has optimum conditions to develop a strong agriculture to support the state economic sector. All this will be possible by a surging interest of the authorities to the needs of the citizens, a support of their projects and a real interest in guiding the young farmers. In order to secure the assurance of stability and continuity of the current CAP, so as to facilitate the long-term planning for the operators along the food chain, this should rely on the aspects working well and focus on the adjustments and improvements of the issue of fair allocation of direct payments among the member states.

The policy development should make sure that this one becomes more sustainable and a better balance is possible among its various objectives, agriculture workers and the member states. A more ample reform of CAP should track a stronger concentration upon the environment-related objectives and to the climate change, plus to a gradual abandonment to the income aid for most market measures.

All of the above feature clear, yet different, advantages and disadvantages from the perspective of fulfilling the CAP goals, consisting in both major changes requiring a new project and also an improvement of the elements proved useful within the current policy, thus aiming to become a more sustainable policy, more balanced, better oriented, more simple and efficient, to better respond to the needs and expectations of the EU citizens.

References

[1] Moga, T., Radulescu, C.V., *Dezvoltarea complexa a spatiului rural*, vol.1, Publishing ASE, Bucharest, 2006
[2] http://europa.eu/pol/agr/index_ro.htm
[3] http://www.europarl.europa.eu
[4] http://mmediu.ro

THE INFLUENCE OF HEAVY METALS ON BIOGAS PRODUCTION DURING THE ANAEROBIC DIGESTION PROCESS

Mirela DINCĂ[1,*], Georgiana MOICEANU[1], Gigel PARASCHIV[1], Gheorghe VOICU [1]
Nicoleta UNGUREANU[1], Laura TOMA[1], Mariana IONESCU[1]
[1]University POLITEHNICA of Bucharest, Faculty of Biotechnical Systems Engineering, Biotechnical Systems Research and Development Center
* E-mail: mirela_dilea@yahoo.com

ABSTRACT

Availability of heavy metals plays a very significant role in the performance and stability of biogas digesters, which are operated with energy crops, organic fraction of municipal solid wastes or any other type of organic waste. Heavy metals are present in significant concentrations in animal manure and in some industrial wastewaters. Heavy metals can be stimulatory, inhibitory, or even toxic in biochemical reactions, depending on their concentrations. A trace level of many metals is required for activation or functioning of many enzymes and co-enzymes. Excessive amounts, however, can lead to inhibition or toxicity, [3].

The aim of this paper is to investigate the effect of heavy metals on biogas production during the anaerobic digestion process of biomass resources, such as animal manure and the organic fraction of agriculture waste.

1. INTRODUCTION

Production of biogas through anaerobic digestion is considered to be the optimal treatment for animal manure, as well as of a wide variety of organic wastes suitable for this purpose, because these substrates are converted into renewable energy and into fertilizer for agriculture, [1].

The main constituents of biogas are methane and carbon dioxide, but it can also contain, depending on the source's composition, trace or significant quantities of undesirable contaminants, such as hydrogen sulphide, ammonia and siloxanes whose presence can cause corrosion, erosion, and fouling to the thermal or thermocatalytic device and generate hazardous emissions. Therefore, biogas quality (purity and composition) is very important, and its purification represents a crucial final step of the overall production process in view of its final application. The processes currently employed for biogas purification are physicochemical (chemical absorption in aqueous solutions and adsorption on solid adsorbents, catalytic oxidation over activated carbons, and scrubbing with solvents or other liquid phases) or biological. The latter processes are widely used for the removal of H_2S from biogas and are considered economical and ecological, [2].

Biogas installations, processing agricultural substrates, are some of the most important applications of anaerobic digestion today.

The European Directives relating to the renewable energy production, the reduction of greenhouse gas emissions and sustainable waste management is based on the commitment of Member States to implement appropriate measures to reach them. Biogas production from anaerobic fermentation process and its use has the potential to satisfy all three targets, simultaneously.

Also, the Europe 2020 Strategy for smart growth, sustainable and favorable to inclusión is focused on three major objectives of the E.U., namely: the Member States have pledged to reduce by 20% greenhouse gas emissions (GHG), to increase to 20% the share of renewable energy in the EU energy mix and fulfill the objective of increasing energy efficiency by 20% until 2020.

The biogas production by anaerobic fermentation process and its use provides many socio-economic benefits, but also environmental, such as, [1]:

- ✓ renewable energy source;
- ✓ reduced greenhouse gas emissions and mitigation of global warming;
- ✓ contribution to the integration with the European Union for energy and the environment;
- ✓ reduction of biodegradable waste by their recovery as biogas and digestate (excellent fertilizer for agriculture);
- ✓ reduction of odors from zootechnical manure and from other organic wastes;
- ✓ is monitored the complex relationship health - environment;
- ✓ additional source of income for the agricultural sector.

The aim of this work was to investigate the role of the heavy metals concentration on the production of biogas during the anaerobic digestion of animal manure combined with fresh residual biomass.

2. FUNDAMENTALS OF MICROBIOLOGY IN ANAEROBIC DIGESTION PROCESS

The anaerobic degradation process has been used for years for energy production and waste treatment. Anaerobic digestion is the process of decomposition of organic matter by a microbial consortium in an oxygen – free environment. Anaerobic digestion involves a series of metabolic reactions such as hydrolysis, acidification, acetogenesis and methanogenesis which are conducted by various groups of microorganisms, [4].

Three major groups of microorganisms have been identified with different functions in the overall degradation process, as can be seen in the Figure 1, [5].

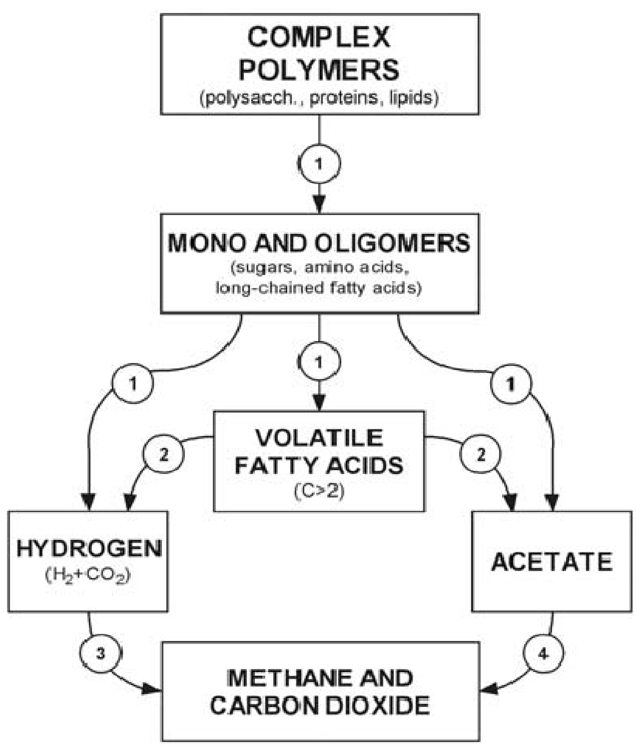

Figure 1: Schematic diagram of the anaerobic degradation process, [5]

1. The hydrolyzing and fermenting microorganisms are responsible for the initial attack on polymers and monomers found in the waste material and produce mainly acetate and hydrogen, but also varying amounts of volatile fatty acids (VFA) such as propionate and butyrate as well as some alcohols, [5].
2. The obligate hydrogen-producing acetogenic bacteria convert propionate and butyrate into acetate and hydrogen, [5].
3. Two groups of methanogenic Archaea produce methane from acetate or hydrogen, respectively, [5].

.

3. FACTORS INFLUENCING THE ANAEROBIC DIGESTION PROCESS

In order to obtain high yields of biogas is necessary to ensure the control of environmental and technological factors favorable to vital activity of methanogenic bacteria, and an equilibrium between the communities of microorganisms that coexist and operate in the anaerobic digester. Otherwise, methano-bacterial activity is hindered and, in extreme cases, stop completely, [6].

The biogas process as a complex biological process is influenced by several environmental factors such as: temperature, pH, substrate composition, pressure, agitation, nutritive elements, inoculation and heavy metals. Under conditions of unstable operation, intermediates such as volatile fatty acids and alcohols accumulate at different rates depending on the substrate and the type of perturbation causing instability, [7].

The most important environmental factors that can significantly influence the biogas production during the anaerobic digestion process are temperature, pH and heavy metals. Further on, will be analyzed how these parameters affect the biogas production.

3.1. Temperature

Temperature is one of the main environmental factors affecting bacterial growth during the anaerobic digestion process. Treatment of waste in anaerobic reactors is normally carried out within two temperature ranges: around 25 – 40^{0}C, known as the ***mesophilic range,*** and higher than 45^{0}C, known as the ***termophilic range***. Methanogenesis is also possible under ***psychrophilic conditions*** (below 25^{0}C) but at lower process rates, [7].

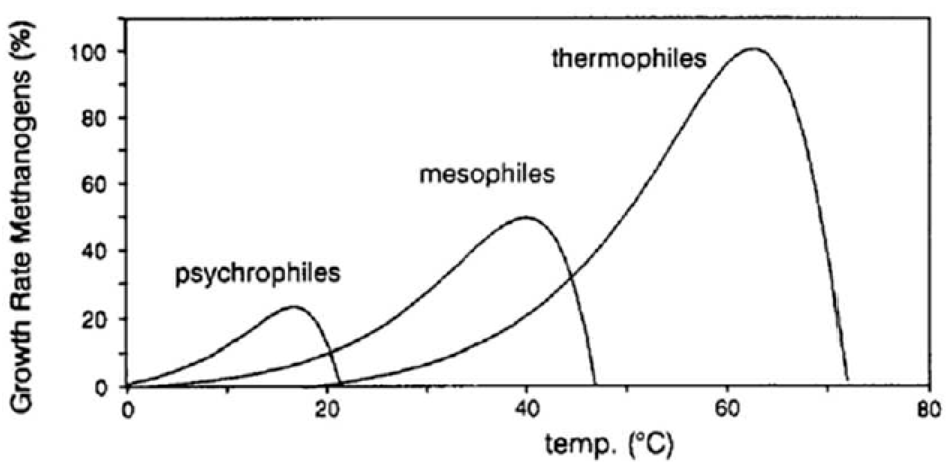

Figure 2: The dynamics of biogas production at different temperatures, [1]

Waste such as sewage sludge, manure or household waste contains many different populations of anaerobic or facultative anaerobic microorganisms. Most of these microbes are mesophilic and only a very small number of true thermophiles is present.

Fermenters fed with organic waste from agriculture can work in certain situations, in all temperature ranges. Biogas plants for rural households, of small capacity are not equipped with internal heating, therefore, the temperature in the fermenter varies, being influenced by ambient temperature. Sudden changes in temperature negatively influence the microbiological activity in the fermenter. If these variations are too large or prolonged, biogas production may stop completely. Such situations occur more frequently in small capacity biogas plants during the cold season, [6].

The optimum temperature for small capacity biogas plants from temperate zone is considered to be in the range 19 ÷ 20°C. Characteristic of these systems is long duration of substrate retention in digester which varies from 30 to 90 days.

The medium and large capacity biogas plants operate in the mesophilic and thermophilic field. These thermal regimes are ensured and maintained relatively constant with the help of internal sources of heat and insulation.

The digesters that work in the thermophilic range, produce biogas with a speed greater than those operating in the mesophilic range. The speed of biogas production shortens the retention time of the organic substrate in the digester, required to obtain the same amount of biogas.

In the experiments performed, the optimum temperature to which the methanogenic bacteria growing is 35 ° C, [8].

3.2. Alkalinity and pH

The parameter that by far most heavily affects the anaerobic fermentation process is the pH value. The pH value of the anaerobic digestion substrate influences the growth of methanogenic microorganisms and affects the dissociation of some compounds of importance for the anaerobic digestion process (ammonia, sulphide, organic acids), [1].

In a properly operating anaerobic digester, a pH of 6.8 to 7.2 occurs as volatile acids are converted to methane and carbon dioxide. Digester stability is enhanced by alkalinity concentration, [9]. The buffering capacity of the environment, namely the material ability to resist to changes in pH, depends on the present alkalinity. It controls the pH fluctuations due to the accumulation of volatile acids (acetic acid, butyric acid, propionic acid), whose acidity neutralizes it. If the present alkalinity and the buffering capacity is insufficient to control the effect of the accumulation of acids, the pH will drop. As a result, in the first phase will increase in biogas the proportion of the carbon dioxide compared to methane until the end of the process for the production of biogas. To maintain the optimum pH in the optimal range to prevent excessive acidification is indicated introduction of alkalizing substances, such as: lime water, calcium carbonate, sodium hydroxide, [6].

3.3 Heavy metals concentration

Heavy metals can be stimulatory, inhibitory, or even toxic for biochemical reactions, depending on their concentration.

Microelements (trace elements) like iron, nickel, cobalt, selenium, molybdenum or tungsten are equally important for the growth and survival of the anaerobic digestion microorganisms as the macronutrients carbon, nitrogen, phosphor, and sulphur. The optimal ratio of the macronutrients carbon, nitrogen, phosphor, and sulphur (C:N:P:S) is considered 600:15:5:1. Insufficient provision of nutrients and trace elements, as well as too high digestibility of the substrate can cause inhibition and disturbances in the anaerobic digestion process, [1].

Some researchers, [10,11,12] investigated the role of iron, nickel and cobalt in the production of biogas during the anaerobic digestion of a sludge. These metals were chosen considering their role in the anaerobic metabolism during the anaerobic fermentation. These metals constitute the active centre in several enzymes which play a key role in the complex methanation process. In particular, nickel is the active centre of the methyl-coenzyme M reductase (known as F430) and several H2-consuming hydrogenases as well as acetate formation enzymes. Iron is part of different hydrogenases (H_2 uptake or evolution), and of the carbon monoxide dehydrogenase (CODH) enzyme, a central enzyme in the formation of acetic acid by anaerobic bacteria, that contains Fe_4S_4. Cobalt is part of cobalamin which catalyses the transfer of methyl-groups. All these enzymes work together for the production of methane and carbon dioxide during the anaerobic digestion.

In other studies [7], was found out that the most common inhibitor for the anaerobic process is ammonia. Many substrates used for anaerobic treatment often contain ammonia in toxic concentrations. Such substrates include pig and poultry manure, slaughterhouse waste, potato, juice, highly proteinaceous sludge, wastewater from shale oil.

E. Zaleckas et al., [13], investigated the effect of heavy metals on biogas production using anaerobic sewage sludge microflora in the presence of Ni, Cu, and Zn ions. They reported that after 14 days of anaerobic digestion an approximately 12% lower biogas amount was observed in the reactor containing the highest amount of zinc compared to the control reactor containing no addition of heavy metal. Nickel whose amounts could be found in sewage sludge does not produce any negative effect on the fermentation process. Additive of nickel has increased the biogas production. However, copper additive has not enhanced further biogas production. After 14 days of anaerobic digestion of sewage sludge and rapeseed cake mixture the methane content in biogas has varied from 64.5 to 70%, [13].

4. CONCLUSIONS

The economy of a biogas plant is directly linked to the amount of biogas produced per unit of raw material treated in the plant.

Biogas production by anaerobic fermentation is considered to be the optimal treatment for agricultural waste, manure and for a wide variety of organic waste, because these substrates are converted into renewable energy and organic fertilizer for agriculture.

Processing biogas from organic matter in anaerobic fermentation process is one of the main priorities of the European strategy regarding biofuels and renewable energy.

Methanogens are commonly considered to be the most sensitive to toxicity of the microorganisms in anaerobic digestion.

It should be pointed out that the heavy metals in high concentration affect heavily the action of methane bacteria during the anaerobic digestion process. It was found out that the addition of Fe, Ni and Co could be beneficial for improving the methanation process within given concentration limits.

Excessive amounts of heavy metals can lead to inhibition or toxicity density of biogas production during the anaerobic fermentation.

In order to prevent falls in the digestion yield, the temperature should be kept strictly constant and the pH value should be kept in the range 6.8 - 7.2.

References

[1] Al Seadi, T., Rutz, D., Prassl, H., Köttner, M., Finsterwalder, T., Volk, S., Janssen, R., *BIOGAS – Handbook*, University of Southern Denmark, 2008, ISBN 978-87-992962-0-0.

[2] A. Converti, R.P.S. Oliveira, B.R. Torres, A. Lodi a, M. Zilli, *Biogas production and valorization by means of a two-step biological process*, Bioresource Technology 100 (2009) 5771–5776.

[3] Kumar A., Miglani P., Gupta R.K., Bhattacharya T.K., *Impact of Ni(II), Zn(II) and Cd(II) on biogassification of potato waste*, Journal of Environmental Biology, 27 (1), pp. 61-66, 2006.

[4] Khalid A, Arshad M, AnjumM, Mahmood T,Dawson L. *Review—the anaerobic digestion of solid organic waste*,Waste Manage2011;31:1737–44.

[5] Birgitte K. Ahring, *Perspectives for Anaerobic Digestion*, Advances in Biochemical Engineering/ Biotechnology, Vol. 81, Springer – Verlag Berlin Heidelberg, 2003.

[6] I.Păunescu, G.Paraschiv, Instalații pentru reciclarea deșeurilor, Editura AGIR, București, 2006.

[7] Irini Angelidaki, Lars Ellegaard, Birgitte Kioer Ahring, Applications of the Anaerobic Digestion Process, Advances in Biochemical Engineering/ Biotechnology, Vol. 82, Springer – Verlag Berlin Heidelberg, 2003.

[8] M. Dilea, G. Paraschiv, Gh. Voicu, S.Șt. Biriş, N. Ungureanu, L. Toma and M. Ionescu, *Biogas, the most effective technology for biomass*, pp. 386 – 390, Research people and actual tasks on multidisciplinary sciences, 12 – 16 JUNE 2013, ISSN 1313 – 7735, Lozenec, Bulgaria.

[9] Jactone Arogo Ogejo, Zhiyou Wen, John Ignosh, Eric Bendfeldt, E.R. Collins, *Biomethane Technology*, Virginia Polytechnic Institute and State University, 2009, VirginiaTech Invent the Future.

[10] Michele Aresta, Marcella Narracci, Immacolata Tommasi, *Influence of iron, nickel and cobalt on biogas production during the anaerobic fermentation of fresh residual biomass*, Chemistry and Ecology, 19: 6, 451 — 459, 2003.

[11] Aresta, M., Quaranta, E. and Tommasi, I., *Reduction of co-ordinated carbon dioxide to carbon monoxide via protonation by thiols and other broensted acids promoted by Ni-systems: a contribution to the understanding of the mode of action of the enzyme carbon monoxide dehydrogenase*, Journal of Chemical Society, Chemical Communications, 450–451, 1988.

[12] Hippler, B. and Thauer, R. K. (1999). The energy conserving methyltetrahydromethanopterin: coenzyme M methyltransferase complex from methanogenic archaea: function of the subunit MtrH. FEBS Letters, 449, 165–168.

[13] Ernestas Zaleckas, Egle Sendzikiene and Ruta Ciutelyte, *Evaluation of Heavy Metals Influence on Biogas Production,* Environmental Research, Engineering and Management, 2012. No. 4(62), P. 14-20.

MATHEMATICAL MODELING OF VERTICAL OSCILLATION OF A TRACTOR FOR A MODEL WITH FOUR DEGREES OF FREEDOM WHEN TRAVELING ON AN AGRICULTURAL LAND AND AN UNPAVED ROAD

PhD. Eng. Mihaela Florentina Duţu – University Politehnica of Bucharest, Faculty of Biotechnical Systems Engineering[1],
PhD. Eng. Gabriela Simion - University Politehnica of Bucharest, Faculty of Biotechnical Systems Engineering[2]
PhD. Eng. Iulian Duţu – Hydraulics and Pneumatics Research Institute, INOE 2000-IHP[3]
PhD. Stud. Eng. Alexandru-Dorin David - National Institute of Research - Development for Machines and Installations Designed to Agriculture and Food Industry – INMA[4]
Sanda Maiduc (Osiceanu) - University Politehnica of Bucharest[5]

ABSTRACT

This paper aims to study mathematical modeling of vertical oscillations of a tractor for a model with four degrees of freedom. In this respect, it was developed a modeling program that enables determining wheel oscillations, oscillations of the center of mass of the tractor for its different speeds when moving on different roads.

In this case, given that the model is approximating the real tractor, there will be followed the trend of variation of different parameters and their values. Values determined with the developed program will be verified in experimental tests of agricultural mobile machines.

The modeling program was run for 10 speeds of the tractor when moving on agricultural land and unpaved road. Movement and the data obtained were recorded and presented below, in tables.

1. INTRODUCTION

In this paper, the authors have studied the motion of a tractor on agricultural land and on unpaved road, in order to compare, using a mathematical modeling program, the variation of amplitude of the oscillation of the mass center of the tractor, the variation of amplitude of the rotation angle of the tractor around its mass center, the variation of the amplitude of driven wheel oscillation when the tractor is moving and the variation of the amplitude of oscillation of the driving wheel.

2. MOVEMENT STUDY OF THE TRACTOR ON AGRICULTURAL LAND

The modeling program was run for 10 speeds of the tractor; the data recorded is presented in Table 1.

Figure 1 shows the variation of the amplitude oscillation of the center of mass of the tractor in respect to the movement speed. The variation curve can be approximated with:

$$z = 0{,}0675\, v^{-1{,}627} \tag{1}$$

Considering that the phase shift of the disturbance due to terrain undulations, on driving wheels is π, the amplitude oscillation of the rotation angle of the tractor in the plan is:

$$\theta = 0{,}0093\, v^{-1{,}5324} \tag{2}$$

[1] Splaiul Independenței, nr.313, corp D, sector 2, București, +4021.402.9637, dutumihaelaflorentina@gmail.com
[2] Splaiul Independenței, nr.313, corp D, sector 2, București, +4021.402.9637, gacsimion@gmail.com
[3] Str.Cutitul de argint nr.14, sector 4, Bucuresti, +4021.336.39.91, dutu.ihp@fluidas.ro
[4] Bd. Ionescu de la Brad Ion, 6, Bucuresti-Sector 1, somy_alex_07@yahoo.com
[5] Splaiul Independentei nr.313, sector 6, Bucharest; +4021.402.97.42, sanda.osiceanu@gmail.com

Figure 3 shows the variation of the amplitude oscillation of the driven wheel of the tractor in respect to the moving speed. Variation curve is approximated with:

$$z_f = 0{,}2813\, v^{-1{,}8449} \qquad (3)$$

Table 1: Movement parameters of the tractor on agricultural land, considered as a model with four degrees of freedom

Speed v	Oscillation frequency	Oscillation wheels		Center of mass oscillation		Vertical force	
		z_f	z_s	z	θ	F_f	F_s
2,58	3,44	0,055	0,06	0,026	0,0026	1,12	17
3,83	5,11	0,024	0,03	0,014	0,0012	8	28
4,16	5,55	0,021	0,026	0,013	0,001	9	30
5,78	7,72	0,01	0,016	0,008	0,0006	11,8	38
6,17	8,24	0,01	0,015	0,008	0,00055	12	42
7,68	10,25	0,006	0,0011	0,006	0,00038	13	50
8,56	11,43	0,005	0,0095	0,005	0,00032	13	52
11,38	15,2	0,003	0,0065	0,004	0,0002	14,5	70
18,18	24,28	0,0013	0,004	0,0024	0,00011	16	106
26,94	35,97	0,00075	0,0026	0,0016	0,00007	18	150

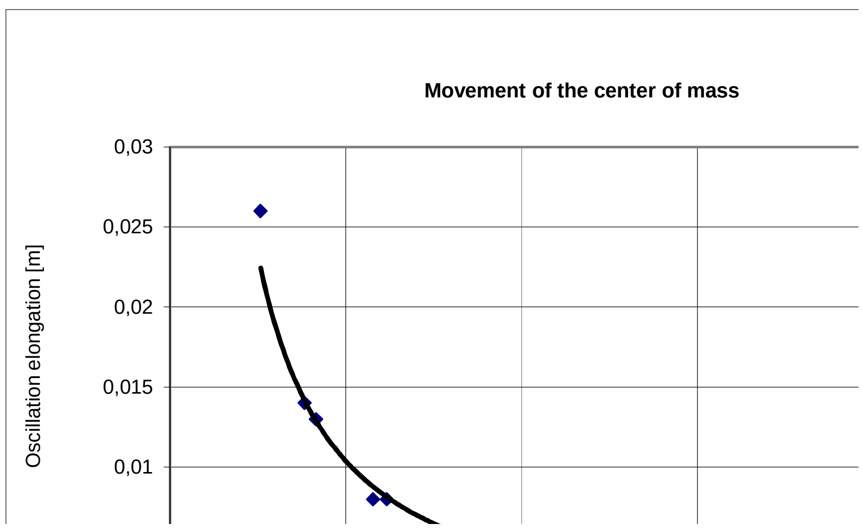

Figure 1: Variation of the amplitude oscillation of the center of mass of tractor

Amplitude variation of oscillation of the driving wheel in concordance with the movement speed of the tractor is shown in Figure 4. The variation curve is approximated by:

$$z_s = 0{,}1415\, v^{-1{,}3296} \qquad (4)$$

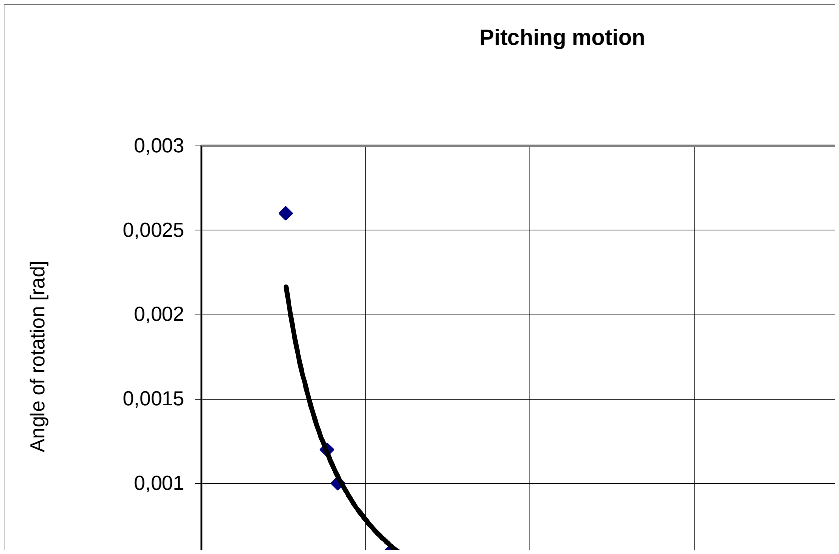

Figure 2: Variation of the amplitude oscillation of the rotation angle of the tractor in the longitudinal plan

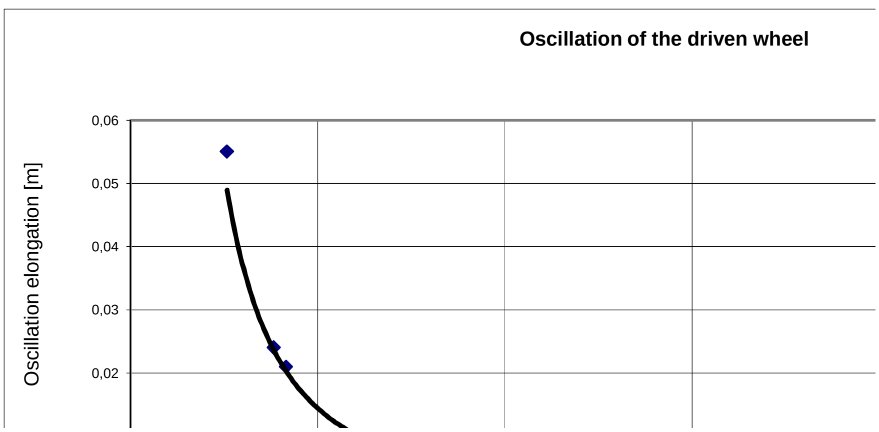

Figure 3: Variation of the amplitude oscillation of the driven wheel in respect to the moving speed of the tractor

3. MOVEMENT STUDY OF THE TRACTOR WHEN DRIVING ON UNPAVED ROAD

After running the modeling program for 10 speeds of the tractor on unpaved road there was obtained the data given in Table 2.

Variation of the amplitude oscillation of the center of mass of the tractor is shown in Figure 4 and the amplitude variation of the rotating angle in the vertical plan of the tractor is shown in Figure 5.

The curves above can be approximated by:

$$z = 0{,}0592\, v^{-1{,}0637} \tag{5}$$

$$\theta = 0{,}0052\, v^{-1{,}3} \tag{6}$$

Variation of the amplitude oscillation of the driven wheel is shown in Figure 6. Variation curves of amplitude oscillation of the tractor wheels in respect to the movement speed on unpaved land are:

$$z_f = 0{,}1401\, v^{-1{,}6928} \tag{7}$$

Table 2: Movement parameters of the tractor on unpaved land

Speed v	Oscillation frequency	Oscillation wheels		Center of mass oscillation		Vertical force	
		z_f	z_s	z	θ	F_f	F_s
2,58	6,63	0,033	0,046	0,023	0,0018	24	80
3,83	9,85	0,016	0,026	0,014	0,0009	29	110
4,16	10,7	0,013	0,023	0,013	0,0008	30	120
5,78	14,86	0,007	0,015	0,009	0,00048	32	150
6,17	15,87	0,006	0,014	0,0082	0,00046	34	165
7,68	19,75	0,004	0,011	0,0065	0,00034	35	195
8,56	22,01	0,003	0,01	0,006	0,0003	36	220
11,38	29,27	0,002	0,007	0,0045	0,00022	40	290
18,18	46,76	0,001	0,0045	0,0028	0,00012	50	442
26,94	69,3	0,0007	0,003	0,0018	0,00008	64	690

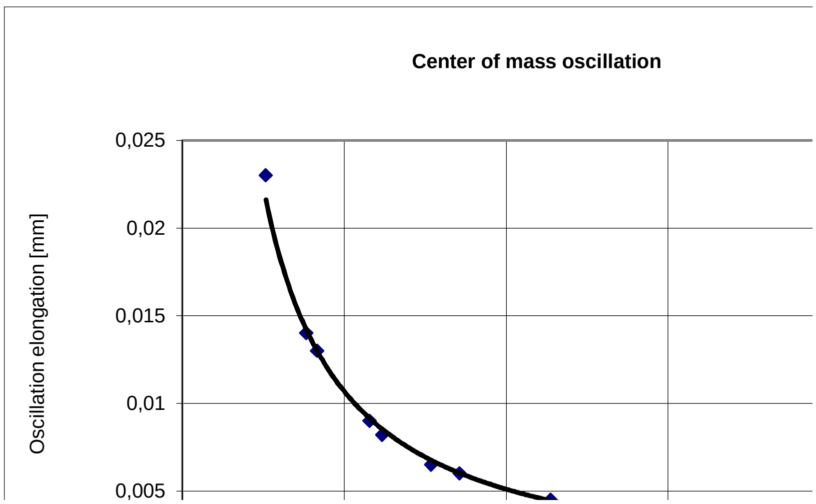

Figure 4: Variation of the amplitude oscillation of the center of mass in respect to the movement speed of the tractor

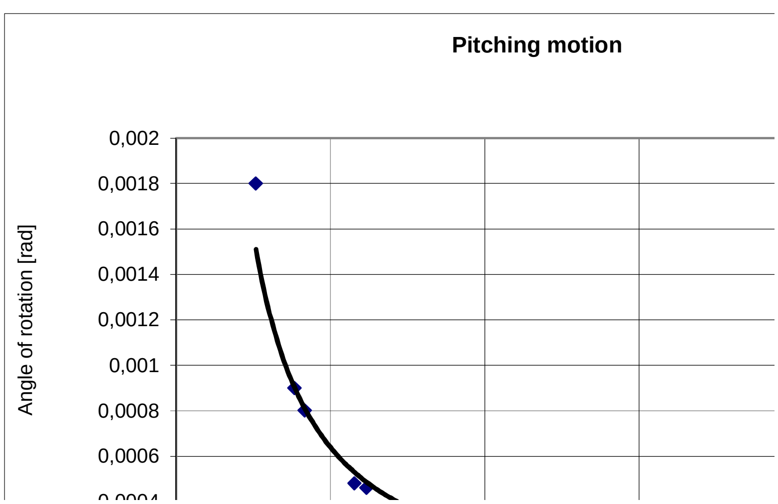

Figure 5: Amplitude variation of the rotation angle of the tractor in longitudinal plan for various movement speeds

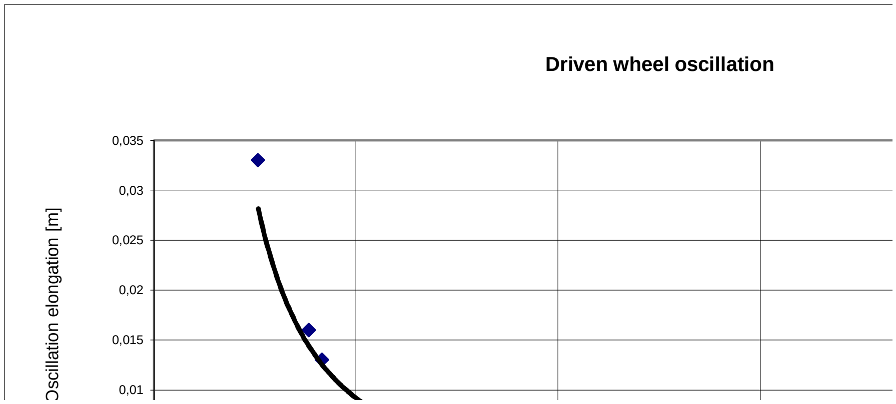

Figure 6: Variation of the amplitude oscillation of the driven wheel in respect to the movement speed of the tractor on unpaved land

4. CONCLUSIONS

4.1. Variation of the amplitude of oscillation of the center of mass of the tractor when driving on unpaved land is higher than when the tractor is moving on agricultural land, for all movement speeds. When analyzing small movement speeds, the variation of amplitude is closer (Figure 7).

4.2. Amplitude variation of the angle of rotation of the tractor in longitudinal plan around of the center of mass is closer to the movement of the tractor on the two field types (Figure 8).

4.3. Amplitude oscillations of the driven wheel are higher when moving on agricultural land than moving on unpaved land for movement speeds less than 12 km/h. For higher movement speeds, the amplitude oscillation on both field types is similar (Figure 9).

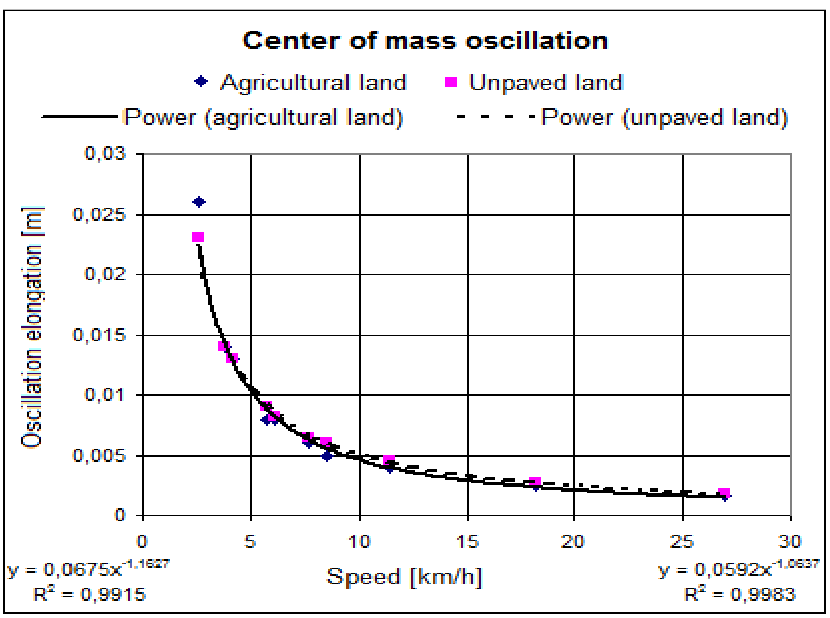

Figure 7: Variation of the amplitude oscillation of the center of mass of the tractor when moving on both types of land

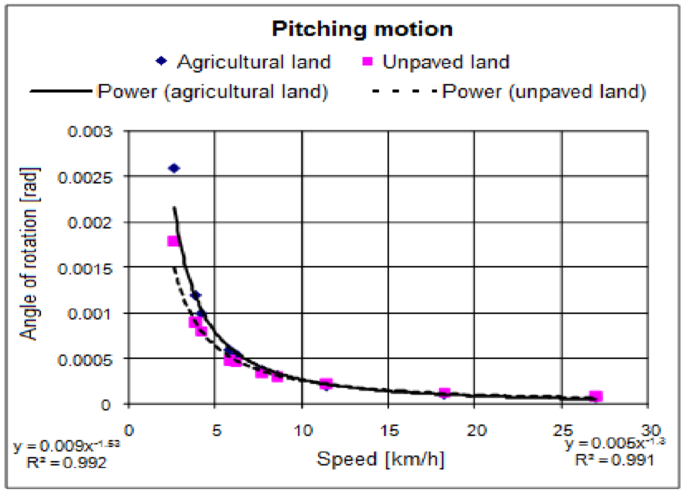

Figure 8: Variation of the amplitude oscillation of the rotation angle of the tractor in longitudinal plan for two field types

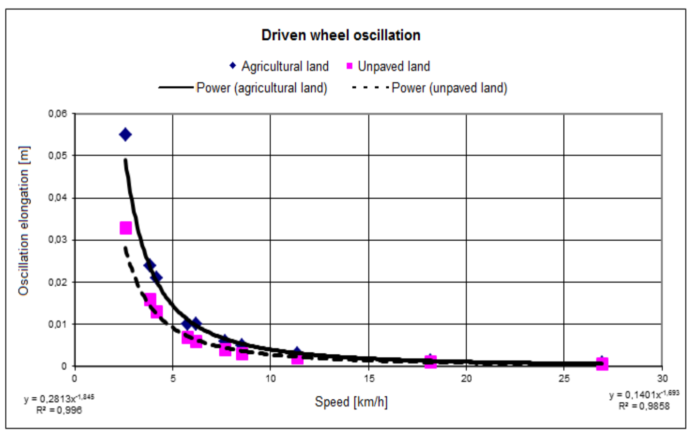

Figure 9: Variation of amplitude of oscillation of driven wheel for two field types

References

[1] Borcilă D., *Studii şi cercetări privind determinarea pe cale analitică şi experimentală a performanţelor de tracţiune şi economice a tractoarelor*, Rezumatul tezei de doctorat, 2001

[2] Benaroya H., *Mechanical Vibration*, Prentice Hall, 2001.

[3] David M.F. , *Contribuţii la studiul dinamicii agregatelor agricole mobile*, Teza de doctorat, Bucuresti, 2007.

[4] Deciu E., Enescu N., Ion C., ş.a. , *Probleme de vibraţii mecanice*, Vol I-II, UPB, 1981.

[5] Frăţilă Gh., *Calculul şi construcţia automobilelor*, Editura Didactică şi Pedagogică, Bucureşti, 1977.

[6] Năstăsoiu S., ş.a., *Tractoare*, Editura Didactică şi Pedagogică, Bucureşti 1983;

[6] Rao S.S. , *Mechanical Vibrations*, 2nd, Ed., Addison-Wesley, Reading, MA, 1990.

[7] Weaver W., Timoshenko S.P., Young D.H., *Vibration Problems in Engineering*, 5th ed., Wiley-Interscience, New York 1990;

[8] *** *Studiu documentar privind perfecţionarea sistemei de maşini pentru transportul produselor din fermele agricole şi zootehnice prin integrarea unui echipament tehnic universal*, Contract 38, Program AGRAL, 15.10.2001.

[9] *** *Analysis and Design of Foundations for Vibrations*, Edited by P.J.Moore, University of Melbourne, 1990.

ANTIMICROBIAL ACTION OF SOME ESSENTIAL OILS FROM INDIGENOUS FLORA AGAINST FUNGAL CONTAMINANTS IN FOOD

Mariana Ferdes [1], Augustina Pruteanu[2]

Abstract

Essential oil plants and culinary herbs include a broad range of plant species that are used for their aromatic value in aromatherapy, as flavorings in foods and beverages and as fragrances in pharmaceutical and industrial products. Essential oils derive from aromatic plants of many genera distributed worldwide. Essentials oils obtained from plant material have been used for centuries as antimicrobial agents. The increase of microbial resistance to antibiotics and the efforts to develop natural preservatives in food manufacturing has increased interest in possible applications of these compounds.

The aim of this study was to determine antimicrobial activity of essentials oils against some fungal food-borne and agricultural strains belonging *Aspergillus*, *Penicillium* and *Fusarium* genera.

The antifungal effect of volatile phase of essential oils was evaluated in vitro by measuring the diameter of the mold colony growth in Petri dishes, on potato dextrose agar. Mycelial growth assay showed fungistatic and fungicidal activity of cinnamon, mint, basil and thyme. Orange and lemon oils show a weak inhibitory activity on these fungi. On microscopic slides were observed alterations of normal appearance of conidiospores and hyphal system. Spores production was inhibited by the essential oils tested and the hyphae are thinner than normal, with large vacuoles.

Key words: essentials oils, antifungal effect

1. INTRODUCTION

Interest in essential oils has revived in recent decades with the popularity of aromatherapy, a branch of alternative medicine which claims that the specific aromas carried by essential oils have curative effects. Essential oils extracted from medicinal plants are known for their beneficial effects in humans (Burt, 2004; Bakkali et al., 2008).

An essential oil is a concentrated, hydrophobic liquid containing volatile aroma compounds from plants. Essential oils are also known as volatile, ethereal oils or simply as the "oil of" the plant from which they were extracted, such as oil of clove. Volatile compounds from plants, especially essential oils, have antimicrobial, fungicidal and insecticidal activities (Pawar W.C. et al., 2007). The effectiveness of aromatic plants generate volatile C10 and C16 terpenes, which are derived from isoprene unit.

Essential oils are volatile compounds produced by plants as secondary metabolites in particular cells or formed as glandular hairs (Hili et al. 1997). The antimicrobial properties of essential oils depend on genus, species, and geographical area (climatic factors) of spices.

[1] PhD., Faculty of Biotechnical Systems Engineering, Department of Biotechnical Systems, University POLITEHNICA of Bucharest, e-mail: marianaferdes@yahoo.com, 0729821256
[2] INMA, Bucharest

Various essential oils have been used medicinally at different periods in history. (Tisserand, 1995; Moreira et al., 2005; Atrea et al.,2008). Medical application proposed by those who sell medicinal oils range from skin treatments to remedies for cancer, and are often based on historical use of these oils for these purposes. Such claims are now subject to regulation in most countries, and have grown vaguer to stay within these regulations.

The most common genera of fungi in food are *Aspergillus, Penicillium* and *Fusarium*. Several species of these genera are able to produce mycotoxins, which are of concern to public health (Ungureanu et al., 2010). Among them, ochratoxin A produced by *Aspergillus ochraceus* is nefrotoxic and carcinogenic to some animals and has been detected in different types of foods. *Penicillium hirsutum* can produce roquefortine and *Fusarium roseum* synthesizes zearalenone under certain conditions.

2. MATERIAL AND METHODS

Strains

Three food-borne fungal strains were tested for the antimicrobial activity of essential oils from thyme, basil, mint, lemon, orange and cinnamon: *Aspergillus ochraceus, Fusarium roseum, Penicillium hirsutum* from the Laboratory of Microbiology, University Politechnica of Bucharest. These strains are well known for the spreading on food and agricultural products and can produce damages and food-contaminating micotoxins such as ochratoxin, roquefortine, zearalenone.

Culture media

These strains were cultivated onto potato-dextrose agar, in tubes, at 30 ºC, for about 10 days to complete sporulation. The growth rate was evaluated by measurement of diameters of colonies in Petri dishes, on potato-dextrose agar, at 30 ºC.

Inocula were prepared from 10 day old cultures grown on potato dextrose agar (PDA). A suspension of spores was prepared in a phosphate buffer (pH 7.2) with 0.1% of Tween 80. 2 microliters of suspension of each fungus was inoculated separately, on the centre of each culture medium. Plates were incubated at temperature of 30ºC.

Antimicrobial vapor assay

The base of the Petri dish containing culture medium was inoculated with molds. 2, 5, 20 μL of the essential oil were placed in center of the cover of the Petri dish. The dishes were tightly closed with adhesive tape and incubated at 30ºC for 10 days. The diameter of fungal colony was measured in milimeters every day with a ruler.

Radial growth rate and inhibition ratio

In order to estimate the radial growth rate of strains the maximum diameter of colonies was measured after 240 hours (or when the colony diameter is equal to the dish diameter) and the ratio diameter/time was calculated.

The inhibition ratio was estimated using the formula:

$$\text{Inhibition ratio (\%)} = \frac{C - E}{C} \cdot 100$$

where C is the diameter of mold colony from control plate and E is the diameter of the mold colony growth in experiment plate which contains the essential oil.

3. RESULTS AND DISCUTIONS

The aim of this investigation was to determine antimicrobial activity of six essential oils against *Aspergillus ochraceus, Penicillium hirsutum* and *Fusarium roseum* known as food contaminant molds.

The diameter of fungal colonies was measured to draw the growth curve for each mold in control plates as well as in the presence of essential oils. The figures 1-3 shows the growth curves for the control plates without oils and for samples, in Petri dishes with 2, 5 and 20 µl of essential oils.

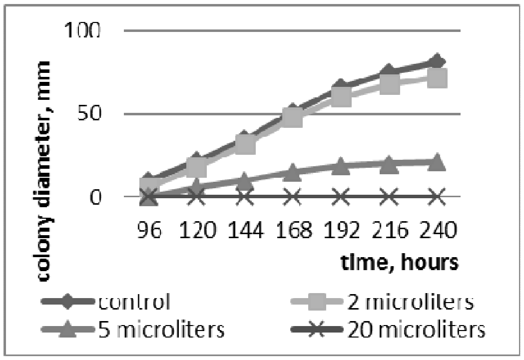

a)

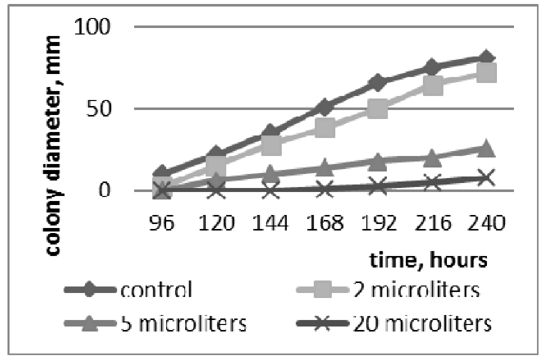

b)

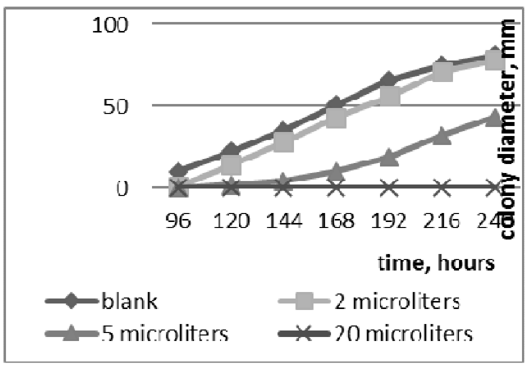

c)

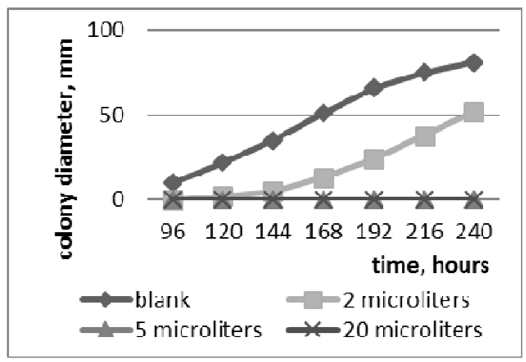

d)

Fig 1. Growth curve of *Aspergillus ochraceus* colonies in presence of a) thyme oil; b) basil oil; c) mint oil; d) cinnamon oil;

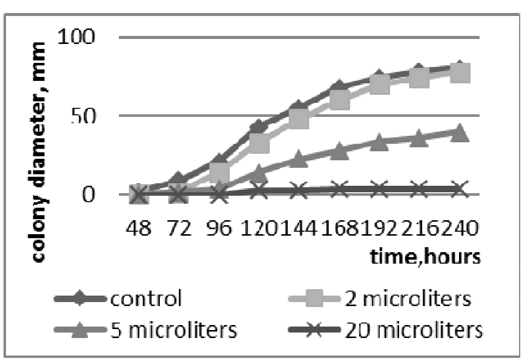

a)

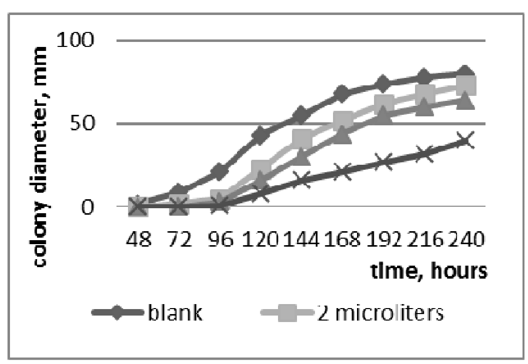

b)

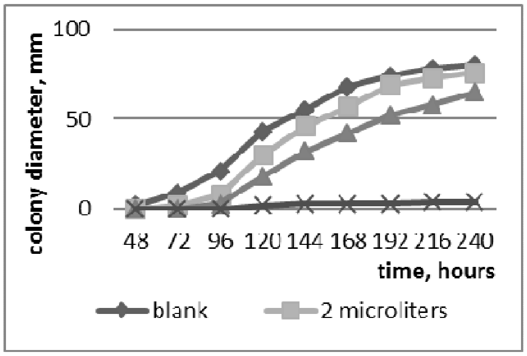

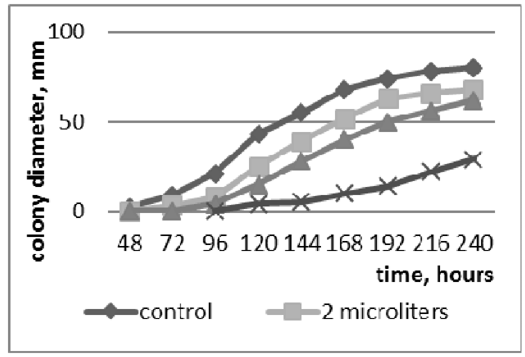

c) d)

Fig 2. Growth curve of *Penicillium hirsutum* colonies in presence of a) thyme oil; b) basil oil; c) mint oil; d) cinnamon oil;

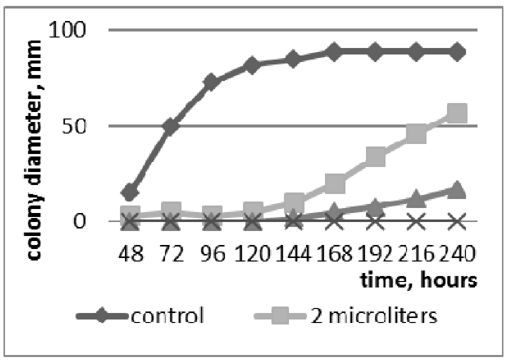

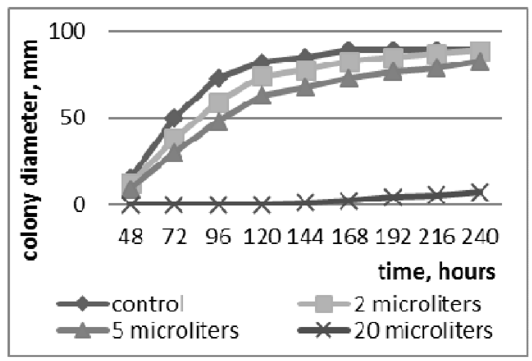

a) b)

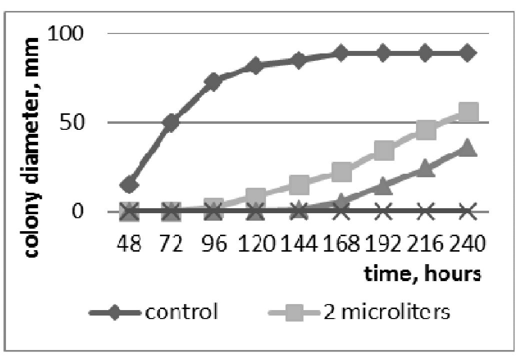

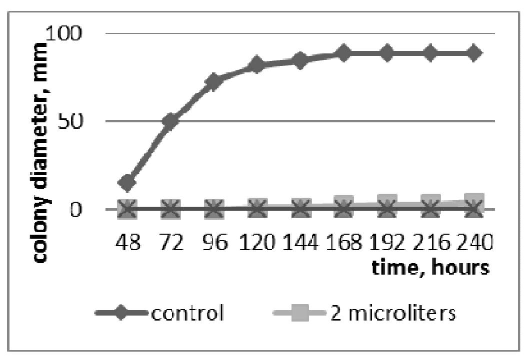

c) d)

Fig 3. Growth curve of *Fusarium roseum* colonies in presence of a) thyme oil; b) basil oil; c) mint oil d) cinnamon oil;

The figures 1-3 present the growth of fungal colonies in control plate and in Petri dishes with essential oils. The diameters varies depending of the type of oil and the strain. It seems that the most effective oils that reduce growth are the thyme, basil and cinnamon oil, while lemon and orange oil are less effective. Some cultures are totally inhibited by the presence of oils and the diameter is considered zero. The volume of added oil on the cover of Petri dish significantly influences the colony size, though is not determined a proportionality between these values.

Radial growth rate

The diameter of colonies was measured in control dishes and in the experimental plates containing the essential oil and there were calculated the average of growth rates (Tables 1-3).

Table 1 The average growth rate for the *Aspergillus ochraceus* colonies

Aspergillus ochraceus	**Concentration, µl**			
	0	2	5	20
	Growth rate, mm/h			
Thyme oil	0,34	0,3	0,1	0
Basil oil	0,34	0,3	0,11	0,03
Mint oil	0,34	0,32	0,18	0
Cinnamon oil	0,34	0,22	0	0
Lemon oil	0,34	0,29	0,25	0,16
Orange oil	0,34	0,33	0,25	0,2

Table 2 The average growth rate for the *Penicillium hirsutum* colonies

Penicillium hirsutum	**Concentration, µl**			
	0	2	5	20
	Growth rate, mm/h			
Thyme oil	0,33	0,32	0,17	0,02
Basil oil	0,33	0,30	0,27	0,17
Mint oil	0,33	0,28	0,26	0,12
Cinnamon oil	0,33	0,32	0,27	0,02
Lemon oil	0,33	0,28	0,26	0,17
Orange oil	0,33	0,32	0,32	0,27

Table 3 The average growth rate for the *Fusarium roseum* colonies

Fusarium roseum	**Concentration, µl**			
	0	2	5	20
	Growth rate, mm/h			
Thyme oil	0,53	0,24	0,07	0
Basil oil	0,53	0,37	0,34	0,03
Mint oil	0,53	0,23	0,15	0
Cinnamon oil	0,53	0,02	0	0
Lemon oil	0,53	0,36	0,33	0,2
Orange oil	0,53	0,35	0,30	0,22

The growth rate depends on the amount of oil and mold species. The thyme, basil, mint, cinnamon, lemon, orange oils show different antifungal activities; the most effective against all tested strains was the cinnamon oil. The diameters of treated colonies were smaller than the control, depending on the volume of oil added on the cover of Petri dish.

For 20 µl of added oil, most fungal cultures are totally inhibited and the growth rate is zero. Only lemon and orange oil have a weaker action and the fungi still growth. The most resistant mold seems to be the *Penicillium hirsutum* strain and the most sensitive was *Fusarium roseum.*

4. CONCLUSIONS

Volatile compounds from plants, especially essential oils, have antimicrobial activity against a variety of food borne fungi. In this study, it was tested the effect of essential oils on in vitro mycelial growth of *Aspergillus ochraceus, Fusarium roseum* and *Penicillium hirsutum*. It was also investigated the effect of essential oils on hyphal morphology under light microscopy.

The results of this study confirm that essential oils from aromatic plants such as thyme, basil, mint, lemon, orange and cinnamon presents antimicrobial activity.

These essential oils show different antifungal activities; the most effective against all tested strains was the cinnamon oil. The diameters of treated colonies were smaller than the control, depending on the volume of oil added on the cover of Petri dish.

The volatile oils presents considerable inhibitory effects against all the microorganisms under test while their major components demonstrated various degrees of growth inhibition.

These inhibitory effects are interesting in connection with the prevention of mycotoxin contamination in many foods and they could be used instead of synthetic antifungal products.

References

- Bakkali F., Averbeck S., Averbeck D. and Idaomar M. (2008), Biological effects of essential oils – A review, Food and Chemical Toxicology,vol. 46, no. 2, pp. 446-475
- Burt S., (2004).Essential oils: Their antibacterial properties and potential applications in foods – A review, International Journal of Food Microbiology,vol. 94,no. 3, pp. 223-253.
- Moreira M.R., A.G. Ponce A.G.,Del Valle C.E., Roura S.I., (2005), Inhibitory parameters of essential oils to reduce a foodborne pathogen, LWT - Food Science and Technology, vol. 38**,** no. 5, pp. 565-570
- Pawar W.C., Thaker V. S., (2007), Evaluation of the anti-Fusarium oxysporum f. sp cicer and anti-Alternaria porri effects of some essential oils, World J Microbiol Biotechnol 23:1099–1106 DOI 10.1007/s11274-006-9339-6
- Tisserand R., (1995), Essential Oil Safety: A Guide for Health Care Professionals. Churchill Livingstone
- Ungureanu C.,Ferdeş M., (2010), Antibacterial and antifungal activity of red rice obtained from Monascus purpureus, Chemical Engineering Transactions, vol. 20, pp. 223-228

CONVECTION DRYERS WITH INCREASED ENERGY INDEPENDENCE

Iulian – Cezar Gîrleanu, Gheorghe Sovăială, Gabriela Matache

ABSTRACT

This paper shows the advantages of using modular convective dryers type drying chamber, as well as their performance in terms of energy. These are meant for dehydration of vegetal products, in line with the global trend concerning the conservation through the thermal and hydric technology of enzyme inactivation (dehydration).

In this paper there are promoted two strictly present-day concepts in the current context of globally deepening of the energy and food crisis: the concept of energy independence, the concept of food security and safety for consumers.

1. INTRODUCTION

Vegetables and fruits along all of human history were key elements in nutrition, as they contain proteins, lipids and carbohydrates, minerals such as potassium, sodium or magnesium etc., their consumption all year long being good for health. Soil and climate and also landscape conditions in Romania enabled that on this territory to be grown a wide range of high importance vegetables and fruits, grouped into more than 15 botanical families. But these products are seasonal, harvesting periods are relatively short, and in most of them perishability is a very high or medium one, making their use as fresh products be possible only after exquisite storage, which considerably increases their costs. [1]

Good tradition has been developed by the Romanian people, on drying preservation of important fruits and vegetables, such as plums, apples, bean pods, mushrooms, carrots etc. In the rural households drying was done naturally, using solar heat, so that the costs of preservation were pretty low. Switching to removal of water excess from vegetables and fruits through controlled dehydration, in technical equipment of high capacity, proved beneficial for the possibility of storage and use of the products thus preserved for long periods of time, particularly in winter and spring, when fresh products are scarce and expensive and the human body needs more their contents. But dehydration is an energy intensive process, which made that in many countries, including Romania, this process to be used less and less, being even on the verge of disappearing. Facing this situation, researchers in developed countries have found new solutions of technical equipment for drying fruits and vegetables, with higher productivity and ensuring for the finished products ever higher nutrition and sensory properties. [1]

Drying is one of the traditional and yet always modern ways for storage on long periods of time of fruits and vegetables for direct consumption or for industrial purpose without addition of preservatives and low power consumption for storage and reprocessing. Convective drying is a technology which greatly consumes heat energy, which in many cases makes it dependent on the heat sources as cheap as possible, this being one reason for super concentration of drying plants. Rapid decline in price of automation devices, development of automatic control software, and the development of machine building engineering and technologies led to a decentralization of processing by drying fruits and vegetables, to the displacement of drying facilities at the location of harvest of the products to be dried. This

makes the use of mobile dryers be dependent on the use of diesel fuel and LPG, fuels with high energy density, but sources of pollution through emission of CO_2. [2]
Currently the emphasis is on reducing the emission of CO_2 into the atmosphere by use of renewable energy, solar, biomass, wind or geothermal energy. With totally negative balance there are the wind plants and the solar thermal and photovoltaic ones, but they produce energy when there is light or wind, which requires obstructing and very expensive devices for storage of energy produced. Since biomass can be stored and used when energy is needed, even if it has an almost null CO_2 balance, this remains the most versatile energy source for agricultural farms which are direct producers of biomass used to generate energy. By using the micro-gasification process TLUD (Top-Lit-Up-Draft) type, from biomass there result fuel gas and residual vegetal coal – currently called biochar. Conversion into thermal energy of the completely gasified biomass part is made with an outturn of 95%, and in biochar there remains about 25% of the input energy and of the carbon in biomass. [2]
To produce electricity in energy independence conditions there are used collapsible, light and low weight photovoltaic panels. One can thus obtain energy independence of dryers, an effective valorization in economical and ecological terms of the mountain spontaneous flora products, as well as an increase in the use of labor force in rural areas. [2]

2. METHODOLOGY

The importance of drying preservation of fruits and vegetables
Dried fruits and vegetables were frequently used in former Romanian traditional diet. The climatic conditions specific to the area where Romania is located, with the four seasons (winter, spring, summer and fall), with a single agricultural crop per year, determined that since ancient times people have concerns about the preservation of fruit and vegetables in order to secure their food in between two crops, especially during the cold seasons.
Among fruits there were dried apples, pears, plums, apricots and grapes (seedless grain). They were used as foodstuff in the most diverse and attractive ways. Among vegetables there were dried especially those which could not be preserved otherwise, but were often used in nutrition, such as: green bean pods, peppers (red peppers, chili peppers, Kapia peppers, 'Sheepnose Pimento' peppers), dill, savory, mushrooms (especially the forest Porcini mushrooms).
Drying of fruits and vegetables in Romania has a history just as extensive as the growing of fruit trees and vegetables. It stands to reason that the human being early faced the problem of preserving for cold periods the products harvested in summer and autumn. Progressively, there were invented the most effective methods to dry some of the fruit and vegetable crops, using rudimentary methods at the beginning and later improved, such as: drying on grillages, drying on covered grillages, drying between vertical grillages, drying on multi-stage grillages, drying on rooftops - arranged platforms, drying on specially built platforms, equipped with tilts, drying in strings, drying in textile meshes. [1]

Fig. 2.1 - Dried apricots, plums and apples [1]

The main advantages of vegetables and fruits preserved by drying

Drying of fruits and vegetables is the healthiest solution for keeping them for a long time. Another advantage of dehydrated fruits and vegetables is that they have a far greater validity than the frozen or canned ones. Actually, dehydrated and stored in optimal conditions, fruits and vegetables can be eaten even after several years. An important economic aspect of dehydrated fruits and vegetables is that their storage poses no great problems, because their volume is reduced significantly after the drying process.

For example, two kilograms of raw fruit upon drying will have only a quarter of the initial volume. Almost all fruits and vegetables can be dehydrated. Exceptions are those rich in vegetal fats, which can become viscous. Grapes, plums, apples, pears, peaches, apricots, pineapple, bananas, tomatoes, carrots and herbs are best suited for this operation. [1]

Convective drying

Convective drying currently remains the best known and widely used method for removing moisture from the material, both due to the simplicity of the process, and especially for the many opportunities to get, at low cost, good quality of drying, in a short time.

The wet material gets in contact with the drying agent – hot air or combustion gases – from which it receives, by convection, 80—90% from the total amount of heat necessary for the drying process. The parameters of the drying agent (speed, temperature, relative humidity etc.) as well as the connection between humidity and material condition the heat and mass transfer in the drying process. Usually, during the process the drying agent changes its temperature over time, the relative humidity and even the travel speed, and the wet material changes its specific heat, density, thermal conductivity and even sizes. Also during the process there vary the coefficients of heat and mass transfer, water viscosity, surface tension etc., so that for getting exact knowledge on the functioning of the process there is required correlation between the theoretical known results and direct experimental research , conducted for each material.

Experimentally, particularities of the drying process of wet materials are given by the drying curves (which shows the variation in moisture content over time), the drying speed rate curves (variation of speed rate of drying with moisture or over time), the variation in temperature of the material and the drying agent over time etc. Experimental curves give the possibility of examining the influence of various parameters on the drying process, in order to establish economic regimes for drying.

The mechanism of drying procedure inside the convective drying plant

For removing water from vegetables and fruits, during the drying process, two core phenomena occur:

- heat transfer, providing energy required to convert the water to vapors;
- mass transfer through transfer of water or water vapors through the cells and then out of the product.

In order to be dried products must first be heated. The heat is brought to produced either by hot air (convection), or by heating the surface on which the products lie, from which they take over the heat (conduction). If heating products directly from sunlight, heat transfer is made through radiation. Water vapors gone out of the product are taken by the air, which becomes mass transfer environment.

In drying plants, water evaporation takes place both on the basis of the difference in temperature between the one of the product under drying and the one of heated air, and especially by the difference between the pressure of vapors inside the tissues and the one of vapors comprised by the air in the installation. Evaporation is influenced also by the surface tension (force) of water vapor inside the product. This takes place until equilibrium is reached between the vapor pressure of the two environments, in other words, until the hot air in the system was saturated with water vapors. The amount of vapors which may be absorbed by the air is closely related to the temperature of the air in the system that is the warmer the air is, a larger amount of vapors it can absorb. [4]

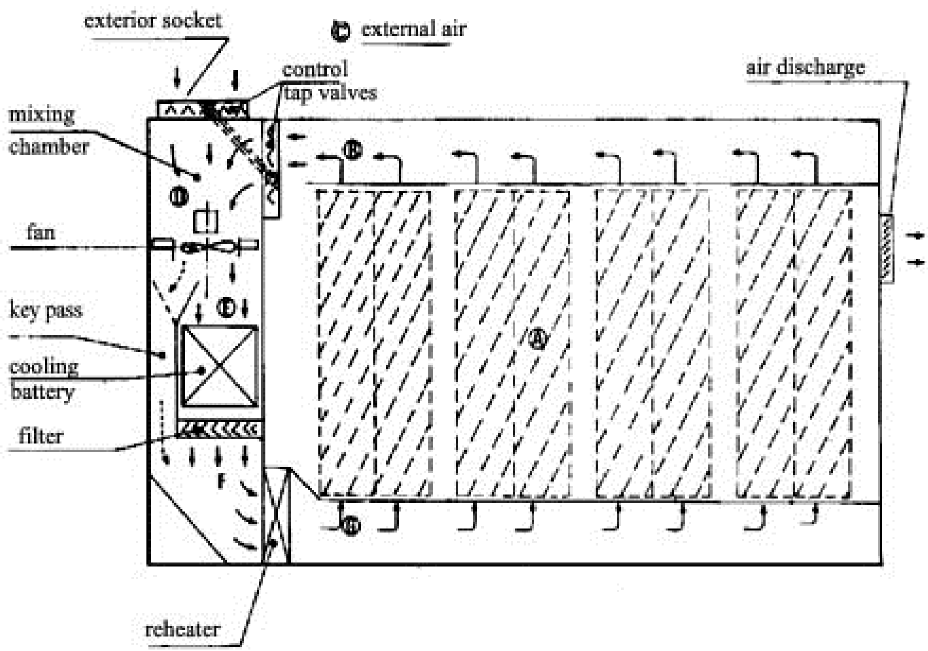

Fig. 2.2. - Convective dehydration plant

When there was set the balance between product moisture and saturation of air with water vapors inside the plant, and the product is still not dried, the drying process can continue only by creating a new imbalance between the moisture of the two environments. This imbalance may be achieved by one of the following technological measures:

- either by raising the air temperature in the system — if this is technologically possible;
- or by ventilating the air in the system, causing it to lose a certain amount of water vapors it is filled with.

Water loss from the tissues of vegetables and fruits has a profound influence on their structural-textural and physicochemical characteristics. Plant tissues alive have the property of turgidity; each cell is maintained unstrained, due to its content in the liquid and has a structure strong enough.
Cell walls are under tension, and their content under compression. Cell walls have strength and elasticity, but if the elastic stress rises above a certain, moderate, value, the structure fails partially and irreversibly. These plastic deformations occur regardless of the method used for

drying plant or animal cells except for lyophilization*, where the original sizes are maintained.

If the cells are killed by scalding, cell walls become slightly permeable, turgidity may disappear, and permanent deformation by drying may become even greater. These processes take place in three phases:

- *The phase of heating* the raw materials under drying; during this phase, there is virtually no phenomenon of evaporation of water from the product, but it is intended overcoming the equilibrium between the relative humidity of the air in the drying plant and the moisture of the product to be dried; heating the air in the system creates its ability to absorb a larger amount of vapors, and through heating the product there decreases the surface tension of the vapors from its surface.
- *The drying phase,* when the evaporation of the water occurs as a result of the imbalance created between the moisture of two environments and also as a result of decrease in the surface tension of vapors from the surface of the product. Evaporation will be achieved in a shorter period of time if air circuit for the elimination of water vapors, which have been overtaken from the product, will be carried out at a faster pace and it will be a closed circuit without heat loss.
- *The final phase* is considered from the moment when the product begins to loosen the bound water; At this stage, the evaporation of water from products greatly slows the drying curve, it registering decreases. Moisture diffusion from the mass of the product becomes increasingly difficult; it depends on the solubility of substances in cell water, the structure of the product, its capillarity, the size of the product pieces subjected to drying.

In this final phase, the molecules of water, adsorbed on the internal surfaces of solid constituents, are removed in a process of diffusion active across blades or solid fibers, in the direction of the surfaces with lower vapor potential.

In this process, a molecule of water, which through exchange gets an impulse higher than average, in its continuous thermal vibration, can jump from its place of absorption in a vacant near place, and, on average, there will be more vacant places in the direction of low vapor pressure. The process will, however, grow slower, until there is reached equilibrium with ambient humidity.

3. CONCLUSIONS

Convective dryers have a wide use due to their high efficiency and simplicity of their construction. Although the variety of constructive designs is large, they can be divided into two large groups, taking into account the mode of operation:

- continuous operation dryers;
- periodic operation dryers.

The pressure of the drying agent is equal to the atmospheric pressure or slightly different from it. If vacuum is created inside the machine, convection effect is greatly reduced, heat transfer to the material being achieved by conduction and radiation.

If natural drying the core thermal agent is solar heat or other renewable energy sources, in dehydration there is used mainly electric power or the one contained mainly in non renewable sources and less in renewable ones. There can be noted research conducted recently on the use with increased efficiency of energy consumed in the processes of dehydration, but also the use of energy from renewable sources or use of energy regarded as a residual of the other technological processes.

Dehydrated products have a reduced volume, less weight, increased energy value, are easy to prepare, bring savings in storage and warehousing, are easily handled and transported, but they lose some aromatic substances and some vitamins are partially destroyed.

The set of phenomena that occur during drying leads to concentration of dry matter, reduction in volume of raw materials used, increased food value per unit of weight and physicochemical changes more or less substantial in the state of membranes and cellular components, which externalize through the rehydration capacity limits.
One of the easiest ways to keep the quality of fruits and vegetables is the preservation by drying or dehydration. While drying is based on the natural heat transfer of water from vegetal products to the outside environment, dehydration involves that same transfer is performed under strict human control, by using appropriate technical equipment.

REFERENCES

[1] Eng. Andreea Lavinia R.I. MARIN, *Cercetari privind optimizarea energetică a procesului de conservare prin uscare a fructelor si legumelor* (Research on energy optimization of the process of preservation by drying of fruits and vegetables), Brasov 2012;
[2] Erol Murad, Aurelian Crăciunescu*, Georgeta Haraga, *Uscatoare mobile pentru zona montana cu impact ecologic redus* (Mobile dryers for the mountain area with low environmental impact), POLITEHNICA University of Bucharest;
[3] Bratu A. , *Operaţii şi utilaje în industria chimică* (Operations and equipment in the chemical industry), Technical Publishing House, Bucharest, 1970
[4] Banu C., *Manualul inginerului de industrie alimentar*ă (Handbook for the Food Industry engineer), Technical Publishing House, Bucharest, 1998
[5] Dascalescu Aurelia - *Uscarea si aplicatiile ei industriale* (Drying and its industrial applications).
[6] Dănescu Al., Nicolescu, Tr., *Termotehnică şi instalaţii termice în agricultură (*Heat engineering and heating installations in agriculture*)*, Didactic and Pedagogical Publishing House, Bucharest.
[7] Davidescu – *Schimbul de caldura in instalatiile industriale* (Heat exchange in industrial installations).
[8] Hazi, Gheorghe; Hazi, Aneta, *Modelarea şi optimizarea procesului de uscare (*Modeling and optimization of the drying process*)*. Plumb Publishing House, Bacău 1999.
[9] Ion Marinescu, Brad Segal, Al. Georgescu, A. Ciobanu, M. Olaru, A. Hobincu - *Tehnologii moderne în industria conservelor vegetale* (Modern technologies in vegetal canning industry), Technical Publishing House, Bucharest, 1976.

PARAMETERS INFLUENCING THE SCREW PRESSING PROCESS OF OILSEED MATERIALS

Mariana Ionescu *, Gheorghe Voicu, Sorin-Ştefan Biriş,
Cristina Covaliu, Mirela Dincă, Nicoleta Ungureanu
University POLITEHNICA of Bucharest, Department of Biotehnical Systems, Biotechnical Systems Research and Development Center

ABSTRACT

Vegetable oil, one of the most important component for both food and non-food industry, is contained by the oleaginous plants in seeds, pulp, stone fruits, in the tubers or sprouts. Depending on the nature of material and their oil content, various methods can be used for oil extraction from oleaginous material. Mechanical continuous presses are the most commonly used machines for the pressing of oleaginous materials in oil industry. These presses have the following advantages: continuous working, high working capacity, operating without major shocks and vibrations, easy adjustment of the working pressures, etc.The request for the vegetable oil increases as a result of the increasing number of applications that it can have. Thus, to satisfy the vegetable oil demand, it is necessary that the oil extraction methods to be faster and more efficient. Processes and phenomena that occur during the pressing process of the oleaginous materials are very complex. For the optimization the pressing process it is useful to know the main variables affecting the oil recovery and oil quality. This study aims to summarize the influence and impact of the main variables on the pressing of oilseed materials.

1. INTRODUCTION

Oil products industry, one of the most important components of modern agriculture, produces edible and inedible oils. About 2/3 of total oil products are the edible oils, which are used directly in food industry as follows: manufacture of margarine, mayonnaise, bakery and pastry products, cooking fats, preserves etc. The remaining 1/3 of the total volume of produced oil is represented by the technical oils, used in the production of various products, such as: detergents, paint, glycerin, fatty acids, varnish, pharmaceuticals or cosmetics, [3].

There are a wide range of raw materials for oils industry. In the vegetable reign are more than 100 oleaginous plants, but only 40 of them can be are used for oil expression. The other plants are unprofitable, as they have low oil content in their seeds or as they require a difficult expression process. The most important oleaginous plants are: sunflower, soya, rape, cotton, poppy, almond, sesame, nut, palm, coconut, olive, flax, castor, [2].

Worldwide, for extraction of oil from seeds, fruits and nuts, four basic methods are used, as it follows:

- chemical extraction (which is a method based on the use of enzymes or solvent to extract the oil from the raw material),
- extraction using high pressure carbon dioxide (i.e. supercritical fluid extraction, SFE),
- steam distillation (the method used for the extraction of 93% from the essential oils),
- mechanical expression (which requires the application of pressure to force oil out of the oil bearing material), [9,11].

Separation of oil from oilseeds is an important processing operation. The process employed has a direct effect on the quality and quantity of protein and oil obtained from oilseeds. Two general terms “expression” and “extraction” are used frequently when discussing about vegetable oil separation. Expression is the process of mechanically pressing liquid out of liquid-containing solids. Extraction is the process of separating a liquid from a liquid-solid system with the use of a solvent. There has been some confusion in the literature between the operations of “expression” and “extraction”. The latter word has been rarely used to designate either operation. This tendency has been so extensive that the distinction between the two terms appears to be disappearing from the literature. The term ”extraction” is also used for mechanical oil expression, [5].

Mechanical pressing and solvent extraction are the most commonly used methods for commercial oil extraction. Screw pressing is used for oil recovery up to 90-95%, while solvent extraction is capable of extracting 99%. In spite of its slightly lower yield, screw pressing is the most popular oil extraction method as the process is simple, continues, flexible and safe, [4].

Mechanical oil extraction (also known as ***pressing***) is based on mechanical compression of oleaginous materials. Through pressing, oil is separated from the oleaginous material (solid-liquid mixture) under the action of compressive external forces that arise in special machines called presses. This method ensures extraction of a non-contaminated, protein-rich low fat cake at relatively low-cost. The disadvantage of this method is that the mechanical presses do not have high extraction efficiencies, about 8-14% of the available oil remain in the press cake, [1].

Pressing operation may be conducted by using hydraulic presses, which are driven by fluid pressure, or in screw presses, where the pressing force is created by a helical body (worm) which rotates in a closed space (press chamber). The hydraulic presses were replaced with continuous screw presses and continuous solvent extraction plants, which are less labor intensive. The olive oil industry still utilizes hydraulic press in the present.

The first screw oil press was developed in 1900 by V.D. Anderson in the United States. This press allows continuous operation of hydraulic presses which resulted in greater capacities with smaller equipments and less labor, [3].

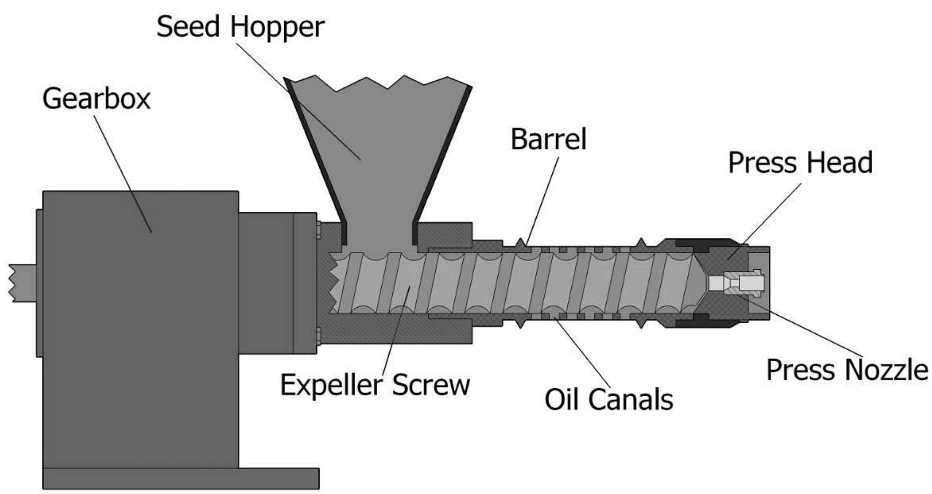

Figure 1: Screw press design, [12]

The mechanical screw press consists of a vertical feeder and a horizontal screw with increasing body diameter to exert pressure on the oilseeds as it advances along the length of the press. The barrel surrounding the screw has slots along its length, allowing the increasing internal pressure to first expel air and then drain the oil through the barrel. Oil is collected in a trough under the screw and the de-oiled cake is discharged at the end of the screw. The main advantage of the screw press is that large quantities of oilseeds can be processed with minimal labor, and it allows continuous oil extraction, [10].

Before the pressing process, the oilseed materials are subjected to various pre-treatment, such as cleaning, conditioning, heating, flaking, dehulling, in order to improve the quantity and the quality of the oil obtained from the raw material. Considerable efforts have been made in the past to improve the oil extraction efficiency of screw presses. Most of them have focused on optimization of process variables such as applied pressure, pressing temperature and moisture conditioning of the fed samples, [1]. Others improvements on oil screw presses were made for the design of the presses and for the material of presses construction.

2. DISCUSSIONS ON THE PARAMETERS INFLUENCING THE SCREW PRESSING PROCESS

When discussing about screw pressing process, a number of parameters had to be taken into account for optimization of the oil production. This study is a short overview of the scientific literature regarding the parameters influencing the pressing process. Literature data show that the most important parameters which influence the pressing process are: screw speed, restriction size, hull content, moisture content, cooking process, temperature, pressure.

Screw speed

The increase of the screw speed leads to the increase of the throughput, while the residual oil content in the press cake will be higher due to the fact that less time is available for the oil to drain from the solids. Also, at higher speed of the screw the viscosity remains lower resulting in less pressure build-up, which leads to the obtaining of relatively high residual oil content, [6]. At slower screw speed, the extraction efficiency will be higher and the oil left in the meal will be lower. In the case of cold pressing, a slower speed is often necessary because as screw speed increases, the temperature of the oil and meal moving through the machine also increases, [12].

At the pressing process of rapeseed using a Mini-40 Rosedown Simon press, [14], it was found that the residual oil from the cake will decrease at a lower screw speed. The decrease of the residual oil may be a consequence of the residence time increasement that occurs as a result of the decrease of the transport speed. An additional reason may be the fact that there is an increase in pressure at the cake outlet nozzle as a result of the increase in the viscosity of the material at lower speeds.

Using a twin screw extruder for pressing sunflower seeds, [8], it was studied the influence of working conditions on the yield of oil obtained. Thus, it was observed that if the screw speed was reduced, for several values of throughput or pressing chamber temperature, there has been a rise in the yield of oil extracted. Energy consumption has also increased with increasing of screw speed, due to the increasement of the specific mechanical energy.

Restriction size

When the restriction size (the dimension of the press nozzle) is reduced the pressure in the pressing chamber increases (because a higher force is required to overcome the restriction) and that will conduct to a higher oil yield, [4,6].

During the experiments conducted by Vivek S. Vadke, [14], it was observed that with decreasing of choke opening (nozzle size) will decrease the amount of residual oil in the cake. This is explained by the fact that when the nozzle size is smaller, the pressure is higher due to higher flow resistance. It was also shown that press productivity will decline if the choke opening will be reduced.

Another study, [7], has revealed the influence of choke opening on the press performance (press with 100 kg/h throughput produced by ICAERD) when pressing the jatropha seed with a moisture content of 15%. The experiments were carried out using different size for the choke opening, such as 6, 7 and 8 mm. It is noted that the varying of the choke opening had a significant influence on the processing capacity of the press. However, by increasing the size of nozzle achieved a reduction in the yield of oil extracted. Therefore, when increasing the nozzle size from 6 to 8 mm, the oil yield decreases from 30.4% to 25.8%.

Hull content

The hull content of the raw material subjected to the pressing process is expected to affect both oil recovery and energy requirement. Removal of the hull, which is a hard material, would require less energy for breaking and compressing and result in zero presence of hull fibers in the crude oil. However, the oleaginous material needs to contain a certain percent of hull, because, seeds without hull will turn into a paste inside standard expellers, which sticks to the worm and keeps rotating along with it. As the hull of the oleaginous seeds contains a low percent of oil, the removing of hull may lead to decreased absorption of oil, which will mean the increasing in oil recovery, [4,6].

In order to study the influence of seeds dehulling on the pressing process, experiments using flaxseeds, variety Omega, were conducted, [16]. After the pressing process has finished has been observed that, although the oil yield obtained from dehulled flaxseeds was smaller than the oil yield obtained from whole flaxseeds (72.0% to a moisture content of 10.5%), the oil productivity for dehulled seeds was higher. It also has been observed that the temperature of the oil and the cake obtained from dehulled flaxseeds was much lower than for whole seeds. Thus, the pressing of dehulled flaxseeds presents several advantages for the production of organic flaxseed oil.

To analyze the necessary energy to press whole or dehulled seeds, [17], a study was conducted on a S 87G Komet screw press. The study revealed that the decrease of the fraction of hull removal (FHR) led to significant increases in oil and cake temperature. This is due to the fact that the lower fiber content of the dehulled seeds leads to smaller friction during the pressing process. When pressing whole flaxseeds, specific mechanical energy (SME) was much higher than in the case of dehulled flaxseeds pressing. The oil yield obtained at dehulled flaxseeds pressing was lower than that obtained at the whole seeds pressing, but taking into account that the specific mechanical energy and the oil/cake temperature obtained from dehulled seeds is lower we can consider that pressing dehulled seeds is a convenient process.

Moisture content

The moisture content of the oleaginous material is another important factor affecting the pressing process. An optimal moisture level for oil expression is expected to exist. In the literature, it is considered that in case of rapeseed the optimum moisture level is close to 7%, while for flaxseed the optimal moisture content is expected to be around 6%, [4]. The increasing of the moisture content of the oilseeds leads to the increasing of the yield until a maximum point. After this point, the increasing of moisture content will conduces to the decrease of the oil yield. This phenomena is explained by the fact that the increasing of the moisture content make the cell walls more permeable (which increases the yield), but it also cause a plasticization of the seed material which reduces the oil yield, [15].

In a study whose objective was to analyze the necessary energy for pressing Omega flaxseeds, whole or dehulled, [17], it was used a S 87G Komet screw press and experiments were carried out in four stages, where the process variables were the moisture content of the seeds and the fraction of hull removal (FHR). Moisture content of the seeds take the values from 6.3 to 12.6% (dry basis) and the fraction of hull removal was 20%, 62% and 85%, in a first step whole seeds being pressed to. It is noted that, for pressing the whole seeds, reducing the moisture content from 12.6 to 6.3% (dry basis) resulted in increased yield of extracted oil , the maximum yield (89.4%) being obtained at the lower moisture content of the seed (6.3%). Instead, when pressing dehulled seeds, the maximum oil yield was not achieved at the minimum moisture content. It was also observed that the decrease in moisture content resulted in significant increases in oil and cake temperature; also, the specific mechanical energy (SME) increased significantly from 81.1 to 104.7 kJ/kg when the moisture content of the whole flaxseeds decreases from 12.6% to 6.3%.

Temperature

In order to obtain good quality oil, the temperature of the material during the pressing process should not exceed maximum allowable values. This is necessary in order to prevent undesired cell wall components polluting the oil. The higher temperatures on the pressing process leads to the dissolving of the phosphor in the oil, [6]. Therefore, it is desirable to obtain the high yields at lower temperatures, [15].

In a study regarding the influence of moisture content and cooking on the pressing process of crambe seeds, [13], it was observed that at moisture content in the range of 3.6 and 9.2%, the extracted oil yield from cooked crambe seeds was higher than the uncooked seeds. For the same values of the moisture content, the processing capacity of the press was higher for the uncooked seeds. Another conclusion of this study was the fact that in the case of uncooked seeds, the residual oil in the cake was higher than for the cooked seeds, while the foot content of the oil was higher for cooked seeds.

Pressure

The radial pressure which arises in the pressing chamber is a parameter directly proportional with the oil yield. Therefore, with the increasing of the pressure, the oil yield increases reaching a maximum limit at higher pressures. This maximum is dependent on the type of seed, pre-treatment applied to the seed and the equipment used. Generally, the specialty literature presents data which limite the pressures below 35 MPa, with a few exceptions, [15].

The effects of compressive stress, feeding rate and speed of shaft screw press on palm kernel oil yield were studied, [1]. They used an expeller with a rated capacity of 180 kg/h for experiments which were conducted by using a factorial experimental design with 3 variables at 3 levels: compressive stress (10, 20 and 30 MPa), feeding rate (50, 100 and 150 kg/h) and shaft screw press speed (50, 80 and 110 rpm). A maximum efficiency of 94,5 % (meaning a maximum oil yield of 46,3%), was obtained at 30 MPa compressive stress, 150 kg/h feed rate and 110 rpm of screw speed, while the minimum express efficiency of 33,6 %, (which represents a 16,3% oil yield) was obtained at 10 MPa compressive stress, 150 kg/h feed rate and 50 rpm of screw speed. For the studied range, oil yield increases with increase in speed of shaft screw press and in feeding rate. Oil yield is directly proportional to compressive stress while influence of speed is marginal, and also it is possible to predict a further increase in oil yield with an increase in compressive stress.

3. CONCLUSIONS

Vegetable oils have a great importance for human health as well as to the oil chemistry. Vegetable oils can be obtained from many oleaginous materials using various technological processes, chemical and mechanical. Solvent extraction technology is still the most widely used process and the one with higher extraction efficiency, but due to the fact that this method use chemicals which affect the environment and human health, new technologies have been researched. The object of this study is the screw pressing method of obtaining oil from oleaginous seeds, which is a simple process that obtain high quality oil at a lower cost. In order to optimize the pressing process, it is important to know the parameters that have the higher influence on the process. Analyzing the literature, the most important parameters which influence the pressing process are: screw speed, restriction size, hull content, moisture content, cooking process, temperature, pressure.

References

[1] Bamgboye, A., Adejumo, A., *Development of a sunflower oil expeller,* Agricultural Engineering International: the CIGR Ejournal. Manuscript EE 06 015, vol IX, September 2007.

[2] Banu, C., *Manualul inginerului din industria alimentară*, vol. I și II, Editura Tehnică, București, 1999.

[3] Bargale, P.C., *Mechanical oil expression from selected oilseeds under uniaxial compression*, Ph.D. Thesis, University of Saskatchewan, Canada, 1997.

[4] Beerens, P., *Screw-pressing of Jatropha seeds for fuelling purposes in less developed countries*, Ph.D. Thesis, Eindhoven University of Technology, the Netherlands, 2007.

[5] Biris, S.St, Manea, M., Maican, E., Ungureanu, N., Toma, L.M., *Studies regarding the use of finite elements method for the working process modeling of the oil presses*, Proceeding of the 37th International Symposium „Actual Tasks on Agricultural Engineering", Croaţia, Opatija, pg. 485-496, 2009.

[6] Cramer, J., The Jatropha Handbook From Cultivation to Application, FACT, ISBN 978-90-815219-1-8, The Netherlands, 2010.

[7] Harmanto, A., Hendriadi, E., Rahmarestia, Mardison, Wiyono, J., *Performance test of a screw-press machine for extracting jatropha curcas seed into crude oil as an alternative energy source,* Indonesian Journal of Agriculture 2(I): 35-40, 2009.

[8] Kartika, I.A., Pontalier, P.Y, Rigal, L, *Extraction of sunflower oil by twin screw extruder: Screw configuration and operating condition effects,* Bioresource Technology 97, 2302-2310, 2006.

[9] Masango, P., *Cleaner production of essential oils by steam distillation*, Journal of Cleaner Production, 13, pg. 833-839, 2005.

[10] Nurhan, D., *Oil and Oilseed Processing II,* Robert M. Kerr Food & Agricultural Products Center, FAPC-159.

[11] Ogunsina, B.S., Owolarafe, O.K., Olatunde, G.A., *Oil point pressure of cashew (Anacardium occidentale) kernels*, International Agrophysics, 22, pg. 53-59, 2008.

[12] Schaufler, D, *Oilseed Fact Sheet: Oilseed Presses,* Dept. of Agricultural and Biological Engineering, Penn State College of Agricultural Sciences.

[13] Singh, K.K., Wiesenborn, D.P., Tostenson, K, Kangas, N., *Influence of moisture content and cooking on screw pressing of crambe seed*, Journal of the Amercian Oil Chemists' Society, vol. 79, nr.2, 2002.

[14] Vadke, V.S., Sosulski, F.W., Shook, C.A., *Mathematical simulation of an oilseed press,* Journal of the American Oil Chemists' Society, v. 65, p. 1610-1616, 1988.

[15] Willems, P., *Gas Assisted Mechanical Expression Of Oilseeds*, Ph.D. Thesis, University of Twente, the Netherlands, ISBN: 978-90-365-2502-2, 2007.

[16] Zheng, Y.l., Wiesenborn, D.P., Tostenson, K., Kangas, N., *Screw pressing of Whole and Dehulled Flaxseed for Organic Oi*l, Journal of the American Oil Chemists' Society, v. 80, p. 1039-1045, 2003.

[17] Zheng, Y.l., Wiesenborn, D.P., Tostenson, K., Kangas, N., *Energy analysis in the screw pressing of whole and dehulled flaxseed*, Journal of food engineering, v. 66, p.193-202, 2005.

MICRO GREENHOUSE CLIMATE MANAGEMENT BASED ON THE ARDUINO

George IPATE[1], Gheorghe VOICU, Elena Madalina STEFAN,
Nicoleta UNGUREANU, Cristian NUTESCU
University POLITEHNICA of Bucharest

ABSTRACT

The plants in a greenhouse impose their own needs, significantly affect their ambient conditions in a nonlinear way, and add long-time constants to the system response. Our work presents a low-cost indoor climate acquisition system, based on the Arduino hardware platform; the hardware and software components are presented, together with experimental evaluation. This system was designed to be integrated in an environmental evaluation platform based on inexpensive device signals that will be used for monitors and control and management the climate greenhouse. The experimental evaluation revealed that this system is not only capable of climate signal acquisition, for our purposes, but it can also be used as a generic platform for other environmental applications, greatly extending its applicability. The tests revealed that the sensor selected provided excellent agreement with a far more expensive air and soil monitor. In this paper we describe the proposed platform, with special emphasis on the design principles and functionality. Future work will focus on further developing our hardware, targeting its integration in a prototype system for environmental evaluation platform.

1. INTRODUCTION

Accurate sensors have become available, offering the opportunity of gaining insight into the relations between the crop and its environment. The present climate conditioning equipment allows for a wide range of modifications of the climatic factors relevant for crop growth, such as the temperature, humidity level, carbon dioxide concentration and radiation level in the greenhouse and the availability of water and nutrients in the root environment. Finally, developments in the field of analog and digital electronics have resulted in a high level of automation of greenhouse climate control.

There are multiple hardware choices available; however the Arduino is currently the most flexible and easy-to-use hardware and embedded software platform, with low cost, easy communication, and software running on a computer or other devices.

Nowadays, the use of the Arduino in agriculture and environmental applications has been widely explored for simple usage scenarios. One particular example is available at (Shaker, 2013), where the Arduino is used to monitoring climate greenhouse, (Nugroho, 2011) who proposed an intelligent control system for a greenhouse and many other examples. Therefore, this project will contribute to the creation of a new system, modular, multi-purpose, easily accessible and with the possibility to be assembled by anyone interested on greenhouse control. In the following sections we describe the acquisition system, designed especially for greenhouse climate data collection.

2. METHODOLOGY

The sensors used inside our experimental greenhouse model were soil moisture sensor, temperature and humidity sensors, but parallel we have monitored the air quality in the

[1] Corresponding author email : ***puiuipate@yahoo.com***

greenhouse. Inside temperature and humidity were measured in the air, on the ground surface and 20 cm inside the ground. Other type of sensors, like barometric pressure, outside weather conditions or lighting sensors can be connected too. The temperature and humidity inside the greenhouse could be controlled using heaters and overheat protection devices (ventilators) system. The soil moisture and water purity could be controlled using pumps and hydrocyclone devices. Laboratory experimental greenhouse is schematically shown on figure 1 and figure 2 shows the laboratory greenhouse model.

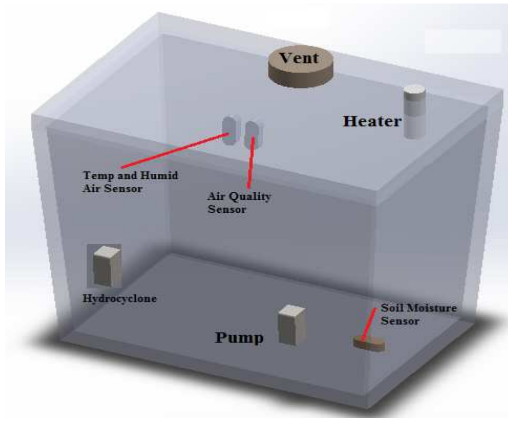

Figure 1. Micro Greenhouse model schematic

Figure 2. Laboratory experimental greenhouse

The proposed acquisition system has two main parts: Hardware and Software. In this particular work, the hardware is composed by the Arduino platform and environmental sensors. The diagram represented in Figure 3 synthesizes the overall architecture of the hardware subsystem, showing a schematic of the main components.

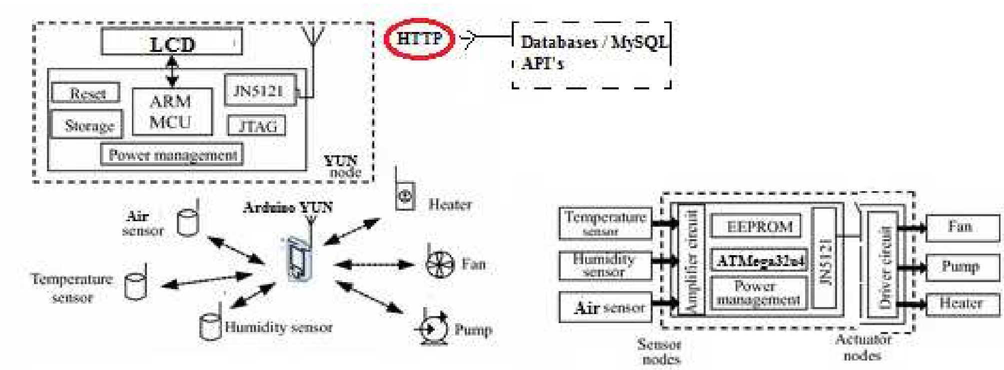

Figure 3. Global architecture system (adapted from Zhang, 2010)

HARDWARE. The main component of this section is the **Arduino Yun**. The Arduino Yún is a microcontroller board based on the ATmega32u4 and the Atheros AR9331. The Atheros processor supports a Linux distribution based on OpenWrt named OpenWrt-Yun. The board has built-in Ethernet and Wi-Fi support, a USB-A port, micro-SD card slot, 20 digital input/output pins (of which 7 can be used as PWM outputs and 12 as analog inputs), a 16 MHz crystal oscillator, a micro USB connection, an ICSP header, and a 3 reset buttons.

In the case of ***soil moisture*** acquisition (figure 4.a), the electrical activity of the soil is captured using electrodes placed on there. Those signals are acquired through the analog input ports on the Arduino board, and subsequently converted using the internal analog-to-digital converter. Then, the digitalized data is sent via Wi-Fi to the database station (e.g. https://thingspeak.com).

The ***TP 401A indoor air quality sensor*** (figure 4.b) is connected to one of the Arduino analog input pins. This sensor is designed for comprehensive monitor over indoor air condition. It's responsive to a wide scope of harmful gases, as carbon monoxide, alcohol, formaldehyde and so on. Due to the measuring mechanism, this sensor cannot output specific data to describe target gases' concentrations quantitatively. But it's still competent enough to be used in applications that require only qualitative results, like auto air cycling systems.

Grove Temperature and Humidity Sensor Pro (DHT22) is a high accuracy sensor used in home conditions. It consists of a capacitive sensor element used for measuring relative humidity and a negative temperature coefficient (NTC) thermistor used for measuring temperature. Small dimension, ultra low power consumption, more than 20m's signal transmission distance makes it a good selection for various application environments. The accuracy of this module can gets up to 0.3 degree in temperature and 2% in relative humidity.

Water Flow Sensor uses a simple rotating wheel that pulses a Hall Effect sensor. By reading these pulses and implementing a little math, we can read the liquids flow rate accurate to within 3%.

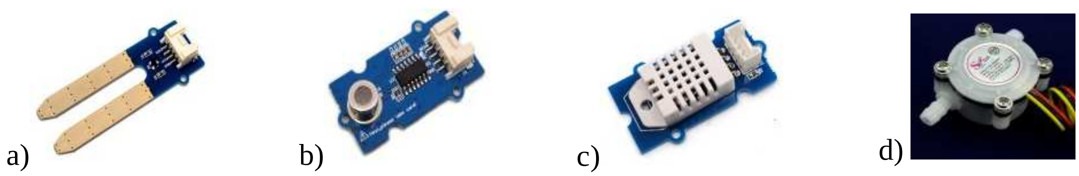

Figure 4. Environmental sensors: soil moisture; air quality; air temperature and humidity; water flow

SOFTWARE. Regarding the software, there are two main programs developed: the Arduino Firmware, which controls its operation, and an Application Programming Interface (API), which communicates with the Arduino, controls the acquisition process, allows the access to the collected raw data and enables high-level applications to access both the device and the data. The firmware development performed in our work was designed to define the behavior of the Arduino microcontroller, setting its parameters, such as sampling rate, baud rate and communication protocol. The open source Arduino environment makes it easy to write code and upload it to the I/O board, which is one of the main reasons why this platform was chosen as the base for our system (Alves, 2010).

In a new system design, system hardware will be chosen according to the overall requirements of the system. Application software needs to be developed in order to achieve the required system functionality. System designer must compromise between hardware and software solutions for each problem. Hardware solutions are easier to design, faster and more accurate in operation. Software solution results in smaller production cost and system modifications are simpler. Particularly, connection to Internet must be considered. When embedded processor is located in the vicinity of local network installation, 150Mbps Wi-Fi interface is chosen.

3. RESULTS AND DISCUSSION

This section presents the experimental results obtained for the micro greenhouse climatic control problem. The control system works such as described in Figure 3, where the controller only calculates a control signal when an event happens. Two types of control procedures were applied: a) simple switch on – switch off control of all actuators using output relays; b) the time on – off control. This type of control is especially important for wetting system but it could be used for any actuator. The users choose the time moments when one of actuators would be switched on and time duration of its active state.

Tests were performed to the final system, to check and evaluate its validity. Various scenarios and possible conditions that occur in the field was tested using the systems such as manual management mode, failure of Internet connections, changes of settings configuration via network, and so on. The experiment was conducted using devices as follow: Arduino Yun board, variable resistors, network devices and relay actuation.

Variable resistor is considered as the input of indoor air temperature and soil moisture content that can be changed as scenario condition. Variable resistor operated manually to set the value of input as well as behavior of soil moisture content and temperature during cultivation. Value of input was carefully observed as the collected information either online mode. Furthermore, changing of system settings (delay reading sensor, limit of minimum value) was also tested.

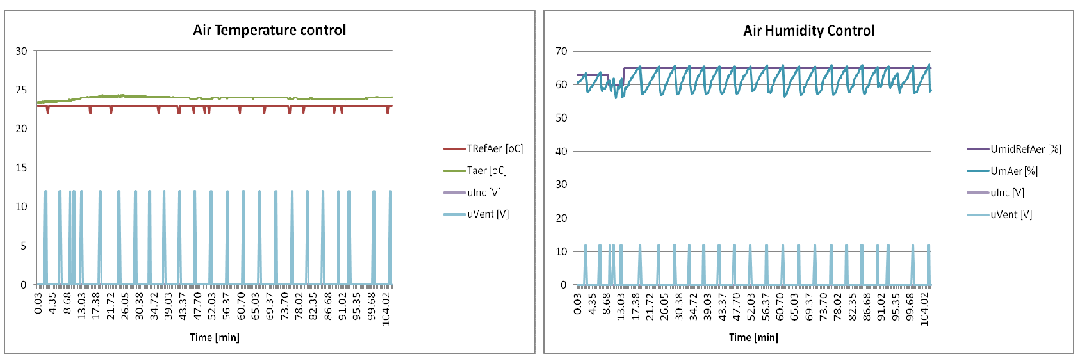

Figure 5. Temperature and Humidity Air control

Figure 5 shows two control examples. The first one, shown in Fig.5a) is temperature air control using heater and the second one, shown in Fig.5b) is humidity air control using cooling devices (ventilators).

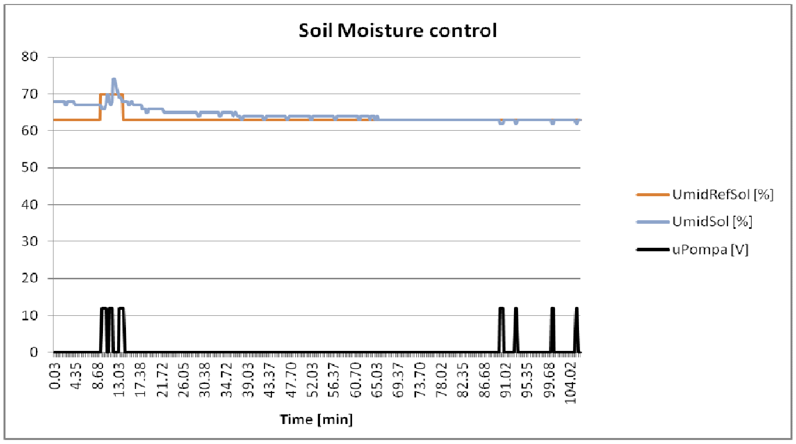

Figure 6. Soil moisture control

In Figure 6, where the control results for the approximately two hours are shown, it can be observed that the soil moisture signal is within acceptable ranges for the event based controller (errors of less than 1 %). The main advantage of bipositional controller is reflected in the resulting control signals, where the number of commutation is considerably smaller.

The Yún has a number of built-in capabilities for networking, but some of the most exciting aspects are working with other online platforms.

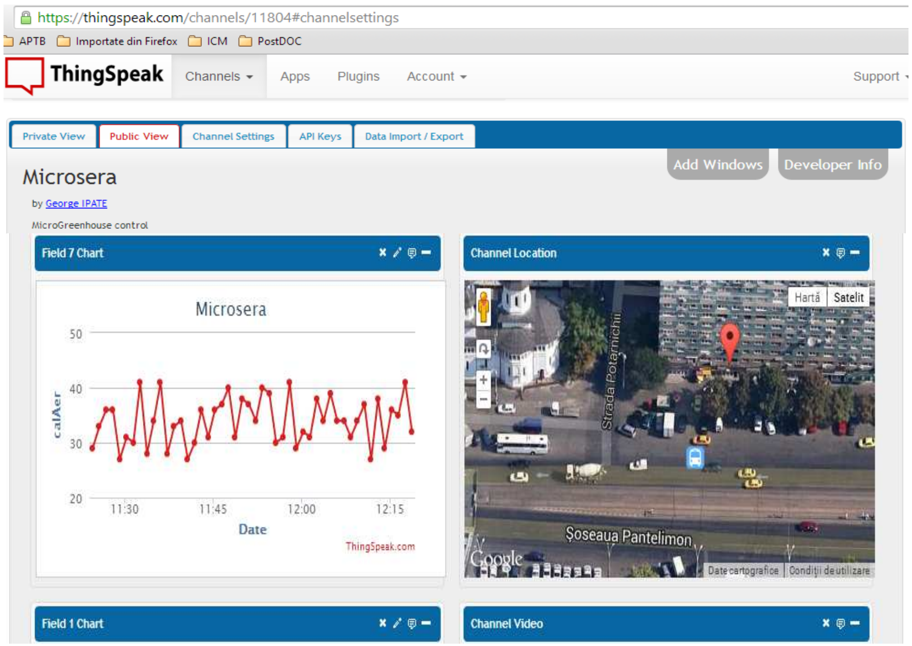

Figure 7. Online platforms - displaying archive air quality

As the Embedded Web Server memory is not big enough to store archive files, they are stored to another standard Web server. ThingSpeak is an open source "Internet of Things" application and API to store and retrieve data from things using HTTP over the Internet or via a Local Area Network. With ThingSpeak, we can create sensor logging applications, location tracking applications, and a social network of things with status updates. Figure 7 shows one example of displaying archive air quality data.

4. CONCLUSIONS

The quality and productivity of plants inside the greenhouse is highly dependent on the management quality. Therefore, continues monitoring of the conditions near to the plants and water irrigation adjusting will allow for maximum crop yield.

We have designed and implemented a network embedded greenhouse monitoring and control based on embedded Web server unit which gather and route data from local sensor/actuator network to global network - Internet. applicable to all environmental applications. Experimental results have shown that the data collected through the proposed system, preserves the waveform properties that are used by the dynamic systems.

The developed experimental system, based on Arduino YUN embedded Web client, collect data from distributed sensors and activate connected actuators using simple 1-wire local network. However, in its current state, this prototype system is already prepared for deployment in real-world test beds, and is an adequate low-cost alternative for large-scale data acquisition.

References

[1] Alves, A. P., Silva, H., Lourenc A., Fred, A., *BITtalino: A Biosignal Acquisition System based on the Arduino*, Academic Press, Published by Elsevier Inc., 2010.

[2] Gonda, L., Cugnasca, C.E., *A Proposal of Greenhouse Control Using Wireless Sensor Networks*, Computers in Agriculture and Natural Resources, Proceedings of the 4th World Congress Conference, pp 229-233, 2006.

[3] Shaker, M., Imran, A., *Greenhouse Micro Climate Monitoring Based On WSN with Smart Irrigation Technique*, Intern. Journal of Electrical, Electronic Science and Engineering, Vol 7, No. 12, pp15-20, 2013.

[4] Nugroho, A.P., Okayasu, T., *Development of Intelligent Control System for Greenhouse, www.researchgate.net*.

[5] Stipanièev, D., Èiæ, M., Marasoviæ, J., *Networked Embedded Greenhouse Monitoring and Control*, Biomass and Bioenergy, Vol 13., No. 3, pp141-146, 1997.

[6] Zhang, Q., et al., *A wireless solution for greenhouse monitoring and control system based on ZigBee technology*, Journal of Zhejiang University SciA, pp 1584-1587, 2007.

THE USE OF ELECTRIC FIELD FOR POLLUTANT REMOVAL FROM CONTAMINATED SOILS

Irina-Aura Istrate[1], Talida Mirona Oprea[2]
[1] University POLITEHNICA of Bucharest, Faculty of Biotechnical Systems Engineering, Department of Biotechnical Systems
[2] University POLITEHNICA of Bucharest, Faculty of Power Engineering, Department of Hydraulics, Hydraulics Machines and Environmental Engineering

ABSTRACT

In our days the pollution of air, water and soil represents a big problem for human society. Even if soil is very important for many human activities, the pollution of the subsurface has not received as much attention as for air and water. As a consequence, soil and groundwater are being degraded as a result of pressure coming from nearly all economic sectors. In the present paper two situations will be presented: the first one is related to an artificial contamination of soil and the second one to a natural contamination one. Also, the behavior of the organic contaminants will be studied.

1. INTRODUCTION

In our days the pollution of air, water and soil represents a big problem for human society. Even if soil is very important for many human activities, the pollution of the subsurface has not received as much attention as for air and water. Soil is an extremely complex medium and different soil fractions and constituents have very variable degrees of reactivity to any introduced compounds [1, 2]. Thus the simplicity of the “cause and effect” situations that can be obvious in air and water pollution incidents is usually unattainable. Major problems in Europe include: loss of top-soil due to erosion or building activities, contamination, and acidification. As a consequence, soil and groundwater are being degraded as a result of pressure coming from nearly all economic sectors. Industrial activities had released to the environment many toxic chemicals, that is, heavy metals and persistent organic pollutants, due to accidental spills or improper management. It was noticed that many conventional in situ remediation technologies are found to be ineffective and/or expensive to remediate sites with low permeability and heterogeneous subsurface conditions and contaminant mixtures [1, 2, 3].

This study aimed at evaluating the effectiveness of electrochemical oxidation as a single treatment of different types of hydrocarbons polluted soils.

2. METHODOLOGY

2.1. Electrochemical treatment

Electrokinetic remediation, variably named as electrochemical soil processing, electromigration, electrokinetic decontamination or electroreclamation uses electric currents to extract radionuchdes, heavy metals, certain organic compounds, or mixed inorganic species and some organic wastes from soils and slurries [3, 4, 5].

[1]Splaiul Independentei, 313, 0723542609, ia_istrate@yahoo.com

Empirical evidences indicate that the reaction rates are inversely proportional to grain size, such that this remediation technique is particularly effective in saturated low permeability soils (like clays and silts), which are often more difficult to treat with conventional chemical methods (such as chemical oxidation or soil flushing), because of their low permeability and their high sorption capacity [4].

For this research were used as a material three kinds of soils: kaolin (clay), sand and sediments. In the first two cases the contamination was artificial and for the last one was natural.

Clay minerals are common weathering products of rocks and sols, characterized by small-size particles with very high specific surfaces. They are composed of a layer structures, named as phyllosilicates. Each phyllosilicate is composed by unit cells which bond to each other form sheets and layers [5,6,7].

The type of clay used in the present research is the kaolinite known also as kaolin. The kaolin, used in the experimental research is composed from particles with dimensions that range between 2μm e 75μm (for 40%) and less than 2 μm (for 60%).

The kaolin that was used for this research has a cation exchange capacity (CEC) of about 8.3 meq/100g and a pH of about 6. Because it was necessary to be know what influence has the content of metals from the soil on the system efficiency, it was determined the quantity of iron and manganese from the kaolin; 2794 mg/kg$_{dw}$ of iron and 34 mg/kg$_{dw}$ of manganese. The main characteristics of the kaolin used during this research, are presented in table 6.2.

The sand that was chosen for this research is dried silica sand. The sand was acquired by the Laboratory of Hydraulics of Faculty of Engineering of Trento from the company Va.Ga. S.r.l. (Pavia). Was chosen this type of sand because, from all available products, this one had the most uniform and fine granulometry; we looked a sand that was characterized by small particles because, as seen in other research, was observed that electrochemical remediation is more efficient for soils that are characterized by a very low hydraulic conductibility and a fine granulometry.

The sand has undergone a series of treatments, done by the company Va.Ga. S.r.l., such as:

- initially the inert are extracted and brought into the screening and washing;
- after that the material is passed through a crushing installation, equipped with two mills, a primary and a secondary that allows the selection and the control of the material that will be crushed and allow the recovery of the coarse parts of the extracted inert;
- at the end, the material arrives in a drying installation where it is inserted in a rotary oven at 1100 C; after that the sand is cooled down and cleaned.

As for the mineralogical composition of the Vaga12 we have: main compound is quartz – 61.8%; granite rocks – 16.5%; feldspar – 12.7%; the rest of about 9 %, is formed from other types of minerals.

The granulometric analysis showed that the particles have a diameter that range between 0.01 mm to 0.20 mm, so can be classified as sand. Vaga 12 has a cation exchange capacity (CEC) of 0.7 m$_{eq}$/100g of soil, a very low value if we compare with CEC of kaolin (8.3 m$_{eq}$/100g).

The sand used for experimentation, is a dissolved material, monogranulare, without particles of clay, without content of organic matter (TOC negligible amounts to 0.23g/kg$_{dw}$) and poor in nutrients (shortage of potassium, calcium and magnesium), because of these characteristics the sand have a low cation exchange capacity and consequently a low power buffer.

The experimental research performed foresees the application of electrooxidation on matrix of artificial contaminated soil with diesel. The diesel used was purchased from petrol station from Trento. The diesel, as almost all the hydrocarbons, is a product of distillation fractional of crude oil, or is produced by cracking (operation through which the hydrocarbons of high molecular weight are fragmented in the presence of a catalyst). In diesel, generally, there are several classes of hydrocarbons such as paraffin, naphthenic and aromatic, whose proportions vary from diesel to diesel: generally, is a mixture containing aliphatic hydrocarbons (including cyclical) from 13 to 18 carbon atoms and is composed of approximately 75% from saturated hydrocarbons (mainly paraffins) and 25% aromatic hydrocarbons. The choice of diesel as a contaminant of soil appeared from the need to represent environmental pollution caused by oil spills and various oil products; indeed the most frequent sources of contamination are made up of losses of oil, which may arise from industrial activities, refineries and oil spills fuel. The diesel, used in this project it appears light-colored, slightly amber and over time saw gradually reduce its sulphur content of up to 0.33%.

2.2. Experimental research

The treatment was applied on three different soil matrixes: sand, kaolin and a mixed sample. Each of the experiments will be presented separately and after the conclusions will be drawn. All the tests had the same main parameters, which are the treatment period was of about 28 days, the applied voltage of 10 V and the distance between electrodes is of about 10 cm.

2.2.1. Test on kaolin matrix

Test ET_K, which aimed at investigating the variation of contaminant removal with test duration, was performed with a constant voltage of 10 V (1 V/cm) for 4 weeks. The initial current flowing across the soil specimen was 17 mA (the measurement was done at the beginning of the test, after 20 minutes).

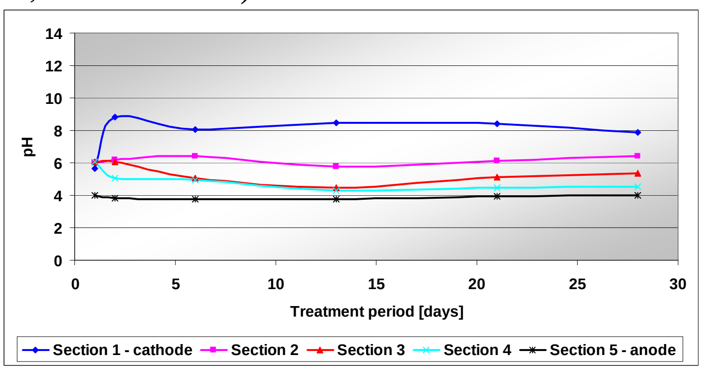

Figure 1: pH variation during test ET_K

TOC removal increased with the increase of the treatment time from 45% to 54 %, and for TPH the removal percentages are higher from 50 to 80%. The results are presented in table 1.

Table 1: The removal percentages obtained during the test ET_K

Elapsed time [d]	TOC [g/kgss]	TPH [mg/kgss]	TOC Removal [%]	TPH Removal [%]
0	208.1	130.977	-	-
7	113.6	64.966	45%	50%
14	109.2	60.338	48%	54%
21	107.8	30.873	48%	76%
28	95.5	26.566	54%	80%

2.2.2. Test on sand matrix

The test ET_S has been performed on a sample of sand Vaga 12 of about 1.8 kg, artificially contaminated by diesel fuel. During the test, on the sample was applied a constant potential difference of 10 V, which corresponds to a specific voltage of 1 V/cm, for a period of 28 days. The initial sample of soil had the humidity equal to 23.9% and a pH of 8.88.

At the beginning of the test, the current was measured and presented a value of 3.98 mA. The behavior of the current was similar with the one observed during the test ET_S and also with the one observed with the tests performed with clay. This behavior was characterized by a modest increase of the current in the first hours of the tests and after that a rapid decrease of the current in time was noticed after several hours from the beginning of the test. This decrease was observed until the current reached a constant value were remained until the end of the test (steady state value).

Contrarily with what was noticed with the clay, in sand case, the electroosmotic flux it is formed after some days from the beginning of the sample (more precise after 94 hours). Moreover, the flux collected at the cathode increased for a maximum 8 days from the beginning of the test, after which stopped. This behavior is justifiable because in between the third and the eight days of the test the current increased and reaches a value a little bit higher than the initial one (4 mA) and it is maintained almost constant for a few days after which starts again to decrease. The quantity of the electroosmotic flux was too small to be analyzed in the laboratory.

In this test, the removal percentages were modest (20% for the TOC and 27% for TPH) and lower than the results obtained in the previous test, were the applied voltage was lower (figure 2). So it can be noticed that an increasing of voltage does not always produce increasing pollutant removal.

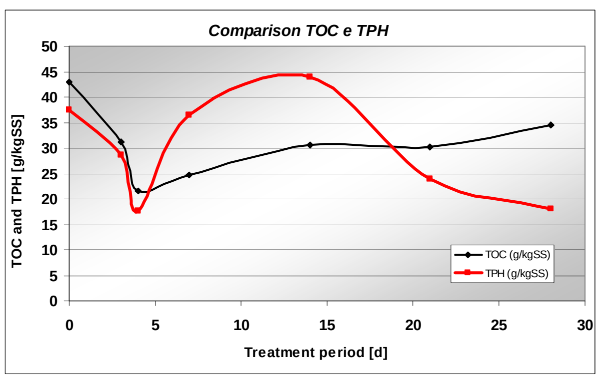

Figure 2: Comparison between the TOC and TPH evolutions in time for test ET_S

2.2.3. Test on mixed matrix

The test ET_M is a test performed on stratified sample. The layers of soil were placed horizontal in the electrochemical reactor, precisely on the bottom of the reactor we have sand and on the top kaolin as shown in figure 3.

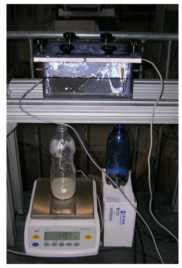

Figure 3: The sample configuration for test ET_M

After a modest initial peak in the first hours of the test the current began to decrease, arriving at his initial value after two days. Afterwards, the current value remained constant for a few days, then return to decrease, after 14 days, arriving to values between 11 - 8 mA. Moreover, during the test, it was noticed the formation of an electroosmotic flux that was developed in the early days of the test, specifically after four days of the test the flux become negligible, because the current is low, and it is stopped on a value of 125.9 mL (figure 4).

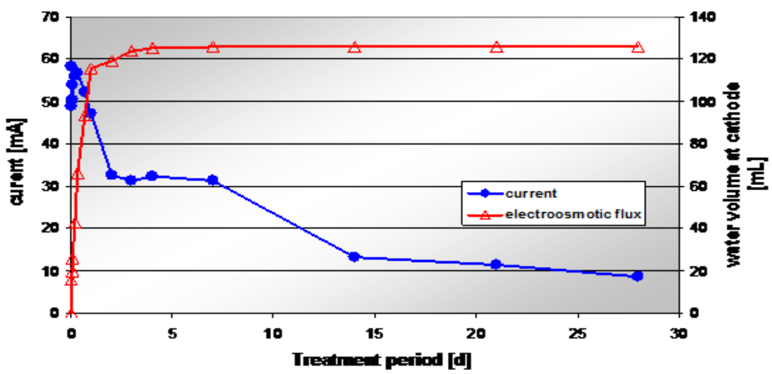

Figure 4: The current and electroosmotic flux measured during the test ET_M

Table 2: Contaminant concentrations and removal percentages obtained after test ET_M in sand layer

Time [d]	TOC [g/kg$_{ss}$]	TPH [g/kg$_{ss}$]	Removal TOC [%]	Removal TPH [%]
0	87.6	67.6	-	-
28	53.4	20.9	39	69

Table 3: Contaminant concentrations and removal percentages obtained after test ET_M in kaolin layer

Time [d]	TOC [g/kg$_{ss}$]	TPH [g/kg$_{ss}$]	Removal TOC [%]	Removal TPH [%]
0	64.1	39.9	-	-
28	58.0	30.0	9	25

The kaolin shows a modest decline in TOC and TPH at the end of treatment, while the sand shows a good removal (table 2 and table 3). This fact leads us to believe that, again, has witnessed the phenomenon of exchange of pore water between sand and kaolin. During this test, the kaolin had a final humidity of about 8 percentage points lower compared to its initial humidity. Even the sand presents a decreasing in humidity at the end of the process. The fact that the kaolin has failed to recover all the quantity of water lost through electroosmosis underlines the fact that the clay is able to take the water from the sand, because the kaolin is located above the sandy layer and have to defeat the gravitation in order to move the water from one layer to another.

This most likely has reduced the exchange between sand and kaolin also in terms of the contaminant. In this way, the electrooxidation could act, however, leading to some removal of contaminants in kaolin.

3. CONCLUSIONS

This study was conducted to assess the effectiveness of electrochemical oxidation for the remediation of different organic pollutants from sediments, fine-grain soils and sand. The research started with the aim of identifying the optimum parameters for the application of electrochemical treatment.

For the tests performed on a single type of matrix, was noted that the contaminant removal increases significantly with the duration of the process, or better said longer last the treatment, bigger are the results. Indeed in the removal variation in time it is noted that the line is in continuous growth even after 28 day treatment. Concentration profile along the sample is not always uniformly distributed; sometimes some areas present a higher remediation than others. This probably is also due to the fact that the diesel, in a matrix of sand, is characterized by a quite high hydraulic conductibility and because of that tends to migrate at the top of the sample.

In the electrooxidation tests, conducted on a stratified sample composed by sand and kaolin, it was noticed that after 28 days of treatment it was noticed a higher removal in sand than what was obtained in the same type of test on kaolin. In fact, the sand has reached during the tests with only electrooxidation to an efficiency of about 39% in terms of TOC and 69% in terms of TPH. In addition, it was observed that the removal percentages in sand for this test are higher than the ones obtained at the end of a test performed with only electrooxidation, with the same voltage, on a sand sample (percentages ranging between 20-35% for both TOC that TPH). The non-uniformity in contaminant removal, which is observed between sand and kaolin, can be attributed to an exchange of interstitial flow that moves from sand towards kaolin, due to the formation of electroosmotic flux in kaolin, resulting in the creation of an negative pressure gradient. This exchange of pore water between sand and kaolin depends on the sand and clay distribution (vertical layers, horizontal layers, the kaolin position respect to the sand position);

References

[1] Istrate, I.A., *Advanced chemical and electrochemical techniques for the remediation of petroleum contaminated sites*, co-tutele PhD thesis, 2010.

[2] Alshawabkeh, A. N., Basics and applications of electrokinetic remediation, Handouts Prepared for a Short Course. Federal University of Rio de Janeiro, Rio de Janeiro, Brazil, 19-20 November 2001.

[3] Acar, Y. B., Gale, R. J., Alshawabkeh, A. N., Marks, R. E., Puppala, S., Bricka, M., Parker, R., Electrokinetic remediation: basics and technology status, Journal of Hazardous Materials, vol. 40, 1995, 117–137.

[4] U.S. AEC, In-situ electrokinetic remediation of metal contaminated soils - technology status report, U.S. Army Environmental Center, Report Number: SFIM-AEC-ET-CR-99022, 2000.

[5] De Battisti, A., Electrochemical remediation, Proceedings of the ESSEE 4, 4th European Summer School on Electrochemical Engineering, 17-22 September 2006, Palic, Serbia and Montenegro.

[6] Doering, F., Doering, N., Iovenitti, J. L., Hill, D. G., McIlvrideW, A., Electrochemical remediation technologies for soil, sediment and ground water, Proceedings of the International Containment and Remediation Technology Conference and Exhibition, 10- 13 June 2001, Orland, FL, USA.

[7] Reddy, R. K., Cameselle, C., Electrochemical remediation technologies for polluted soils, sediments and groundwaters, Published by Wiley, 2009, 732 pages, ISBN: 978-0-470-38343-8.

CURRENT STATE OF FUEL CELLS AND HYDROGEN FOR EUROPEAN ROAD TRANSPORT SECTOR

Edmond MAICAN[1]
Politehnica University of Bucharest, Faculty of Biotechnical Systems Engineering, Biotechnical Systems Research and Development Centre

ABSTRACT

Following the European Strategic Energy Technology Plan (SET Plan) which aims to accelerate the development and deployment of low carbon technologies, the European transport system is subject to a wide decarbonisation action. By 2050 the EU Commission's roadmap targets a 80% decrease of total CO_2 levels compared to 1990, and a 60% decarbonisation of the road transport sector. Leading European energy companies and automotive manufacturers understood that hydrogen will play a major role as fuel and as an energy storage medium, responding directly to the societal challenges identified in the EU 2020 Strategy. It is also agreed that such transformation of the transport sector and related industries will require huge efforts and involvement of all public and private stakeholders. For short and mainly for long distance travel, the cleanest alternative is offered by electric vehicles powered by fuel cells working with hydrogen.

1. INTRODUCTION

Today the transport fuel in Europe is dominated by oil (94%) which is proven to last around 40 years [1]. 84% of it is imported, raising the European bill to €1 billion/day [2]. On the same time, despite the fuel efficiency continuous improvement of internal combustion engines (ICE) leading to reduction in CO_2 emissions, total CO_2 emission level from transport increased by 24% between 1990 and 2008. And it is expected a rise in the number of passenger cars of up to 273 million [3] in Europe by 2050, and 2.5 billion worldwide. In 2010 about 420.000 premature deaths in EU were estimated to happen due to air pollution.

2. EU INITIATIVES

Several main measures were taken at EU level in order to overcome these challenges. The European Strategic Energy Technology Plan establishes an energy technology policy for Europe whose target is to accelerate the development and deployment of low carbon technologies, including the transport sector. One of the Industrial Initiatives under the SET Plan is the Fuel Cell and Hydrogen Joint Undertaking (FCH JU), which mobilizes research and innovation in order to accelerate the development of fuel cell and hydrogen technologies in Europe to enable their commercialization.

In 2011 the European Commission adopted the 2050 Transport Strategy, aiming to reduce EU transport's dependence on oil [4]. It establishes 40 transport initiatives to increase mobility and remove major barriers in key areas. Battery and fuel cell electric vehicles are mentioned as a solution for reducing both air emissions and noise. They are considered essential technologies for the 60% cut in transport emissions by 2050. In 2013 the European Commission published a Communication on Energy Technologies and Innovation [5], stressing among others the need for further accelerating innovation in cutting edge low-carbon technologies, including those based on fuel cells and hydrogen.

---

[1]Spl.Independentei 313, 060042 Bucharest, Romania; phone: +40721.090.813; email: edmond.maican@upb.ro

Also in 2013 EU reviewed its policies regarding air quality in an attempt to further improve it and reduce corresponding threats to human health and environment. One of the outcomes was the European Commission's Clean Power for Transport Communication and an accompanying legislative proposal [6] which provides the framework for the development of alternative fuels (natural gas, electricity and hydrogen), whom are considered the only solution to decarbonize transport. After several amendments made by various Committees and negotiations between the European Parliament, European Commission and representatives of member states, a final form [7] establishes that each Member State that decides to include hydrogen refueling stations accessible to the public in their national policy framework should take the necessary steps to ensure that a sufficient number of refueling points are available by 31 of December 2025 at the latest, "with distances not exceeding 300 km, including one refueling point per 250 000 inhabitants in urban areas".

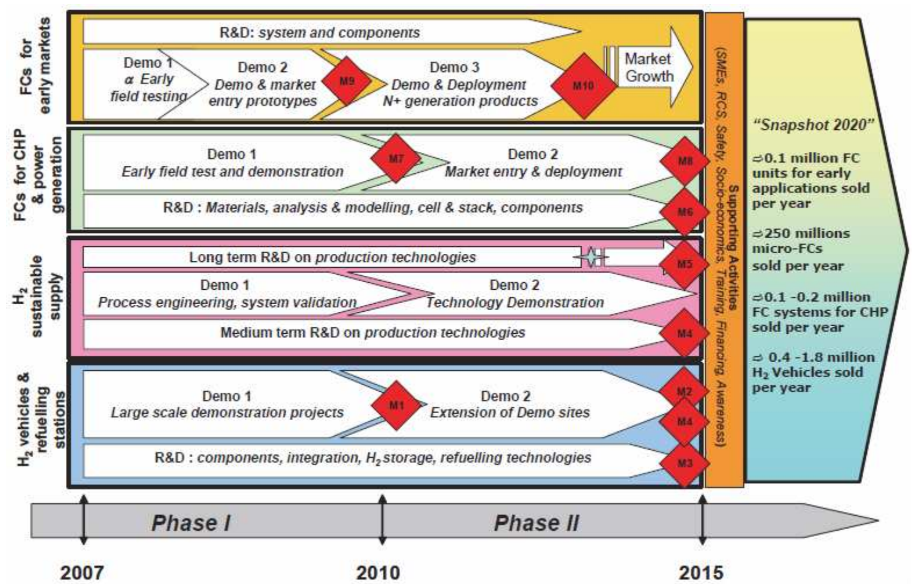

Figure 1: European Roadmap for development and deployment of fuel cell technologies [8]

3. HYDROGEN AND FUEL CELLS TECHNOLOGY

At present petrochemical plants produce large quantities of hydrogen which can be leveraged for public infrastructure. Hydrogen is seen as a clean universal energy carrier and can be produced using all primary energy sources, therefore creating the opportunity for many countries to reduce their dependence on imported energy. It has an energy density of 33 kWh/kg, compared to only 0.22…0.26 kWh/kg in case of batteries. Hydrogen powered fuel cells efficiency is at least double compared to an internal combustion engine (ICE). Currently the main method of H_2 production is steam methane reforming, followed by water-gas shift. The two-stage process extracts hydrogen both from methane and water, with a conversion efficiency of up to 80%. Fuel cell electric vehicles using hydrogen produced from natural gas reduce greenhouse gas emissions by 60%, compared to ICE [9]. 250 million fuel cell cars could be fuelled using current world hydrogen production [10]. Steam methane reformers (SMR) proved to be the most amenable to down-scaling, for hydrogen production directly at the refueling stations. In 2010, the available on-site SMRs were able to deliver hydrogen at 0.35 to 0.70 €/Nm^3, depending on capacity, natural gas cost, utilization rate and investment cost [11]. Furthermore, various industrial processes generate hydrogen as a by-product.

Especially interesting for hydrogen production through electrolysis is the use of a large share of renewable energy and of energy from power plants including carbon capture and storage (CCS). At the European level, 50% of hydrogen for energy applications should be produced by means of CO_2 emission-free methods. It is expected that production costs will be further reduced by 30% to 50% in the next 40 years. The automotive technology based on fuel cells is currently ready for market entry. To date more than 400 fuel cell electric vehicles have covered over 15 million km [1]. Storage, heat management, cold weather start, platinum quantity, hydrogen purity, were major hurdles that have been resolved. Moreover, economies of scale and further innovations in design will reduce the fuel cells cost by 90% by 2020 [12].

4. FUEL CELL ELECTRIC VEHICLE MANUFACTURERS

On 8-th of September 2009 seven of the world's largest automakers (Daimler, Ford, Honda, Hyundai-Kia, General Motors, Renault-Nissan and Toyota) signed a joint letter of understanding, signaling their intent to start commercialization of fuel cell electric vehicles (FCEVs) in 2015. This timeline corresponds with the European Roadmap for development and deployment of hydrogen and fuel cell technologies (fig. 1). In the meantime the basic refueling infrastructure is developed mainly in central and western EU countries.

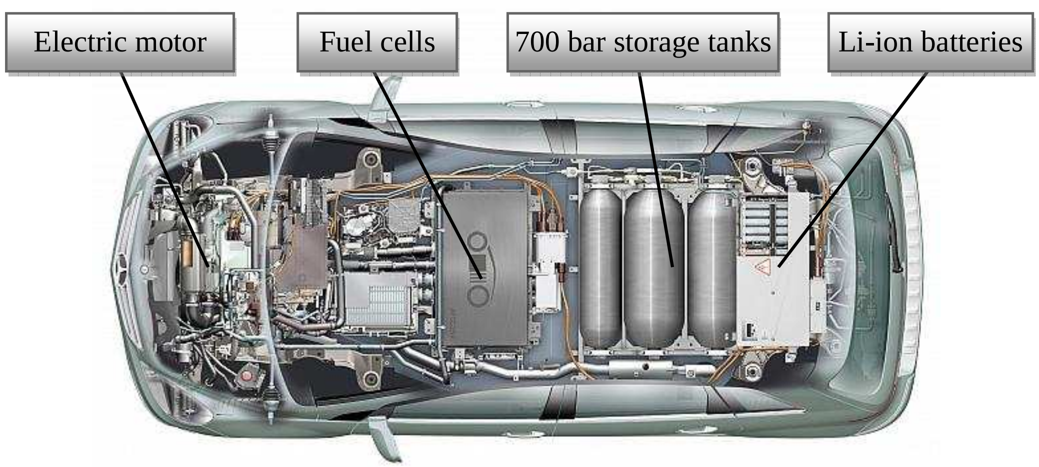

Figure 2: Mercedes-Benz B-Klasse F-CELL model fuel cell electric vehicle

Figure 2 shows the current zero-emission technical solution for a FCEV, widely adopted by the main car manufacturers. Inside fuel cells stack reaction between hydrogen and oxygen from air generates water, heat (70-85 °C) and electricity, powering the electric motor. Usually tanks from passenger vehicles store hydrogen at 700 bar, while in case of fuel cell busses it is stored at 350 bar. Refueling is achieved in about 3 minutes. The battery stores energy from fuel cells and from regenerative braking and provides additional power during acceleration. For an annual milleage of 15000 km the current life time of a fuel cell is around 10 years [13].

The technology is now ready for market introduction, with several models waiting for market deployment: Hyundai ix35 FCEV, Hyundai Intrado, Mercedes-Benz B-Klasse F-CELL, Honda FCX Clarity, Honda FCEV, Toyota FCHV, GM Hydrogen4 etc. Major car manufacturers marketing plans provide scaling up to mass production volumes by 2020. Table 1 summarizes the energy consumption and range [13].

Table 1: Former, current and future expectations for energy consumption and range

Parameter	2010	2015	2035
Hydrogen consumption (kg H_2/100 km)	1	0.8	0.6
Gasoline equivalent (l/100 km)	3.8	3	2.3
Range (per refueling)	400-500	500-800	800-1000

5. HYDROGEN REFUELLING INFRASTRUCTURE

The Directive of the European Parliament and of the Council on the deployment of alternative fuels infrastructure has just been approved, setting up the legislative framework, standards and timelines on building alternative fuels infrastructure, including hydrogen. Due to numerous large scale demonstration projects involving mainly fuel cell buses and taxis that have been under way since 2003, more than 120 refueling stations are already available across EU (figure 3 [14]). This network serves as a basis for building the basic EU stations network. Linde, Air Liquide, Shell, OMW, H2Logic, BP, Total, Hydrogenics, Air Products, are some of the companies engaged during the last years in building hydrogen refueling stations (HRS).

Initial investment is comparable with recharging stations for battery electric vehicle. The average capital cost of one HRS ranges between € 0.6 – 1.6 million [15] depending on number of refilling points and hydrogen source, leading to a total cost of €1.7 billion for the entire EU network to be built by 2020. Usually two refueling pressure alternatives are available at each station: 35Mpa and 70Mpa. Hydrogen is supplied by truck and/or is produced on site. Hydrogen purity and vehicle refueling process are both in line with SAE J2601 and 2719 as well as with ISO specifications.

6. MEMBER STATES GOVERNMENTAL SUPPORT

Ambitious targets are already adopted by some Member States regarding initiatives on infrastructure build-up, and progress is now visible. Other Member States have just started discussion on initiatives and a few did not announced any measure or intention in this direction. However, due to the binding targets from the recently approved Directive on the deployment of alternative fuels infrastructure, it is expected that Member States will take the necessary measures to attract private investment into infrastructure roll-out, thus avoiding to burden public budgets. Following some of the main national initiatives and policies where governments and regional authorities are involved to a large extent are presented.

Germany: Regional and local authorities are directly involved in hydrogen efforts, co-financing many of the first refueling stations for bus and car public fleets. The federal government also supported electric vehicles and refueling stations test projects implemented by Clean Energy Partnership (CEP[2]). German H2 Mobility initiative was initiated in 2009 by Linde, OMW, Shell, Daimler, EnBW, Total, Vattenfall and NOW (National Organization for Hydrogen and Fuel Cell Technology - the interface to the federal government). The number of stations in Germany is going to raise from the existing 26 (plus 11 under construction) to 100 over the next 3 years (50 by 2015).

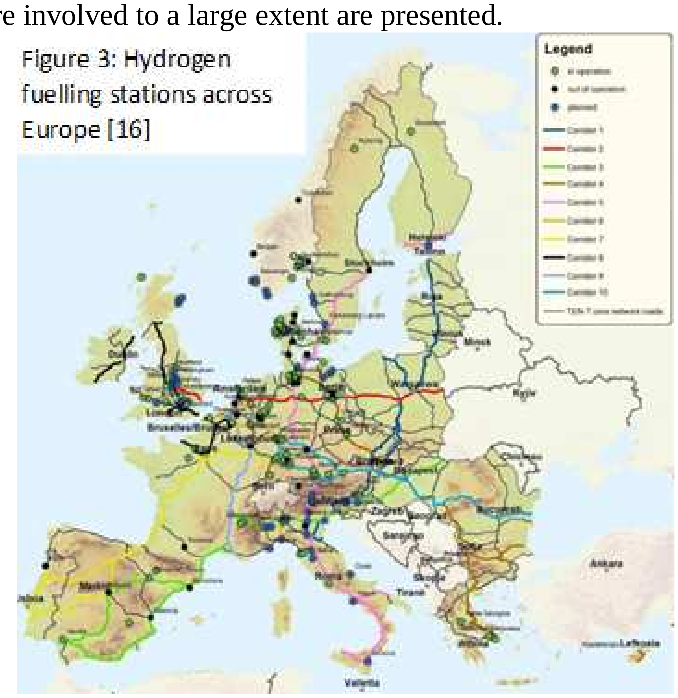

Figure 3: Hydrogen fuelling stations across Europe [16]

[2] CEP members: Air Liquide, BMW, Daimler, EnBW, Ford, GM/Opel, Hamburger Hochbahn, Honda, Hyundai, Linde, Shell, Siemens, Total, Toyota, Vattenfall Europe and Volkswagen; Others: Nissan and Intelligent Energy

A recent agreement of six partners (Linde, Daimler, Total, Air Liquide, Shell and OMW) set up a specific action plan for the construction of 400 stations by 2023. It is expected that a total investment of around €400 million will be required for this project.

The **UK Government** is investing £400 million to support the development of hydrogen infrastructure and vehicles. Over £30 million for similar projects including green hydrogen production based on wind and solar energy are financed by the UK government and the Technology Strategy Board. The UK H2Mobility project gathers three Governmental Departments (Dept. of Energy and Climate Change, Dept. for Transport, Dept. for Business Innovation & Skills), the Greater London Assembly, the Devolved Administrations and also industrial representatives. Four stages are covered: (1) evaluation of potential for hydrogen transport (ended in March 2013); (2) business case development (ended in January 2014); (3) implementation plan (ending in Summer 2014); (4) Building hydrogen refueling infrastructure – to start on 2014. Results indicated that 65 stations across the UK could provide sufficient initial coverage to start the market. By 2030 a number of 1150 will be built, with total costs of £418 million. The "Hydrogen Network" was initiated in 2010 by the Mayor of London and includes: six new refueling sites in London; 50 vehicles operated by Transport for London, the London Development Agency, the London Fire and Emergency Planning Authority, the Metropolitan Police Authority.

In 2013 **France** launched the Mobilité Hydrogène France infrastructure programme. The consortium has twenty members (government departments, regional authorities, gas production, storage and energy utilities companies). The French approach is similar to the initiatives in Germany, Great Britain and the USA, targeting a deployment scenario based on regional clusters connected together, and is co-funded by the stakeholders and the European Union within the Hydrogen for Transport Infrastructure (HIT) framework project. 10 more filling points will be built by 2015, up to 250 HRSs by 2020 and up to 800 by 2030.

Governments of **Denmark**, **Sweden** and **Norway** as well as regional and local authorities joined their financial efforts with industry and research institutions in order to support the Scandinavian Hydrogen Highway Partnership (SHHP). It aims to link the already existing hydrogen routes from the three countries and to deliver by the end of 2015: 15 HRSs (12 already operational and 2 under construction), 30 satellite stations, 100 busses, 500 FCEVs, 500 specialty vehicles. There were also adopted some of the most attractive financial tax exemption schemes in Europe, for fuel cell and battery electric vehicles.

In order to support the introduction of low and zero emission transport solution, Transnova was established by the **Norwegian** Government to fund the establishment of the initial infrastructure. Transnova's support scheme is up to 45% of total budget cost (2013 budget: €10.5 million). Also in Norway, The City of Oslo and Akershus County Council will contribute to the regional build-up of hydrogen infrastructure, in order to deliver access to hydrogen by the end of 2018 for at least 350 FCEVs (including taxis) and 30 hydrogen buses. Phase one (2014-2018) has a budget of €30 million. In **Sweden**, the Swiss Federal Office supports the H2-Mobility Swiss Initiative. Phase 1 (2013-2015) involves the development of the necessary framework, demonstration sites and vehicles, as well as the preparation of Phase 2 (July 2015-December 2020), comprising the rollout of the initial infrastructure and FCEVs.

In **Netherlands** the hydrogen infrastructure will be built through the H2NL initiative. Public bodies involved are the Ministry of Infrastructure and Environment (I&M), Ministry of Economic Affairs and Ministry of Finances. Hydrogen production, refueling stations and fuel cell electric vehicles are considered. Activities are part of the larger HIT project, coordinated by the Netherlands and signed by the Ministries of Transport and Infrastructure of Sweden, Denmark and France, being supported by the EU TEN-T programme.

Large projects delivering fuel cell busses (FCB) in regular public transport and corresponding HRSs were implemented starting with 2001 in **Italy, Switzerland, Spain,**

Iceland, UK, Norway, Germany, Netherlands, Portugal, Sweden, regional and local authorities being involved. Some of the most important projects from this category are CUTE/ECTOS (2001-2005; 30 FCBs deployed), HyFLEET:CUTE (2006-2009; 47 FCBs deployed; over 2.6 mln. km covered) and CHIC-High VLO-City (2010-2014; 31 FCBs) [16].

There are also signs of interest coming from other European countries. **Hungary** is developing two electric buses on the Mabi premises near Budapest with support from the Hungarian government. **Slovenia** presented its first hydrogen station located at a petrol filling station in Lesce near Lake Bled. It is valued at close to €0.5 million, and was supported by the European fund for regional development. The Ministry of Transport in **Czech Republic** is part of a project developing the FCZ-H2BUS fuel cell bus at Škoda Electric premises.

7. CONCLUSIONS

Hydrogen and fuel cell technology in transport systems offer a very reliable alternative to meet EU2020 targets. Based on former research and demonstration projects, this technology is now mature. The Directive of the European Parliament and of the Council on the deployment of alternative fuels infrastructure sets up the legislative framework, standards and timelines on building alternative fuels infrastructure, including hydrogen. Hydrogen powered fuel cell vehicles have similar performances with classic internal combustion vehicles in terms of refueling time, acceleration and comfort. Hydrogen can be cost-effectively produced both on small and large scale. Moreover, electrolysis allows the use of renewable energy for hydrogen production with a possibility to achieve effective zero emission greenhouse gases “from well to wheel”.

Due to numerous large scale demonstration projects mainly targeting fuel cell buses and taxis that have been under way since 2003, more than 120 refueling points are already available across EU. They serve as a basis for building up the basic EU network of HRSs. Some Member States were already involved in supporting research and implementation of hydrogen network. Starting with 2015, increased financial support for more ambitious targets are adopted by many governments aiming hydrogen infrastructure deployment.

References

[1] *Future Transport Fuels* – Report of the European Expert Group on Future Transport Fuels; January 2011.
[2] COM(2013) 17 – *Clean Power for Transport: A European alternative fuels strategy*; Brussels, 24.01.2013.
[3] *Parc Auto Survey 2009; Global Insight 2010*; study analysis.
[4] *Roadmap to a Single European Transport Area – Towards a competitive and resource efficient transport system*; EC White Paper; Brussels, 28.03.2011.
[5] COM(2013) 253 - *Energy Technologies and Innovation*; Brussels, 02.05.2013.
[6] COM(2013) 18 – *Directive of the European Parliament and of the Council on the deployment of alternative fuels infrastructure*; Brussels, 24.01.2013.
[7] *Draft Report on the proposal for a directive of the European Parliament and of the Council on the deployment of alternative fuels infrastructure*; Brussels, 30.07.2013.
[8] *European Hydrogen & Fuel Cell Technology Platform: Implementation Plan*; European Technology Platform for Hydrogen and Fuel Cells (HFP).
[9] *FCT Hydrogen Production: Natural Gas Reforming*; eere.energy.gov. 15 December 2008. October 19, 2009.
[10] *Fuel Cell Electric Vehicles: The Road Ahead*; Report-European Electro-mobility Observatory; August 2012.
[11] *Small-scale reforming systems for hydrogen refueling stations*; Technology Watch Report; February 2010.
[12] *McKinsey Report Overview: Process and Outcomes*; DOE Hydrogen and Fuel Cell Technical Advisory Committee; February 18, 2011.
[13] *Action Plan 2012-2015*; The Norwegian Hydrogen Council, 2012.
[14] http://www.netinform.net/H2/H2Stations/H2Stations.aspx?Continent=EU&StationID=-1
[15] *Infrastructure for Alternative Fuels*; Report, European Expert Group on Future Transport Fuels; Dec.2011.
[16] Reijalt, Marieke, *Building H2 Corridors: the role of National and Regional Clusters in Linking the First Hydrogen Hubs*; International Workshop „"Hydrogen fuel cell based mobility and fuel cell bus development in Central Europe” Budapest, 2014.

THE POTENTIAL OF BIOMASS FROM AGRICULTURAL ACTIVITIES AVAILABLE FOR ENERGY PURPOSES

Grigore Marian[1], Alexandru Muntean[1], Andrei Gudîma[1], Andrei Pavlenco[1]
The State Agrarian University of Moldova

ABSTRACT

This article refers to improving of the estimation methodology of biomass potential for obtaining solid biofuels. Purpose of this paper is to evaluate the energy potential of biomass, obtained from the main agricultural activities.

The estimation methodology of biomass potential for energy purposes is based on the estimation of the biomass flow depending on respective crops production, losses from harvesting, transportation and use for other purposes than energy. For the crops taken in the study was determined the calorific value of the biomass at zero moisture content and 10% of humidity.

Researches were carried out in the Laboratory of solid biofuels of SAUM. It was found that the energy potential of biomass formed from growing agricultural residues wheat, barley, corn and sunflower seeds is 598 361 TEP (tones equivalent petroleum).

For what purposes will this potential be used depends on the specific technical and economic conditions, and perspectives of agricultural development in the coming years.

1. INTRODUCTION

The amount of agricultural residues depends directly on the global harvest of agricultural crops, which greatly is influenced by climatic conditions, land structure, crop rotation, use of organic and mineral fertilizers etc.. However, to forecast the bioenergy development are needed data regarding the potential of biomass available to be used for energy purposes and its dynamics of change over time.

2. METHODOLOGY

Methodologies for appreciation of biomass potential derived from agricultural waste are based on the estimation of fluxes of these depending on production of respective crops. The necessary data can be obtained from information sources such as the Statistical Yearbook of the Republic of Moldova, The Land Cadastre of the Republic of Moldova or by assessment in land made for specific soil - climatic conditions and for certain agricultural crops . Existing methodologies of estimation are based on three types of data: theoretical, technical and economic [1].

The total amount of agricultural residues can be calculated with the equation:

$$M_{rez.} = M_{p.b.} \cdot K_{rez.}, \qquad (1)$$

[1]**The Faculty of Agricultural Engineering and Auto Transportation, the State Agrarian University of Moldova, 44 Mircesti st., Chisinau, republic of Moldova, +37322312207,** marian@uasm.md**,** alexmuntean@inbox.ru**, andreigudima@rambler.ru.**

where - $M_{p.b.}$ is the mass of basic products; $K_{rez.}$ – unitary factor of conversion (it is also called the coefficient of residues).

Unitary factor of conversion is a dimensionless value and is determined with the ratio between the mass of respective crop residues and the mass that basic biomass (harvest). The calculations of unitary conversion factor are realized for zero humidity, both of the biomass derived from residues as well as of that derived from basic production.

Since the mass of residues derived from agricultural crops depends on the mass of basic production, the unitary conversion factor for a certain crop should be quite stable. Unfortunately, this is not observed in the presented data in the literature [2-7]. The big difference between the values of unitary conversion factor can be explained by the fact that, often, is not specified what kind of initial data were used: the theoretical, technical or economical. Also, is not specified humidity of basic biomass and for that resulted from residues when was determined the conversion factor.

A similar situation also refers to data relating to the calorific value of different types of biomass. In most cases it is not specified which calorific value is presented- the higher or the lower and which was the humidity of evaluated samples [2, 5 ,9-12]. Obviously that this situation leads to quite heterogeneous appreciations relating to biomass potential possible to be used for energy purposes. For this reason, it is recommended that the energy potential of biomass to determine for dry substance (humidity 0), can be recalculated for any value of the moisture.

A significant part of the biomass derived from agricultural activities is used for other purposes than that energetic (forage for animals, raw materials for various industrial fields, organic fertilizers etc..). For this reason, the determination of the amount of biomass, available for use as raw material for production of biofuels, is used availability factor of the biomass for energy purposes $K_{d.e.}$. This factor varies from one crop to another and it is determined for specific conditions based on the technical, social, economic etc.. For account of the inevitable losses from harvesting, transportation, storage, is used coefficient $K_{per.}$.

Thus the amount of biomass resulted from agricultural residues, available for energy purposes, will be calculated by using of the formula:

$$M_{rez.s.ener.} = M_{rez.} \cdot K_{rez.} \cdot K_{d.e.} \cdot (1 - K_{per.}) \cdot \qquad (2)$$

Total energy potential of biomass in dry basis (in MJ) is determined by the relationship:

$$P_{t.} = M_{rez.dry} \cdot NCV_{dry}, [MJ] \qquad (3)$$

In which $M_{rez.dry}$ is total mass of biomass residues with moisture 0, in kg, NCV_{dry} - net calorific value of biomass with moisture 0, MJ/kg.

As the biomass used in the production of biofuels possesses certain moisture content, represents interest the know ledge of energy potential of the biomass with respective moisture, as an example, the processing moisture of biomass or moisture of the finished product in the usage phase.

Thus the total energy potential of biomass with moisture W is determined by the relationship:

$$,P_{t.W} = M_{rez.W} \cdot NCV_{w}, [MJ] \qquad (4)$$

where $M_{rez.W}$ is total mass of waste of biomass resource with moisture W, in kg,

NCV_W - net calorific value of the biomass, with moisture W, MJ/kg.

The energy potential of biomass in dry basis and with moisture W, available for energy purposes, is determined by the relationships:

$$P_{sener.dry} = M_{rez.s.ener.dry} \cdot NCV_{dry}, [MJ] \quad (5)$$

$$P_{s.ener.w} = M_{rez.s.ener.w} \cdot NCV_{w} [MJ] \quad (6)$$

In many cases it is necessary to assess biomass resources related to agricultural areas in different localities by highlighting the areas available for energy purposes. Usually these surfaces are valued differently depending on local characteristics, economic considerations, trends. Also quantification of energy production derived from specific land surfaces can vary depending on land use and types of cultivated crops on this land.

To estimate the value of annual energy potential ($P_{s.ener,S.}$), related to a specific area of culture can be used the expression:

$$P_{s.ener.S.} = S_i \cdot M_{p.b.i.} \cdot K_{rez.} \cdot K_{d.e.} \cdot \left(1 - K_{per}\right) \cdot NCV, MJ/an \quad (7)$$

S_i is the area in which it is estimated the energy potential of biomass, ha; $M_{p.b.i}$ - the mass of annual basic production from one annual basis hectare, K_{rez}. - unit conversion factor for respective crop; $K_{d.e}$ - availability factor of biomass for energy purposes for respective crop, K_{per} - coefficient of inevitable losses from harvesting, transportation and storage, NCV - net calorific value of the respective biomass.

Table 1 presents the areas sown with agricultural crops in the Republic of Moldova, for 2007-2011 years, residues of which can be used as biomass for energy purposes. This table shows that the largest area is sown with corn - on average 433.5 thousand ha, which constitutes 29.4% of total area sown with agricultural crops, followed by seeded with wheat (23.2%) and sunflower (16.5%). In view of the above, in continuation we will examine more thoroughly the issues related to the availability of these cultures from point of view of the energy potential.

Table 1. Sown areas with agricultural crops, waste of which can be used as biomass for energy purposes [13]

Year	**2007**	**2008**	**2009**	**2010**	**2011**	**average value for 5 years**
Sown areas with agricultural crops, thousand hectares	1499,2	1500,3	1464,1	1460,3	1447,2	1474,2
Sown areas with agricultural crops, %	100	100	100	100	100	100,0
Total cereals and leguminous crops, thousand hectares	955,4	1005,8	951,6	919,6	894	945,3
Total cereals and leguminous crops,, %	63,7	67,0	65,0	63,0	61,8	64,1
Wheat, thousand hectares	314,5	412,3	353,2	328,2	301,8	342,0
Wheat, %	21,0	27,5	24,1	22,5	20,9	23,2
Winter and spring barley, thousand hectares	127,6	130,2	155,7	132,6	103,5	129,9
Winter and spring barley, %	8,5	8,7	10,6	9,1	7,2	8,8
Grain maize, thousand hectares	466,2	428	401,8	415,9	455,5	433,5

Grain maize, %	31,1	28,5	27,4	28,5	31,5	29,4
Leguminous crops, thousand hectares	39,3	27,8	32,6	34,9	27,9	32,5
Leguminous crops, %	2,6	1,9	2,2	2,4	1,9	2,2
Total industrial crops, thousand hectares	368,2	342,1	365,4	388,3	412,4	375,3
Total industrial crops, %	24,6	22,8	25,0	26,6	28,5	25,5
Sunflower, thousand hectares	233,6	228	226,6	252,4	277	243,5
Sunflower, %	15,6	15,2	15,5	17,3	19,1	16,5

Since the data concerning to energy potential, in many cases, are compared to those obtained from other sources, these can be estimated in conventional units, as an example, tcc and t.e.p.

Table 2 shows the result of calculation of the energy potential of several herbaceous agricultural crops which are more widespread in Moldova. The energy potential is calculated for biomass on wet basis and converted to moisture content of biomass equal to 10%.

The comparative estimations concerned to the energy potential of solid biofuels is necessary to be used the data for the moisture content 10%, because, at the burning of them, on average, can have moisture content $W = 10 \pm 2\%$.

3. CONCLUSIONS

Analyzing the data from the table shown and taking into consideration that in the year 2012, according to the National Bureau of Statistics in RM were imported natural gas with 42.54 PJ potential is obvious that just from the efficient use of residues resulted from cultivation of wheat, oats, corn, vegetables and sunflower can be significantly reduced imports of natural gas and other energy carriers. Adding to these figures the potential energy that can be produced from biomass resulted from cutting and care of fruit trees, and the vine, as well as forestry and industrial activities can confidently say that this potential is comparable to the annual consumption of natural gas.

Table 2. The average of biomass potential derived from herbaceous agricultural crops, available for energy purposes, grown in the Republic of Moldova

The name of crop	**S_i**	**$M_{p.b.i.}$**	**$K_{rez.}$**	**$K_{d.e}$**	**$K_{per.}$**	**NCV**		**Energy potential of biomass on a dry basis for area S_i**			**Energy potential of biomass on wet basis (W-10%) for the area Si**		
						W=0	**W=10%**	**$P_{s.ener,Si}$, MJ**	**$P_{s.ener,Si}$, PJ**	**$P_{s.ener,Si}$, tep**	**$P_{s.ener,Si}$, MJ**	**$P_{s.ener,Si}$, PJ**	**$P_{s.ener,Si}$, tep**
Wheat	342	2290	0,85	0,25	0,1	16,8	14,91	2,52E+09	2,522	60031,90	2,23E+09	2,233	53151,76
Winter and spring barley	129,9	1780	0,75	0,25	0,1	16,5	14,62	6,45E+08	0,645	15341,22	5,7E+08	0,570	13576,80
Grain maize	433,5	2790	1,2	0,75	0,25	16,8	14,86	1,37E+10	13,699	326036,33	1,21E+10	12,132	288730,62
Leguminous crops	32,5	9700	1,3	1	0,1	16,7	14,79	6,16E+09	6,160	146600,14	5,46E+09	5,455	129833,30
Sunflower	243,5	1340	1,25	1	0,3	18,8	16,64	5,36E+09	5,356	127474,00	4,75E+09	4,751	113068,62
Average								2,84E+10	28,38166	675483,585	2,51E+10	25,14122	598361,1

References

[1] ГЕЛЕТУХА, Г.Г.: Желєзна, Т.А.: Жовмір, М.М.; Матвєєв, Ю.Б.; Дроздова, О.І. Оцінка енергетичного потенціалу біомаси в україні. частина 1. відходи сільського господарства та деревна біомаса. În: *Пром. теплотехника, 2010, т. 32, №6, p. 58-65*.

[2] Energie din biomasă: tehnologii şi mijloace tehnice/ Ion Hăbăşescu, Valerian Cerempei, Vasile Deleu et. al; red. şt.: Ion Hăbăşescu. Min. Agriculturii şi Industriei Alimentare, Acad. de Ştiinţe a Moldovei, Inst. de Tehnică „Mecagro". – Ch.: Bons Offices, 2009. – 368 p.

[3] ГАВРЛАНД, Б.; Побединский, В.М. Биомасса для энергетического использования. Прага, CzechAid: 2008. 154 с.

[4] ГЕЛЕТУХА, Г.Г.; Желєзна, Т.А.; Жовмір, М.М.; Матвєєв, Ю.Б.; Дроздова, О.І. Оцінка енергетичного потенціалу біомаси в україні. частина 1. відходи сільського господарства та деревна біомаса. În: *Пром. теплотехника, 2010, т. 32, №6, p. 58-65*.

[5] ION V. ION and Ion Dana-Ioana. Energie din biomasă. În: *Tehnica instalaţiilor*, 2006, nr.7(38). p. 14 – 30.

[6] КЛЮС, С.В.; Забарный, Г.Н. Оценка и прогноз потенциала твердого биотоплива Украины. În: Компрессорное и энергетическое машиностроение. Nr. 2(24), июнь 2011, pp. 8-13.

[7] ТЕХНОЛОГИИ ОБЕСПЕЧИВАЮЩИЕ ЗАДЕЛКУ СОЛОМЫ В ПОЧВУ. Широко распространенный опыт в Швеции включительно по 2012 год.. Instituted for jordbruks – och miljoteknik. bellona.org/files/fil_Gunrus.pdf [citat 08 Sep. 2013].

[8] Strategia privind valorificarea potenţialului de biomasă şi direcţii de acţiune pentru dezvoltare şi utilizare pentru anii 2911 -2015.

[9] DANCIU A.; Vlăduț V.; Voicea I., Postelnicu Elena. Possibilities of using solid biomass, agricultural and forestry for reducing pollution soil and water (*posibilități de utilizare a biomasei solide, agricole și forestiere pentru reducerea poluării solului și apei)* Lucrări științifice (INMATEH), vol.27, nr. 1, București, 2009, p.86-92.

[10] ANDRÉ FAAIJ, Joep van Doorn, Toine Curvers, Lars Waldheim, Eva Olsson, Ad van Wijk, Cees Daey-Ouwens. Characteristics and availability of biomass waste and residues in The Netherlands for gasification. În. *Biomass and Bioenergy,*Volume 12, Issue 4, 1997, Pages 230.

[11] BRYAN M. JENKINS and James M. Ebeling. Termochemical properties of biomass fuels. În: California agriculture, may-june 1985. P.14-16.

[12] VALTER FRANCESCATO, Eliseo Antonini, Luca Zuccoli et al. Wood fuels handbook. AIEL, p20. 2009.

[13] Anuarul Statistic al Republicii Moldova ediţia 2012. http://www.statistica.md/public/files/publicatii_electronice/Anuar_Statistic/2012/anuar_2012

BIOGAS, THE FUTURE OF MODERN SOCIETY

Georgiana Moiceanu[1], Mirela Dincă[1], Gigel Paraschiv[1], Gheorghe Voicu[1], Mihai Chiţoiu[1]
[1]University POLITEHNICA of Bucharest, Faculty of Biotechnical Systems Engineering, Biotechnical Systems Research and Development Center
* E-mail: moiceanugeorgiana@gmail.com

ABSTRACT

An indispensable part of any society, but mostly modern society in represented by energy. Although technology nowadays has developed at an alarming rate, there are still some parts of the world where the energy comes from biomass resources like firewood, crop residues etc. burned in traditional stoves. It is well known that these regions need a cleaner environment and a sustainable development. In order to do so, it is necessary to upgrade the existing biomass resources to more efficient carries (biogas from anaerobic digestion) which can provide reliable energy, in the same time being cleaner and preserving the environment. Biogas technology can be modernized only through governmental and non-governmental sectors collaboration. This paper intents to highlight the importance of biogas as an major part of modern society by presenting the biogas technology, development, challenges, pretreatment.

1. INTRODUCTION

The comfort of modern society is given by energy, which most of the time is taken for granted. As the number of people increases the demand for energy increases, so it is necessary to say that about 1.5 billion people still lack access to basic energy services despite of nowadays technology. 90% of household energy consumption consists in biomass. The development of these parts of the world where these live will contribute to waste increase. [9]

The overall pollution prevention targets, the objectives of the Kyoto agreement as well important issues related to human and animal health and food safety require increasingly sustainable solutions for handling and recycling of animal manure and organic wastes, where biogas from anaerobic co-digestion of animal manure, combined with pre- and post-treatment technologies, play an increasing important role. [4]. Biogas comes from animal manure, and is perhaps the ultimate win-win energy source, allowing farmers to produce their own electricity and reduce the water contamination, odor pollution, and global warming emissions caused by animal waste.[10].

According to a biogas survey done in 2012/2013, *Biogas to Energy 2012/2013 – The World Market for Biogas Plants*, the international biogas boom will continue in the years to come. It is said that a growth of 60% through the years 2012 to 2016 will happen. Another aspect expected to grow refers to the number of plants, increasing from 9,700 to 13,500 plants. The main reason for this growth is the support of renewable energy that is increasing throughout the world. It is a well-known fact that more countries are now able to create the necessary framework conditions for a fast growth of the biogas industry. Also according to studies Europe will remain the world's most dynamic market. [11].

This paper aims to present the importance of biogas, by showing the way this energy works and the a few aspects regarding anaerobic digestion. It is a general review of the main ideas about biogas.

[1]Spl. Independentei, no. 313 , phone number 0745 201 365, email moiceanugeorgiana@gmail.com

2. HOW BIOGAS ENERGY WORKS

The biogas process is part of a biological waste treatment method used commonly in waste treatment plants anywhere in the world. The only difference is that instead of releasing the gases produced during the fermentation process, the gases are collected and utilized as a gaseous fuel product.[12]

Biogas can be produced from nearly all kind of biological feedstock types, within these from the primary agricultural sectors and from various organic waste streams from the overall society. The largest resource used for obtaining biogas is represented by animal manure, according to studies in Europe these resources being about 65% from the total amount. Although these are a very large percentage, energy crops can also be used as raw material for biogas. If the animal manure is poorly managed or untreated, it becomes a source of water and air pollution. 65% of anthropogenic nitrous oxide and 64% of anthropogenic ammonia emission originates from the worldwide animal production sector [8].

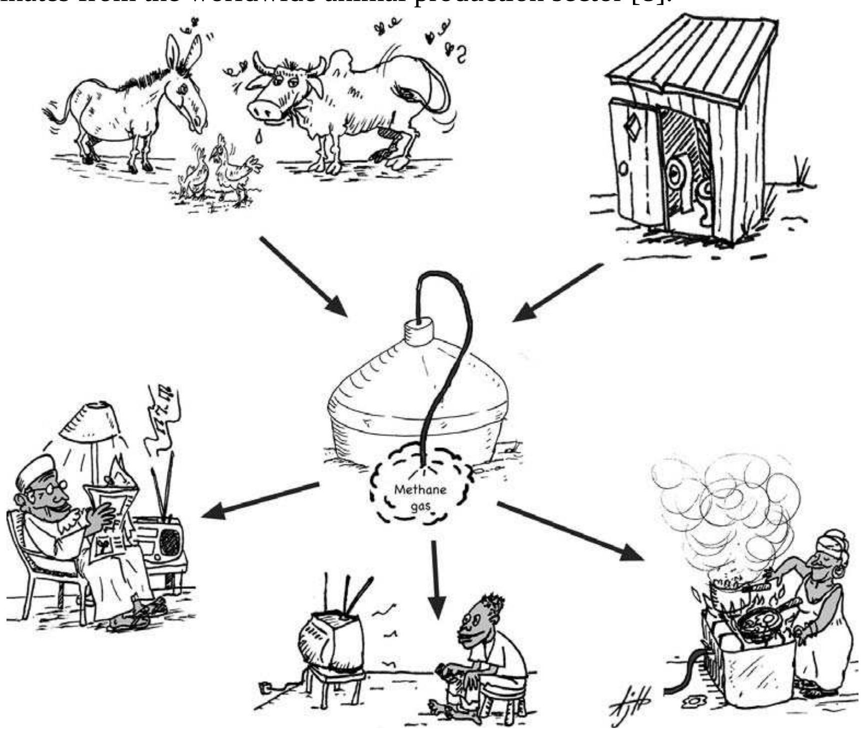

Figure 1. Materials used for biogas and biogas distribution16]

Biogas recovery systems have a few main components: a manure collection system, an anaerobic digester, usually a covered lagoon or tank, which stabilizes the manure and optimizes methane production; a biogas handling system that pipes the resulting gas to the device it will fuel, such as a generator; and a storage tank for the remaining discharge. [10].

There are a few types of digesters: covered anaerobic lagoons are pond-like basins, often earthen, that are covered to retain the biogas. The most popular biodigesters are lagoons which are also the simplest, but they are limited to warmer climates (colder temperatures can suppress methane production). Plug-flow digesters are long, narrow, heated tanks, often installed partially underground to retain the heat. These units work only with dairy manure. Complete-mix digesters are heated tanks made of reinforced concrete or steel with a mechanical, hydraulic or gas-powered mixing system. They generally require a diluted manure mix, such as manure mixed with process water [10].

The conversion of organic matter into biogas is carried out by a consortium of microorganisms through a series of metabolic stages (namely, hydrolysis, acidogenesis, acetogenesis and metha - nogenesis).

Tabel 1: Chemical composition of biogas and properties of components [2]

Components	**Concentration**	**Properties**
CH_4	50 – 75% (v/v)	Energy carrier
CO_2	25 -50% (v/v)	Decrease heating value Corrosive, especially in presence of moisture
H_2S	0 – 5000 ppm (v/v)	Corrosive Sulfur dioxide emission during combustion
NH_3	0 – 500 ppm (v/v)	NO_x – Emissions during combustion
N_2	0 -5% (v/v)	Decrease heating value
Water vapor	1 -5% (v/v)	Facilitate corrosion in presence of CO_2 and sulfur dioxide (SO_2)

3. ANAEROBIC DIGESTION

3.1. Anaerobic digestion – general view

Anaerobic digestion is a very common practice in term of waste management treatment strategy from two points of view, environmental and social benefits. Among these benefits it can be included odor removal, mass reduction, pathogen reduction, less energy use and the energy recovery in the form of methane [1]. Much of the fermentation used industrially to produce food and drink products, as well as home fermentation, uses anaerobic digestion. Anaerobic digestion also occurs naturally in some soils and in lake and oceanic basin sediments, where it is usually referred to as "anaerobic activity".[5,6].

Anaerobic digestion is a collection of processes by which microorganisms break down biodegradable material in the absence of oxygen. [13]. Anaerobic digestion is a highly sophisticated process in which a variety of microorganisms play various roles in the decomposition of organic material and production of methane and CO_2.

3.2. Stages of anaerobic digestion

Anaerobic digestion can be subdivided into four phases, as illustrated in Figure 2 and 3 and described below [7].

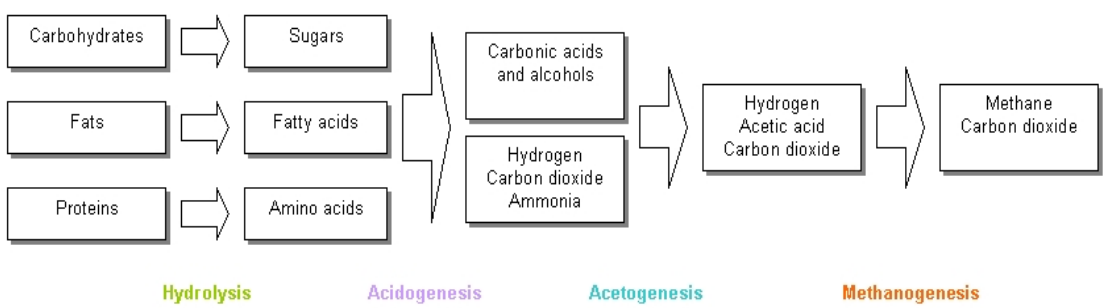

Figure 2. Stages of anaerobic digestion[14]

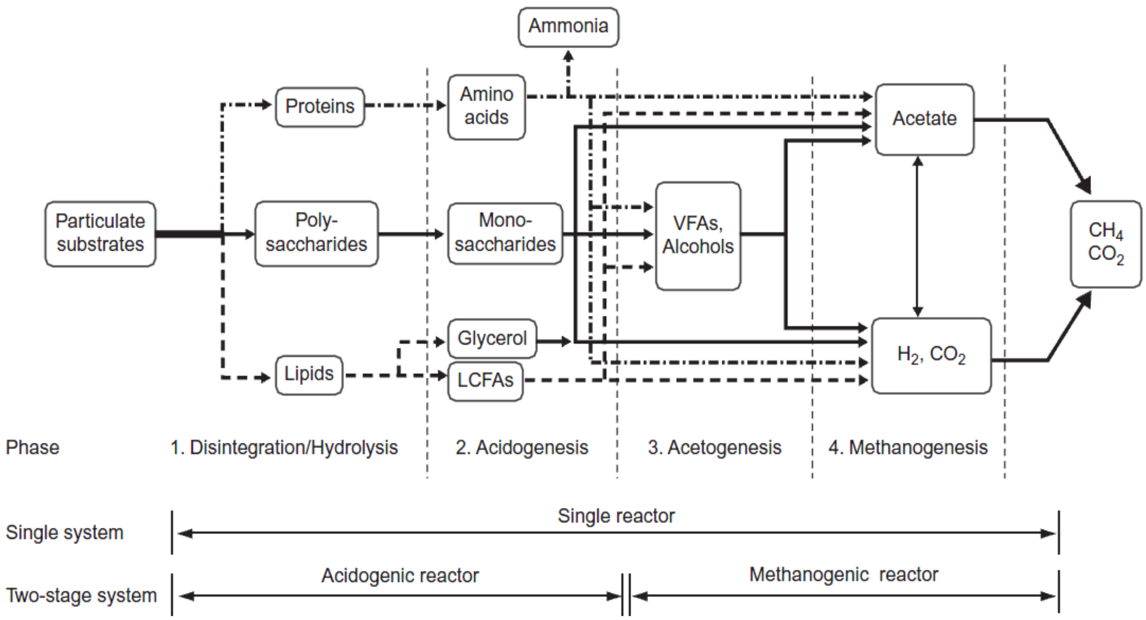

Figure 3. Schematic representation of anaerobic digestion. Disintegrated to lipids, polysaccharides proteins and in the same time hydrolyzed to amino acids, long chain acids and monosaccharides are the particle substrates in the water. The hydrolyzed compounds are then fermented. After this part the volatile fatty acids are oxidized to acetate, H_2 and CO_2 by particular acetogenic bacteria. Using acetoclastic and hydrogenotrophic methanogens the acetate, H_2/CO_2 are converted in CO_2 and methane. [3].

Anaerobic digestion treats a variety of organic wastes. Taking these into consideration, anaerobic digestion systems are classified according to mixing method, percentage of total solids in the waste and operation temperature.

Converting organic residues from animal manure through anaerobic digestion we can obtain two types of valuable products:

- Biogas used to produce green energy;
- Digested substrate or digestate used as a fertilizer in agriculture.

3.3. Environmental benefits of anaerobic digestion

According to studies made with the purpose to compare environmental impact and aspect of various technologies for treatment of biogenic waste (anaerobic digestion, tunnel composting, combinations of anaerobic digestion and composting) the most recommended was to treat biogenic wastes with biotechnology, mostly anaerobic process.[15]

Among the environmental benefits provided from the anaerobic digestion of organic waste and manure we can name:

- Less air pollution;
- Less leakage of nutrient salts to ground or water surface;
- Energy saving by producing a renewable energy sourse – biogas;
- Less greenhouse gas emissions;
- Sanitation of wastes an manure;
- Usage of digestate as a fertilizer, etc.

Biogas has definite advantages, even if compared to other renewable energy alternatives. It can be distributed through the existing natural gas infrastructure and used in the same applications like the natural gas. Biogas can replace fossil fuels in the transport sector, apart from utilization for renewable electricity and heat production.

4. CONCLUSIONS

The greatest challenge in biogas technology progress it is represented by education. In order to use biogas as a sustainable option for modern society, the people need to be taught about the merits of biogas technology among which we can mention economic potential, health, social and environmental merits. These merits can only be presented through the presentation of successful implemented biogas technologies in other countries all around the world.

Modern society needs to be aware of the biogas great potential in terms of reduced environmental impacts, clean and reliable energy, job creation, all these contributing to the improvement of current life quality.

Taking into consideration the organic substances discharged from animal residues and also food industry, it is necessary to transform these biogas resources in order to obtain energy. The most common technology for recovery of cost-effective energy and chemicals is anaerobic digestion. Operation parameters affect the operational stability of an anaerobic digestion system. Microbial physiology and ecology of the process along with the technologies for plant development and operation need to be understood so that the anaerobic digestion system and process performance improves.

Advantages of Biogas for Romania[17]

- *Presently 3 mil ha or 30% of total 8,8 mill ha are not being cultivated, part of this land can be utilized to grow energy crops;*
- *If biogas reaches a level of 10% of total renewable energy (like Germany in 2008) under 2% of the available agricultural area will be necessary to satisfy the substrate demand;*
- *No competition with food production to be expected;*
- *Jobs and agricultural revenues*

References

[1]. Ackmez Mudhoo, *Biogas Production - Pretreatment methods in anaerobic digestion*, Scrivener Publishing LLC, ISBN 978-118-06285-2;

[2]. Braun R. *Anaerobic digestion: a multi-faceted process for energy, environmental management and rural development*, In Ranalli P, editor Improvement of crop plants for industrial end uses. Netherlands:Springer;2007.p.335–416;

[3]. de Mes,T.Z.D.,Stams,A.J.M.,Reith,J.H.,Zeeman,G.,2003.*Methane production by anaerobic digestion of waste water and solid wastes*, In:Reith, J. H., Wijffels, R. H., Barten, H.(Eds.), Bio- methane & Bio-hydrogen. Dutch Biological Hydrogen Foundation, The Hague, pp.58_102;

[4]. J.B. Holm-Nielsen, T. Al Seadi, P. Oleskowicz-Popiel, *The future of anaerobic digestion and biogas utilization*, Elsevier - Bioresource Technology 100 (2009) 5478–5484;

[5]. Koyama, Tadashiro (1963). "*Gaseous metabolism in lake sediments and paddy soils and the production of atmospheric methane and hydrogen*". Journal of Geophysical Research 68(13): 3971–3973,

[6]. Pamatmat, Mario Macalalag, and Bhagwat, Ashok M. (1973). *"Anaerobic metabolism in Lake Washington sediments"*. Limnology and Oceanography 18 (4). pp.611–627. 2013;

[7]. Naomichi Nishio and Yutaka Nakashimada, *Manufacture of Biogas and Fertilizer from Solid Food Wastes by Means of Anaerobic Digestion*, Treatment Of Solid Food Wastes, pp. 121 - 133;

[8]. Steinfeld, H., Gerber, P., Wasenaar, T., Castel, V., Rosales, M., de Haan C., 2006. Livestock's long shadow. Environmental Issues and Options. Food and Agriculture Organisation (FAO) of United Nations;
[9]. K.C. Surendra,DevinTakara,AndrewG.Hashimoto,SamirKumarKhanal, *Biogas as a sustainable energy* source for developing countries:Opportunities and challenges, Elsevier - Renewable and Sustainable Energy Reviews 31(2014) 846–859;
[10]. http://www.nrdc.org/energy/renewables/biogas.asp;
[11].http://www.ecoprog.com/en/publications/energy-industry/biogas-to-energy.htm?gclid=CMHAztm2hb4CFVLItAodr3gAwA;
[12]. http://www.integratedenergyindustries.com/biogas-process.html;
[13]. http://en.wikipedia.org/wiki/Anaerobic_digestion;
[14]. http://en.wikipedia.org/wiki/File:Stages_of_anaerobic_digestion.JPG;
[15] http://www.iea-biogas.net/files/daten-redaktion/download/publi-task37/managementpaw3.pdf.
[16]. www.paceproject.net
[17]. http://www.biogest.at/biogaz-romania/Bilder/biogas_in_romania_100425.pdf

EXPERIMENTAL RESEARCH REGARDING CHAMOMILE INFLORESCENCES MECHANIZED HARVESTING PROCESS

Adriana Muscalu[1], Augustina Pruteanu [1], Ladislau David [2]
1) National Institute of Research- Devlopment for Machines and Installations designed to Agriculture and Food Industry - INMA, Bucharest
2) Politehnica University, Bucharest – Biotechnical Systems Engineering Faculty

ABSTRACT

Lately, the utilization of medicinal plants have known an unprecedentedly growth. This particular concern determined higher and higher requirements in terms of vegetal raw materials, rich in active principles, designed to industries of pharmaceutical products, cosmetics, perfume and also food industry. Therefore, extending the surfaces cultivated by these plant species, modernizing and adapting the crop technologies to current demands become a must.

In medicinal plants case, the quality conditions imposed to collected material are very strict. But, for species cultivated, the mechanized harvesting can guarantee profitable productions.

The paper presents a synthesis of experimental researches performed within INMA, researches related to mechanized harvesting of wild chamomile inflorescences, with different active parts typo-dimensions. Results obtained constitute an important step in achieving performance specialized equipment, appropriate to sustainable agriculture principles and practices.

1. INTRODUCTION

Cultivation of medicinal plants on scientific basis creates the conditions for applying the scientific results as well as the previous experience in the field, aiming to:

- acclimatizing certain medicinal plants species, which do not spontaneously grow in our flora;
- preserving rare species, already declared as natural monuments;
- obtaining large quantities of raw material, more homogenous and richer in active principles;
- avoiding substitutions and frauds;
- performing harvesting at optimum moment, when the content of plant active principles is maximum. [1]

Chamomile (*Matricaria recutita L.*) is one of the oldest and most wide-spread medicinal plants. It is cultivated for its flowers (inflorscences) therapeutical importance, which is due to high content of essential oil, rich in azulene, bisabolol and other valuable components[2]. At world level, approximately 20,000 ha of field are cultivated by chamomile, the main producers being Argentina, Egypt, Italy, Hungary, Germany, Serbia etc. An important chamomile production can be obtained only by mechanized harvesting. Thus, at the present moment, different producing countries such as, Argentina, Slovakia, Serbia, Italy and Germany, are using techniques of mechanized harvesting, based on different types of pickers.[3]

Following the expertise gathered in the field and after numerous researches, it has been found that the main part appropriate to chamomile harvesting is considered to be the comb.[4] Therefore, from the constructive point of view, the pickers can be of drum type or conveyor type.

[1]amuscalis@yahoo.com

Drum-type pickers may have the combs arranged as it follows:

- parallel to the axis of rotation of cylinder and equidistant to generatrix;
- obliquely to generatrix, on external surface.

Conveyor-type picker is, in fact, a band and blades conveyor, represented by combs and their support.

Because of working parts type, the working process is, in fact a raking (scraping) process, which comprises, as all the processes of the kind, the following stages:

a) Combs penetrating into the layer of stems;
b) Combs displacement along the stems;
c) Combs coming from the stem layer.[5]

For medicinal plants the harvested material quality influences its therapeutic action. Chamomile flowers are harvested on nice weather days, after the early morning dew had disappeared (after 9^{00} A.M), when 50% out of tubular flowers from capitulum are opened, and long corolla flowers have a fresh appearence and are horizontally placed. Material harvested must contain min. 75% flowers with peduncle < 2 cm. The rest is represented by impurities of max. 5% stems and leaves, flowers with peduncle >2cm max 5%,crushed flowers , foreign organic bodies of max 2%, mineral impurities 0.3%.[1]

2. METHODOLOGY

The harvesting system is the main sub-assembly from chamomile harvesting machines manufacturing. Its functional role consists in detaching the inflorescences from stems and introducing them in machine technological flow.

In figure 1 are shown the constructive scheme and the main elements comprised in harvesting system: 1- supporting frame; 2 – conveyor-type picker raking combs; 4 – cylindrical brush; 5 – inflorescences captor system; 6 –propping support; 7 – mechanical transmission; 8 – working height limiting device; 9 – front guard.

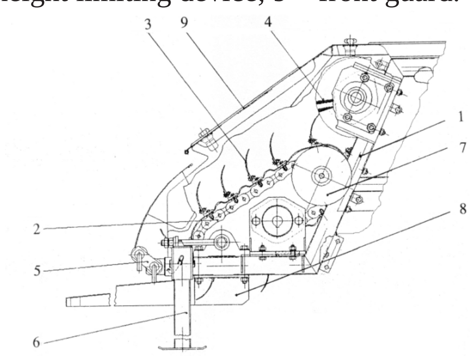

Figure 1: Mechanical system for harvesting chamomile inflorescences

The harvesting system is made of an inflorescence picker as main active part, which is endowed with active parts of raking combs type. Several types of raking combs with straight teeth (fig.2 a) and, respectively, bended teeth (fig.2 b) have been manufactured and tested. At both teeth types the gap between teeth is rounded “U”-shaped, this shape being the most used. [4] Gap adjusting ray is equal to half of distance between teeth.

For identification, the following symbols were used:

a) straight teeth combs- M_1; N_1;O_1; S_1;T_1;V_1.

b) bended teeth combs- M_2; N_2;O_2; S_2;T_2;V_2.

Symbols used in figure 2a and 2b have the following significations:

p – teeth pace; L – teeth length; d – distance between two consecutive teeth; b – teeth width; R – radius of curvature of combs with curved teeth, R=L.

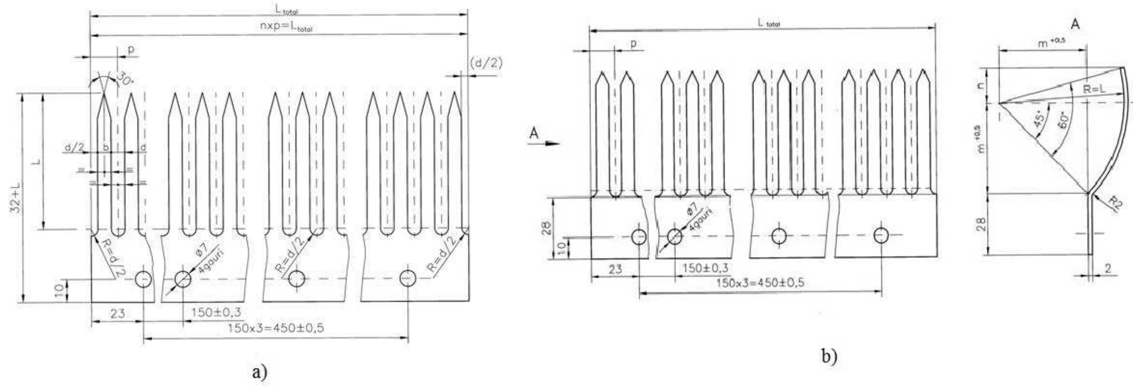

Figure 2 Combs shape: a) with straight teeth; b) with curved teeth

Dimensional characteristics of combs have the following values for:
1) d=6 mm
M_1 and M_2: p=12 mm; L=60 mm; b=6 mm; R_{M2}=60 mm;
N_1 and N_2: p=14 mm; L=80 mm; b=8 mm; R_{N2}=80 mm;
O_1 and O_2: p=16 mm; L=100 mm; b=10 mm; R_{N2}=100 mm;
2) d=4 mm
S_1 and S_2: p=10 mm; L=60 mm; b=6 mm; R_{S2}=60 mm;
T_1 and T_2: p=12 mm; L=80 mm; b=8 mm; R_{T2}=80 mm;
V_1 and V_2: p=14 mm; L=100 mm; b=10 mm; R_{V2}=100 mm;
Characteristics of machine used in experiments are shown in table 1.

Table 1: Characteristics of chamomile harvesting machine

Machine type	towed
Tractor power [HP]	45
Working width [mm]	2000
Brush gyro frequency [min^{-1}]	327÷400
Linear velocity of conveyor type picker [m/s]	0.5; 0.76;1.08
Working speed [km/h]	0.5÷1.22
Transport speed[km/h]	15
Working personnel [number of persons]	1

Chamomile harvesting machine works in offsetting conditions against the tractor, the working process running as following: the picker moves toward the plant rows, the active parts being in operation (raking combs) . They achieve a parallel movement to plan, which results from the displacement of aggregate, on which the picker's [5] rotation movement superposes. Therefore, the plants are combed from down to up, resulting in the inflorescences detachment from stems. The raking combs action comprises the upper parts of flower to be harvested. Chamomile inflorescences collected during harvesting are taken over by a conveyor, to be to be spilt into the machine hopper .Its unloading is made at ground level, by swinging a mobile wall driven by hydraulic cylinder.

For obtaining different linear velocity of picker band (v_1=0.52m/s; v_2=0.76 m/s; v_3=1.08m/s) the movement displacement ratio to band has been modified by putting into operation interchangeable chain wheels with different number of teeth (Z=12;21;29)

Characteristics of chamomile crop where tests were performed are shown in table 2.

Table 2: Characteristics of chamomile culture

Variety	Margaritar
Average number of chamomile[pcs/m^2]	326
Average number of weeds [pcs/m^2]	12
Average number of mature flowers [pcs/m^2]	1986
Average number of buds which have not blossomed[pcs/m^2]	46
Average production of fresh inflorescences [kg/ha]	3204
Average mass of 100 inflorescences[g]	13.2
Average diameter of inflorescences [mm]	19.4
Minimum and maximum height between which the flowers grow [mm]	298...583

As the most valuable substances of chamomile are in its flowers, when establishing and evaluating the qualitative working indexes of inflorescences harvesting equipment, it was first envisaged to perform an as complete as possible harvest (the active parts being designed for this very purpose). The inflorescences harvesting degree is expressed in percentages(%) and is defined as being the ratio between the number and/or quantity of flowers detached from stems during harvesting and number and/or quantity of flowers existing on plants before harvesting.

In figures 3, 4, 5 the harvesting degree is shown comparatively to combs types of d=6mm and d=4mm, for each band linear velocity, in different working speed conditions v_l=0.5; 0.76; 1.04 km/h and low harvesting (the harvesting height is H=0.300m).

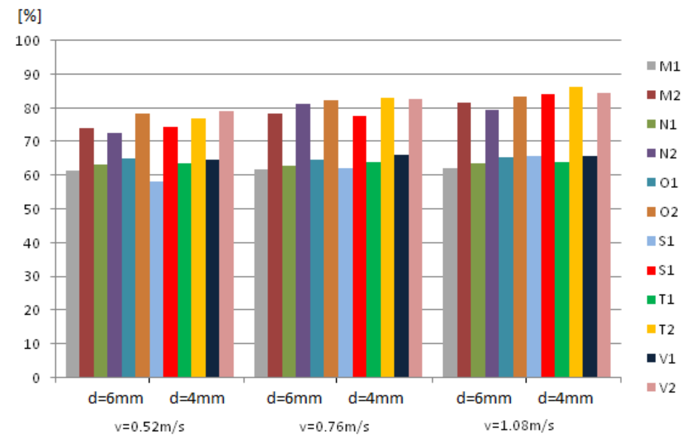

Figure 3: Harvesting degree for v_l=0.5 km/h and H=0.300 m

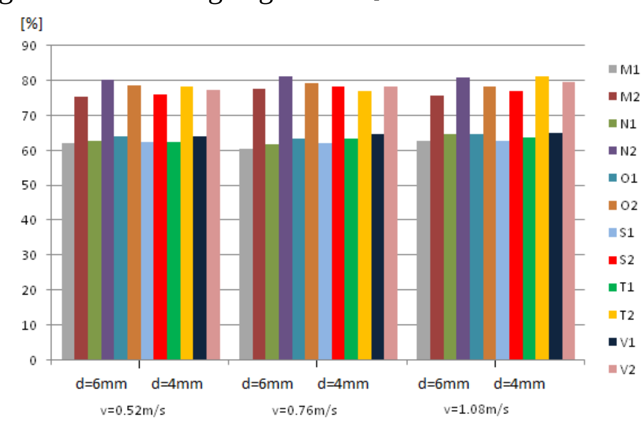

Figure 4: Harvesting degree for v_l=0.76 km/h and H=0.300 m

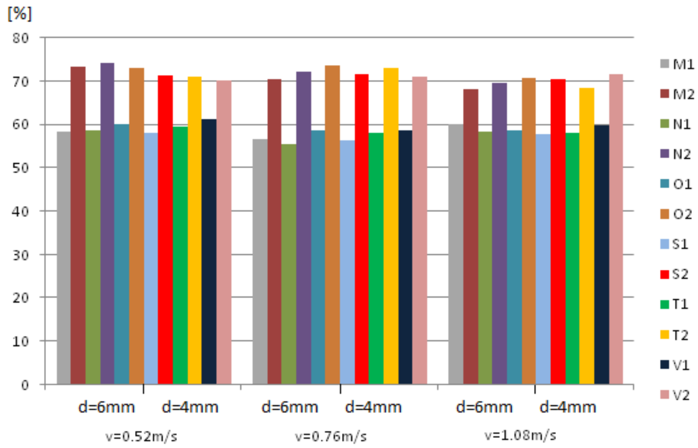

Figure 5: Harvesting degree for v_l=1.04 km/h and H=0.300 m

In figures 6,7 the harvesting degree is comparatively presented for combs types of d=6mm and d=4mm, for each linear velocity of band, under maximum and minimum working speed and high harvesting (harvesting height is H=0.450m).

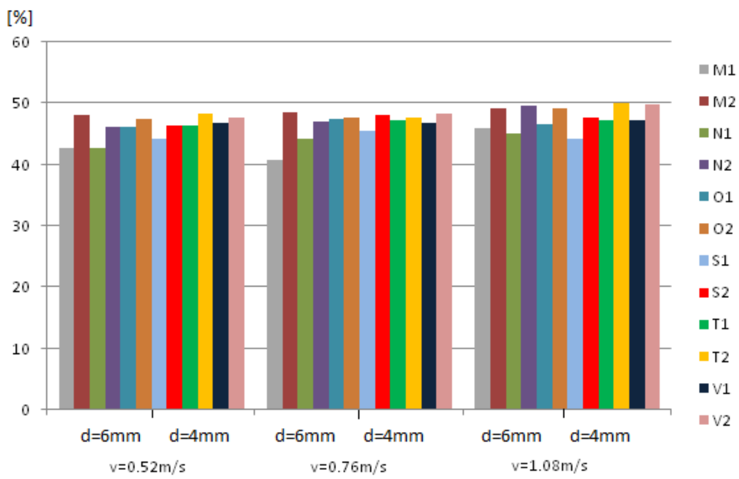

Figure 6: Harvesting degree for v_l=0.50km/h and H=0.450 m

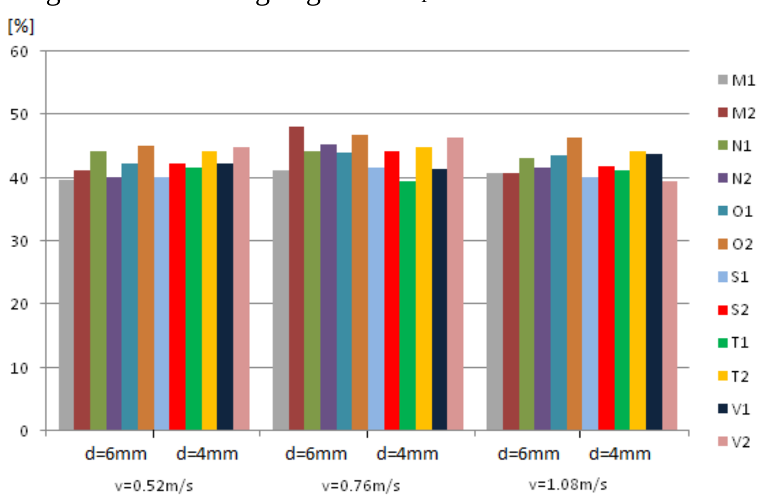

Figure 7: Harvesting degree for v_l=1.04 km/h and H=0.450 m

3. CONCLUSIONS

Analysis of experimental research results shown in figures 3;4;5;6;7 emphasizes the following aspects:

Harvesting degree has higher values for "low harvesting" in comparison with “high harvesting", the differences between the two harvestings being of about 20%, in favour of the low harvest(picker working height H=0.300m).

Harvesting degree has decreasing values along to working speed increase, for the same type of active parts and similar operating regime, the variation domain framing between 5...8%.

Increasing peripheral speed of active parts (raking combs) beneficially influences the inflorescences harvesting degree, with values comprised between 1...10%.

Harvesting degree of active parts of comb with curved teeth -type is superior to that of straight teeth combs, by approx.14%.

- the most advantageous situation in terms of harvesting degree is in case of using curved teeth, variants S_2, T_2, V_2. For these variants, the harvesting degree has maximum values, framing between 84.2% and 86.4%, in case of low harvesting, with minimum working speed (v_l=0.5km/h), at maximum linear velocity of band (v=1.08m/s).

Results obtained during tests have enabled to find the optimum typo-dimensional variants of active parts used in chamomile inflorescences harvesting, under kinematic indexes scientifically established and according to features of respective crop.

Results obtained represent an important step in achieving efficient specialized equipment, designed to harvest chamomile inflorescences, as well as an argument in relaunching chamomile crop in Romania, in the contex of sustainable devlopment.

References

[1] Muntean L.S. *Medicinal and aromatic plants cultivated in Romania*, Editura Dacia Publishing, Cluj, 1990.
[2] Verzea M. And all., *Culture technologies for medicinal and aromatic plants* Editura Orizonturi Publishing, Bucharest, 2002.
[3] Brabandt H., Ehlert D. - *Chamomile harvesters: A review,* Industrial Crops and Products 34, Elsevier, 2011.
[4]. Ehlert D. and col. - *Influence of comb parameters on picking properties for chamomile flowers* Industrial Crops and Products 33, Elsevier, 2011
[5] Neculăiasa V. Dănilă I.*Working processes and harvesting machines,* Editura A92 Publishing, Iaşi, 1995;

RESEARCH ON OPTIMIZATION OF PARAMETERS OF PLOWS WITH VARIABLE WORKING WIDTH

Cristian Nuţescu
Polytechnic University of Bucharest of Romania, Faculty of Biotechnical Systems Engineering; Splaiul Independentei, no.313, District 6, Bucharest, Romania

ABSTRACT

This paper has as main objective the development of theoretical and experimental research on dynamic behavior and energy of plowing aggregates.

The aggregates are formed by a wheeled tractor and a plow wear, which can highlighted the influence of the adjustment systems of the working width, on the dynamics and energetics of the plowing aggregates, to travel on different soil types in different conditions.

1. INTRODUCTION

For the tehnological and energetical optimization of the plowing aggregates it requires a scientific theoretical and experimental analysis about the influence of the formation method and the operating parameters of the plowing aggregate.

It requires a summary of the most representative international achievements of the theoretical and experimental research on the dynamics and energy of the plowing aggregates.

2. METODOLOGY

It has been presented the physical and mechanical interaction between the soil and plow working active organs in certain soil types. It gives an overview of the soil, soil structure, soil characteristics and soil types found throughout the globe [1].

SOIL PHYSICAL AND MECHANICAL PROPERTIES

1. General presentation

1.1 Overview

Soil is the top, loose, lithosphere layer , which is a continuously evolving under the influence of pedogenicals factors representing the layer of Earth's on which plant life develops.

Fertile soil contains nutrients and is composed of humus and loess.

It can also come from soil mulci .The soil who lacks a sufficient amount of nutrients is called oligotrophic [6].

Science which studies the genesis, evolution, structure and distribution of soils is called pedology.

Temporarily or permanently frozen soil are called gelisoils .The below part, that remains permanently frozen, is called permafrost or pergelisoil.The surface that thaws in summer, is called molisoil.The areas who are deeply affected by frost forms criolitoarea.

In areas with thick pergelisoil, repeated freeze-thaw process gives rise to an ordered anarchy microrelief (like fort) called criocarst or termocarst. By gelisoil's study deals geocriologia [3].

Other types of soils are:

- alluvial soil: type soil with a varied structure that appears on floodplains. They are highly productive soils rich in nutrients.

- azonal soil: soils evolutionary stages, without distinctive horizons formed in recent deposits, scattered small areas.
- caleimorfic soil: type of soil that is situated above of a rich in calcium ground layer .
- hydromorphic soil - type of soil whose pedological processes are dominated by the presence of abundant amounts of water.
- sundre soil-it is found in humus
- grey soil- it is found in few places in the desert where vegetation is present, very small thickness.
- red soil - found in areas where developing subecuatoriale savannas, they have a good fertility but degrades quickly.
- laterite soil - is found in equatorial areas, poor in humus, red.

1.2 Soil fertility

Fertility is the ability of soil to supply plant in continuous mode, the need for water, nutrients and air they need in order to normal growth and development.

Fertility is determined by the properties of the chemical, physical and mechanical properties of soil.[1]

1.3 Soil structure

From the physico-chemical point of view, soil is a heterogeneous poly-dispersive layer that consists in three distinct phases which in turn have several components.[4]

The soils of the land for crops can differentiate between them by different structure of layers, each with different thickness and composition .Those layers called horizons and the thickness and structure is different for each soil type separately.

Three-phase composition of the soil is shown in the diagram in Figure 1. It shows that the weight of the solid phase represented by the content of minerals and organic is majority and has a value of about 50%. The other two phases, the gas phase (air) and liquid (water) are shown in the voids, pores and the capillary spaces of the mass of soil.

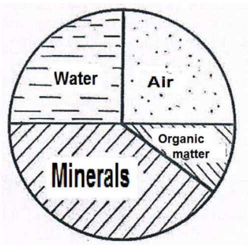

Figure1 Three-phase composition of the soil [6]

2. PHYSICAL AND MECHANICAL PROPERTIES OF THE SOIL.

2.1 Specific weight (density) soil

Depending on the internal structure of materials which are compact and have pores inside them can be characterized by the absolute density, respectively apparent density.

Absolute density (ρ) is the unit volume of the soil mass, in a compact form without pores. Determine by the relation:

$$\rho = \frac{m_s}{V_s} \text{ [kg/m}^3\text{]} \quad (2.1)$$

where: m is solid phase weight [Kg]; V-solid phase volume, in [m^3].

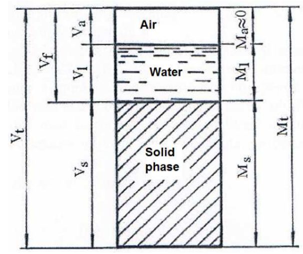

Figure 2 The three phases of soil constituents [2]

Apparent density (ρ_a) is the unit weight of the soil volume in the natural state, loose and determine by the relation:[3]

$$\rho_a = \frac{m_s}{V_t} \text{ [kg/m}^3\text{]} \qquad (2.2)$$

where,V_t is the total probe soil volume [m^3].

2.2 Soil porosity

Soil is the solid material poroscare is crossed by a complex network of macro and microscopic cavities canales, which gives a quality specifications called porosity.

Total porosity ψ is defined by the relation:

$$\Psi = \frac{V_l + V_a}{V_t} \cdot 100 = \left(1 - \frac{\rho_a}{\rho}\right) \cdot 100[\%] \qquad (2.3)$$

where, V_l is the pore volume occupied by water; V_a is the pore volume occupied by air.

2.3 Soil cohesion

Soil cohesion soil property that is both elementary particles and soil structural elements are maintained stuck together due to mutual attraction forces. Cohesion forces are of the Van der Wals and occurs between molecules of the same substance.

Soil physical properties (texture, structure, density, etc..) influences the value of cohesion. Finer the particles, higher the number of contact points and the cohesion forces will be higher. Cohesion depends on the degree of compaction, organic content and relative humidity value of moisture. Dependency cohesion of different soil types is shown in the figure below.It is shown that for sandy soils cohesion variation is less dependent on moisture.[2]

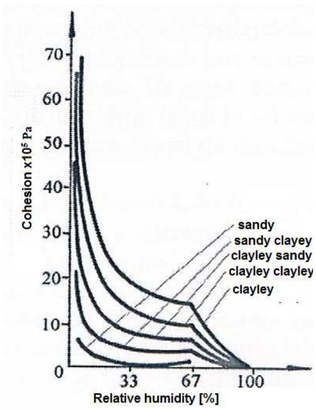

Figure 3 Cohesion variation depending on soil moisture [2]

2.4 Soil moisture(humidity)

Soil moisture should be analyzed from two points of view: the availability and use of water from the soil by plants and soil workability.

Humidity is a conventional size that characterizes the amount of water contained in the mass of a body. Humidity can be relative or absolute.

Absolute humidity (w) este is defined as a ratio between the amount of water that m_a that can be removed by drying in oven and solid phase mass m_s.It is determine by the relation:

$$W = \frac{m_a}{m_s} \cdot 100 \ [\%] \qquad (2.4)$$

where m_a is the solid phase weight (water) [Kg]; m_s - solid phase weight [Kg].

Relative humidity of the soil w_r is defined as the ratio of absolute humidity and moisture corresponding field capacity.

$$W_r = \frac{m_{ae}}{m_{ac}} \cdot 100 \ [\%] \qquad (2.5)$$

Interval in which the relative humidity is situated soil is dependent on soil texture.

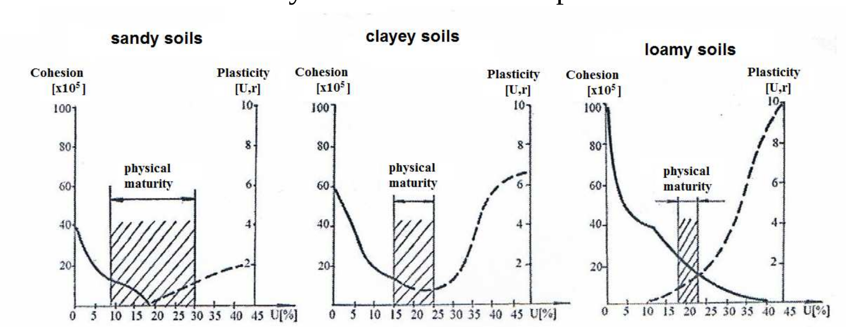

Figure 4 Adequate soil moisture state of physical maturity [4]

2.5 Soil Plasticity

Plasticity is the soil property can be modeled under the action of mechanical forces and nurturing form obtained by modeling (without breaking) after the causes that produced it stopped. Soil plasticity is subject to humidity and clay content. Sandy soils or those with low plasticity clay does not have plasticity.

2.6 Soil friction forces

Both cohesion and adhesion are also the result of frictional forces.

Friction forces are manifested in two forms: *internal friction,* that occurs in soil particles; *external friction,* that occurs between the surface and the ground surface active bodies.[5]

Experimental research has shown that in addition to working bodies roughness and friction coefficient of soil type and soil moisture depends.

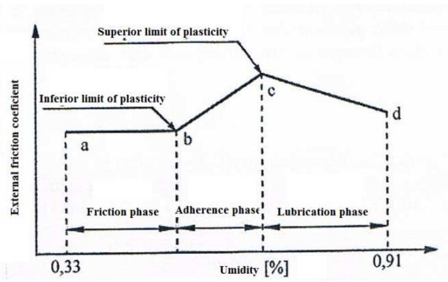

Figure 5 Variation of friction coefficient μ depending on humidity external [5]

2.7 Compressive Strength

During the working process, the soil is subject to mechanical stress under the influence which is mobilized and deformed to a certain depth.

Ground reaction to these requests is on compressive strength and is a manifestation of consistency of soil.In after compressing the soil is brought to a mechanical tension σ, depending on the type and moisture content of soil.

For a given deformation z, the soil will have different tension and the tension depending on the deformation can be done by a function σ=f(z).

$$\sigma = c \cdot z^n \quad (2.6)$$

where z is the deformation of the soil,in m; c- volume deformation coefficient, in N/m^3;

n- exponent which depends on the soil type and the request;

Volume deformation coefficient c is numerically equal to the tangent of the angle α formed by the tangent to the curve at the origin of the coordinate axes.[2]

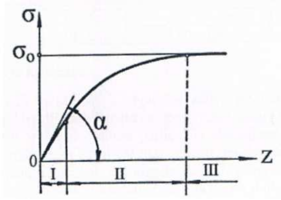

Figure 6 Addiction normal stress σ according to soil deformation [2]

2.8 Shear Strength

As a result of mechanical action organs active during processing of agricultural machine, soil suffer deformities caused by compressions, subsidence, etc. They produce residual deformations, after breaking the links between elementary particles or gromerular due to shear stresses exceeding. In the most general case, the shear stress τ depends on the degree of compaction or pressure in the soil, soil deformation, its physical properties, mechanical etc. Expressing the shear stress τ by deformation x in direction OX, fig 7 shows that the shear stress dependence of the strain can be divided into several areas.[6]

In compact soils (curve a), from the sandy-loam texture, to the clay loam texture, the shear tension τ_p is proportional to the shear deformation x_p. In plastic soils respectively when their moisture approaches saturation limit (curve b), maximum shear stress is found for large values of the deformation curve not having a maximum.[7]

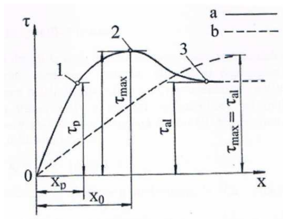

Figure 7 Strain dependence of shear stress of the soil:
a-compact soil; b-plastic soil [7]

The maximum shear unified effort can be expressed by the relation:

$$\tau_{max} = c + \tau_{al} = c + \sigma tg\theta \tag{2.7}$$

where:c-the coefficient of soil cohesion; τ_{al}-slip unit effort;
θ -angle of internal friction between soil particles; compression-tension τ.

2.9 Specific resistance plowing

Resistance plowing soil, includes all resistances determinated by cutting, bending, compression, torsion, rupture and lateral displacement of a unit volume of soil. Plowing soil resistance relates to the cross section of the furrow, yielding a indicator that is called *specific resistance plowing (k_0)*, wich is determine by the relation:

$$k_0 = \frac{F_t}{a \cdot b} \quad [\text{N/m}^2] \tag{2.8}$$

F_t= strength of a troop,in N; a= deep furrow,in m; b= furrow width, in m.

Plowing specific resistance is dependent on structure, texture, moisture content, cohesion and adhesion of soil.[8]

It should be noted that repeated passages of wheels over the soil surface increases the degree of soil compaction, which increases the resistance to ground-work.

3. CONCLUSION

In this paper presents and briefly analyzes those physical and physico-chemical properties of the soil that have direct influence on the interaction of plowing working bodies and the soil that undergoes the plowing process, including qualitative and energetic parameters of the technological process.

References

[1]Vladut V., Nicolescu M., Voicu Gh., Matache M., Biris S., Danciu A., Voicea I., Paraschiv Gh., Persu C. *"Aided Testing biotechnical systems"* - Editura Terra Nostra, Iasi 2012

[2]Caproiu St., Scripric V., Babiciu P., Ciubotoru C., Ros V. "*Agricultural machinery for soil, sowing and crop maintenance*" -Editura Didactica si Pedagogica, Bucuresti 1982

[3] Krasnicenko A. V., Segarceanu M. *"Handbook manufacturer of agricultural machinery"* -Editura Tehnica, Bucuresti 1964

[4]Girma,G. *Measurement and prediction forces on plough bodies 1- Measurement of forces and soil dynamic parameters. In: Land and Water Use* (Dodd V A; Grace P M,eds), Balkema, Rotterdam,(1989)

[5]Guskov, V. V. *Traktori, Ciasti. II.* Teoria. Vaseisaia skola, Minsk,1977

[6]Gus,P. si col. *Agrotehnica.* Edit. Risoprint, Cluj-Napoca,2004

[7]Nastasoiu S.,Popescu S, *Tractors*, Editura Didactica si Pedagogica, Bucuresti, 1983

[8]Ormenisan N. *Considerations influence the steering wheel size on the dynamics and energetics of agricultural tractors. INMATEH vol. III*, Bucuresti 2006

THE SHREDDING OF SOFT-TEXTURED FOOD MATERIALS BY MEANS OF UNHEATED METAL WIRE CUTTING

Ciprian Olaru[1], Valentin Nedeff[1], Mirela Panainte - Lehăduș [1]*,
Ionel Olaru [1], Elena Ciobanu [1]
[1]"Vasile Alecsandri"University of Bacău, Calea Mărăşeşti, 157, RO-600115, Bacău, Romania

ABSTRACT

Abstract: The cutting of food materials must not damage the material properties, as in the cutting process there should not appear any excessive heating or any breaking of the material due to the choice of an inadequate cutter. Previous studies and research on the cutting of soft-textured food materials refer to the phenomena that are produced during the process of cutting by means of unheated metal wire, the influence of the diameter of the cutting metal wire on the quality of the shredding, the analysis of the cutting aspect, the analysis of quantitative material losses and the determination of the energy necessary for the shredding.

In the shredding process of such materials, the resulting cutting surfaces are more regular, lower cutting forces are needed, while resulting juice and material losses are also reduced.
Keywords: cutting, food material, texture, metal wire.

1. INTRODUCTION

The shredding process implies the possibility to separate soft-textured food materials in several smaller components. The main preoccupation of food experts is to design equipment and technologies for an optimal shredding (the achievement of the desired degree of shredding with the least power consumption possible). Thus, food materials should not be broken or suffer any loss during the shredding process [1, 2, 3].

Few studies in the field have thoroughly investigated the behavior of soft-textured food materials during the shredding operation. In general, the main preoccupation was to test the bending of soft-textured cheeses and to study their behaviour at low temperatures [4, 7]. However, in the case of soft-textured food materials at room temperature, when they have a high degree of unevenness and low viscoelastic forces and rigidity, it can be difficult to apply the conventional tests of breaking; therefore metal wire cutting tests can be used as an alternative [6].

To understand how food materials are shredded in the cutting process it is necessary to develop computer simulations for the testing of several types of soft-textured food materials that have different rheological properties, so that the phenomena that take place during the shredding process should be elucidated. [5, 8, 9].

In this paper was to examine the way in which the shredding of the material is produced, the released quantity of juice, the cutting aspect, the shredding energy value.

2. METHODOLOGY

For a better understanding of the phenomena occurring during the shredding of soft-textured food materials, various materials with various textural properties were used in this experiment.

[1] corresponding author: Mirela PANAINTE-LEHĂDUȘ, "Vasile Alecsandri"University of Bacău, Calea Mărăşeşti, 157, RO-600115, Bacău, Romania, phone number: +40723291670, e-mail address: mirelap@ub.ro

Table 1: Soft-textured food materials used in the study

No.	Soft-textured food materials	Type/variety
1.	Curdled cheese	Sheep cheese
2.	Tomatoes	Unibac
3.	Peeled oranges	Valencia
4.	Strawberries	Elsanta
5.	Peeled bananas	Cavendish
6.	Turkish delight	Bucharest

To study the shredding of soft-textured food materials by using cutting metal wires of different diameters (0.4 mm, 0.3 mm and 0.2 mm) at 20°C, a laboratory stand was used (Fig. 1), which made it possible to produce various shredding degrees for various food materials. In this study we used a working speed of 2.5 mm/s.

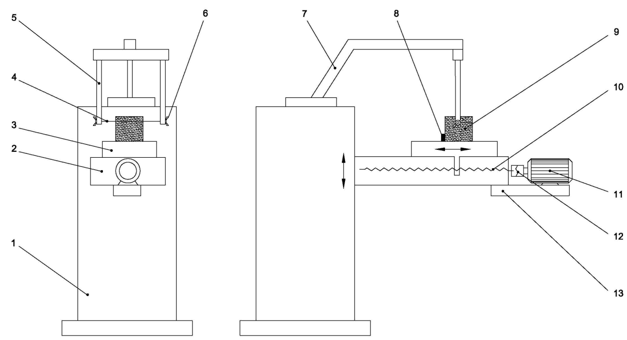

Figure 1: Scheme of laboratory stand:
1. frameworks; 2. longitudinal table; 3. mobile sled; 4. cutter; 5. fixing frame of metal wire cutting; 6. attachment device; 7. support framework; 8. stop for cutting material; 9. cutting material; 10. bolt for driving the mobile sled; 11. electric motor; 12. coupler; 13. support device for the electric engine

The cutting device is made up of the framework 1, on which the longitudinal table 2 is placed, it being possible that the latter be moved vertically; on the table 2, the mobile sled 3 is mounted, which can move longitudinally as a result of its being controlled by the electric engine 11 through the drive bolt 10.

The transmission of the rotation movement from the electric engine positioned on the support device 13 to the drive bolt is made through the coupler 12. To achieve the continuity of the shredding process, the engine can be operated in both directions thereby moving the mobile sled in both directions.

The cutting device is composed of the fixing frame of the metal wire cutting 5, the metal wire cutter 4, which is fastened by the attachment device 6. The whole cutter assembly is attached to the framework by the support framework 7. In order that the cutting material 9 should not move on the mobile sled surface, the latter is provided with the stop for cutting material 8.

The horizontal moving of the cutting machine is made by means of an electric engine provided with a gearbox with a worm mechanism/worm drive wheels incorporated in the motor housing.

In order to analyze the parameters resulted from the shredding of soft-textured food materials, the experimental stand is provided at one end of the metal cutting wire with a metal blade made of a material with elastic properties. On this blade two tensometric marks were attached, which take over the deformation of the metal blade and transmit it through an electrical signal to the SPIDER 8 type data acquisition board.

For the calculation of the shredding energy in the case of the food materials studied above, Bond's law was used [10]:

$$E_m = k \cdot \left(1/\sqrt{D_f} - 1/\sqrt{D_i}\right) \text{ [J]} \tag{1}$$

According to Bond's law, the shredding energy is equal to the difference between the energy contained in the material before and after the shredding. The k parameter can be expressed in the form [8]:

$$k = 2 \cdot F \cdot S_{nc} \tag{2}$$

Inserting Bond's constant (2) in equation (1) the following relation will result:

$$E_m = 2 \cdot F \cdot S_{nc} \cdot \left(1/\sqrt{D_f} - 1/\sqrt{D_i}\right) \text{ [J]} \tag{3}$$

where:

E_m is the shredding energy, [J];
D_i – the dimensions of the material before shredding, [m^3];
D_f – the dimensions of the material after shredding, [m^3];
F – the shredding force, [N];
S_{nc} – the new created surface, [m^2].

Because we can't accurately determine the final dimension of the material, the initial and final dimensions of the material are replaced in equation 3, according to the corresponding density and weight.

$$D_i = m_i/\rho\,;\; D_f = m_f/\rho \tag{4}$$

where:
m_i is the weight of the material before shredding, [kg];
m_f – the weight of the material after shredding, [kg];
ρ – the material density, [kg/m^3].

The density of each material is determined and thus the relation for the determination of the shredding energy will appear as follows:

$$E_m = 2 \cdot F \cdot S_{nc} \cdot \left(1/\sqrt{m_f/\rho} - 1/\sqrt{m_i/\rho}\right) \text{ [J]} \tag{5}$$

- In the case of food materials that are considered spherical:

$$S_{nc} = 2 \cdot \pi \cdot D_i^2/4 \text{ [m}^2\text{]} \tag{6}$$

- In the case of food materials that are considered rectangular:

$$S_{nc} = 2 \cdot a \cdot b \text{ [m}^2\text{]} \tag{7}$$

where:

a is the width of the soft-textured food materials that are shredded, [m];

b – the length of soft-textured food materials that are shredded, [m].

3. Results

Using data obtained through experimental results the value of the shredding energy was calculated, with relation (5), for all six soft-textured food materials under analysis, the results being rendered in a graphical form in Figure 2.

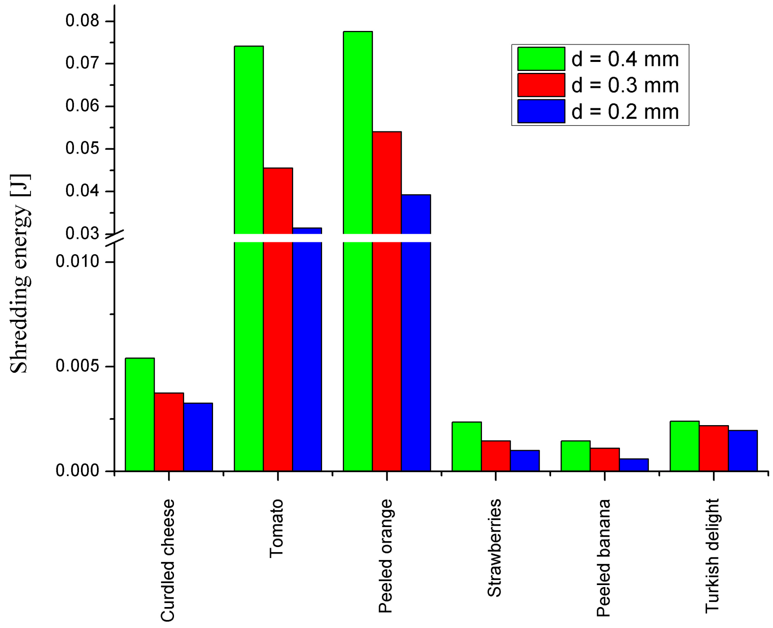

Figure 2: The variation of shredding energy for food materials shredding by means of metal wires with different diameters.

As it can be seen in Figure 2, the value of the shredding energy in the case of soft-textured food materials under analysis varies according to the material properties, the metal wire diameter etc.

By using the analytical balance and by the visual analysis of the cutting aspect of soft-textured food materials having undergone metal wire shredding at a temperature of 20°C, we examined a series of indicators such as the adherence to the cutter, the cutting aspect, the quantitative material losses (Table 2, Table 3 and Table 4).

Table 2: Working indices obtained for the shredding of soft-textured food materials by means of a metal wire with a diameter d = 0.2 mm

No.	Food material	Average cutting surface *a* x *b* (d^2) [mm^2]	Weight before cutting [g]	Weight after cutting [g]	Percentage of losses [%]	Adherence to the cutter	Cutting aspect
1	Curdled cheese	30 x 30	28.5	28.42	0.28	Small	Regular
2	Tomatoes	50 x 50	84.2	83.48	0.86	Small	Irregular
3	Peeled oranges	60 x 60	108.91	108.25	0.61	Small	Irregular
4	Strawberries	25 x 25	20.86	20.84	0.12	Small	Regular
5	Peeled bananas	30 x 30	35.26	35.22	0.11	Small	Regular
6	Turkish delight	35 x 35	39.22	39.19	0.07	High	Regular

Table 3: Working indices obtained for the shredding of soft-textured food materials by means of a metal wire with a diameter d = 0.3 mm.

No.	Food material	Average cutting surface *a* x *b* (d^2) [mm^2]	The weight before cutting [g]	The weight after cutting [g]	Percentage of losses [%]	Adherence to the cutter	Cutting aspect
1	Curdled cheese	30 x 30	30.1	30.01	0.30	Small	Regular
2	Tomatoes	50 x 50	90.15	89.35	0.89	Small	Irregular
3	Peeled oranges	60 x 60	105.89	105.20	0.65	Small	Irregular
4	Strawberries	25 x 25	16.76	16.74	0.14	Small	Regular
5	Peeled bananas	30 x 30	28.4	28.36	0.13	Small	Regular
6	Turkish delight	35 x 35	43.22	43.19	0.08	High	Regular

Table 4: Working indices obtained for the shredding of soft-textured food materials by means of a metal wire with a diameter d = 0.4 mm

No.	Food material	Average cutting surface *a* x *b* (d^2) [mm^2]	Weight before cutting [g]	Weight after cutting [g]	Percentage of losses [%]	Adherence to the cutter	Cutting aspect
1	Curdled cheese	30 x 30	38.15	38.01	0.37	Small	Regular
2	Tomatoes	50 x 50	89.35	88.49	0.96	Small	Irregular
3	Peeled oranges	60 x 60	101.23	100.53	0.69	Small	Irregular
4	Strawberries	25 x 25	19.3	19.27	0.18	Small	Regular
5	Peeled bananas	30 x 30	29.1	29.06	0.15	Small	Regular
6	Turkish delight	35 x 35	44.24	44.20	0.10	High	Regular

The analysis of tables with working indices referring to the shredding of soft-textured food materials by means of metal wire revealed that significant losses (juice/material) were recorded in the case of shredded tomatoes (0.86% ÷ 0.96%) and oranges (0.61% ÷ 0.69%). because of their high percentage of juice content. but these values were decreased by reducing the metal wire cutter diameter.

For the other types of materials analyzed (curdled cheese - 0.28% ÷0.37%. Turkish delight - 0.07% ÷0.10%. strawberries - 0.12% ÷ 0.18%. peeled bananas - 0.11% ÷ 0.15%). due to their homogeneous composition. low shredding loss percentages were registered.

4. CONCLUSIONS

The experimental results obtained after the shredding of soft-textured food materials revealed the following:

- In the case of shredding energy the higher values were registered for the inhomogeneous food materials (tomatoes and oranges), and the lower values, for food materials such as curdled cheese, strawberries, peeled bananas, and Turkish delight.
- As to the metal wire cutter diameter, it was found that the highest shredding energy values corresponded to the largest diameter, i. e., d = 0.4 mm, for all six analyzed food materials, and that the value of the shredding energy decreased in direct proportion to the reduction of the metal wire cutter diameter.
- It was concluded that Turkish delight, bananas, strawberries and curdled cheese are the most suitable for the cutting by means of metal wires, due to their degree of homogeneity and structural properties. In the case of such materials, the cutting was smooth from the

beginning to the end due to their relatively uniform composition, and the reducing of the metal wire cutter diameter led to lower cutting forces, to the improvement of the quality of the cutting surface and to reduced material and juice losses.

Thus it can be concluded that metal wire shredding is more suitable for soft-textured food materials that have a more uniform composition. By using the metal wire cutting method, the shredding process was improved, as the resulting cutting surfaces were more regular, the cutting forces were lower, and the juice and material losses were reduced.

References

[1] Atkins, T., *Food and Food-Cutting Devices and Wire Cutting, Chapter 12*, The Science and Engineering of Cutting, 283–306, 2009.

[2] Brown, T., *Cutting forces in foods: experimental measurements*, Journal of Food Engineering, 70, 165–170, 2005.

[3] Brown, T., et al., *Improving food cutting systems*, In Proceedings of IChemE Food and Drink, 103–106, 2000.

[4] Charalambides, MN., et al., *The analysis of the frictional effect on stress–strain data from uniaxial compression of cheese*, Journal of Material Science, 13–21, 2001.

[5] Gipsy, T.M., Gustavo, B.C., *Rheology for the food industry*, Journal of Food Engineering, 67, 147–156, 2005.

[6] Goh, S.M., *On the mechanics of wire cutting of cheese*, *Engineering Fracture Mechanics*, 931–946, 2005.

[7] Imbeni, V. et, al., *Rate and temperature dependence of the mechanical properties of Cheddar cheese*, In: Proceedings of 10th International Conference on Fracture, ICF1001101 PR, 2001.

[8] Panainte, M., *Cercetări privind optimizarea procesului de mărunţire a produselor agroalimentare*, PhD thesis, Universitatea Tehnică „Gh, Asachi" Iaşi, 2008.

[9] Panainte, M., Nedeff, V., Olaru, C., Tomozei, C., Irimia, O., *Study the behavior of food materials with soft textured subject to shred by cutting through the texture analysis method*, Proceedings of the 5th International Conference on Advanced Concepts in Mechanical Engineering ACME, 2012.

[10] Thompson, M., *Procesul de mărunţire*, Curs, Universitatea Politehnica Bucureşt, 2005.

EFFICIENTLY EXTRACTION OF BIOACTIVE COMPOUNDS FROM MEDICINAL PLANTS USING ORGANIC AND SUSTAINABLE TECHNIQUES

A. Pruteanu[1], A. Muscalu [1)] M. Ferdes [2)],
[1)]INMA Bucharest / Romania; [2)]P.U. Bucharest / Romania

ABSTRACT

At present, the demand for natural bioactive compounds is increasing as a result of their use in the food and pharmaceutical industry, including different functional activities of them, such as: the antioxidant, antimicrobial, antitumoral, antihypertensive activity etc. The medicinal herbs are the most popular natural sources for this type of bioactive compounds, which can only be obtained by the operation of extraction. The qualitative and quantitative studies on bioactive compounds from medicinal plants is based on the choice of an extractive technique appropriate and of performance, which ensures an operation completely and efficiently. This paper presents synthetically the organic and sustainable extraction techniques, in order to obtain bioactive compounds from medicinal plants, as well as the current trends in the field.

1. INTRODUCTION

The medicinal plants represent the oldest class of therapeutic remedies that accompanied mankind throughout its historical evolution. Also, plants have played a dominant role for millennia in the treatment and cure of various diseases [7], being recommended the products that do not affect the organism in conditions of imbalance caused by disease.[1]

Natural remedies that are based on medicinal plants have come to the forefront because they contain bioactive compounds and that make them useful in the treatment of various diseases. At the base of herbal medicinal plant efficiency sits the relation between the bioactive compound and the therapeutic action.[6] These compounds originating from plants offer a less aggressive treatment and more complex upon the human body, but requires a longer time to obtain the expected results.[7]

At present has increased the interest for the search for bioactive compounds of natural origin, which prove their effectiveness against many diseases. The classes of bioactive compounds present in the medicinal plants include: vitamins, minerals, alkaloids, flavonoids, saponins, glycosides, terpenes, tannins, volatile oils etc.[2]

The amount of bioactive compounds from the plant is conditioned by environmental factors, by the zoning of the species, by the culture technology, by the biological value of the cultivated varieties and not the least, by the modalities of processing. The knowledge of bioactive compounds as well as their extraction technique is important in order to be able to assess the complex therapeutic value of the medicinal plants.[6]

The current trend regarding the extraction of bioactive compounds from medicinal plants is that of replacing the classical technologies, which are quite complicated, inefficient and expensive, with new and efficient methods for obtaining the vegetal extracts. The application of ecological and sustainable extraction techniques have the purpose of determining the bioactive natural compounds, to improve the extraction efficiency and to reduce the environmental impact.[5]

---

[1] INMA, Bucharest, ROMANIA, 6 Ion Ionescu de la Brad, Blv, sector 1, Bucharest 71592, OP 18, Phone: 004021-269.32.55, e-mail : pruteanu_augustina@yahoo.com

In this paper is analyzed various studies describing the efficiency of the extraction process using two organic and sustainable techniques: the extraction with pressurized liquid and the extraction with super-critical fluids, in order to obtain natural bioactive compounds from different medicinal plants.

2. METHODOLOGY

The use of bioactive substances in various trade sectors such as: pharmacies, food and chemical industry, led to the need to find a suitable technique for extracting these bioactive compounds from the medicinal plants.

Extraction is the operation of separation partially or totally of the components of a mixture based on the difference in solubility in one or more solvents.

The extractive solutions from plants are prepared containing the components extracted from vegetal products by means of solvents through techniques ensuring an appropriate extraction.

The quality of the bioactive substances contained in the obtained extract is influenced by parameters depending on the vegetal material, on solvent, on equipment and on the used method to determination, figure 1.[4]

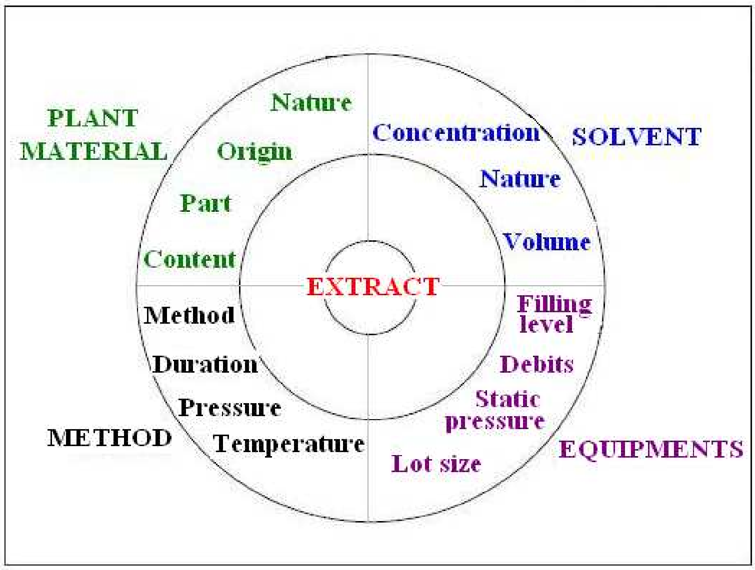

Figure 1 – Influence of parameters on the extract [4]

The vegetal material consists of medicinal and aromatic plants cultivated or harvested from the wild flora. The parts from plants that are used for the extraction can be: strains, roots, rhizomes, seeds, shell, fruits, leaves, flowers or herb. It can be used both fresh plants and dried plants, which are minced and / or chopped, then there are separated on different size fractions, according to Romanian Pharmacopoeia.[9]

The solvent used must to dissolve and extract the majority of bioactive components. It must have a boiling point as decreased so that the use of it to be as economical.

The most solvents in the industry of used vegetal extracts are: the water (for salts of alkaloids, glicoids, sugars, pectin mucilaginous material, protidics or colorants, enzymes, tannins, etc..), ethylic alcohol (for volatile oils, hydrocarbons , tannins, alkaloids, bases and salts of their, glicoids, resins, chlorophyll etc.), ethyl ether (for alkaloid bases, resins, volatile oils, etc.).[9]

The main mechanism of the process of extraction of the bioactive compounds from medicinal plants, Figure 2, consists of:[3]

a) Direct dissolution of protoplasmic constituents

This phenomenon occurs when the solvent comes into contact with the broken cell. As the degree of crushing plant is higher the percentage of substances arrived in contact with the solvent is greater.

b) The actual extraction

It is a complex process and is produced by the influence of the solvent on the intact cells. After drying of the vegetal product, the protoplasm loses water and a part of protoplasmic substances precipitates as an amorphous form or crystalline, situation in which the cell loses the osmotic ability. By the penetration of the solvent into the cell (process facilitated by the intermicelare spaces that are created in the cellulosic membranes than by drying and solvent contact) are restored some of the initial conditions. Thus, the solvent dissolves part of the cellular constituents after which migrates through the membrane into the interstitial spaces (due to osmosis) based on the difference of concentration of the liquids from the two sides of the membrane (intracellular and extracellular space).

The extraction takes place until the concentrations of the solutions in the two spaces become equal.

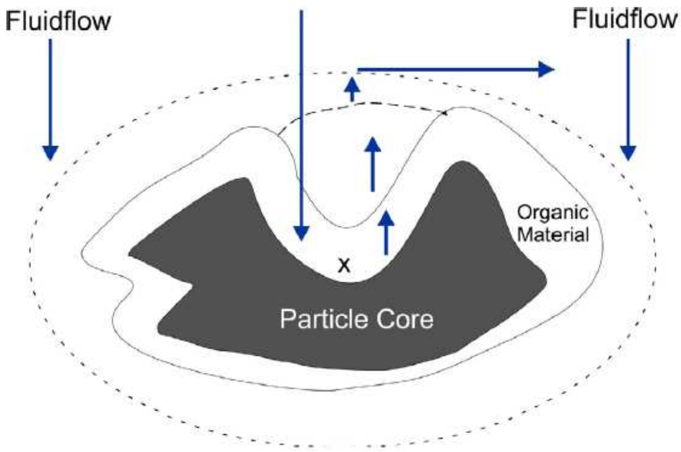

Figure 2 - The extraction mechanism [3]

For the extraction of bioactive substances from medicinal plants there are various conventional and unconventional techniques.

Conventional techniques are classic and they are based on the power extraction using different solvents and applying heat and / or mixing. The reference technique used is Soxhlet extraction and maceration, percolation, hydrodistillation too.

The unconventional techniques are more *environmentally friendly* due to the use in a short time of synthetic organic chemical substances, with high productivity and very good quality. Thus, in order to increase the efficiency of extraction of bioactive substances from medicinal plants are used the following unconventional extraction techniques: with ultrasound, with electrical pulses, by extrusion, by enzymatical digestion, with microwaves, with subcritical and supercritical fluids, but also accelerated extraction with solvents.[3]

Accelerated – solvent extraction (**ASE**) or **Pressurized – liquid extraction** (**PLE**) is a new extraction technique based on the use of high temperature and pressure to accelerate the kinetics of dissolution and break bonds analyte-matrix interactions. In addition, by increasing the temperature decreases the viscosity of the solvent which makes it easier to penetrate the solid matrix of the sample. In this way, the extraction time is reduced from tens of minutes to a maximum of a few minutes, and the samples can be extracted in small quantities.

This technique is an alternative to the Soxhlet extraction or at the supercritical fluids extraction.

The devices in which such an extraction is performed must withstanding at high pressures, the samples and the solvent being introduced into a closed and heated enclosure. The high temperature (50-200°C) accelerates the diffusion of solvent molecules in the sample texture, and the high pressure which is obtained maintains the solvent in liquid state. The operation is realized in extraction cell ,which must to resist the high pressure.[6]

The main stages of a solvent extraction procedure (ASE) are the following:[6]

- introduction of the sample into the extraction cell;
- filling with solvent;
- heating and pressurizing of the cell;
- emptying the cell by purging with a gaseous flow (N_2);
- collecting the extract in one vial for its analysis.

The ASE systems are fully automated. The scheme of a system based on accelerated solvent extraction, Figure 3 a, was performed for the first time by Dionex Corporation.[6]

Supercritical – fluid extraction (**SFE**) is a technique developed in the last years for use at analytic scale, constituting an alternative to the classical solvent extraction.

The extractions with supercritical fluids are carried out most frequently with CO_2, but also with ethanol, methanol, etc. The solvation power of a supercritical fluid is dependent on the density, which can be influenced by small variations of the pressure and temperature. Having a critical temperature of $31,1^0$C and a critical pressure of 73,8 bar, the carbon dioxide is a popular and environmental supercritical fluid, which is inexpensive, non-toxic and non-flammable.[6]

The components of an extraction system with supercritical fluids shown in figure 3 b are the following: a source of pure carbon dioxide, an oven with extraction vessel, a pressure regulator and a collection vessel for the recovery of the extracted analytes. The collection of samples can be done by passing the extract through a solvent, or over a suitable adsorbent, such as Florisil. [8]

Supercritical fluid extraction has two integrated parts: one is the extraction of the analyte from the sample matrix and the other is the collection or the covering of the analytes. There are three main ways of collecting: (1) collection in a tank containing the solvent; (2) covering on a cartridge packed with absorbent material in the solid phase and (3) collection in a device which is connected on-line with the chromatographic system, so that the entire extract is introduced into this system .[8]

Due to the high efficiency of this type of extraction it has become increasingly used by the food industry and by the industry of fragrances and flavors.

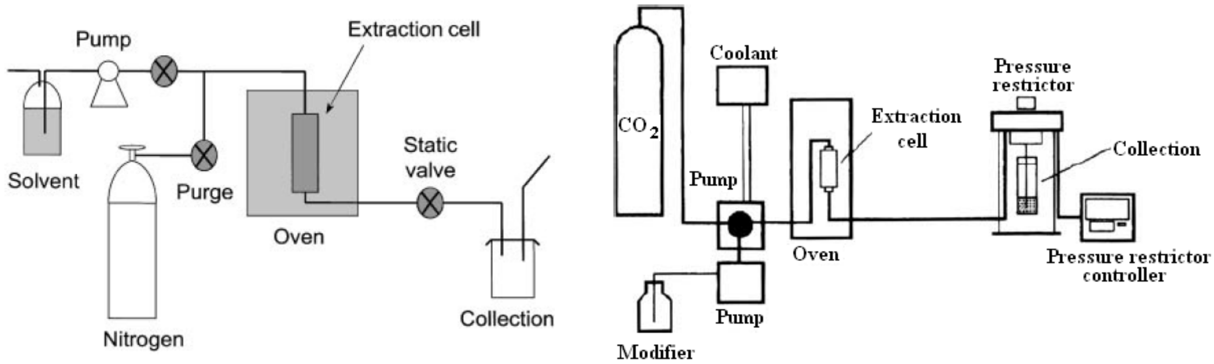

a) Extraction system with liquids under pressure [6] b) Extraction system with supercritical fluids [8]

Figure 3. Ecological extraction systems

3. RESULTS

The tables below present the most relevant applications of the extraction systems with liquids under pressure (PLE), Table 1, and with supercritical fluids (SFE), Table 2, on obtaining bioactive compounds from natural sources.

Table 1 Applications of the system for pressurized - liquid extraction (PLE) [2]

Product	**Compounds of interest**	**Solvent**	**Tempera-ture (^{0}C)**	**Pressure (MPa)**	**Pressure mode**	**Extraction time (min)**
Hylocereus undatus (flowers)	Flavonoids	methanol	120	10	static	15
Olea europaea (olive leaves)	Phenolics	ethanol	150	10	static	20
Mentha piperita (Peppermint)	Phenolic compounds	75 % acetone	100	10	static	10
Plants of the Family *Apiaceae*	Coumarins	metanol	110	-	static	10
Rosmarinus officinalis (Rosemary)	Phenolic compounds	ethanol	150	10	static	20
Origanum vulgare (Oregano)	Phenolic compounds	ethanol	200	10	static	20
Plants of the Family *Lamiaceae*	Phenolic compounds	56 % methanol	129	10	static	5
Spinacia oleracea (Spinach)	Flavonoids	70 % ethanol	150	13	static	5
Thymus vulgaris (Thyme)	Essential oil	n-hexane	100	6	static	10

Table 2 Applications of the system for supercritical - fluid extraction (SFE) [2]

Product	**Compounds of interest**	**Solvent**	**Tempera-ture (^{0}C)**	**Pressure (MPa)**	**Pressure mode**	**Extraction time (min)**
Hemerocallis disticha (Wild lily)	Lutein, zeaxanthin	CO_2	80	60	static and dynamic	30; 30
Plants of the Family *Lamiaceae*	Essential oil	CO_2	40	30	dinamic	90
Magnolia officinalis	Magnolol	CO_2	80	40	static and	60; 40

(Magnolias)					dynamic	
Rosmarinus officinalis (Rosemary)	Phenolic compounds	CO_2	40	30	dynamic	300
Rosmarinus officinalis (Rosemary)	Phenolic compounds	CO_2 and ethanol	40	15	static	120
Salvia officinalis (Sage)	Essential oil	CO_2	40	30	dynamic	80
Mentha spicata (Peppermint)	Essential oil	CO_2	35	9	static	30
Mentha spicata (Peppermint)	Essential oil	CO_2	50	30	dynamic	180
Thymus vulgaris (Thyme)	Volatiles	CO_2	40	9	dynamic	240

4. CONCLUSIONS

This paper presents two ecological and sustainable extraction techniques that can be applied to obtain bioactive compounds. The principles and applications of these techniques environmentally friendly are developed, as shown, within several published scientific works. Therefore, the adoption of these techniques presents several advantages:
- the extraction technique with liquids under pressure uses a high pressure and temperature, but decreases the time and solvent consumption, thus improving the extraction yield;
- the extraction technique with supercritical fluids is realized at low temperatures, avoiding the distortion of bioactive compounds due to the heating, the pressure and time are high, and the solvent used is cheap, safe and easy to recycle;
- both techniques are environmentally friendly, safe, give high yield, are suitable for thermally labile substances, have standardized extraction duration leading to a profitable extraction;
- high cost of equipment necessary for the work under pressure, when using both ecological extraction techniques are compensated by the benefits of the quality of the bioactive compounds obtained, important for the human health.

The application of the extraction techniques shown is justified by: technological efficiency, use of green technologies and the quality of the extracts obtained.

References:

[1] Grigore Gheorghe, Grigore Corina, *The guide of the medicinal plants and the disease treated with plants*, Bic All Publishing House, Bucharest, Romania, (ISBN 978-973-571-729-2), 2007

[2] Herrero Miguel, Castro-Puyana María, Mendiola A. Jose´, Elena Ibañez, *Compressed fluids for the extraction of bioactive compounds*, Trends in Analytical Chemistry, Vol. 43, 2013

[3] Ming Yuan Heng, Swee Ngin Tan, Jean Wan Hong Yong, Eng Shi Ong, *Emerging green technologies for the chemical standardization of botanicals and herbal preparations*, Trends in Analytical Chemistry 50, 1-10, 2013

[4] Mompon -Vannes Bernard, *Methods of extraction and purification of natural products*, The transformation of medicinal plants, Canada; www.archimex.com, 2006

[5] Mustafa Arwa, Turner Charlotta, *Pressurized liquid extraction as a green approach in food and herbal plants extraction: A review*, Analytica Chimica Acta 703 8– 18, 2011

[6] Păun Gabriela, Gheorghe Oana, Diaconu Mirela, *Medicinal plants advanced processing (guide)*, MedPlaNet Project, www.medplanet.ro, 2012

[7] Roman Gheorghe Valentin, Toader Maria, Epure Lenuta Iuliana, *Cultivation of medicinal and aromatic plants in organic farming conditions*, Ceres Publishing House, Bucharest, Romania, (ISBN 978-973-40-0823-0); 2009

[8] Sjaak de Koning, Hans-Gerd Janssen, Udo A. Th. Brinkman, *Modern Methods of Sample Preparation for GC Analysis*, Chromatographia Supplement Vol. 69, 10.1365/s10337-008-0937-3, 2009

[9] *** *Romanian Pharmacopoeia*, Medical Publishing, Bucharest, 1993

RESULTS FROM IMPLEMENTATION OF ENERGY SAVING MEASURES IN THE EDUCATIONAL BUILDINGS OF UNIVERSITY OF FOOD TECHNOLOGIES. BLOCK 4

Violeta Rasheva, Nikola Kalojanov,
Stanialava Tasheva, Mincho Minchev, Georgi Valtchev

1.INTRODUCTION: Climate change and security of energy supply are two major challenges needing urgent action. They have common causes and common solutions. Except of that the future seems marked by permanently rising prices of energy, which we use in all areas of our own life.

Analyses based on Euro stat data show retardation of Bulgaria in basic energy-economical indicators for sustainable development. Bulgaria is the most energy-intensive country in Europe - respectively 7,46; 6,81; 6,37; 6,81; 7,41; 6,12; 2,62 и 4,7 times more energy intensive than Austria, Denmark, France, Germany, Italy, Greece, Hungary and Turkey. Except of that Bulgaria is one of the most dependent countries with regard to import of energy resources in Europe – 71, 6 %. Heating in buildings is the largest consumer of energy and generator of CO_2 emissions, released into the environment. The new EU member countries use more than 40% of their energy in buildings. In fact up to 80% of this energy can be saved by renovating the existing buildings and implementation of cost-effective energy conservation measures (ECMs).

2.THE AIM of this paper is reporting the results from implemented in block 4 of University of Food Technologies (UFT) ECMs according to the project "Energy efficiency, improve access for people with disabilities in UFT and modernization of information services", realized with the financial support of OP "Regional Development", co financed by European Union through European Regional Development Fund, as well as dissemination of good practice.

3.MATERIALS AND METHODS: The above mentioned project has been developed and won on the base of carried out in 2010 energy audit of educational buildings of UFT. The building of **Block 4** is a monolithic building with 4 flours. Offices, classrooms and laboratories are situated in it. A Science laboratory and a Boiler room are situated in adjacent to main building one-store buildings. The building is inhabited average of 100 students and 70 employees. Classes are held five days a week from 7:00 to 18:00, totally 11 hours per day. The total built area is 1740 m^2, unfolded area - 5310 m^2, heated area - 5044 m^2 (boiler room is not heated), and the gross heated volume is 19398,5 m^3.

In the energy audit, it was found that heating system type «Tichelman» is in bad condition. Supply and return lines were located in a technical channel below the ground floor and were in very bad condition, in places with compromised insulation, also there were leaks. There were difficulties with the correct maintenance of supply and return lines. Losses in the distribution network was estimated at 12,4 %. Internal heating system was strongly amortized, with glider cast iron radiators. The required temperature could not be maintained in premises with a northern exposure. The lack of thermostatic room temperature control did not allow regulating the heat supply in the two branches of the installation – north and south. The windows were in poor condition – with deformed frames and unsealed. The fourth floor inhabited many years by another organization and after being released it was found that some of the windows have been left open for a long time. The Science laboratory (former gymnasium) was with switch heating off because of the many leakages. The following ECMs have been provided as a result of the energy audit, and then they were realized at the implementation of the project:

1.Thermal insulation of all outside walls: with 7 cm fibrane outside the walls.

2.Replacement of windows: with aluminum frames, interrupted thermal bridge and double glass package having 1 "K" glass.

3.Thermal insulation of the roof: for the main building - of the inside of the ceiling plate with 10 cm mineral wool and gypsum-paper wall, and for the two adjacent one-stored buildings - outside with 12 cm mineral wool.

4.Thermal insulation of the floor (oriel): from the outside with 7 cm fibran.

5.Replacement of the horizontal distribution network of the heating system (and removing them over level 0). Installation of three horizontal circles: one northern and two southern circles (for the ground floor and the other floors). Replacement of vertical pipes and radiators: with aluminum once. Installation of energy-efficient variable-speed pumps the boiler room.

6.Replacing the heat source – passing from central heating towards a condensing boiler of a new generation, operating on natural gas.

Data for areas of the surrounding constructions and their coefficients of overall heat transfer before and after implementation of the foreseen ECMs are presented in table 1.

Table 1

Building envelope element	Area, m^2	Coefficient of overall heat transfer, $W/(m^2.K)$		
		Before energy audit	Reference values	After implementation of ESMs
Walls	1799	1,65	0,35	0,34
Windows	1085	4,08	1,99	1,81
Ruff	1474	1,08	0,29	0,25
Floor	1474	0,54	0,39	0,33

The project was implemented from September 2011 until the end of April 2012. As a result of the project implementation today we have a beautiful and energy efficient building with a modern heating system. This heating system is also used for the training of students.

4. RESULTS AND DISCUSSION:

Two full heating seasons have passed after implementing the ECMs. The data from invoices for heating of Block 4 for three consecutive years before the project implementation (2009, 2010 и 2011), as well as for November and December of 2012, for the whole 2013, and for January, February and March of 2014 in the natural and financial terms were collected and processed. These data are presented in Table 2. Heat consumption during the project implementation (from September 2011 to April 2012) is not subject to this study.

Table 2

Year	Months	I	II	III	IV	Total for I, II, III and IVmonths	X	XI	XII	Total for X, XI and XIImonths	Total for the year
2014	thousants nm^3	3,113	2,400	0,858	-	6,371					
	MWh	28,95	22,327	7,98	-	59,257					
	BGN	3242,92	2492,79	893,07	-	6628,78					
2013	thousants nm^3	3,015	2,711	0,926	0,048	6,70	-	0,912	2,243	3,155	9,855
	MWh	28,05	25,220	8,61	0,446	62,33	-	8,48	20,86	29,34	91,68
	BGN	3138,19	2821,76	963,85	48,49	6972,29		920,32	2263,44	3183,76	10156,05
2012	thousants nm^3	-	-	-	-	-	-	0,834	2,287	3,121	
	MWh	-	-	-	-	-	-	7,75	21,27	29,02	
	BGN	-	-	-	-	-	-	940,01	2578,45	3518,46	
2011	MWh	66,12	77,49	60,69	-	204,30	-	-	-	-	
	BGN	6587,74	7720,02	6046,89	-	20354,65	-	-	-	-	
2010	MWh	57,81	77,45	56,25	-	191,51	-	-	42,90	42,90	234,41
	BGN	5161	6914	4933,34	-	17008,34	-	-	4509,14	4509,14	21517,48
2009	MWh	44,02	57,60	48,33	-	149,95	-	32,17	46,83	79,54	229,49
	BGN	4549,27	6091,72	5006,16	-	15647,15	-	2694,36	3893,71	6588,07	22235,22

The results from Table 2 are shown graphically in fig. 1 (in natural form).

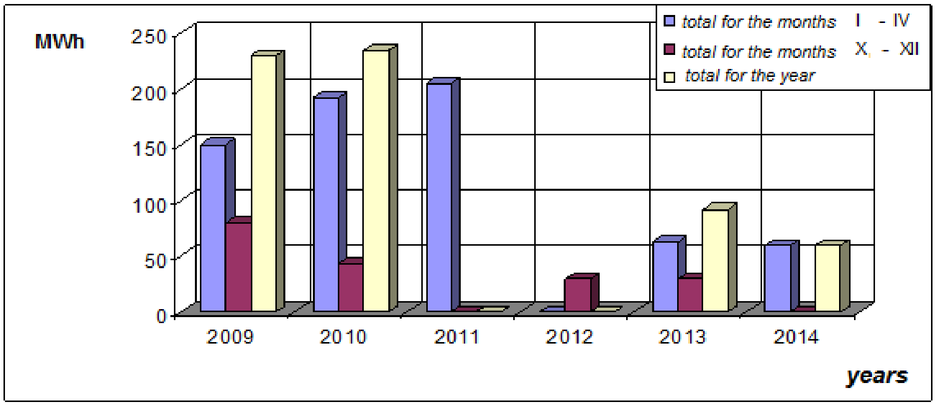

Fig. 1 Energy consumption for heating (in MWh) of Block 4 for 2009, 2010, 2011 г, and for the heating seasons 2012/2013 and 2013/2014

The results of Table 1 show that the total consumption of thermal energy for heating of Block 4 for I, II, III and IV months of 2009 year is е 149,95 MWh, respectively for 2010 year – 191,51 MWh and for 2011 year – 207,30 MWh. The average value of this three years for the same months is 182,92 MWh. The monthly consumption of thermal energy for heating in total during I, II, III and IV months of 2013 is 62,33 MWh, respectively for 2014 year – 59,257 MWh. The average value of these two years for the same months is 60,793 MWh. The decrease in the heat energy consumed for heating after the implementation of ECMs is 66,76%. Similarly the total consumption of thermal energy for heating during the XI and XII months of 2009 year is 79,54 MWh, respectively for 2010 year – 42,9 MWh (there was no heating in November 2010 year) and the average value of these 2 years – 62,22 MWh. The consumption of thermal energy for heating in total for XI and XII months of 2012 is 29,02 MWh, respectively for 2013 year – 29,34 MWh, and the average consumption of these two years for the same months is 29,18 MWh. The decrease in the heat energy consumed for heating after the ECMs is 52, 34%.

Reduction in the annual consumption of heating energy in 2013 compared to 2009 is 60,05%, and toward 2010 – 60, 88%.

It should be noted that for the period 2009 – 2011 years the University of Food Technologies has larger winter holidays, as follows: in 2009 year – 15 days, in 2010 year – 14 days and in 2011 year - 13 days and there was no consumption of heat energy for the building during this periods. There was no such a large winter holidays during the heating seasons 2012/2013, and 2013/2014. Therefore, for fair comparison it is necessary to increase the consumption of heat energy for the heating period 2009 – 2011 with the inevitable heat consumption of these non-operating periods. Thus the share of saved energy for space heating after the implementation of energy saving measures will increase really more.

In order to avoid uncertainty in the interpretation of data from invoices the data for consumption of heating energy referred to the heating degree days (DD) for the same heating period are presented in table 3.

Table 3

Year	Heat Energy, MWh	Degree Days, DD	Heat Energy per 1 Degree Day, MWh/DD
2009	229,49	1765	0,130023
2010	234,41	1513	0,154931
2013	91,22	1993	0,04577

Energy consumption for heating in 2009 is 229,49 MWh, the degree days - 1765, and the specific energy consumption - 0,130 MWh/DD. Similarly at 1513 degree days for 2010 the energy consumption is 234, 41 MWh, and the specific energy consumption - 0,155 MWh/DD.

These data compared to the figures from 2013 (specific energy consumption - 0,04577 MWh/DD) show a real decrease of energy consumption (the impact of the climate change has been avoided by heating degree days) after the implementation of the ECMs with 64.8% compared to 2009 year and with 70,46% compared to 2010 year.

This means that 37,568 tons harmful emissions of $CO_{2,}$ emitted into the atmosphere have been saved compared to 2009 year and respectively 38,905 tons CO_2 have been saved compared to 2010 year.

5. CONCLUSION:

1. University of Food Technologies in Plovdiv develops wins and implements the project **"**Energy efficiency, improving access for people with disabilities at the University of Food Technologies - Plovdiv and modernization of information services**",** BG161PO001/1.1-07/2009/010, as the prescribed energy saving measures have been implemented.

2. As a result of implemented according to the project energy saving measures in Block 4 the consumption of heat energy has been reduced really with 67,88%, compared to the average heat consumption for 2009 and 2010. And the saved emissions of CO_2, emitted in the environment are in average 38, 24 tons yearly.

References:

1. Valtchev, G. Energy Efficiency and Protection of the Environment. Scientific Conference 2010, University in Town of Chanak Kale, Turkey, 2010.
2. Valtchev, G., N. Kalojanov, M. Minchev, V. Rasheva, S. Tasheva. Analysis of the Potential of Energy Consumption in Student Hostel "Maritza 3" of University of Food Technologies – Plovdiv, Scientific Conference with International Participation «Food Science, Equipment and Technologies» UFT – Plovdiv, 2010, p.p. 509-514.
3. Valtchev, G., N. Kalojanov, V. Rasheva, M. Minchev, S. Tasheva. Study of Energy Efficiency of Educational Buildings of University of Food Technologies – Plovdiv, Scientific Conference with International Participation «Food Science, Equipment and Technologies» UFT – Plovdiv, 2010, p.p. 499-508.
4. Kalojanov, N., G. Hristov and others. Analysis of the Alternative Possibilities for Energy Saving in 142 Secondary School "St. Methodij" – Sofia. TU – Sofia, Proceedings of Scientific Conference with International Participation EMF'2000, Volume II, 25 – 28 June, 2000, Varna, p.p. 15 – 23.
5. Kalojanov, N. and others. Utilization of Geothermal Water for Heating of Administrative Buildings in Town of Kyustendil. TU – София, Proceedings of Scientific Conference with International Participation EMF'2002, Volume II, 18 – 20 септември, 2002, Varna, p.p. 84 – 92.
6. Kalojanov, N., V. Sharankov and others. Guide for Energy Efficiency Audit and Certification of Buildings. TU – Sofia, 2006.

[1]University of Food Technologies - Plovdiv
Bulgaria, 4000, Plovdiv, 26, Maritza Blvd; Tel. (032) 603 699; Fax (032) 44 01 02,
Assoc. Prof. PhD, Eng. Violeta Dimitrova Rasheva - E-mail: v_rasheva@abv.bg
Assoc. Prof. PhD, Eng. Stanislava Tzankova Tasheva - E-mail: st_tasheva@abv.bg
Assoc. Prof. PhD, Eng. Mincho Stojanov Minchev - E-mail: minchev_m@abv.bg
Prof. PhD, Eng. Georgi Ivanov Valtchev – Rector, E-mail: g_valtchev@abv.bg;

[2]Technical University of Sofia
Prof. PhD, Eng. Nikola Georgiev Kalojanov – E-mail: ngk@tu-sofia.bg

CHARACTERIZATION OF RAINFALL WITH RAINFALL INDICES IN THE CITY OF BUCHAREST IN (2009-2012)

Carmen Otilia Rusănescu
Polytechnic University of Bucharest of Romania, Faculty of Biotechnical Systems Engineering; Splaiul Independentei, no.313, District 6, Bucharest, Romania

ABSTRACT

In this paper is analyzed rainfall regime with rainfall indices: the Martonne precipitation index is calculated Lang, Mayr tetratherm is plotted as an arithmetic average of the warmest four months in a row. We calculated the eco-climatic indices for the city of Bucharest, a city with a lot of vegetation, parks, and green spaces to highlight issues tend aridity of the region. According to the data processed, the city of Bucharest has a temperate continental climate. Specific four seasons, winter, spring, summer and autumn. Bucharest winters are very mild with little snow and relatively high temperature, while in recent years are very hot summers, very hot with little precipitation. Rainfall was recorded by the weather station.

1. INTRODUCTION

Bucharest City is located in south-eastern Romania, between Ploiesti at north and Giurgiu at south . The city is in Vlasiei Plain, which is part of the Romanian Plain. To the east lies Baraganul , in the western part lies Burdea Găvanu Plain and in south it is bordered by Burnazului Plain .[8]

Bucharest is a city of lowland flora and fauna temperate continental climate, steppe grass. The climate and topography of the surroundings of Bucharest are very suitable for agriculture. Growing grain, vegetables and fruit trees. In addition a number of plants growing wild, damaging crops and which man tries to destroy them (weeds). The forests grow a wide variety of fungi, ferns and moss. [8].

Rainfall is one of the most important features of the climate, which largely reflects the geographical landscape and agricultural economy of a region. On average, precipitation falls within Bucharest in 120 days / year.

Ecometrici climatic indices are formulas for climatic suitability, taking into account the actual values of key climatic factors. Classification and calculation of indices arid climates, rainfall are issues that have concerned some of the most prominent climate scientists of the twentieth century (the Martonne, Thornthwaite, Gaussen). In order to find a generally applicable mathematical expressions of ecological valence of a site arose a series of formulas and tables for interpretation, some based on climatic factors, others on the biogeography [5].

Drought is a complex natural phenomenon caused by climate variability and elements that can turn into factor climate risk by exceeding tolerance limits of natural systems [1].

And other authors have studied their works rainfall in different regions of the world [6, 9].

2. METHODOLOGY

Based on data recorded by the weather station 24 hours out of 24, we performed statistical analysis, and calculated the tetratherm Mayr knowing the temperatures in the months V, VI, VII, VIII.

Mayr tetratherm (T_M) represents the arithmetic mean of the temperatures registered in May, June, July, and August [7].

$$T_M = \frac{t_V + t_{VI} + t_{VII} + t_{VIII}}{4} \quad (1)$$

Mayr tetratherm is the arithmetic average of the mathematical expression corresponding to the warmer temperatures four consecutive months overlapping period of maximum biological activity.

Values Mayr tetratherm reveal restrictive climate for certain configurations of a complex plant (by continentalism, altitude, exhibition etc.)

Using real data, we calculated the following Mayr tetratherm for the weather station from Biotechnical Systems Engineering Faculty of Bucharest.

All values calculated indicates that in Bucharest in the maximum biological activity (May, June, July, August) are registered optimum temperature for plant growth (herbaceous steppe), but at the same time, these values are some indicators regarding the type of vegetation that grows predominantly in Bucharest, namely forest vegetation type. There are forests at Baneasa, Tunari, Andronache, Cernica, Snagov forest, Bufteanca, Vlasia Pascani Bigiara, Surlari, Nuca, Ciolpani , Caldarusani, Cocioc, Cioglia,Pasarea, Pustnicu, Mogosoaia, Rosu. Existing forests are composed of a mixture of different species of hardwood: Quercus robur, Carpinus betulus, Tilia argentea, Quercus cerris, Quercus frainetto etc. Forest trees around the capital are represented by Horn (Cornus mas), Sanger (Cornus sanguinea), elder (Sambucus nigra), gherghinar (Crataegus monogyna), blackthorn (Prunus spinosa), privet (Liqustum vulgare).

Herbaceous aquatic vegetation present in lacustrine complexes, forming associations of white and yellow water lilies, Frogs, algae and submerged. Shore vegetation deeper lakes, represented by thick reeds to 1 m [7].

$$T_{MayrBucharest\,2009} = \frac{19.4 + 22.9 + 25.4 + 24.6}{4} = 23.075\,[^0\mathrm{C}]$$

$$T_{MayrBucharest\,2010} = \frac{19.9 + 20.5 + 24.6 + 26.8}{4} = 22.95\,[^0\mathrm{C}]$$

$$T_{MayrBucharest\,2011} = \frac{17.7 + 22.5 + 24.9 + 24.5}{4} = 22.4\,[^0\mathrm{C}]$$

$$T_{MayrBucharest\,2012} = \frac{19.5 + 21.3 + 25 + 24.6}{4} = 22.6\,[^0\mathrm{C}]$$

Spatial variation tetratherm values is illustrated with a simple graph type line (figure 1). The values resulting from calculations are very close: 23.075 [^{0}C] in 2009, 22.95 [^{0}C] in 2010, 22.4 [^{0}C] in 2011, 22.6 [^{0}C] in 2012 and demonstrates us that we stand in a steppe.

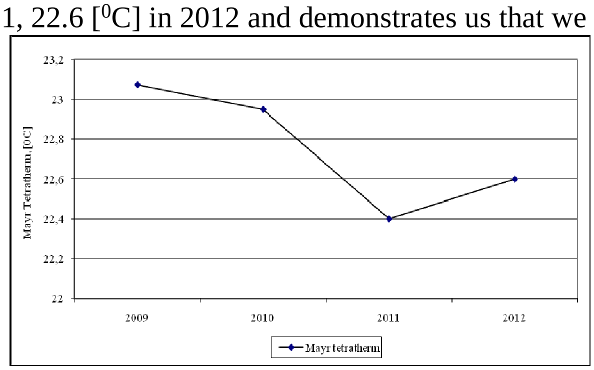

Figure 1: Mayr tetratherm values within the Bucharest in 2009, 2010, 2011 and 2012

We calculate the annual aridity index of Martonne. De Martonne aridity index eloquently emphasizes the features of the vegetal cover. Its mean annual value is relatively homogenous (Table 1).

$$I_a = \frac{P}{T+10} \tag{2}$$

P – the annual amount of precipitation
T – the mean annual temperature
10 – a coefficient that is added in order to obtain positive values
This index was firstly used by De Martonne [2]. It is used for emphasizing the restrictive character of the climate with regard to certain vegetal formations: values ≤5 correspond to desert areas, those close to 10 to the steppe areas, those above 30 indicate the forest steppe area, while the values ≥40 the forest areas [3,4]. Values between 30 and 40 indicate predominant forest vegetation. Values below 30 indicate the existence of conditions of formation of steppe.

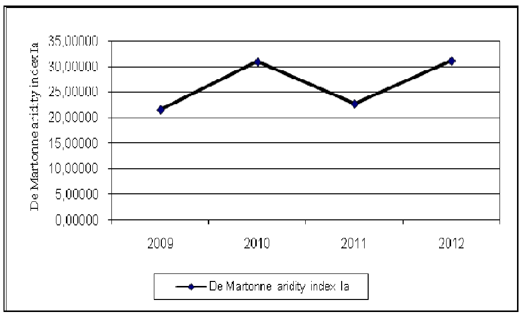

Figure 2: Annual aridity index variation within Bucharest in the years 2009, 2010, 2011, 2012

Based on calculations of index annual Martonne observe that Bucharest is semi-humid climate, all values being less than 31, steppe and steppe vegetation.

$$I_{a2009} = \frac{560}{15.99251+10} = 21.54467$$

$$I_{a2010} = \frac{713}{13.09113+10} = 30.87766$$

$$I_{a2011} = \frac{507.8}{12.36822+10} = 22.70185$$

$$I_{a2012} = \frac{722}{13.2452+10} = 31.06018$$

We calculate the index Lang rain Lang rain index, also called the pluviothermal index, indicates the atmospheric moisture degree, as well as its variation; it can be calculated at an annual, summer or vernal level [3,4]. It increases with the altitude up to the condensation level, as the precipitation amounts get bigger and the temperature lower.

$$L = \frac{P}{T} \tag{3}$$

P = precipitation (mm)
T = temperature (^{0}C)
0 <L <20 arid climate
20 <L <40 Mediterranean climate

40 <L <70 semiarid climate
70 <L <1000 humid climate
P – the annual precipitation amount
T– the mean annual temperature

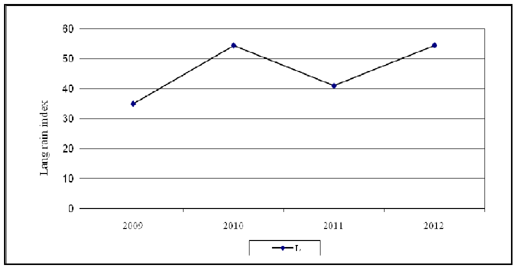

Figure 3: Lang rain index in 2009, 2010, 2011 and 2012 in Bucharest

20 <L <40 In 2009, the year the climate is Mediterranean
40 <L <70 years 2010, 2011, 2012 are years semiarid climates

3. CONCLUSIONS

According Mayr tetratherm observed that in Bucharest are registered optimum temperature for plant growth (herbaceous steppe), but at the same time, these values are some indicators regarding the predominant type of vegetation that grows in Bucharest, namely forest vegetation type. Based on calculations rainfall in this paper came off the Romanian capital city of Bucharest has a temperate continental climate. We calculated the index of aridity of Martonne and got the corresponding values of forest vegetation. Based on the index Lang noted that the city of Bucharest is a Mediterranean climate.

References

[1]Barbu I, Popa I., *Temperature and precipitation regime in 2003 in the Romanian forests* Magazine forests, 4; 2004
[2]De Martonne E., *Une nouvelle fonction climatologique: L'indice d'aridité*, La Meteorologie, 449-458; 1926
[3]Dumitraşcu M., *Changes in the landscape Oltenia plain*, Romanian Academy Publishing House, Bucharest; 2006
[4] Gaceu O., *Elements of practice climatology*, University of Oradea 2002
[5] Minea I, Stângă IC., *Analysis of spatial variability of indices for assesing drought risks and disasters*, Volume III :138-149 Book House Science, Cluj Napoca, ISSN 1584-5273; 2004
[6]Ghermec O., Ghermec C., Dubovan S., Rusănescu C.O. *Improving the environmental performances of iron powders carburizing process in a methane-bearing atmosphere*; Environmental Engineering and Management Journal October 2013, Vol.12, No. 10, 2019-2023
[7]Stănescu SV, Gavriloaie C. *Aspects of the vegetation and fauna Colentina river route from Bucharest Romanian* Ecoterra 27 ; 2011
[8]Vlăduţ A., *Ecoclimatic indexes within the Oltenia plain* Forum geographically. Studies and research in geography and environmental protection 9 : 49-56 49; 2010
[9]Vasilica M, Capsa D, Covaci I, Nedeff V, Bârsan N, Panainte M, *A case study on heavy rainfall in the central-southern Moldavia region, Romania,* Environmental Engineering and Management Journal December , Vol.11, No.12, 2151-2158; 2012

LAGOON SYSTEMS FOR EXTENSIVE WASTEWATER TREATMENT PLANTS FROM THE RURAL AGGLOMERATIONS

Victor-Viorel Safta [1], Mirela Dincă [1], Gabriel-Alexandru Constantin [1], Adrian Boureci[2]
[1]University POLITEHNICA of Bucharest, Department of BIOTECHNICAL SYSTEMS
[2] Captain Nicolae Pleşoianu High School of Râmnicu Vâlcea

ABSTRACT

Taking into account that implementation in the rural area of sewage systems and wastewater treatment in classic form, involves considerable investments, there are presented as particularly attractive alternatives, viable and significantly cheaper, both in construction and in operation, the use of modern and efficient sewage solutions and the use of *extensive wastewater treatment plants.*

In the present paper there are presented the construction, operation, the characteristics and performances of some extensive wastewater treatment plants with *lagoons systems*.

1. INTRODUCTION

Extensive treatment processes are wastewater treatment processes which are very close to the natural processes of water purification (self-purification processes) where the main role is played by microorganisms (bacteria). Naturally, into the contaminated water there are microscopic algae which use solar energy to produce the required oxygen by photosynthesis necessary to the bacterial cultures which are found dispersed or fixed on different supports in the water subjected to the process, to achieve the purification of water by a biological process. Therefore, the extensive treatment processes present the great advantage that the vast majority of them, don't need external input of energy for carrying out wastewater treatment processes, making it very economical in use. Also, the extensive wastewater treatment plants have the advantage of very high efficiency to remove the organic loads and the nutrients from water that is subjected of treatmnent providing high quality effluent, that can be discharge without danger to natural watercourses. Another advantage of the the extensive wastewater treatment plants is that they have a very natural appearance (not like an industrial plant), fit perfectly into the natural landscape, without affecting this one at all.

It is to be noted that extensive wastewater treatment plants have been developed in different European countries (France, Germany, Spain, Netherlands, and so on) usually for serving small communities with a population of around 500 equivalent inhabitants [1,2].

In the present paper are presented the construction, operation, the characteristics and performances of some extensive wastewater treatment plants with *lagoons systems*. For this purpose will be analyzed the most common types of lagoons systems, namely: *stabilisation ponds systems (mycrophyte lagoons systems)* and *aerated lagoons systems.*

Will be given representative exemples of extensive wastewater treatment plants with lagoon systems from the country and the world, highlighting the constructive features and the performances obtained.

2. OPERATING PRINCIPLES, CONSTRUCTION AND PERFORMANCE OF LAGOONS SYSTEMS

Generally, lagoons are extensive installations where the wastewater subjected to treatment is purified (treated) of the organic pollutant load by the biological activity of the bacterial culture, essentially an aerobic type, which are dispersed in the water. The oxygen required for aerobic fermentation process may be available, depending on the circumstances, from natural or artificial sources, the aeration mode giving the extensive installation type designation, which may be with *natural or aerated lagoons.*

2.1. Stabilisation ponds systems (natural lagoons systems)

Extensive natural lagoon systems (also called stabilization ponds) are lagoons systems in which two populations of micro-organisms proliferate interdependent, namely: aerobic bacteria and planktonic algae, the latter being called "mycrophyte". The oxygen required for the developing and maintaining the aerobic bacteria biomass is produced naturally through photosynthesis by algae biomass that develops in the layer of water from lagoon in the vicinity of the free surface (mirror) of water, which it is exposed to the solar radiation (light) (see the scheme in Figure 1).

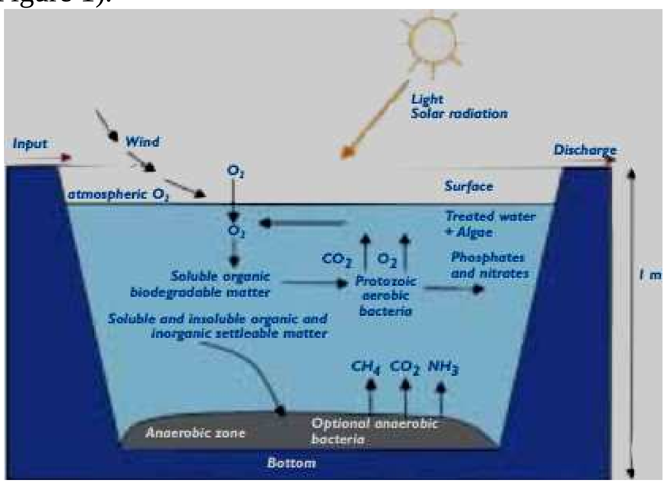

Figure 1: The biological process scheme from inside a natural lagoon, [2]

By means of its metabolism, aerobic bacteria decompose the organic matter from the waste water in which they are dispersed, which converts and synthesizes for their development, by removing significant amounts of carbon dioxide and water. The carbon dioxide produced by the aerobic bacteria, as well as the mineral salts contained in wastewater subjected to the process, allow the planktonic algae to multiply and develop.

This biological process is self-maintained as long as the system receives solar energy and organic matter through the wastewater influent. It should be noted that in the lagoon bottom, in the vicinity of their bottom, where sunlight does not penetrate, is developing the anaerobic bacteria biomass that decompose the sedimented organic sludge. As a result of this process, anaerobic fermentation of organic matter, carbon dioxide and methane are released in the form of fermentation gas. This natural biological processes are carried out relatively slowly, and therefore, in order to obtain a satisfactory degree of purification of the water subjected to the process, it requires a high retention time.

Usually, the extensive systems with natural lagoons are formed from several lagoons (ponds) placed in series through which the water subject to treatment flows.

In practice, natural lagoon system configuration most commonly encountered is the one with 3 ponds. However, using configurations of systems with 4-6 ponds, besides getting a purity of the effluent, is also achieved an effluent disinfection.

In these systems, the roles of each of the different ponds are: first pond provides, above all, a significant reduction of the organic load of the waste water; the second pond ensure the removal of nitrogen and phosphorus (nutrients); the third pond refines the wastewater treatment and makes the system reliable, in case of failures occurred in the first two tanks or during the maintenance of the system.

The performances obtained by wastewater treatment plants with natural lagoons are the following: reduction of more than 75% of the organic matter load in the effluent, calculated on the basis of the influent pollutant loading values, which corresponds to a filtered COD concentration of 125 mg/l; the concentrations in total nitrogen at the discharge level are very low in the summer, but can reach several dozen mg/l (expressed in N) in the winter; the reduction in phosphorus is noticeable over the first few years (> 60%), then dwindles down to zero after about 20 years; the natural lagoon effluent disinfection is important, especially in summer (reduction in microbial load over 10000).

The main advantages of using extensive treatment systems with natural lagoons are: a supply of energy is not necessary if exists a difference in level favorable to the gravitational movement of the water in the system; the natural lagoons systems operating is simple, on the condition that maintaining general cleaning; it eliminates a large part of nutrient pollution (nitrogen and phosphorus), especially in summer; it provides a very good elimination of pathogenic organisms in summer (4-5 logs) and good removal in winter (3 logs); constructions and installations necessary for the establishment of the natural lagoon systems are not very complex engineering required to achieve them remaining simple; it integrates well into the landscape; absence of noise pollution; sludge from cleaning is well stabilised (except that from at the head of the first basin) and is easy to spread on agricultural land.

2.2. Aerated lagoons

The extensive aerated lagoons systems are lagoons systems in which the oxygen required for the development and maintenance of the aerobic bacteria biomass, taken up from the air, is introduced by means of mechanical surface aerators or pneumatic insufflation systems.

It should be noted that for aerated lagoons systems is needed the energy supply for conducting the working process, the energy consumption being similar to the intensive plants with activated sludge aeration basins, with values in the range of 1.8 - 2 kW / kg BOD5 removed. The major mechanisms that realize the working process in the aerated lagoons are the following:

- *the aeration* required to produce and conduct the aerobic fermentation process, where the water to be treated comes in contact with the aerobic micro-organisms (bacteria and fungal species similar to those present in activated sludge instalations), that consume and assimilate the pollutant loading of organic matter and the nutrients from water;
- *the settling*: suspended solids, that are found in the water subjected to the treatment process in the form of groups of microorganisms, fermentation products and solid particles embedded, with density higher than that of water, are settled forming a biological sludge.

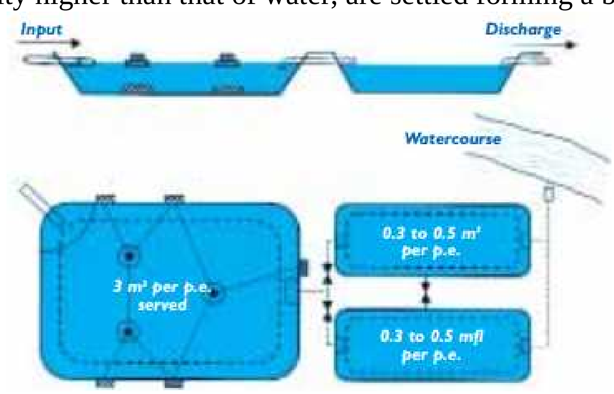

Figure 2: Aerated lagoons extensive systems (principle and dimensioning schemes), [2]

The performances obtained by wastewater treatment plants with aerated lagoons are the following:

- ensure a good quality of the effluent from the point of view of the organic load (a reduction by more than 80% of the BOD);

- for nutrients, removal is limited to bacterial assimilation and remains around 25-30%; this performance can be improved by the use of physical and chemical additives to eliminate the orthophosphates.

The main advantages of using extensive treatment systems with aerated lagoons are the large variation in hydraulic loading to the influents; influents with extremely high pollution loads; uneven dispersion of active bacterial biomass in water leading to obtaining some effluents with variable nutrient content; influents obtained from mixing wastewaters, easily biodegradable, with wastewaters from industrial discharges, [2].

3. REPRESENTATIVE EXAMPLES OF LAGOONS SYSTEMS

3.1. Stabilization ponds systems (natural lagoons)

Waste stabilization ponds are one of the main natural wastewater treatment methods. Further, there are presented representative examples of stabilization ponds systems (natural lagoons), used in different countries.

The governments of Tanzania in collaboration with the World Bank, through Urban Sector Rehabilitation Project (USRP), expanded and rehabilitated the network and constructed wastewater treatment plant known as waste stabilization ponds. Currently there are 2080 customers who are connected to this sewerage network, which can be seen in figure 3.

Figure 4 shows a waste stabilization pond system at Ginebra in southwest of Colombia (population is around 9.000 and wastewater flow is about 27 l/s). The resulted effluent is used for the irrigation of sugar cane.

Figure 3: Construction of waste stabilization ponds in Tanzania, [3]

Figure 4: Waste stabilization ponds in Colombia (a) and Embankment protection with stone (b), [4]

In figure 5 is presented another example of stabilization pond from Fortaleza, norteast of Brazil. In this case, the influent flow is about 10.000 m^3/day and around half the flow is from local textile factories.

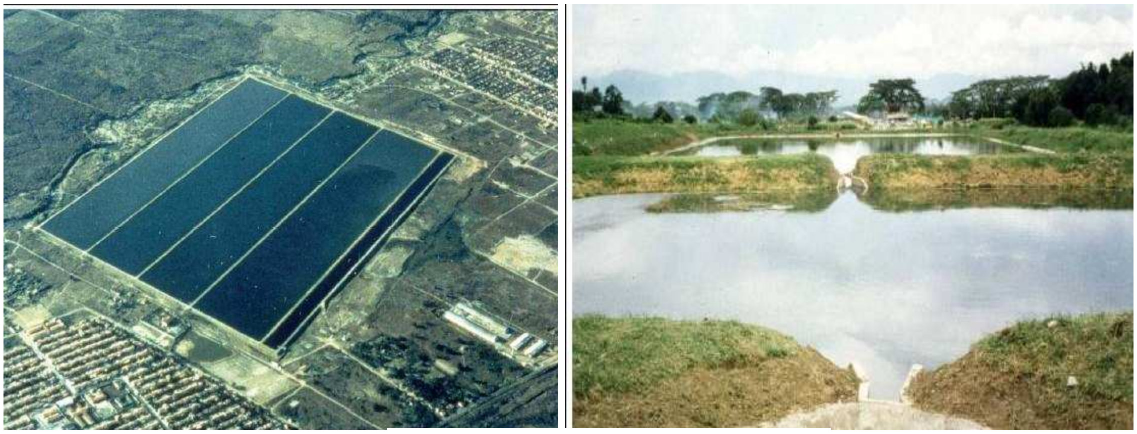

Figure 5: Waste stabilization ponds in Brazil, [4]

3.2. Aerated lagoons for the treatment of municipal wastewater

Up to now several new methods of wastewater treatment in rural districts have been applied. The oldest and easiest type of wastewater treatment plants are sedimentation and oxidation lagoons, also referred to as “oxidation ponds”, “anaerobic ponds” or “naturally aerated ponds” respectively.

A treatment plant for domestic wastewater should consist of a fine screen, two aerated lagoons in series and at least one polishing lagoon. Aerated lagoons for municipal wastewater are designed according to the volume load and the retention time.

Further, there are presented representative examples of aerated lagoons for the treatment of municipal wastewater, used in Europe.

In figures 6 and 7 there are presented aerated lagoons used in Germany, [5].

In the figure 6 there are 2 aerated lagoons, 2 polishing lagoons and the inlet zone is equipped with scum baffle and walkway made of concrete.

Figure 6: The construction of an aerated lagoon in Germany, [5]

In figure 7 is presented an example with 2 aerated lagoons, 1 polishing lagoon and the inlet zone with scum baffle and walkway made of wood.

Figure 7: Aerated lagoon, Germany, [5]

Figure 8: Aerial view of the aerated lagoon system, Veazie, United States, [6]

4. CONCLUSIONS

In the present paper there was presented aspects regarding the construction, operation and the characteristics and performances of some extensive wastewater treatment plants with lagoon systems, namely stabilization ponds (natural lagoons) and aerated lagoons.

Using the extensive wastewater treatment plants with lagoon systems represent one of the most practical and inexpensive method that is widely adopted in many countries around the world. This, has proved to be an effective method in the removal of suspended and dissolved organic substances and nutrients up to 80%.

References

[1] Safta, V.V., *Procedee extensive de epurare a apelor uzate,* Note de curs la disciplina Dezvoltare rurală durabilă şi protecţia mediului (Facultatea Ingineria Sistemelor Biotehnice, licenţă anul IV, Specializarea Dezvoltare rurală durabilă) - anul universitar 2013-2014.

[2] *******Guide, *Extensive Wastewater Treatment Processes - adapted to small and medium sized communities (500 to 5000 population equivalents),* Office of official publications of the European Community, Luxembourg , 2001.

[3] http://www.muwsa.or.tz/index.php/sewerage_services/category/sewerage-general-info.

[4] http://web.deu.edu.tr/atiksu/ana52/ani4044-7.html – stabilization ponds.

[5] FUCHS Enprotec GmbH, *Aerated lagoons for the treatment of municipal wastewater,* Germany, www.fuchs-germany.com.

[6] http://web.deu.edu.tr/atiksu/ana52/ani4044-13.html.

HACCP APPROACH TO PASTRY PRODUCTS

Assoc.Prof.dr.eng. Gabriela-Cristina SIMION [1], lecturer dr.eng. Mihaela Florentina DUȚU[2]
Biotechnique Systems Departament, University Politehnica of Bucharest

ABSTRACT

HACCP (Hazard Analysis and Critical Control Point) is a method that enables a company to prevent food contamination throughout the technological process , beginning with raw materials and ending with the reception of the final product .This preventive approach to food control is applied at all stages of food industrial processes. The case study, the production of the pie sheet analyzes the risks that occur in the production chain. Hazards can be prevented by following the established procedure of control step by step. It is important a decision tree analysis which will include: respect for hygiene, sanitation compliance program, compliance with good practice and compliance with product handling prescriptions working.

1. INTRODUCTION

HACCP (Hazard Analysis and Critical Control Point) is a method that enables a company to prevent food contamination throughout the technological process, beginning with raw materials and ending with the reception of the final product. We are interested in identifying and controlling hazards in food transmitting the disease to humans. HACCP test steps are:

• Identification of potential contaminants (random potential);
• Assessment of hazards significance (analysis);
• Determining Critical Control Points (CCP);
• Determining appropriate control measures;
• Setting standards and critical limits for each CCP;
• Monitoring the production process;
• Determining appropriate corrective actions;
• Setting appropriate documents, records and procedures for verifying the effectiveness of the HACCP control.

The case study ,the production of the pie sheet analyzes the risks that occur in the production chain (reception of raw materials, storage of raw materials, dosing of raw materials, mixing, dough relaxation, manual portioning and food extruder; extrusion; transport tape dough; distribution starch; tape collection dough; timing sheets of dough, packaging, freezing, storage, delivery).

Risks involved in the manufacture of sheets of pie are different:

-chemical hazards , such as raw material specific hazards, excessive humidity that fosters the growth of mycotoxin content in, the possibility of contamination with disinfectants and pest control, overdose, contamination with cleaning agents, disinfectants contamination during storage;

-physical risks, such as the presence of foreign objects (metal, glass, wood, masonry, plastic), pests (rodents, insects) contamination of disinfectants;

[1] Splaiul Independenței, nr.313, corp D, sector 2, București, telefon 021.402.9637, gacsimion@gmail.com
[2]Splaiul Independenței, nr.313, corp D, sector 2, București, telefon 021.402.9637, dutumihaelaflorentina@gmail.com

-biological hazards , such as increased temperatures and relative humidity contribution to the generation and growth of microorganisms; infected with Escherichia coli, Salmonella, Staphylococcus, the presence of pests, reception of raw materials.

The increase in temperature and the relative humidity above the permissible limits favors the growth of microorganisms.

Hazards can be prevented by following the established procedure of control step by step. It is important a decision tree analysis which will include: respect for hygiene, sanitation compliance program, compliance with good practice and compliance with product handling prescriptions working.

Establish critical limits for control and care for pie sheets case study is based on analysis of the product manufacturing process steps bakery.

2. HACCP METHOD

Submitting the necessary documentation is in compliance with HACCP seven principles of HACCP stated below:

Principle 1. Hazard assessment associated with used raw materials and ingredients, processing, handling, storage, distribution and consumption of food is addressed by conducting a systemic analysis of all food products manufactured and the ingredients used in their manufacture. The purpose of the analysis is the hazard identification of pathogenic microorganisms in food, parasites, chemicals or foreign bodies that may affect consumer health.

Hazard assessment is carried out in two stages:

• evaluating the type of product depending on its risks;

• hazard assessment according to their degree of severity.

Product inclusion in a specific category of endangered note the following details:

• the product contains sensitive ingredients;

• containing manufacturing stage it is possible to effectively destroy dangerous microorganisms or other risks identified;

• danger of contamination of the product after manufacture;

• danger of improper handling during transport, sale and preparation of food , transforming into a dangerous product for consumption;

• the product is longer apply heat treatment after packaging.

Each hazard found falls into a category of danger.

Principle 2. Determination of critical points which can control the risks are addressed by identifying processes points in the loss or lack of control could result in endangering consumer health. These points are identified with particular care in all phases of processes deployed in production of the manufacturing.

Principle 3. Establish critical limits that must be observed in each critical control point is addressed by establishing one or more critical limits for each critical control point identified. The criteria that were used to establish critical limits are choosing measurable parameters (temperature, humidity, etc.).

Principle 4. Setting of monitoring procedures at critical control points CCP is addressed by the fact that the monitoring of critical control points must be achieved by means and rapid methods to be permanently secured to provide timely information . Also keep in mind that the actual monitoring results must be well documented and interpreted correctly.

Principle 5. Establish corrective actions to be applied when the monitoring of critical control points is detected a deviation from critical limits. Corrective actions are agreed with the competent decision.

Principle 6. Establish an efficient system of keeping records is considering the need for records to establish appropriate corrective measures. Retrieving records necessary to establish traceability and availability for inspection bodies for this purpose is implemented integrated with ISO 9001.

Principle 7 - Establish procedures to verify that the HACCP system is working correctly through the need to demonstrate that all risks are identified and controlled. Verification methods are based on microbiological, physical, chemical and sensory actions.

3. CRITICAL CONTROL LIMITS

Hazards can be prevented by following the procedure beginning with received raw materials. It provides a decision tree analysis which will include: respect for hygiene, sanitation compliance program, compliance with good practice and compliance with product handling prescriptions working.

Establish critical limits for control and care for pie sheets case study is based on analysis of the product manufacturing steps.

Manufacturing type critical limit risk is very important for monitoring procedures corrective measures

1. Reception of raw materials:

- The presence of foreign bodies or pests
- The presence of pathogenic microorganisms
- Maxim and tolerance: according to current regulations
- Inspection of incoming raw materials.
- Tracking analysis reports.
- Not receiving products whose packaging is damaged.
- Unloading and handling of raw materials will be made according to procedures.
- Rejecting the reception of raw materials accompanied the report of damages.
- Document monitoring reception.

2. Storage of raw materials

- Storage flour
- Increasing temperature and humidity favor the development of fungi and pests specific flour
- temperature: 200C target value limits admitted -5, +50 C
- Humidity: 70 % target value limits admitted: -5 , +5 %
- Damage to packaging
- Temperature measurement by thermometry and humidity with hygrometer inspection. Ventilation or air conditioning of storage space.
- Eliminating the causes.
- Monitoring sheet.

3. Mixing

- Temperature rise above the permissible limit favors the growth of microorganisms
- Target Value 180C
- Permissible limits: -2, +20 C
- Temperature measurement by thermometry.
- Check the temperature of the ingredients and adding water and ice flakes.
- CCP monitoring sheet

4. Divide dough and food extruder

- Physical presence of foreign bodies
- Target Value: absent
- Inspection Monitoring.

5. Dough extruder, dough formation and tape transport, dispersion starch dough physically present collection of foreign bodies.

- Target Value: absent
- Inspection Monitoring and eliminating causes.

6. Shaping dough

- Physical presence of foreign bodies
- Target Value: absent Inspection.
- Monitoring data deletion causes.

7. Making pies

- Physical presence of foreign bodies
- Target Value: absent
- Inspection Monitoring
- Data Deletion causes.

8. Packing

- Physical presence of foreign bodies
- Target Value: absent Inspection Monitoring Data Deletion causes.

9. Freezing

Bacteriological product conservation.

- Deep freeze quickly.
- The target: the core product - 180C
- Permissible limits: -3, +30 C
- Temperature measurement by thermometry.
- Time prolonged freezing.
- Checking frigorific unit. CCP monitoring sheet.

10. Biological conservation stockpiles above the target temperature.

- Target Value: - 180C
- Permissible limits: -3, +30 C temperature measurement by thermometry.
- Checking frigorific unit. CCP monitoring sheet.

11. Delivery of finished products.

- Physical damage to the pack by improper handling.
- Inspection and removal causes

3. CONCLUSIONS

Implementation of Hazard Analysis and Critical Control Points System in Bread Industry become effective when its principles are correctly and broadly applied in all stages of the production. Implementation of Hazard Analysis and Critical Control Points System in the food industry has an important impact on safety food products and the environment protection, especially on utilities using.

In terms of the food industry, two other factors should also be included: the need to ensure food safety and the need to protect consumers' health. Therefore, the existence of a system that ensures food safety is crucial to preserve a company's image and reputation and to increase local and international market shares.

References

[1] Cãtoiu I.,Teodorescu N ., *Comportamentul consumatorului*, Editura Uranus, Bucuresti 2003.

[2] Albu A.,*introducerea controlului managerial pe baza sistemului HACCP în unitãtile alimentare din România*, Editura Sagitarius, Bucuresti, 1998.

[3] World Health Organization. Food safety and food borne illness.

[4] http://www.who.int/ foodsafety/foodborne_disease/in/ . 2007

STUDY ON THE SPECIFIC ENERGY CONSUMPTION FOR DRYING BLUEBERRIES IN CONVECTIVE SOLAR DRYER

Dimitar Stoev, Atanas Tashev, Nikolay Penov
UFT-Plovdiv, Bulgaria

ABSTRACT

A full factorial drying experiment of blueberries in convective dryer with air solar collector was conducted. The influence of three factors - temperature of the drying agent, rate frequency of air recirculation and loading of the drying chamber on the specific energy consumption was investigated. To perform the experiments an additional energy source simulating solar radiation was used. The obtained experimental results are presented in tabular and graphic form. A regression equation describing the influence of these factors on the response function is also presented.

1. INTRODUCTION

Solar energy is a renewable energy that is practically inexhaustible. Its potential in Bulgaria is significant, although there are differences in the intensity of solar radiation by regions [4]. To achieve the economic importance of the use of solar energy is necessary to develop technologies and equipment, ensuring its efficient conversion into another form of energy according to the needs of the consumers. One of the most energy-intensive processes in the food industry is the drying process.

Bilberry (*Vaccinium myrtillus* L.) is one of the most important wild berry species in Europe and is widespread in Bulgaria occurring in the semi-mountain regions at 1200–1500 meters of altitude. Their bioactive components have received considerable interest due to their health-promoting effects such as antioxidant, antimutagenic, antiinflammatory, antiproliferative and antimicrobial activities [1]. Besides the issue of seasonal availability, fresh wild berries generally have a short shelf life and they are processed into various products. Drying is one of the most common methods employed to extend the availability of berries out of season.

Purpose of the work

The aim of this work is the experimental determination of the specific energy consumption for drying blueberries at various regime parameters in convective solar dryer. These results are important for future design of solar convective dryers with air solar collector built into the roof construction.

2. METHODOLOGY

Frozen bilberry (*Vaccinium myrtillus* L.) fruits were obtained from Ekovita Ltd. (Pazardjik, Bulgaria). After thawing and rinsing with water, the bilberries were dried using a pilot scale solar convective dryer (Figure 1). Final moisture content of the dried bilberries was 7–10%. Experiments were conducted with electric power only in order to accurately measure the specific energy consumption for drying. To measure the amount of electricity a digital meter for electrical quantities Reichelt company - Germany with a basic error ± 0,01 % has been used. Temperature control in the drying chamber is done by controller TC 800 Comeco company, managing electric heaters. The device has a basic error ± 0,4%.

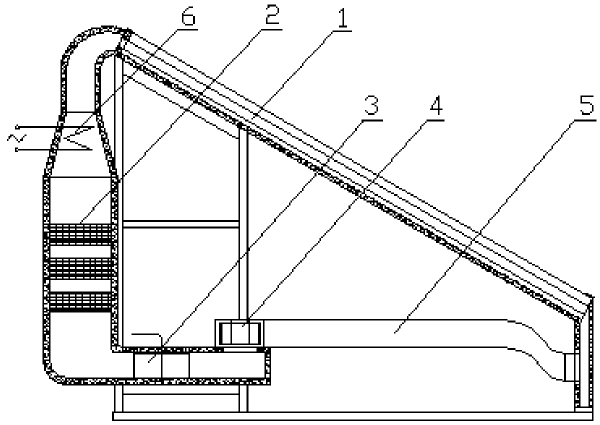

Figure 1. Schematic presentation of the pilot scale dryer: 1 - air solar collector; 2 – drying chamber; 3 – control unit; 4 - centrifugal fan; 5 – air ducts; 6 - electric heater

Full factorial experiment

The main goal in the multifactorial planning is to create a mathematical model of the research process [2].

For the objective function is defined specific energy consumption for drying - q, [kJ/kg e.w.]. It is known that a substantial influence on the kinetics of the process and the energy consumption for drying, have the following values:

- Air temperature - t, ^{0}C ;
- Air velocity - v, m/s;
- Relative humidity – φ, %;
- loading of the drying chamber – m, kg/m^2.

Factors, whose influence was studied in FFE are adopted on the basis of literature data [3] and the preliminary experiments. They are:

1. Rate frequency of air recirculation (indirectly influences relative humidity) - k, % - X_1. For lower level of this factor is set the value of 50% and an upper level - 90%
2. Air temperature (drying agent) - t, ^{0}C - X_2. The values of the lower and upper temperature level are selected according to the characteristics in utilization of solar energy. The selected values are respectively 40^{0}C for lower level and 60^{0}C for upper level.
3. Loading of the drying chamber - m, kg/m^2 collector area - X_3 with lower level - 1 kg/m^2 and upper level - 2 kg/m^2. Loading is per unit collector area for ease of using results in the design of convective solar dryers.

Experimental results.

The test results for the specific energy consumption and drying time for all variants are presented in Table 1.

Table 1. Specific energy consumption and drying time for variants of FFE

Variant of the FFE	Rate frequency of air recirculation	Air Temperature	Loading of the drying chamber	Specific energy consumption	Time for drying
№	X_1	X_2	X_3	kJ/kg.e.w.	h
1	+	+	+	10708	12
2	+	+	-	17751	9
3	+	-	+	9716	26
4	+	-	-	16574	22
5	-	+	+	12266	11
6	-	+	-	19753	8
7	-	-	+	13248	26
8	-	-	-	23571	22

In figures 2, 3 and 4 are presented reflecting surfaces and isolines, describing the variation of the specific energy consumption depending on the mutual influence of the pairs of factors.

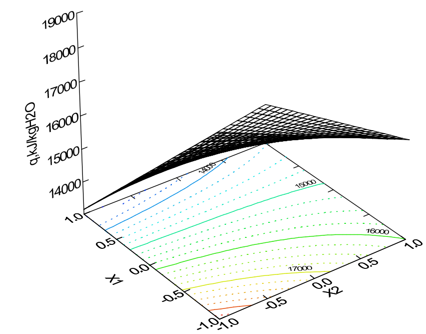

Figure 2. Reflecting surface and isolines, describing the variation of the specific energy consumption, depending on the factors rate frequency of air recirculation (X_1) and air temperature (X_2)

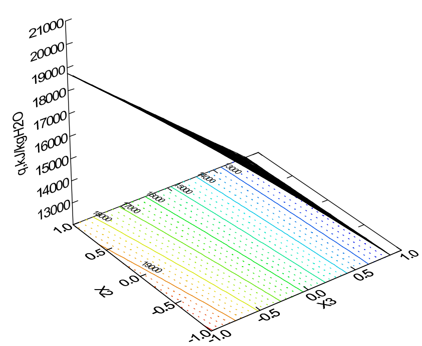

Figure 3. Reflecting surfaces and isolines, describing the variation of the specific energy consumption depending on the factors air temperature (X_2) and loading of the drying chamber (X_3)

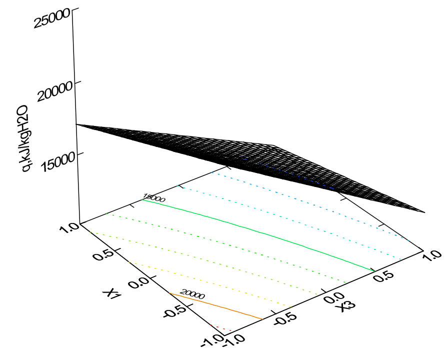

Figure 4. Reflecting surface and isolines, describing the variation of the specific energy consumption depending on the factors rate frequency of air recirculation (X_1) and loading of the drying chamber (X_3)

Regression equation is obtained:

$q = 15448.5 - 3964.01X_3 - 328.65X_2 - 1760.84X_1 + 331.14X_3X_2 + 488.57X_3X_1 + 871.08X_2X_1$ [kJ/kg.e.w.]

3. CONCLUSIONS

1. For different regimes of drying specific energy consumption is in the range 9716-23571 kJ/kg.e.w.
2. The time required for drying the product at various regime parameters is between 8 and 26 hours.
3. Increasing the rate frequency of air recirculation from 50% to 90% in the variants with a high temperature (60°C) results in minimal increasing in the drying time (one hour). In the variants with a low temperature (40°C) the drying time is not changed.
4. Significant savings of energy (up to 30%) in all variants of the FFE with the high level of rate frequency of air recirculation (90%) has been observed, compared to those with low level of rate frequency of air recirculation (50%). Therefore, maintaining the high rate frequency of air recirculation is appropriate on drying of blueberries.

References

[1] Badjakov I., Nikolova M., Gevrenova R., Kondakova V., Todorovska E., Atanassov A., Bioactive compounds in small fruits and their influence on human health. Biotechnology and Biotechnological Equipment, 22, 581, 2008.

[2] Lambrev, At., Fundamentals of engineering experiment in the study of machines and equipment for the food industry, (in Bulg.), Plovdiv, 1994

[3] Minchev, M., Drying equipment, (in Bulg.)Academic Publishing UFT - Plovdiv, 2012

[4] Stamov, St., Handbook of heating, heat and gas, Part II, (in Bulg.)Engineering, Sofia, 2001

SPECIAL CONSTRUCTION AUTONOMOUS STATION FOR THE DYNAMIC MONITORING OF SURFACE WATER QUALITY INDICATORS

Constantin VÎLCU[1], Gheorghe VOICU[2], Gigel PARASCHIV[2], Andreea PETCU[1], Adrian NEDEA[3]
[1]INCD Gas Turbines – COMOTI, [2]UPB – Biotechnical Systems Engineering, [3]University of Southampton UK

ABSTRACT

The monitoring station described represents a newly designed floating structure, "Buoy Monitoring" model, for the continuous monitoring of surface waters. Autonomous and adaptable to meteorological conditions in situ for the areas with continental climate, the floating station is designed for the real-time monitoring of the quality indicators of river water and is able to work with reduced maintenance in isolated locations. The floating structure, with possibility of immersion for protection against frost incorporates the multi-parameter probes and the hardware-software system of data (quality indicators) acquisition, processing and wireless transmission for the monitored water body. The evaluation of the river water "health status" is thus made continuously in situ with the scope of warning in case of ecological risk for the situations of accidental pollution of the investigated environment.

1. INTRODUCTION

Today, the integrated systems of surface waters quality monitoring are real-time systems which perform continuously the physicochemical and biological structural monitoring of the water body. In case of ecological risk, for situations of accidental pollution, the system warns in deterministic time the decision factors in order to reduce the impact and the negative effects. The dynamic monitoring in situ is made through a network of sensors distributed after the micro-scale placing topography in the investigated impact area. The monitoring of the environment according to the Environment Protection Law from the 29.12.1995, represents a "*system of surveillance, prognosis, warning and intervention, which takes into consideration the systematic evaluation of the qualitative features, dynamics of the environmental factors, in order to acknowledge these ones quality status and ecological significance, the evolution and social implications of the changes produced, followed by measures which are necessary*" [1,3]. Today's tendency in the design and/or realization of the systems of environment integrated monitoring is of decentralizing through data measuring and validation directly in situ, of these ones, "on-line" transmission to the regional centres for "off-line" processing and analysis, of performing in real time the warnings to environment protection agencies and institutions for emergency situations when the medium values of environment polluters exceed the values of the alert thresholds prescribed by European laws [2, 4].

2. STATIONS AND METHODS FOR MONITORING RIVER WATER QUALITY

The classical method for monitoring river water quality is made by taking samples and laboratory analyses. Although it offers a better accuracy, the method is expensive in time and costs (samples collection and transport for complex laboratory analyses).

*Corresponding author, 0720/392341, email ; constantin.valcu@comoti.ro

It can not be replaced especially for pollutants that do not have sensors and measuring techniques to allow determinations on site. The advantages of the measurements in situ (taking samples on site) are that they offer an instantaneous quality indicator of the physicochemical and biological conditions of the investigated water body. From this point of view, the continuous monitoring is more and more frequently used. The flexibility of equipping the continuous monitoring stations depending on the monitoring needs in situ, allow obtaining a large amount of data of water environment components at a low cost. The method of continuous monitoring allows the evaluation of the real status of river water in situ and the warning in real-time in case of ecological risk for the situations of accidental pollution (fig. 1.c).

a) Lab Sampling / Prelevare de probe de laborator; b) Spot Sampling / Prelevare de probe la fața locului; c) Continuous Monitoring / Monitorizarea continuă

Fig. 1 **–** Methods for monitoring of river water quality *(www.ysi.com)*

The terrestrial stations designed for the monitoring of river water quality (fig. 2) are generally robust buildings situated as near as possible to the water. They have large and various capacity of sensors and samples analyzers, connection facilities to the electrical network and Internet access. They need permanent operating personnel for maintenance and exploitation. The high costs of obtaining the amount of data of water environment component for these stations recommend them as nodes in the monitoring relays of hydrographical basins or as regional centres of acquired data validation, analysis and processing.

a) Land fixed stations / *Stații terestre fixe*; b) Land semi-mobile stations / *Stații terestre semi-mobile*; c) Land stations – fixed platforms / *Stații terestre – platforme fixe*

Fig. 2 – Land stations for monitoring of river water quality *(a, b - www.hach-lange.ro ; c – www.nexsens.com)*

The floating stations designed for the monitoring of river water quality (fig. 3) are floating structures: pontoon platforms with monitoring modules (PPM); buoy monitoring (BM); autonomous underwater vehicles (AUV). They are dedicated to continuous monitoring. The embedded real-time monitoring systems make from these structures, ideal operational instruments for optimization of the monitoring infrastructure of the surface water quality indicators (including rivers sub-system).

a) Ponton Platforms Monitoring (PPM) / *Platforme ponton de monitorizare*; b) Buoys Monitoring (BM) / *Geamanduri de monitorizare*; c) Autonomous Underwater Vehicle (AUV) / *Vehicule subacvatice autonome*

Fig. 3 – Floating stations for monitoring of river water quality *(a, c - www.ysi.com; b – www.anhydre.org)*

3. BUOY MONITORING FLOATING STATION

3.1. BM structure and functioning. Embedded sub-systems of the floating structure

BM is a floating structure for the dynamic monitoring and warning of surface flowing water pollution (fig. 4). The structure of the floater is interiorly compartmented so that it can partially allow its automatic flooding with water at the board controller command, for total immersion and protection sinking under freezing limit. Two electrical generators, each of them actuated by a propeller, are intubated and mounted diametrically opposed on the floating structure. Continuously immersed in the flowing water of the monitored river, the hydro-generators produce the electrical energy necessary for the BM autonomy.

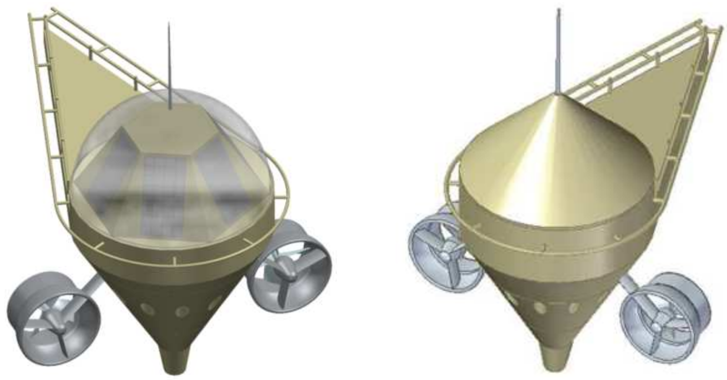

Fig. 4 – BM floating stations for the monitoring of river water quality

The BM structure is equipped with intelligent sensors (IQ) for the continuous monitoring of quality indicators and with a real time modular and scalable controller (DAQS) for the acquisition and processing of measured data. So equipped, the BM floatable structure allows "Real Time" dynamic monitoring, acquisition and processing of environmental data, remote transmission and warning (by SMS) in case of pollution. The structure and the embedded sub-systems of the BM floating structure are presented in fig. 5.

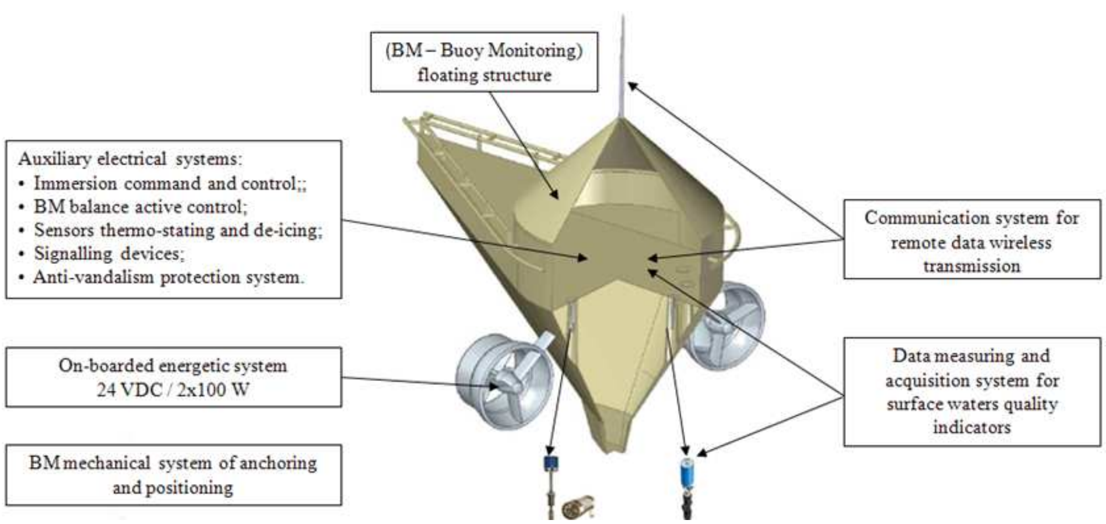

Fig. 5 – Buoy Monitoring embedded systems

3.2. IQ sensors for water bodies monitoring

The most important water quality parameters are continuously measured and analyzed when the general features that describe the ecosystem *health status* are evaluated. The selected parameters which allow the dynamic or real-time monitoring, must give enough vital information regarding the status of the ecosystem. So, they can often be used as a primary measure of water body quality evaluation or they can offer an early warning regarding the deviation from the status normal conditions due to contamination, measurable ecological or biological changes [1].

In fig. 6 there are presented intelligent sensors for the monitoring of river water. The parameters specifications and the performances of YSI 6820V2 multi-parameters probe are:

- ROX (Optical Dissolved Oxygen): 0 to 500%;
- DO (Dissolved Oxygen): 0 to 50 mg/l;
- Conductivity: 0 to 100 mS/cm;
- pH: 2 to 14 units;
- Temperature: -5 to +50°C;
- Turbidity: 0 to 1000 NTU resolution 0.1 NTU;
- ORP: -999 to +999 mV, resolution 0.1 mV;
- Depth: 0 to 61m, resolution 0.001 m;
- Ammonium/ammonia/Nitrate/nitrogen: 0 to 200 mg/L-N;
- Chloride: 0 to 1000 mg/l, resolution 0.001 to 1 mg/l;
- Rhodamine: 0 to 200 μg/l, resolution 0.1 μg/l;
- Chlorophyll: 0 to 400 μg/l, resolution 0.1 μg/l. [5]

The multi-parameters probes consist of a battery of sensors mounted in a single device, easily to be installed in situ. Used in the integrated monitoring systems, they allow a dynamic monitoring (live) of the quality indicators of surface waters.

Fig. 6 – Multi-parameter probes for water quality monitoring *(a, b -* www.intellitect-water.co.uk*; c - www.ysi.com)*

3.3. Hardware si software BM

For the evaluation of water quality, the number of sensors and measuring lines in unified analogical signal is generally of 40 ± 10%, depending on the monitoring scope and program. For this fact, it has been integrated as hardware a National Instruments [10] modular platform, scalable for the flexibility of the application, CompactRIO System model, which will represent the DAQS of the BM in situ. This allows through the elaborated program, the automatic load of the local database implemented in the NI platform of the BM. The data server of the integrated system of real time monitoring and warning of water quality from the monitored area of the investigated hydrographical basin will be situated onshore in the monitoring network node, where Internet connection is available. The configuration of DAQS-BM modular platform of the system of environmental data acquisition and processing for the real-time application of surface water quality monitoring is given in fig. 7. a).

At the BM installation in situ and commissioning, it is made the software configuration of the DAQS-BM data acquisition and processing system. This activity consists of the geostationary parameterization of the BM floater location, inclusively the identification through IDs of the quality indicators files with the samples continuously measured by IQ sensors. For the automatic registration of the environmental data in DB-BM local database, the program presented in fig.7.b) performs the software configuration of the DAQS integrated in the BM structure for various monitoring locations.

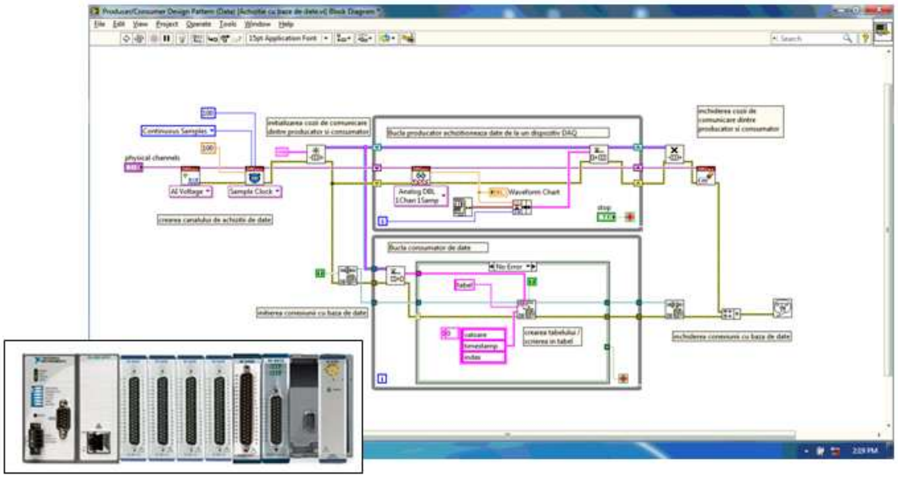

a) Configuration hardware DAQS-BM / *Configurare hardware DAQS-BM*

b) Configuration software DAQS-BM / *Configurare software DAQS-BM*

Fig. 7 – DAQS-BM hardware-software configuration

Locally, DB-BM is a sum of environmental data files relationally organized. Each file corresponding to a pollutant continuously monitored in situ, spatially localized, is registered and stored in NI-CompactRIO System unit of the BM. The local database is managed (creation, query and maintenance) by a relational database management system with implementations for Linux, Unix and Windows operation systems.

The determinations made in situ through reliable measurements for a large amount of parameters, corroborated with the wireless transmission through IT communication devices to the environmental data analysis and processing centres, gives the following potential benefits:

- Pro-active approach to the surface waters quality management;
- The possibility of real-time monitoring of the problems of surface waters quality (fig.8);
- The possibility of evaluation and contamination risks, generally ecological risks minimization.

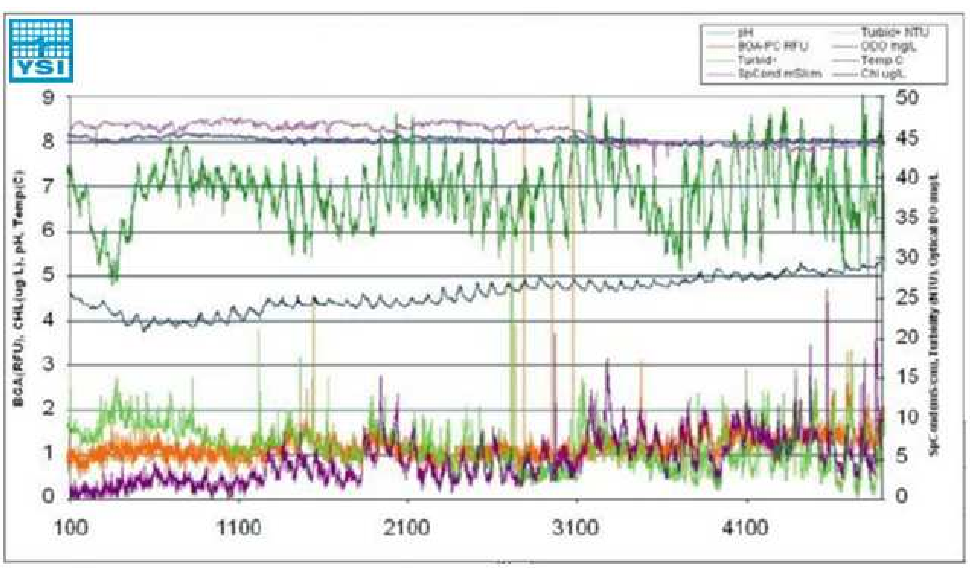

Fig. 8 – The graphical interface of the data operator *(www.ysi.com)*

4. REZULTATE

Data validation in situ and real-time warning in case of ecological risk

The hardware-software configuration of the DAQS platform which equips the BMs in the network of the monitoring and warning system of waters pollution in an area of the investigated hydrographical basin, allows, through the software implemented in the NI-Compact Rio "Real-Time" central unit, the data validation and release of the warnings from situ level. Even though typically the process is slow, characteristic to open systems, the pollution warnings signalized from situ since the phase of acquisition and processing for data validation, save significant time for the reaction of the operators for emergency situations in maintaining the ecological balance in the monitored hydrographical basin.

5. CONCLUSIONS

The floating station (BM) can be considered novelty element in the optimization of infrastructure of monitoring networks of surface water bodies quality indicators, as:

- BM is energetically independent. Equipped with two hydro-generators for the local production of electrical energy necessary for the operation autonomy (24 VDC), BM can function in situ in isolated locations;
- BM is adaptable to environmental variations. In winter, for protection against frost, in case of deep waters, BM is automatically immersed at the board controller command when the water temperature is of 0°C descending;
- More BMs topographically situated in a mesh type network allow, through NI on-boarded hardware with LabVIEW implemented software equipment, the automatic insertion of data in existent environmental databases, relational and distributed, spatiotemporal and interactive;
- BM structure allows the realization of distributed sensors networks and implicitly the obtaining of an informational global network of hydrographical basins monitoring.

6. ACKNOWLEGEMENT

The paper is proposed for founding within the competition Collaborative Applicative Research Projects PCCA and registered with the code number PN-II-PT-PCCA-2013-4-1165.

BIBLIOGRAFIE

[1]. Cioplan, O., *Monitoringul integrat al sistemelor ecologice*, Editura Ars Doceni, Bucuresti, 2005;
[2]. Dobriceanu, M., Olteanu, D., *Sisteme informatice de supraveghere a mediului. Ingineria si Managementul Calitatii si Mediului*, Craiova, 2007;
[3]. Rojanschi, V., Bran, F., Diaconu, G., *Protectia si ingineria mediului.* Bucuresti, Editura ECONOMICA, 1997;
[4]. ***, *Sistem integrat pentru monitorizare dinamica si avertizare in caz de riscuri tehnologice in zona transfrontaliera România-Bulgaria*, www.project-react.eu., 2012;
[5]. ***, www.ysi.com, 09.10.2013;
[6]. ***, www.hach-lange.ro, 08.10.2013;
[7]. ***, www.nexsens.com, 07.10.2013;
[8]. ***, www.anhydre.org, 08.10.2013;
[9]. ***, www.intellitect-water.co.uk, 09.10.2013;
[10]. ***, http://sine.ni.com/.../n24:cRIO/, 10.10.2013.

EXPERIMENTAL RESEARCH ON THE DETERMINATION OF THE LOWER CALORIFIC POWER OF THE MISCANTHUS BRIQUETTES COMPARED WITH THAT OF THE SAWDUST BRIQUETTES

PhD. Std. Eng. I. Voicea.[1], Prof. PhD. Eng. Gh. Voicu, PhD. Eng. V. Vladut,
Eng.G. Găgeanu, Math. P Cârdei
[1)] INMA Bucharest; [2)] Politehnica University of Bucharest

ABSTRACT:

Burning is the oldest and most used technology for obtaining the energy in form of heat. The biomass can be burned directly (as is burnt the wood for heating or the waste incineration) or can be burned simultaneously with the coal (co-burning). The briquettes are obtained by pressing the sawdust mixed with chips, tree branches or shells by means of a piston or screw press. A unique alternative to achieve of fossil fuel in the form of briquettes for the Romanian space is the cultivation of the plant called Miscanthus. This is a very high perennial herb (reaching 3.5 m at maturity), increasingly popular in Europe as a source of green energy. For the determination of caloric power was used a calorimetric system type CAL 2K. The experimental data resulted showed the fact that although misacanthus briquettes shows a lower value of the the lower calorific power than those of sawdust may be a viable alternative to the fossil fuel until recently used exclusively (wood, coal, etc.), without issuing dangerous pollutants in the environmental atmosphere.

1. INTRODUCTION

The alteration of air and water quality has resulted in deterioration of population health, registering an increase of cardio respiratory deseases at alarming levels of the morbidity and mortality worldwide, together with the thermal stress produced by the heat waves and the increase of spreading of infectious diseases in tropical climates to other locations because of the global warming.

The technologies based on renewable energy have the great advantage that it use practically inexhaustible resources, cleaner, with a negligible contribution to climate changes. In addition, their use reduces the dependency on the conventional resources wich will be exhausted in a not too distant future, [2]**.**

Even if clean energy is currently more expensive (due to high investment costs and lower performance), in the last period of time were recorded major technological leaps, giving the hope that in the near future this will be a viable alternative to the traditional sources. The biomass is the first form of energy used by humans with the discovery of the fire. The energy incorporated into biomass is released by various methods, which however in the end represents the chemical process of combustion. The biomass represents the vegetal component of the nature. As a form of storing of the sun energy in chemical form, the biomass is one of the most popular and universal resource on the Earth. It ensures not only food but also energy, building materials, paper, fabrics, medicines and chemicals. The biomass has been used for energy purposes since the discovery of the fire by humans. Today the fuel from biomass can be used for different purposes: from the heating of rooms up to the production of electricity and of fuels for cars.

The term of biomass is used to name alive or dead biological material that is used to produce fuel or industrial production. Most often the term of biomass refers to the matter obtained from plants, necessary to obtain ecological fuel, but this term includes also the

[1] 6 Ion Ionescu de la Brad Bld, Bucharest, +40752161780, voicea_iulian@yahoo.com

animal or vegetable matter from which are obtained fibers, chemicals or heat. The energetic biomass is represented by plants like hemp, corn, poplar, willow, reed, mischantus, etc. Although the solid fuels originate in biomass, they are not considered as part of it because they contain carbon that has not been included in the natural circuit for a long time, [5].

A unique alternative to the Romanian space is the cultivation of the plant called Miscanthus (Fig. 1). This is a perennial plant very high (reaching at maturity 3.5 m), becoming more popular in Europe as a source of green energy. Grows best within a breezy climate. Can be harvested once a year with technical equipment currently used in the conventional agriculture (eg the sugar cane cultivation equipment). It is common and in its hybrid form, Miscanthus giganteus [7].

This plant is particularly suitable for the manufacture of the pellets because it has a low moisture content, property which is acquired and by the pellets at the end of the manufacturing process, regardless of the used raw material. Recently are used technologies for its compaction in the form of briquettes. The annual production (calculated after the drying in ovens of the harvested plant) is of 10-20 tons per hectare.

Figure 1: Miscanthus - an alternative source of energy

In the last ten years, in the developed countries are completed the technologies and equipment required in manufacturing and efficient burning of briquettes from sawdust, straw, miscanthus, grasses and other forms of biomass.

Currently, these lighters are economically competitive compared to generic fossil fuel and natural gas, further having the advantage of being neutral from the point of view of the earth heating, due to lower emissions of greenhouse gases. It is considered that at burning the briquettes are emitting into the atmosphere the same amount of carbon dioxide that the plants have absorbed from the atmosphere in the process of photosynthesis which has generated the biomass used in the production of pellets.

The coordinates of the Energy Policy for Europe (EPE) agreed upon by the heads of state and government in Brussels during the European Council of 8 and 9 March 2007 are the achievement of the following targets by the year 2020, 20-20-20-10, videlicet: [3].

- reduction of greenhouse gas emissions by 20%;
- reduction of energy consumption in Europe by 20%;
- the use of renewable energy to reach 20%;
- 10% of the transportation to be achieved with biofuel.

2. METHODOLOGY

Starting from a raw material consisting of sawdust from forest debris and miscanthus chips with different granulations and moistures, aimed the obtaining of cylindrical briquettes in a mold with a piston by pressing (fig.2). At the beginning of the compression process, the end of the compressed biomass output is keep closed up to the reaching of a threshold pressure of pressing by the piston, after which it opens allowing the release (discharge) of the formed briquette. For the actuation of the piston a machine of force was used with a maximum capacity of 100 kN. The machine of force used as a compaction system (Figure 3) being assisted by a computer, allowed the controling of the moving speed of the piston and respectively the recording of the force-displacement diagram.

Figure 2: Cylinder with piston for compaction

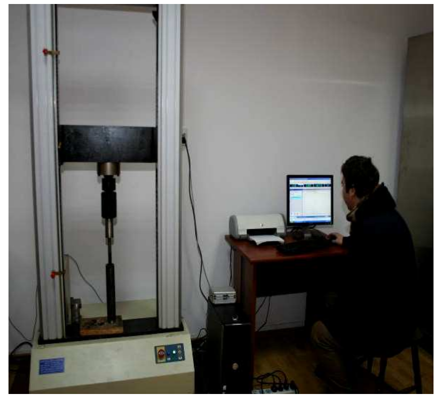

Figure 3: Installation for the biomass compaction at a reduced scale

Carrying out the experiments in the conditions described above, led to obtaining of briquettes from miscanthus chips (Figure 5) respectively of sawdust from forestry residues (Fig. 4).

Figure 4: Sawdust briquette

Figure 5: Miscanthus briquette

To determine the lower calorific power it is used a calorimetrical system type CAL 2K, Figure 6 and 7, consisting of:

- calorimeter itself;
- calorimetrical bomb;
- nacelle;
- burning adapter;
- oxygen station;
- analytical balance with the accuracy of 0.1 mg.

Figure 6: Sample weighing with the analytical balance

Figure 7: Calorimetrical bomb CAL 2K

Working Mode

The sample of material is inserted into nacelle for determining the calorific power and weigh it. A cotton thread is attached in the center of the ignition wire and insert the other end into the sample, in order to propagate the combustion inside it. The nacelle located in its holder is inserted into the calorimetrical bomb and is hermetically sealed. The bomb is then filled with oxygen at a pressure of 20-30 bar by means of the oxygen station, connected to an oxygen cylinder. To the bomb is attached the ignition adapter being then inserted inside the calorimeter vessel. Pour about 2 liters of demineralized water into the tank of the calorimeter, following the level indicator.

Figure 8: Determining the lower calorific power using the calorimetrical bomb

For the preparation of the measurement shall be inserted into measurement menu the measured weight of the sample, the type of operation that will be performed (calibration or proper measurement), the type of the calorimetrical bomb and the correction values for the heat generated by the combustion of cotton thread (the default value is 50 J) or from other sources.

When everything is ready, the lid of the calorimeter is closed and the device starts the measuring operation. First, the inner vessel is filled with water, and then is performed the combustion, the final step consisting of the equalization of the temperatures of the inside and outside vessel, by the transfer of heat from the inside to the outer vessel. When this happened, the measurement process is over and the value of the measured calorific power is displayed.

The device calculates the lower calorific power according to the following assumptions:

- the temperature of fuel and of the combustion products is 25 °C;
- the water contained in the fuel and the water formed by combustion of hydrogen is in the liquid state at the end of the process (the device measures the calorifical power);
- the atmospheric nitrogen was not oxidized;
- the gaseous products of combustion are: O_2, N_2, CO_2 and SO_2;
- it may form ash.

There are two types of calorific power:

- the upper calorific power (Q_s) in which the water vapors formed during combustion are condensed giving their latent heat of vaporization [2];
- the lower calorific power (Q_i) in which the water vapors formed during combustion remains in gaseous form and therefore does not give their latent heat of vaporization [1].

It is considered that the water vapor resulting from the burning are coming from the combustion of hydrogen, and from the water initially contained in the fuel. At the fuels not containing hydrogen or water, for example the carbon, the carbon monoxide and the sulfur, because during the combustion was is not formed water, the upper and lower calorific powers are equal. In thermoenergetics until recently was not economical the water vapor condensation resulting from the burning, so it was simple and convenient that the design and operation to be based on the lower calorific power. With the advent of condensing boilers emerged the need to use the upper calorific power.

The upper calorific power at constant volume of sample ($Q_{s,V}^{a}$)of a fuel is the number of units of heat released by the complete combustion of a unit of mass from the fuel prepared for analysis, in the atmosphere of oxygene, into the calorimetrical bomb, under standard conditions. The products of combustion are formed by carbon dioxide, sulfur dioxide, nitrogen and oxygen in gaseous form, water in liquid form in equilibrium with its vapor and saturated with carbon dioxide and solid ash [6]. $Q_{s,V}^{a}$, are experimentally determined by the complete combustion in the calorimetrical bomb of a known amount of fuel, the heat released by combustion being ceded to the calorimetrical system containing a known quantity of water, whose temperature is recorded [4].

OUTCOMES

Lower calorific power at constant pressure of the original sample ($Q_{i,p}^{i}$)of a fuel represent the number of heating units which would be released by the complete combustion of a unit of mass from the fuel in the initial state, in oxygen atmosphere, at constant pressure. The products of combustion are all at a temperature of 25 °C and consist of carbon dioxide, sulfur dioxide, nitrogen and oxygen in gaseous form, water in vapor state and solid ash. The value of $Q_{i,p}^{i}$ is obtained by calculation:

$$Q_{i,p}^{i} = (Q_{s,V}^{a} - 212H^{a} - 0,8O^{a})\frac{100 - W_{t}^{i}}{100 - W^{a}} - 24,5W_{t}^{i} \quad (1)$$

where:

- H^a and O^a are the percentages of hydrogen and oxygen,
- W_t^i and W^a are percentages of moisture from the initial weight, respectively of the mass for analysis,
- and the coefficients 212, 0,8 and 24,5 take into account massic heat of the water and water vapor, respectively of the latent massic heat of vaporization of the water, expressed in SI units [6].

The size which interests usually in energetics is $Q_{i,p}^{i}$, which in everyday language is called lower calorific power and is denoted Q_i . For condensing boilers interested the gross calorific power at constant pressure of the initial sample $Q_{s,p}^{i}$, usually denoted Q_s.

The calorific power of solid fuels is related to 1 kg of fuel and is expressed in MJ/kg [6].

Following the completion of the experimental testings were determined the following values for the calorific power for the sawdust briquettes compared with those of miscanthus.

Table 1: Lower caloric power

Test No.	Lower caloric power Sawdust Briquettes [MJ/kg]	Lower caloric power Miscanthus Briquettes [MJ/kg]
1.	19.990	15.164
2.	19.664	14.829
3.	20.051	15.507
4.	20.075	15.432
5.	20.070	15.679
6.	19.671	15.445

By processing the experimental data obtained and shown in Table 1 using the Excel program , resulted the graphs below:

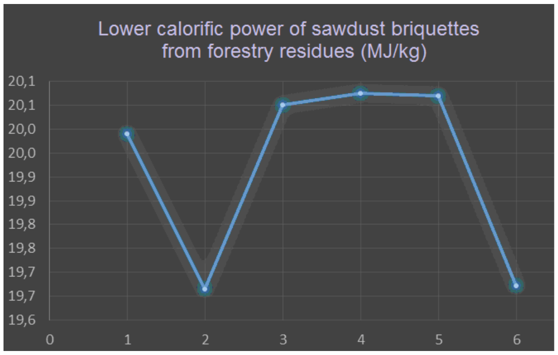

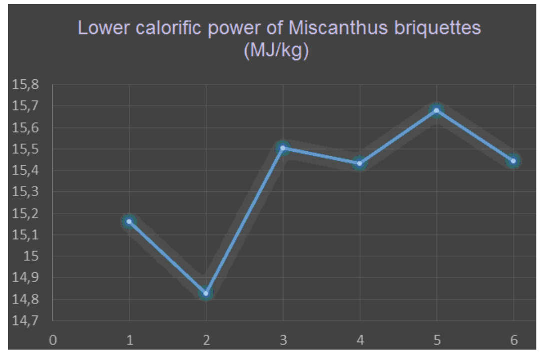

Figure 9: Graphical representation of the lower calorific power

3. CONCLUSIONS

The calorific power (the heat of combustion) represents the number of units of heat released by the complete combustion of a unit of mass of fuel as provided by standards. The chemical reaction of burning is usually an oxidation of the hydrocarbons, resulting carbon dioxide, water and heat.

The calorific power of solid fuels (and of those liquids, heavies which does not evaporate) is measured with the calorimetrical bomb, and that of the gaseous fuels (and liquids, volatiles) with the calorimeter with circulation of water. It can be calculated as the difference between the enthalpy of the combustion products and that of the fuel, dacă acestea sunt cunoscute.

Following the data experimentally determined with the help of the calorimetrical bomb, was obtained an average value of the lower calorific power for the briquettes of sawdust from forest residues 19.921 MJ/kg. In comparison the average value of the lower calorific power of Miscanthus briquettes was of 15.432 MJ/kg.

The superior value of the lower calorific power of the briquettes of sawdust from forest residues is due to the high content of lignin from their composition compared to the briquettes of Miscanthus. As it can be see from the last position in Figure 8, the burning of the miscantus briquette is incomplete due to the high content of silicon from the plant composition. The extraction of the silicon from the soil by the plant occurs in periods of prolonged drought, a phenomenon met in 2013.

References

[1]. Bazil, P. et al - *Handbook of termotehnician engineere (MIT)*, vol 1, Bucharest: Technical Publishing, 1986;

[2]. Danciu A. and others - *Technology for harnessing agricultural and forestry solid biomass to achieve clean energy and reduce emissions of greenhouse gases*, Research Report, Contract 21-008, 2007-2010;

[3]. Romanian Government, *Energy and Environment. Energy Policy for Europe. Spring European Council conclusions*, eu-ro newsletter no. 17/11.03. 2007,

[4]. Ionel I - *The management of energetic recovery of biomass,* Timisoara, Publisher "Politehnica" 2007;

[5]. Ministry of Economy, Trade and Business Environment - Romania; NL Agency- Netherlands; ENERO - Romania - *Romania biomass Master Plan, Version 2, (2010);*

[6]. SR ISO 1928:1995 - *Solid mineral fuels. Determination of upper calorific power by the bomb calorimetrical method and calculation of the lower calorific power;*

[7]. Voicu E. and others - *Technology to promote energy plant in Romania Miscanthus as sources in order to increase competitiveness and security energetice*. Raport research, contract no. 21-038, 2007-2010.

THE STUDY OF MISCANTHUS RHIZOMES DISTRIBUTION AT THE SEMIAUTOMATIC PLANTERS

Gheorghe VOICU[1], Gigel PARASCHIV[1], Petru CÂRDEI[2], Mirela DINCĂ[1,*], Ion – Cristian POENARU[1]

[1]University POLITEHNICA of Bucharest, Faculty of Biotechnical Systems Engineering, Biotechnical Systems Research and Development Center
[2] National Institute of Research - Development for Machines and Installations Designed to Agriculture and Food Industry - INMA Bucharest
*E-mail: mirela_dilea@yahoo.com

ABSTRACT

At the semiautomatic miscanthus rhizomes planters, the rhizomes distribution is carried out manually at regular time intervals through the leading tubes to the coulters. The whole movement of clamping the rhizome, transport over the mouth of launch of the leading tube and the release into the tube, influences its trajectory and obviously the quality of the working process of the miscanthus rhizomes planter.

This paper presents a mathematical model for determining the movement equations of the rhizomes at their fall through the tube, modeling the rhizome as a one-dimensional rigid bar of length *l*, with free movement in space being done comparative analysis of possible situations of the rhizomes launching and dropping through the tube, for several initial conditions, physico- mathematical modeling being done on the computer. Also, are made recommendations in order to achieve a proper distribution process, so as not to affect the quality of the working process.

1. INTRODUCTION

The quality of planting work performed by the miscanthus rhizomes planter is determined, among other parameters, and those of the kinematics and dynamics of stalk miscanthus movement into the machine planted tube. Obvious that it depends on the launch mode: the operator’s hand gives the movement conditions of the rhizomes in the tube, all the hand movements being correlated with the forward speed of the aggregate tractor – miscanthus rhizomes planter.

2. THEORETICAL ELEMENTS

In order to estimate the role of the parameters involved in the planting process, with direct effects in the distance between the rhizomes on the row and even in their correct alignment, a simple mathematical model is approached, in which the rhizome (stalk) is shaped as a rigid solid, which falls under the action of gravity through the launch tube and is deposited in the soil channel digged by the coulter, as a consequence of potential energy converted into the kinetic energy and, finally, in the penetration energy of the soil. Would be ideal that the rhizome free fall, with zero initial conditions (namely, the relative speed at launch tube to be zero, and the position of the mass center to be in center of the tube or near the end of the tube from the front of the aggregate.

At the MPM – 4 machine, the rhizomes guide tubes have a length of about 775 mm and the inferior circumference is about 200 mm above the soil. The diameter of the guide tubes is 167 mm. The detail of the tube in a section of the same machine can be seen in Figure 1, a.

The absolute reference system is the system xOy which have the origin in the projection point on the on the unprocessed soil surface O and which moves along with the aggregate, to its operating speed. The *Ox* axis of the absolute reference system, coincides with the direction of travel of the aggregate. The reference system $\xi o \eta$ is integral with the rhizome.

If the rhizome is modeled as a one-dimensional rigid bar of length *l*, then according to [1,2,3,4,5], the motion equations of the free rigid bar in space are:

$$m \cdot \ddot{\xi} = 0,\ m \cdot \ddot{\eta} = -G,\ J_{\theta}\ddot{\theta} = 0 \tag{1}$$

where: *m* is the mass of the rhizome; ξ, η, are the coordinates of the mass center of the rhizome model, and θ is the angle between the rhizome axis and the Ox axis of the absolute coordinate system. These three coordinates modeling the rhizome parallel plan movement, into a first approximation of the real phenomenon. Equations (1) are easily integrated and lead to the solution:

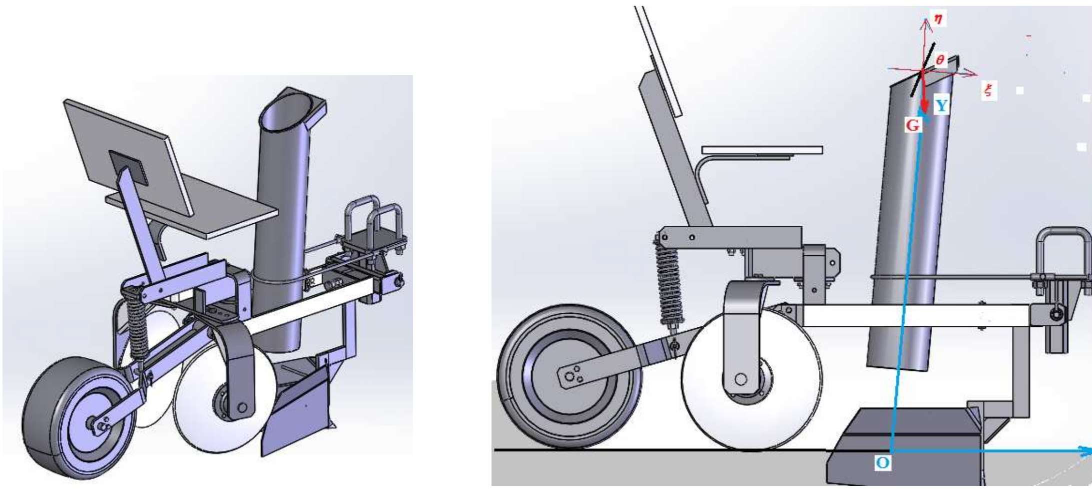

a b

Figure 1: Detail of a miscanthus rhizomes planter working section – a and scheme of reference system and the forces acting on the rhizome - guide tube

$$\xi(t) = \dot{\xi}_0 t + \xi_0,\ \eta(t) = -\frac{g}{2}t^2 + \dot{\eta}_0 t + \eta_0,\ \theta(t) = \dot{\theta}_0 t + \theta_0 \tag{2}$$

where: $\dot{\xi}_0$ - the initial speed after horizontal axis of the mass center of the rhizome's mathematical model; ξ_0 - the initial horizontal coordinate of the mass center of the rhizome's mathematical model when launching; g - gravitational acceleration; $\dot{\eta}_0$ - the initial speed on the absolute reference system vertical; η_0 - the initial coordinate (when launching) of the rhizome center; $\dot{\theta}_0$ - the initial angular speed of the rhizome; θ_0 - the rhizome's initial angle with the absolute coordinate system horizontal. In interpreting the model should also consider that, in relation to an absolute reference with the origin linked to a point in the working field, the launch tube also has speed v_0.

The initial parameters of the rhizome movement are generated by the manner of handling by the miscanthus rhizomes planter operator.

Thus, the way he moves his arm, forearm and fingers that catch the rhizome will give values for $\dot{\xi}_0$, ξ_0, $\dot{\eta}_0$, $\eta_0, \dot{\theta}_0, \theta_0$, that is, the initial linear speeds or the rotation speeds and for the intial translations and the initial rotation.

The following explanations will show that in order to avoid undesirable phenomena, the operator must manipulate the rhizome so that this initial values to be zero. Therefore, the manipulation should be as quiet as possible, namely, even if the rhizome is brought over the mouth of feed tube at high speed, there must be braked (a moment of silence) and then must release the rhizome, as parallel as possible to the tube walls. By undesirable phenomena is meant any rhizome trajectories in which it touches the guide tube walls, being thus subjected to some forces and shocks with friction, and what is worse is that, generally, these have a random character, duration of action being undetermined due to the collision character of the rhizome - guide tube contact.

Another important issue that must be considered in the modeling of miscanthus rhizome launching onto the guiding tube is that the operator does not catch the rhizome so that its mass center be placed between the fingers of the operator, but somewhat random, as not all the rhizomes have not the same size. For this reason, the initial conditions must be applied at an arbitrary point of the rhizome, point that in model should be noted.

Thus, by *r* will denote the distance on the bar from the bar mass center that represents the rhizome model, at its point of clamping by the operator. If u_0, v_0, $\dot{u}_0$, $\dot{v}_0$, θ_0, $\dot{\theta}_0$, are the coordinates and speeds, respectively the rotation angle and the angular speed of rotation, known of the rhizome clamping point among the fingers of the operator, then the initial conditions at the rhizome mass center is calculated by formulas:

$$\xi_0 = u_0 - r \cdot \cos\theta_0,\ \eta_0 = v_0 - r \cdot \sin\theta_0 \tag{3}$$

$$\dot{\xi}_0 = \dot{u}_0 - r \cdot \dot{\theta}_0 \sin\theta_0,\ \dot{\eta}_0 = \dot{v}_0 - r \cdot \dot{\theta}_0 \cos\theta_0 \tag{4}$$

Obviously, for *r* = 0, the rhizome clamping point by the operator is precisely its mass center.

3. NUMERICAL SIMULATION OF THE RHIZOMES TRAJECTORIES INTO THE GUIDE TUBE

The equations of movement (2) was used to simulate the miscanthus rhizome movement in the guide tube. The program with which was conducted simulation is Mathcad. The movement whose trajectory is shown graphically in Figure 2, is studied having as absolute benchmark a reference system solidary with the machine, so the travel speed is eliminated. The reason for that it takes the absolute benchmark solidary with the machine is that is studied the rhizome movement in relation to the guide tube.

If all the initial speeds, the inclination angle and the initial rotation speed are all zero, then the rhizome follows a trajectory like in Figure 2, a. The term of trajectory is unsuitable for a rigid solid correctly described by a beam trajectories of all his points, but we used only for simplicity of language which is so complicated. It is noted that all the points follow the same trajectory, that is the axis of the guide tube. The time in which the lowest point of rhizome touches the soil is 0.432 s. In Figure 2, the possible trajectories of the rhizome are included in a box whose side walls represent the vertical walls of the guide tube. More specifically, they are located between 0.2 and 0,975 mm vertical quotas. If the operator's hand catch the rhizome from 5 cm above its mass center and move in such a way that at the starting point of the movement (when the rhizome is released) is printting in the point of clamping a horizontal speed of only 0.2 m / s, then the rhizome touch the soil at the same time as the movement in the case „a" of Figure 2, but on a parabolic trajectory of the mass center, as can be seen from Figure 2, b. It also notes that the the rhizome does not touch the walls of the tube before reaching the soil. If the initial horizontal speed (in the direction parallel to the direction of the aggregate movement) is 0.3 m / s, then the fall takes place on the trajectory of Figure 2, c. It is noted that somewhere in the middle of the tube height, the rhizome hits the tube wall. After the moment of impact the equations of movement should be rewritten and must recalculate with new initial data. To calculate new initial data must be solved the problem of collision between the rhizomes and the tube surface. To solve this problem it is necessary to know some impact properties of the two surfaces (the rhizome and sheet metal tube). The collision can be considered elastic or elasto - plastic (where, for example, the rhizome can slide on the tube wall with friction), but these would be only hypotheses to be verified experimentally. Is very possible that collisions that will occur to produce random phenomena very likely due to the configuration of the rhizome. The formulated mathematical model can be used to set the initial conditions in which the collision with the walls does not occur. If the collision with walls occurs, another importan problem o consider would be the consequences of contact on the rhizome: it will hurt or not?

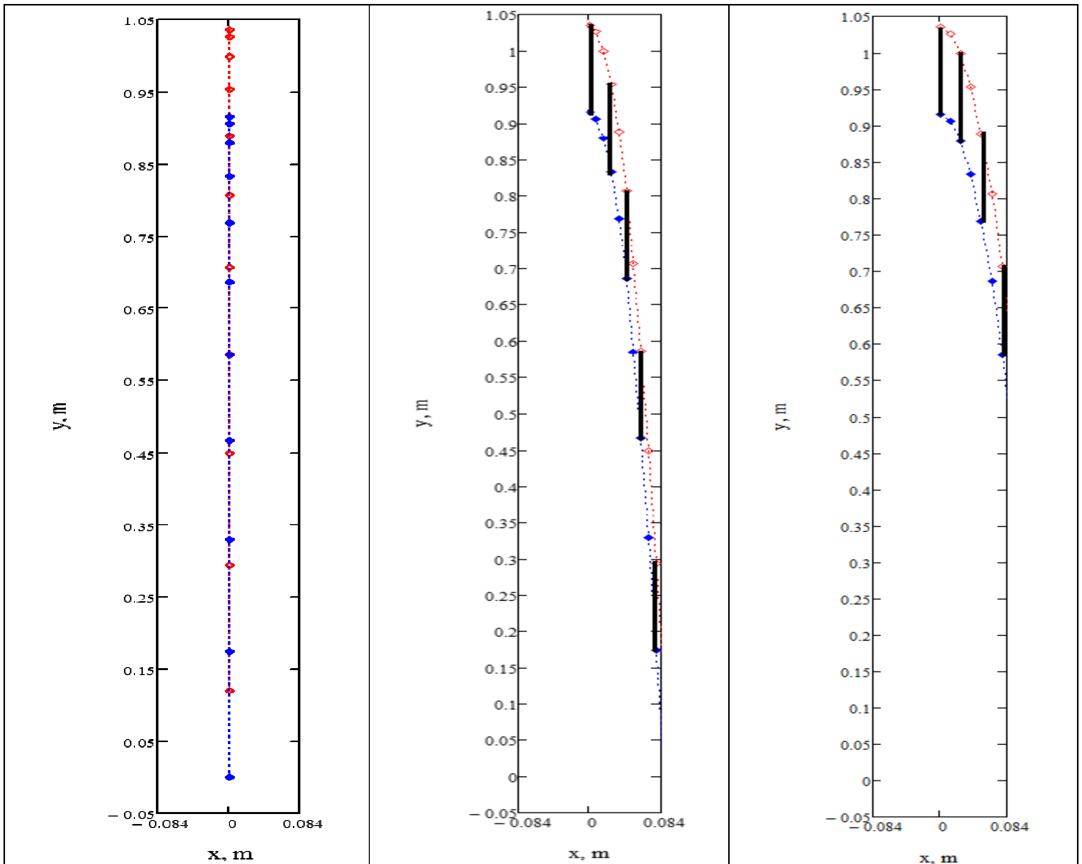

a: v_x= 0 b: v_x= 0,2 m/s c: v_x= 0,3 m/s

Figure 2: The fall of the rhizome through guide tube

The collision of the rhizome with the guide tube can happen and if, in addition to the initial horizontal speed in the direction of the aggregate forward speed, it also introduces a non-zero vertical component (the operator's hand from the miscanthus rhizomes planter section is moving vertically up when the rhizome is released in the center of the guide tubeupper base). If the vertical component has the value 0.3 m / s, then the descent time will increase to 0.464 s, but it will be a bit longer because the rhizome will collide with the tube wall somewhere near the lower base. Another important case, for both model verification, and its practical consequences is that (quite unlikely) the operator launches the rhizome from the horizontal position of it. In this case, (without taking into account the aerodynamic process, which would make the model more complicated), the calculations show that the rhizome is reaching the soil after 0,446 s (is changed the vertical dimension of the the rhizome) also in a horizontal position without touching the walls of the tube. If the planting in this position is correct from agronomic point of view then this type of release is not contraindicated, but, otherwise, should be specified the optimal position to launch the rhizome. It has been demonstrated that, in this case, the rhizome remain permanently parallel to the initial direction. The same phenomenon is happening and if the rhizome is released from an oblique position in relation to the tube walls. Released centered, the rhizome will not touch nor in this case the walls of the tube, and the descent time will have 0,434 s value. If, besides the oblique orientation to the axis of the guide tube (initial inclination of 30º to the axis of the tube guide), to the rhizome is applied also an initial horizontal speed with the value of 0.1 m / s, then the rhizome trajectory will change. It was observed that under these conditions, the rhizome reaching the soil without touching the walls of the guide tube (the descent time has also the value of 0.434 s). If the initial speed component on the horizontal doubles (0.2 m / s), to the previous case, the rest of the initial conditions are similar then, the rhizome will descend freely only until the half of the tube, colliding in this area of the wall, and then follows a trajectory probably with friction for whose determination model must be reformulated in a manner specified above. It is not done this analysis in this material because comparing the effort with the possible results, there is not a sufficient reason.

If the release is made from an oblique position in relation to the axis of the tube and with the horizontal initial speed of 0.1 m / s, but also imposes an initial speed in the vertical direction to the value of 0.7 m / s (caused, for example, by a section passing over an obstacle that confers a shock on the vertical's operator), the rhizome trajectory will change substantially. The rhizome reaches in this case on the soil without touching the walls of the guide tube, in 0.511 s. It is noted that due to the positive vertical component, the rhizome initially going in the positive direction of the vertical, then returns on the downward trajectory. In the case of the initial rotation speed is non-zero, through an initial rotation imparted by the operator's fingers, the rhizome will come down rotating. For example, for an initial rotation speed about 0.7 rad / s (less than 40 ° / s, what is still more, but we chose this value to make more visible the effect), the rhizome descent way is shown in Figure 3, a.

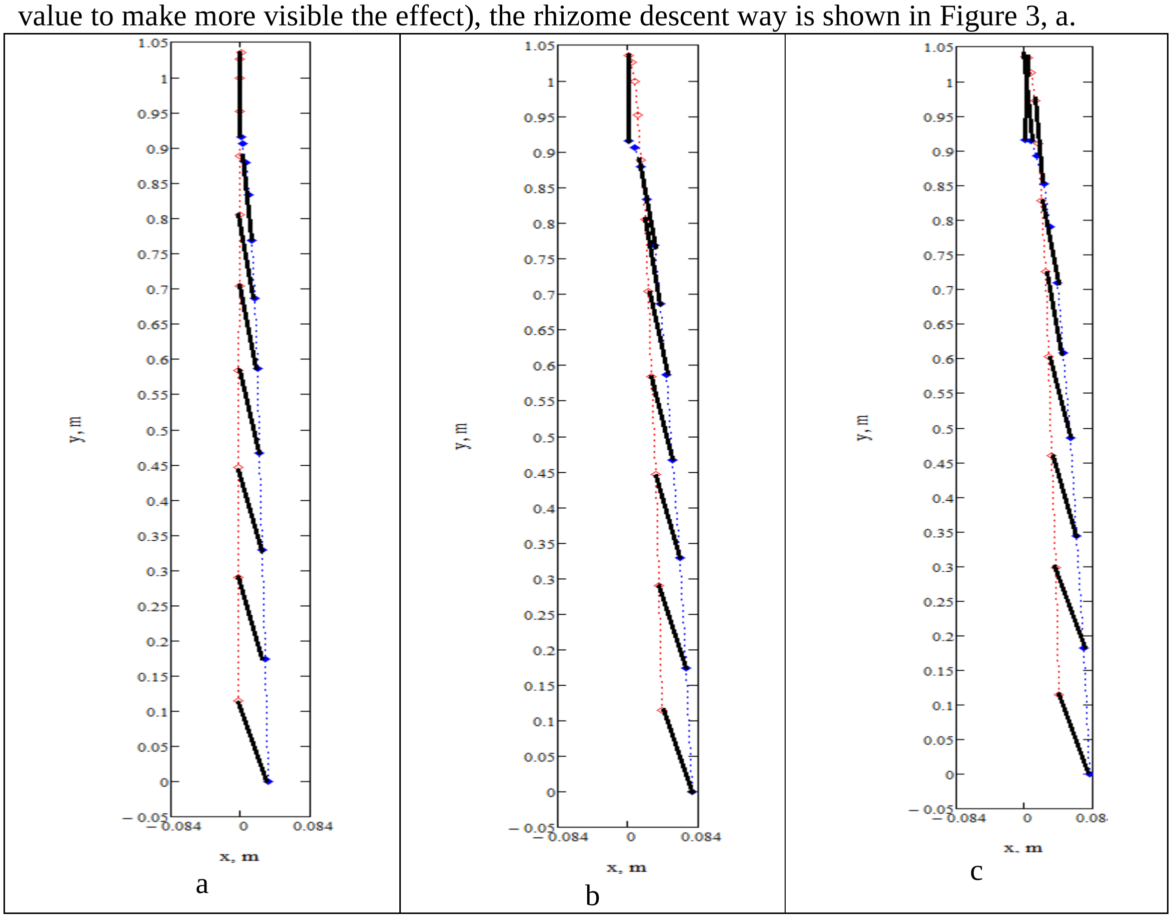

Figure 3: Sequences from the descent process of the rhizome through the tube

If to this non-zero initial condition is added the horizontal initial speed with the value about 0.1 m / s, the rhizome descent into the tube takes place after the trajectory from Figure 3, b. In both cases, the descent time is 0,433 s and the rhizome touch the ground without colliding the tube walls.

Finally, if the vertical speed is a positive value 0.2 m/s, then, immediately after launching, the rhizome rises slightly then descends easily rotating, the whole movement lasting for 0,453 s.

The whole movement of clamping the rhizome, transport over the guide tube's mouth and releasing in the tube, influence its trajectory and obviously, the quality of the working process of the miscanthus rhizomes planter.

4. CONCLUSIONS

Some simple reasonings made for this chapter show that it is indicated that the rhizome to be released at a point located in the vicinity of the center tube, preferably between the center of the section and the generator from the front of the guide tube.

It is recommended that, prior to launch, the rhizome to be kept a short moment in the launching point for any initial speed to cancel, and thus the rhizome trajectory to be the simplest possible. Is contraindicated launching from points located in the vecinity in the tube wall because the rhizome trajectory becomes uncontrollable, that is take place multiple collision with the walls of the tube which may generate deviation from the optimum place for planting or even affect the plant. It is recommended that the aggregate speed to be small enough so that the operators can launch the rhizomes taking into account the indications above.

The land where mischantus is planted should be as well processed so that not generate in the aggregate and, especially, in the miscanthus rhizomes planter shocks that could unbalance the operators, so that to carry out wrong launches or even to fall off the chair.

The launch process requiring attention and maximum concentration, for the good activity progress, is recommended short periods of rest for operators.

AKNOWLEGEMENT

The work has been funded by the Sectoral Operational Programme Human Resources Development 2007-2013 of the Romanian Ministry of Labour, Family and Social Protection through the Financial Agreement POSDRU/107/1.5/S/76903.

References

[1] Dobrescu C., *Optimizarea parametrilor agregatelor agricole in scopul reducerii consumului de energie*, Redactia de propaganda tehnica agricola, Bucuresti, 1981.

[2] Gioncu V., Ivan M., *Teoria comportării critice şi postcritice a structurilor elastice*, Editura Academiei, Bucureşti, 1984.

[3] Letosnev M.N., *Masini Agricole*, Ministerul Agriculturii si Silviculturii, Editura Agro-Silvica de Stat, Bucuresti, 1959.

[4] Mocanu V., Hermenean I., *Experimental reserches concerning dynamics and energetic of two – wheel tractor – mower systems*, INMATEH, 31(2), 2010, 93-98.

[5] Tompkins F.D., Bledsoe B.L., *Vibratory furrow opening tool for minimum tillage planters*, Transactions of the ASABE, 22(3), 1979, 0498-0503.

BIODEGRADABILITY OF HYDRAULIC FLUIDS

Sava ANGHEL[1], INOE 2000 – IHP; Dipl.Eng. Alina Iolanda POPESCU, INOE 2000 – IHP; Ph.D.Eng. Cezar Iulian GARLEANU, INOE 2000 – IHP

ABSTRACT

Hydraulic fluids problem is a current research topic generated by their interface with the environment and their action with hydraulic equipment they serve. Environment imposes conditions of rapid degradation of hydraulic fluid and hydraulic systems require keeping a longer period of time fluid drive performance. To solve environmental conditions occurring biodegradable liquid. Normally should be introduced control means of liquids performance and their influence on hydraulic equipment.

1.INTRODUCTION

Agricultural machinery, construction machinery and transport bodies working for operating hydraulic systems. In these systems drive fluids are harmful to the environment. Agent is using hydraulic fluids based on mineral oil or synthetic and biodegradable fluids. If using simple mineral oils or additives, it was observed that while they suffer physical and chemical changes that decrease the safe operation of facilities and equipment; oils degrade, aging and become worn. Oil degradation is due to internal changes (thermal and chemical degradation of hydrocarbon components and additives, the breakdown electric field) and external - contaminants in the external environment (produced by incomplete combustion, soot, water, metallic particles, etc.). Biodegradability in the event of accidental oil discharges or spills is the ability of a substance, a lubricant to be decomposed by organisms or bacteria that live in soil and in surface water. Combined action effects of these factors are: decreases of lubrication and flow properties, increases of organic acidity and saponification number as well as decreases of flammability temperature.

2. METHODOLOGY

Assessment of oil degradation and replacement criteria of used oil are established by comparing periodic physico-chemical characteristics relative to baseline. Sometimes, changing the oil is determined experimentally and indicated by used oil production company and is done after a certain period of time or after a certain distance (for vehicles).

Located in the EU and in the U.S. waste oils are collected systematically and recovered by regeneration. Regeneration is performed after a preliminary purification physics (" pre heat ") which consist of oil vacuum distillation or treatment with selective solvents or chemical reactions with H_2 treatment. Synthetic oils is of interest to obtain better characteristics or different from mineral oils. Are used alone or mixed with mineral oils where they do not give good results. Currently used at very low temperatures (polar regions) or above 200^{o}C (have much higher thermal resistance than mineral oils due to Si-O bonds , C-F bonds, C-O bonds), for fine mechanisms or supersonic aircraft. Are used suitable additives for intended domain.

Have the following physico-chemical characteristics:
- linear structure as flexible , with very few side chains without polar groups that can determine the association of molecules; - high - boiling point , low freezing , high flame-retardant ; - high - thermal-oxidative stability; - compatibility with substances and materials in contact .

[1]Cutitul de Argint Street, No.14, District 4, Bucharest, tel.+4021 /3366420 , sava.ihp@fluidas.ro

The most performant are silicone oils with excellent lubricating qualities, used to working mechanisms at high temperature variations in supersonic aircraft, vacuum technology, precision instruments, compressors and hydraulic fluids. LUBASYST company produces a wide range of high performance biodegradable hydraulic oils.

PLANTO ENVIRO HYD 46 HVI

Hydraulic fluid, high performance, rapidly biodegradable ester based saturated selected with high stability, thermal and oxidation, meets and exceeds the requirements of ISO 15380 : HEES 46, nontoxic, received European Ecolabel (Euro Marguerite) according to European 2005/360 EC .

PLANTO ENVIRO HYD 46 S

Hydraulic fluid, high performance, rapidly biodegradable ester based fluid, clean water (according to German law), meets and exceeds the requirements of ISO 15380 : HEES 46, nontoxic , received European Ecolabel (Euro Marguerite) European Directive 2005 / 360 EC.

PLANTOHYD 40 N

A hydraulic fluid based on vegetable oil containing additives to improve the resistance to oxidation and stability to aging. Rapidly biodegradable. Temperature range: - 270ºC to +700 ºC. Exceeds ISO 15380 specifications HETG. VDMA 24 568 change recommendations should be followed. Hydraulic oil formulated based on rape. Environmental Recognized by label -Blue Angel .

PLANTOHYD S – NWG

Hydraulic and organic oils, based on synthetic, special esters. Series PLANTOHYD S- NWG meets ISO 15380 HEES and German legal requirements on clean substances for water . VDMA 24 569 change recommendations should be followed.

PLANTOHYD S

Hydraulic and general oils, lubricating, based on synthetic ester. Temperature range : -35 ºC to +900 ºC. Rapidly biodegradable. Exceeding ISO 15380 HEES. VDMA 24 569 change recommendations should be followed. Approved by BOSCH REXROTH(BRUENINGHAUS) and SAUERSUNDSTRAND .

PLANTOLUBE POLAR S

Hydraulic oil based on synthetic esters, saturated. Environmentally it is rapidly biodegradable. Very low freezing point. Universally applied at temperatures ranging from - 550ºC to +900 ºC. Exceeds ISO 15380 HEES . VDMA 24 569 change recommendations should be followed.

PLANTOSYN 3268

Universal hydraulic oil, multigrade, rapidly biodegradable synthetic esters based, fully saturated. Environmental Recognized by tag - Blue Angel .

ECO 3268 PLANTOSYN

Universal hydraulic oil, multigrade, rapidly biodegradable ester based. Environmental Recognized by tag - Blue Angel .

PLANTOSYN 46 HVI

Ester -based hydraulic oil completely saturated. Environmentally because it is rapidly biodegradable. Suitable for all hydraulic systems. Excellent EP performance. Tested and approved by BOSCH REXROTH (BRUENINGHAUS) at axial piston pumps and SAUER - SUNDSTRAND . Exceeds ISO 15380 HEES 46. Change recommendations VDMA 24 569 must be respected.

In the case of a pollution accident of the environment with hydraulic oil based on petroleum, its biodegradation in time consists in decomposing under the action of bacteria and fungi and oxidative transformation. Degradation coefficient is dependent on the temperature, O_2 availability of nutrients and also on the type of oil. Lighter components degrade faster, the temperatures most favorable microorganisms growth are situated above value of 25 ^oC. A part of the carbon present in the oil is used by microorganisms in the process of feeding and forming of biomass, which requires, among other nitrogen and phosphorus:

1kg HC+2.6kg O_2 +70g N ------------- 1,6kg CO_2+ 1kgH_2O+ 1kg biomass

Biodegradation of oil is a natural phenomenon of degradation that occurs very slowly and can be incomplect.

Another factor that matters when hydraulic oil is the pollution and pollutants holding capacity of soil depending on the soil type, presented in the following table.

Table1: Pollutants holding capacity of soil depending on the soil type

Soil type		**Pollutants holding capacity of soil , R, 1/m^2**
Coarse gravels		5
Coarse gravels and sands		8
Medium coarse sands		15
Fine and medium sands		25
Fine sands		40

Hydraulic equipment from hydraulic drive systems of machinery is designed to achieve certain operating parameters which are closely related to performance of used hydraulic drive liquids. While these parameters may vary due to degradation. Therefore occurs the problem of finding solutions to determine wear of hydraulic fluids and wear of hydraulic equipment caused by the action of various components of the liquids on the equipment. For this in Romania to INOE 2000 IHP in collaboration with SC LYRA PROD SRL was made a device that can determine the wear of hydraulic fluid or hydraulic equipment in time: Stand for comparative testing at endurance of hydraulic systems with hydrostatic rotary pumps.

Fig.1 Stand for comparative testing at endurance of hydraulic systems with hydrostatic rotary pumps

Stand executed after the programme INNOVATION, by winning a a check is based on a patent for comparative testing at endurance of hydraulic systems with hydrostatic rotary pumps. You can test different types of liquids by comparing them with standard liquid. It can test at endurance and determine interaction of different types of fluids on hydraulic equipment wear or premature wear of biodegradable fluids. It is used the following testing stand scheme:

M	Electric engine
Man	Pressure gauge
V	Beaker
B	Tank
P	Pump
S	Pressure valve

Testing Stand Scheme

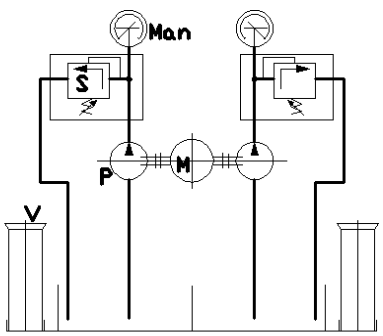

The stand consists of two separated hydraulic circuits, each formed from a pump, a tank, a pressure valve, a pressure gauge and a beaker. Tests are made by comparing the wear of liquids or of pumps that worked in identical conditions, on a circuit being used sample liquids and on the other being used standard liquids. The electric motor is 0.75 kW, 2750 rev / min , with two shaft ends, pressure valves can be adjusted to the maximum pressure of 220 bar, beaker is 1 dm^3 .

By comparing the leaks in beaker in the two circuits under identical conditions can be determined the liquids wear by varying the viscosity of liquids or pumps wear in operation after some time.

The stand is designed also to be used transducers of moment, pressure, flow and temperature the test being performed through your PC using an appropriate software.

It can run following types of comparative and endurance tests:

- Determining the performance of a liquid by comparison with a standard liquid
- Determining the interaction of a liquid on the hydraulic equipment
- Determining the performance of a hydraulic fluid at low temperatures
- Determining the performance of a liquid at different operating pressures

3. CONCLUSION

By making the testing stand by INOE 2000 IHP in collaboration with SC LYRA PROD IMPEX SRL has created the possibility of solving the conflicting problem regarding the quality of hydraulic drive fluids from the machinery systems used in agriculture, transport or construction.

References

[1]. LUBASYST Catalogue

[2]. http://www.rmri.ro/EU_2850/Downloads/Depol/SuportCurs2.pdf

[3].Vlăduţ V., Matache G., Bungescu S., Biriş S., Paraschiv G., Atanasov At. – *The analysis of lubrificants wchich can be used in agriculture and food industry. The development of some biodegradable lubrificants, Proceedings of the Second International Conference* "RESEARCH PEOPLE AND ACTUALTASKS ON MULTIDISCIPLINARY SCIENCES", vol. 2, pag. 142-152, ISSN 1313-7735, 10-12 Iunie 2009, Lozenec, Bulgaria**;**

STUDY OF OPTICAL FIBER SENSORS REGARDING CORROSION DETECTION FOR BUILDING EFFICIENCY IMPROVEMENT

Andrei Badea[1], Florin Dragan[2], Laurentiu Fara[3], Paul Sterian
Polytechnics University of Bucharest, Faculty of Applied Sciences

Abstract: Steel corrosion resulting from the penetration of chloride ions or carbon dioxide is a major cause of degradation for reinforced concrete structures. In the last decades, fiber optic based sensing technology has come up with may solutions to this problem by finding simpler and cost effective methods of implementation as well as, increasing the accuracy level in structural health monitoring of concrete structures . In this work, the principle of a Fiber Optic Sensor (FOS) based on Enhanced Fiber Optic Corrosion Sensor (EFOCS) is being discussed. This method aims to detect, measure and obtain the drawbacks in concrete structures and also quantify the corrosion level. Finally, a unique and special coating material (PDMS) is being applied on the EFOCS sensor for performance and accuracy enhancement [1]. Comparison between traditional corrosion detection methods and the EFOCS approach emphasizes the advantages of this method regarding building efficiency improvement for some types of concrete structures.

1. INTRODUCTION

In recent years, the demand for the development of new materials to strengthen, upgrade and retrofit existing aged and deteriorated concrete structures has increased rapidly. The continuing deterioration and functional deficiency of existing civil infrastructure elements represents one of the most significance challenges facing the world’s construction and civil engineers. Deficiencies in existing concrete structures caused by initial flawed design due to insufficient detailing at the time of construction, aggressive chemical attacks and aging of structural elements enhance an urgent need of finding an effective means to improve the performance of these structures without additionally increasing the overall weight, maintenance cost and time. In the last 60 years, a large number of civil concrete structures have been built; many of these structures, particularly in off-shore regions have now deteriorated and require repair in a short period of time. Moreover, the increase of traffic volume and population in many developing countries is causing the demand to upgrade existing concrete structures to increase [5]. The damage of reinforced concrete (RC) structures through reinforcement corrosion and residual capacity are the most important issues that concern engineers. These problems occur not only in constructed concrete structures but also in structures strengthened by externally bonded steel reinforcements.

The durability and practicability of reinforced concrete structures is one of the primary concerns in the present day science. Because, majority of modern physical infrastructures are being constructed of reinforced concrete structures. These concrete structures can be degraded or

[1]badea_an@yahoo.com
[2]dr.florin28@yahoo.com
[3]lfara@renerg.pub.ro

deteriorated for various reasons such as low funding, population growth, tighter health and environmental needs, substandard installation, insufficient inspection and maintenance, and lack of uniformity in design, construction and operation practices usually have adverse effects on reinforced concrete structures [1]. There are various types of concrete degradation but steel corrosion is one primary cause for concrete deterioration. Naturally, inside concrete structures, steel is surrounded by the alkaline environment and also in a passive condition with a negligible corrosion rate. Nevertheless when the concrete cover of the steel is being infiltrated by carbon dioxide and chlorides to get in touch with the steel, the corrosion rate also gets accelerated. To avoid such situation, a proper, effective and accurate steel corrosion detection method is highly required to be developed. In this paper, we analyze a number of new fiber optic based sensing methods for detecting the onset of steel corrosion inside reinforced concrete structure with particular application on concrete structures.

The novel corrosion detection method is based on the simple principle of light reflection illustrated in Figure 1. An optical fiber is stripped and cut with a cleaver to produce a flat surface at its end that is perpendicular to the fiber axis. Using the ion sputtering technique, an iron thin film (thickness around one hundred to several hundred nanometers) is deposited on the cleaved fiber end. Light is then sent through the optical fiber and the reflected light intensity is monitored as a function of time. Initially, the iron film at the end of the fiber acts like a mirror and all or most of the light is reflected (Figure 1a). As corrosion occurs, the film thickness decreases with time. Consequently, the reflected signal also drops (Figure 1b). Finally, after the film is completely removed, the reflected light intensity will return to the level for the cleaved glass surface [3].

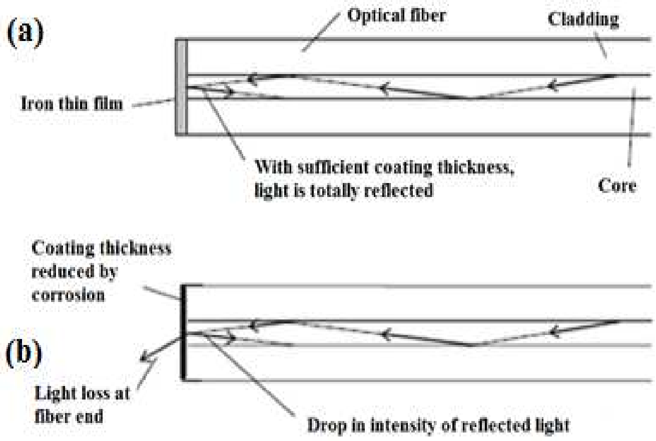

Fig. 1.Illustration of the corrosion sensing principle.

Compared to other corrosion sensors, the ‘reflection’ sensor possesses a number of advantages. Since the principle is very simple, interpretation of results is easy and direct. It is applicable to corrosion induced by either chloride penetration or carbonation. The technique does not require the use of special optical fibers, so low-cost single mode telecommunication fibers can be employed. In the sputtering process, a large number of fibers can be placed in the sputtering chamber and coated at the same time. Mass production of the sensor at low cost should therefore be possible. Moreover, with the small size of the sensor, it can be retrofitted to existing structures. Two plausible ways to install the sensor are illustrated in Figure 2.

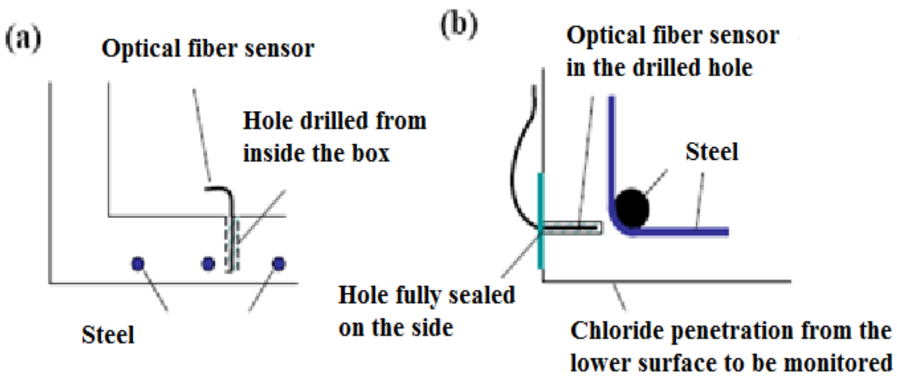

Fig. 2. Plausible ways for retrofitting the sensor on an existing structure with (a) boxed section, (b) solid section.

For a bridge with boxed section, a hole of required depth can be drilled from the inside of the box for placement of the sensor (Figure 2a). To monitor chloride or carbon dioxide penetration from a surface of a solid section, the hole can be drilled on a perpendicular surface and sealed (Figure 2b). With these approaches, the drilled hole will not act as an easy diffusion path that will affect the monitoring results.

2. SCIENTIFIC INNOVATION AND RELEVANCE OF THE WORK

In reinforced concrete infrastructure, the steel corrosion occurs due to penetration of chloride ions or carbon dioxide. This is one of the most important causes of deterioration of reinforced concrete structures and usually has a very negative effect on modern science both in safety issues and economically. The objective of the present investigation is to develop a low-cost FOS based sensing technology for detecting steel corrosion inside reinforced concrete infrastructures and also measure the level of the corrosion occurred in the specific section so necessary steps can be taken effectively. Over the time, different type of approaches is being studied, applied and tested to detect the steel corrosion effectively and also measure the corrosion rate appropriately. All the above proposed method and technology certainly lacked in three most important areas while detecting steel corrosion inside concrete structures [1].

First, installations of all these sensing methods are very complicated and often required professional assistance.

Second, most of these methods are only applicable in newly constructed concrete structure. That means, these sensing methods need to be installed while constructing the structure which is a huge limitation.

Third, excessive high cost is needed for designing and fabricating these methods. So to overcome these problematic areas, a new FOS based sensing method to detect corrosion inside concrete structures has been studied and presented in this paper.

3. OBJECTIVES

The main objectives of this study are as follows:
1. To analyze the design and fabrication of a novel and unique FOS based sensing technology to detect and measure the level of corrosion inside concrete structures.
2. Can be applied both in new and used concrete structure.
3. Application of PDMS as a coating of optical fiber cable and analysis of overall performance.
4. Making sure of overall performance by verifying the output results with provided data.
5. Overcome the durability and feasibility issue.
6. Enhancement of proposed sensor with PDMS coating and output analysis.

4. A DESIGN OF FOS BASED ENHANCED FIBER OPTIC CORROSION SENSOR (EFOCS)

An Enhanced Fiber Optic Corrosion Sensor (EFOCS) is being applied here [9]. It is manufactured of one FBG sensor and two specific sized identical reinforcing bar and then it is essential to package up with the sample concrete slab in a particular method. These two rebars are a special type of screw-thread steel. First, rebar 1 is split in to R1-1 and R1-2, and rebar 2 is split in to R2-1 and R2-2. Second, a FBG sensor is set vertically to the twin rebar axis and bonded on their planed surface after R1-2and R2-2 are placed alongside. Third, R1-1 and R2-1 are attached to R1-2 and R2-2, respectively. Last, the FBG sensor and twin rebar elements are installed together with concrete structure. Usually, the output of the corrosion of the twin rebar represents in the shift of the maximum wavelength of the grating because of their volume growth. With the purpose of balancing this specific temperature effect, a fiber optic temperature sensor (FOTS) is applied here. Fig. 3 represents the standard schematic diagram of enhanced fiber optic corrosion sensor [8].

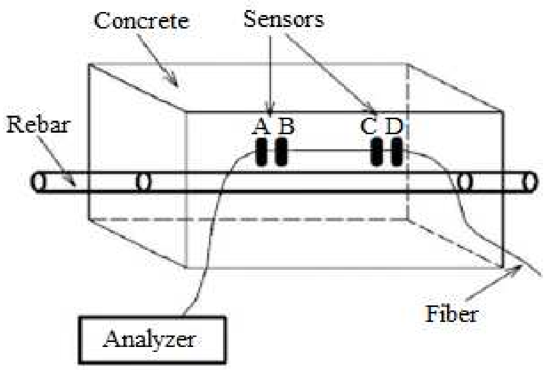

Fig. 3. A standard schematic diagram of enhanced fiber optic corrosion sensor (EFOCS).

5. PDMS COATED FBG SENSOR METHOD

In the recent years, FOS based fiber Bragg grating (FBG) sensors have been studied, researched and experimented extensively for sensing and measuring several types of physical parameters such as strain, bending, pressure, temperature, and chemicals. By applying FBG sensors, the environmental perturbations on the FBG sensors, such as strain, temperature, and pressure, can be straightforwardly calculated by monitoring the degree of the Bragg wavelength shift induced by the amount of the FBG bend. Nonetheless, for chemical sensing purpose, ordinary FBGs are not entirely suitable for practical applications because optical fibers do not respond to chemical solutions. Furthermore, traditional FBGs are intrinsically not sensitive to a surrounding-medium refractive index (SRI) variation because optical fields are well-bound within a fiber core and a light coupling with the SRI is screened by a thick cladding layer. So to overcome these problems, long- period fiber gratings (LPFGs) are generally used for chemical sensing applications, where the light couplings between the core and the cladding modes are present, associated an optical interaction linking the cladding and an external medium. Here, the Figure 4 represents the standard schematic diagram of PDMS coated FBG sensor [1].

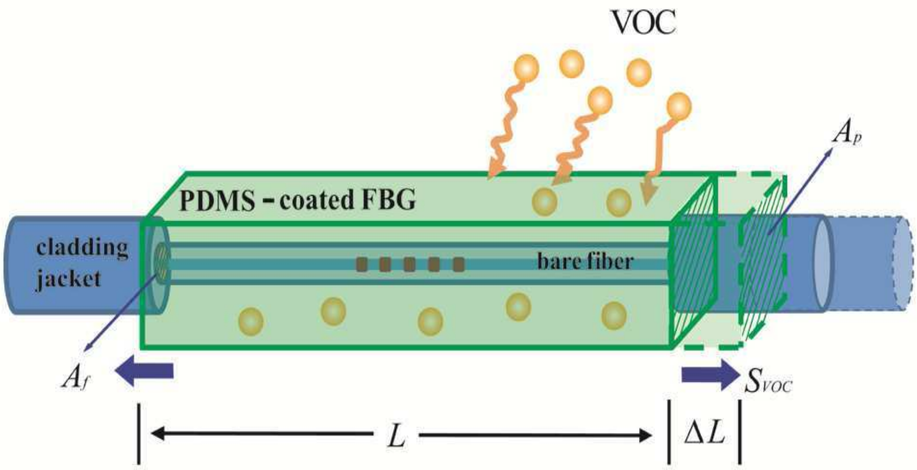

Fig. 4. A standard schematic diagram of PDMS-coated FBG sensor.

So, to effectively determine the corrosion level of a concrete structure, here a special FBG sensor has been applied with specific PDMS coating for enhanced sensing and measuring the concrete corrosion. After applying the special PDMS coating on the FBG sensor, it will be introduced into the EFOCS. After that, the output results from half cell method, standard EFOCS method and enhanced PDMS coated EFOCS method will be observed, analyzed and verified. Then the accuracy of these three proposed methods will be compared and further scope of improvements will be discussed.

6. CONCLUSIONS

All existing electrical instruments and most fiber optic sensors are ‘point’ sensors that can only detect changes at local points in a structure. Such ‘point’ measurements can provide information on the behavior of the structure, and areuseful for the verification of design assumptions. Also, the measured data may be employed in a feedback loop to facilitate the active control of a structure. However, for health monitoring of concrete structures, ‘point’ measurements are not effective. Degradation of concrete structures occurs through the formation and propagation of localized cracks. Since cracks in reinforced concrete structures have little effect on structural stiffness, the displacement, strain or corrosion at a particular sensing point is insensitive to cracking unless the point is very close to the damage location. To guarantee the detection of each potential corrosion affected spots, the required number of sensing points will be excessively large for any monitoring scheme to be practical [2].

There are different types of concrete degradation but steel corrosion is one of the major reasons for severe concrete deterioration. Traditional detection methods are not very effective and user-friendly comparing to the modified sensor based technologies. Especially, FOS based technology is very easier to operate and durable. Here, a unique coating of PDMS material for the fiber optic sensor has been proposed and with appropriate research and further study, the detection accuracy enhancement will be analyzed.

In the near future, we are thinking to analyze the EFOCS utilization possibilities for improvement of efficiency of Romanian building materials, integrating the results of these high-performance optical sensors in the world with the research of Romanian scientists in the field.

References

[1] O. Sidek, S. Kabir, M. H. Bin Afzal, “*Fiber Optic-based Sensing Approach for Corrosion Detection*”, PIERS Proceedings, Suzhou, China, September 12–16, 2011

[2] C.K.Y. Leung ,“*Fiber optic sensors in concrete: the future?*”, NDT&E International 34, 85–94, 2001

[3] C.K.Y. Leung, K. T. Wan, L. Chen, “*A Novel Optical Fiber Sensor for Steel Corrosion in Concrete Structures*”, Sensors, Vol. 8, 1960-1976, 2008

[4] P. L. Fuhr, D. R. Huston, “*Corrosion detection in reinforcedconcrete roadways and bridges viaembedded fiber optic sensors*”, Smart Mater. Struct.7, 217–228, 1998

[5] K.T. Lau, “*Fibre-optic sensors and smart composites forconcrete applications”*, Magazine of Concrete Research, 55, No. 1, February, 19–34, 2003

[6] S. Kabir, P. Rivard, D.C. He, and P. Thivierge, “*Damage assessment for concrete structure using image processing techniques on acoustic borehole imagery*”, Construction and Building Materials, Vol. 23, 3166-3174, 2009.

[7] J. P. Broomfield, *Corrosion of Steel in Concrete*, E & FN SPON, London, 1997.

[8] 19. Park, C.-S., Y. Han, K.-I. Joo, Y. W. Lee, S.-W. Kang, and H.-R. Kim, Optical detection of volatile organic compounds using selective tensile effects of a polymer-coated fiber Bragg grating," Optics Express, Vol. 18, No. 24, 24754, 2010.

AN INNOVATIVE TECHNIQUE OF CAR NOISE ANALYSIS BASED ON MULTIRESOLUTION ALGORITHMS

(a) Luigi Maxmilian Caligiuri[1], (b) Francesco Lamonaca, (a) Alfonso Nastro, (c) Monica Vasile

(a) Department of Chemistry and Chemical Technologies, University of Calabria, Rende (CS), Italy; (b) Department of Informatics, Modelling, Electronics and System Engineering, University of Calabria, Rende (CS), Italy; (c) Medical School, Ovidius University, Costanta, Romania.

ABSTRACT

The most part of acoustics signals associated to real world phenomena are non - stationary. A particularly important example is represented by signals associated to motor vehicular transits, whose noise environmental impact is evaluated by considering the features associated to each of them. The traditional noise signal analysis techniques, based on Fourier transform and digital filtering, are generally not be able to adequately characterize such non stationary signals. In this paper we'll discuss the use of multiresolution time-scale and time-frequency analysis, based on Wigner-Ville transforms, to the study of noise signal produced by automotive traffic, showing that the suitable employ of these techniques is able to properly characterize the motor vehicular features and their environmental noise impact.

1. INTRODUCTION

Acoustic and vibrations measurement are fundamentally printed to provide quantitative physical description of such phenomena in order to extract the required to control their effects on environmental and public health such as annoyance, hearing damage, mechanical stress and so on. Most of the acoustical and vibrational processes able to generate environmental pollution and adverse health effect are represented, when expressed in terms of short L_{eq} [1] , by non - stationary signals, namely whose spectral content varied with time without a predictable trend, as for example noise generated by urban and extra - urban car, track and motorbike traffic.

This type of noise generally represents the main contribution to the overall noise level in the middle and big town but it can be also extremely important in small cities when the background noise level is low. The annoyance due to traffic noise is not only related to the overall acoustic energy generated during a given time interval, but also to the spectral content of each vehicular passing that is different among the different vehicular categories. For this reason is fundamental, to ensure the validity of the measurements and realize adequate health safeguard actions, to properly recognize and characterize the noise events produced by vehicular transits, in particular distinguish them from those produced by other sources (this is particularly important, for example, for the measurements made in absence of operators).The evaluation of noise impact generated by vehicular traffic is usually achieved by means of the A - weighted equivalent sound pressure level L_{Aeq} associated to day and night reference time intervals respectively.

Nevertheless, the use of energy - integrated quantities as Leq doesn't give us the possibility to characterize the time - frequency content of the specific noise events associated to urban traffic. Even considering the time - history of sound pressure level, expressed as

[1]Arcavacata di Rende (CS) - ITALY, +390984492105, max.caligiuri@gmail.com.

short - time Leq, the traditional noise signal analysis techniques based on the Fourier Transform, as Fast Fourier Transform (FFT), and digital filtering (1/n of octave) implemented in most of the frequency analyzers on the market, face some critical description limitations when the signals to be analyzed are highly non-stationary, because they does not tell about the time location of the frequency components of the spectra. In order to overcome these difficulties time-frequency and/or time-scale analysis techniques, getting the spectra associated to samples of signal that can be considered sufficiently stationary, must be applied.

The Wigner-Ville transform (WVT) represent one of the most important examples of these techniques. In this work we'll discuss the application of Smoothed Wigner-Ville Transform (SWVT) to the noise signals associated to the transits of the most important types of vehicles that constitute urban traffic.

We'll show that, with a suitable choice of parameters related to these transforms we can be able to adequately study the main features of urban vehicular noise sources. The work represents a further application of the analogous study already performed on railway noise some years ago [2].

2. FUNDAMENTALS OF MULTIRESOLUTION ANALYSIS

The WVT is a quadratic form and represents a time-frequency energy density computed by correlating the original signal by a time and frequency translation of itself [3,4]:

$$P_{WV}(t,\omega)=\int_{-\infty}^{\infty} f\left(t+\frac{\tau}{2}\right) f^{*}\left(t-\frac{\tau}{2}\right)e^{-i\tau\omega}d\tau \tag{1}$$

The application of the WVT, in the native form above, is nevertheless limited by the presence of interferences terms of negative energy due to the non linearity of the transformation. In order to attenuate these effect we have introduced a “smoothing” kernel q that regularises the WVT, obtaining the so called Smoothed Wigner – Ville Transform (SWVT):

$$P_{SWV} f(t,\omega)=\int_{-\infty}^{\infty}\int_{-\infty}^{\infty} P_{WV} f(\bar{t},\bar{\omega})\theta(t,\bar{t},\omega,\bar{\omega})d\bar{t}d\bar{\omega} \tag{2}$$

The kernel function θ can be composed by introducing a function Σ such that:

$$P_{SWV} f(t,\omega)=\int_{-\infty}^{\infty}\int_{-\infty}^{\infty}\Sigma(\alpha,\tau) f\left(t+\alpha-\frac{\tau}{2}\right) f^{*}\left(t+\alpha+\frac{\tau}{2}\right)e^{-i\omega\tau}d\alpha d\tau \tag{3}$$

with

$$\Sigma(\alpha,\tau)=g(\alpha)\otimes h(\tau) \tag{4}$$

where g is called “time smoothing window” and h is called “frequency smoothing window”, whose widths can be separately adjusted.

3. ANALYSIS OF THE MEASUREMENT RESULTS

In the figures 1-3 are shown the time-histories of the signals s_1, s_2, s_3 respectively associated with the transits of:

1) CAR;
2) MOTORBIKE;
3) TRUCK.

On the x axis is represented time, on the y axis the normalized amplitude in arbitrary units.

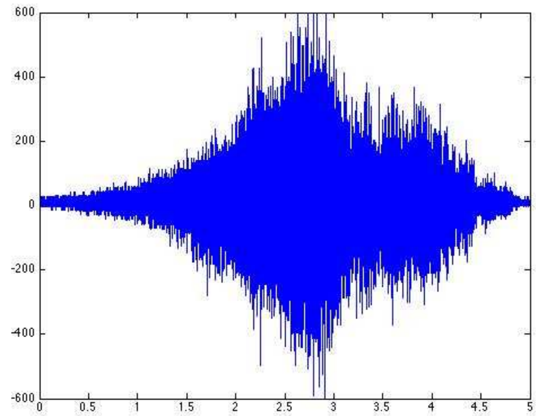

Figure 1: time history of signal s_1

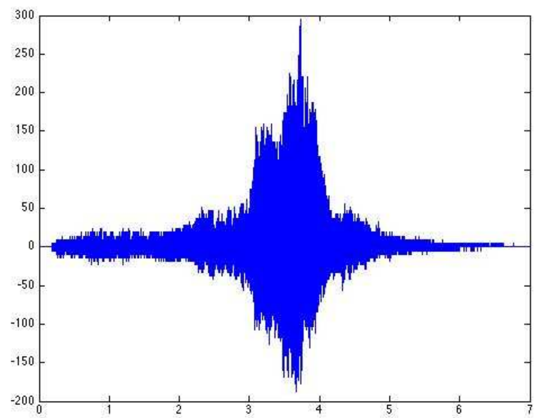

Figure 2: time history of signal s_2

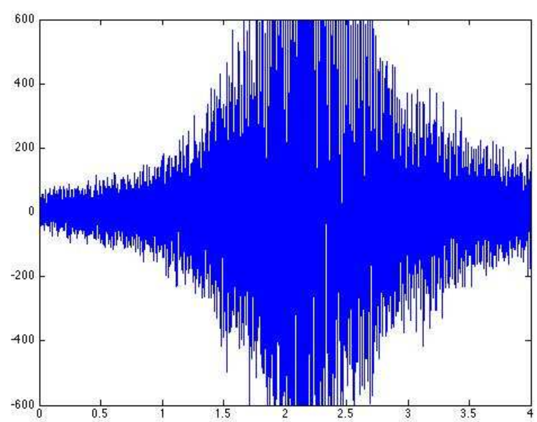

Figure 3: time history of signal s_3

The results obtained by means of this analysis strongly depend on the g and h windows widths. It has been shown [5] that the use of rectangular windows of length $g = 80$ points and $h = 256$ points achieves a good compromise between simultaneous time - frequency resolution and image clarity.

The fig. 4, 5 and 6 show the time-frequency energy distributions corresponding to the SWVT of the signal s_1, s_2 and s_3 obtained by means of rectangular smoothing windows. On the x axis time (s) is represented, on the y axis the frequency (Hz) and, as before, the image points intensity is proportional to SWVT coefficients.

The fig. 4 clearly shows the time behaviour of the frequency spectrum of signal associated to the car transit, prevalently characterized by the presence of low and middle frequency components ($f < 2kHz$). We can observe the “red shift” of the frequencies due to the Doppler effect.

In the transit of the motorbike (fig. 5), the most important feature is represented by the “two - zones” spectrum one placed at middle frequencies and another placed at very high frequencies: the first one ($f < 1kHz$) is substantially produced by aerodynamic noise while the second one by the very high ($f > 7.5kHz$) engine rpms.

Finally, the fig. 6 shows that, during the truck pass – by, the low frequencies components are the most important ones and determine a “three – zones” spectrum whose particular form is associated to the track shape and speed which, in this case, creates a less pronounced Doppler effect.

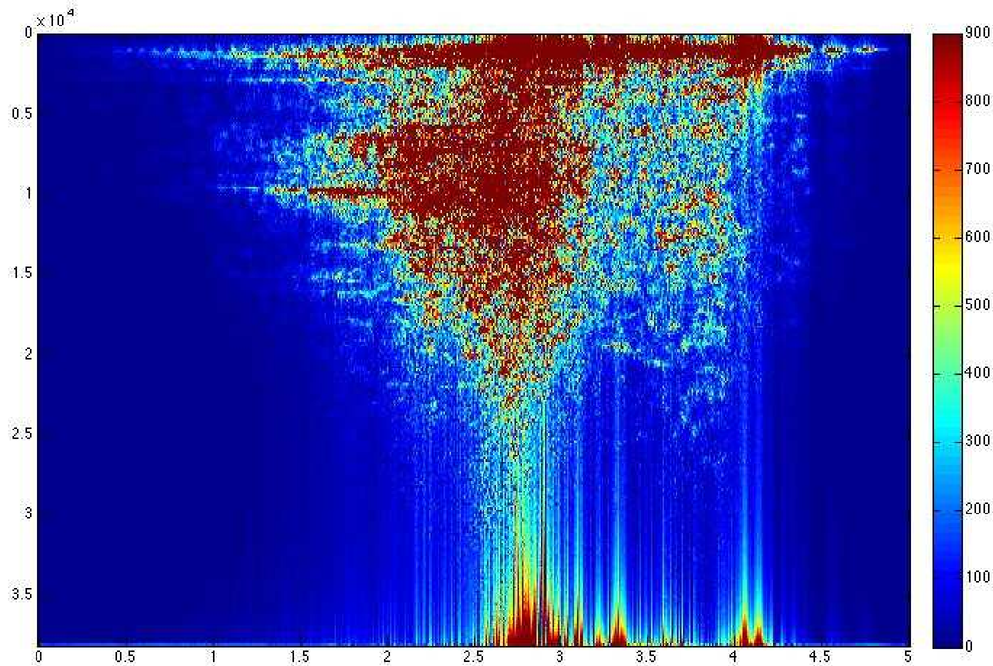

Figure 4 :SWVT of signal s_1. Time window 80 points, frequency window 256 points.

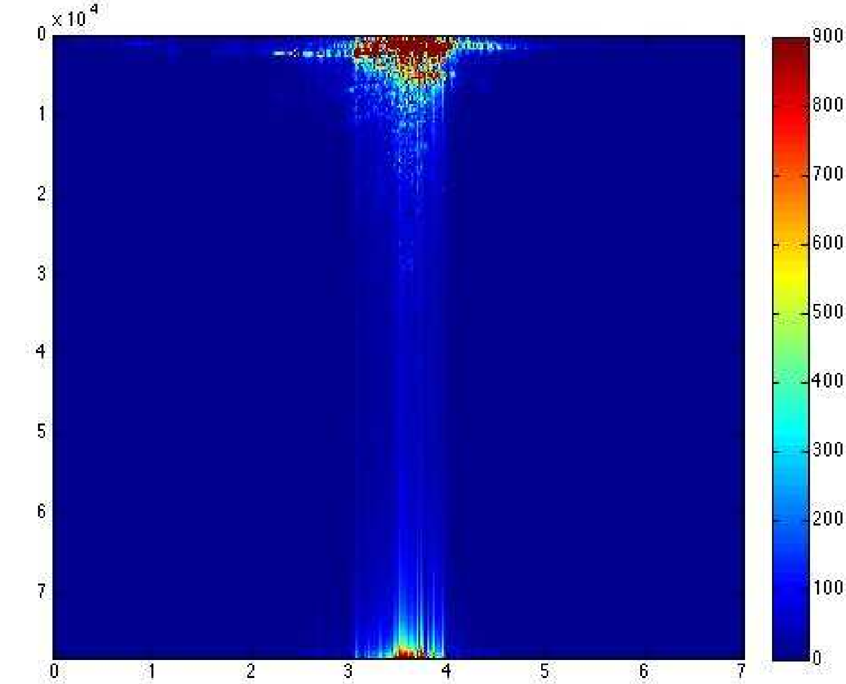

Figure 5: SWVT of signal s_2. Time window 80 points, frequency window 256 points

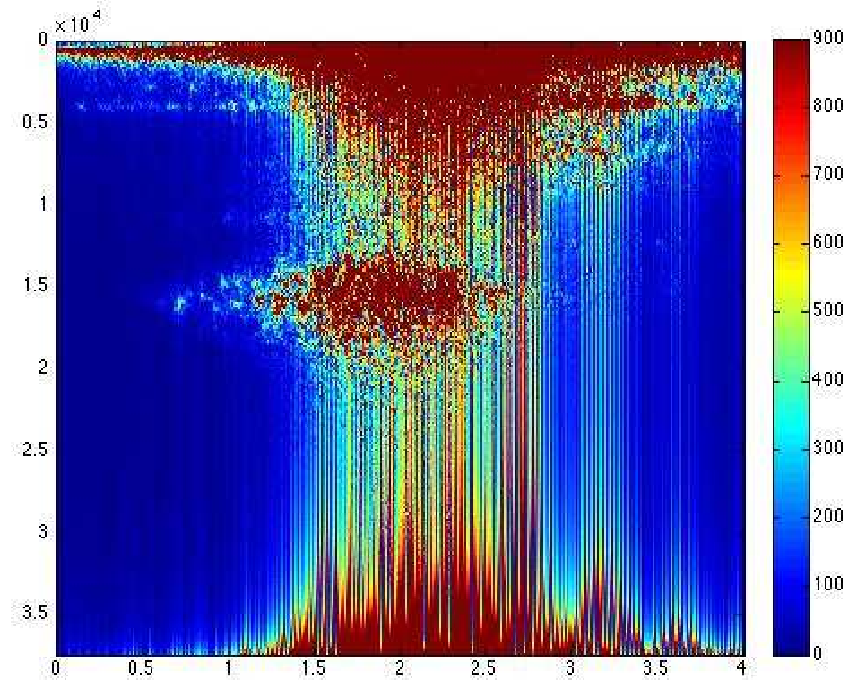

Figure 6: SWVT of signal s_3. Time window 80 points, frequency window 256 points

4. CONCLUSIONS

As we have seen a suitable choice of the parameters related to SWVT allow us to properly analyse the noise signals associated to the transits of motor vehicles, making us able to distinguish the different noise events one from another, and deduce the relevant features of these noise sources.

Furthermore we must remind that generally it is advisable to make use of both these analysis techniques, especially considering their very different features as regards resolution and the SWVT computational difficulties in the case of long duration signals.

References

[1] ISO 1996-1 (1982) "Acoustics – Description and measurements of environmental noise – Part 1: Basic quantities and procedures".

[2] L.M. Caligiuri and A. Sabato, Multiresolution analysis of environmental noise signals: an application to railways noise, *Proceedings of IMTC 2004, The 2004 Instrumentation and Measurement Technology Conference" IEEE, Como, ITALY*

[3] S. Mallat, A wavelet tour of signal processing (Academic Press,1999)

[4] W. Meyer, Wavelet Algorithms and Application (SIAM, Philadelphia, 1993)

[5] L.M. Caligiuri and A. Sabato, Time-scale and time-frequency analysis of complex noise scenario by means of Wavelet and "smoothed" Wigner-Ville transforms, *Proceedings of INTERNOISE 2003, South Korea, August 25-28, 2003*

COMBINED SYSTEMS USING RENEWABLE SOURCES – A SOLUTION FOR INCREASED ENERGETIC AUTONOMY

Cătălin Dumitrescu[1], Hakon Sundt[2], Petrin Drumea [1],
Liliana Dumitrescu[1], Corneliu Cristescu[1]
[1] INOE 2000 – IHP, Bucharest, Romania
[2] SINTEF ENERGY RESEARCH, Trondheim, Norway

ABSTRACT

The article examines the possibilities of fulfillment by Romania of targets assumed by Directive 2009/28/EC, about the use of renewable energy in the perspective of 2020. Romania has significant renewable energy resources, type wind, solar, biomass, etc.; this allowed that the situation at the end of 2013, also presented in the article, to be very good, taking into account the fulfillment of national commitments. The article also presents several solutions of renewable hybrid type systems that can help ensure energy independence of consumers in remote areas; it is intended that these solutions form the basis of a joint project between Romanian and Norwegian research units

1. INTRODUCTION

Quality of EU member country involves aligning to the general and punctual objectives of European policy; such a set of targets is assumed in the field of renewable energies.

Romanian goals in the domain take into account the EU Directive for the use of energy from renewable sources (2009/28/EC – RES Directive). This directive is part of the package "Energy - Climate Change", which sets a series of targets for the EU by 2020, known as "20/20/20 objectives": by 2020, at Community level, should be reduced by 20% the greenhouse gas emissions, energy efficiency must increase by 20% and 20% of energy consumption should be from renewable sources.

On the other hand, Romania has significant quantities of renewable resources that were far under-exploited until now.

2. RENEWABLE RESOURCE SITUATION IN ROMANIA

Romania has a high potential of renewable energy sources, as can be seen in the table below.

Table 1: Romania’s energy potential of various renewable

Renewable type	Annual energy potential	Economic equivalent in energy (thousand Tep)	Application
Solar energy:			
- thermal	60×10^6 GJ	1.433,0	Thermal energy
- photovoltaic	1.200 GWh	103,2	Electricity
Wind energy	23.000 GWh	1.978,0	Electricity
Hydro Power	40.000 GWh	3.440	Electricity
Biomass and biogas	318×10^6 GJ	7.597,0	Thermal energy

[1] Cutitul de Argint nr. 14, sector 4, Bucuresti, 021 336 39 91, dumitrescu.ihp@fluidas.ro

Wind power, like other forms of renewable energy, knew in recent years an intensive use; in 2010, it covered 2.5% of world energy and growth in recent 2 years has been about 20% per year. The national strategy for the use of renewable energy said the wind potential is 14,000 MW (installed capacity), which can provide an amount of energy of about 23,000 GWh/year. This potential is used only to a limited extent, although there are many favourable areas in the country, where the wind speed exceeds 5 m/s, thus ensuring proper functioning. More important is the positioning of our country in the ranking of countries producing electricity using wind power; are noted large increases in recent years, as can be seen in Table 2.

Table 2: Installed wind capacity in various countries (MW).

Installed wind power capacity (MW)											
#	**Nation**	**2006**	**2007**	**2008**	**2009**	**2010**	**2011**	**2012**	**2013**	**last yr % growth**	**5 yr avg % growth**
-	European Union	48,122	56,614	65,255	74,919	84,278	93,957	106,454	117,289	10.2	12.5
1	China	2,599	5,912	12,210	25,104	44,733	62,733	75,564	91,424	21	53.1
2	USA	11,603	16,819	25,170	35,159	40,200	46,919	60,007	61,091	1.8	20.1
3	Germany	20,622	22,247	23,903	25,777	27,214	29,060	31,332	34,250	9.3	7.5
4	Spain	11,630	15,145	16,740	19,149	20,676	21,674	22,796	22,959	0.7	6.6
5	India	6,270	7,850	9,587	10,925	13,064	16,084	18,421	20,150	9.4	16.1
…	……………	……..	……..	……..	……..	……..	……..	……..	……..	……..	……..
19	Romania	2	7	10	14.1	462	982	1,905	2,600	36.5	692.1

From the table above we can see that Romania is ranked 19 in the world, and analyzing the full version of the table we see that in the EU, our country ranks 10.

Regarding solar energy, Romania enjoys very favourable conditions, more than half the year having an average over 1 kWh/m^2/day, with maximum values in June (1.49 kWh/m^2/day) and minimum values in February (0.34 kWh/m^2/day). A similar situation is registered in the biomass field, our country having significant resources, as can be seen in Table 1. In 2013 Romania obtained about 35% of electricity from hydropower, and the goal for 2020 is a share of 43%.

Due to these favourable conditions, the production of renewable energy reached a record level at the end of 2013, the total capacity of the existing projects in this sector exceeded 3,757 MW, 60% more than at the end of 2012. This value was achieved through the exploitation of wind turbines (2,459 MW), PV panels (740 MW), small hydro (505 MW) and biomass (53 MW).

Accelerate the exploitation of renewable resources can be realized using combined energy systems – for this is necessary to propose viable concepts tailored to the situation in Romania. Increasing the amount of energy (heat, electricity) that can be used in a certain area can provide user autonomy, the more important when centralized network is not available.

Decision-making bodies of all EU member countries are placed in front of the targets to be achieved by 2020, and for this purpose have been developed National Action Plans. In Romania was elaborated National Action Plan on Renewable Energy (PNAER), in 2010, by Ministry of Economy, Trade and Business Environment.

The final document was elaborated by a consortium led by the Institute for Energy Research and Modernization - ICEMENERG, under a project funded by the Ministry of the Economy Sectoral Plan for Research and Development in Industry. Besides these institutions, there are several entities with interests in renewable energy, in the categories of research institutes, technical and economic universities, state authorities, etc.

Beyond 2020, the Romanian Government is taking into account the elaboration of a strategy in the field, to predict the development of the energy sector until 2035. The new installed capacities on Renewable Energy Sources (according PNAER) are estimated to reach of 5,515 MW by 2035, which means a necessary investment of about EUR 9 billion, of which about 7 billion by 2020. According to the strategy, 4,440 MW will be represented of wind power. It is expected that 2,640 MW will be installed during 2011 to 2015, 800 MW in 2016-2020, 500 MW in 2021-2025, 300 MW in 2026-2030 and 200 MW in 2031-2035.

On the other hand, on the Romanian territory are eight development regions. In each region operates one agency that aims strategic planning to economic and social development of the region. Valorisation of renewable energy is an important component of regional strategies. Regional Development Agencies (ADR) manage development funds allocated to the regions by the EU. But there is not strategy / regional programs intended exclusively for energy from renewable sources. Such strategies in question are included in programs with broader themes (sustainable development, modernization of infrastructure, etc.).

3. TYPES OF EQUIPMENT USED IN ROMANIA, IN THE RENEWABLE ENERGY DOMAIN

Currently, renewable exploitation in Romania to produce large amounts of energy is made in the classic, mono-energetic systems, and the most used resources are hydro, wind, solar and biomass, in this order, and work systems are hydropower and small hydropower, wind farms, fields of solar panels and biomass plants. Exploitation of hydro and wind energy is performed in order to obtain electric power; solar panels, which are found in solar farms, are also used for electricity production and the biomass is used for heat production.

Using a type of renewable energy in a given area is depending on the availability of the resource; for Romania, several areas can be estimated by use of renewable energies, as shown in Figure 1.

Use of solar panels to produce thermal energy is limited, due to the lack of sunrise during the night and in some periods of the year. The disadvantage of solar panels can be removed if it works with another energy source.

Figure 1: Renewable energy in different areas of Romania

Legend:
I. Danube Delta (solar energy);
II. Dobrogea (solar energy, wind);
III. Moldova (micro-hydropower, solar energy and biomass);
IV. Carpaţi Montains (biomass, micro-hydropower);
V. Transylvanian Plateau (micro-hydropower);
VI. Western Plain (geothermal);
VII. Subcarpathians (biomass, micro-hydropower);
VIII. Southern Plain (biomass, geothermal and solar).

In last years, in the small size installations domain, intended for individual users, have appeared systems that combine the classic fuel burning (usually gas) with renewable sources (biomass or solar energy). The scheme of such an installations is presented below.

The installation comprises a main circuit in which thermal energy is produced using solar thermal panels and a secondary classic circuit (auxiliary), which can be electrically or with gas fuel (central thermal energy). These systems use storage tanks, electric pumps and a control panel. In the presented example, the quantities of heat produced by the two sources are collected in a bivalent boiler.

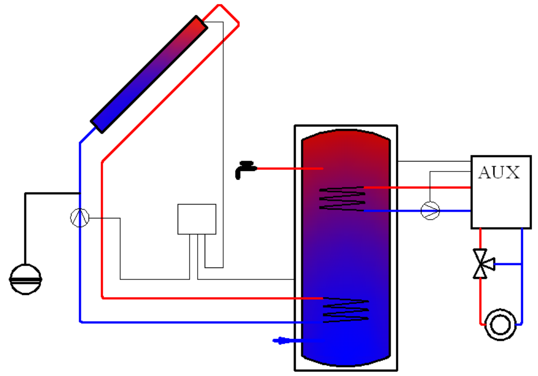

Figure 2: Schematic diagram of a system that uses solar panels and a classical source

Regarding the use of solar energy for the production of heat or electricity, in this moment the principle solutions are well-defined and hard to be improved. So, the solar thermal panels are achieved in two technologies: flat thermal panels, respectively evacuated (vacuum) tubes panels. The former has as main argument the price more affordable, but offers limited opportunities to exploit solar radiation in the absence of guidance system; using copper for absorbing radiation surfaces increases the efficiency, but raises the price.

Vacuum tube panels offer a higher yield, because the round shape of vacuum tube section and principle of operation allows higher exploitation of solar radiation, but their price is higher and thus less accessible to consumers. In this area, INOE 2000-IHP participated in a project to implement a solution for thermal panels having flat absorber made of aluminum, with a special geometry, that allows a higher recovery of solar radiation.

Regardless of the type of active element of the system, all variants for producing energy using thermal panels are based on the transfer of heat between the panels and a storage tank, by means of a heat transfer fluid.

It is therefore necessary coupling panels with an other system for producing thermal energy, during the night, in cloudy days and in cold season. The diagram below represents the materialization of Figure 2, the classical heat source being a gas burner.

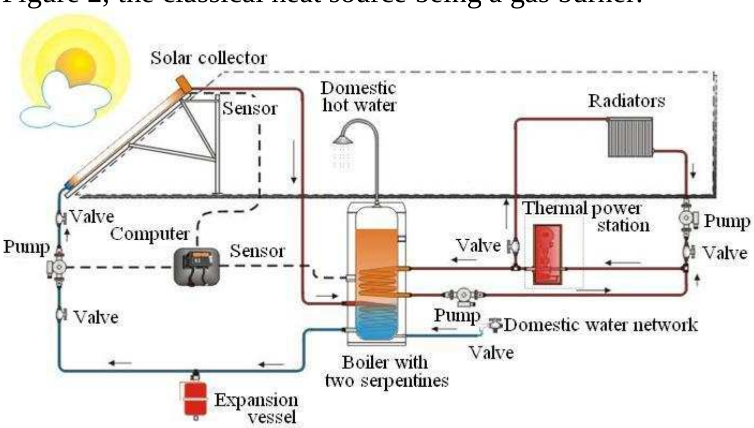

Figure 3: Solar thermal installation with thermal panels + boiler

If the classic power source is electricity, it is necessary an electric resistance heater mounted in the monovalent boiler, a polluting and expensive solution. In Figure 4 is shown an alternative, based on a patent application of INOE 2000-IHP.

A solution to increase the thermal energy is to combine thermal panels with a biomass energy module (gas generator + burner for biomass), that will provide thermal power during periods when sunlight is lacking or insufficient (figure 4).

In this case, the storage cylinder with one coil is replaced by a buffer tank with two coils, to store the energy from both sources - solar panels and biomass burner. Solar panels 1 heat the fluid that is moved by hydraulic unit 8. Pump in this unit is controlled by a controller 3, based on information from transducers 6 and 7. With the energetic module (consisting of gas generator 2 and burner 4), the energy produced by the solar panels is summed with that from biomass, by using the pump unit 9. If the heat produced is more than necessary to obtain DHW, the surplus is used for heating, with radiators 11 and the unit 10. Ordering of all actuating elements (pumps) is performed by the controller 3. Installation so designed, with 2 solar panels and an energy module approx. 10 kW, can cover the needs of a family of four members, at an average of 50 liters/day/person, for the most part of the year.

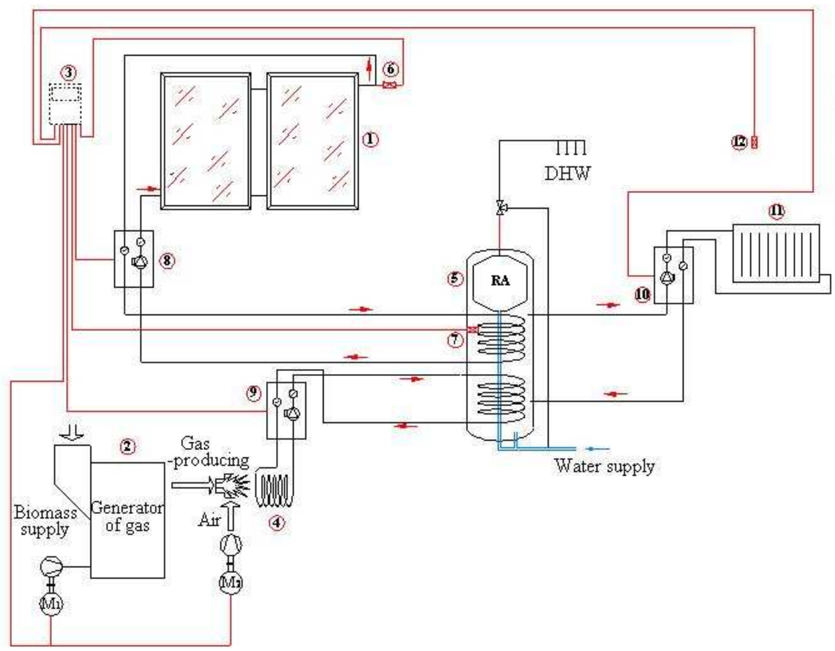

Figure 4: Installation using solar collectors + energy module

The energetic module of combined installation must allow the functioning with primary wood chips but also with pellets. Production of the thermal energy from biomass using the process taken into account consists of two phases: first - the chemical and thermal gasification and two - burning the fuel gas produced. An energetic module is composed of a gas-producing connected to a gas burner. For biomass gasification of agricultural origin process will use TLUD (Top-Lit-Up-Draft) method, designed by Thomas Reed in 1985, titled gasification co-current reversed (downdraft inverted gas generator), adapted for low power.

In the field of electricity generation from renewable sources, the most suitable option for Romania is the combination of wind - PV panels with battery storage and local use (for remote locations) or injection into the grid when there is an electrical connection.

In the picture below, a hybrid system consists of a solar PV and a wind turbine, which drive a water pump. This provides a possible solution for energy and water problems in remote rural areas. The main features:

- Electricity: solar & wind hybrid power system with rechargeable battery
- Water: stand-alone solar pumping system
- Supply micro-grid to households
- Prevent water-borne diseases such as dysentery, typhoid fever, and viral infections
- Supply water to irrigation system for small farms.

The system can be supplemented by a generator, consisting of a diesel engine and an electrical generator; this leads to full insurance of electricity needs in isolated location.

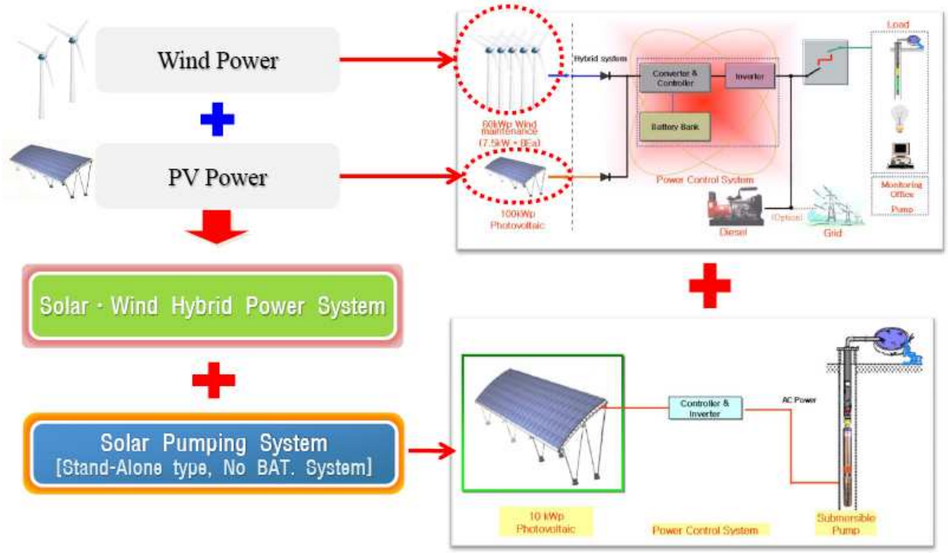

Figure 5: Hybrid wind + PV panels system

4. CONCLUSIONS

- Analysis of the possibilities of using renewable energy in Romania shows that our country has huge potential, but insufficiently capitalized; combined use of two or more types of renewable energy, with or without the contribution of a classic energy sources (eg PV panels + wind + diesel-electric generator), can ensure the autonomy of isolated consumers or significantly reduce costs
- Currently, most of the electricity produced from renewable sources is obtained from hydropower; it is estimated that in the total quantity of consumed electricity, the one produced in this way will have in 2015 a share of 35% and in 2020 accounted for 38%
- The past years have seen remarkable progress in renewable energy; the required and assumed targets for 2020 can be met in 2014
- Developing systems to exploit renewable energy, mono-energetic or hybrid (two or more combined energy), is in the attention of several types of organizations: state authorities, institutes and technical / economic universities, companies interested by the production and operation of the systems.

INOE 2000-IHP is part of the research institutes concerned with green energy, for which it developed a new research direction. Activities in recent years have targeted fields of wind, solar, biomass, in projects in cooperation with national or international partners.

References

[1] David Toke, *The EU Renewables Directive - What is the fuss about trading?*, Energy Policy, ISSN 0301-4215, 2008, Energy Policy, Volume 36, Issue 8, pp. 3001 – 3008.

[2] Government of Romania, *Elements Energy Strategy for the period 2011-2035. Directions and strategic objectives in the electricity sector*, Bucuresti, 2010

[3] Ministry of Economy, Trade and Business Environment, *Planul National de Actiune in Domeniul Energiei din Surse Regenerabile / National Action Plan on Renewable Energy (PNAER)*, București 2010

[4] Global Wind Energy Council, *Wind Energy Report 2013*, February 2014

[5] *Romania's Green Energy Newsletter*, 5th edition, January 2014

[6] Park Moon-Hee, *Renewable Energy Business Model for KAZAKHSTAN*, The 6th KAZENERGY EURASIAN FORUM, October 5. 2011. Astana

[7] Drumea, P., Dumitrescu, C., Ion Guta, D. D., *Renewable energy – a huge generator of business opportunities*, Hidraulica Magazine, nr. 3/2010

ANALYSIS OF CHARGE TRANSPORT IN DYE-SENSITIZED SOLAR CELLS (DSSC) USING A MONTE CARLO SIMULATION

Constantin Dumitru[1], Vlad Muscurel[2], Laurentiu Fara[3], Paul Sterian
Polytechnics University of Bucharest, Faculty of Applied Sciences

ABSTRACT

A Dye-Sensitive Solar Cell (DSSC) is a thin film solar cell, comprised of a semiconductor formed from an electrolyte and a photo-sensitized anode. In this type of cell, recombination should be avoided to achieve a better performance, thus the charge separation should be attained by charge transport. In this paper we will try to realistically model the diffusion and recombination of electrons in a TiO_2 solar cell, using the Monte Carlo simulation. We will address the specifics of electron transport and recombination in a TiO_2 DSSC cell and evaluate the electron diffusion coefficient for this cell. We conclude that this method can be adapted to analyze the solar cell nonlinear behavior and to optimize its performance.

1. INTRODUCTION

Dye-Sensitized Solar Cells (DSSC) made of TiO_2 have received increasing attention since O'Regan and Gratzel published their work in Nature in 1991. Dye-Sensitized Solar Cells, represent solar cells of the third generation first presented in 1988 [1]. They use nanostructured semiconductors like TiO_2 , resulting in cells that can be processed at low temperature and cost less to produce.

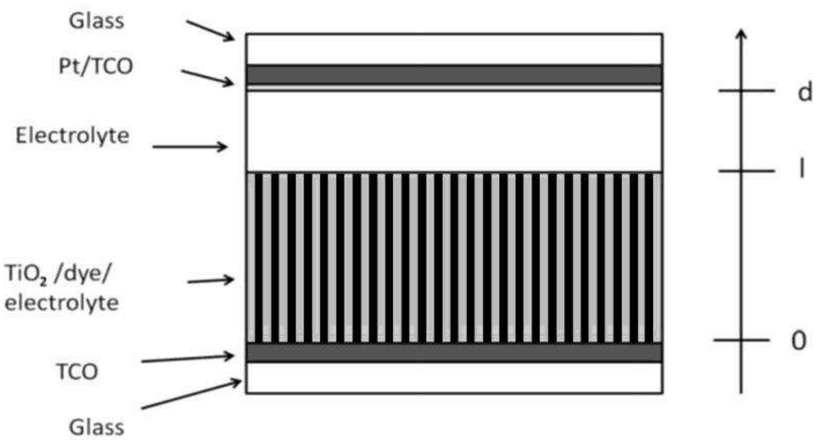

Fig. 1 *Base schematic of a DSSC*

The Dye-Sensitized Solar Cell basic structure is schematically shown in Figure 1. There is a photoanode made of a semiconductor mesoporous substance (TiO_2), immersed into a liquid electrolyte (redox mediator), which is covered at the surface by a monolayer of dye molecules

[1] condumitru@gmail.com
[2] vmuscurel@yahoo.com
[3] lfara@renerg.pub.ro

which in turn make the oxide photoactive. Then we have a region of electrolyte in liquid form, in contact with a counter electrode covered with a thin platinum or graphite layer which acts as a catalyst for the redox reaction [8]. The mesoporous characteristic comes from sintering 15-20 nm diameter nanoparticles of TiO_2.
The smaller the TiO_2 nanoparticle size, the more defects in the nanoparticles which results in electron loss to iodide solution. However, the smaller the nanoparticle for a fixed volume, the more surface area you can coat with dye.
A lower density of nanoparticles will have the same result, but that also means electrons will have fewer path to take to the anode. Optimizing the size and density of the nanoparticles is one of the challenges in building a DSSC, having the maximum amount of surface area while also creating the maximum number of safe pathways for the electrons.

In comparison with a conventional PN junction-based solar cell, the impurity in the semiconductor of a DSSC causes less adverse effect on the cell performance because the important electron injection and recombination processes occur at the TiO_2/electrolyte interface.
Presently, DSSC can achieve as much as 15% energy conversion efficiency (EPFL prototype).
Another advantage of this cells is that they are semiflexibile and semitransparent offering the possibility of integrating them in buildings.

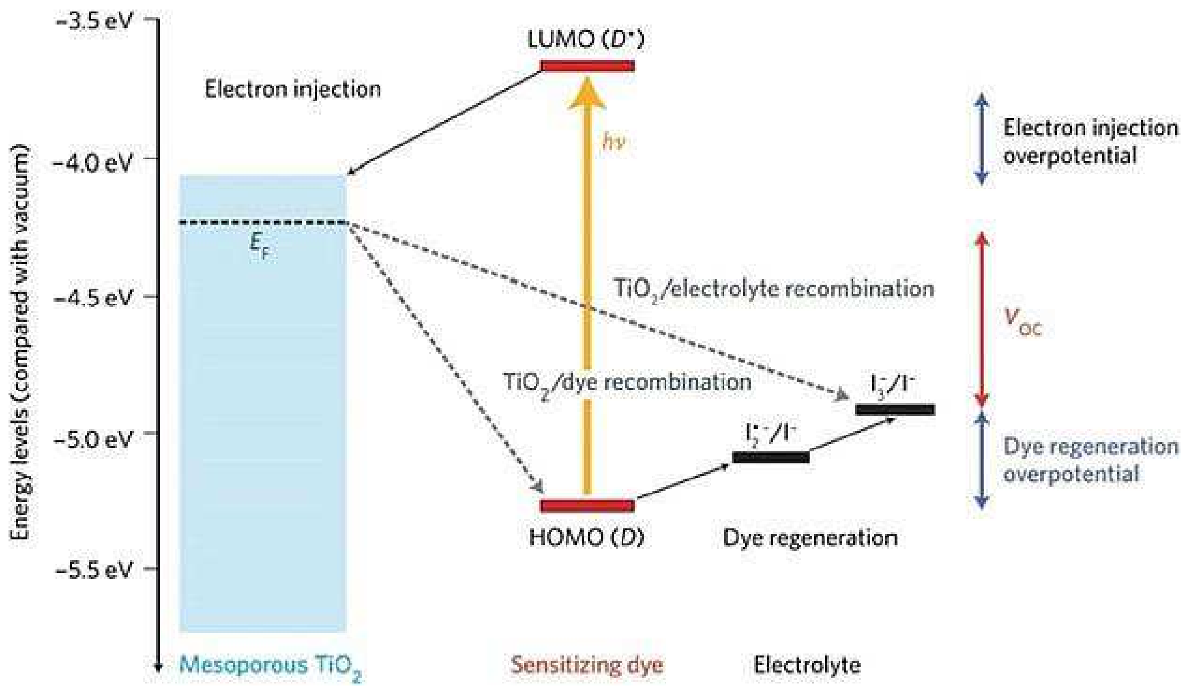

Fig. 2 *Diagram showing energy levels in conventional DSCs* [4]

The collection of energy is separated from the charge transport, and these DSSC cells work by absorbing a photon with the layer of dye (or quantum dots), creating an exciton.
The oxidation of the iodide ions regenerates the molecule by transferring this positive charge to the system. The electrons that were generated flow to the electrode where they power a load, after that reentering the device via a counter electrode.

We can see the energy levels needed for the processes in Figure 2, the voltage being obtained from the difference between the quasi Fermi level E_F for the injected electrons in the TiO_2 film and the redox potential for the $I3^-/I^-$ reaction in the electrolyte.

2. METHODOLOGY AND SIMULATION RESULTS

Monte Carlo simulation methods are known as stochastic. A stochastic method is one that uses probability statistics to examine phenomena and solve problems.
For example, the first use of Monte Carlo computer simulation was in the 1940s, when physicists used it to estimate the probability of chemical chain reactions being successful.
Another famous problem that can be "solved" using Monte Carlo simulation is the area of an irregular 2D shape that cannot be easily calculated. Monte Carlo would assume first circumscribing the irregular shape with a square with well known area, then randomly selecting points within the square. The ratio of the number of points that happen to fall within the irregular shape to the total number of points set in the square, multiplied by the known area of the square, is the Monte Carlo simulated solution to the area within the irregular shape. Area of irregular shape is determined by the area of the square times the ratio, where the ratio is

$$\frac{\text{\# random points in irregular shape}}{\text{total \# random points applied to square}}$$

Problems involving integration, where the integral is too complex to algebraically compute and evaluate, can be addressed with a Monte Carlo simulation (see Fig. 3) to obtain an accurate numerical approximation. An advantage of this technique is that it can be considered as an idealized experiment carried out on samples of arbitrarily adjustable computational parameters.

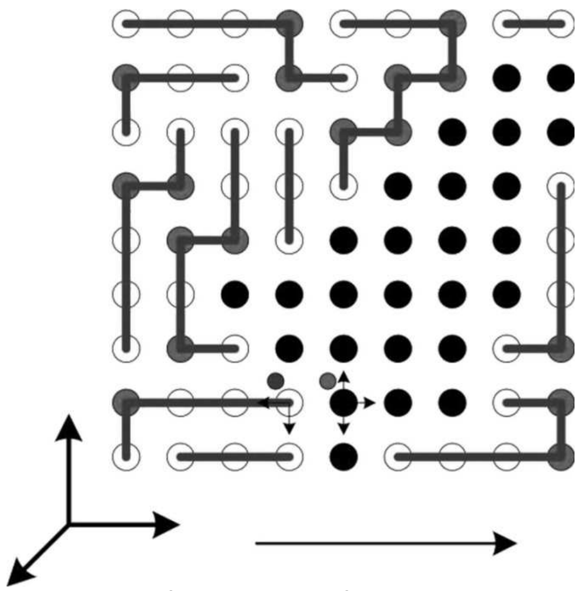

Fig. 3 *Scheme of the model used for the MC calculations*

The performance of these Dye-Sensitized Solar Cells depends on the charge separation which produces high photocurrents and photovoltages. This charge separation is achieved by having a material that conducts photogenerated carriers and if there aren't too many current losses due to electron-hole recombination.

These processes are controlled by the charge transfer mechanisms, electron diffusion and lifetime, depending on the density of charges and the illumination of the cell [6], [7].

In TiO_2 this electron transport mechanism has been explained using a *Multiple Trapping* model, the transport and recombination being correlated.

When it is assumed that tunnelling transitions of carriers between localized states are less probable than transitions between localized and extended states then the carrier transport and energy relaxation can be easily described in the framework of the so-called multiple trapping model. In this model, it is assumed that localized states do not contribute to the transport and carriers can move only via extended states above Ec. The role of localized states is then to slow down charge carriers by a succession of trapping-detrapping events (see Fig. 4).

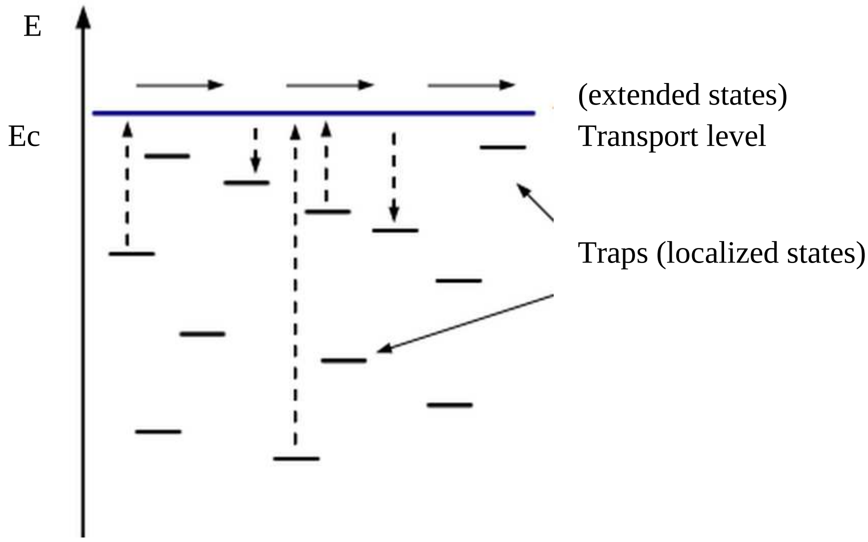

Fig. 4 *Multiple-trapping mechanism of transport*

Charges move through extended states but conduction is slowed down by successive trapping/detrapping events.

The first part of the simulation was done in MatLab, where for a generic organic cell, the BHJ, bulk heterojunction layer thickness of 13.5 * 10^{-8} m, and a wavelength between 400 and 900 nm, the carrier density boundary conditions (hole and electron concentration at the anode and cathode) were defined.

The boundary conditions along with the mobility, non-geminate recombination coefficients and permittivity of the BHJ film are used to solve the current continuity equation which are further used to find the recombination profile.

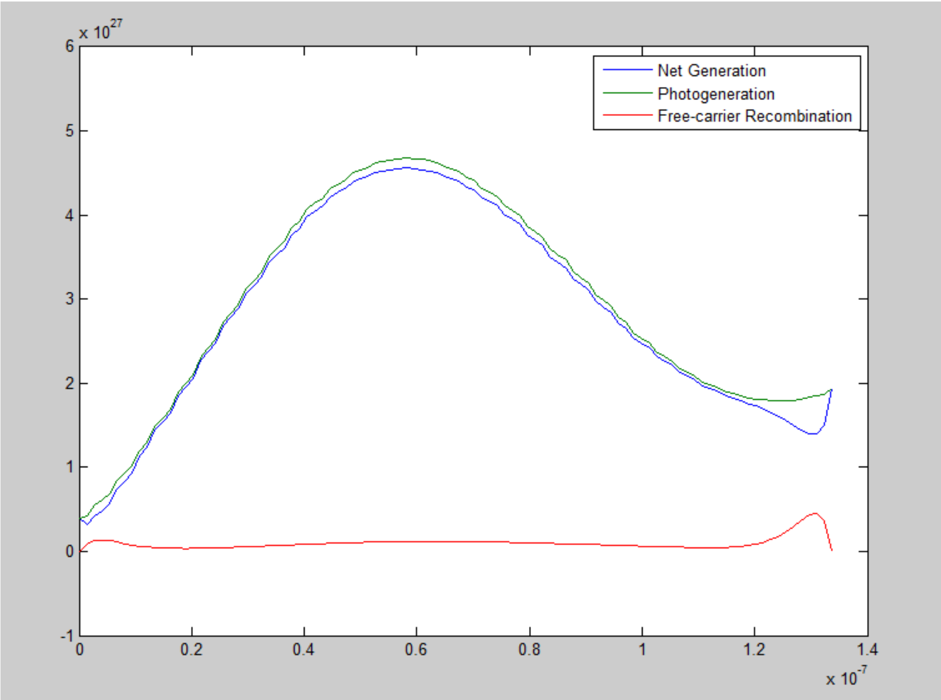

Fig 5 *Generation and recombination rates as a function of position*

We are able to see these recombination and generation rates in Fig. 5, the only spike in the recombination rate appearing towards the end of the scale.
We are using our own Monte Carlo simulations to verify and obtain a result similar to the one in Fig 6.
Preliminary calculations show similar results to the work done in the paper by Vasquez J.P. [9]

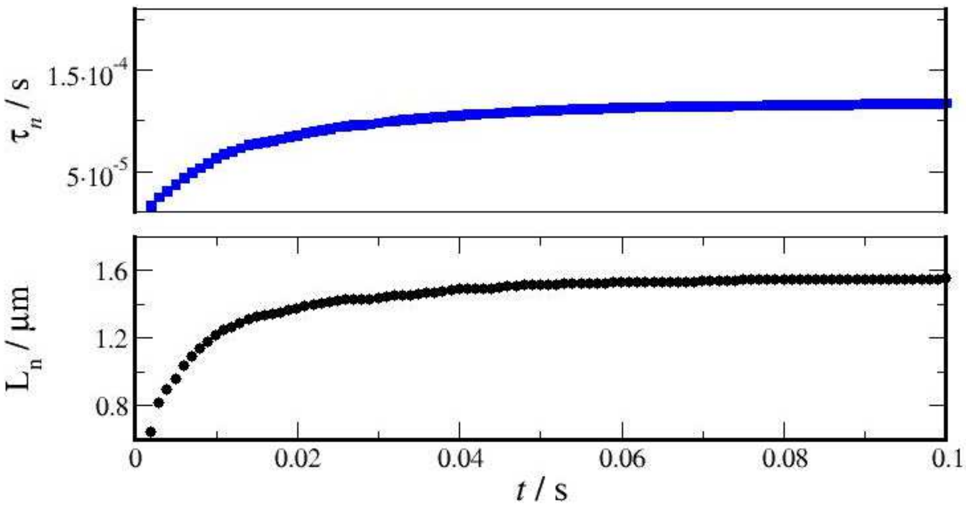

Fig 6 *Electron lifetime and electron diffusion length. Data for a multi-electron calculation with 50 electrons in a simulation box of 18 × 18 × 18 nm^3*

3. CONCLUSIONS

We confirm that the diffusion length maintains a constant value despite varying the Fermi level, upon which, the electron lifetimes entail an exponential dependence, in agreement with previous experimental and theoretical studies.
As future work it is recommendable to realize a simulator that runs on GPUs for obtaining faster computing time, thus a huge number of electrons could be realized as threads and run concurrently**,** resulting in a more accurate Monte Carlo simulation. Graphics Processing Units based massively parallel computing techniques are extremely fast compared to the traditional single-threaded CPU-based simulations. Graphic cards provide much more processing cores to a lower price in comparison to CPUs, because the GPU has thousands of individual computational units. After finalizing our results we expect to confirm the slowing down of the lifetime by the trapping-detrapping process.

References

[1] O'Regan B. and Gratzel M., "*A low-cost high-efficiency solar cell based on dye-sensitized colloidal TiO2 films*", Nature, vol. 353:737-740 (1991)
[2] Fara L. et al. "*Modelarea si simularea numerica a celulelor solare nanostructurate*" ,Punct Publ.House (2008)
[3] Mehdi A., Juan A.,and Ezatollah A. "*Conditions for diffusion-limited and reaction-limited recombination in nanostructured solar cells*", J. Chem. Phys. 140, 134702 (2014)
[4] Walker A.B. "*Monte Carlo Studies of Electronic Processes in Dye-Sensitized Solar Cells*", Top. Curr. Chem. Springer-Verlag Berlin Heidelberg (2013)
[5] Hardin B., Snaith H.J., McGehee M.D. "*The renaissance of dye-sensitized solar cells"*, Nat. Photon. 6:162–169 (2012)
[6] de Jongh P.E. and Vanmaekelbergh D., Phys. Rev. Lett. 77, 3427 (1996)
[7] Fisher A.C., Peter L.M., Ponomarev E.A., Walker A.B., and Wijayantha K.G.U., J. Phys. Chem. B 104, 949 (2000)
[8] Smestad G., Bignozzi C. and Argazzi R., "*Testing of dye sensitized TiO2 solar cells I: Experimental photocurrent output and conversion efficiency*", Solar Energy Materials and Solar Cells, vol. 32:259-272 (1994)
[9] Vasquez J.P. - "*Random walk numerical simulation of electron dynamics in solar cells based on disordered materials*" Ph.D. Thesis (2012).

HYDROTHERMAL TREATMENT FOR THE PRODUCTION OF CALCIUM PHOSPHATE BIOMATERIALS

D. Grimaldi[1], D. L. Carnì[1], F. Lamonaca[1], A. Nastro[2], M. Vasile[3]
[1] Department of Computer Science, Modeling, Electronic and System (DIMES), University of Calabria, Rende (CS), Italy
[2] Chemical and chemical technology department, University of Calabria, Rende (CS), Italy
[3] Medical School, Ovidius University of Constanta, Romania.

ABSTRACT

The mineral part of the human bone is composed by calcium phosphates and hydroxyapatite embedded in amorphous matrix. For this reason the hydroxyapatite is used as spacer or filter to the defected bones in orthopedic surgery and in several oral and maxillofacial applications. Nevertheless the sinterized hydroxyapatite is characterized by high crystallinity that makes it difficult to integrate in the bone turnover. In the paper is proposed hydrothermal treatment for the production of calcium phosphate biomaterials with particular reference to hydroxyapatite. The particularity of the proposed approach is the low crystallinity of the resulting biomaterials.

1. INTRODUCTION

The mineral part of the human bone is composed by hydroxyapatite embedded in an amorphous matrix. The hydroxyapatite Calcium phosphates, with particular reference to hydroxyapatite, has been used during the last years as spacer or filter to the defected bones in orthopedic surgery and in several oral and maxillofacial applications [1]. Generally, this material is obtained through sinterization processes that characterizes it by high crystallinity.

Sinterized hydroxyapatite differs from that of the natural bone component because of its high crystallinity [2], so it hardly integrates in the bone turnover after implantation. Moreover, the hydroxyapatite crystals are a common cause of particular disease [3]. To overcome this problem in the paper is proposed a method to produce hydroxyapatite with low crystallinity. The production methodology is based on hydrothermal treatment at relatively low temperatures (120°C maximum) of pre-shaped mixtures of calcium phosphates. The hydrothermal treatment provides two advantages. The first advantage comes from the low temperature of the hydrothermal treatment that offers new interesting possibilities in the introducing in the starting mixture collagen components of the bone. These last would not be altered during the hardening process and could contribute to the osteo-inductive properties of the final product. The second advantage is that the hardening of the materials is obtained though dissolution and precipitation reactions resulting in a very limited increase of the crystallinity of the original calcium phosphate powders.

In the paper, in order to characterize the sinterized hydroxyapatite X-ray powder diffraction (XRD), and scanning electron microscopy (SEM) instrumentations are used. These instrumentations are typically applied to study civil engineering materials XRD is typically used in mineralogy and material science [4]. The proper use of commercial measurement instruments allow assessing the traceability of the measurement, i.e. the experimental results depend on the material under test, only, and not by the specific measurement method or measurement instruments pointed out.

The paper is organized as follows. Initially, the materials and the methods used to obtain the hydroxyapatite are explained. Successively, the characterization method is synthetized. Following, the results of the experimental tests are described. Finally, the conclusions are drawn.

2. MANUFACT PREPARATION METHOD BASED ON HYDROTHERMAL TREATMENT

Calcium phosphate manufacts were prepared by mixing variable amount of hydroxyapatite (Ca10(PO4)6(OH)2) and monetite (CaHPO4), powders humidified by distilled water. The hardening of the materials is obtained though dissolution and precipitation reactions resulting in a very limited increase of the crystallinity of the original calcium phosphate powders.

Besides, the low temperature of the hydrothermal treatment offers new interesting possibilities of introducing in the starting mixture collagenic components of the bone which would not be altered during the hardening process and could contribute to the osteo-inductive properties of the final product.

The mixtures made of only hydroxyapatite and only monetite are indicated as H 100% and M 100%, respectively; the mixtures of both hydroxyapatite and monetite indicated as the percent in weight of hydroxyapatite are: H 90%, H 80%, H 70%, H 60%, H 50% and H 30%. To the powders mixtures were added low amount of water to obtain the final manufact, as Tab.1 shows.

Manufacts were produced by compacting the mixtures in a steel die at 36 Mpa. They resulted as cylindric shape with a diameter of 12.7 mm and height of about 6 mm. Then they were hydrothermally treated throughout 72 hours in water steam saturated environment at low temperatures (at 37°, 60°, 80°, 100° and 120°C).

Table 1: Water amount for powders grams

Mixture	ml/g
A 100%	0.62
A 90%	0.32
A 80%	0.32
A 70%	0.26
A 60%	0.17
A 50%	0.16
A 30%	0.13
M 100%	0.13

3. MANUFACTS CHARACTERIZATION

All calcium phosphate manufacts are characterized by XRD, and SEM.

The XRD measurements are carried out by CuKα radiation (α= 0.154050 nm) in the Philips X-ray diffractometer 1730/10 (at 20 mA and 40Kv), from 5 to 25 °Θ degree, and SEM Jeol JSM-T330.

Moreover, the two starting powders of calcium phosphate used to prepare manufacts: hydroxyapatite and monetite are produced by Aldrich and they are characterized by solubility tests, XRD and SEM.

The hydroxyapatite and monetite powders are subjected to solubility tests after that, 15 grams of each powders in 500 ml of distilled water is stirred at 25°C for three days. The calcium and phosphate ions concentrations dissolved are determined in order to evaluate the hydroxyapatite and monetite solubility: the calcium ion concentration is determined by a complessometric titration with Ethylenediaminetetraacetic acid by spectrophotometry method and molibdate [5]. The ions concentration is expressed as mmoli/l.

For the XDR, the X-ray traces of the powders under examination are compared with the information provided by the American Society for Testing and Materials International (ASTMI) and shown in Fig.1. In particular, the XDR traces are shown in Fig.1a and Fig.1b represent the XDR trace for the hydroxyapatite and monetite powders. Each peak corresponds exactly with those of pure hydroxyapatite and monetite by the ASTM. In Fig.1c is reported the X-ray pattern of the hydroxyapatite powder treated at 1000°C for two hours. This last figure shows as the cristallinity of hydroxyapatite increases by about three times during the sintering treatment.

The same XRD test is used to study manufacts obtained with and without the proposed methodology obtained starting from the same materials, and two samples selected as reference. The reference samples used in the experiments are compact bovine bone and commercial calcium phosphate, employed as filter in orthopedic surgery. The results of XDR test are shown in Fig.2. In particular, in Fig.2a and Fig.2b the XRD traces of two manufacts, H 80% untreated and after hydrothermal treatment at 60°C are shown. In Fig.2c and Fig.2d the XDR trace for (i) compact bovine bone and (ii) commercial calcium phosphate samples are reported, respectively.

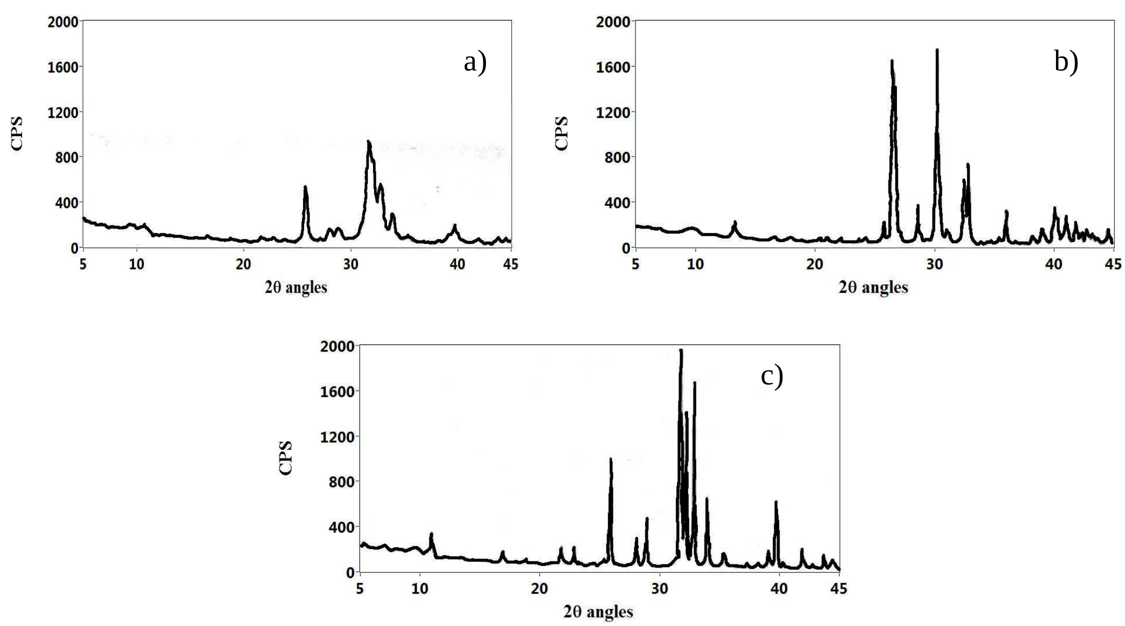

Figure 1: XRD patterns of: a) commercial hydroxyapatite; b) commercial monetite; c) commercial hydroxyapatite treated at 1000°C/2h.

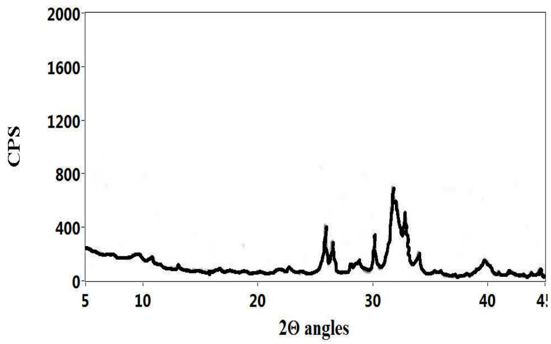

a)

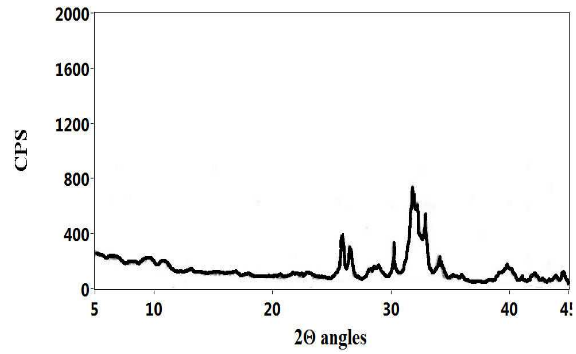

b)

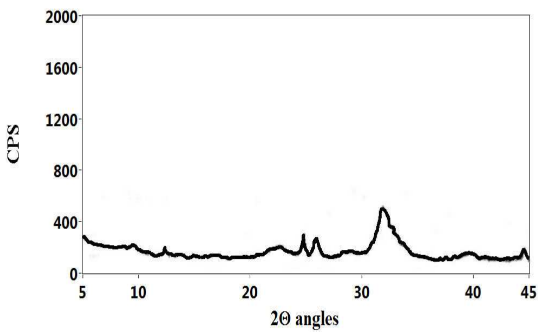

c)

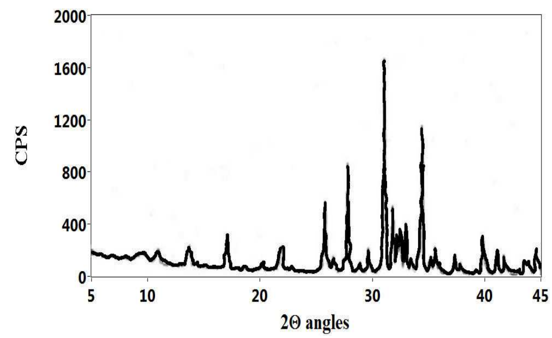

d)

Figure 2: XRD patterns of: a) H 80% untreated, b) after hydrothermal treatment at 60°C, c) a sample of compact bovine bone, and d) the sample of commercial calcium phosphate.

The XRD traces of two manufacts shows the typical peaks of hydroxyapatite and monetite powders, which don't modify their intensity after hydrothermal treatment.

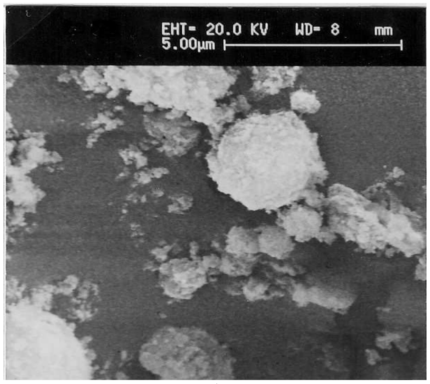

a)

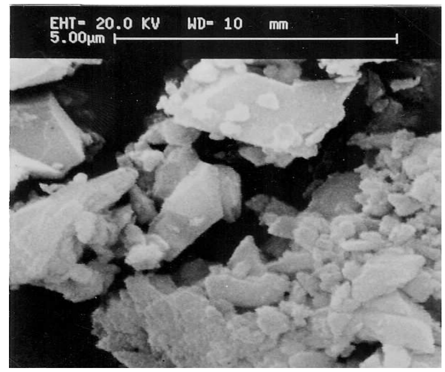

b)

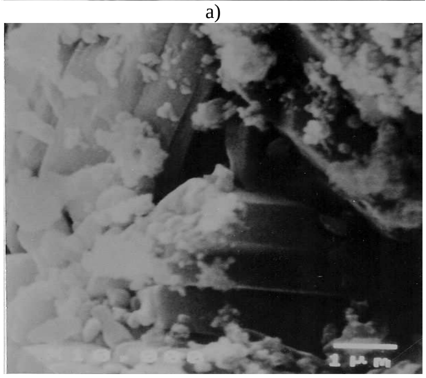

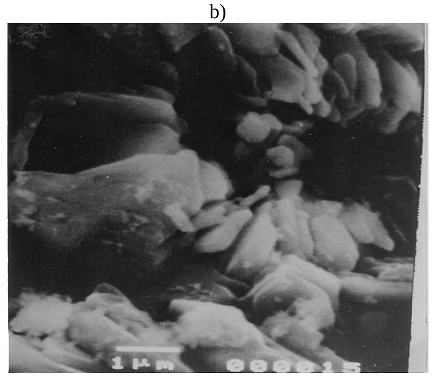

The diffraction pattern of compact bovine bone shows that the mineral phase of bone corresponds to an amorphous hydroxyapatite kind. The sample of calcium phosphate commercial subjected to X-ray diffraction results be composed by a mixture of whitlockite ($Ca9(MgFe)(PO4)6PO3OH$) and hydroxyapatite ($Ca10(PO4)6(OH)2$). The peak-to-background ratio of the XDR shows the similar value for the material obtained with the proposed method and the bovine bone this means that the crystallinity is about the same of the bone samples. Instead, the peak-to-background ratio of the XDR of the commercial calcium phosphate is really high than the bovine bone sample, this means that the crystallinity is higher than the bone samples.

The hydroxyapatite and monetite gains size are examined by using SEM. From the study by SEM the hydroxyapatite powder results constituted of grains that are between 400 to 7000 Å size. In particular the analysis highlight that:

- grains that are less than 2000 Å represent the 34%;
- gains that are more than 2000Å represent about the 66%;
- aggregates which are less than 2000Å are composed of smaller grains which have size about 100Å.

In fact, monetite powder is composed of two groups of aggregates: the first is constituted of grains which are 1000-2600 Å size and they represent about the 52%; the second is constituted of grains which are 3-6 micron size and they represent about the 48%. Fig.3 shows SEM images of: a) hydroxyapatite powder, b) monetite powder, c) sample of hydroxyapatite 40 steered at 120°C, d) sample of hydroxyapatite 80 steered at 120°C.

4. CONCLUSIONS

In the paper a method to obtain through hydrothermal treatment, calcium phosphate manufacts which have mechanical, chemical and physical characteristics much similar to the human bone ones. Particularity of the method is that the cementation of starting powder is obtained through a dissolution/crystallization process that involves a very small part of material; so this process leads to a very small increasing of the starting crystallinity of the calcium phosphate. This is the characteristic that distinguishes our method from the generally used one, because this second method consists in a sinterization treatment at temperature of about 1000°C, and it has, as a result, marked increasing crystallinity in the final manufact. To conclude, the cementation process of the calcium phosphate manufacts is due mainly to a gradual superficial dissolution of the two starting powders and to a subsequent preferential precipitation of the less soluble phase, in our case it is the hydroxyapatite (HPA).

All these processes produce a very little increasing of phosphate crystallinity. Low crystallinity of manufacts hydrothermally obtained is extremely important in order to use such a materials in the orthopaedic surgery because it can make them to be more reactive and so more osteoinduttive after their implantation.

The suggested method results extremely promising for another important characteristic represented by physical properties of manufacts, evaluated by means of X-ray powder diffraction and scanning electron microscopy which are more similar to the bone ones than to the sinterized products.

References

[1] N. M. Zainuddin, Z. A. Rahim, R. Anwar, M. S. Mujir, and O. H. Hassan, "Conceptual framework of hydroxyapatite for damaged skull through design approach," presented at the IEEE Business Engineering and Industrial Applications Colloquium (BEIAC), 2012.

[2] M. Gindre, D. Le Guillou-Buffello, A. Sewing, R. Bareille, J. Amedee, and P. Laugier, "Adhesion of human osteoprogenitor cells on peptide immobilization onto titanium monitored a quartz crystal resonator technique," presented at the IEEE International Workshop on Medical Measurement and Applications (MeMea 2006), 2006.

[3] J. A. Bonavita, M. K. Dalinka, and H. R. Schumacher, "Hydroxyapatite deposition disease", *Radiology,* vol. 134, pp. 621-625, 03/ 1980.

[4] B. Fultz and J. Howe, "Diffraction and the X-Ray Powder Diffractometer," in *Transmission Electron Microscopy and Diffractometry of Materials*, ed: Springer Berlin Heidelberg, 2013, pp. 1-57.

[5] C. P. Klein, J. M. de Blieck-Hogervorst, J. G. Wolke, and K. de Groot, *Studies of the solubility of different calcium phosphate ceramic particles in vitro* vol. 11, 1990.

MEDIUM AND HIGH PRESSURE ACTUATORS PNEUMATIC SYSTEM

Gabriela Matache[1], Gheorghe Sovaiala, Radu Radoi, Ioan Pavel

ABSTRACT

This paper presents the research concerns of Hydraulics and Pneumatics Research Institute (IHP) in Bucharest on knowing the specific phenomena and processes regarding the operation of medium and high pressure actuators, in order to increase energy efficiency of pneumatic drive systems. At IHP, in the Laboratory of Pneumatics, there have been performed tests on the experimental model (EM) of a pneumatic system with medium and high pressure actuators. The following tests have been conducted on this EM: Response of the pneumatic drive system with medium pressure actuator to step signal, for various values of the PID controller and controlled load and there have been developed the attenuation - frequency chart and phase – frequency chart (the BODE diagram)

1. INTRODUCTION

Currently, **at global level** research in the field of pneumatics is focused on **three important directions: miniaturization, use of intelligent techniques and increase of energy efficiency** in pneumatic parts and systems. In all these cases the virtual modeling techniques have a crucial role, especially where the classical methods of design and testing can no longer cope on their own with the requirements regarding the functional quality of the components and systems required by modern technical applications.

Among the ways to improve, in terms of dynamics and energy, the process complex pneumatic systems we mention the use of components with superior operating characteristics (for instance: components with very low pressure drop and null losses of flow), structural optimization of circuits, very good quality of the work agent used, etc.

The particularities that pneumatic systems present (difficulty in flow controlling, sensitivity to external disturbance) lead to instability of energy parameters if there is no real time control upon them.

Control of complex technological processes, in which they are increasingly being used, require for their design and testing to be a high performance one (for example: for robotized of work lines, medical applications, IT apps, etc.)

2. DEVELOPMENT OF THE SPECIFIC DIAGRAM FOR TESTING THE EM OF A PNEUMATIC SYSTEM WITH MEDIUM AND HIGH PRESSURE ACTUATORS

In order to test the EM of a pneumatic system with medium and high pressure actuators there has been developed the testing diagram achieving the load controlled through a proportional pressure controller valve, which controls the pressure values in the chambers of the load actuator, Fig. 1.

Based on the testing diagram of pneumatic systems with medium and high pressure actuators, with load controlled by means of a pressure controller proportional valve, there was made configuration for the testing device.

In the structure of the testing device with load controlled via a proportional pressure controller valve, Fig. 2, the following components can be found:

[1] Cutitul de Argint Street, No. 14, sector 4, Bucharest, phone: +40213363991, e-mail: fluidas@fluidas.ro

-GPA1- air preparation block, which includes the pressure regulator RP1 and the filter F1; this group contains no air lubrication device, as for the pilots of the proportional equipment in the stand structure is recommended to use dry air

-RP- proportional pressure regulator MPPE-3-1/2-10-010-B provides an output pneumatic pressure proportional to the input electrical signal

-DP1- flow proportional directional control valve (regulator) MPYE-5-1/8HF-010-B; allows for controlled flow rates

-TP_1, TP_2- pressure transducers PMP 1400 read the pressure values in the chambers of the actuator being tested, convert them into analogue signals voltage type and convey them to the computer via the data acquisition board USB-6218;

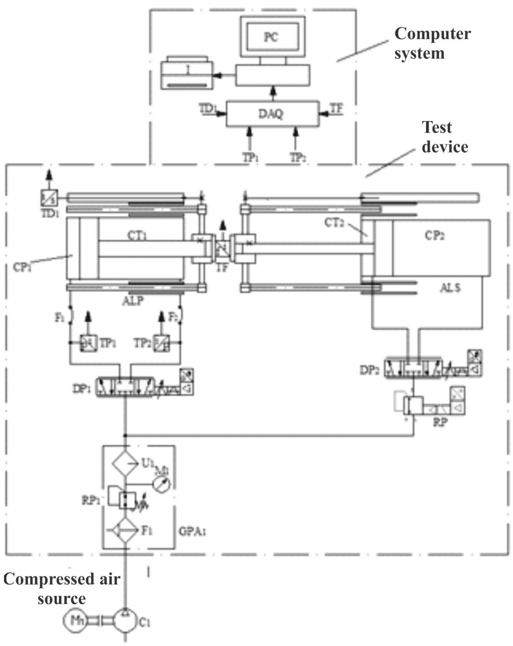

Fig. 1 Diagram for testing the automated pneumatic systems with load controlled via a proportional pressure controller valve

Fig. 2 Device for testing the pneumatic systems with medium and high pressure actuators with load controlled via a proportional pressure controller valve

-ALP- pneumatic linear servo actuator to be tested DNCI-32, equipped with **incremental displacement transducer TD_1**

-ALS-load pneumatic linear servo actuator DNCI-32, equipped with **incremental displacement transducer TD_2**

- pressure in the chambers of the drive actuator is adjusted to the testing value by means of the pressure regulator RP1 in the structure of the air preparation block;

-$CP_{1/2}$-piston chambers of the pneumatic actuators to be tested/of the load actuators;

-$CT_{1/2}$-rod chambers of the pneumatic actuators to be tested/of the load actuators;

-$DRT_{1,2}$- throttles with bypass valve

-TF-force transducer CTOL 500, is mounted between the rods of the pneumatic actuators to be tested and of the load actuators and is intended to allow testing of the thrust/traction force at the actuator under tests, as well as positioning tests and tests of speeds under load. Combined error of the transducer: < +/- 0,03 %

- the air flow that the drive actuator chambers are fed with is preset and adjusted by the associated proportional flow regulator;

- the proportional pressure controller valve allows setting and maintaining constant value of pressure in the pressurized chamber of the load actuator, regardless of the position of the piston, which by moving in the direction of reducing continuously the volume of air determines a continuous increase of pressure;

-the proportional flow regulator interposed between the proportional pressure controller valve and the load actuator chambers acts like a simple pneumatic directional control valve and allows feeding/discharging them from/to the atmosphere.

3. DEVELOPMENT OF THE METHODOLOGY FOR TESTING THE EM OF A PNEUMATIC SYSTEM WITH MEDIUM AND HIGH PRESSURE ACTUATORS

The pneumatic systems with medium and high pressure actuators go through two kinds of tests:

1. Static tests, aiming at:

- determining the minimum pressure for the piston of the pneumatic actuator driving the system to start moving, for both directions of travel (rod chamber and piston chamber);
- determining the thrust/traction forces of the pneumatic drive actuator;
- speed test at preset pressure, with pneumatic spring type load;
- speed test at preset pressure, with load generated by proportional pressure controller valve;

2. Dynamic tests, aiming at:

- response of the pneumatic drive system with double effect actuator to sine wave signal, for preset values of the parameters of PID controller and load controlled via proportional pressure controller valve; drawing the Bode diagrams (attenuation - frequency, phase - frequency).

The influence of the PID controller parameters on the positioning accuracy of the drive system with servo pneumatic actuators

The test sofware has been developed with LabVIEW. On the input of the data acquisition board USB-6218 there are entered voltage type signals from the pressure transducers (associated to the two chambers of the drive actuator), force transducer, displacement transducer, proportional pressure controller valve. One of the two analog signal outputs of the acquisition board is used for controlling the proportional pressure regulator, and the other one for controlling the proportional directional control valve in the test diagram.

The test device allows conducting tests on drive systems with simple pneumatic actuators, respectively medium and high pressure servo actuators, both in static and in dynamic regime.

Feeding the electromagnets of proportional equipment and the sensors of the data acquisition board is made from a dual-channel voltage source.

For testing with the software developed in LabVIEW, value of the testing pressure has been determined via a command given to the proportional pressure regulator. The proportional directional control valve is controlled via a step type signal to perform strokes in both directions with a preset frequency.

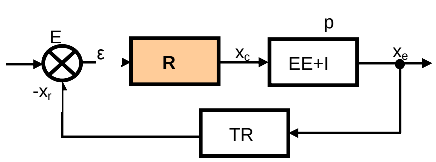

Fig. 3 Block diagram of the automatic control system

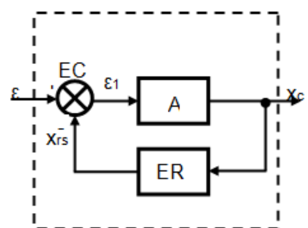

Fig.4. Block diagram of an automatic controller

When pressing the stop button, the software asks for the path and file name. The data type file contains columns with all the values acquired during testing.

These can be further used for processing and plotting other types or combinations of graphs.

In an automatic control system, the automatic regulator (RA) is designed to operationally process the error signal ε (got upon the linear - additive comparison of the input parameter x_i

with the reaction parameter x_r in the comparison element) and to generate an output control signal x_c for the execution element. It is placed on the direct route, between the comparison element and the execution element, as in the block diagram of the automatic control system shown in Figure 3.
Current information on the automated process is obtained using the reaction transducer TR and it is processed by the automatic regulator RA according to a certain law which defines the automatic adjustment algorithm (the adjustment law).
Although there are a wide variety of regulators, any regulator will include the following components (Figure 4): amplifier (A); secondary reaction element (ERS); the secondary comparing element (ECS).
To highlight the influence of the type of regulator on the behaviour of an SRA, in Figure 5 there have been plotted the responses over time of an SRA output parameter, $x_e(t)$, for a step variation of the input parameter x_i, for the cases when there are used the P, PI, PD and PID controllers.

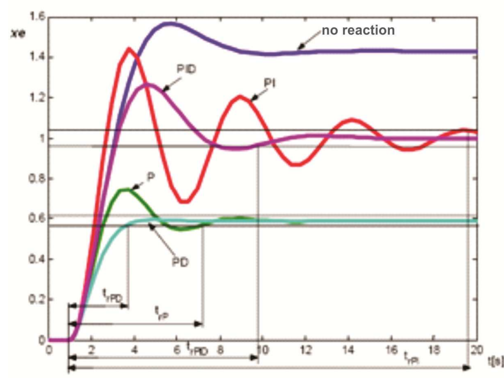

Fig.5 Unit step responses of a SRA for various linear continuous controllers

Comparing the response curves, the following considerations can be made:
• the *P* type controller appreciably reduces the overshoot, leads to a short transient time, but introduces a high stationary ε_{st} error;
• by introducing the component *I*, the *PI* type controller cancels the stationary error at step input, but leads to overshoot higher than at the *P* controller and an increased value of response time;
• by introducing the component *D*, the *PD* type controller improves the dynamic behaviour (overshoot σ and the transient regime duration are small), but it maintains a high stationary error;
• the *PID* type controller, combining the effects P, I and D, gives superior performance both in stationary and transient regime.

Response of the pneumatic drive system with double effect actuator to sine wave signal

The methodology for plotting the BODE diagrams (attenuation - frequency, phase-frequency) is based on the response of the pneumatic drive system with double effect servo actuator to sine wave signal, for preset values of the PID controller parameters and load controlled via a proportional pressure controller valve.
Tests have been performed in dynamic regime, on the device configured based on the pneumatic diagram with load controlled via a proportional pressure controller valve.

The attenuation – frequency chart (response to sine wave signal)

It consists of the analysis of positioning system response when there is applied a sine wave variation of the electrical control signal, within a relevant frequency range.
The operations performed are the following:

a) The pneumatic cylinder piston is placed halfway the stroke, acting on the offset manual adjustment in the software application window;

b) By means of the signal generator there is applied a sine wave signal of amplitude ± 3V and frequency 0.02 Hz. Using the data acquisition system is recorded variation over time of the electric control signal of position and stroke made by the positioning system rod.

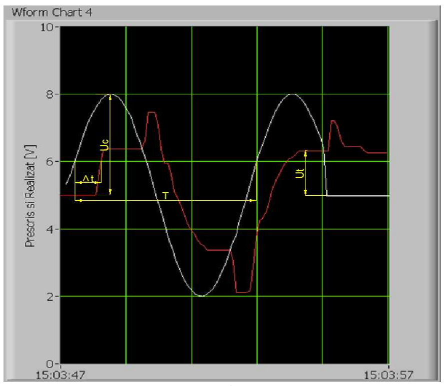

Fig. 6. Presentation of parameters used in the calculation of attenuation at frequency

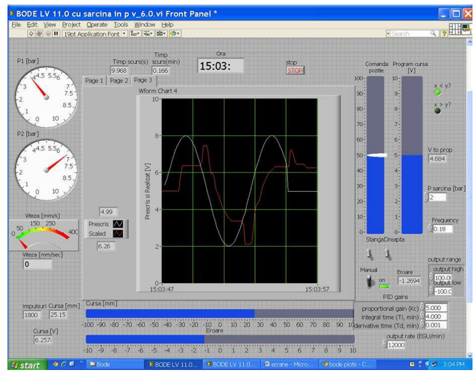

Fig. 7. Screen capture while performing tests in order to plot the Bode diagrams

c) Repeat the operations of point b, incrementing the frequency in steps of 0.04 Hz.

d) The attenuation – frequency chart is plotted as follows:

- after reading amplitude values on the diagram, Fig. 6, for each frequency incremented in steps of 0.04 Hz, there is calculated the ratio of oscillation amplitude at linear pneumatic actuator rod U_t and oscillation amplitude at power signal U_c and it is inserted in the attenuation to frequency calculation, A:

$$A\ (dB) = -20\ \lg \frac{U_t}{U_c}$$

where: U_t – oscillation amplitude at cylinder rod.
 U_c – oscillation amplitude in control signal.

With the values obtained there is plotted the attenuation-frequency curve on the chart of the BODE diagram.

In Fig. 7 is shown a screen capture with the window where there are presented: the position sine wave signal applied to the proportional flow directional control valve from which are supplied the chambers of the system drive servo actuator (the preset one) and system response, received from the incremental position transducer of the drive servo actuator (the achieved one). The two signals are electrical type (voltages).

The offset – frequency chart is plotted as follows:

After reading the values Δt and T on the chart, for each frequency incremented in steps of 0.04 Hz, there is calculated the offset between the cylinder stroke and the control signal:

$$\varphi[\circ] = \frac{\Delta t}{T} x 360^{\circ}$$

where:

φ - offset

Δt – time difference between intersection of the time axis and the control signal curve and intersection of the time axis and cylinder stroke on a half-period.

T – control signal period.

Points are recorded until attenuation decreases by 15 dB or offset exceeeds 120^0. With the values obtained there is plotted the offset-frequency curve on the chart of the BODE diagram.

The BODE diagram

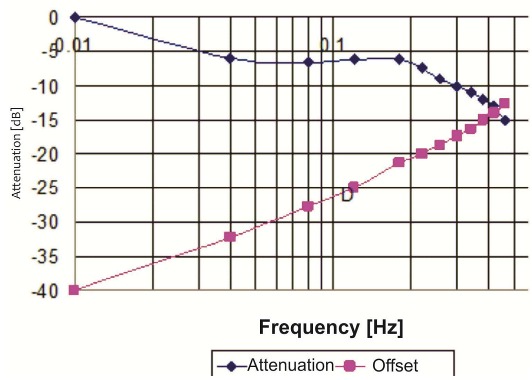

Fig. 8 The BODE diagram

There are plotted on the same chart the curves highlighting the variations of offset and attenuation depending on frequency on the logarithmic scale.

4. CONCLUSIONS

Following the tests conducted on **the pneumatic drive system with medium and high pressure actuators, load controlled,** the following conclusions have been reached:

• *P* type controller sensibly reduces the offset, leads to a short transient period, but introduces a high stationary error ε_{st};

• by introducing the component *I*, the *PI* type controller cancels the stationary error at step input, but leads to overshoot higher than at the *P* controller and an increased value of response time;

• by introducing the component *D*, the *PD* type controller improves the dynamic behaviour (overshoot σ and the transient regime duration are small), but it maintains a high stationary error;

• the *PID* type controller, combining the effects P, I and D, gives superior performance both in stationary and transient regime.

The tested system had a steady behaviour for values of the PID parameters ranging between: k_c=4.000-6.000; T_i=5.000-6.000; T_d=0.001.

5. REFERENCES

[1] Avram M: “Acţionări hidraulice şi pneumatice - Echipamente şi sisteme clasice şi mecatronice”, University Publishing House – Bucharest, 2005;

[2] Belforte, Bertetto, Mazza: “Pneumatico - curso completo”, Techniche nueve Publishing House, Milan, 2004;

[3] Banu, Demian: “Motoare pneumatice liniare si rotative”, Technical Publishing House, Bucharest, 1994;

[4] Banu, Stanescu Atodiroaiei, Gaburici: “Sisteme de automatizare pneumatice”, Technical Publishing House, 1997;

[5] SMC Romania: “SMC International Training-Introducere in pneumatica”, SMC Romania 2004;

[6] Diaconescu E -“Controlul Pozitiei cu Labview”, Publisher University of Pitesti’ 2006

ELECTRO HYDRAULIC SYSTEM FOR SPEED CONTROL OF A HYDRAULIC MOTOR USING A PI CONTROLLER

R. I. Rădoi[1], I. C. Duţu [1]
[1] Servotechnics and Electronics Department, Hydraulics & Pneumatics Research Institute (INOE 2000 - IHP), Bucharest, Romania

ABSTRACT

Some industrial applications which use hydraulic actuations require precise and constant maintaining of a regulated parameter. Such an application can be for a hydraulic motor speed control from a particular installation (eg winder, conveyor, etc.)
For this are required particular actuating hydraulic diagrams and electronic control modules equipped with certain controllers. These drive systems can be part of complex installations and can be operated via PLC or industrial computer. An important feature of such a control system is related to the dynamic performances. The article presents the construction of a stand such a system for experimentation, hydraulic and electric diagram of the system and functional characteristics obtained using the stand.

1. INTRODUCTION

Industrial applications of variable speed rotary motors use specialize modules or can be can be implemented and operated by means of PLCs.

To achieve experimenting of such a system has developed a hydraulic and control scheme that use existing components from endowment.

Hydraulic components used are a vane hydraulic motor and a 4/4 hydraulic proportional directional valve size NG 6. As controller were used a Virtual Instrument application implemented in LabVIEW.

2. HYDRAULIC AND CONTROL SCHEME

The scheme for the experimental system (Fig. 1), consists of a mechanical-hydraulic part and an electrical / electronic part. For the mechano hydraulic section were used, an hydraulic vane motor and a 4/4 proportional directional valve. Hydraulic motor is the model M2-210 with a displacement of 25 cc/rev produced by the Vickers. The hydraulic proportional directional valve 4WRPEH, NG 6 produced by Bosch Rexroth.

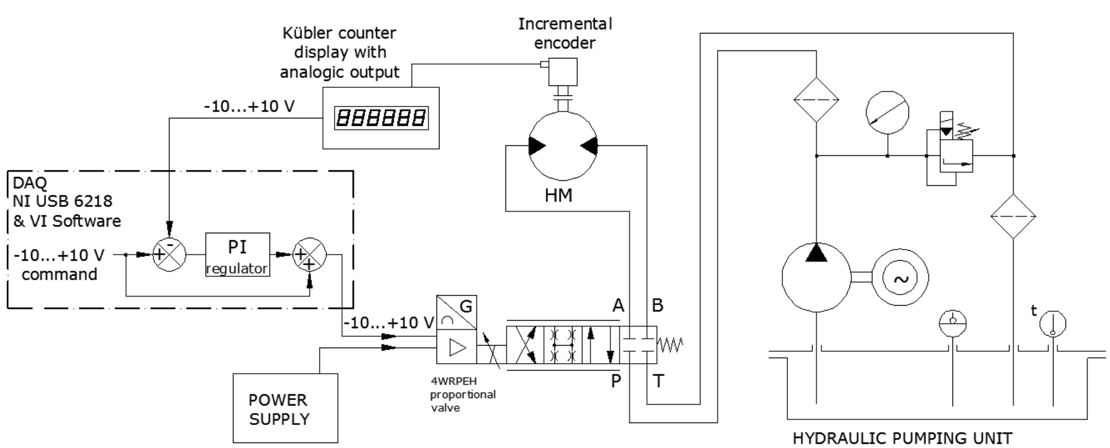

Figure 1: Hydraulic and control scheme

Electric part is composed of: incremental encoder type 8.3700, counter with analogic output, National Instruments DAQ type USB-6218 as interface between system and the VI software and 24 V dc power supply. The Virtual Instrument software allows adjusting the nominal speed of motor and monitoring and recording of speed variation. Also in the VI software was implemented the speed control circuit with PI controller.

From the speed value set in the VI window is subtracted the feedback value from the motor through a subtraction block. The result is applied to the PI controller input. Command signal exiting from PI controller enters in a summation block. Also the speed set in the VI window is transmitted directly to summation block bypassing PI controller. The value from the summation block output go through the medium of analog output in the form of voltage in a range of -10…10 V to the connector of the proportional directional valve. This feedforward term adjustment scheme provide better dynamic, the controller intervening only for the difference between the set value and feedback value.

For the system to function all values of signals must be correlated. There must be determined the maximum speed that can be achieved with proportional directional valve to a maximum + / - 10 V command to a flow rate provided by the pumping group. Analog feedback signal must be scaled so that to maximum speed of the system to be equal to the maximum speed that can be adjusted.

3. EXPERIMENTAL STAND AND RESULTS

The system was assembled on the table of a stand for testing hydraulic equipments. The electrohydraulic proportional directional valve was connected via hoses to the source of flow, to the tank connection and to the two connections of the hydraulic motor.

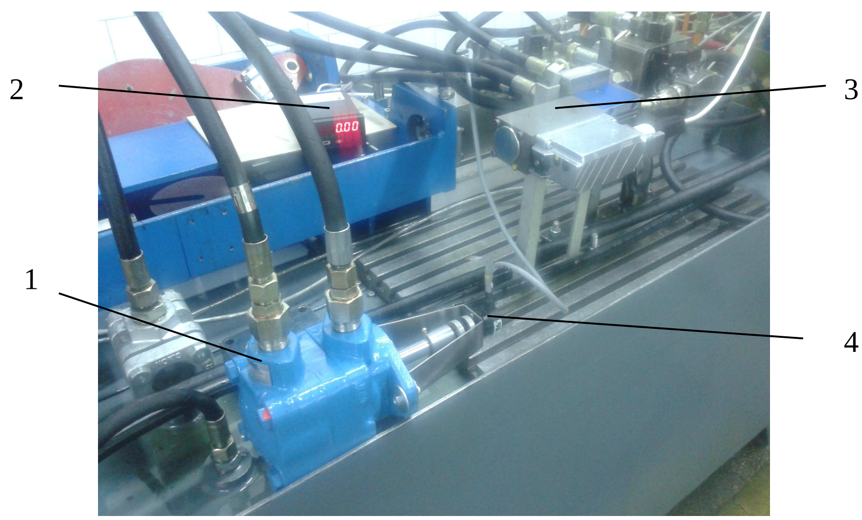

Figure 2: The system for speed control during the experiments

In Figure 2 it can be observed the following system components: 1 – rotary hydraulic motor; 2 – RPM meter with analog output of the incremental encoder 4; 3 – proportional directional valve type 4WRPEH and in position 4 – incremental encoder type 8.3700 produced by Kubler.

For incremental encoder mounting was made a support and a coupling piece to motor shaft (Fig. 3). Encoder was coupled through a flexible coupling.

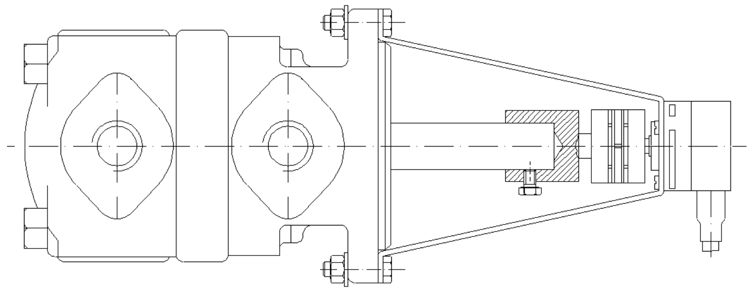

Figure 3: The method of attachment of the incremental encoder to the motor shaft

Virtual instrument application for controlling the hydraulic motor speed was achieved in LabVIEW development enviroment. The application was based on the block diagram in Figure 5. This allows setting the speed by a numeric control box. The motor speed can be read from a speed gauge and is recorded on a wave chart. The signal for control the proportional directional valve is sent to an output port of a data acquisition board through DAQ assistant block configured as voltage output in a range of ±10 volts. The analog signal from RPM meter of incremental encoder was connected through an analog input port of the data acquisition board also by means of an DAQ assistant block configured as an voltage input in the range of -10...10 V. For controller and display part of the aplication have performed a series of scaling of the signals.

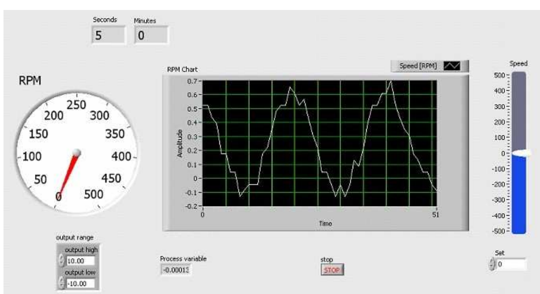

Figure 4: Command and speed recording window

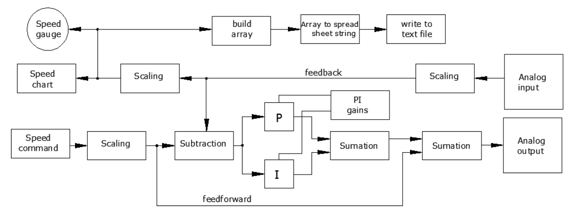

Figure 5: Block diagram of VI application

The controller part from the VI application processes the error resulting from difference between the commanded speed and the actual motor speed according to equations (1) and (2), the operator has the possibility to modify the proportional K_P and integral K_I gain terms, in order to tune the controller.

$$P = K_p * e(t) \tag{1}$$

$$I = K_I * \int e(t) d\tau \tag{2}$$

In Figure 4 you can see the window of VI application by which the operator can control the desired speed value. Speed variation can be seen on a speed gauge. On completion of probation after the stop button is pressed the VI application asks for the name and path for the text file in which are saved recorded data.

The controller was tuned after a series of input values for the terms K_P and K_I so as not to occur oscillations and stationary errors. After that was obtained the diagram in Figure 6 in which were recorded a few speed steps.

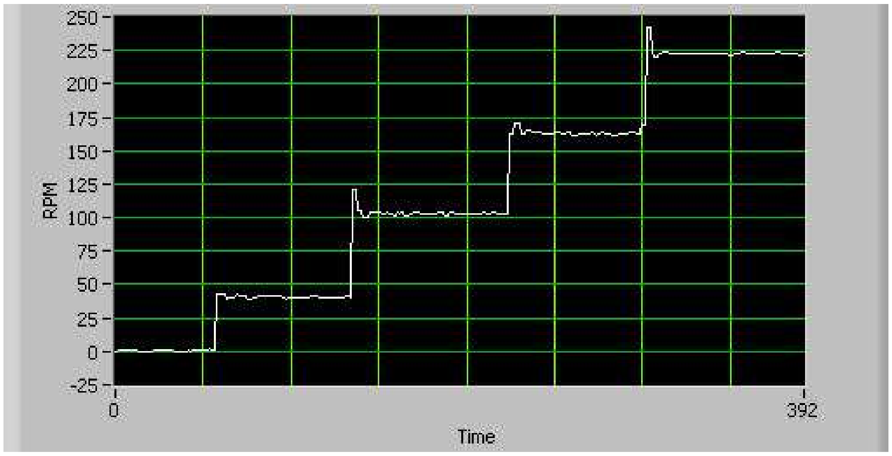

Figure 6: Recorded speed steps

4. CONCLUSIONS

The system allows adjusting the speed of a hydraulic motor and recording of speed variation in time.

The system can be tuned by changing the terms of K_P and K_I in order to obtain an optimal response.

Research can continue by realizing a module for creating load to the motor shaft and tracking the system behavior when the load to the motor shaft varying.

References

[1] Marin, A., *Regulatoare de Turație Pentru Turbine Hidraulice*, Printech, Bucharest, 2006.
[2] Afrăsinei, M., Chiriță, C., Damaschin, V., Grama, A., *Experimental Research to Validate Simulation Model of Constant Speed at Low Power Axis Wind Turbine*, Hervex Conference Proceedings, Călimănești-Căciulata, ISSN 1454-8003 November 2012.
[3] Popescu, T.C., Ion Guță, D., *"Hydrostatic Transmision with Mixed Adjustment"*, Hervex Conference Proceedings, Călimănești-Căciulata, ISSN 1454-8003 November 2010.
[4] Dorr, H., Ewald, R., Hutter, J., Kretz, D., Hydraulic Trainer – Proportional and Servo Valve Technology, Mannesmann Rexroth GmbH 1986
[5] National Instruments USB-6218 data sheet, http://sine.ni.com/ds/app/doc/p/id/ds-9/lang/ro
[6] Kubler compact incremental 3700 optic encoder
http://www.kuebler.com/PDFs/leaflet/drehgeber/english/3700-3720_en.pdf

IMPACT OF NOISE AND VIBRATIONS ON THE SHIP MICROCLIMATE

Krisztina Uzuneanu[1], Ion V. Ion
"Dunărea de Jos" University of Galaţi, Romania
Department of Thermal Systems and Environmental Engineering

Abstract

Noise pollution of the vessel microclimate means values of noise and vibration beyond the normal ones, reaching damaging thresholds. As sources of noise and vibration are considered the power plants, auxiliary facilities, drive propellers and the action of waves. Preventing noise is a problem to be treated differently depending on the noise sources, acoustic energy propagation medium and receivers. Among the methods of combating this type of pollution we identified active and passive means of protection.

1. Types of noise and their propagation pathways

Ship noise issue must be considered from two points of view. Firstly, in terms of providing appropriate working conditions for the ship crew which is very important in terms of physiological action on the service personnel , as well as technically . A high level of noise is not only harmful to the human body but can be the cause for failing to hear signals and commands, an indirect cause of damage to the various mechanisms or the ship as a whole. Secondly this issue should be examined in terms of creating favorable conditions for the rest time of the off-duty crew.

Typically, on board of a ship noise sources can be considered all mechanisms and machines with moving parts that generate vibration and aerodynamic disturbances. Transmission of noise from the source of its generation can be done by air and throughout the hull as vibrations (Fig. 1). Thus, in production problems both airborne noise (represented in the figure below the line discontinuous -----) and the structural noise (represented by arrows →) must be properly dealt with.

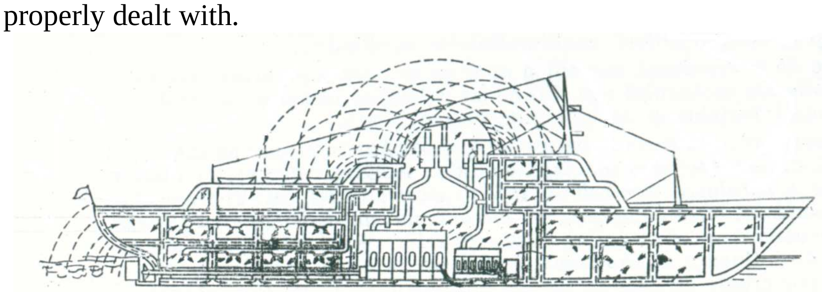

Fig. 1. Transmission of noise on shipboard.

Airborne noise occurs when sound sources, such as a machine tool, give rise to vibrations that propagate as waves in air. Airborne sound transmission between two rooms separated by a bulkhead occurs when waves bring into vibrations - with large enough amplitudes – the bulkhead and its vibrations are thus transferred to the air in the adjoining room. Other pathways of airborne noise in rooms are openings for doors and windows, openings in walls and floors, ventilation channels and holes around plumbing and electrical pipes.

Structural noise arises when the vibration source itself excites the structural/building elements, this is the case of shock or impact in ceilings and floors. Due to transversal waves that occur, ceilings and floors become noisy acoustic radiators producing airborne noise in the surrounding air when the vibration frequency is higher than 20 Hz. If the vibration frequency is below this limit they cause trepidations. Structural noise can be generated by machinery and

[1] Galati, 47 Domneasca St., E-mail: kristina.uzuneanu@ugal.ro

equipment, doors slamming. Structural noise can be reduced if the continuity of the propagation pathway is interrupted. The propagation pathways of noise from a source on shipboard are shown in Fig. 2.

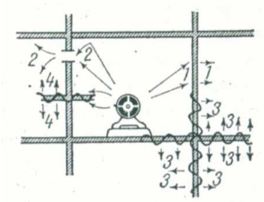

Noise propagation pathways:
1 – air-bulkhead-air;
2 – air-orifices- air;
3 – foundation-floor- bulkhead-air;
4 – air- floor- -air.

Fig. 2. Propagation of noise on shipboard.

The impact noise is a form of structural noise caused by forces acting on the ceilings and floors of buildings causing vibrations that propagate through the solid media. When coming across surfaces able to radiate acoustic energy, these vibrations are converted into audible air noise. Instant vibration energy of impact is much higher than the usual sources of noise generated by air.

Contemporary ship builders give more and more importance to noise reduction inside the rooms. Until recently, almost all attempts in this direction have been focused on noise generated by engines [2]. These tests however used to neglect other interacting mechanisms thus generating unacceptable noise levels. Approaching the issued of ship noise and vibration requires consideration of all noise sources and materials used in the construction of ships. To comply with both the criteria of effectiveness and price, solutions must be adapted to the navigation particulars. Techniques for noise control have been developed, including energy absorbing material adapted to interdependent sources of ship noise.

Through extensive analysis of noise and their transmission through the ship structure, using digital technology to measure noises, it was possible to identify the actual sources and propagation pathways within. These analyses include measurement of sound pressure, sound intensity and structural vibration under ship march.

A less expensive control method is to isolate noise as close as possible to the source of noise or vibration. This means insulation of the structure vibration is to be transmitted through with wet materials before vibrations are radiated as noise. By carefully selecting materials for isolating the largest noise sources and their propagation paths, it is possible to achieve an effective treatment method with better performance than traditional systems.

Vibrational energy is transmitted through the hull by the propulsion system. This energy enters the hull through transmission fluids such as exhaust gas or the propeller fixed connections.

In order to alleviate both types of induced vibration, hydrodynamic and mechanical, vibro insulation materials will be applied on the underside of the support plane. They should be centered between the support framework and the mechanism.

2. Vibrations due to the effects of the sea. Solutions to reduce excitation sources

The effect of the swell of the ship hull can be considered as an excitation source and vibration generator of the ship structure (Fig. 3). There are two kinds of excitations: whipping and springing.

Whipping phenomenon is best known and is the result of the impact of hydrodynamic shocks applied to the bottom of the ship in the bow area. They usually occur in situations where hydro-meteorological conditions allow significant movement of the stem so as to cause impacts. Depending on where the impact occurs, this can be:

- slamming - shock occurs on the plane area of the ship's bottom when it falls back into the sea after emersion;

- slapping - the bow shock is produced without emersion.

Springing phenomenon is the second type of excitation due to variable hydrodynamic forces and is related to a phenomenon of entering into free vibrations maintained by the hull. This occurs when the natural frequency of the framework, which vibrates according to the first mode of vibration, is within the frequency range of the ship/swell intersection for which the spectral energy density of the swell is high enough.

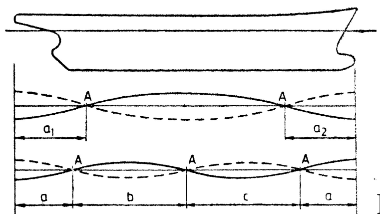

Fig. 3. Ship vibration due to the swell of the ship hull.

Vertical bending vibrations of two or three knots may become dangerous because of the disruptive forces and moments. Estimation of the springing effects can be done analytically, but at the same time there are reserves about their accuracy as in the case of whipping. The law accuracy of the methods estimating the excitation forces correlated with reduced information about the influence of hull shape on their level, do not allow precise recommendations to prevent springing and whipping.

Regarding the phenomenon of whipping, although a major influence in its production is that of the hydro-meteorological conditions, as early as the design stage the following can be taken into account:

- flat or "U" pronounced shape of the hull bottom and too steep slopes of the dead work cause slamming or slapping;
- maintaining draught under any navigational conditions to the recommended level;
- presence of bulb should be avoided if possible;
- phenomenon is sensitive to the length of the ship and its speed in some cases.

With respect to the phenomenon of springing there is no method for its reduction, as it is dependent on the speed and length of the ship, as well as the distribution of cargo and ballast. Reducing the two excitation sources can be done by changing the speed and route of the ship. For whipping through a proper ballasting it can be obtained an increase in the forward draught, and for springing by changing the cargo distribution.

3. Torsional vibration dampers to reduce the shaft line

The machine crankshaft together with intermediate shafts and propeller shaft represent the shaft line of a ship propulsion plant. Together with a crank rod mechanism of the cylinders and the rotating mass (flywheel, propeller) the shaft line is a flexible system, where torsional vibrations occur due to the action of torque, inertia forces and translating masses. These vibrations can be very strong at certain speeds called critical shaft speed. To remove critical speed or to reduce vibration amplitudes in case of operation at critical speeds, vibration dampers can be used [4]. In practical use there are several types of dampers. Any of them has a wheel or an element of high inertia that can move relative to the shaft whose vibration should be damped and to which is connected by: dry friction; viscous friction; dry or viscous friction and springs; centrifugal force equivalent to a spring (pendulum damper/absorber).

Each of these types of dampers generates torques in opposition to excitation torques. The simplest damper and widely used on marine engines is the auxiliary mass damper with dry friction and not adjusted as shown in Fig. 4.

The damper comprises a cylindrical housing J inside of which there is a flywheel J_d. Between the flywheel and housing are very small h_1 and h_2 clearances and the housing is filled with oil so that the flywheel J_d can rotate freely relative to the housing. Silicone oil is used because of its high viscosity: IV = 150-250 and the fact that the viscosity of the oil varies very little with temperature. Viscosity index is denoted by IV (index viscosity) and is a parameter defined in relation to how viscosity varies with the temperature of two reference oils, as follows:

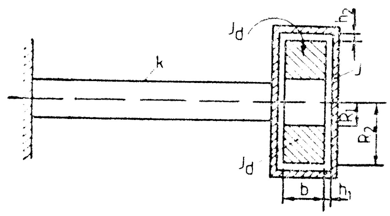

Fig. 4. Vibration damper.

- IV = 0 for high oil viscosity variation with temperature;
- IV = 100 for oil whose variation with temperature is relatively small.

The calculation of viscosity index is:

$$IV = \frac{v_1 - v_0}{v_1 - v_2} \times 100 \tag{1}$$

To measure the viscosity, the measurable parameter is the ratio of the dynamic viscosity η and density, ρ, called the kinematic viscosity parameter:

$$v = \frac{\eta}{\rho} \ [\mathrm{m^2/s}] \tag{2}$$

For oils having viscosity higher than 100 a similar index is used defined by the relation:

$$IV_E = 100 + \frac{10^N - 1}{0.00715} \tag{3}$$

where:

$$N = \frac{\log(v_2) - \log(v_0)}{\log(v_3)} \tag{4}$$

Variation of kinematic viscosity with temperature, in analytical forms is expressed by Reynolds' equation:

$$\eta = A \cdot e^{-\beta T} \tag{5}$$

4. CONCLUSIONS

The ship noise problem must be examined from two viewpoints. Firstly, in terms of creating appropriate conditions of the crew employment which is very important both in terms of physiological action on the servicing staff and technically. A high level of noise is not only harmful to the human body but may cause hearing problems as regards signals and commands, an indirect cause of damage to different mechanisms or the ship as a whole. Secondly, this issue should be examined in terms of creating favorable rest conditions for the crew which is out of service. Typically, on shipboard all the mechanisms and machinery with moving parts that generate vibration or aerodynamic disturbance may be considered sources of noise.

References

1. Alexa F., *Introducere în tehnica sunetului*. Editura de Vest, Timişoara, 1999.
2. Bodolan D., Buzbuchi N., *Modelarea, predicţia şi controlul emisiilor poluante ale motoarelor navale,* Ed. Nautica, Constanţa, 2005.
3. Dinu D., Dinu V., *Prevenirea poluării mediului marin*, Ed. Fundației Universitare "Dunarea de Jos", Galati, 2004.
4. Howard D.M., Angus J., *Acoustics and Psychoacoustics,* Focal Press, 1996.
5. Turner J.D., Pretfore A.J., *Acoustic for Engineers,* MacMillian Education Ltd., 1991.
6. Uzuneanu K., *Poluarea sonoră*, Ed. Didactica şi Pedagogică, Bucureşti, 2005.

With more than 20 years of experience, Sartorom offers complete solutions for laboratories from all industries (R&D, production, quality control), being the first lab instruments provider that has been certified ISO 9001 in Romania

Our offices:

- Bucharest: Sales, service and calibration laboratory
- Timisoara: Sales and calibration laboratory
- Cluj: Sales
- Craiova: Sales and service
- Brasov: Sales
- Iasi: Sales and service

Certifications:

- ISO 17025:2005 Calibration laboratory for balances and weighing platforms
- ISO 17025:2005 Calibration Laboratory for pipettes
- ISO 17025:2005 Calibration laboratory for testing machines and extensometers
- ISO 17025:2005 Calibration laboratory for calorimeters
- Integrated Management System ISO 9001/ISO 14001/ISO 18001 TÜV Hessen

SARTOROM is exclusive dealer of:

NETZSCH - The Analyzing & Testing business unit of the NETZSCH group develops and manufactures a complete high-precision instrument line for thermal analysis and thermophysical properties measurement, as well as offering world class commercial testing services in our laboratories. Our instrumentation is employed for research and quality control in the polymer sector, the chemical industry, the areas of inorganic and building materials, and environmental analysis.

Simultaneous Thermogravimetry - Differential Scanning Calorimetry (STA)

Thermogravimetry TG

HFM 436 Lambda

Zwick Roell For over 150 years the name of Zwick Roell has stood for outstanding technical expertise, innovation, quality and reliability in materials and component testing.

INFORS HT is your specialist for bioreactors, incubation shakers and bioprocess control software. You benefit from sophisticated systems, in which your cell lines or microorganisms develop their full potential in a reproducible way, thus contributing to your success.

FRITSCH Since many decades FRITSCH laboratory instruments for sample preparation convince with comfort, dependability and precision

IKA® has gained a leading position in the world market with its innovative magnetic stirrers, mixers, overhead stirrers, shakers, homogenizers, mills, rotary evaporators, calorimeters, laboratory reactors and specially developed software for laboratory and analysis applications.

Angelantoni INDUSTRIE MORE THAN TECHNOLOGY

ACS, world-famous since 1952 for its design and manufacture of a comprehensive range of environmental test chambers , including high-tech test equipment such as high vacuum chambers for aerospace applications and calorimeters.

A few of our reference customers:

- University Politehnica of Bucharest
- University Politehnica of Timisoara
- West University of Timisoara
- "Gheorghe Asachi" Technical University of Iaşi
- "Aurel Vlaicu" University of Arad
- Transilvania University of Brasov
- "P. Poni" Institute of Macromolecular Chemistry
- "Ilie Murgulescu" Institute of Phisical Chemistry
- National Institute for R&D in Electrical Engineering ICPE-CA
- National Institute of Research & Development for Technical Physics
- Biotehnos S.A.
- Dacia S.A.
- Autoliv Brasov

The underlying company's motto is: "Quality is the difference".

Analytik Jena is a leading provider of high-end analytical instruments and bio-analytical systems for industrial and scientific applications.

The company is represented in more than 100 countries and has its roots in the Zeiss-company with the headquarters in Jena, Germany.

It has more than 150 years of experience in the field of optical spectroscopy and elemental analysis.

Area of product applications are including materials research, cosmetic industry, food industry, pharmacy, research and education, agriculture, water analysis, metallurgy, petrochemical industry, chemical industry, galvanic industry, medicine.

The products of Analytik Jena have an intelligent design and enhanced quality because:

- The optics are quartz coated
- Usage of certified high end components only in the manufacturing process
- The optical systems are complete encapsulated

Analytik Jena is the only company which offers 10 years warranty on optical components.

Analytical instruments produced by Analytik Jena includes:

- Optical Emission Spectroscopy: PlasmaQuant® PQ 9000
- Atomic Absorption Spectroscopy: novAA®, ZEEnit, contrAA®
- Atomic Fluorescence Spectroscopy: mercur
- Sample Preparation: microwave digestion systems (TOPwave®)
- UV VIS Spectroscopy: SPECORD® and SPEKOL®
- Photochemiluminescence: PHOTOCHEM®
- Sum Parameter Analysis: - multi N/C® – TOC/TN, multi X® – AOX/TOX, EOX, POX
- Elemental Analysis: Carbon, Sulfur, Nitrogen and Chlorine (multi EA® series)

Analytik Jena is taking more than a decade of excellence in high-resolution (HR) spectrometer design to the next level introduction an HR Array ICP OES of unparalleled resolving power: PlasmaQuant® PQ 9000. Standing for unsurpassed quality instrumentation entirely made in Germany, PlasmaQuant PQ® 9000 masters the most difficult analytical challenges in atomic spectroscopy with superiority in terms of convenience, flexibility and precision. PlasmaQuant PQ® 9000 is the most powerful ICP OES wich combines robust hig-resolution technology and a revolutionary small design.

Persuasive characteristics:

- Smart bench-top instrument design
- Innovative high-end technology
- Impressive analytical performance
- Competitive sampling efficiency
- A new generation in operator comfort
- Premium quality made in Germany

*PlasmaQuant® PQ 9000— Continuing the Success

Analytik Jena brings an innovation on the market – the contrAA® series – which exceeds the performance of conventional AA spectrometers in all parameters. The HR-CS AAS contrAA® 700 it's a new instrument concept, using a high-intensity xenon short-arc lamp as continuum radiation source, a high-resolution double monochromator (a prism and an Echelle grating) and a CCD array detector. It finally closes the gap between ICP-OES and AAS.

HR-CS AAS contrAA® 300 for flame and hydride techniques, contrAA® 600 for graphite furnace technique and contrAA® 700 for flame, hydride and graphite furnace techniques are capable of analyzing liquid as well as solid samples. This instruments combines intelligent design with premium functionality and persuasive performance characteristics:

- Just one light source for all elements
- Sequential multi-element routine as standard
- Unique simultaneous background correction
- New information content

The contrAA® 600 and contrAA® 700 permits automated direct solid sample feeding and allows easy conversion for liquid sample analysis.

Analytical advantages of solid samples includes:

- Analysis of original samples
- Use of small amounts of samples
- No dilution
- Detection limits in the pg and fg ranges
- No sample digestion needed

Thanks to their unique precision, innovative technologies and durability an increased number of companies are putting their trust in technology from Analytik Jena AG. We can mention in here companies like: Abbott, Akzo Nobel, Altana, AstraZeneca, Braun, BASF, Baxter, Bayer, BMW, Boehringer Ingelheim, BP, Buderus, Coca-Cola, Dea, Degussa, Dow, Esso, Fresenius Fuji, Gsk, Henkel, Honeywell, Knoll, The Linde Group, Mercedes, Merck, Mitsubishi Motors, Nissan, Novartis, Roche, Samsung, Sanofi Avensis, Sasol, Schering, Schott, SGS, Shell, Siemens, Solvay, Thyssenkrupp, Volskwaggen, Wacker and many more.

HEAT RECOVERY SYSTEMS AND EQUIPMENT

Our company **Turboexpert SRL** is involved in research and development of heat recovery systems and equipment. We design equipment, we install it (turn key projects) and we offer consulting and technical assistance. One of our areas of expertise is energy recovery, obtaining significant fuel economies and minimizing environmental impacts. We recover waste heat, especially from flue gases released to atmosphere at high temperature 150 to 400degrees C. Such applications are steam boilers, furnaces, internal engines

We also recover steam under pressure for producing electricity (CHP).Such applications are industrial boilers over 20t/hr steam capacity and delivery pressure over 16 bar.

For waste heat recovery **Turboexpert SRL** has designed an original recuperator. It consist of a modular solution that can work in economizer or condensation mode, based on the flue gas temperature and its dew point.

The major advantage of our recuperator is that have a very competitive price, can be located in restrained locations, can operate under different thermal regimes, and require a very low maintenance. Return on investment can be obtained in a very short period, 5 to 8 months of operation.

Please contact us with your energy recovery problems, we can turn waste heat in significant profits

Economical efficiency of our recuperators is very high. The investment is recovered overall for heat recovery systems in 5-8 months of nominal operation

www.turboexpert.ro

Eng. Dan ANDREESCU
Mobil: (004) 0722 229 638
Fax: (004) 021/ 252 18 59
Email: turboexpertromania@rdslink.ro
office@turboexpert.ro
Eng. Elisabeta CERCHEZ
Mobil: (004) 0741 01 39 71
Email: elisabeta_cerchez@yahoo.ro